

DEVELOPMENT OF LARGE HIGH-STRENGTH REINFORCING BARS WITH STANDARD HOOKS AND HEADS

By

Ali Banaeipour, David Darwin
Matthew O'Reilly, Rémy D. Lequesne
~~Andres Lepage~~, Matthew Blessent

A Report on Research Sponsored by



**CHARLES PANKOW
FOUNDATION**

Charles Pankow Foundation Research Grant Agreement #05-18, D17
ACI Foundation, BarSplice Products,
Headed Reinforcement Corporation, nVENT Lenton,
CRSI Education and Research Foundation,
Precast/Prestressed Concrete Institute,
Commercial Metals Company, Nucor Corporation

Structural Engineering and Engineering Materials
SM Report No. 153
July 2023



THE UNIVERSITY OF KANSAS CENTER FOR RESEARCH, INC.
2385 Irving Hill Road, Lawrence, Kansas 66045-7563

**DEVELOPMENT OF LARGE HIGH-STRENGTH REINFORCING BARS WITH
STANDARD HOOKS AND HEADS**

By
Ali Banaeipour
David Darwin
Matthew O'Reilly
Rémy D. Lequesne
Andres Lepage
Matthew Blessent

A Report on Research Sponsored by



**CHARLES PANKOW
FOUNDATION**

Charles Pankow Foundation Research Grant Agreement #05-18, D17

**ACI Foundation, BarSplice Products,
Headed Reinforcement Corporation, nVENT Lenton,
CRSI Education and Research Foundation,
Precast/Prestressed Concrete Institute,
Commercial Metals Company, Nucor Corporation**

Structural Engineering and Engineering Materials

SM Report No. 153

THE UNIVERSITY OF KANSAS CENTER FOR RESEARCH, INC.

LAWRENCE, KANSAS

July 2023

ABSTRACT

Hooked and headed reinforcing bars are viable alternatives for development of reinforcing steel when member geometry does not allow for a straight deformed bar to fully develop its yield strength. Current design provisions in ACI 318-19 Building Code impose limitations on the use of hooked and headed bars larger than No. 11 (that is, No. 14 and No. 18 bars), mainly due to a lack of experimental data. This research continues a comprehensive study of the anchorage and development of high-strength hooked and headed bars to expand the available data to include No. 14 and No. 18 bars. Forty-two large-scale simulated beam-column joint specimens containing No. 11, No. 14 and No. 18 hooked and headed bars are tested. Of the 42 specimens, 12 contain hooked bars and 30 contain headed bars. The effects of bar size, bar spacing, bar location, embedment length, confining transverse reinforcement in the joint region, placement of bars within the cross-section, concrete compressive strength, compression strut angle, and effective beam depth on anchorage strength are investigated. Two loading conditions are used. In loading condition A, the joint shear is 80% of the total applied force to the bars, simulating the forces in an exterior beam-column joint with the beam located at the midheight of the column. The joint shear is reduced to ~69% of the total applied force in loading condition B. All hooked bar specimens and 15 headed bar specimens are tested under loading condition A, while the other 15 headed bar specimens are tested using loading condition B. Concrete compressive strengths range from 6,390 to 15,770 psi for hooked bars and from 5,310 to 16,210 psi for headed bars. Bar stress at failure ranges from 87,300 to 130,600 psi for hooked bars and from 54,900 to 148,300 psi for headed bars. Center-to-center bar spacing, s , ranges from $3.5d_b$ to $10.6d_b$ for hooked bars and from $2.7d_b$ to $10.6d_b$ for headed bars, where d_b is the nominal hooked or headed bar diameter. Confining reinforcement, A_{th} , or parallel ties, A_t , in the joint region ranges from 0 to $0.465A_{hs}$ and 0 to $0.827A_{hs}$ for hooked and headed bars, respectively, where A_{th} or A_t equal the total cross-sectional area of tie legs within $10d_b$ from the top of the bars and A_{hs} is the total area of the bars being developed. Headed bars with net bearing areas between 4.2 and 4.4 times the bar area are used.

The test results are compared with the current provisions for the development length of hooked and headed bars in Chapter 25 of ACI 318-19. Descriptive equations to characterize anchorage strength of hooked and headed bars developed previously for No. 11 and smaller bars are evaluated. New descriptive equations are developed to represent the anchorage strength for bars as large as No. 18. The equations are compared with the test results in the current study and available in the literature. New design provisions for development length are developed for hooked

and headed bars and evaluated with respect to test results and ACI 318-19 provisions.

The descriptive equations for hooked and headed bars developed in this study accurately account for concrete compressive strength, confining reinforcement, and bar spacing. The ability of the equations to accurately represent anchorage strength is insensitive to variations in compression strut angle and effective beam depth. While the contribution of confining reinforcement to anchorage strength increases with bar size, the effect of increasing confining reinforcement for headed bars is much lower than for hooked bars and much lower for headed bars than observed in prior studies. Under loading condition A, all hooked bar specimens, even those without confining reinforcement, carried the joint shear and exhibited an anchorage failure, whereas shear-like failures were observed in some headed bar specimens under similar conditions. These observations reveal the distinct role of the tail of the hook in helping to carry the joint shear, and indicate the difference in joint shear under loading conditions A and B is a key factor in the type of failure and anchorage strength of headed bars. Larger headed bars need confining reinforcement on the order of $0.5A_{hs}$ to carry the joint shear demand under loading condition A.

The development length provisions in ACI 318-19 are unnecessarily conservative for No. 14 and No. 18 hooked and headed bars. For both hooked and headed bars, providing confining reinforcement below the minimum amounts required by ACI 318-19 contributes to anchorage strength. Similar to No. 11 and smaller hooked and headed bars, the effect on anchorage strength of concrete compressive strength is best represented by the 0.25 power for design. The bar location factor ψ_o of 1.25 in ACI 318-19, applied to bars terminating inside column longitudinal reinforcement (column core) with side cover < 2.5 in. or bars with side cover $< 6d_b$, can be safely reduced to 1.15 for design. The proposed design equations for hooked and headed bars are applicable to concrete with compressive strengths up to 16,000 psi, steel with yield strengths up to 120,000 psi, and bars as large as No. 18. The proposed modification factors for confining reinforcement (expressed as A_{th}/A_{hs} or A_{tt}/A_{hs}) and bar spacing (expressed as s/d_b), in the form of a single expression or simplified expressions that address the effects of confining reinforcement and bar spacing independently, provide more flexibility for designers to take advantage of a range of values for A_{th}/A_{hs} or A_{tt}/A_{hs} and s/d_b and, ultimately, permit the use of shorter development lengths than the provisions in ACI 318-19 for all bar sizes.

Keywords: anchorage, beam-column joint, bond, development length, headed bar, high-strength concrete, high-strength steel, hooked bar, large-scale testing

ACKNOWLEDGEMENTS

This report is based on a thesis presented by Ali Banaeipour in partial fulfillment of the requirements for the Ph.D. degree from the University of Kansas. Support for the study was provided by the Charles Pankow Foundation under Research Grant Agreement #05-18, the ACI Foundation, BarSplice Products, Headed Reinforcement Corporation, nVENT Lenton, the CRSI Education and Research Foundation, the Precast/Prestressed Concrete Institute, Commercial Metals Company, and Nucor Corporation.

Additional support was provided by Dayton Superior, Midwest Concrete Materials, and Grace Construction Products. Thanks are due to Jack Moehle, Amy Trygstad, Javeed Munshi, and Andrew Taylor who served on the advisory panel.

TABLE OF CONTENTS

ABSTRACT	iii
ACKNOWLEDGEMENTS	v
TABLE OF CONTENTS	vii
LIST OF FIGURES	xii
LIST OF TABLES	xxv
CHAPTER 1: INTRODUCTION	1
1.1 GENERAL	1
1.2 BACKGROUND AND PREVIOUS RESEARCH.....	3
1.2.1 Reinforcing Bars with Standard Hooks	3
1.2.2 Headed Reinforcing Bars	14
1.3 CURRENT CODE PROVISIONS AND DESIGN GUIDELINES	29
1.3.1 Reinforcing Bars with Standard Hooks	30
1.3.2 Headed Reinforcing Bars	36
1.4 OBJECTIVE AND SCOPE	43
CHAPTER 2: EXPERIMENTAL WORK	45
2.1 MATERIAL PROPERTIES.....	45
2.1.1 Hooked and Headed Bars.....	45
2.1.2 Reinforcing Steel Properties.....	46
2.1.3 Concrete Properties.....	47
2.2 TEST SPECIMENS.....	48
2.2.1 Specimen Design	48
2.2.2 Test Parameters.....	52
2.2.3 Specimen Designation.....	53
2.2.4 Specimen Fabrication.....	54
2.2.5 Specimen Instrumentation.....	58
2.3 TESTING APPARATUS.....	59
2.3.1 Loading Conditions.....	59

2.3.2 Reaction Frame.....	61
2.3.3 Bearing Plates.....	67
2.3.4 Bar Displacement Measurement.....	68
2.3.5 Load Cells.....	69
2.3.6 Testing Procedure.....	69
2.3.7 Summary of Test Program.....	71
CHAPTER 3: TEST RESULTS	73
3.1 CRACKING PATTERNS.....	73
3.1.1 Hooked Bars.....	73
3.1.2 Headed Bars.....	75
3.2 FAILURE MODES.....	79
3.2.1 Hooked Bars.....	79
3.2.2 Headed Bars.....	81
3.3 STRAIN DEVELOPED IN REINFORCEMENT.....	87
3.3.1 Ties.....	87
3.3.2 Hooked Bars.....	90
3.3.3 Headed Bars.....	92
3.4 ANCHORAGE STRENGTH.....	93
CHAPTER 4: ANALYSIS AND DISCUSSION: HOOKED BARS.....	96
4.1 COMPARISON OF TEST RESULTS WITH ACI 318-19.....	96
4.2 COMPARISON OF TEST RESULTS WITH DESCRIPTIVE EQUATIONS DEVELOPED BY AJAAM ET AL. (2017, 2018).....	99
4.3 NEW DESCRIPTIVE EQUATIONS.....	101
4.3.1 Widely-spaced Bars Without Confining Reinforcement.....	101
4.3.2 Closely-spaced Bars Without Confining Reinforcement.....	103
4.3.3 Widely-spaced Bars with Confining Reinforcement.....	107
4.3.4 Closely-spaced Bars with Confining Reinforcement.....	109
4.3.5 Summary.....	111

4.4 EVALUATING DESCRIPTIVE EQUATIONS.....	113
4.4.1 Bar Location	113
4.4.2 Confining Reinforcement.....	118
4.4.3 Bar Spacing	121
4.4.4 Strut Angle	122
4.4.5 Effective Beam Depth.....	125
4.4.6 Embedment Length.....	127
4.5 SPECIMENS NOT USED TO DEVELOP DESCRIPTIVE EQUATIONS	128
CHAPTER 5: ANALYSIS AND DISCUSSION: HEADED BARS	136
5.1 COMPARISON OF TEST RESULTS WITH ACI 318-19.....	137
5.2 COMPARISON OF TEST RESULTS WITH DESCRIPTIVE EQUATIONS DEVELOPED BASED ON TESTS OF NO. 5 THROUGH NO. 11 HEADED BARS	140
5.3 NEW DESCRIPTIVE EQUATIONS.....	144
5.3.1 Widely-spaced Bars Without Parallel Ties	145
5.3.2 Closely-spaced Bars Without Parallel Ties.....	146
5.3.3 Widely-Spaced Bars with Parallel Ties	149
5.3.4 Closely-Spaced Bars with Parallel Ties.....	151
5.3.5 Summary	154
5.4 EVALUATING NEW DESCRIPTIVE EQUATIONS FOR NO. 14 AND NO. 18 BARS...	156
5.5 EFFECT OF TEST PARAMETERS.....	162
5.5.1 Loading Condition	162
5.5.2 Parallel tie Reinforcement.....	172
5.5.3 Bar Spacing	175
5.5.4 Placement of Bars Within the Cross-section.....	176
5.5.5 Compression Strut Angle	179
5.5.6 Effective Beam Depth.....	180
5.5.7 Embedment Length.....	182
5.5.8 Bar Location	183

5.6 BEAM-COLUMN JOINT SPECIMENS NOT USED TO DEVELOP DESCRIPTIVE EQUATIONS	188
CHAPTER 6: DESIGN APPROACH.....	194
6.1 HOOKED BARS.....	194
6.1.1 Simplified Descriptive Equations	194
6.1.2 Design Equation for Development Length.....	199
6.1.3 Evaluating Proposed Design Equation.....	207
6.2 HEADED BARS	218
6.2.1 Simplified Descriptive Equations	218
6.2.2 Design Equation for Development Length.....	224
6.2.3 Evaluating Proposed Design Equation.....	229
6.3 COMPARISONS WITH ACI 318-19	238
6.3.1 Concrete Compressive Strength	238
6.3.2 Required Development Length.....	240
CHAPTER 7: SUMMARY, CONCLUSIONS, AND FUTURE WORK	248
7.1 SUMMARY	248
7.2 CONCLUSIONS	249
7.3 FUTURE WORK	252
REFERENCES.....	253
APPENDIX A: NOTATION.....	258
APPENDIX B: HOOKED BAR BEAM-COLUMN JOINT SPECIMENS	262
B.1 DRAWINGS AND REINFORCEMENT LAYOUTS FOR NO. 14 AND NO. 18 BAR SPECIMENS TESTED IN CURRENT STUDY	263
B.2 DETAILED PROPERTIES AND TEST RESULTS FOR NO. 14 AND NO. 18 BAR SPECIMENS TESTED IN CURRENT STUDY	275
B.3 SPECIMENS TESTED AT THE UNIVERSITY OF KANSAS	279
B.4 SPECIMENS TESTED IN OTHER STUDIES	315
APPENDIX C: HEADED BAR BEAM-COLUMN JOINT SPECIMENS.....	324

C.1 DRAWINGS AND REINFORCEMENT LAYOUTS FOR NO. 14 AND NO. 18 BAR SPECIMENS TESTED IN CURRENT STUDY325

C.2 DETAILED PROPERTIES AND TEST RESULTS FOR NO. 14 AND NO. 18 BAR SPECIMENS TESTED IN CURRENT STUDY353

C.3 SPECIMENS TESTED AT THE UNIVERSITY OF KANSAS361

C.4 SPECIMENS TESTED IN OTHER STUDIES384

LIST OF FIGURES

Figure 1.1. Anchorage mechanism of hooked bars (adapted from Marques and Jirsa 1975)	4
Figure 1.2 Crack progression observed in the beam-column joint specimens containing hooked bars (Sperry et al. 2015b, 2017a). Breakout failure is preceded by bond slip of the straight portion of the bars and cracking of the concrete.....	4
Figure 1.3 Schematic of test specimens used by Marques and Jirsa (1975); Type 1: Hooked bars inside column core without confining reinforcement, Type 2 and 4: Hooked bars outside column core without confining reinforcement, Type 3: Hooked bars outside column core with No. 3 ties, and Type 5: Hooked bars outside column core with No. 3 ties plus cross-tie	6
Figure 1.4 Strut angle as defined by Joh et al. (1995).....	7
Figure 1.5 Schematic of specimens (a) side view (b) cross-section without confining reinforcement, and (c) cross-section with confining reinforcement, where ℓ_{eh} is the embedment length and d_b is bar diameter	10
Figure 1.6 Schematic of the reaction frame (Sperry et al. 2015b).....	11
Figure 1.7 Primary failure modes observed in hooked bar specimens (Sperry et al. 2015b).....	12
Figure 1.8 Steel congestion in an external beam-column joint caused by staggered hooked bars (https://www.sefindia.org).....	14
Figure 1.9 Different types of headed bars (Shao et al. 2016)	15
Figure 1.10 Previous limits on headed bar obstructions (ASTM A970/M970-16)	15
Figure 1.11 Current dimensional limits for obstructions or interruptions in headed bars (ASTM A970/M970-18)	16
Figure 1.12 Anchorage and bond of headed bars (Shao et al. 2016)	16
Figure 1.13 Crack progression observed in the beam-column joint specimens containing headed bars. Breakout failure is preceded by bond slip along the straight portion of the bars and cracking of the concrete (Shao et al. 2016, Ghimire et al. 2019a).....	17
Figure 1.14 (a) Side view of specimen proportions used by Chun et al. (2017a) and Chun and Lee (2019); (b) Side view of the specimen proportions used by Sim and Chun (2022b); (c) Side view of the specimen proportions used by Sim and Chun (2022a).....	20
Figure 1.15 Schematic of headed bar specimens (a) side view (b) cross-section, where h and w are column height and width, respectively, and ℓ_{eh} is the embedment length (Shao et al. 2016)	23

Figure 1.16	The loading frame and test setup of headed bar specimens (Shao et al. 2016)	24
Figure 1.17	Concrete breakout (a) cone-shaped (b) back cover spalling (Shao et al. 2016).....	25
Figure 1.18	Side-face blowout (a) side view (b) back view (Shao et al. 2016).....	26
Figure 1.19	Confining reinforcement contributing to anchorage strength of headed bars anchored in beam-column joints (Shao et al. 2016, Ghimire et al. 2019).....	28
Figure 1.20	ACI 318-14 provisions for ties or stirrups placed perpendicular (left) or parallel (right) to the hooked bar being developed (ACI 318-14)	30
Figure 1.21	Ratio of test-to-calculated stress $f_{su}/f_{s,ACI}$ versus f_{cm} for hooked bars without confining reinforcement (Sperry et al. 2015b)	31
Figure 1.22	Ratio of test-to-calculated stress $f_{su}/f_{s,ACI}$ versus f_{cm} for hooked bars with No. 3 ties spaced at $3d_b$ in the joint region (Sperry et al. 2015b)	32
Figure 1.23	Confining reinforcement placed parallel (left) or perpendicular (right) to the hooked bar being developed as defined in ACI 318-19 (from ACI 318-19).....	35
Figure 1.24	Ratio of test-to-calculated stress $f_{su}/f_{s,ACI}$ versus f_{cm} for two widely-spaced headed bars without confining reinforcement, where $f_{s,ACI}$ is based on ACI 318-14 (from Shao et al. 2016)..	37
Figure 1.25	Ratio of test-to-calculated stress $f_{su}/f_{s,ACI}$ versus f_{cm} for two widely-spaced headed bars with No. 3 hoops spaced at $3d_b$, where $f_{s,ACI}$ is based on ACI 318-14 (Shao et al. 2016).....	38
Figure 1.26	Bars located outside (left) or inside (right) of the column core	40
Figure 1.27	Parallel tie reinforcement that contribute to anchorage strength of headed bars as defined in ACI 318-19 (ACI 318-19).....	41
Figure 2.1	Different types of headed bars used in the study	45
Figure 2.2	Schematic of the specimens with hooked bars, side view (left) and top view (right).	49
Figure 2.3	Schematic of the specimens with headed bars, side view (left) and top view (right) .	50
Figure 2.4	Dimensional proportions of the specimens; For specimens with No. 14 bar, $x_{mid} = 28.56$ in. and $h_0 = 14$ ft, and for specimens with No. 18 bar, $x_{mid} = 38.15$ in. and $h_0 = 18$ ft	51
Figure 2.5	Double overlapping tie configuration.....	53
Figure 2.6	Example specimen designation	54
Figure 2.7	Cross-sectional dimensions and variable callouts of specimens.....	54
Figure 2.8	Vertical formwork for No. 14 bar specimens and sawhorses to hold the bars	55
Figure 2.9	Clamping system to brace the vertical forms for No. 14 bar specimens	56
Figure 2.10	Horizontal formwork for No. 18 bar specimens	56

Figure 2.11 A typical reinforcement cage (steel cage).....	57
Figure 2.12 No. 14 hooked (left) and headed (right) bars tied to steel cages.....	57
Figure 2.13 No. 18 hooked (left) and headed (right) bars tied to steel cages.....	58
Figure 2.14 Side view (left and middle) and top view (right) of strain gauge locations.....	59
Figure 2.15 Forces applied to specimens by the reaction frame during the test.....	60
Figure 2.16 Side elevation of the reaction frame for the No. 14 bar setup	62
Figure 2.17 End-elevation of the reaction frame for the No. 14 bar setup.....	63
Figure 2.18 The reaction frame (No. 14 bar setup) and applied forces.....	64
Figure 2.19 Plan view and cross-section of the built-up section	65
Figure 2.20 Load cells, washer plates, and couplers for No. 14 bar test setup.....	66
Figure 2.21 Alternative test setup used in widely-spaced No. 18 bar specimens.....	67
Figure 2.22 Setup for using the LVDTs.....	68
Figure 2.23 Load cell for No. 14 and No. 18 bars	69
Figure 3.1 Example of cracking pattern in hooked bar specimens (front face, specimen H14-15): (a) Horizontal cracks likely initiating due to bar slip, (b) Cracks radiating from the hooked bars, and (c) Cracks radiated from the hooked bars connected to each other along with local concrete damage.....	74
Figure 3.2 Example of cracking pattern in hooked bar specimens (side face, specimen H14-15): (a) Vertical crack likely initiating due to bar slip, (b) and (c) Cracks propagating and branching towards upper and lower bearing members, (d) Cone-shaped cracking pattern near failure (see arrows.).....	75
Figure 3.3 Example of cracking pattern in headed bar specimens (side face, specimen 18-3): (a) Vertical crack likely initiating due to bar slip, (b) Cracks branching towards bearing members, (c) First diagonal crack due to shear in joint, (d) and (e) Cracks propagating throughout the joint, (f) Cone-shaped cracking pattern after failure. (Note: Extension of diagonal cracks along the back face of the specimen towards the top of the column are marked by dashed lines.).....	77
Figure 3.4 Example of cracking pattern in headed bar specimens (top face, specimen 18-3): (a) Crack between bars likely initiating due to bar slip, (b) Cracks branching towards bearing members, (c) First diagonal crack due to shear in joint, (d) and (e) Cracks propagating throughout the joint.....	78
Figure 3.5 Side view of a concrete breakout failure in hooked bars with tail kickout (H14-7) ...	80

Figure 3.6 Side view of a side-splitting failure for hooked bars (H14-8)	81
Figure 3.7 Primarily concrete breakout failure (top: specimen 14-10, bottom: specimen 18-5). (Note: Dashed lines highlight the cracks extending beyond the joint and along the back face of the column or towards the upper bearing member)	82
Figure 3.8 Primarily side-splitting failure (left: specimen 14-3, right: specimen 18-4)	83
Figure 3.9 Combination of concrete breakout and side splitting (specimen 14-15)	84
Figure 3.10 Concrete breakout accompanied by side splitting and compression failure of concrete between bearing face of the head and lower bearing member (specimen 14-16B)	84
Figure 3.11 Shear-like failure in headed-bar specimen 14-16. (Note: The specimen shows no indication of a breakout or side-splitting failure.)	85
Figure 3.12 Examples of strain developed in parallel ties in hooked bar specimen H14-2 (left) and headed bar specimen 14-6 (right)	88
Figure 3.13 Specimens H14-2 at failure showing location of ties and strain gauges	89
Figure 3.14 Parallel ties trapping the first diagonal cracks and their strain gauge labels in the headed bar specimen 14-6	90
Figure 3.15 Strain developed in one hooked bar in specimens H14-2 (left) and H14-15 (right). (Note: T1 was mounted just before the bend in the tail, and T2 mounted 1 in. from the front face of the column)	91
Figure 3.16 Strain developed in one headed bar in specimen 14-16C (left) and 18-8 (right) (Note: T1 was mounted 1.5 in. from the bearing face of the head, and T2 was mounted 1 in. from the column front face)	92
Figure 4.1 Ratio of test/calculated bar stress (ACI), $f_s/f_{s,ACI}$ versus concrete compressive strength f_{cm} for No. 14 and No. 18 hooked bar specimens (using values of ψ_r permitted for No. 11 and smaller bars, as shown in Table 4.1)	99
Figure 4.2 Ratio of test-to-calculated bar force at failure T/T_c versus concrete compressive strength for hooked bar specimens with widely-spaced bars (center-to-center spacing $\geq 6d_b$) without confining reinforcement	102
Figure 4.3 Test-to-calculated bar force at failure T/T_c versus ratio of center-to-center spacing to bar diameter s/d_b for widely- and closely-spaced hooked bars without confining reinforcement	104

Figure 4.4 Ratio of test-to-calculated failure load T/T_c versus concrete compressive strength for hooked bar specimens having widely- and closely-spaced bars without confining reinforcement	106
Figure 4.5 Ratio of test-to-calculated bar force at failure T/T_h versus concrete compressive strength for hooked bar specimens having widely-spaced ($s/d_b \geq 6d_b$) bars with confining reinforcement	108
Figure 4.6 Test-to-calculated bar force at failure T/T_h versus ratio of center-to-center spacing to bar diameter s/d_b for widely- and closely-spaced hooked bars with confining reinforcement ...	109
Figure 4.7 Ratio of test-to-calculated bar force at failure T/T_h versus concrete compressive strength for hooked bar specimens having widely- and closely-spaced bars with confining reinforcement	111
Figure 4.8 Measured versus calculated bar force at failure based on new descriptive equations for hooked bars, Eq. (4.5) and (4.7)	112
Figure 4.9 Confining reinforcement layouts in specimens with hooked bars placed outside the column core: (a) hooks outside the confining ties (Chun et al. 2017b), (b) hooks inside confining ties (Chun et al. 2017b), and (c) hooks inside confining ties (Sperry et al. 2015b)	116
Figure 4.10 Test-to-calculated ratio T/T_h based on new descriptive equations, Eq. (4.5) and (4.7), for hooked bars versus confining reinforcement ratio A_{th}/A_{hs}	118
Figure 4.11 Comparing anchorage strength of No. 14 hooked bars for confining reinforcement. T/T_h ratios shown based on Eq. (4.5) and (4.7). Center-to center spacing is $3.5d_b$ for specimens H14-7 and H14-8 (closely-spaced), and $10.6d_b$ for all other specimens (widely-spaced)	120
Figure 4.12 Comparing anchorage strength of No. 18 hooked bars for confining reinforcement. T/T_h ratios shown on top of each bar. Hooked bars have center-to-center spacing of $6d_b$	120
Figure 4.13 Test-to-calculated ratio T/T_h versus ratio of center-to-center spacing to bar diameter s/d_b based on Eq. (4.5) and (4.7), for hooked bar specimens used to develop the equations.....	122
Figure 4.14 Definition of compression strut angle (θ) for hooked bars.....	123
Figure 4.15 Test-to-calculated T/T_h ratio based on Eq. (4.5) and (4.7) versus compression strut angle θ for hooked bar specimens used to develop descriptive equations (not including specimens with $d_{eff}/\ell_{eh} > 1.5$).....	124
Figure 4.16 ℓ_{eh}/d_b versus compression strut angle θ for hooked bar specimens used to develop descriptive equations, Eq. (4.5) and (4.7).....	125

Figure 4.17 Effective beam depth d_{eff} for hooked bars (Ajaam et al. 2017).....	126
Figure 4.18 Test-to-calculated T/T_h ratio based on Eq. (4.5) and (4.7) versus effective beam depth to embedment length d_{eff}/ℓ_{eh} ratio for hooked bar specimens used to develop descriptive equations plus specimens with $d_{eff}/\ell_{eh} > 1.5$	127
Figure 4.19 Test-to-calculated T/T_h ratio based on Eq. (4.5) and (4.7) versus embedment length to bar diameter ℓ_{eh}/d_b ratio for hooked bar specimens used to develop descriptive equations.....	128
Figure 4.20 Schematic of the forces applied to specimens by (a) Marques and Jirsa (1975) and (b) University of Kansas studies (Searle et al. 2014, Sperry et al. 2015a, 2015b, 2017a, 2017b, 2018, Yasso et al. 2017, Ajaam et al. 2017, 2018) (Note: drawings are not to scale)	131
Figure 4.21 No. 11 hooked bar specimen proportions and applied forces: (a) University of Kansas (Searle et al. 2014, Sperry et al. 2015a, 2015b, 2017a, 2017b, 2018, Yasso et al. 2017, Ajaam et al. 2017, 2018), and (b) Marques and Jirsa (1975) (Note: T is the total applied force, and the force in the lower tension member is neglected).....	134
Figure 5.1 Ratio of test/calculated bar stress $f_s/f_{s,ACI}$ applying the ACI 318-19 provisions to No. 14 and No. 18 headed bar specimens versus concrete compressive strength f_{cm} , excluding specimens that failed in shear.....	139
Figure 5.2 Test versus calculated force per bar at failure for No. 14 and No. 18 headed bar specimens based on descriptive equations by Shao et. al (2016)	144
Figure 5.3 Ratio of test-to-calculated bar force at failure T/T_c , with T_c based on Eq. (5.4), versus concrete compressive strength for headed bar specimens with widely-spaced bars without parallel ties	145
Figure 5.4 Test-to-calculated bar force at failure T/T_c versus ratio of center-to-center spacing to bar diameter s/d_b for widely- and closely-spaced headed bars without parallel ties with T_c based on Eq. (5.4).....	147
Figure 5.5 Ratio of test-to-calculated bar force at failure T/T_c , based on Eq. (5.5), versus concrete compressive strength for headed bar specimens with widely- and closely-spaced bars without parallel ties.....	148
Figure 5.6 Ratio of test-to-calculated bar force at failure T/T_h versus concrete compressive strength for headed bar specimens with widely-spaced bars with parallel ties with T_h based on Eq. (5.6)	150

Figure 5.7 Test-to-calculated bar force at failure T/T_h versus ratio of center-to-center spacing to bar diameter s/d_b for widely- and closely-spaced headed bars with parallel ties with T_h based on Eq. (5.6).....	152
Figure 5.8 Ratio of test-to-calculated bar force at failure T/T_h versus concrete compressive strength for headed bar specimens with widely- and closely-spaced bars with parallel ties with T_h based on Eq. (5.7).....	153
Figure 5.9 Measured versus calculated bar force at failure using new descriptive equations for all headed bar specimens, excluding those with a shear-like failure, with the calculated bar force, T_h , based on Eq. (5.5) or (5.7).....	156
Figure 5.10 Measured versus calculated bar force at failure using new descriptive equations for No. 14 and No. 18 headed bar specimens, excluding those with a shear-like failure, with the calculated bar force, T_h , based on Eq. (5.5) or (5.7)	159
Figure 5.11 Ratio of test/calculated ratio T/T_h versus concrete compressive strength f_{cm} for No. 14 and No. 18 headed bar specimens, with the calculated bar force, T_h , based on Eq. (5.5) or (5.7)	160
Figure 5.12 Ratio of test/calculated ratio T/T_h versus parallel tie reinforcement ratio A_{tt}/A_{hs} for No. 14 and No. 18 headed bar specimens, with the calculated bar force, T_h , based on Eq. (5.5) or (5.7)	161
Figure 5.13 Ratio of test/calculated ratio T/T_h versus ratio of center-to-center spacing to bar diameter s/d_b for No. 14 and No. 18 headed bar specimens, with the calculated bar force, T_h , based on Eq. (5.5) or (5.7).....	162
Figure 5.14 Shear-like failure observed in specimen 14-16 ($A_{tt}/A_{hs} = 0.178$) tested under loading condition A: (a) after failure and (b) after dissection.....	164
Figure 5.15 Anchorage failure observed in specimen 14-15 ($A_{tt}/A_{hs} = 0$) tested under loading condition B	165
Figure 5.16 Additional No. 11 longitudinal bars in specimen 14-16A.....	166
Figure 5.17 Shear-like failure observed in specimen 14-16A ($A_{tt}/A_{hs} = 0.178$) tested under loading condition A	166
Figure 5.18 Shear-like failure observed in specimen 14-1A ($A_{tt}/A_{hs} = 0$) tested under loading condition B	167

Figure 5.19 Anchorage failure observed in specimen 14-2A ($A_{tt}/A_{hs} = 0.267$) tested under loading condition B	167
Figure 5.20 Anchorage failure observed in specimen 14-16B ($A_{tt}/A_{hs} = 0.178$) tested under loading condition B	168
Figure 5.21 Anchorage failure observed in specimen 14-16C ($A_{tt}/A_{hs} = 0.356$) tested under loading condition B	169
Figure 5.22 Double overlapping No. 5 ties in specimen 14-16D; (a) top view, (b) front view .	170
Figure 5.23 Anchorage failure observed in specimen 14-16D ($A_{tt}/A_{hs} = 0.827$) tested under loading condition A (after removal of loose concrete).....	170
Figure 5.24 Anchorage failure observed in specimen 14-16E ($A_{tt}/A_{hs} = 0.551$).....	171
Figure 5.25 Comparing anchorage strength of headed bars with and without parallel ties (Note: L.C. = Loading Condition, and the number below L.C. denotes $A_{tt,ACI}/A_{hs}$).....	172
Figure 5.26 Double No. 5 ties used in specimen 14-16F	173
Figure 5.27 Comparing side splitting failure modes of specimens 14-16E with parallel ties with middle legs (top) and 14-16F with only external legs (bottom), both with $A_{tt}/A_{hs} = 0.551$	174
Figure 5.28 Comparing the anchorage strength (average force per bar at failure) of No. 14 and No. 18 headed bars based on bar spacing	175
Figure 5.29 Concrete breakout observed in specimen 14-17 ($A_{tt}/A_{hs} = 0.551$) with increased side cover to the bar and decreased bar spacing	176
Figure 5.30 Comparing failure modes of specimen 18-1 with 3.5 in. side cover to the bar (top, side splitting) with specimen 18-5 with 6.5 in. side cover to the bar (bottom, concrete breakout), both with $A_{tt}/A_{hs} = 0.543$	177
Figure 5.31 Comparing failure modes of specimen 18-2 with 3.5 in. side cover to the bar (top) with specimen 18-6 with 6.5 in. side cover to the bar (bottom), both with $A_{tt}/A_{hs} = 0.543$	178
Figure 5.32 Compression strut angle (θ) for headed bars (x_{mid} is 28.56 and 38.15 in. for No. 14 and No. 18 bars, respectively, and ℓ_{eh} is the embedment length)	179
Figure 5.33 Comparison of strut angle θ versus test-to-calculated ratio T/T_h based on Eq. (5.5) and (5.7) for large (No. 11, No. 14, and No. 18) headed bars for specimens with $d_{eff}/\ell_{eh} < 1.5$	180
Figure 5.34 Effective beam depth d_{eff} for headed bars (Shao et al. 2016).....	181
Figure 5.35 Comparison of d_{eff}/ℓ_{eh} versus test-to-calculated ratio T/T_h based on Eq. (5.5) and (5.7) for large (No. 11, No. 14, and No. 18) headed bars.....	182

Figure 5.36 Comparison of ℓ_{eh}/d_b versus test-to-calculated ratio T/T_h for based on Eq. (5.5) and (5.7) for large (No. 11, No. 14, and No. 18) headed bars 183

Figure 5.37 Parallel tie layouts in specimens with headed bars placed outside the column core tested by Chun et al. (2017) and Sim and Chun (2022a, 2022b): (a) heads outside parallel ties (“unconfined”), (b) heads inside parallel ties (“confined”), and (c) heads outside parallel ties but “confined” by hairpin transverse reinforcement..... 185

Figure 5.38 Specimen proportions and applied forces: (a) current study; (b) Bashandy 1996 (Note: the bottom drawing is not to scale, L.C. = Loading condition, V_J = Joint Shear) 192

Figure 5.39 Schematic of the reinforcement layouts used by Bashandy (1996): (a) Headed bars outside the column core and parallel ties (specimens T10, T12, and T13); (b) Headed bars inside the column core and parallel ties (specimens T14 and T25); and (c) Headed bars inside column core but ties were not wrapped around column longitudinal bars (rest of the specimens) 193

Figure 6.1 Test-to-calculated bar force at failure T/T_c based on simplified Eq. (6.2) versus ratio of center-to-center spacing to bar diameter s/d_b for widely- and closely-spaced hooked bars without confining reinforcement used to develop descriptive equations, Eq. (4.5) and (4.7) 195

Figure 6.2 Ratio of test-to-calculated bar force at failure T/T_c based on simplified descriptive equation Eq. (6.3) versus concrete compressive strength f_{cm} for hooked bar specimens with widely- and closely-spaced bars without confining reinforcement used to develop descriptive equations, Eq. (4.5) and (4.7)..... 196

Figure 6.3 Test-to-calculated bar force at failure T/T_h based on simplified Eq. (6.5) versus ratio of center-to-center spacing to bar diameter s/d_b for widely- and closely-spaced hooked bars with confining reinforcement used to develop descriptive equations, Eq. (4.5) and (4.7) 197

Figure 6.4 Ratio of test-to-calculated bar force at failure T/T_c based on simplified Eq. (6.6) versus concrete compressive strength for hooked bars with widely- and closely-spaced bars with confining reinforcement used to develop descriptive equations, Eq. (4.5) and (4.6) 198

Figure 6.5 Test-to-calculated bar force at failure T/T_c based on Eq. (6.19) versus ratio of center-to-center spacing to bar diameter s/d_b for widely- and closely-spaced headed bars without parallel ties 219

Figure 6.6 Ratio of test-to-calculated bar force at failure T/T_c based on simplified descriptive equation, Eq. (6.20), versus concrete compressive strength f_{cm} for headed bar specimens with

widely- and closely-spaced bars without parallel ties used to develop descriptive equations, Eq. (5.5) and (5.7)	220
Figure 6.7 Test-to-calculated bar force at failure T/T_c based on Eq. (6.22) versus ratio of center-to-center spacing to bar diameter s/d_b for widely- and closely-spaced headed bars with parallel ties used to develop descriptive equations, Eq. (5.5) and (5.7)	222
Figure 6.8 Ratio of test-to-calculated bar force at failure T/T_c based on simplified descriptive equation, Eq. (6.23), versus concrete compressive strength f_{cm} for headed bar specimens with widely- and closely-spaced bars with parallel ties used to develop descriptive equations, Eq. (5.5) and (5.7).....	223
Figure 6.9 Ratio $f_{s,Descriptive}/f_{s,calc}$ versus concrete compressive strength f_{cm} for No. 8 bars headed bars with $s = 6d_b$ and $A_{th}/A_{hs} = 0$ for ACI 318-19 and proposed design provisions	240
Figure 6.10 Required development lengths of No. 8 hooked bars for $f'_c =$ (a) 4000 psi, (b) 10,000 psi, and (c) 16,000 psi as a function of s/d_b and A_{th}/A_{hs} based on based on ACI 318-19 and the proposed provisions using the full expression for ψ_r , Eq. (6.14)	242
Figure 6.11 Required development lengths of No. 8 hooked bars for $f'_c =$ (a) 4000 psi, (b) 10,000 psi, and (c) 16,000 psi as a function of s/d_b and A_{th}/A_{hs} based on ACI 318-19 and the proposed provisions using the simplified expressions for ψ_r , Eq. (6.15).....	243
Figure 6.12 Required development lengths of No. 8 headed bars for $f'_c =$ (a) 4000 psi, (b) 10,000 psi, and (c) 16,000 psi as a function of s/d_b and A_{th}/A_{hs} based on ACI 318-19 and the proposed provisions using the full expression for ψ_p , Eq. (6.29).....	245
Figure 6.13 Required development lengths of No. 8 headed bars for $f'_c =$ (a) 4000 psi, (b) 10,000 psi, and (c) 16,000 psi as a function of s/d_b and A_{th}/A_{hs} based on ACI 318-19 and the proposed provisions using the simplified expressions for ψ_p , Eq. (6.30)	246
Figure B.1 Details of reinforcement layout for No. 14 hooked bar specimen H14-1: (a) elevation, (b) cross-section	263
Figure B.2 Details of reinforcement layout for No. 14 hooked bar specimen H14-2: (a) elevation, (b) cross-section	264
Figure B.3 Details of reinforcement layout for No. 14 hooked bar specimen H14-3: (a) elevation, (b) cross-section	265

Figure B.4 Details of reinforcement layout for No. 14 hooked bar specimen H14-3: (a) elevation, (b) cross-section	266
Figure B.5 Details of reinforcement layout for No. 14 hooked bar specimen H14-15: (a) elevation, (b) cross-section	267
Figure B.6 Details of reinforcement layout for No. 14 hooked bar specimen H14-16: (a) elevation, (b) cross-section	268
Figure B.7 Details of reinforcement layout for No. 14 hooked bar specimen H14-7: (a) elevation, (b) cross-section	269
Figure B.8 Details of reinforcement layout for No. 14 hooked bar specimen H14-8: (a) elevation, (b) cross-section	270
Figure B.9 Details of reinforcement layout for No. 18 hooked bar specimen H18-1: (a) elevation, (b) cross-section	271
Figure B.10 Details of reinforcement layout for No. 18 hooked bar specimen H18-2: (a) elevation, (b) cross-section	272
Figure B.11 Details of reinforcement layout for No. 18 hooked bar specimen H18-3: (a) elevation, (b) cross-section	273
Figure B.12 Details of reinforcement layout for No. 18 hooked bar specimen H18-4: (a) elevation, (b) cross-section	274
Figure C.1 Details of reinforcement layout for No. 14 headed bar specimen 14-2: (a) elevation, (b) cross-section	325
Figure C.2 Details of reinforcement layout for No. 14 headed bar specimen 14-3: (a) elevation, (b) cross-section	326
Figure C.3 Details of reinforcement layout for No. 14 headed bar specimen 14-4: (a) elevation, (b) cross-section	327
Figure C.4 Details of reinforcement layout for No. 14 headed bar specimen 14-15: (a) elevation, (b) cross-section	328
Figure C.5 Details of reinforcement layout for No. 14 headed bar specimen 14-16: (a) elevation, (b) cross-section	329
Figure C.6 Details of reinforcement layout for No. 14 headed bar specimen 14-16A: (a) elevation, (b) cross-section	330

Figure C.7 Details of reinforcement layout for No. 14 headed bar specimen 14-1A: (a) elevation, (b) cross-section	331
Figure C.8 Details of reinforcement layout for No. 14 headed bar specimen 14-2A: (a) elevation, (b) cross-section	332
Figure C.9 Details of reinforcement layout for No. 14 headed bar specimen 14-16B: (a) elevation, (b) cross-section	333
Figure C.10 Details of reinforcement layout for No. 14 headed bar specimen 14-16C: (a) elevation, (b) cross-section	334
Figure C.11 Details of reinforcement layout for No. 14 headed bar specimen 14-16D: (a) elevation, (b) cross-section	335
Figure C.12 Details of reinforcement layout for No. 14 headed bar specimen 14-16E: (a) elevation, (b) cross-section	336
Figure C.13 Details of reinforcement layout for No. 14 headed bar specimen 14-16F: (a) elevation, (b) cross-section	337
Figure C.14 Details of reinforcement layout for No. 14 headed bar specimen 14-17: (a) elevation, (b) cross-section	338
Figure C.15 Details of reinforcement layout for No. 14 headed bar specimen 14-5: (a) elevation, (b) cross-section	339
Figure C.16 Details of reinforcement layout for No. 14 headed bar specimen 14-6: (a) elevation, (b) cross-section	340
Figure C.17 Details of reinforcement layout for No. 14 headed bar specimen 14-7: (a) elevation, (b) cross-section	341
Figure C.18 Details of reinforcement layout for No. 14 headed bar specimen 14-8: (a) elevation, (b) cross-section	342
Figure C.19 Details of reinforcement layout for No. 14 headed bar specimen 14-9: (a) elevation, (b) cross-section	343
Figure C.20 Details of reinforcement layout for No. 14 headed bar specimen 14-10: (a) elevation, (b) cross-section	344
Figure C.21 Details of reinforcement layout for No. 18 headed bar specimen 18-1: (a) elevation, (b) cross-section	345

Figure C.22 Details of reinforcement layout for No. 18 headed bar specimen 18-2: (a) elevation, (b) cross-section	346
Figure C.23 Details of reinforcement layout for No. 18 headed bar specimen 18-3: (a) elevation, (b) cross-section	347
Figure C.24 Details of reinforcement layout for No. 18 headed bar specimen 18-4: (a) elevation, (b) cross-section	348
Figure C.25 Details of reinforcement layout for No. 18 headed bar specimen 18-5: (a) elevation, (b) cross-section	349
Figure C.26 Details of reinforcement layout for No. 18 headed bar specimen 18-6: (a) elevation, (b) cross-section	350
Figure C.27 Details of reinforcement layout for No. 18 headed bar specimen 18-7: (a) elevation, (b) cross-section	351
Figure C.28 Details of reinforcement layout for No. 18 headed bar specimen 18-8: (a) elevation, (b) cross-section	352

LIST OF TABLES

Table 1.1 Standard hook requirements (ACI 318-19).....	3
Table 1.2 Values for the confinement and bar spacing factor, ψ_{cs} , as proposed by Ajaam et al. (2017) for hooked bars ^[1]	33
Table 1.3 Modification factors for hooked bars as given in Table 25.4.3.2 of ACI 318-19	34
Table 1.4 Values for the confinement and bar spacing factor, ψ_{cs} , as proposed by Shao et al. (2016) for headed bars.....	39
Table 1.5 Modification factors for headed bars as given in Table 25.4.4.3 of ACI 318-19.....	41
Table 2.1 Dimensions of the headed bars.....	46
Table 2.2 Physical properties of reinforcing steel.....	47
Table 2.3 Concrete mixture proportions.....	48
Table 2.4 Values of forces applied to the specimens under the two loading conditions.....	61
Table 2.5 Test program and the main parameters for No. 11, No. 14, and No. 18 bar specimens	71
Table 2.6 Summary of the test program and number of specimens.....	72
Table 3.1 Summary of hooked bar specimens with different failure types	86
Table 3.2 Summary of headed bar specimens with different failure types	86
Table 3.3 Summary of anchorage strength results for hooked bar specimens.....	94
Table 3.4 Summary of anchorage strength results for headed bar specimens	94
Table 4.1 Comparison of No. 14 and No. 18 hooked bar test results with descriptive equations by Ajaam et al. (2018), Eq. (1.1) and (1.2), also Eq. (4.2) and (4.3), and ACI 318-19. Eq. (4.1)	97
Table 4.2 Summary of test-to-calculated ratio for No. 14 and No. 18 hooked bars based on descriptive equations by Ajaam et a. (2017, 2018), Eq. (4.2) and (4.3)	100
Table 4.3 Statistical parameters of T/T_c ratio using Eq. (4.4) for hooked bar specimens with widely-spaced bars (center-to-center spacing $\geq 6d_b$) without confining reinforcement	103
Table 4.4 Statistical parameters of T/T_c ratio using Eq. (4.5) for hooked bar specimens with closely-spaced ($s/d_b < 6d_b$) bars without confining reinforcement.....	105
Table 4.5 Statistical parameters of T/T_c ratio using Eq. (4.5) for hooked bar specimens with widely- and closely-spaced bars without confining reinforcement	106

Table 4.6 Statistical parameters of T/T_h ratio using Eq. (4.6) for hooked bar specimens with widely-spaced ($s/d_b \geq 6d_b$) bars with confining reinforcement	108
Table 4.7 Statistical parameters of T/T_h ratio using Eq. (4.7) for hooked bar specimens with closely-spaced bars with confining reinforcement	110
Table 4.8 Statistical parameters of T/T_h ratio using Eq. (4.7) for hooked bar specimens with widely- and closely-spaced bars with confining reinforcement	110
Table 4.9 Statistical parameters of T/T_h ratio using Eq. (4.5) and (4.7) for all hooked bar specimens used to develop the descriptive equations	111
Table 4.10 Summary of test-to-calculated ratio T/T_h using Eq. (4.5) and (4.7) for No. 14 and No. 18 hooked bar specimens tested in this study	113
Table 4.11 Test-to-calculated T/T_h ratio based on Eq. (4.5) and (4.7) for specimens with hooked bars placed outside column core (Ajaam et al. 2017)	114
Table 4.12 Test-to-calculated ratio T/T_h based on Eq. (4.5) and (4.7) for specimens with No. 14 and No. 18 hooked bars placed outside column core by Chun et al. (2017b)	116
Table 4.13 Test-to-calculated T/T_h ratio based on Eq. (4.5) and (4.7) for specimens tested outside University of Kansas and not used to develop Eq. (4.5) and (4.7)	129
Table 4.14 Bar stresses and slip at failure for No. 7 and No. 11 hooked bar specimens by Marques and Jirsa (1975) along with T/T_h based on descriptive equations, Eq. (4.5) and (4.7)	135
Table 5.1 Comparison of No. 14 and No. 18 headed bar test results with descriptive equations by Shao et al. (2016), Eq. (1.5) and (1.6), also (5.2) and (5.3), and ACI 318-19.....	137
Table 5.2 Summary of test-to-calculated ratio T/T_h for No. 14 and No. 18 headed bars based on bar size and parallel ties with T_h based on Eq. (5.2) or (5.3), excluding specimens that failed in shear	142
Table 5.3 Summary of test-to-calculated ratio T/T_h for No. 14 and No. 18 headed bars tested under loading condition A (all with parallel ties) with T_h based on Eq. (5.3), excluding specimens that failed in shear.....	142
Table 5.4 Summary of test-to-calculated ratio T/T_h for No. 14 and No. 18 headed bars with parallel ties and tested under loading condition B with T_h based on Eq. (5.3)	143
Table 5.5 Statistical parameters for T/T_c ratio for headed bar specimens with widely-spaced bars without parallel ties with T_c based on Eq. (5.4).....	146

Table 5.6 Statistical parameters of T/T_c ratio for headed bar specimens with closely-spaced bars without parallel ties with T_c based on Eq. (5.5).....	148
Table 5.7 Statistical parameters of T/T_c , with T_c based on Eq. (5.5), for headed bar specimens with widely- and closely-spaced bars without parallel ties.....	149
Table 5.8 Statistical parameters of T/T_h ratio for headed bar specimens with widely-spaced bars with parallel ties with T_h based on Eq. (5.6).....	151
Table 5.9 Statistical parameters of T/T_h ratio for headed bar specimens with closely-spaced bars with parallel ties with T_h based on Eq. (5.7).....	153
Table 5.10 Statistical parameters of T/T_h ratio for headed bar specimens with widely- and closely-spaced bars with parallel ties with T_h based on Eq. (5.7).....	154
Table 5.11 Statistical parameters of T/T_h ratio for all headed bar specimens with T_h based on Eq. (5.5) or (5.7).....	154
Table 5.12 Summary of T/T_h values for No. 14 and No. 18 headed bars specimens tested in this study based on the developed descriptive equations, Eq. (5.5) and (5.7)	155
Table 5.13 Summary of test-to-calculated ratio T/T_h for No. 14 and No. 18 headed bars based on bar size and parallel ties, with T_h based on Eq. (5.5) or (5.7), excluding specimens that failed in shear	157
Table 5.14 Summary of test-to-calculated ratio T/T_h for No. 14 and No. 18 headed bars tested under loading condition A (all with parallel ties) with T_h based on Eq. (5.7), excluding specimens that failed in shear.....	157
Table 5.15 Summary of test-to-calculated ratio T/T_h for No. 14 and No. 18 headed bars with parallel ties and tested under loading condition B with T_h based on Eq. (5.7).....	158
Table 5.16 Details and test-to-calculated T/T_h ratios of the specimens tested by Chun et al. (2017) and Sim and Chun (2022a, 2022b) with headed bars outside column core	185
Table 5.17 Test-to-calculated ratio T/T_h based on Eq. (5.5) and (5.7) for beam-column joint specimens tested by Bashandy (1996) (values converted from SI units).....	190
Table 6.1 Statistical parameters of T/T_c ratio using Eq. (6.3) for hooked bar specimens with widely- and closely-spaced bars without confining reinforcement	196
Table 6.2 Statistical parameters of T/T_h using Eq. (6.6) for hooked bar specimens with widely- and closely-spaced bars with confining reinforcement used to develop descriptive equations Eq. (4.5) and (4.7)	199

Table 6.3 Statistical parameters of T/T_h ratio using Eq. (6.3) and (6.6) for hooked bar specimens used to develop descriptive equations Eq. (4.5) and (4.7)	199
Table 6.4 Statistical parameters of T/T_h ratio using Eq. (6.8) with applying $A_{th}/A_{hs} \leq 0.4$ for hooked bar specimens with widely- and closely-spaced bars with confining reinforcement used to develop descriptive equations Eq. (4.5) and (4.7).....	200
Table 6.5 Modification factors for the proposed design equation for development of hooked bars	206
Table 6.6 Statistical parameters of test-to-calculated bar stress at failure $f_{su}/f_{s,calc}$ for hooked bar specimens without confining reinforcement, based on the proposed design equation, Eq. (6.17), and the full expression for ψ_r , Eq. (6.14)	208
Table 6.7 Statistical parameters of test-to-calculated bar stress at failure $f_{su}/f_{s,calc}$ for hooked bar specimens without confining reinforcement, based on the proposed design equation, Eq. (6.17) and the simplified expressions for ψ_r , Eq. (6.15)	209
Table 6.8 Statistical parameters of test-to-calculated bar stress at failure $f_{su}/f_{s,calc}$ for hooked bar specimens with confining reinforcement, based on the proposed design equation, Eq. (6.17) and the full expression for ψ_r , Eq. (6.14).....	209
Table 6.9 Statistical parameters of test-to-calculated bar stress at failure $f_{su}/f_{s,calc}$ for hooked bar specimens with confining reinforcement, based on the proposed design equation, Eq. (6.17) and the simplified expressions for ψ_r , Eq. (6.15).....	210
Table 6.10 Statistical parameters of test-to-calculated bar stress at failure $f_{su}/f_{s,calc}$ for hooked bar specimens, without and with confining reinforcement, used to develop descriptive equations Eq. (4.5) and (4.7), based on the proposed design equation Eq. (6.17) and using the full expression for ψ_r , Eq. (6.14)	211
Table 6.11 Statistical parameters of test-to-calculated bar stress at failure $f_{su}/f_{s,calc}$ for hooked bar specimens, without and with confining reinforcement, used to develop descriptive equations Eq. (4.5) and (4.7), based on the proposed design equation Eq. (6.17) and using the simplified expressions for ψ_r , Eq. (6.15).....	212
Table 6.12 Comparison of hooked bar specimens tested by Marques and Jirsa (1975) versus the proposed design equation, Eq. (6.17) using full and simplified expressions for ψ_r	213
Table 6.13 Comparison of hooked bar specimens tested by Pinc et al. (1977) versus the proposed design equation, Eq. (6.17).....	214

Table 6.14 Comparison of hooked bar specimens tested by Hamad et al. (1993) versus the proposed design equation, Eq. (6.17).....	214
Table 6.15 Comparison of hooked bar specimens tested by Ramirez and Russell (2008) versus the proposed design equation, Eq. (6.17).....	215
Table 6.16 Comparison of hooked bar specimens tested by Lee and Park (2010) versus the proposed design equation, Eq. (6.17).....	216
Table 6.17 Comparison of hooked bar specimens tested by Chun et al. (2017b) versus the proposed design equation, Eq. (6.17).....	216
Table 6.18 Statistical parameters of $f_{su}/f_{s,calc}$ for hooked bar specimens tested outside University of Kansas, based on the proposed design equation Eq. (6.17) and using the full expression for ψ_r , Eq. (6.14).....	217
Table 6.19 Statistical parameters of T/T_c ratio based on simplified descriptive equation, Eq. (6.20), for headed bar specimens with widely- and closely-spaced bars without parallel ties used to develop descriptive equations, Eq. (5.5) and (5.7)	220
Table 6.20 Statistical parameters of T/T_h ratio based on simplified descriptive equation, Eq. (6.23), for headed bar specimens with widely- and closely-spaced bars with parallel ties used to develop descriptive equations, Eq. (5.5) and (5.7).....	222
Table 6.21 Statistical parameters of T/T_h ratio based on simplified descriptive equation, Eq. (6.20) and (6.23), for all headed bar specimens used to develop descriptive equations, Eq. (5.5) and (5.7)	224
Table 6.22 Modification factors for the proposed design equation for development of headed bars, Eq. (6.31).....	228
Table 6.23 Statistical parameters of test-to-calculated bar stress at failure $f_{su}/f_{s,calc}$ based on the proposed design equation Eq. (6.32) and using the full expression for ψ_p , Eq. (6.29) for headed bar specimens without parallel tie used to develop descriptive equations, Eq. (5.5) and (5.7)	230
Table 6.24 Statistical parameters of test-to-calculated bar stress at failure $f_{su}/f_{s,calc}$ based on the proposed design equation Eq. (6.32) and using the full expression for ψ_p , Eq. (6.29) for headed bar specimens with parallel tie used to develop descriptive equations, Eq. (5.5) and (5.7)	231
Table 6.25 Statistical parameters of test-to-calculated bar stress at failure $f_{su}/f_{s,calc}$ based on the proposed design equation Eq. (6.32) and using the simplified expressions for ψ_p , Eq. (6.30) for	

headed bar specimens with parallel tie used to develop descriptive equations, Eq. (5.5) and (5.7)	232
Table 6.26 Statistical parameters of test-to-calculated bar stress at failure $f_{su}/f_{s,calc}$ based on the proposed design equation Eq. (6.32) and using the full expression for ψ_p , Eq. (6.29) for all headed bar specimens used to develop descriptive equations, Eq. (5.5) and (5.7)	232
Table 6.27 Statistical parameters of test-to-calculated bar stress at failure $f_{su}/f_{s,calc}$ based on the proposed design equation Eq. (6.32) and using the full expression for ψ_p , Eq. (6.30) for all headed bar specimens used to develop descriptive equations, Eq. (5.5) and (5.7)	233
Table 6.28 Comparison of beam-column joint test results by Bashandy (1996) versus the proposed design equation Eq. (6.32) (values converted from SI units)	234
Table 6.29 Comparison of headed bar specimens tested by Chun et al. (2017a) and Chun and Lee (2019) versus the proposed design equation, Eq. (6.32)	235
Table 6.30 Comparison of headed bar specimens tested by Sim and Chun (2022b) versus the proposed design equation, Eq. (6.32)	236
Table 6.31 Statistical parameters of $f_{su}/f_{s,calc}$ for all headed bar specimens tested outside University of Kansas (Bashandy 1996, Chun et al 2017a, Chun and Lee 2019, Sim and Chun 2022b) based on the proposed design equation Eq. (6.32), excluding specimens with shear failure and those with headed bars that yielded	237
Table B.1 Detailed properties and test results for No. 14 and No. 18 bar specimens tested in current study	275
Table B.2 Detailed properties and test results for hooked bar specimens having widely-spaced bars without confining reinforcement tested at the University of Kansas	279
Table B.3 Detailed properties and test results for hooked bar specimens having closely-spaced bars without confining reinforcement tested at the University of Kansas	288
Table B.4 Detailed properties and test results for hooked bar specimens having widely-spaced bars with confining reinforcement tested at the University of Kansas	291
Table B.5 Detailed properties and test results for hooked bar specimens having closely-spaced bars with confining reinforcement tested at the University of Kansas	301
Table B.6 Detailed properties and test results for hooked bar specimens with bars placed outside column longitudinal reinforcement (column core) tested at the University of Kansas	307

Table B.7 Detailed properties and test results for hooked bar specimens with effective beam depth to embedment ratio $d_{eff}/\ell_{eh} > 1.5$ tested at the University of Kansas	313
Table B.8 Detailed properties and test results for hooked bar specimens tested outside the University of Kansas	315
Table C.1 Detailed properties and test results for No. 14 and No. 18 bar specimens tested in current study	353
Table C.2 Detailed properties and test results for headed bar specimens having widely-spaced bars without parallel ties tested at the University of Kansas	361
Table C.3 Detailed properties and test results for headed bar specimens having closely-spaced bars without parallel ties tested at the University of Kansas	367
Table C.4 Detailed properties and test results for headed bar specimens having widely-spaced bars with parallel ties tested at the University of Kansas	373
Table C.5 Detailed properties and test results for headed bar specimens having closely-spaced bars with parallel ties tested at the University of Kansas	379
Table C.6 Detailed properties and test results for hooked bar specimens tested outside the University of Kansas	385

CHAPTER 1: INTRODUCTION

1.1 GENERAL

The bond between the reinforcing steel and concrete is a critical factor in reinforced concrete structures and must be sufficient so that forces can transfer between the two materials. Development length is defined as the “length of embedded reinforcement...required to develop the design strength of reinforcement at a critical section” (ACI 318-19) (such as the face of column in a beam-column joint connection). In some cases, such as in an external beam-column connection, it is possible that the member geometry does not allow for a straight deformed bar to fully develop its yield strength (that is, the required development length is longer than the column width). To address this issue, hooked and headed reinforcing bars are commonly used to mechanically anchor the bar within the connection. For both hooked and headed bars, a bearing force from the bent portion of the hook or from the head participates in transferring the force in the bar to the concrete, in addition to the force transferred along the straight portion of the bar, allowing for a shorter overall development length than can be achieved with a straight bar alone. The use of conventional hooked bars, however, can be problematic where steel congestion is a concern (for example, in a heavily reinforced beam-column joint). In such cases, headed bars can be used as an effective alternative.

The provisions for the development length of hooked and headed bars are provided in Sections 25.4.3 and 25.4.4, respectively, of the ACI 318-19 Building Code Requirements for Structural Concrete. Earlier editions of the ACI Code, including ACI 318-14, contained a number of restrictions applied to the use of hooked and headed bars, mainly due to limited test data and a limited range of material properties. For hooked bars, the yield strength was limited to 80,000 psi and the concrete strength was limited to 10,000 psi for use in calculating the development length. For headed bars, the steel yield strength was limited to 60,000 psi and concrete strength to just 6,000 psi. In addition, headed bars were required to be placed with a minimum clear spacing of $4d_b$ with a minimum cover of $2d_b$, where d_b is the nominal diameter of the bar.

The provisions in ACI 318-14 did not allow for the use of high-strength reinforcing steel and concrete, despite their expanding use in construction. High-strength steel helps reduce reinforcement congestion, and high-strength concrete yields smaller member sizes and increased usable floor area. A comprehensive study at the University of Kansas (Searle et al. 2014, Sperry et al. 2015a, 2015b, 2017a, 2017b, 2018, Yasso et al. 2017, Ajaam et al. 2017, 2018, Shao et. Al

2016, Ghimire et al. 2018, 2019a, 2019b) expanded the experimental database on hooked and headed bars in beam-column joints to provide a better understanding of their behavior and improve the Code provisions. The study included 338 simulated beam-column joint specimens with hooked bars and 202 specimens with headed bars tested to investigate the effect on anchorage strength of key parameters, including concrete compressive strength (3,960 to 16,510 psi), bar stress at failure (22,800 to 153,200 psi), bar size (No. 5, No. 8, and No. 11), number of bars (2, 3, 4, and 6 bars in one or two layers), bar spacing (1.7 to $11.8d_b$), embedment length (3.5 to 26.3 in.), and the amount of confining reinforcement (stirrups and ties for hooked bars and parallel ties for headed bars) in the joint region (none to No. 3 or No. 4 hoops or ties spaced at $3d_b$). Based on the test data, descriptive equations for anchorage strength of hooked and headed bars were developed that cover a wide range of material strengths and member properties. The descriptive equations were then simplified to propose new provisions for development length of hooked and headed bars that allow the safe use of high-strength reinforcing steel (up to 120,000 ksi) and concrete (up to 16,000 psi).

The findings at the University of Kansas became the basis for developing current Code provisions in ACI 318-19. Limitations, however, remain on the use of hooked and headed bars larger than No. 11 (that is, No. 14 and No. 18 bars), mainly due to a lack of experimental data. For both hooked and headed bars, the current provisions still limit concrete compressive strength to 10,000 psi for the purpose of calculating development length. For hooked bars, the Code gives no credit to confining reinforcement for hooked bars larger than No. 11, and for headed bars, bars larger than No. 11 are not permitted. These limitations were the motivation for the current study.

The research reported here is a continuation of the comprehensive study began at the University of Kansas on the anchorage of high-strength hooked and headed reinforcing bars. This study expands the available data on the anchorage strength of high-strength headed and hooked bars to include No. 14 and No. 18 bars, the largest sizes currently permitted in the ACI Building Code. These results are used as a basis for new design criteria.

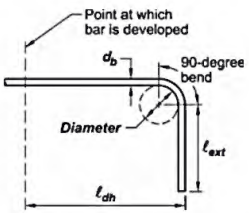
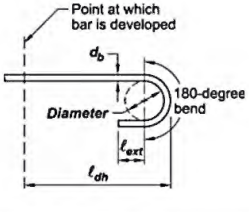
In this chapter, the background and relevant research work on the development of hooked and headed bars are provided, followed by a discussion of the current Code provisions, their development, and limitations. Finally, a summary of the objectives and scopes of this study is presented.

1.2 BACKGROUND AND PREVIOUS RESEARCH

1.2.1 Reinforcing Bars with Standard Hooks

When member dimensions do not allow for development of a straight bar, such as within an external beam-column joint, bars with a standard hook at their end (tail of the hook) can be used to provide anchorage to concrete. Standard hooks have 90° or 180° bends that meet the dimensional requirements specified in Table 25.3.1 of the ACI 318-19 Code, as shown in Table 1.1. The development length for hooked bars, ℓ_{dh} , is measured from back of the tail.

Table 1.1 Standard hook requirements (ACI 318-19)

Type of standard hook	Bar size	Minimum inside bend diameter, in.	Straight extension ^[1] ℓ_{ext} in.	Type of standard hook
90-degree hook	No. 3 through No. 8	$6d_b$	$12d_b$	
	No. 9 through No. 11	$8d_b$		
	No. 14 and No. 18	$10d_b$		
180-degree hook	No. 3 through No. 8	$6d_b$	Greater of $4d_b$ and 2.5 in.	
	No. 9 through No. 11	$8d_b$		
	No. 14 and No. 18	$10d_b$		

^[1]A standard hook for deformed bars in tension includes the specific inside bend diameter and straight extension length. It shall be permitted to use a longer straight extension at the end of a hook. A longer extension shall not be considered to increase the anchorage capacity of the hook.

Hooked bars provide anchorage force by engaging the concrete, as shown in Figure 1.1, with the anchorage strength governed, not ultimately by bond, but by the breakout or side-splitting strength of the concrete, as shown in Figure 1.2, which can be enhanced by confining reinforcement.

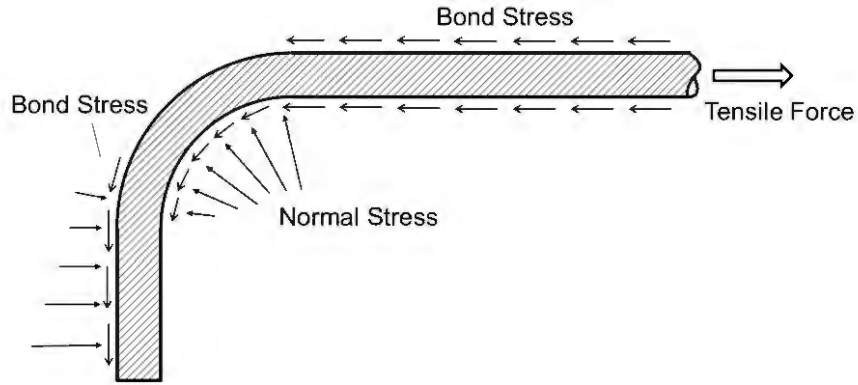


Figure 1.1. Anchorage mechanism of hooked bars (adapted from Marques and Jirsa 1975)

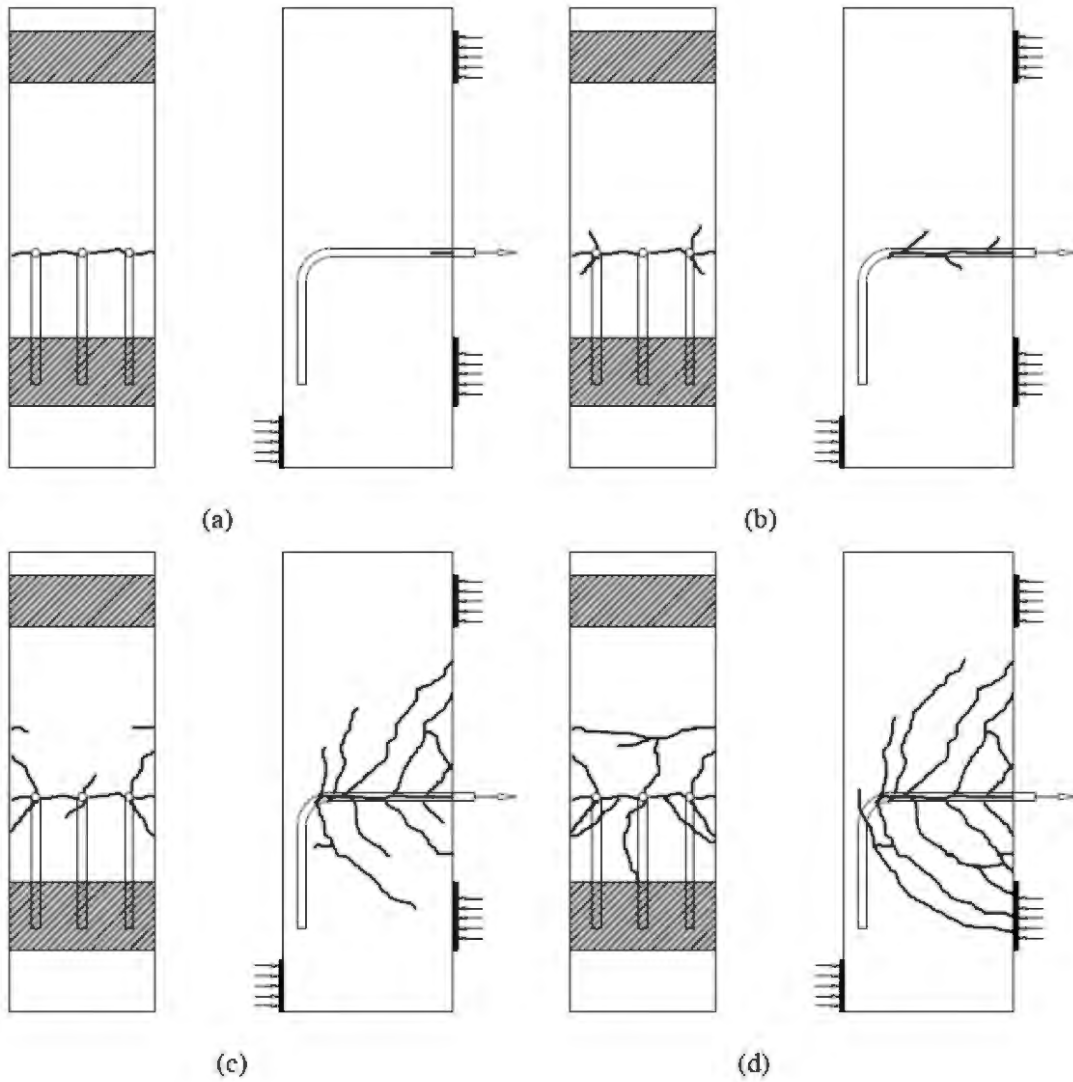


Figure 1.2 Crack progression observed in the beam-column joint specimens containing hooked bars (Sperry et al. 2015b, 2017a). Breakout failure is preceded by bond slip of the straight portion of the bars and cracking of the concrete

Marques and Jirsa (1975) studied No. 7 and No. 11 hooked bars anchored in simulated exterior beam-column joint with a width of 12 and 15 in. and a depth of 12 in. The study included twenty-two specimens with concrete compressive strengths of 3,600 to 5,100 psi, embedment lengths of 6.5 to 9.5 in. for No. 7 and 3 to 6 in. for No. 11 hooked bars, clear spacing between the two bars of 3.4 to 7.25 in., confining reinforcement in the joint region consisting of No. 3 ties spaced at 2.5 or 5 in., placement of hooked bars inside or outside of the column core), concrete side cover of 1.5 or 2.875 in., and an axial load of 135 to 450 kips. A schematic of the test specimens is shown in Figure 1.3. Marques and Jirsa (1975) found that increasing the embedment length increased the anchorage strength but that axial load variations and placement of hooked bars inside or outside of the column core had no noticeable effect on the anchorage strength.

As shown in Figure 1.3, the specimens had unconventional geometry and reinforcement layouts. All specimens were narrow, with a column width of 12 in. The side cover was almost 3 in. for the majority of specimens (Types 1, 2, 3, and 5), representing nearly half the specimen width. The hooked bars were placed outside column core, except in the Type 1 specimens. Also, in specimens with confining reinforcement, Types 3 and 5, there was a noticeable gap between the No. 3 bar tie legs and the column longitudinal reinforcement, uncommon in practice. The specimen proportions and location of applied forces along the height were also unrealistic, resulting in the joint carrying only 54% of the total force applied to the bars, significantly lower than would occur in a joint in a reinforced concrete frame structure, leading to unrealistically high anchorage strengths. These specimens are investigated in detail in Section 4.5. However, despite the unusual specimen geometry and reinforcement layouts, which were likely the result of the early nature of this research, the work by Marques and Jirsa (1975) paved the way for the many studies that followed.

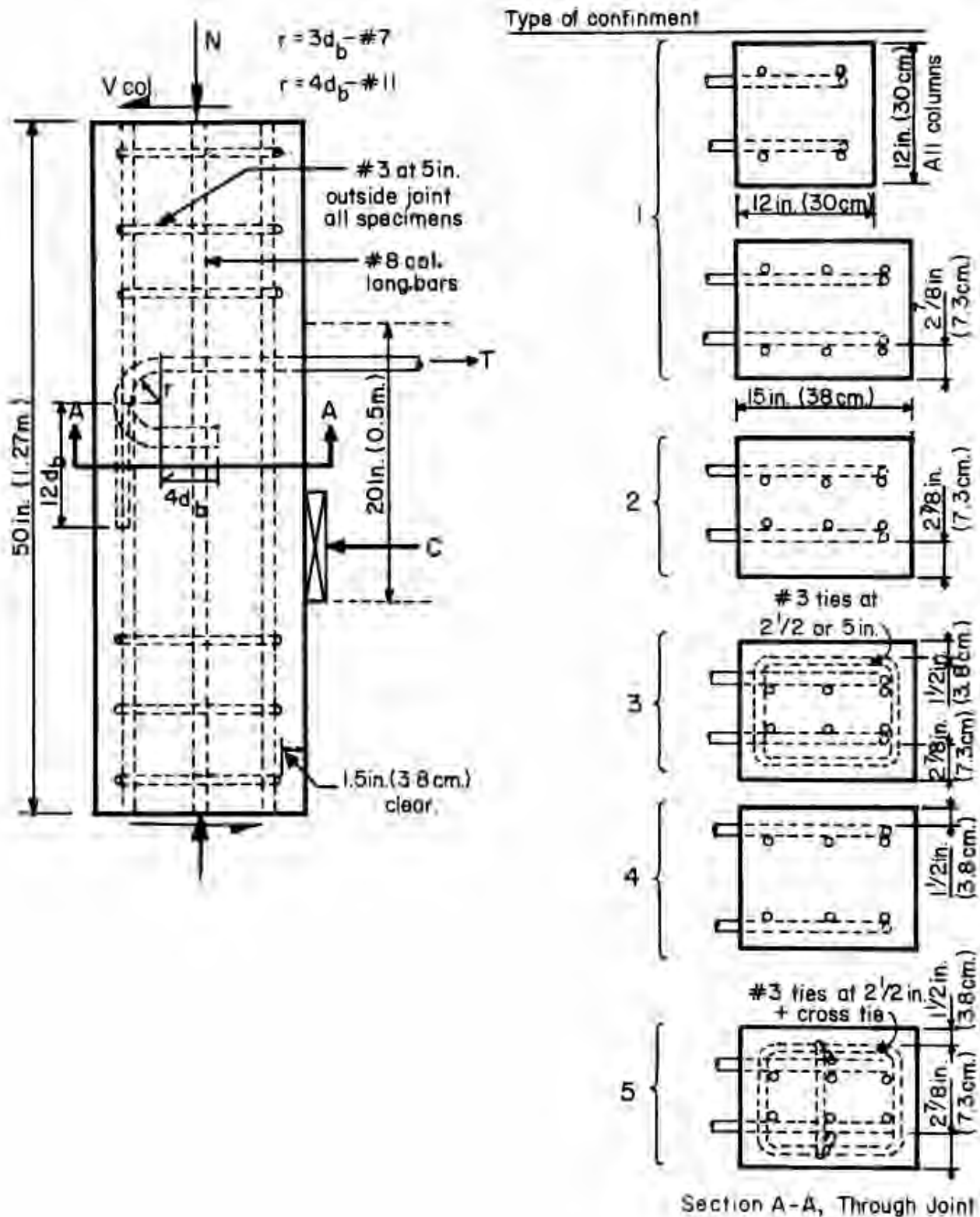


Figure 1.3 Schematic of test specimens used by Marques and Jirsa (1975); Type 1: Hooked bars inside column core without confining reinforcement, Type 2 and 4: Hooked bars outside column core without confining reinforcement, Type 3: Hooked bars outside column core with No. 3 ties, and Type 5: Hooked bars outside column core with No. 3 ties plus cross-tie

Pinc et al. (1977) tested 16 beam-column joint specimens, each with two hooked bars. No. 7, No. 9 and No. 11 hooked bars were used in normalweight and lightweight concrete. Concrete compressive strength ranged from 3,600 to 5,400 psi, clear bar spacing ranged from 3.4 to 4.0 in., and the side cover was $2\frac{7}{8}$ in. The specimens had no confining reinforcement in the joint region. A constant axial load (108 to 230 kips) was applied to specimens during the test. Pinc et al. concluded that embedment length was the key factors affecting the anchorage strength of hooked bars, and that the loss of side cover is the main factor governing the failure of hooked bars.

Joh et al. (1995) tested 19 beam-column specimens with 19 mm hooked bars; all but one contained four hooked bars. A single specimen contained eight hooked bars in two layers. Joh et al. investigated the effects of embedment length (nominally 5.2 to 13.0 in.), distance to the reaction representing the compression zone of the beam (nominally 9.0 to 16.9 in.), column depth (nominally 11.8 to 19.7 in.), spacing of the bars (1.9 to 2.6 in.), concrete side cover (2.54 to 14.5 in.), ratio of the confining reinforcement in the joint (0.2%, 0.4%, 0.8%), column axial stress (0 to 900 and 1887 psi, equal to 16.7% and 33.3% of the concrete compressive strength of the corresponding specimens), loading type (cyclic or monotonic), and concrete compressive strength (4,490 to 10,720 psi). Joh et al. found that applying a column axial stress equal to 16.7% ($1/6$) of concrete compressive strength increased the anchorage strength more than double (unlike Marques and Jirsa 1975), but increasing the axial stress from 16.7% ($1/6$) to 33.3% ($1/3$) of the concrete compressive strength had no effect on anchorage strength. They also found that anchorage strength increases proportionally with the addition of confining reinforcement, and that anchorage strength is proportional to the square root of the concrete compressive strength and the reciprocal of the sine of the compression strut angle (from the centroid of the compression zone of the beam to the bent portion of the hooked bar, as shown in Figure 1.4).

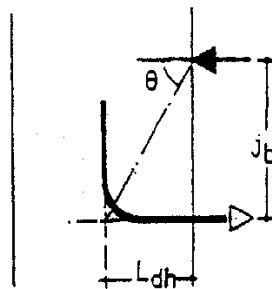


Figure 1.4 Strut angle as defined by Joh et al. (1995)

The work by Joh et al (1995) was continued by Joh and Shibata (1996), in which 13 beam-column specimens were tested. Each specimen had four 19-mm diameter hooked bars. The specimen parameters were concrete compressive strength (3,380 to 8,060 psi), center-to-center bar spacing (nominally 2.2 in.), side cover on the hooked bars (nominally 2.5 to 10.4 in.), and column axial stress (0 to 1,860 psi, equal to 0 to 33% of the concrete compressive strength of the corresponding specimens). The column ties were placed around the column longitudinal bars with a clear cover of 0.75 in. Joh and Shibata observed an increase in anchorage strength of hooked bars in specimens subjected to column axial stress compared to those with no axial stress. For pairs of specimens with similar concrete strengths and subjected to axial stress, however, increasing the axial stress beyond 8% of the corresponding concrete compressive strength (as opposed to 16.7% of the compressive strength in the previous research by Joh et al. 1995) did not have a noticeable effect on the anchorage strength. Anchorage strength also increased with increasing concrete side cover. However, when the side cover on the hooked bars was so large (10.4 in. versus 2.5 in.) that the breakout region ahead of the hooked bars (angle with respect to the longitudinal direction of the hooked bars of about 40°) did not reach the sides of the column, the effectiveness of the ties at the column boundaries decreased.

Twenty-one beam-column joint specimens were tested by Ramirez and Russell (2008). The specimens were cantilever columns with no axial load. The parameters included bar size (No. 6 or No. 11), confining reinforcement in the joint region (none to No. 3 ties spaced at $3d_b$), side cover (3.5 in.), back cover to the hook (0.75 to 2.5 in.), concrete compressive strength (8,910 to 16,500 psi), and embedment length (6.5 to 15.5 in.). They proposed increasing the modification factor 0.7 to 0.8 for No. 11 and smaller bars with a minimum side cover to the bar of 2.5 in. and cover to the back of the hook of 2 in. in ACI 318-05 and the AASHTO LRFD Bridge Specifications. Ramirez and Russell stated that the limit on concrete compressive strength could be increased to 15,000 psi in ACI 318-05 and the AASHTO LRFD Bridge Specifications if ties spaced at $3d_b$ are provided as confining reinforcement in the joint region.

To expand the available data to include a wide range of material properties, including high-strength concrete and reinforcing steel, a comprehensive study was initiated at the University of Kansas on the anchorage strength of standard hooked bars. The study included work by Searle et al. (2014), Sperry et al. (2015a, 2015b, 2017a, 2017b, 2018), Yasso et al. (2017), Ajaam et al. (2017, 2018). A total of 245 simulated beam-column joint specimens were tested in normalweight

concrete to investigate the effects of key parameters on the anchorage strength of hooked bars. The parameters included the number of hooked bars (2, 3, 4, or 6), arrangement of hooked bars (one or two layers), bar size (No. 5, No. 8, and No. 11), bar spacing (2 to $11.8d_b$ center-to-center), hook bend angle (90° or 180°), embedment length (3.5 to 26.3 in.), confining reinforcement in the joint region (none to nine No. 3 hoops spaced at no greater than $3d_b$), location of hooked bar within the column depth (hooks on the far side of the column or extending only to the middle of the column), placement of hooked bar inside or outside the column core (the area of concrete inside the column longitudinal reinforcement), bar stress at failure (22,800 to 141,600 psi), concrete compressive strength (4,300 to 16,510 psi), clear concrete side cover (1.5 to 4 in., with most values between 2.5 and 3.5 in.), cover to the tail of the hook (2 to 18 in.), and ratios of beam effective depth to embedment length (0.6 to 2.13).

A schematic of a specimen simulating an exterior beam-column joint with hooked bars placed inside the column core is shown in Figure 1.5. Tension and compression forces are applied using a self-reacting frame. The hooked bars represent the longitudinal reinforcement of a simulated beam, and the adjacent compression force represents the beam compression region.

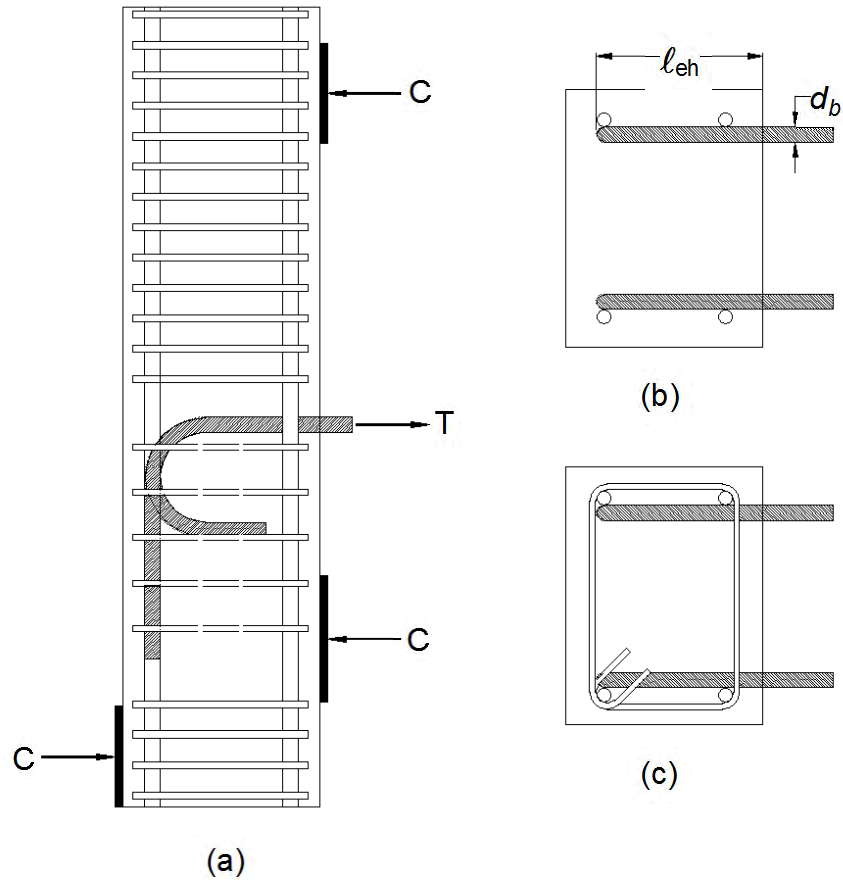


Figure 1.5 Schematic of specimens (a) side view (b) cross-section without confining reinforcement, and (c) cross-section with confining reinforcement, where l_{eh} is the embedment length and d_b is bar diameter

The reaction frame to simulate the axial, tensile, and compression forces, shown in Figure 1.6, was a modified version of that used by Marques and Jirsa (1975). The beam compression zone was simulated using bearing member, and the upper compression and lower tension members prevented rotation of the specimen.

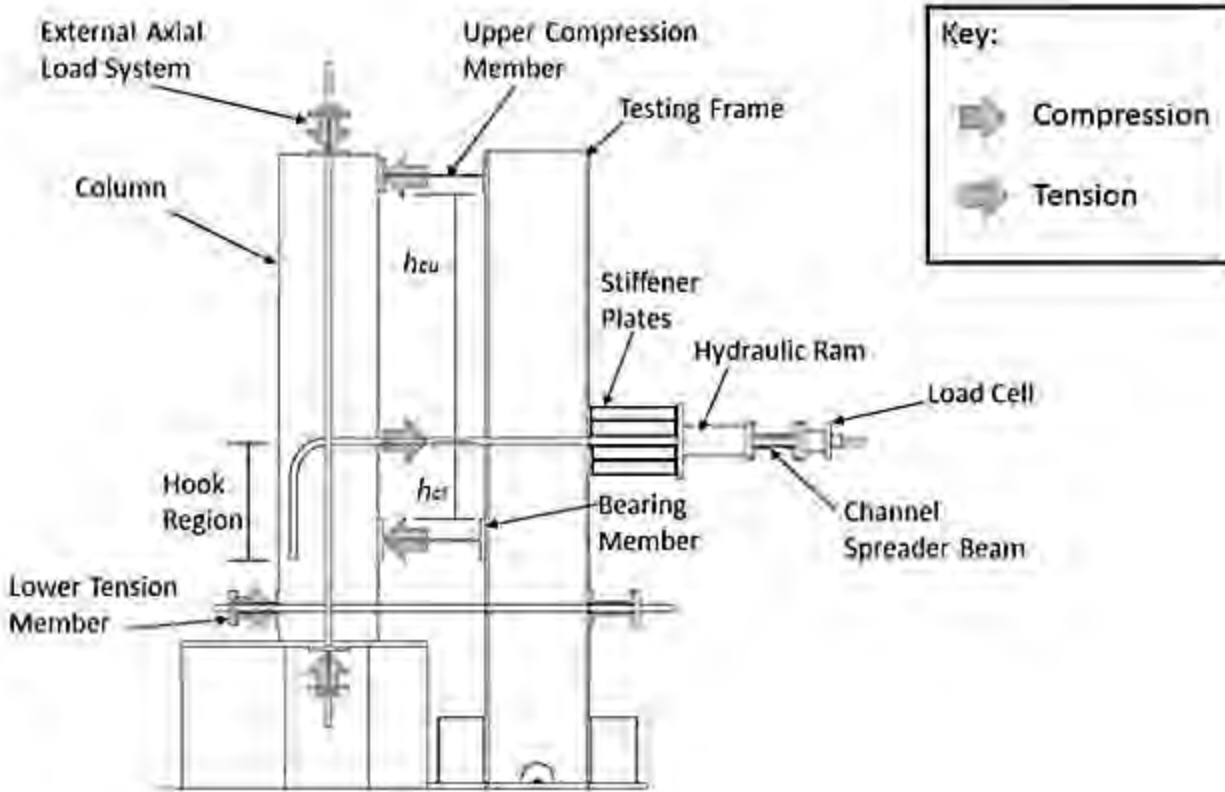


Figure 1.6 Schematic of the reaction frame (Sperry et al. 2015b)

Crack progression and the failure mechanism for the specimens is illustrated in Figure 1.2. The first cracks initiated from the hooked bars on the front face of the column due to slip of the straight portions of the bars and propagated horizontally on the column side face (Figure 1.2a). With an increase in load, the front face cracks continued to grow, radiating from the hooked bars. On the column side face, cracks continued to grow horizontally along the straight portion of the bars (Figure 1.2b). With more load, inclined cracks propagated on the column side face, in a cone-shaped manner, towards the bearing members (Figure 1.2c). These cracks further propagated and were widened near as the specimen got close to failure (Figure 1.2d).

Two primary failure modes were observed, namely concrete breakout and side splitting, as shown in Figure 1.7. Concrete breakout is characterized by a mass of concrete being pulled out along with the hooked bar from the front face of the specimen. Side splitting is marked by the side cover on the hooked bar separating from the specimen due to wedging action of the hook. In some specimens, a secondary failure mode, tail kickout, occurred along with other failure modes, marked by the concrete over being pushed off the back of the column by the tail of the hook, causing the

cover to spall and exposing the tail. Tail kickout occurred subsequent to the peak load and did not affect anchorage strength.



Figure 1.7 Primary failure modes observed in hooked bar specimens (Sperry et al. 2015b)

Based on the test results, descriptive equations were developed to characterize the anchorage strength of hooked bars, as shown in Eq. (1.1) and Eq. (1.2) for bars without and with confining reinforcement, respectively (Ajaam et al. 2017):

$$T_h = 294 f_{cm}^{0.295} \ell_{eh}^{1.0845} d_b^{0.47} \left(0.0974 \frac{s}{d_b} + 0.391 \right) \quad (1.1)$$

$$\left(0.0974 \frac{s}{d_b} + 0.391 \right) \leq 1.0$$

$$T_h = \left(294 f_{cm}^{0.295} \ell_{eh}^{1.0845} d_b^{0.47} + 55,050 \left(\frac{A_{th}}{n} \right)^{1.0175} d_b^{0.73} \right) \left(0.0516 \frac{s}{d_b} + 0.6572 \right) \quad (1.2)$$

$$\left(0.0516 \frac{s}{d_b} + 0.6572 \right) \leq 1.0$$

where T_h is the anchorage strength of hooked bars (lb); f_{cm} is the measured concrete compressive strength (psi); ℓ_{eh} is the embedment length of the hooked bar measured from the face of the column to the end of the hook (in.); d_b is the hooked bar diameter (in.); A_{hs} is the total area of the hooked bars (in.²); A_{th} is the effective confinement and defined as the area of confining reinforcement (in.²) within $8d_b$ from the top of the hooked bar for No. 8 bars and smaller or within $10d_b$ for No. 9 bars

or larger; n is the number of hooked bars in the joint; and s is the center-to-center spacing between hooked bars. The maximum effective value for A_{th}/A_{hs} is 0.2 when using the descriptive equations. [Note: The definition of A_{th} differs from that used in ACI 318-19.] The equations were used as the basis for the design provisions in ACI 318-19, allowing the use of high-strength concrete and reinforcing steel. The Code provisions for hooked bars in ACI 318-19 are discussed later in this chapter. The descriptive equations were also used in the current study as the basis for the design and evaluation of specimens with No. 14 and No. 18 hooked bars.

In addition to developing the descriptive equations and proposing new design provisions for ACI 318 Code, some of the key findings of the study at the University of Kansas were:

- Closely-spaced hooked bars (center-to-center spacing below $6d_b$) are weaker, individually, than widely-spaced hooked bars.
- Hooked bars with 90° and 180° bends have similar anchorage strengths.
- Confining reinforcement parallel and perpendicular to the bar increases the anchorage strength of hooked bars.
- Confining reinforcement contributes more to anchorage strength for closely-spaced bars than it does for widely-spaced bars.
- The provisions in ACI 318-14 did not accurately represent the anchorage strength of hooked bars in terms of the effect of bar size and the contributions of confining reinforcement and concrete compressive strength.
- The contribution of concrete compressive strength on the anchorage strength of hooked bars is best represented by a 0.295 power rather than by the square root of compressive strength (as used in ACI 318). For design purposes, compressive strength to the 0.25 power can be safely used.
- Specimens with a ratio of beam effective depth to the hooked bar embedment length (d_{eff}/ℓ_{eh}) greater than 1.5 had low anchorage strengths with respect to the descriptive equations, which were developed based on specimens with $d_{eff}/\ell_{eh} \leq 1.5$.
- Concrete breakout was the dominant failure mode, but side splitting tended to increase as the bar size increased.

1.2.2 Headed Reinforcing Bars

As discussed in the previous section, hooked bars can be used when straight bars cannot be fully developed. In some cases, such as a heavily reinforced region, however, hooked bars can cause congestion. When several and/or staggered hooked bars are required, the tail extension of the bars can cause steel congestion, which in turn can adversely affect the construction quality and structural performance of the member. An example of steel congestion in the presence of staggered hooked bars in an external beam-column joint is shown in Figure 1.8.



Figure 1.8 Steel congestion in an external beam-column joint caused by staggered hooked bars (<https://www.sefindia.org>)

A viable solution to the steel congestion problem is the use of headed reinforcing bars, which permit the tail extension of the hook to be eliminated. Instead, a head is forged or attached to one or both ends of the bar. The head can have a round, elliptical, or rectangular shape, and can vary in size, as shown in Figure 1.9.

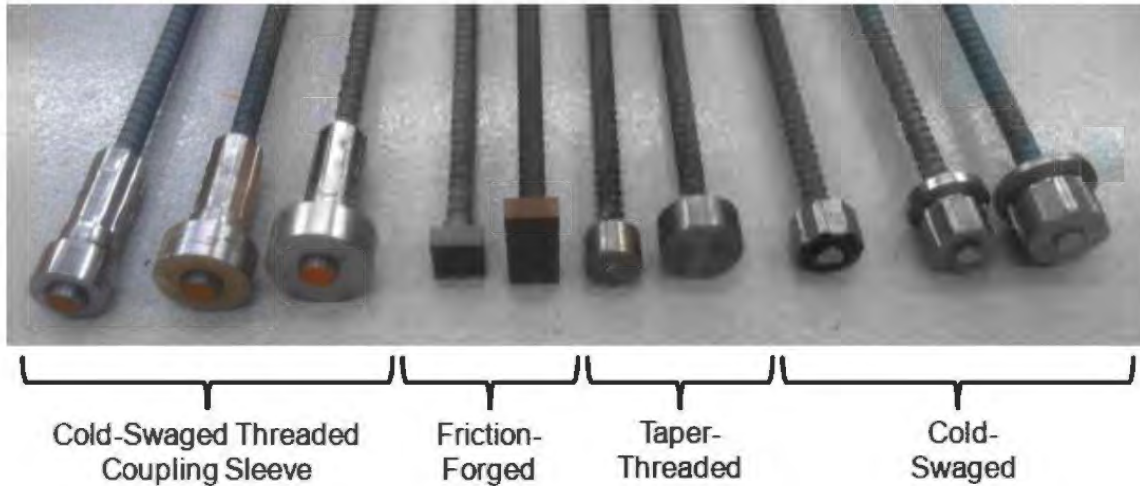


Figure 1.9 Different types of headed bars (Shao et al. 2016)

ACI 318 only permits the use of heads conforming to the Class HA requirements in ASTM A970. Based on these requirements, the net bearing area of the head, A_{brg} , must be at least four times the area of the bar, A_b . Net bearing area is defined as the gross area of the head minus the nominal area of the bar plus, in certain cases, any obstructions of the head induced by the manufacturing process. Prior to 2016, ASTM A970 required obstructions to have a width less than $1.5d_b$ (Figure 1.10). Shao et al. (2016) and Ghimire et al. (2018) found that some headed bars with obstructions exceeding the ASTM A970-16 dimensional limits provided adequate anchorage strength; as a result, the requirements were modified and updated in ASTM A970-17. The current requirements (ASTM A970-18) are shown in Figure 1.11.

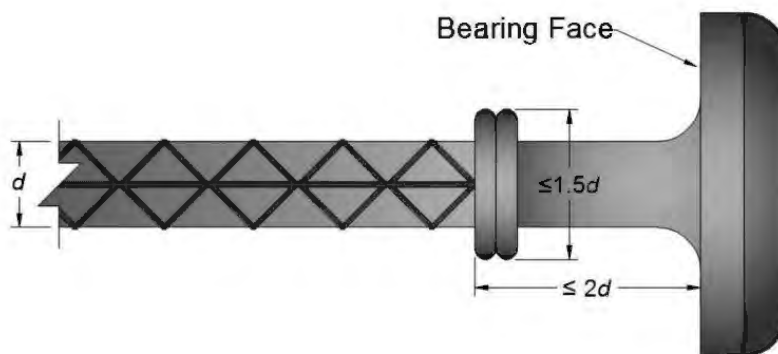


Figure 1.10 Previous limits on headed bar obstructions (ASTM A970/M970-16)

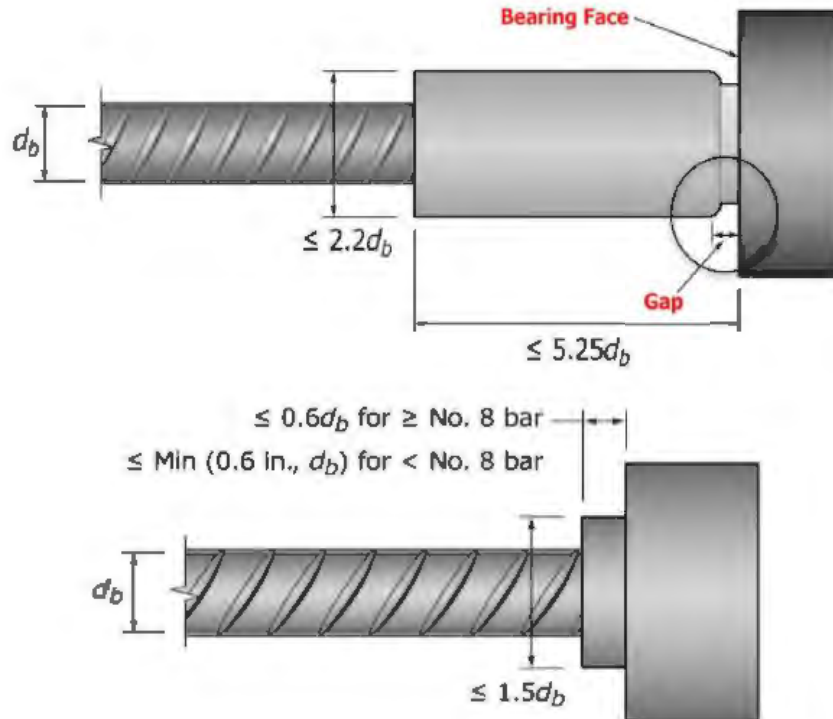


Figure 1.11 Current dimensional limits for obstructions or interruptions in headed bars (ASTM A970/M970-18)

Headed bars achieve anchorage by engaging the concrete through a combination of bond along the deformed bar length and the bearing of the head on concrete, as shown in Figure 1.12. Much like hooked bars, anchorage strength is governed by the breakout strength of the concrete, by mechanisms illustrated in Figure 1.13, which is enhanced by the presence of confining reinforcement. For headed bars, development length is measured from the face of the head, not the back of the head.

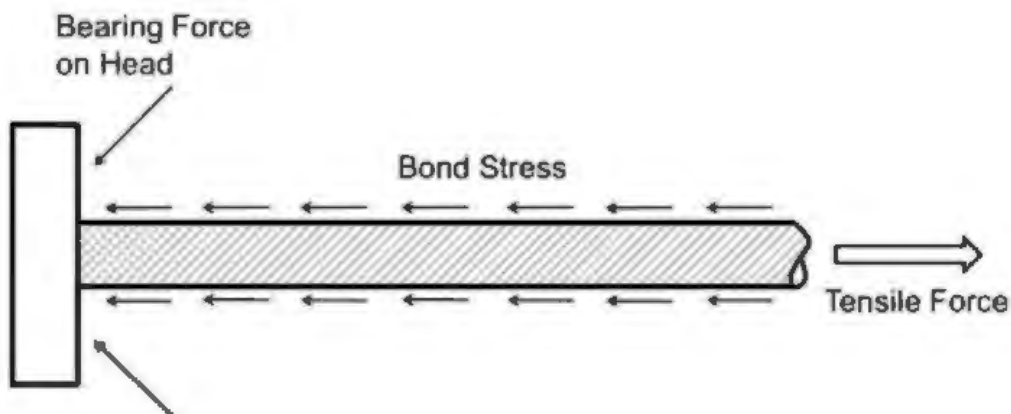


Figure 1.12 Anchorage and bond of headed bars (Shao et al. 2016)

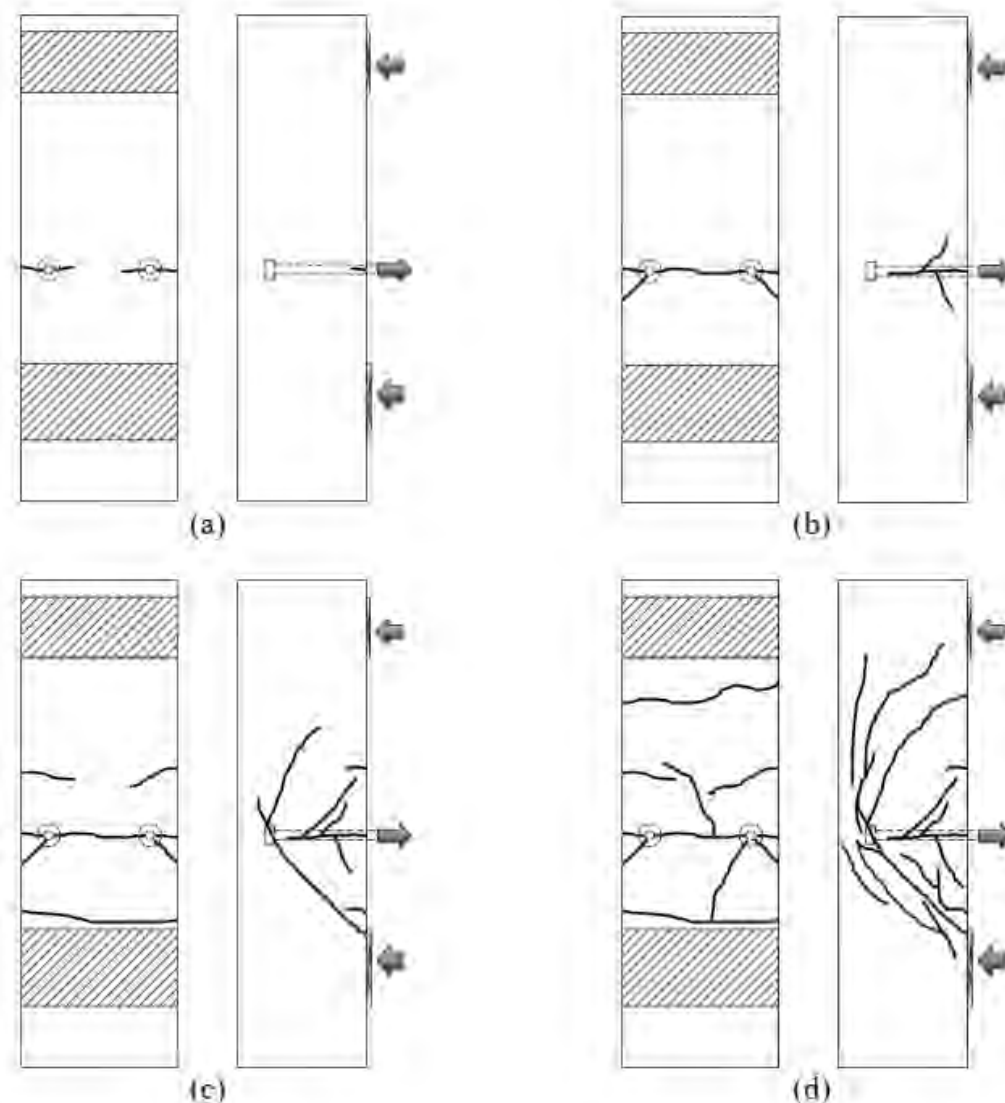


Figure 1.13 Crack progression observed in the beam-column joint specimens containing headed bars. Breakout failure is preceded by bond slip along the straight portion of the bars and cracking of the concrete (Shao et al. 2016, Ghimire et al. 2019a)

Previous studies on headed bars include tests on slab and column-like specimens, splices, compression-compression-tension (CCT) nodes, and beam-column joints under monotonic or cyclic loading. DeVries (1996), Bashandy (1996), and Wright and McCabe (1997) conducted beam-end tests, pullout tests, shallow- and deep-embedment tests, and simulated beam-column joint tests and proposed anchorage provisions. The first design provisions for headed bars were introduced in the 2008 edition of the ACI 318 Building Code, based primarily on the work by Thompson et al. (2005, 2006a, 2006b) in which CCT node tests and lap splice tests were conducted. Since the thrust of the current study is external beam-column joints under monotonic loading, the relevant literature is discussed next.

Bashandy (1996) tested thirty-two simulated beam-column joint specimens, each containing two headed bars, to investigate the effects of embedment length (8.5 to 17 in.), confining reinforcement in the joint region (26 specimens without confining reinforcement and 6 specimens with No. 3 ties spaced at 2 to 4 in.), bar size (No. 8 and No. 11), head size (2 to $7.1A_b$), concrete compressive strength (3,200 to 5,800 psi), and placement of headed bars (inside or outside the column core). The two main failure modes observed were side blowout (spalling of the concrete side cover, in 18 specimens) and along the diagonal cracks formed in the joint region (along the diagonal strut between the head and the top of the bearing plate simulating the beam compressive zone, in 14 specimens). Bashandy (1996) found that the anchorage strength of headed bars increased with increasing embedment length, confining reinforcement, head size, and concrete cover to bar, and that the bar size did not have a noticeable effect. Also, headed bars placed outside the column core had lower anchorage strength than those placed inside the column core.

Chun et al. (2009) tested 30 beam-column joint specimens, of which 24 had headed bars and 6 had hooked bars. Chun et al. investigated bar size (No. 8, No. 11, and No. 18) and embedment length (6.3 to $10.4d_b$ for No. 8 and No. 11 bars and 8.4 to $15.5d_b$ for No. 18 bars). Concrete compressive strength ranged from 3,510 to 3,640 psi. The specimens had a single headed or hooked bar with no confining reinforcement in the joint region. The heads used did not conform to Class HA requirements and had obstructions with a diameter of $1.5d_b$ and a length of $0.75d_b$, reducing the net bearing area of the head adjacent to the obstruction to 2.7 to $2.8A_b$. Concrete side cover to the bar was $2.5d_b$. It was observed that the models proposed by Bashandy (1996), DeVries (1996), and Thompson et al. (2006) for predicting the anchorage strength of headed bars based on failure modes did not provide an accurate prediction of the concrete contribution to anchorage strength. Chun et al. (2009) proposed a new model in which the anchorage strength of a headed bar was the sum of contributions from bond along the bar and head bearing. Chun et al. established the bond along the bar as a function of bar diameter, embedment length, and concrete compressive strength, and the bearing on head as a function of net bearing area, ratio of embedment length to column depth, and concrete compressive strength.

Kang et al. (2010) tested 12 beam-column joint specimens to investigate the effects of head size (large head with net bearing area of $4.5A_b$ and non-HA heads with net bearing area of 2.6 to $2.8A_b$), manufacturing process of the head (welding or threading), and loading condition (monotonic and reversed cyclic loading). The results showed that only the head size, among other

parameters, influenced the anchorage strength. Specimens with larger heads had a higher anchorage strength than those with smaller heads.

Chun et al. (2017a), Chun and Lee (2019), Sim and Chun (2022a, 2022b) tested a total of 53 simulated beam-column joint specimens to investigate the side-face blowout strength of headed bars. The headed bars used did not meet the Class HA requirements and had net bearing areas of 2.7 to $2.9A_b$. All specimens had double overlapping parallel ties in the joint region. The majority of specimens had a single layer of No. 7, No. 10, No. 14, or No. 18 headed bars. Ten specimens had two layers of No. 14 headed bars, with layers spaced at 1 or $2d_b$ on-center. All specimens had two bars per layer, and all bars were Gr. 80. Concrete compressive strength ranged from 5,450 to 16,680 psi. Bar stress at failure ranged from 43.1 to 93.4 ksi. Embedment length ranged from 6 to $20d_b$. Side cover to the bar ranged from 1 to $4d_b$. In these studies, the specimens were designed to force a side-face blowout failure. The schematic of the test setup and specimen proportions used in these studies are shown in Figure 1.14. Figure 1.14.a shows a side view of the specimen proportions as well as the cross section of specimens tested by Chun et al. (2017a) and Chun and Lee (2019), in which the compression reaction of the simulated beam was placed $2/3$ of the embedment length from the headed bars. Figure 1.14.b shows a side view of the specimen proportions used by Sim and Chun (2022b), in which the supports were placed farther from the bars (twice the embedment length, as opposed to one embedment length in the first two studies). A side view of the 10 specimens with two layers of headed bars tested by Sim and Chun (2022a) is shown in Figure 1.14.c, in which the compression reaction of the simulated beam was placed a distance equal to the embedment length (not $2/3$) from the bars, but the supports were placed closer to the bars ($2/3$ of the embedment length).

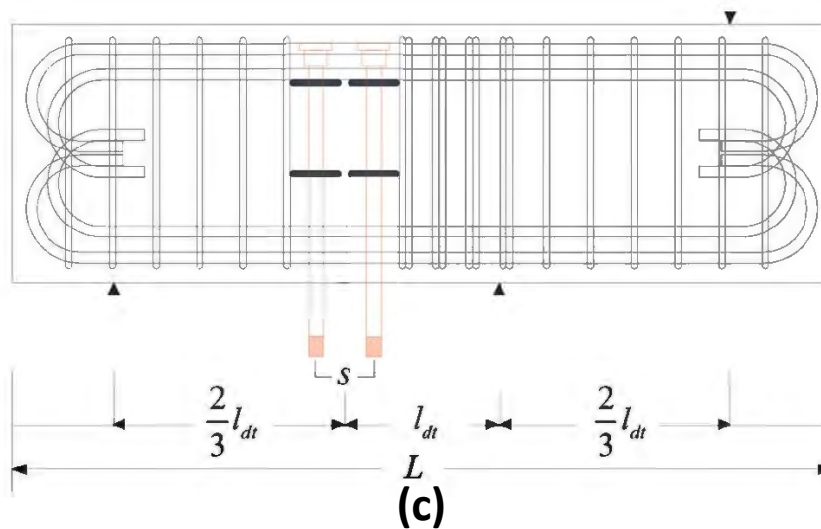
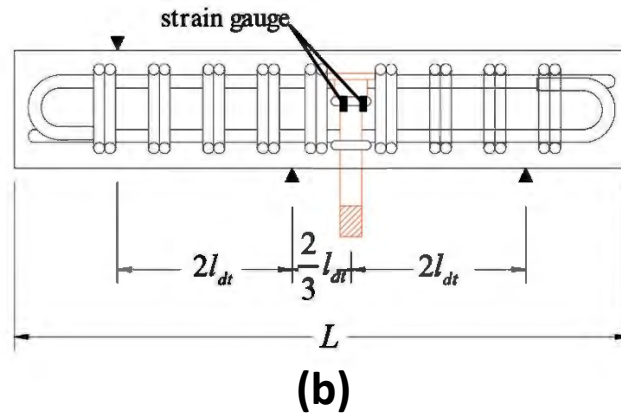
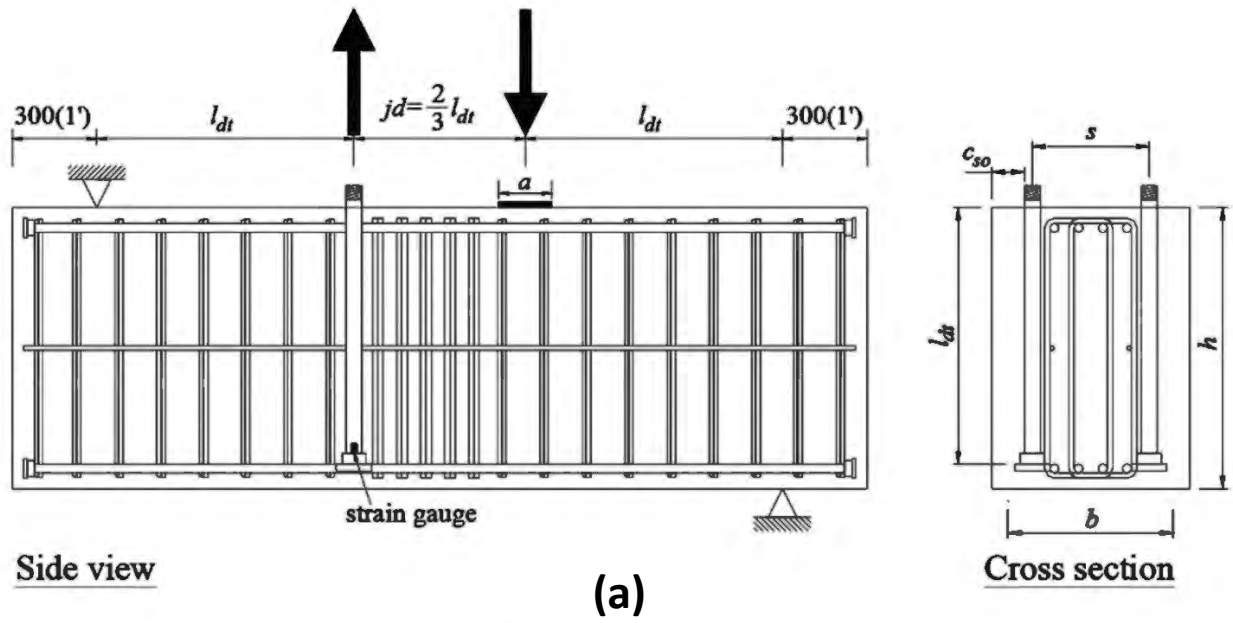


Figure 1.14 (a) Side view of specimen proportions used by Chun et al. (2017a) and Chun and Lee (2019); (b) Side view of the specimen proportions used by Sim and Chun (2022b); (c) Side view of the specimen proportions used by Sim and Chun (2022a)

Chun et al. (2017a), Chun and Lee (2019), Sim and Chun (2022a, 2022b) stated that the anchorage strength of headed bars depends on failure type and member geometry. The two components contributing to side-face blowout strength of headed bars, namely head bearing and bond along the bar, were evaluated. The head bearing contribution was based on the measured strain in the bar $1d_b$ from the bearing face of the head, and the bond contribution was calculated by deducting the head bearing contribution from the bar stress at failure. Initially, bond carried most of the load. As the load increased, the forces carried by both bond and head bearing increased, with head bearing carrying progressively more of the load – the majority at failure – with the load carried by bond dropping off. The researchers found that the bond contribution was linearly proportional to the development length for increases in ℓ_{dt}/d_b above 4.26 (negative intercept of -138 in Eq. (1.3)). The head bearing contribution was not affected by the development length. The side-face blowout strength of headed bars was enhanced with increasing side cover, embedment length, and hairpin-type transverse reinforcement. Simplified and detailed models were proposed for predicting the side-face blowout strength of headed bars, including the effects of side cover and transverse reinforcement. The detailed expression is provided in Eq. (1.3).

$$\begin{aligned}
 f_{dt,p} &= [523\psi_{brg} + (32.4\frac{\ell_{dt}}{d_b} - 138)\psi_b] \sqrt{f'_c} \\
 \psi_{brg} &= 0.7 + 0.3\frac{c_{so}}{d_b} + 0.325\frac{K_{tr}}{d_b} \\
 \psi_b &= 0.78 + 0.22\frac{c_{so}}{d_b} + 0.104\frac{K_{tr}}{d_b}
 \end{aligned} \tag{1.3}$$

where $f_{dt,p}$ is the side-face blowout strength of headed bars (psi), ℓ_{dt} is the embedment length (in.), d_b is the bar diameter (in.), f'_c is the concrete compressive strength (psi), ψ_{brg} is the head bearing factor, ψ_b is the bond factor, c_{so} is the side cover to the bar (in.), and K_{tr} is the transverse reinforcement index defined in Eq. (25.4.2.4b) of ACI 318-19 [$K_{tr} = 40A_{tr}/sn$ where A_{tr} is “total cross-sectional area of all transverse reinforcement within spacing s that crosses the potential plane of splitting through the reinforcement being developed, in.²”, s is the center-to-center spacing of transverse reinforcement, and n is the number of bars being developed.].

Sim and Chun (2022b) proposed a design equation for the development length of headed bars:

$$\frac{\ell_{dt,p}}{d_b} = \frac{f_y}{29\psi\sqrt{f'_c}} - 10 \quad (1.4)$$

$$\psi = 0.75 + 0.25\frac{c_{so}}{d_b} + 0.4\frac{K_{tr}}{d_b}$$

where $\ell_{dt,p}$ is the proposed development length (in.), and ψ is the modification factor for side cover and confining reinforcement. In these equations, K_{tr}/d_b cannot be greater than 0.7, $\ell_{dt,p}$ cannot be less than $6d_b$, f'_c cannot be greater than 17,400 psi, c_{so}/d_b cannot be less than 1.0 or greater than 3.0, and ψ cannot be greater than 1.5.

The work by Thompson et al. (2005, 2006a, 2006b), was used as a basis for the first design provisions for headed bars, in ACI 318-08. Due to the limited range of the material properties in those studies, however, the provisions were very conservative for headed bars such that in ACI 318-08 and ACI 318-14: the concrete compressive strength was limited to 6,000 psi for use in calculating development length and the specified steel yield strength was limited to 60,000 psi. Among other shortcomings, these limitations prevented application of the provisions to high-strength concrete and reinforcing steel. To address these limitations and to provide more experimental data to better understand the anchorage and development of headed bars, a comprehensive study was initiated at the University of Kansas, similar to the studies on the hooked bars (discussed in the previous section). A wide range of material properties (including high-strength concrete and reinforcing steel) and specimen configurations and their effects on the anchorage strength of headed bars were investigated.

A total of 233 specimens were tested by Shao et al. (2016), including 202 simulated exterior beam-column joint specimens, 10 CCT node specimens, 15 column-foundation joint specimens (each slab containing one to three headed bars for a total of 32 tests), and 6 splice specimens. The main variables investigated were bar size (No. 5, No. 8, and No. 11), number of headed bars (2, 3, or 4 per specimen), bar spacing (1.7 to $11.8d_b$ on-center), bar stress at failure (26,100 to 153,200 psi), head size (3.8 to $14.9A_b$), concrete compressive strength (3,960 to 16,030 psi), embedment length (4 to 6 in. for No. 5 bars, 6 to 14.5 in. for No. 8 bars, and 12 to 19.25 in. for No. 11 bars), and amount of confining reinforcement in the joint region (none to six No. 3 ties parallel to the headed bars spaced at $3d_b$). Some of the headed bars used had large obstructions (Figure 1.10) exceeding what were the dimensional limitations of Class HA heads in ASTM A970-16. Side cover to the bars themselves ranged from 2.5 to 4 in., with most specimens having a 2.5

in. side cover. A limited number of specimens had headed bars anchored in the middle of the column, but for the majority of the specimens, the headed bars were anchored at the far side of the column so that the back of the head touched the longitudinal reinforcement of the column.

The specimen design and configuration were very similar to those tested with hooked bars. A schematic of a typical simulated beam-column joint specimen is shown in Figure 1.15.

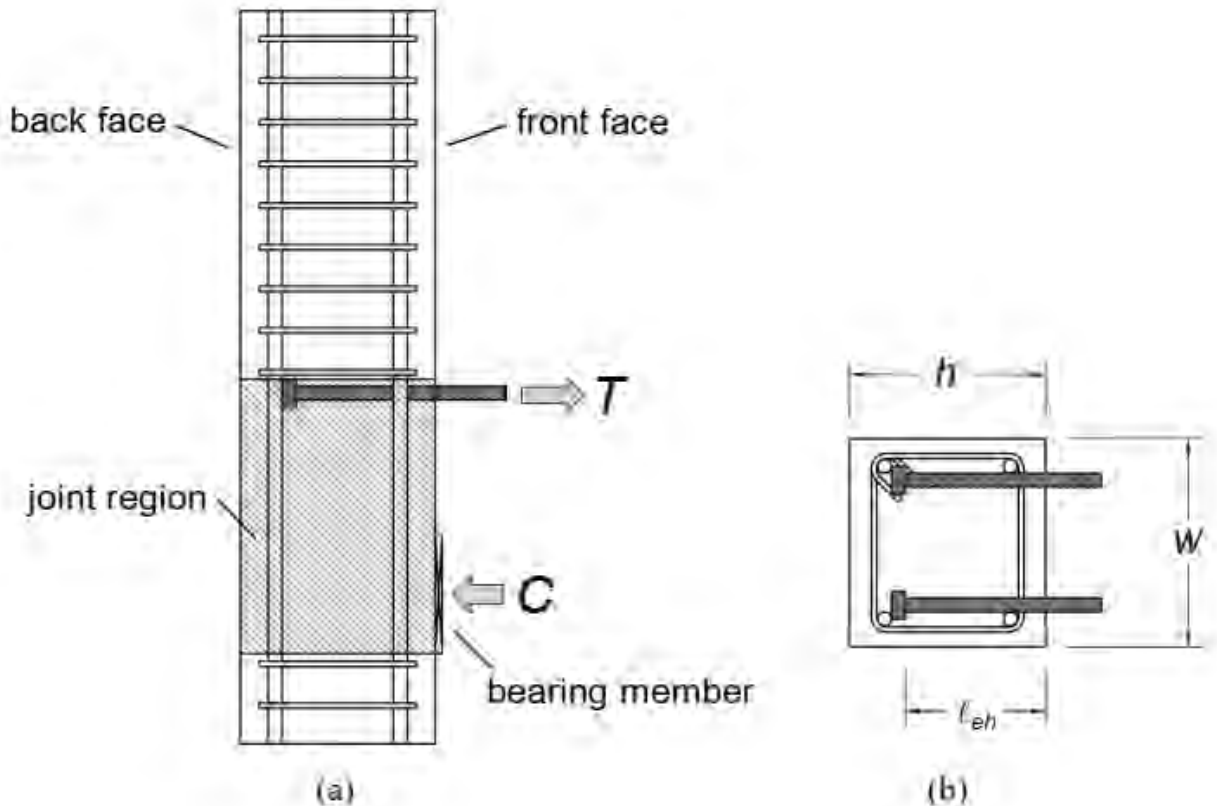


Figure 1.15 Schematic of headed bar specimens (a) side view (b) cross-section, where h and w are column height and width, respectively, and ℓ_{eh} is the embedment length (Shao et al. 2016)

The loading frame was the same as used by Sperry et al. (2015a, 2015b) and Ajaam et al. (2017) for testing simulated beam-column joint specimens containing hooked bars (Figure 1.6). Headed bars represented the top longitudinal reinforcement and the adjacent bearing member represented the compressive zone of the virtual beam, as shown in Figure 1.16. The tensile force applied to the bars and the compressive force by the bearing member acted as a couple, simulating the negative moment acting at a beam-column joint.

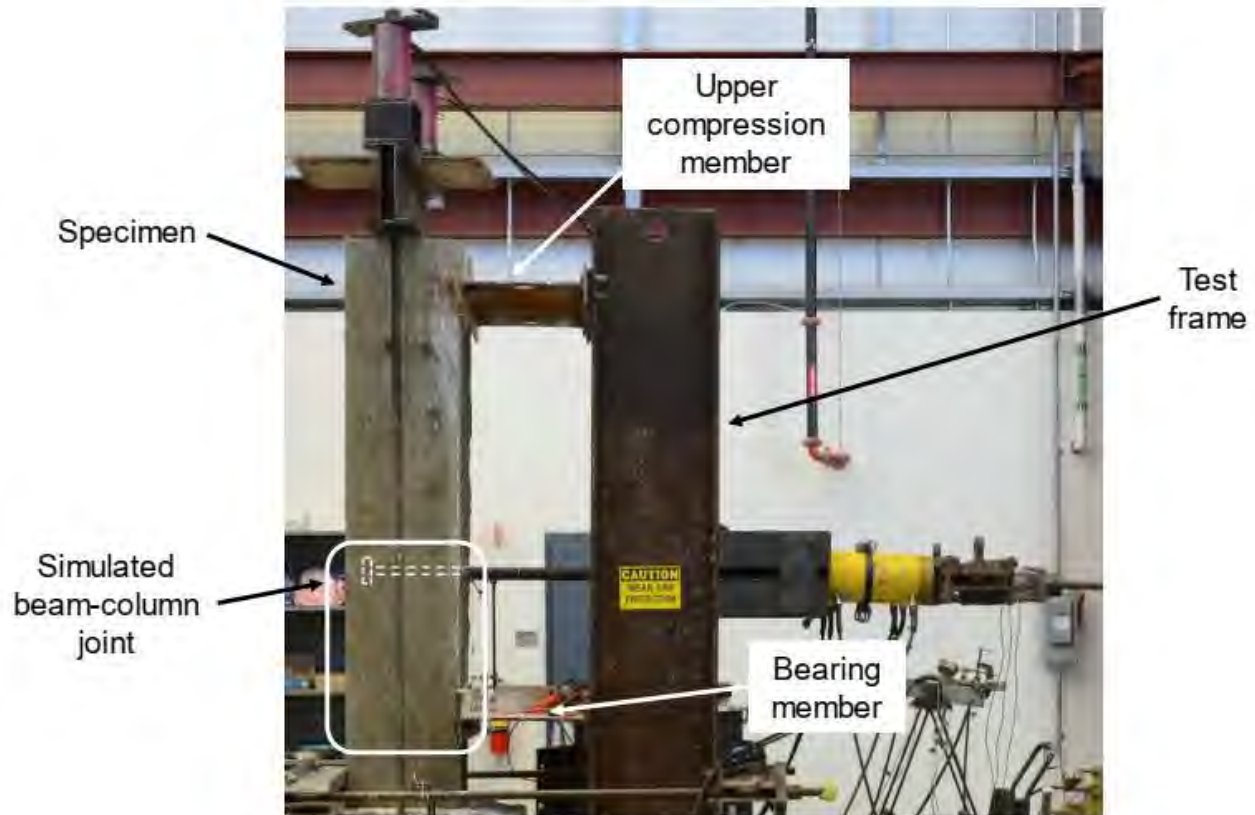


Figure 1.16 The loading frame and test setup of headed bar specimens (Shao et al. 2016)

The headed bar specimens exhibited cracking and failure mechanisms, as shown in Figure 1.13, that were similar to those of the hooked bar specimens (Figure 1.2). Cracking began with a horizontal crack on the front face of the column at the level of the headed bars and extending towards both sides (Figure 1.13a). With increasing load, the horizontal cracks started to connect, with new cracks radiating from the bars. On the sides, the horizontal crack grew along the length of the headed bars, while diagonal cracks started branching towards the upper compression and lower bearing members (Figure 1.13b). As the load continued to increase, more horizontal cracks appeared on the front face, while a large diagonal crack forming in the joint region between the head and the bearing member (Figure 1.13c). Near failure, the existing cracks got wider while new cracks continued to branch from the existing cracks in a cone-shaped form (Figure 1.13d).

Shao et al. (2016) observed two main failure modes, concrete breakout and side-face blowout. Concrete breakout occurred in the majority of specimens (149 out of 196) and was characterized by the separation of the concrete within the column in front of the head. As shown in Figure 1.17, two types of failure surface were observed, namely cone-shaped and back cover

spalling. About half of the specimens had a cone-shaped failure surface. No direct relationship was found between the shape of the failure surface and the anchorage strength of headed bars.

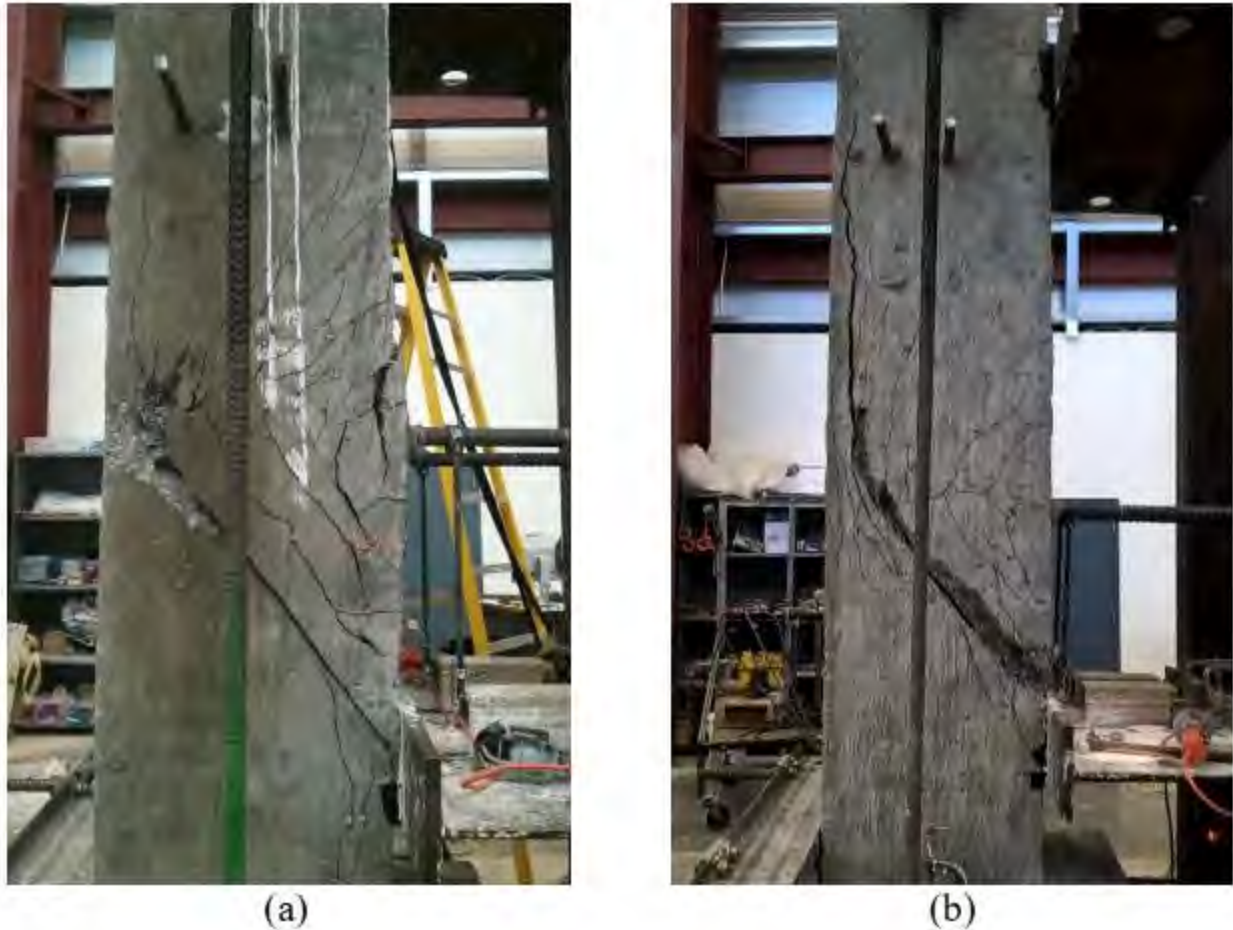


Figure 1.17 Concrete breakout (a) cone-shaped (b) back cover spalling (Shao et al. 2016)

Side-face blowout (in 47 out of 196 specimens) was characterized by local damage to the concrete around the head due to the head movement, resulting in spalling or separation of the concrete cover, sometimes in an explosive manner as shown in Figure 1.18.



Figure 1.18 Side-face blowout (a) side view (b) back view (Shao et al. 2016)

As they were for hooked bars, descriptive equations were developed for headed bars based on a best fit of the experimental data (Shao et al. 2016, Ghimire et al. 2019b). The descriptive equations characterize the anchorage strength of headed bars as a function of concrete compressive strength, bar diameter and spacing, embedment length, and confining reinforcement in the joint region (parallel ties for headed bars). The equations for headed bars without and with confining reinforcement are shown in Eq. (1.5) and Eq. (1.6), respectively:

$$T_h = 781 f_{cm}^{0.24} \ell_{eh}^{1.03} d_b^{0.35} \left(0.0836 \frac{s}{d_b} + 0.344 \right) \left(0.0836 \frac{s}{d_b} + 0.344 \right) \leq 1.0 \quad (1.5)$$

$$T_h = \left(781 f_{cm}^{0.24} \ell_{eh}^{1.03} d_b^{0.35} + 48,800 \left(\frac{A_{th}}{n} \right) d_b^{0.88} \right) \left(0.0622 \frac{s}{d_b} + 0.5428 \right) \left(0.0622 \frac{s}{d_b} + 0.5428 \right) \leq 1.0 \quad \& \quad \frac{A_{th}}{n} \leq 0.3 A_b \quad (1.6)$$

where T_h is the anchorage strength of headed bars (lb); f_{cm} is the measured concrete compressive strength (psi); ℓ_{eh} is the embedment length of the headed bar measured from the face of the column to the bearing face of the head (in.); d_b is the headed bar diameter (in.); A_{hs} is the total area of the headed bars (in.²); A_{tt} is as the area of confining reinforcement (in.²) within $8d_b$ from the top of the headed bar for No. 8 bars and smaller or within $10d_b$ for No. 9 bars or larger (Figure 1.19); n is the number of headed bars in the joint; and s is the center-to-center spacing between headed bars. As shown in Eq. (1.6), Shao et al. (2016) showed that the maximum value of A_{tt}/n that contributes to T_h is $0.3A_b$. Equations (1.5) and (1.6) were used as the basis for the development length provisions in ACI 318-19, allowing the use of high-strength concrete and reinforcing steel. Equations (1.5) and (1.6) were also used as the basis for designing the specimens in this study.

Shao et al. (2016) also compared the descriptive equations with their test results and results from previous studies (exterior beam-column joints by Bashandy 1996 and Chun et al. 2009, CCT nodes by Thompson et al. 2006a, shallow embedment pullout tests by DeVries 1999, and lap splice tests by Thompson et al 2006b and Chun 2015). The test-to-calculated ratio (T/T_h) for the specimens used in the comparison was generally conservative (> 1.0), but low anchorage strength was observed for the specimens tested by Chun et al. (2009) and Chun (2015), assumed to be due to Chun et al. (2009) and Chun (2015) using heads with large obstructions that resulted in net bearing areas of only 2.7 and $2.8A_b$. The descriptive equations, also were shown to be applicable to beam-column joints subjected to reversed cyclic loading (Ghimire et al. 2018). Shao et al. (2016) used Eq. (1.5) and (1.6) to develop design provisions for the development length of headed bars, that applied reinforcing steel with yield strengths up to 120,000 psi and concrete with compressive strengths up to 16,000 psi). The proposed design provisions will be discussed later in this chapter.

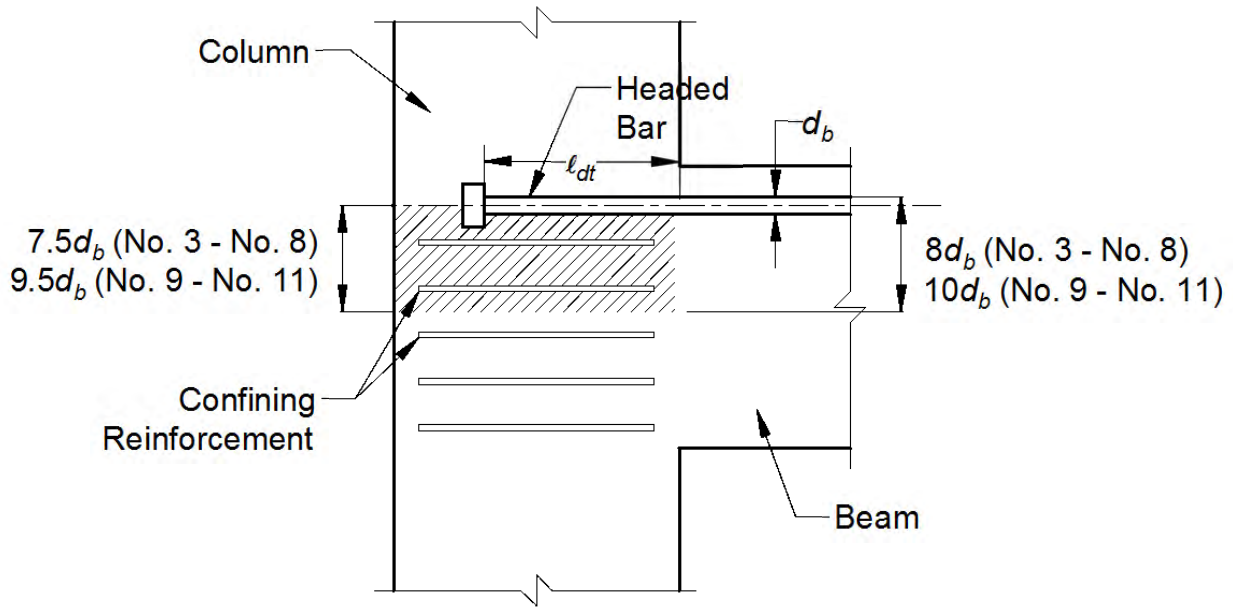


Figure 1.19 Confining reinforcement contributing to anchorage strength of headed bars anchored in beam-column joints (Shao et al. 2016, Ghimire et al. 2019)

In addition to developing descriptive equations and new design provisions, Shao et al. (2016) and Ghimire (2018, 2019a, 2018b) observed that:

- The development length provisions in ACI 318-14 became progressively less conservative as the bar size increased.
- The development length provisions in ACI 318-14 became progressively less conservative as the concrete compressive strength increased. The anchorage strength of headed bars increases with compressive strength to the 0.24 power, rather than the square root of the compressive strength as represented in ACI 318-14.
- Providing confining reinforcement parallel to the headed bars increases the anchorage strength in proportion to the amount of confining reinforcement per headed bar up to $0.3A_b$, as shown in Eq. (1.6).
- When center-to-center spacing of headed bars decreased below $8d_b$, anchorage strength decreased. “Widely-spaced” headed bars were defined as bars with center-to-center spacing was equal or greater than $8d_b$, and closely-spaced heads bars as bars with center-to-center spacing below $8d_b$.

- Headed bars with obstructions exceeding the limitations of HA heads in ASTM A970-16 and prior versions of the specification provided satisfactory anchorage strength, and the findings were incorporated in ASTM A970-17.
- Heads with bearing areas of 12.9 to 14.9A_b provided, on average, 17% and 7% more anchorage strength for No. 5 and No. 8 bars, respectively, than heads with smaller bearing areas between 3.8 and 9.5A_b, but the increase in anchorage strength was not proportional to the bearing area.

Comparing the test results and findings of the studies on the anchorage of hooked and headed bars at the University of Kansas (Searle et al. 2014, Sperry et al. 2015a, 2015b, 2017a, 2017b, 2018, Yasso et al. 2017, Ajaam et al. 2017, 2018, Shao et al. 2016, Ghimire et al. 2018, 2019a, 2019b) provides the following valuable observations:

- Hooked and headed bars have a lot of similarities in terms of anchorage behavior
- For the same embedment length, headed bars provide a higher anchorage force than hooked bars.
- Closely-spaced hooked and headed bars are weaker, individually, than widely-spaced hooked and headed bars.
- Confining reinforcement parallel to the bar increases anchorage strength of hooked and headed bars.
- Confining reinforcement perpendicular to the bar increases anchorage strength of hooked but not headed bars.
- For both hooked and headed bars, confining reinforcement makes a bigger contribution for closely-spaced bars than for widely-spaced bars

1.3 CURRENT CODE PROVISIONS AND DESIGN GUIDELINES

In this section, the provisions in the ACI 318-14 for the development length of both hooked and headed bars are presented, followed by the proposed design provisions based on the studies at the University of Kansas (Sperry et al. 2015a, 2015b, 2017a, 2017b, 2018, Ajaam et al. 2017, 2018, Shao et al. 2016, Ghimire et al. 2018, 2019a, 2019b). Finally, the current Code provisions, in ACI 318-19, and their limitations are discussed.

1.3.1 Reinforcing Bars with Standard Hooks

The provisions for the development length of hooked bars in ACI 318-14 were based on 38 tests of simulated beam-column joints conducted in 1970s with concrete compressive strength ranging from 3.8 to 5.1 ksi and yield strengths of hooked bars of 64 or 68 ksi. Based on these limited experimental data, the following equation was given in ACI 318-14 and Codes dating back to 1983 to calculate the development length of deformed bars with standard hooks in tension (Eq. 1.7):

$$\ell_{dh} = \left(\frac{f_y \psi_e \psi_c \psi_r}{50 \lambda \sqrt{f'_c}} \right) d_b \quad (1.7)$$

where ℓ_{dh} is the embedment length of hooked bar (in.), f_y is the bar yield strength (psi), ψ_e is the coating factor, ψ_c is the concrete cover factor, ψ_r is the confining reinforcement factor, λ is the concrete density factor, f'_c is the concrete compressive strength (psi), and d_b is the bar diameter (in.). For lightweight concrete, $\lambda=0.75$, and for epoxy-coated bars, $\psi_e=1.2$; otherwise, these factors are equal to 1.0. For No. 11 and smaller hooks, $\psi_c=0.7$ if side cover is ≥ 2.5 in. and tail cover ≥ 2 in., $\psi_r=0.8$ if ties or stirrups are provided along or perpendicular the straight portion of the bar and spaced no greater than $3d_b$, as shown in Figure 1.20.

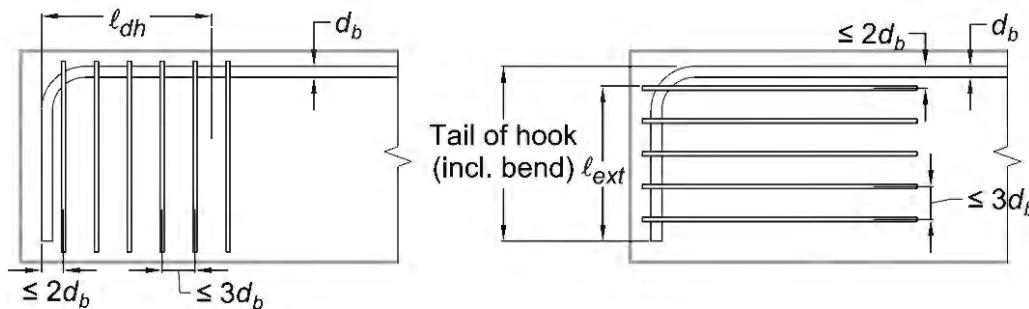


Figure 1.20 ACI 318-14 provisions for ties or stirrups placed perpendicular (left) or parallel (right) to the hooked bar being developed (ACI 318-14)

The ACI 318-14 provisions for hooked bars limited the concrete compressive strength to 10,000 psi and bar yield strength to 80,000 psi. At the University of Kansas, Sperry et al. (2015a, 2015b, 2017a, 2017b, 2018) compared test results from their study and earlier studies with the anchorage strength derived from ACI 318-14 provisions (Eq. 1.7). Specimens included in the analysis had two widely-spaced hooked bars. The yield strength f_y in Eq. 1.5 was replaced by bar stress, $f_{s,ACI}$, and f'_c was replaced by the measured compressive strength, f_{cm} . The equation was

then solved for $f_{s,ACI}$ to calculate the anchorage strength. Figure 1.21 shows the ratio of test-to-calculated stress $f_{su}/f_{s,ACI}$ versus f_{cm} for hooked bar specimens without confining reinforcement.

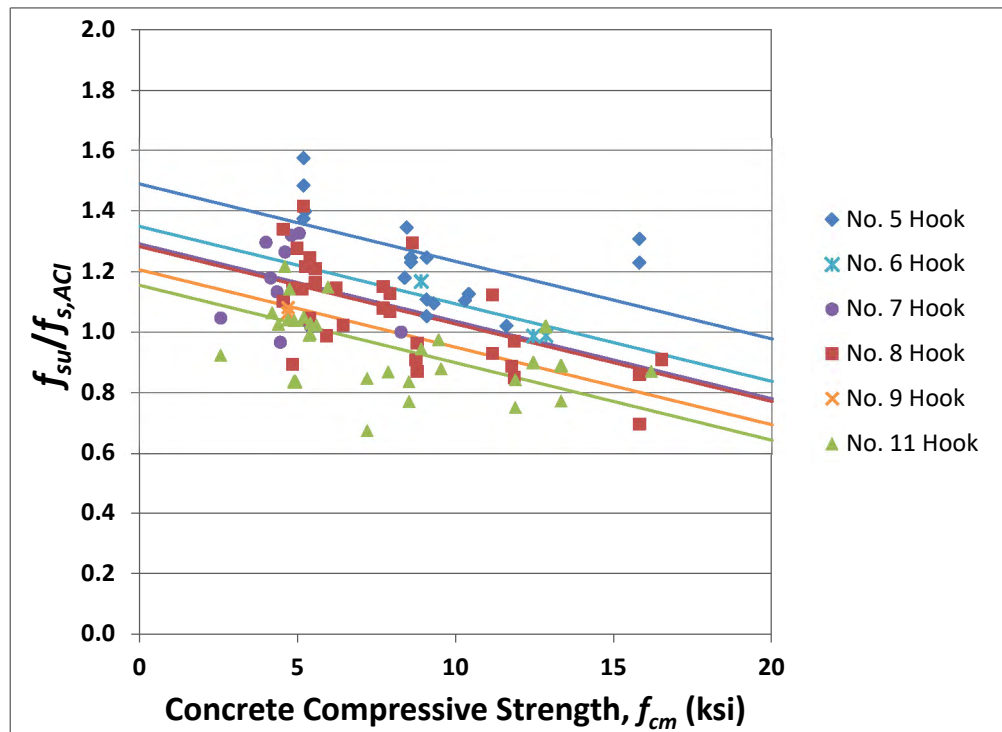


Figure 1.21 Ratio of test-to-calculated stress $f_{su}/f_{s,ACI}$ versus f_{cm} for hooked bars without confining reinforcement (Sperry et al. 2015b)

The trend lines in Figure 1.21 indicate that the test-to-calculated ratio $f_{su}/f_{s,ACI}$ decrease with increasing compressive strength and bar size. For No. 9 and No. 11 hooked bars, the ratio drops below 1.0 at approximately 8,000 and 6,000 psi, respectively. This observation showed that the ACI 318-14 provisions may be unconservative for No. 9 and larger bars in concrete with compressive strengths as low as 6,000 psi.

Figure 1.22 shows the same comparison for widely-spaced hooked bars with No. 3 ties in the joint region spaced at $3d_b$ or less. As shown in Figure 1.22, the $f_{su}/f_{s,ACI}$ ratio decreases as the bar size and compressive strength increase. For No. 8 and No. 11 hooked bars, the ratio drops below 1.0 at compressive strengths of about 11,000 and 5,000 psi, respectively, indicating unconservative designs produced by the ACI 318-14 provisions. Sperry et al. (2015b) concluded that the ACI 318-14 provisions overpredicted the effects of concrete compressive strength and confining reinforcement on the anchorage strength of hooked bars, and the anchorage strength of larger bars. Furthermore, the reduction factors applied to Eq. (1.7) for concrete cover and confining reinforcement, ψ_c and ψ_r , were found to be unconservative.

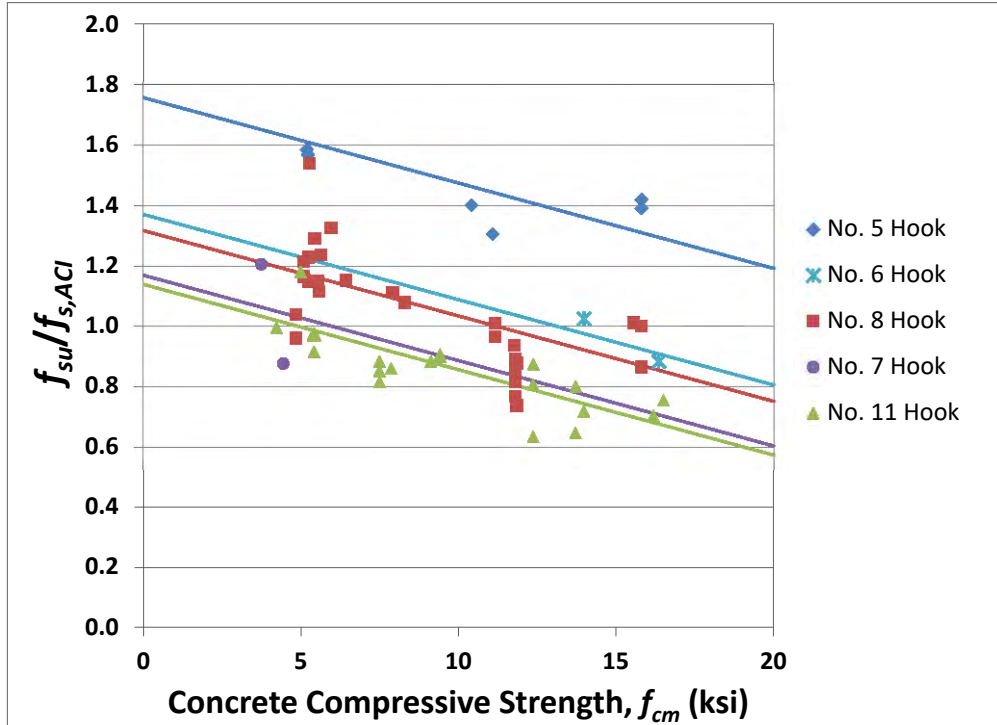


Figure 1.22 Ratio of test-to-calculated stress $f_{su}/f_{s,ACI}$ versus f_{cm} for hooked bars with No. 3 ties spaced at $3d_b$ in the joint region (Sperry et al. 2015b)

Based on these observations, the development length provisions for hooked bars in ACI 318-14 needed to be modified to more accurately reflect the effects of concrete compressive strength and bar size. To do so, Sperry et al. (2015b) and Ajaam et al. (2017) simplified the descriptive equations, Eq. (1.1) and (1.2) to propose a new design equation for the development length of hooked bars. For bars spaced at or greater than $6d_b$ (referred to as widely-spaced bars), the descriptive equations were converted to equations for development length (ℓ_{dh}), and were then accounted for closer bar spacing, confining reinforcement, and bar location within the member. Eq. (1.8) shows the proposed design equation:

$$\ell_{dh} = \left(\frac{f_y \psi_e \psi_{cs} \psi_o}{500 \lambda f_c^{1.25}} \right) d_b^{1.5} \quad (1.8)$$

where ℓ_{dh} is the embedment length of hooked bar (in.), f_y is the bar yield stress (psi), ψ_e is the coating factor, ψ_{cs} is the confinement and spacing factor, ψ_o is the location factor, λ is the concrete density factor, f_c' is the concrete compressive strength, and d_b is the bar diameter (in.). The values of the modification factor for confining reinforcement and spacing, ψ_{cs} , are given in Table 1.2. The bar location factor, ψ_o , is 1.0 if hooked bars with a side cover to the bar of at least 2.5 in. terminate inside the column core, or in a member with a side cover to the bar of at least $6d_b$. In all

other cases, ψ_o is 1.25. The coating factor ψ_e (1.0 for uncoated bars and 1.2 epoxy-coated bars) and the concrete density factor λ (0.75 and 1.0 for lightweight and normalweight concrete, respectively) were retained from ACI 318-14.

Table 1.2 Values for the confinement and bar spacing factor, ψ_{cs} , as proposed by Ajaam et al. (2017) for hooked bars ^[1]

Confinement level	f_y (psi)	s	
		$2d_b$	$\geq 6d_b$
$A_{th}/A_{hs} \geq 0.2$ ^[2] or $A_{th}/A_{hs} \geq 0.4$ ^[3]	60,000	0.6	0.5
	120,000	0.66	0.55
None	all	1.0	0.6

^[1] Linear interpolation may be used for spacing or yield strengths not listed

^[2] Confining reinforcement parallel to straight portion of bar

^[3] Confining reinforcement perpendicular to straight portion of bar

Compared to the ACI 318-14 design equation (Eq. 1.7), the proposed equation incorporated a number of changes. The bar diameter d_b was raised to the 1.5 power rather than 1.0 and concrete compressive strength f'_c to the 0.25 power rather than $\sqrt{f'_c}$ for a more accurate representation of the effects of these two parameters. Also, the proposed equation was shown to provide conservative criteria for the development length of hooked bars for steel yield strengths up to 120,000 psi and concrete compressive strengths up to 16,000 psi, whereas ACI 318-14 limited these values to 80,000 psi and 10,000 psi, respectively.

The findings of the studies at the University of Kansas were used as a basis for developing the design provisions for hooked bars in the current edition of the ACI 318 Building Code, ACI 318-19 (Section 25.4.3). However, a modified version of the equation proposed by Ajaam et al. (2018) was adopted, because ACI Committee 318 did not want to incorporate a double interpolation for the confinement and bar spacing factor, as shown in Table 1.2, and did not want to represent the contribution of f'_c in the form of $f'_c{}^{0.25}$. Currently, Eq. (1.9) is used to calculate the development length of hooked bars in tension.

$$\ell_{dh} = \left(\frac{f_y \psi_e \psi_r \psi_o \psi_c}{55 \lambda \sqrt{f'_c}} \right) d_b^{1.5} \quad (1.9)$$

where ℓ_{dh} is the embedment length of hooked bar (in.), f_y is the bar yield strength (psi), ψ_e is the coating factor, ψ_r is the confining reinforcement factor, ψ_o is the location factor, ψ_c is the concrete strength factor, λ is the concrete density factor, f'_c is the concrete compressive strength, and d_b is the bar diameter (in.). Compared to the ACI 318-14 equation (Eq. 1.7), the bar diameter d_b is now raised to the 1.5 power in ACI 318-19 (as proposed by Ajaam et al. 2017 in Eq. (1.8)). The current Code equation is compared with the results obtained in this study in Chapter 4 and with newly proposed provisions for hooked bars in Chapter 6.

The modification factors for lightweight concrete, λ , and for epoxy-coated bars, ψ_e are 0.75 and 1.2, respectively. The other modification factors are given in Table 1.3.

Table 1.3 Modification factors for hooked bars as given in Table 25.4.3.2 of ACI 318-19

Modification Factor	Condition	Value
Confining reinforcement, ψ_r	$A_{th} \geq 0.4A_{hs}$ or $s^{[1]} \geq 6d_b^{[2]}$	1.0
	Other	1.6
Location, ψ_o	(1) Terminating inside column core with side cover normal to plane of hook ≥ 2.5 in., or (2) With side cover normal to plane of hook $\geq 6d_b$	1.0
	Other	1.25
Concrete strength, ψ_c	$f'_c < 6,000$ psi	$f'_c / 15,000 + 0.6$
	$f'_c \geq 6,000$ psi	1.0

[1] s is minimum center-to-center spacing of hooked bars

[2] d_b is nominal bar diameter

The bar location factor ψ_o is the same as proposed by Ajaam et al. (2017). In Table 1.3, A_{th} is the total cross-sectional area of ties or stirrups confining hooked bars within $15d_b$ of the centerline of the hooked bars and spaced no greater than $8d_b$, as defined in Figure 1.23, and A_{hs} is the total cross-sectional area of hooked bars developed at the critical section. In developing the Code (in both 318-14 and 318-19 editions), it was assumed that confining reinforcement would be uniformly distributed within the joint region. Based on this assumption, the choice was made to convert the maximum effective values based on confining reinforcement within $7.5d_b$ to $9.5d_b$ from the centerline of the hooked bars (as established by Ajaam et al 2017) to an approximate value within $15d_b$ (that is, $A_{th} = 0.4A_{hs}$, in place $0.2A_{hs}$). As shown in Table 1.3, the confining reinforcement factor ψ_r , which replaces the confining reinforcement and bar spacing factor, ψ_{cs} ,

is no longer variable, as proposed by Ajaam et al. (2017), but must be taken as 1.6 unless $A_{th} \geq 0.4A_{hs}$ or the center-to-center bar spacing $s \geq 6d_b$.

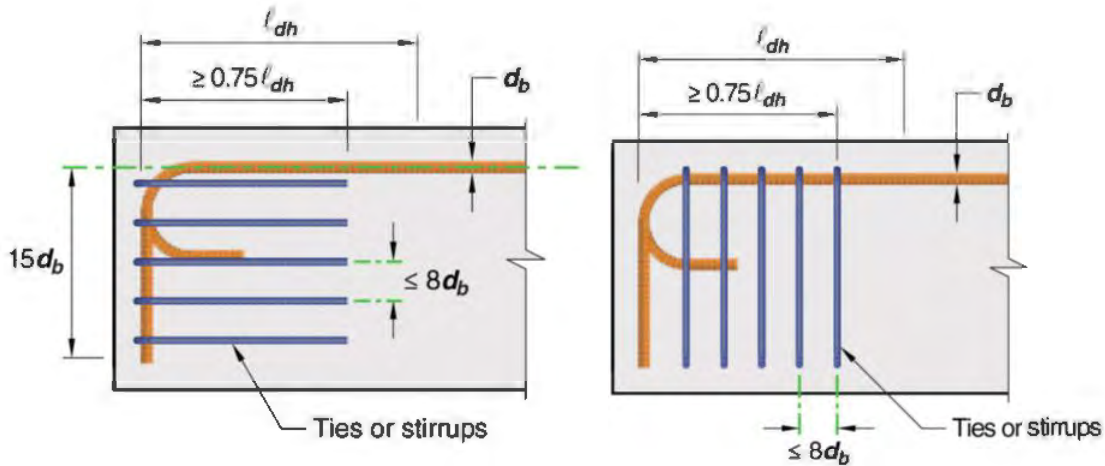


Figure 1.23 Confining reinforcement placed parallel (left) or perpendicular (right) to the hooked bar being developed as defined in ACI 318-19 (from ACI 318-19)

Although it was shown by the studies at the University of Kansas (Sperry et al. 2015b and Ajaam et al. 2017) that the effect of concrete compressive strength on the anchorage strength of hooked bars for design purposes is best represented by compressive strength to the 0.25 power (as reflected in their proposed design equation, Eq. (1.8), ACI Committee 318 chose to stay with the square root of compressive strength ($\sqrt{f'_c}$) in Eq. (1.9) during developing the 2019 edition of the Code. However, to prevent unreasonably long development lengths for the lower concrete strengths normally used in the practice (in the range of 4,000 to 6,000 psi), Eq. (1.9) was modified with the concrete strength factor, ψ_c , as defined in Table 1.2. The current Code equation becomes progressively less conservative as concrete strength increases above 6000 psi, up to 10,000 psi, at which point it begins to become more conservative as f'_c increases to 16,000 psi.

While improved, the Code provisions in ACI 318-19 still have limitations that need to be addressed. The maximum limit on concrete compressive strength is still 10,000 psi for use in calculating the development length, ℓ_{dh} , in Eq. (1.7), to prevent unconservative designs for higher-strength concretes (as discussed earlier, staying with $\sqrt{f'_c}$ in the current Code equation is already unconservative and the design becomes progressively more unconservative as the concrete strength increases to 10,000 psi). The binary choice of 1.6 and 1.0 for the confining reinforcement factor, ψ_r , limits the flexibility of the design; providing more detailed expressions would allow designers to take advantage of confining reinforcement $A_{th} < 0.4A_{hs}$ for bar spacing s less than $6d_b$.

Although there is no limit on the bar size, ACI 318-19 gives no credit to confining reinforcement for hooked bars larger than No. 11. That is, No. 14 and No. 18 hooked bars, even with confining reinforcement, are treated as if no confining reinforcement were present; thus, a ψ_r factor of 1.6 is applied as a penalty (increasing the required development length by 60%), unless the spacing $s > 6d_b$. This is mainly due to a lack of experimental data on No. 14 and No. 18 hooked bars, and one of the motivations for the current study.

1.3.2 Headed Reinforcing Bars

About 100 splice and CCT node tests were the basis for the provisions for the development of headed bars in ACI 318 Code before 2019. In these tests, the concrete compressive strength ranged from 3.5 to 5.5 ksi. The maximum yield strength of the headed bars used in the tests was 69 ksi. This very limited range of material properties and test specimens resulted in very conservative restrictions on the use of headed bars. Concrete compressive strength was limited to 6,000 psi, and the bar yield strength to 60,000 psi, impeding the use of high-strength concrete and reinforcing steel. ACI 318-14 provided the following equation to calculate the development length of headed bars:

$$\ell_{dt} = \left(\frac{0.016 f_y \psi_e}{\sqrt{f'_c}} \right) d_b \quad (1.10)$$

where ℓ_{dt} is the embedment length of headed bar (in.), f_y is the bar yield strength (psi), ψ_e is the coating factor (=1.2 for epoxy-coated reinforcement), f'_c is the concrete compressive strength (psi), and d_b is the bar diameter (in.). Unlike hooked bars, no modification factor was provided to account for confining reinforcement. The net bearing area of the head was required to be greater than or equal to 4 times the bar area ($A_{brg} \geq 4A_b$). The required concrete cover on the bar was $\geq 2d_b$ (same as for straight bars). The clear spacing between headed bars in both horizontal and vertical layers was required to be $\geq 4d_b$, not allowing the use of more closely spaced bars.

To evaluate the headed bar provisions in ACI 318-14, Shao et al. (2016) compared their beam-column joint test results with anchorage strengths based on Eq. (1.8). The bar stress at failure measured in the tests, f_{su} , was compared against the anchorage stress derived from Eq. (1.10), $f_{s,ACI}$. To do so, ℓ_{dt} was replaced with the measured embedment length, ℓ_{eh} , f'_c was replaced with the measured concrete compressive strength, f_{cm} , and f_y was replaced with $f_{s,ACI}$. Eq. (1.10) was then solved for $f_{s,ACI}$, and the test-to-calculated ratio, $f_{su}/f_{s,ACI}$, was used to perform the comparison. To

accurately evaluate the effect of f_{cm} raised to the 0.5 power, the upper limit of 6,000 psi on concrete compressive strength was not applied. Figure 1.24 shows the ratio of test-to-calculated stress $f_{su}/f_{s,ACI}$ versus f_{cm} for 46 specimens with two widely-spaced headed bars without confining reinforcement, and Figure 1.25 shows the same comparison for 35 specimens with two widely-spaced bars with No. 3 hoops spaced at $3d_b$ in the joint region.

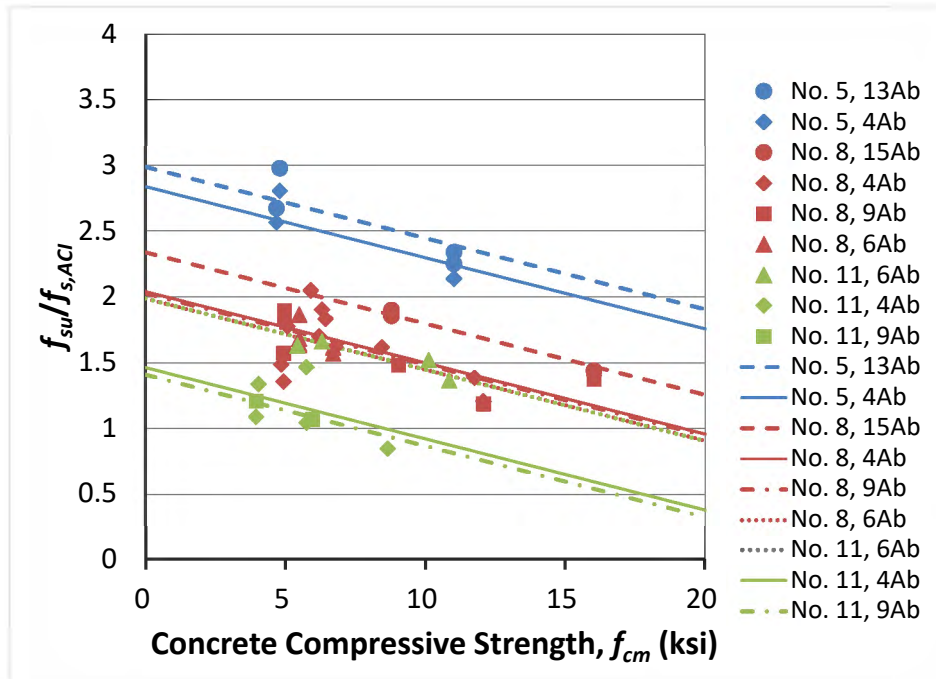


Figure 1.24 Ratio of test-to-calculated stress $f_{su}/f_{s,ACI}$ versus f_{cm} for two widely-spaced headed bars without confining reinforcement, where $f_{s,ACI}$ is based on ACI 318-14 (from Shao et al. 2016)

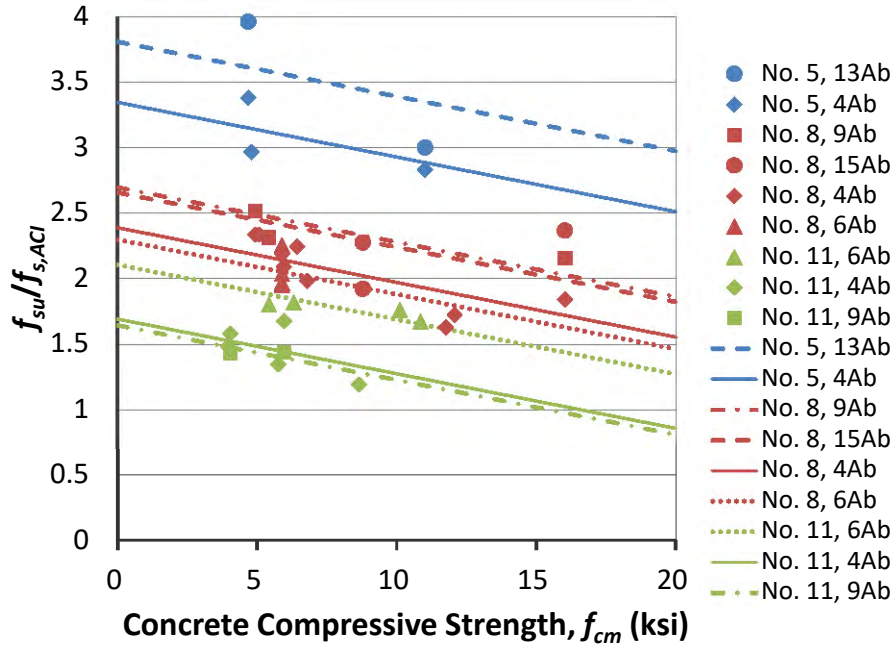


Figure 1.25 Ratio of test-to-calculated stress $f_{su}/f_{s,ACI}$ versus f_{cm} for two widely-spaced headed bars with No. 3 hoops spaced at $3d_b$, where $f_{s,ACI}$ is based on ACI 318-14 (Shao et al. 2016)

In both figures, 1.24 and 1.25, the trend lines have negative slopes, showing the overestimation of the effect of concrete compressive strength to the 0.5 power in the ACI equation. Comparing Figures 1.24 and 1.25 shows that the test-to-calculated ratio $f_{su}/f_{s,ACI}$ values for ACI 318-14 were higher for specimens with confining reinforcement, indicating an improvement in anchorage strength by providing confinement in the joint, a factor not accounted for in the ACI 318-14 provisions. The order of trend lines in both figures reveals that the 1914 Code became less conservative as the bar size increased. With these observations, Shao et al. (2016) concluded that the ACI 318-14 provisions need to be updated for headed bars to include a wider range of material properties and to account for factors such as confining reinforcement.

By converting the descriptive equations, Eq. (1.5) and (1.6), for widely-spaced headed bars (center-to-center spacing $\geq 8d_b$) without confining reinforcement to an equation for development length, ℓ_{dt} , Shao et al. (2016) proposed a new design expression. The expression incorporates the effects of close bar spacing (center-to-center spacing $< 8d_b$), confining reinforcement, and bar location within the member:

$$\ell_{dt} = \left(\frac{f_y \Psi_e \Psi_{cs} \Psi_o}{800 f_c^{0.25}} \right) d_b^{1.5} \quad (1.11)$$

where ℓ_{dt} is the embedment length of headed bar (in.), f_y is the bar yield stress (psi), ψ_e is the coating factor, ψ_{cs} is the confinement and spacing factor, ψ_o is the location factor, f'_c is the concrete compressive strength, and d_b is the bar diameter (in.).

Equation (1.11) is applicable for steel yield strengths up to 120,000 psi and concrete compressive strengths up to 16,000 psi. Equation (1.11) is similar to the proposed equation for hooked bars (Eq. 1.8) in form, with the exceptions of not having the concrete density factor, λ (since headed bars are not currently permitted to be used in lightweight concrete), and in the values of confinement and spacing factor, ψ_{cs} . Like Eq. (1.8), the bar diameter d_b is raised to the 1.5 power and the concrete compressive strength f'_c is raised to the 0.25 power. Table 1.4 gives the values for the confinement and bar spacing factor, ψ_{cs} .

Table 1.4 Values for the confinement and bar spacing factor, ψ_{cs} , as proposed by Shao et al. (2016) for headed bars

Confinement level	f_y (psi)	s	
		$2d_b$	$\geq 8d_b$
$A_{tt}/A_{hs} \geq 0.3$	$\leq 60,000$	0.6	0.4
	120,000	0.7	0.45
None	all	1.0	0.5

In Table 1.4, s is the center-to-center spacing of headed bars, A_{tt} is the effective amount of confining reinforcement in the joint region and is defined as the total cross-sectional area of all the ties parallel to the headed bars within $8d_b$ from the top of the headed bar for No. 8 bars and smaller or within $10d_b$ for No. 9 bars or larger, and A_{hs} is the total cross-sectional area of the headed bars being developed. The maximum limit of 0.3 on A_{tt}/A_{hs} is based on the observation during development of Eq. (1.6) that values of A_{tt}/n above $0.3A_b$ did not contribute to anchorage strength.

The bar location factor, ψ_o , is 1.25 unless the bars are located within the column core (the region inside column longitudinal reinforcement, as shown in Figure 1.26) with side cover ≥ 2.5 in., or in a wall with side cover $\geq 8d_b$, for either of which the factor is 1.0. The value of 1.25 was chosen based on the observations by Shao et al. (2016) that, in general, headed bars located outside the column core had an anchorage strength of about 80% of those within the column core. The value of 1.25 for ψ_o for headed bars matched the findings by Sperry et al. (2015b) for hooked bars.

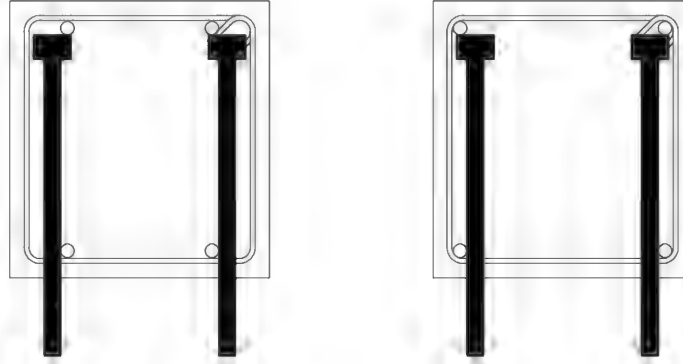


Figure 1.26 Bars located outside (left) or inside (right) of the column core

The expression for calculating the development length of headed bars proposed by Shao et al. (2016) was modified in the ACI 318-19 Code, including retention of $\sqrt{f'_c}$ to represent the contributing of concrete compressive strength rather than incorporating the proposed and more accurate $f_c'^{0.25}$, as shown in Eq. (1.12).

$$\ell_{dt} = \left(\frac{f_y \psi_e \psi_p \psi_o \psi_c}{75 \sqrt{f'_c}} \right) d_b^{1.5} \quad (1.12)$$

where ℓ_{dt} is the embedment length of headed bar (in.), f_y is the bar yield strength (psi), ψ_e is the coating factor, ψ_p is the parallel tie reinforcement factor, ψ_o is the location factor, ψ_c is the concrete strength factor, λ is the concrete density factor, f'_c is the concrete compressive strength, and d_b is the bar diameter (in.). Compared to the ACI 318-14 equation (Eq. 1.10), the current equation has changed significantly. The bar diameter is raised to the 1.5 power (same as for hooked bars), and three new modification factors (ψ_p , ψ_o , and ψ_c) are incorporated. The format of Eq. (1.12) is similar to the expression for development of hooked bars (Eq. 1.9), and the values for modification factors are also the same, as given in Table 1.5.

Table 1.5 Modification factors for headed bars as given in Table 25.4.4.3 of ACI 318-19

Modification Factor	Condition	Value
Parallel tie reinforcement, ψ_p	$A_{tt} \geq 0.3A_{hs}$ or $s^{[1]} \geq 6d_b^{[2]}$	1.0
	Other	1.6
Location, ψ_o	(1) Terminating inside column core with side cover ≥ 2.5 in., or (2) With side cover $\geq 6d_b$	1.0
	Other	1.25
Concrete strength, ψ_c	$f'_c < 6,000$ psi	$f'_c/15,000 + 0.6$
	$f'_c \geq 6,000$ psi	1.0

[1] s is minimum center-to-center spacing of hooked bars

[2] d_b is nominal bar diameter

In Table 1.5, A_{tt} is the total cross-sectional area of ties or stirrups parallel to headed bars within $8d_b$ from the centerline of the headed bars and spaced no greater than $8d_b$, as shown in Figure 1.27, and A_{hs} is the total cross-sectional area of headed bars being developed.

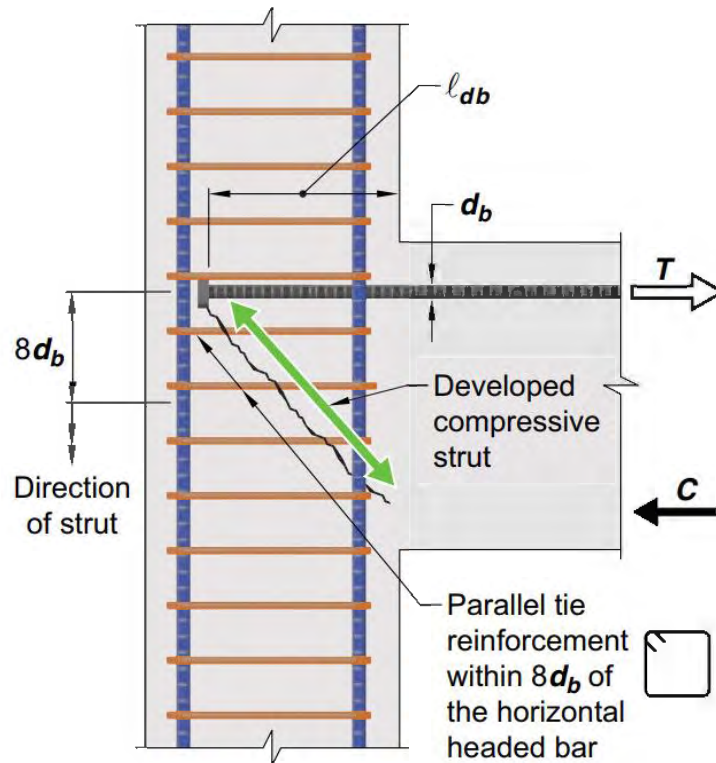


Figure 1.27 Parallel tie reinforcement that contribute to anchorage strength of headed bars as defined in ACI 318-19 (ACI 318-19)

Although the values for confining reinforcement factors for hooked and headed bars (ψ_r and ψ_p , respectively) are the same, the amount of confining reinforcement considered by the Code that contributes to anchorage strength are different. For hooked bars, it should be a minimum of

$0.4A_{hs}$ within $15d_b$ of the centerline of the bars (Figure 1.23), whereas for headed bars it is $0.3A_{hs}$ within $8d_b$ (Figure 1.27). The other difference between the hooked and headed bar equations is the constant multiplier; for hooked bars, it is $1/55=0.018$, whereas for headed bars it is $1/75=0.013$. This indicates that, if all other parameters are equal, headed bars require a shorter development length than hooked bars. The last difference is that, unlike hooked bars, the equation for headed bars does not have a concrete density factor, λ , to account for using lightweight concrete since only the use of normalweight concrete is permitted.

In addition to incorporating the three modification factors discussed above, ACI 318-19 has a few other improvements compared to the ACI 318-14 design provisions for headed bars. The upper limit of 60,000 psi on the bar yield strength is removed (ACI 318-19 currently allows up to 100,000 psi in general). The minimum required clear spacing between the bars has been reduced from $4d_b$ to $2d_b$. Similar to hooked bars, ACI 318-19 stayed with $\sqrt{f'_c}$ rather than incorporating the more accurate $f_c'^{0.25}$ as proposed by Shao et al. (2016), but includes the ψ_c factor to account for the effect of $f_c'^{0.25}$ for $f'_c < 6,000$ psi to prevent excessively long development lengths for lower compressive strengths, as discussed before. The minimum net bearing area of the head A_{brg} is $4A_b$, unchanged from ACI 318-14.

Despite the improvements, the headed bar development length provisions in ACI 318-19 have limitations. The maximum bar size allowed is No. 11 due to a lack of experimental data for larger bars (No. 14 and No. 18), a restriction that is one of the main motivations of the current study. The effect of confining reinforcement and bar spacing, simplified to a binary choice of 1.0 or 1.6 (similar to hooked bars), prevents designers from using values other than 1.6 (that is, shorter development lengths) in cases where the center-to-center bar spacing (s) is less than $6d_b$ and area of parallel ties (A_{tt}) is less than $0.3A_{hs}$. Also, although the concrete compressive strength factor ψ_c , is conservative for concrete compressive strengths below 6,000 psi, as will be shown in Chapter 6, it becomes progressively unconservative as the concrete strength increases from 6,000 to 10,000 psi and makes the development length equations for both hooked and headed bars slightly more complex. If the more accurate $f_c'^{0.25}$ could be used, a more uniform margin of safety would be provided for concrete strengths up to 16,000 psi and there would be no need for a concrete strength modification factor.

1.4 OBJECTIVE AND SCOPE

A comprehensive study has been underway at the University of Kansas since 2012 to investigate the anchorage and development of hooked and headed bars. To date, the study has included up to No. 11 and smaller bars anchored in members with a wide range of material and member properties, including high-strength reinforcing steel and concrete in beam-column joints, lap splices, bars with shallow embedments, and CCT node specimens (Searle et al. 2014, Sperry et al. 2015a, 2015b, 2017a, 2017b, 2018, Yasso et al. 2017, Ajjam et al. 2017, 2018, Shao et al. 2016, Ghimire et al. 2018, 2019a, 2019b). Descriptive equations to calculate the anchorage strength and design provisions for the development length, have been developed that apply to hooked and headed bars with yield strengths up to 120,000 psi and concrete compressive strengths up to 16,000 psi. The findings served as basis for the current design provisions, in ACI 318-19, for the development of hooked and headed bars. There are, however, a number of limitations in the Code provisions. For hooked bars, the provisions in ACI 318-19 give no credit to the contribution of confining reinforcement for hooked bars larger than No. 11. For headed bars, bars larger than No. 11 are not permitted. These limits are mainly due to a lack of experimental data on No. 14 and No. 18 bars. For both hooked and headed bars, $\sqrt{f'_c}$ does not provide an accurate representation of the contribution of concrete compressive strength to the anchorage strength.

The objective of this research is to continue the comprehensive study of the anchorage strength and development of headed reinforcing bars and to expand the available data to include the largest sizes currently permitted in the ACI Building Code, No. 14 and No. 18. The study also includes a limited number of specimens with No. 14 and No. 18 hooked bars to investigate the differences in performance between large hooked and headed bars in external beam-column joints. Test results are compared with anchorage strengths calculated using the descriptive equations developed based on No. 11 and smaller bars and those based on the development length and anchorage provisions in ACI 318-19. The findings are used as a basis for design criteria applicable to No. 14 and No. 18 bars, with the goal of addressing the current Code limitations on both hooked and headed bars.

Forty-two large-scale beam-column joint specimens containing No. 11, No. 14 and No. 18 headed and hooked bars are tested. Of the 42 specimens, 30 contain headed bars and 12 contain hooked bars. The effects of bar size, bar spacing, embedment length, confining transverse

reinforcement in the joint region, side cover, and concrete compressive strength on anchorage strength are investigated.

The 30 specimens containing headed bars include 2 with No. 11, 20 with No. 14, and 8 with No. 18 bars. Of the 20 specimens with No. 14 bars, 13 have two widely-spaced bars (center-to-center spacing $\geq 8d_b$), one has two closely-spaced bars (center-to-center spacing $< 8d_b$), and six have three closely-spaced bars. Of the eight specimens with No. 18 headed bars, four have two widely-spaced bars, two have two closely-spaced bars, and two have three closely-spaced bars. Concrete compressive strength ranges from 5,310 to 16,210 psi. Bar stresses at failure range from 54,900 to 148,300 psi. The center-to-center bar spacing range from $2.7d_b$ to $10.6d_b$. Headed bars from different manufacturers are used with net bearing areas of $4.2A_b$ to $4.4A_b$. The majority of specimens contain ties within the joint, with the total area of tie legs within $10d_b$ from the top of headed bars ranging from $0.178A_{hs}$ to $0.827A_{hs}$, where A_{hs} is the total area of the headed bars being developed. Most specimens have a side cover to the bar of 3.5 in. One No. 14 specimen and four No. 18 specimens have a side cover of 6.5 in.

Of the 12 specimens containing hooked bars, eight contain No. 14 and four contain No. 18 bars. The No. 14 bar specimens include six with two widely-spaced bars and two with three closely-spaced bars. All No. 18 bar specimens have two widely-spaced bars. Bar spacing ranges from $3.5d_b$ to $10.6d_b$. Specimens have concrete compressive strengths ranging from 6,390 to 15,770 psi, and bar stresses at failure range from 87,300 to 130,600 psi. Four No. 14 bar specimens have no confining reinforcement in the joint region. The remaining hooked bar specimens have ties in the joint region ranging from $0.178A_{hs}$ to $0.465A_{hs}$. All specimens have a side cover to the bar of 3.5 in.

CHAPTER 2: EXPERIMENTAL WORK

This chapter describes the details of the experimental work in this study, including the properties of the reinforcing steel (headed and hooked bars, column longitudinal reinforcement and ties) and concrete, specimen design and fabrication, testing apparatus (reaction frame, bearing plates, and load cells), and testing procedure. The testing program is summarized at the end of the chapter.

2.1 MATERIAL PROPERTIES

2.1.1 Hooked and Headed Bars

The hooked and headed bars used in this study were fabricated from No. 11, No. 14, and No. 18 high-strength ASTM A1035 steel. The hooked bars consisted of No. 14 and No. 18 bars with 90° standard hooks, as specified in Table 25.3.1 of the ACI 318-19 (Table 1.1). No. 11, No. 14, and No. 18 headed bars were supplied by three manufacturers. The heads were cold-swaged, taper-threaded, and cold-swaged with a threaded coupling sleeve, as shown in Figure 2.1.

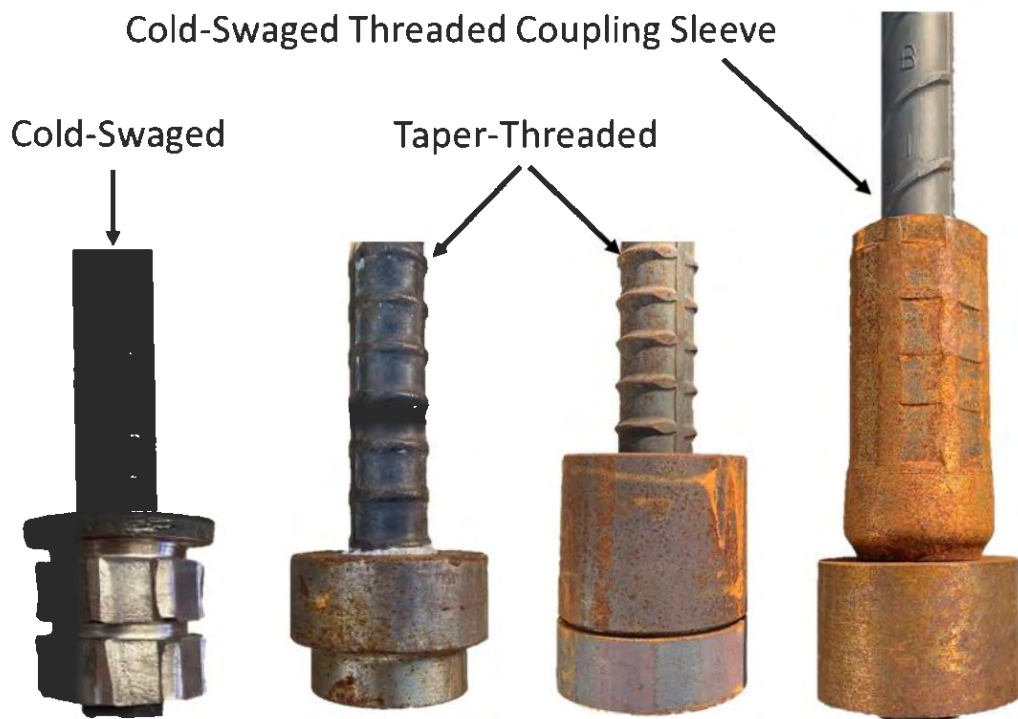





Figure 2.1 Different types of headed bars used in the study

Table 2.1 shows the dimensions of the heads used in this study. Each head has a designation consisting of a letter and a number, representing the head type and the net bearing area,

respectively. The obstruction on the No. 18 headed bar with coupling sleeve (Figure 2.1) was tapered to a smaller diameter adjacent to the head, and this diameter was used when calculating the net bearing area in accordance with ASTM A970-17.

Table 2.1 Dimensions of the headed bars

Head Type	Designation	Bar Size	d_1 (in.)	t_1 (in.)	d_2 (in.)	t_2 (in.)	A_{brg}^1
 Cold-Swaged	B4.2	No. 14	4.125	4.5	-	-	$4.2A_b^2$
 Taper-Threaded	L4.2	No. 14	3.875	2.5	-	-	$4.2A_b$
	H4.4	No. 18	5.25	6.25	-	-	$4.4A_b$
	L4.4	No. 18	5.25	3.25	-	-	$4.4A_b$
 Cold-Swaged Threaded Coupling Sleeve	O4.5	No. 11	3.75	2.125	2.25	6.75	$4.5A_b$
	O4.3	No. 18	6	3.75	3.75	10	$4.3A_b$

¹ Net bearing area

² Nominal area of the bar

2.1.2 Reinforcing Steel Properties

The hooked and headed bars were made of ASTM A1035 Gr. 120 reinforcing steel to ensure that the bars did not fracture prior to bond failure. In all specimens with No. 14 bars, Gr. 60 No. 11 reinforcing bars were used as column longitudinal reinforcement. Due to higher flexural demand in specimens with No. 18 bars, ASTM A615 Gr. 80 or A1035 No. 11 bars were used. For column shear reinforcement outside the joint region, ASTM A615 Gr. 60 No. 4 bars were used in all specimens. For confining reinforcement in the joint region, parallel ties made of ASTM A615 Gr. 60 No. 4 or No. 5 bars were used. Table 2.2 provides the physical properties of hooked and headed bars.

Table 2.2 Physical properties of reinforcing steel

Bar Size	Nominal diameter, d_b (in.)	Type	Yield strength (ksi)	Average rib spacing (in.)	Average rib height (in.)		Average gap width (in.)	Relative rib area ²
					A ¹ (in.)	B ² (in.)		
4 ⁶	0.5	Ties	72.7 ³	–	–	–	–	–
5 ⁶	0.625	Ties	66.7 ³	–	–	–	–	–
11 ⁶	1.41	Long. reinf.	79.6 ³	–	–	–	–	–
11 ⁶	1.41	Long. reinf.	80.4 ⁴	–	–	–	–	–
11 ⁶	1.41	Long. reinf.	120 ⁵	–	–	–	–	–
11	1.41	Head, O4.5	135 ⁵	0.838	0.097	0.092	0.394	0.099
14	1.693	Hook	127 ⁵	1.006	0.079	0.070	0.279	0.062
		Head, B4.2	127 ⁵	1.006	0.079	0.070	0.279	0.062
		Head, L4.2	127 ⁵	1.006	0.079	0.070	0.279	0.062
18	2.257	Hook	131 ⁵	1.449	0.121	0.117	0.312	0.074
		Head, H4.4	136 ⁵	1.502	0.144	0.130	0.316	0.078
		Head, L4.4	131 ⁵	1.449	0.121	0.117	0.312	0.074
		Head, O4.3	131 ⁵	1.449	0.121	0.117	0.312	0.074

¹ Per ASTM A615, A1035² Per ACI 408R- 3³ ASTM A615 Gr. 60⁴ ASTM A615 Gr. 80⁵ ASTM A1035 Gr. 120⁶ Rib area data not obtained

2.1.3 Concrete Properties

The specimens were cast with non-air-entrained ready-mix concrete with the mixture proportions given in Table 2.3. Different high-range polycarboxylate-based water reducers were used in the normal- and high-strength mixtures. The specific gravity (SG) for cementitious materials and the bulk saturated surface dry specific gravity BSG (SSD) for fine and coarse aggregates are also given in Table 2.3. The nominal maximum aggregate size was $\frac{3}{4}$ in. for all mixtures.

Table 2.3 Concrete mixture proportions

Material	Quantity (SSD)				SG or BSG (SSD)
	5,000 psi $w/c = 0.44$	12,000 psi $w/c = 0.26$	15,000 psi $w/cm = 0.21$	16,000 psi $w/cm = 0.21$	
Type I/II Cement, lb/yd ³	600	880	800	498	3.2
Type C Fly Ash, lb/yd ³	-	-	200	-	2.3
Slag Cement, lb/yd ³	-	-	-	373	2.9
Silica Fume lb/yd ³	-	-	-	25	2.2
Water, lb/yd ³	263	228	210	188	1.0
Kansas River Sand, lb/yd ³	1396	1517	1430	1214	2.63
Crushed Limestone, lb/yd ³	1735	-	-	-	2.59
Granite, lb/yd ³	-	1517	1430	1792	2.61
High-range Water Reducer (superplasticizer), oz (US)	40 ¹	44 ¹	147 ²	44 ¹ + 218 ³	-
Viscosity Modifier (VMAR), oz (US)	-	-	20	54	-
Set Retarder ⁴ , oz (US)	12	-	-	27	-

¹ ADVA® 140M² ADVA® Cast 575³ ADVA® Cast 600⁴ DARATARD®

2.2 TEST SPECIMENS

2.2.1 Specimen Design

The specimens represent exterior beam-column joints without casting the beam, similar to those used in previous studies beginning with the work of Marques and Jirsa (1975) and the studies at the University of Kansas by Searle et al. (2014), Sperry et al. (2015a, 2015b), Ajaam et al. (2017), Yasso et al. (2017), Shao et al. (2016). The top longitudinal reinforcement of the simulated beam is represented by the headed or hooked bars embedded in the column, and the compression region of the virtual beam is simulated by the bearing member below the test bars. Figures 2.2 and 2.3 show a schematic of the specimens with hooked and headed bars, respectively. As shown in the figures, a tensile force (T) was applied to hooked and headed bars during the test, and a compressive force (C) was applied through the bearing member below the test bars. The tensile and compressive forces, T and C , represent the forces at the face of the column due to the application of a negative bending moment by the beam.

The embedment length (ℓ_{eh} in Figures 2.2 and 2.3) was calculated based using the descriptive equations for hooked and headed bars, Eq. (1.1) and (1.2), and (1.3) and (1.4), respectively, to achieve a target bar stress so that the anchorage failure would occur prior to

fracture of the test bars. For hooked bars, the embedment length is the distance from the back of the hook to the front face of the column. For headed bars, the embedment length is defined as the distance from the bearing face of the head to the front face of the column. Because the bars were placed to provide the maximum embedment length, the depth of the column, h , equaled the sum of embedment length, head thickness, and cover to back of the head (3.5 in.) for headed bars, and the sum of embedment length and cover to the back of the hook (2 in.) for hooked bars. The column width, b , equaled the sum of out-to-out spacing of test bars and two times the side cover to the bar (3.5 in. for the majority of specimens).

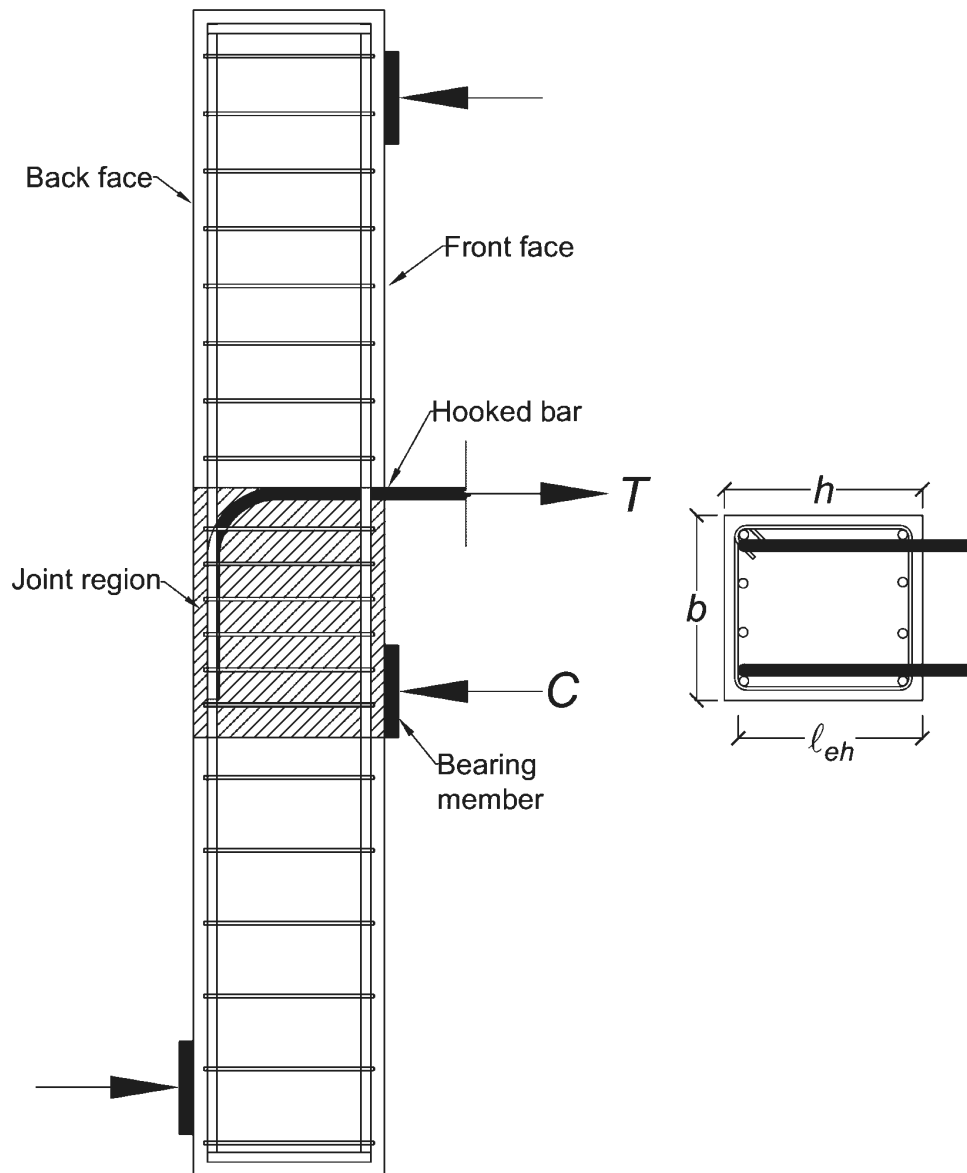


Figure 2.2 Schematic of the specimens with hooked bars, side view (left) and top view (right)

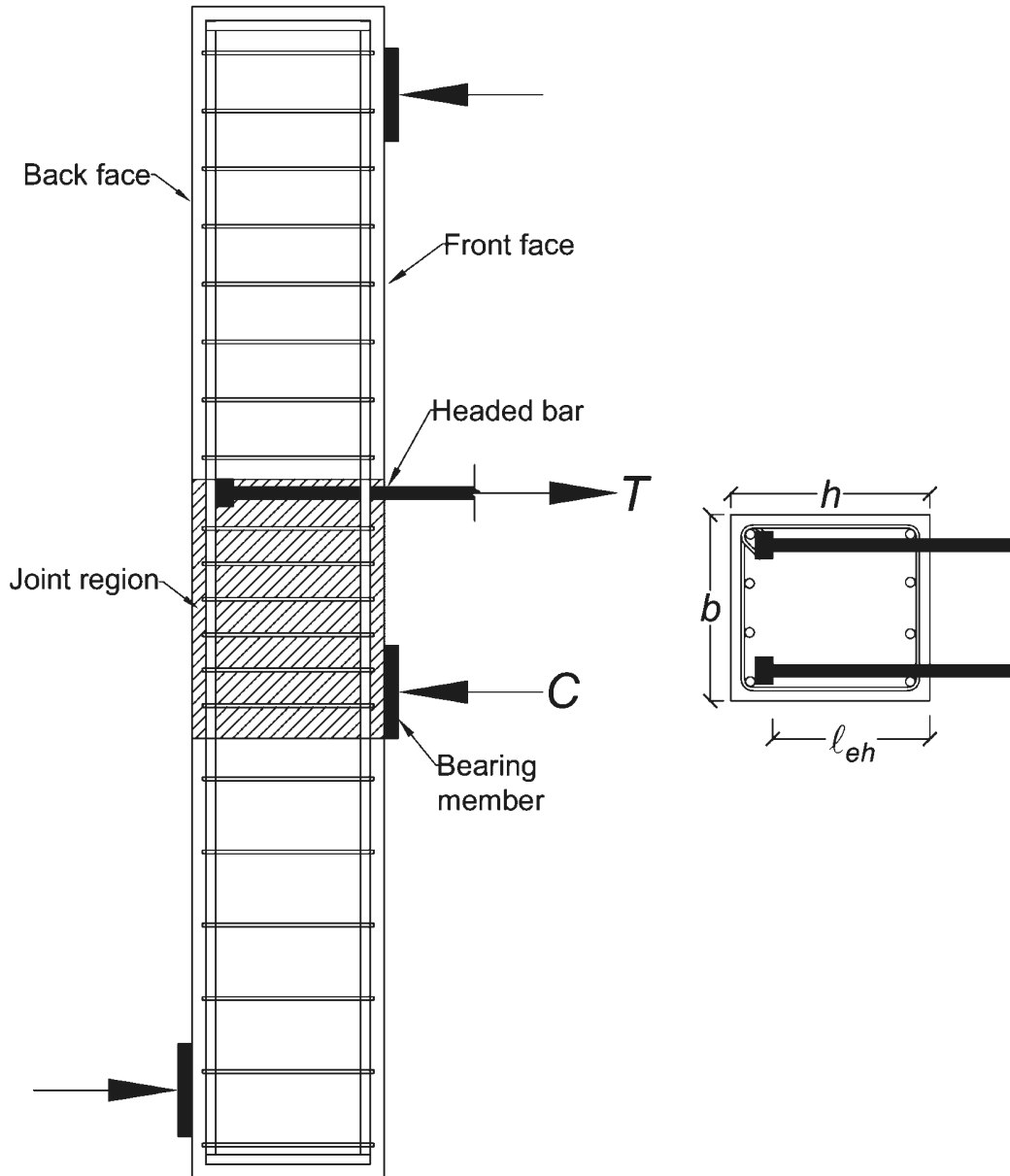


Figure 2.3 Schematic of the specimens with headed bars, side view (left) and top view (right)

The specimen simulated an exterior beam-column joint in a building located halfway between two inflection points. In most cases, load was applied so that the column moment demands above and below the joint were equal and the shear force within the joint region was 80% of the force applied to the hooked or headed bars. In other cases, the joint shear was reduced to about 69% of the force applied to the hooked or bars. Loading conditions are described in detail in Section 2.3.1. The specimens had the proportions shown in Figure 2.4. The dimension x_{mid} was 28.6 and 38.2 in. for specimens with No. 14 and No. 18 bars, respectively. The total height of the column, h_0 , was 14 ft and 18 ft for specimens with No. 14 and No. 18 bars, respectively.

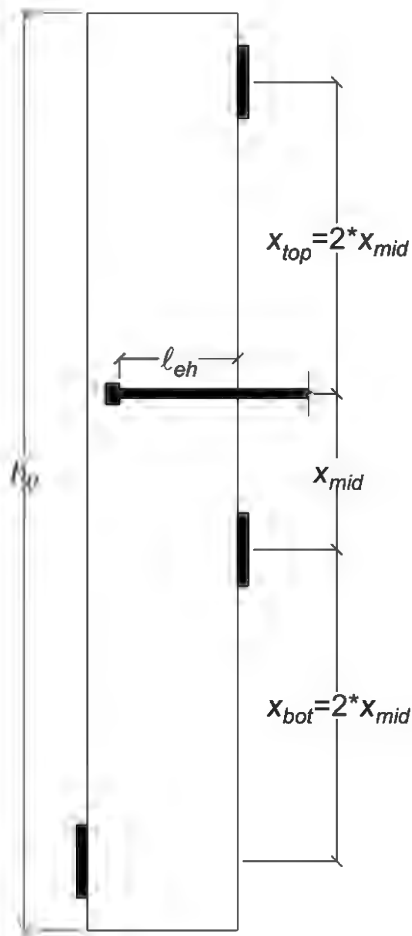


Figure 2.4 Dimensional proportions of the specimens; For specimens with No. 14 bar, $x_{mid} = 28.56$ in. and $h_0 = 14$ ft, and for specimens with No. 18 bar, $x_{mid} = 38.15$ in. and $h_0 = 18$ ft

The quantity of confining reinforcement in the form of ties parallel to the hooked or headed bars within the joint region (number, configuration, and spacing of ties) was one of the test parameters, as described in Section 2.2.2. Outside of the joint region, longitudinal and transverse reinforcement was designed to resist the flexural and shear demands on the column without yielding¹. The design was based on the assumption that all test bars reached the expected anchorage failure stress simultaneously. No axial force was applied because it has been shown to have a negligible effect on anchorage strength (Marquez and Jirsa, 1975, Sperry et al. 2015b).

¹ The contribution of concrete to shear, v_c , was taken as $2bd\sqrt{f'_c}$

2.2.2 Test Parameters

As discussed in Chapter 1, this study investigates the effects on anchorage strength of headed and hooked bars of bar size, number and spacing of bars, concrete compressive strength, embedment length, confining reinforcement within the joint region, and side cover to the bars, as follows:

Bar Size: No. 14 and No. 18 hooked bars; No. 11, No. 14 and No. 18 headed bars.

Number and spacing of bars: The majority of the specimens (32 out of 42) had two hooked or headed bars, and the remaining specimens contained three bars. Of the 32 specimens with two test bars, 29 specimens had widely-spaced bars (ranging from 8.0 to $10.6d_b$ on-center) and 3 specimens had closely-spaced bars ($5.3d_b$ to $7.1d_b$ on-center). All 10 specimens containing three bars had closely-spaced bars, with center-to-center spacing ranging from 2.7 to $3.5d_b$ on-center. Specimens with two widely-spaced bars had a center-to-center bar spacing of 18 in. Specimens with two closely-spaced bars had bars spaced at 12 in. on-center. Center-to-center spacing of bars in specimens with three closely-spaced bars was 6 in.

Concrete compressive strength: The concrete mix designs used (Table 2.3) had target compressive strengths of 5,000, 12,000, 15,000, and 16,000 psi. The measured concrete compressive strength (f_{cm}) ranged from 5,310 to 16,210 psi for the headed bar specimens and from 6,390 to 15,770 psi for the hooked bar specimens.

Embedment length: Nominal embedment lengths of 26.6 and 35.8 in. were used for the No. 14 hooked bars and 27.8 and 37.8 in. for the No. 18 hooked bars. A nominal embedment length of 18.5 in. was used for the No. 11 headed bars and ranged from 20.5 to 31.9 in. for the No. 14 headed bars and from 27.8 to 31.1 in. for the No. 18 headed bars.

Confining reinforcement within the joint region: The majority of specimens had confining reinforcement within the joint region in the form of No. 4 or No. 5 ties parallel to the hooked or headed bars. For the No. 14 hooked bar specimens, the ratio of confining reinforcement (total area of tie legs within $9.5d_b$ from the centerline of test bars, as shown in Figure 1.18) to the total cross-sectional area of the bars being developed, A_{th}/A_{hs} , ranged from 0 to 0.28. For the No. 18 hooked bar specimens, A_{th}/A_{hs} ranged from 0.23 and 0.47. For the No. 14 headed bar specimens, A_{th}/A_{hs} ranged from 0 to 0.83. For the No. 18 headed bar specimens, ranged from 0.23 to 0.54. Most of the No. 4 or No. 5 ties had two legs. Three specimens had double overlapping No. 5 ties (four legs, two internal legs and two external legs), as shown in Figure 2.5, to investigate the effect of having

middle legs within the joint. Three specimens had double No. 5 ties, which consisted of two single ties placed adjacent to each other (four external legs).

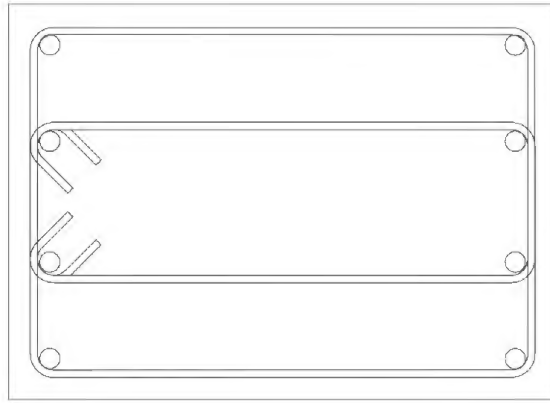


Figure 2.5 Double overlapping tie configuration

Side cover to the bars: Most specimens had side cover to the hooked or headed bars of 3.5 in. One No. 14 and four No. 18 headed bar specimens had a side cover of 6.5 in.

2.2.3 Specimen Designation

Each specimen has a designation denoting the design variables and parameters. For example, the designation shown in Figure 2.6 indicates a specimen containing two No. 14 headed bars with B4.9 heads (refer to Table 2.1) spaced at $10.6d_b$ on-center, cast in concrete with a nominal strength of 15 ksi concrete, and having a total of five No. 4 ties within the joint region. The headed bars were placed inside the column core, with a nominal side cover to the bar (c_{so}) and back cover to the head (c_{bc}) of 3.5 in., and a nominal embedment length (ℓ_{eh}) of 20.6 in. The confining reinforcement designation is removed from specimens without ties within the joint region. For the hooked bar specimens, the head type designation is removed, and the back cover is the cover to the back of the hook.

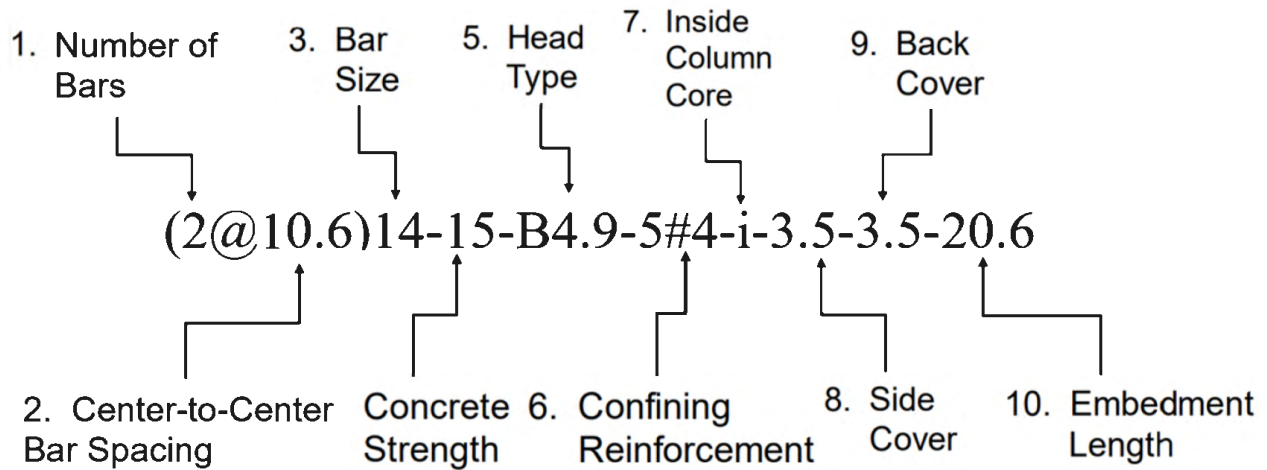


Figure 2.6 Example specimen designation

The cross-sectional dimensions of a typical headed bar specimen with variable callouts are shown in Figure 2.7.

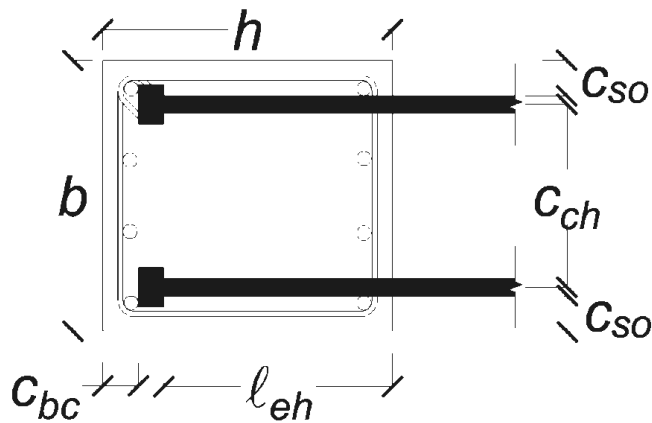


Figure 2.7 Cross-sectional dimensions and variable callouts of specimens

2.2.4 Specimen Fabrication

The formwork for the columns was fabricated using 2×4 dimension lumber and $\frac{3}{4}$ -in. plywood. The lower half of the formwork was braced with clamps consisting of 2×6 dimension lumber and all-thread rods to provide resistance against the lateral hydrostatic pressure of the fresh concrete during concrete placement. Reinforcement cages (steel cages) were built according to the specimen design, with No. 4 or No. 5 ties bent to the specified dimensions and tied to the No. 11 longitudinal reinforcing bars at the designated spacing. The clear cover to the No. 11 longitudinal bars was 2 in. in all specimens, maintained using 2-in. steel chairs that were tied to the reinforcement cages to maintain the side and back cover during casting. After the steel cages were

placed in the formwork, the headed or hooked bars were tied into the steel cage at the desired spacing and height in the column. The No. 14 bar specimens, with a height of 14 ft, were cast vertically, and large sawhorses were built and placed under the test bars to hold them level. The No. 18 bar specimens, with a height of 18 ft, were cast horizontally to ease concrete placement, and a wooden frame was built and bolted/screwed to the form to hold the test bars level vertically. Continuous bracing consisting of 2×6 lumber and all-thread rods was used to resist the lateral pressure of fresh concrete.

The vertical formwork for No. 14 bar specimens and the large sawhorses to hold the test bars is shown in Figure 2.8. The formwork bracing system used for No. 14 bar specimens is shown in Figure 2.9. The horizontal formwork for No. 18 bar specimens is shown in Figure 2.10. A typical reinforcement cage with steel chairs tied to the cage is shown in Figure 2.11. Cages with No. 14 headed and hooked bars tied to the vertical steel cage are shown in Figure 2.12. No. 18 headed and hooked bars tied to the horizontal steel cage are shown in Figure 2.13.

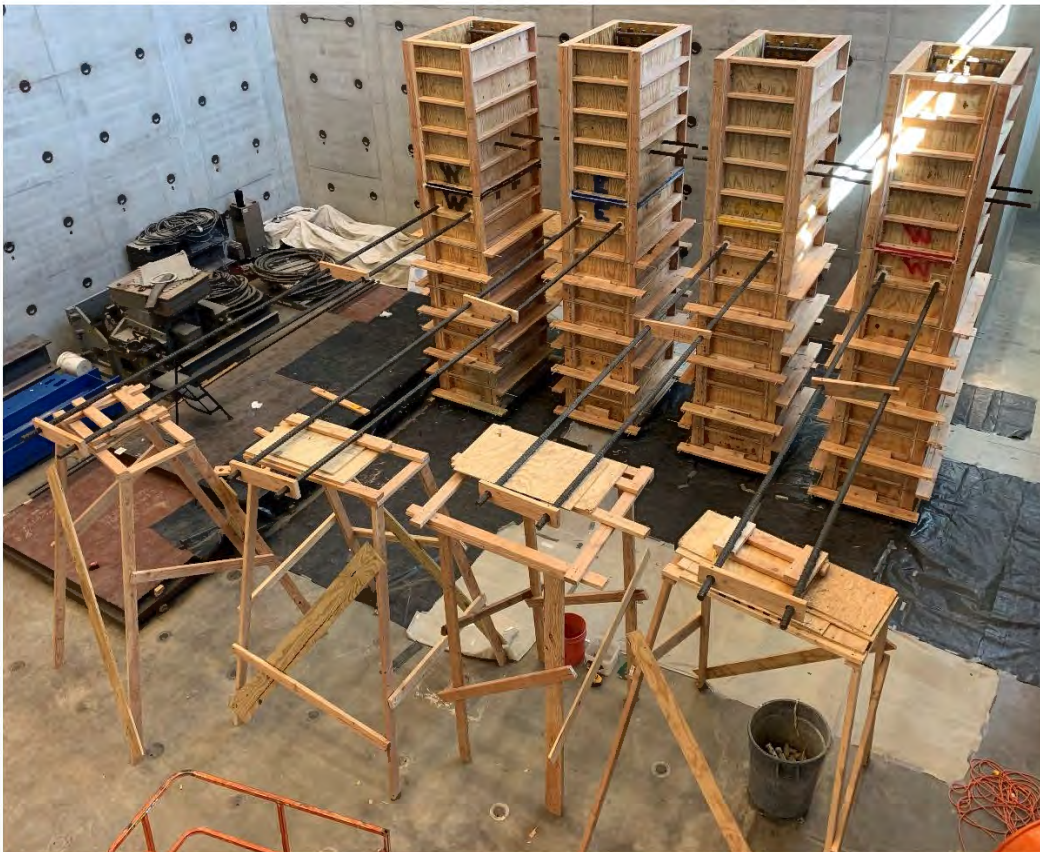


Figure 2.8 Vertical formwork for No. 14 bar specimens and sawhorses to hold the bars



Figure 2.9 Clamping system to brace the vertical forms for No. 14 bar specimens



Figure 2.10 Horizontal formwork for No. 18 bar specimens

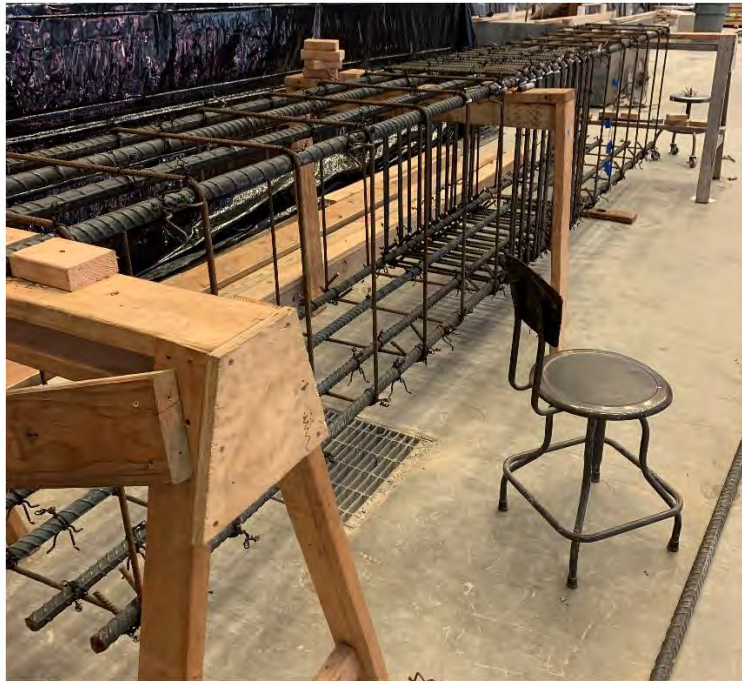


Figure 2.11 A typical reinforcement cage (steel cage)



Figure 2.12 No. 14 hooked (left) and headed (right) bars tied to steel cages



Figure 2.13 No. 18 hooked (left) and headed (right) bars tied to steel cages

2.2.5 Specimen Instrumentation

In all specimens, strain gauges were installed on the first two ties above the joint region, some ties within the joint region, column longitudinal bars, and the headed or hooked bars to monitor the change in strain during the test. As shown in Figure 2.14, the strain gauges were attached to one headed or hooked bar and on the ties on one side of the specimen. In specimens with three test bars, strain gauges were attached to the middle bar in addition to one side bar. Two strain gauges were installed on the test bars. On headed bars, one gauge was placed 1.5 in. from the bearing face of the head (labeled T1) and the second gauge 1 in. from the column front face (labeled T2). On the hooked bars, one gauge was mounted just before the bend in the tail of the bar (labeled T1), and the second gauge 1 in. from the front face of the column (labeled T2). In all specimens, strain gauges were mounted on the first two ties above the joint region (labeled S1 and S2, with S2 being the closest to the test bar), and on the ties within the joint region, starting with S3. On the longitudinal column bars, one gauge was mounted on a corner bar (labeled L1) and the other gauge on an adjacent bar (labeled L2). Gauges L1 and L2 were installed at the location of headed or hooked bars along the length of the column bars.

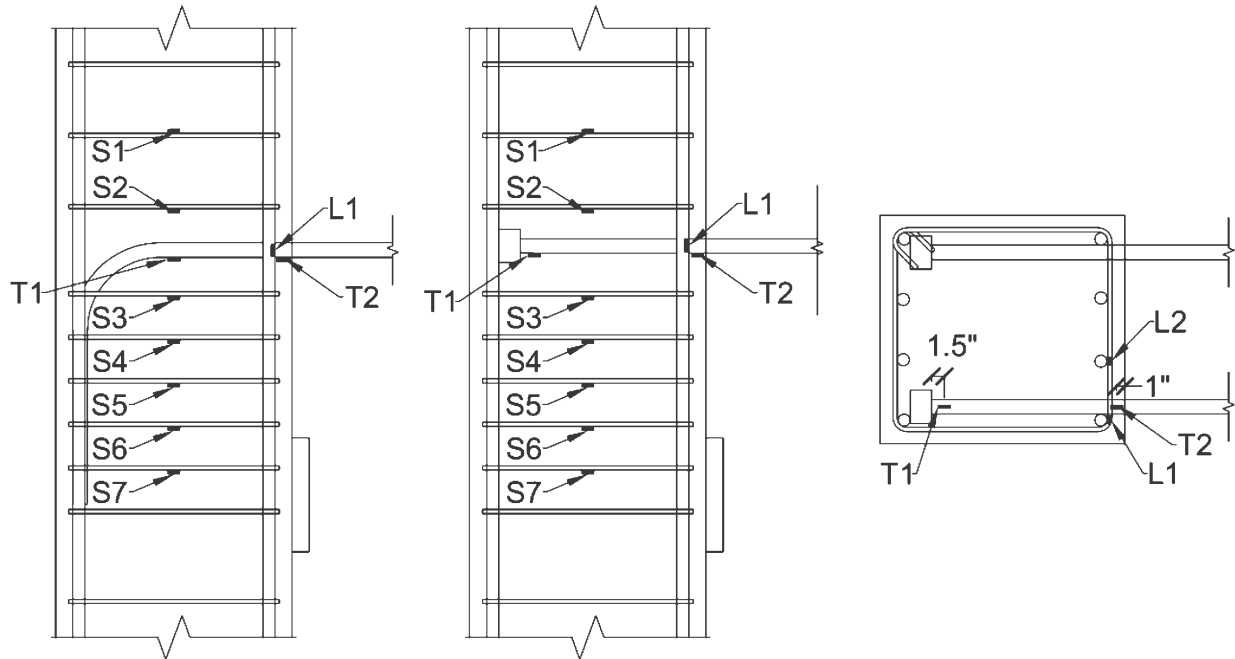


Figure 2.14 Side view (left and middle) and top view (right) of strain gauge locations

2.3 TESTING APPARATUS

2.3.1 Loading Conditions

The specimens were tested in the horizontal position. The forces applied to the specimens by the reaction frame (described in Section 2.3.2) during the test are shown in Figure 2.15. The upward force T was applied to the test bars using hydraulic jacks. The two downward compressive forces, C_1 and C_2 , were applied through bearing plates by bearing members of the reaction frame, and the upward compressive force C_3 was applied through a “lower tension member,” which consisted of two instrumented threaded rods – in some cases the force using a hydraulic jack and in some cases the force was due to the reaction induced in the rods, as explained next.

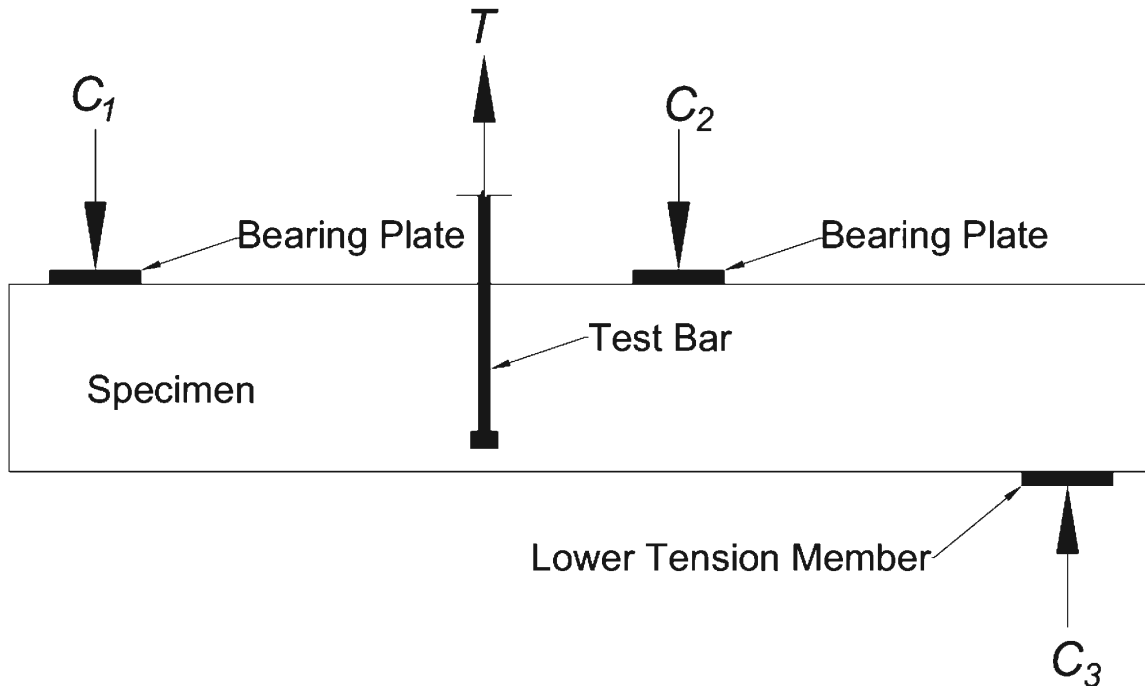


Figure 2.15 Forces applied to specimens by the reaction frame during the test

Two loading conditions were considered by testing the specimens with or without a hydraulic jack applying a load to the lower tension member:

Loading Condition A – Midheight between inflection points: In this loading condition, the specimen was tested with a hydraulic jack applying a load to the lower tension member equal to one-fifth the load applied to the hooked or headed bars, resulting in equal column moments above and below the joint and a shear force within the joint region was 80% of the force applied to the test bars. This loading condition simulates the forces in an exterior beam-column joint with the beam located at the midheight of the column between inflection points.

Loading Condition B – Anchorage only: In this loading condition, the specimen was tested without using a hydraulic jack to apply load to the lower tension member. In this case, the only load applied via the lower tension member, which was always in place and tightened, was due to the strain induced in the member due to deflection of the column as load was applied to the hooked or headed bars. Previous tests on No. 5, No. 8, and No. 11 hooked and headed bar specimens were based on this configuration (refer to Figures 1.5 and 1.14). Without the hydraulic jack applying load to the lower tension member, the force C_3 was approximately $0.04T$ (based on strain gage measurements), and the joint shear was reduced to about 69% of the force applied to the hooked or bars.

Table 2.4 summarizes the values of forces applied to the specimen for the two loading conditions. All 12 hooked bar specimens were tested under loading condition A. Of the 20 specimens containing No. 14 headed bars, nine were tested under loading condition A and 11 under loading condition B. Of the eight specimens with No. 18 headed bars, six were tested under loading condition A, and two under loading condition B.

Table 2.4 Values of forces applied to the specimens under the two loading conditions

Force	Loading Condition A ^[1]	Loading Condition B ^[2]
$C_1^{[3]}$	$0.2T$	$\approx 0.31T$
$C_2^{[3]}$	$T^{[6]}$	$\approx 0.73T$
$C_3^{[4]}$	$0.2T$	$\approx 0.04T$
$V_J^{[5]}$	$0.8T$	$\approx 0.69T$

^[1] Midheight between inflection points, test with the lower tension member

^[2] Anchorage only, test without hydraulic jack applying a load to lower tension member

^[3] Downward compressive forces applied by the bearing members

^[4] Upward compressive force applied by the lower tension member

^[5] Shear force in the joint region

^[6] Total force applied to the hooked or headed bars

2.3.2 Reaction Frame

The loading frame is a larger version of the system used by Shao et al. (2016) (Figure 1.14). The loading frame can apply loads up to 1620 kips and allows for a single row of two or three bars, as well as two rows of two or three bars, to be tested simultaneously. The frame can be modified to test specimens with No. 11, No. 14, or No. 18 bars. Side and end-elevation views of the reaction frame for No. 14 bar test setup are shown in Figure 2.16 and 2.17, respectively. The components of the test frame are described next.

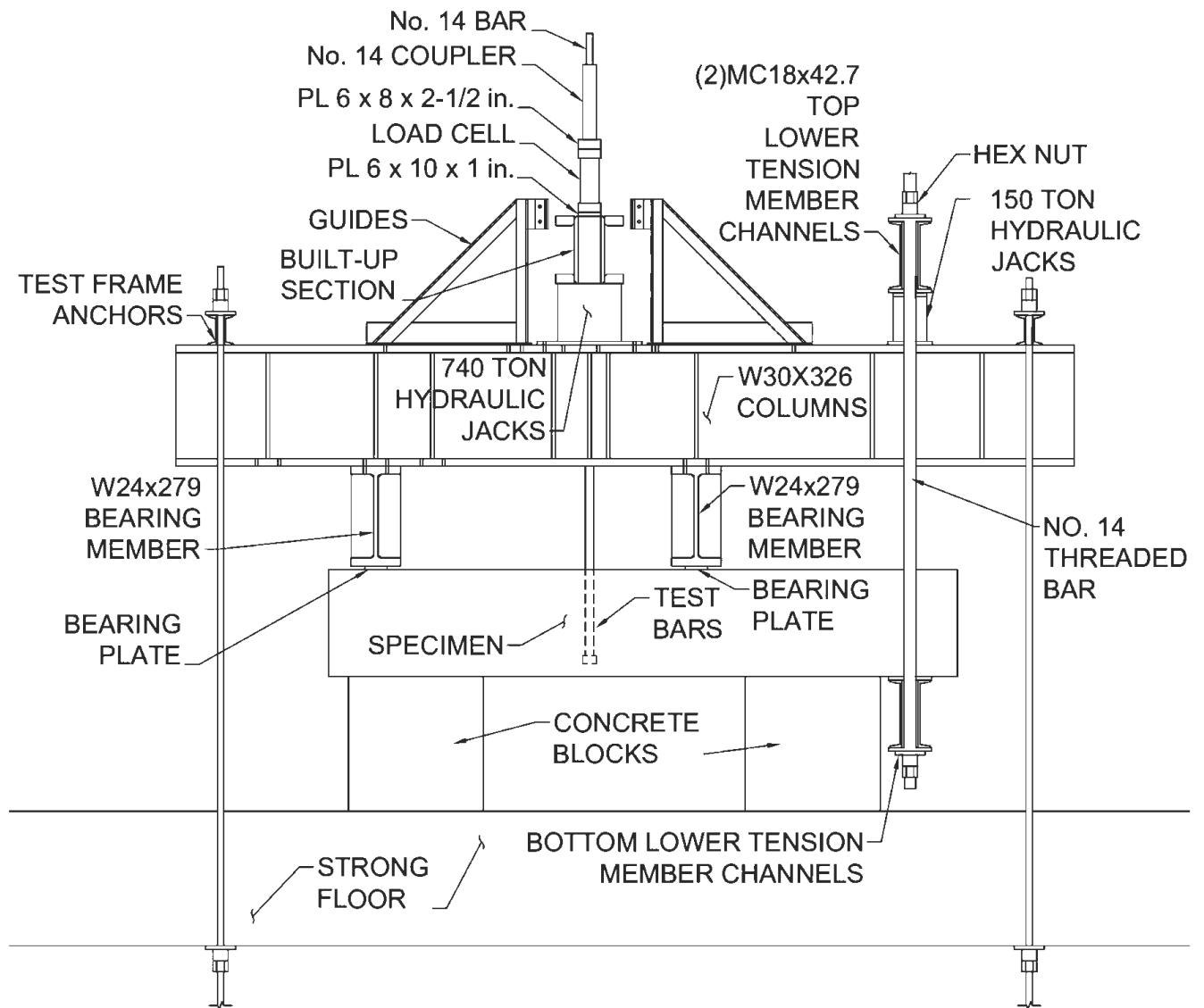


Figure 2.16 Side elevation of the reaction frame for the No. 14 bar setup

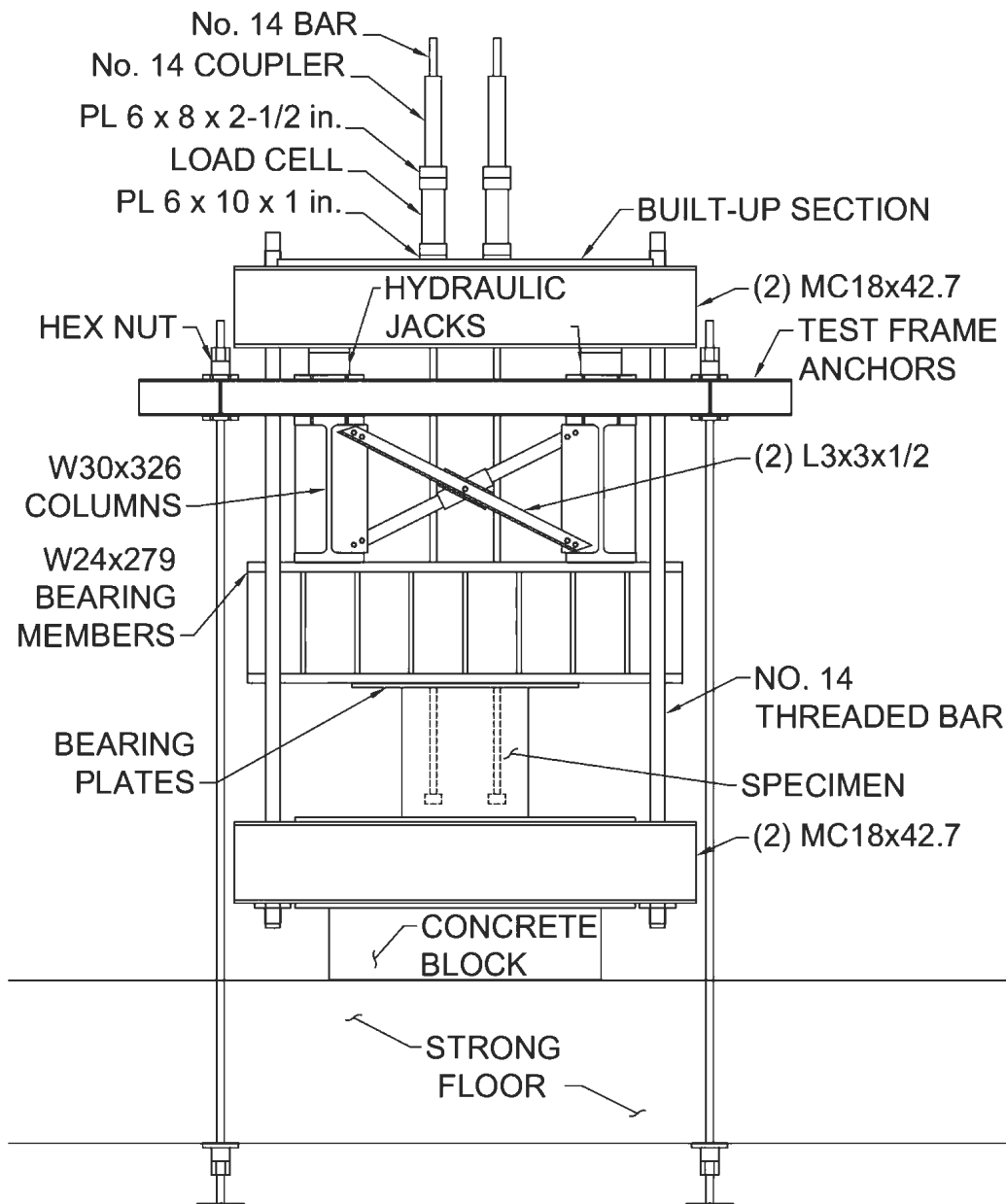


Figure 2.17 End-elevation of the reaction frame for the No. 14 bar setup

For the test, the specimens were placed horizontally on two $3 \times 3 \times 5$ ft concrete blocks with the hooked or headed bars oriented upward, as shown in Figure 2.18. The concrete blocks were cast with the 15,000-psi concrete and were placed so as to avoid applying any load near the tail of the hook. $6 \times 1 \times 36$ -in. steel plates were placed on the concrete blocks and leveled using hydrostone to provide a level surface to support the specimens.



Figure 2.18 The reaction frame (No. 14 bar setup) and applied forces

The two downward compressive forces, C_1 and C_2 , shown in Figure 2.18, were applied by two $W24 \times 279$ bearing members as the load T was applied to the hooked or headed bars anchored in the column. The distances between the downward compressive forces and the hooked/headed bars are shown in Figure 2.4.

The upward compressive force C_3 shown in Figure 2.18 was applied through the lower tension member, using two 150-ton jacks when active (loading condition A, as described in Section 2.3.1). The 150-ton jacks were bolted to the top of each $W30 \times 326$ column. As shown in Figure 2.16, the lower tension member consisted of two sets of two $MC18 \times 42.7$ channels, the two 150-ton hydraulic jacks, and the two No. 14 threaded bar. As shown in Figures 2.16 and 2.18, one set of channels was placed on top of the two 150-ton jacks (across the jacks), and the other set of channels was placed in contact with the back face of the specimens. The No. 14 threaded rods connected the two sets of channels. Strain gauges were installed on these rods to track the force in the lower tension member during the test.

The force on the test bars, T , was applied by two 740-ton hydraulic jacks using an electric hydraulic pump. As shown in Figure 2.16, the jacks were bolted to horizontal W30×326 “columns,” and a built-up section was placed across the jacks, as shown in Figure 2.17. The W30 × 326 columns were bolted to the top of the bearing members, which have a center-to-center spacing of 60 in. that allows for all possible spacings of test bars. The built-up section consists of 1 and 2.5 in. steel plates welded together, and has rectangular openings spaced at 6 in. on-center for the test bars to pass through. The 6 in. spacing between the openings allows for testing specimens with two or three test bars spaced at 6, 12, or 18 in. on-center. As shown in Figure 2.16, two triangular-shaped bracing members were bolted on top of W30 × 326 columns to act as guides for positioning the built-up section prior to testing. The built-up section is shown in Figure 2.19.

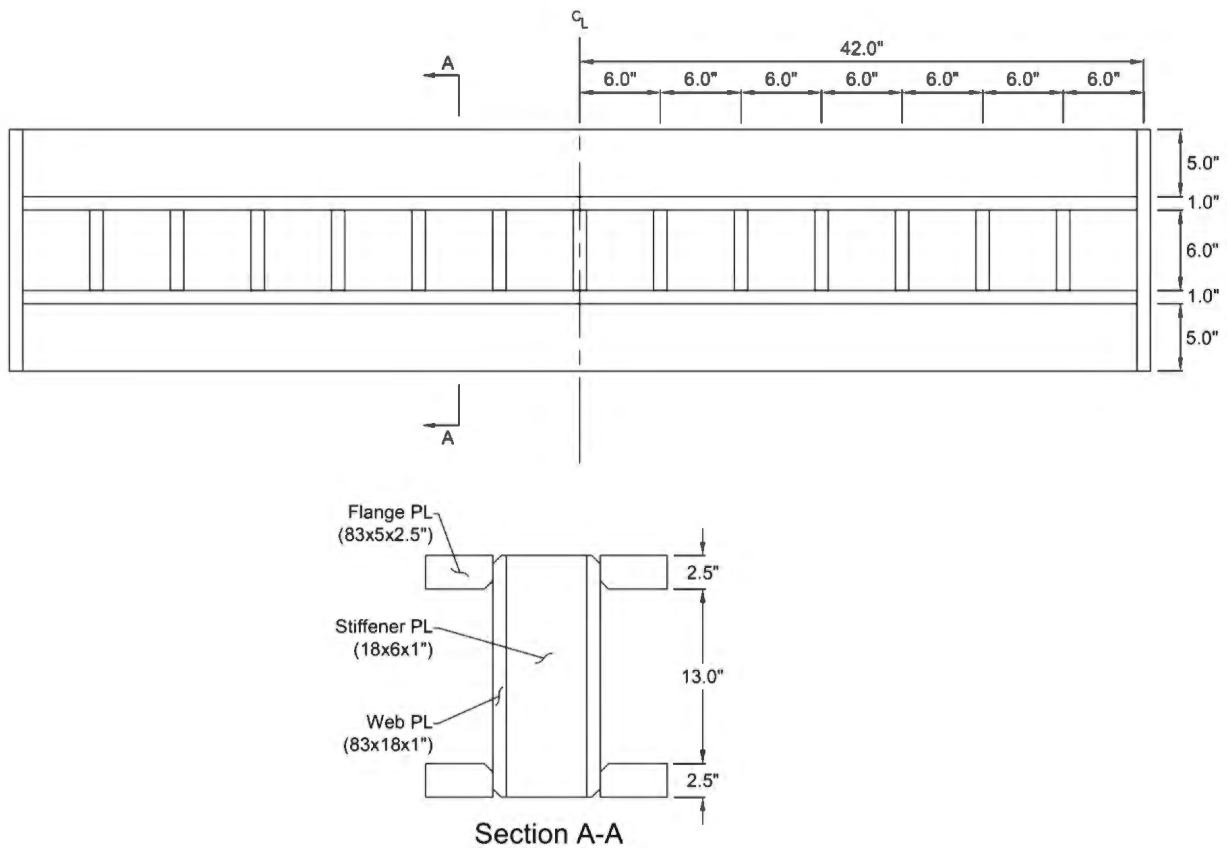


Figure 2.19 Plan view and cross-section of the built-up section

As shown in Figure 2.20 for No. 14 bars, the test bars passed through cylindrical load cells used to measure the applied force on each. A 1-in. thick washer plate was placed under each load cell to transfer the forces to the built-up section. The test bars were gripped at the top using mechanical reinforcing bar couplers. A 2.5-in. thick plate was placed between the couplers and the

load cells. As shown in Figures 2.16 and 2.18, the reaction frame was anchored to the strong floor at all four corners using test frame anchors consisting of C-channels and No. 14 threaded bars. The test frame anchors did not apply any force to the specimen during the test.

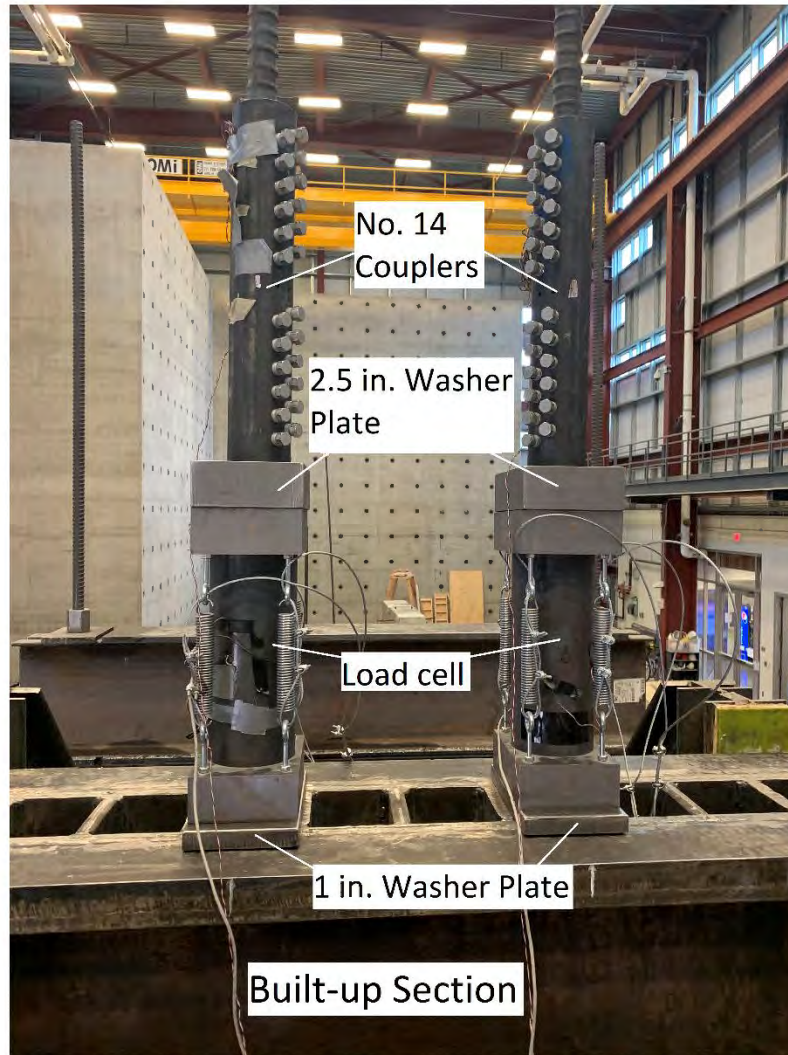


Figure 2.20 Load cells, washer plates, and couplers for No. 14 bar test setup

The test setup shown in Figures 2.16 and 2.18 was used in all No. 14 bar specimens and closely-spaced No. 18 bar specimens. For the widely-spaced No. 18 bar specimens (four specimens with headed bars and four with hooked bars), an alternative configuration was used in which hollow 434-ton jacks were used instead of the 740-ton jacks to apply the force directly to the bars. The alternative test setup is shown in Figure 2.21. In this case as shown in the figure, the built-up section was placed directly on top and across the two W30 × 326 columns. No guides were used for the built-up section in this setup. New 1-in. thick washer plates were placed below and above the hollow jacks to transfer the forces to the built-up section and load cells, respectively. The

dimensions of the new washer plates were chosen to cover the entire area of the bottom of the jacks and the jack pistons at the top. The load cells and couplers in the original test setup were used. The alternative setup, shown in Figure 2.21, was used to test the two No. 11 headed bar specimens in which 150-ton jacks were used in place of the 434-ton jacks and collars with wedges were used instead of couplers as the gripping system.

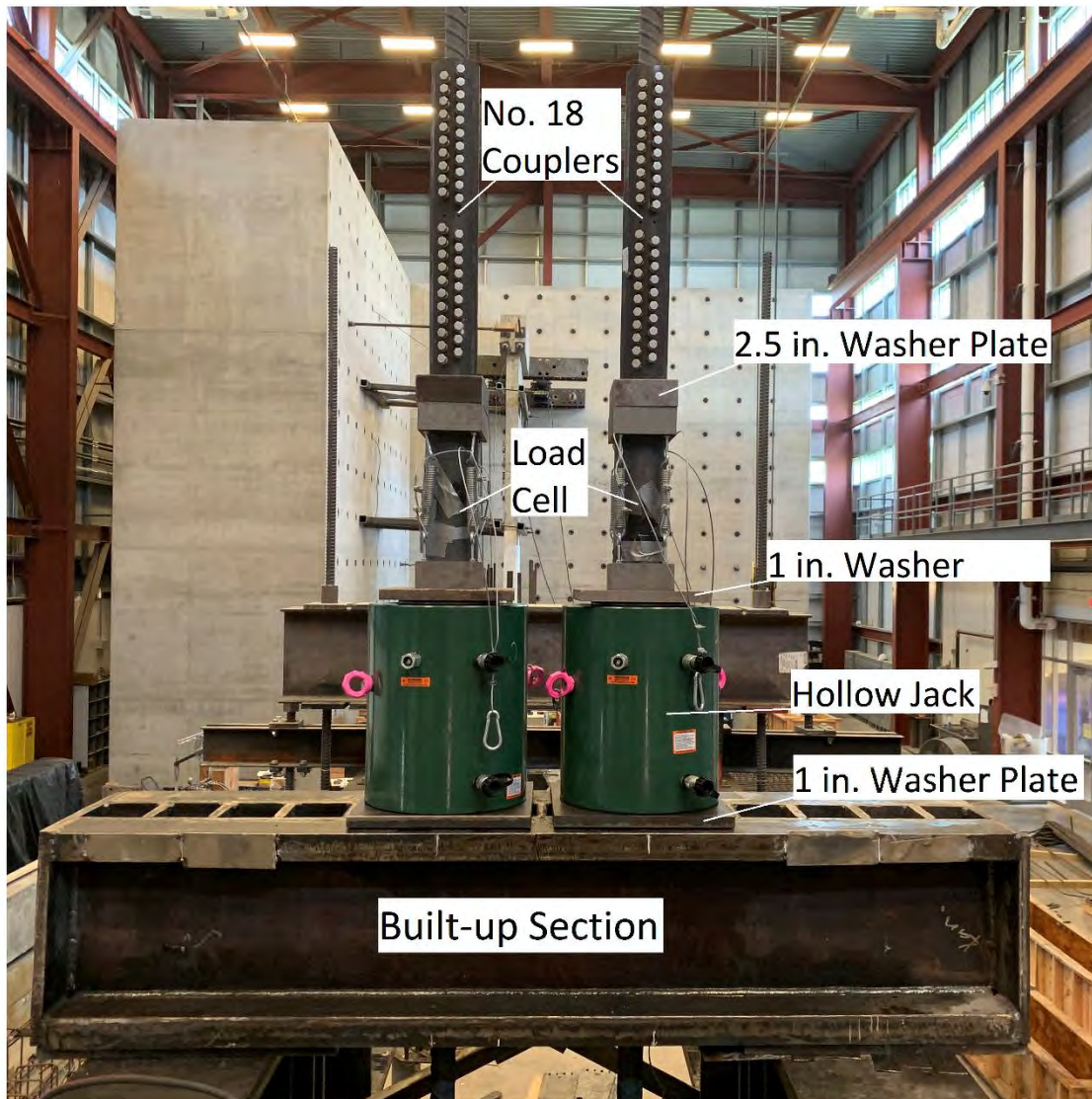


Figure 2.21 Alternative test setup used in widely-spaced No. 18 bar specimens

2.3.3 Bearing Plates

To represent the compression region a beam at the face of a column with depth of the neutral axis c , 1-in. thick by 48-in. long steel plates were placed between the specimen and each of the two $W24 \times 279$ bearing members, as shown in Figure 2.16. Plates with 6, 9, and 12 in.

widths were used when the calculated neutral axis depth was $c \leq 6$ in., $6 \text{ in.} < c \leq 9$ in., and $9 \text{ in.} < c \leq 12$ in., respectively. Based on the dimensional proportions for No. 14 or No. 18 bar setup, the locations of the bearing plates on the front face of the specimen were marked. The plates were then placed at those locations. Hydrostone was used between the plates and concrete surface to ensure plates are set in place level in both directions. The reaction frame is placed on the bearing plates.

2.3.4 Bar Displacement Measurement

The displacement of each test bar relative to the front face of the column was measured using linear variable differential transformers (LVDTs). The LVDTs, shown in Figure 2.22, were attached to 2×4 lumber. The lumber was then clamped to a stiffener on the lower bearing member between its flanges. A $3/8$ -in. solid square steel rod with a $1/8$ -in. thick plate bolted to one end and a steel tube welded to the other end was used. The LVDTs were in contact with the flat plate during the test. Two $3/4$ -in. nuts were welded to the tube so that the tube could be secured on the test bar by tightening the bolts against the bars. The LVDTs were connected to a data acquisition system (DAQ) during the test.



Figure 2.22 Setup for using the LVDTs

2.3.5 Load Cells

Five load cells were built and calibrated to measure the applied force on the test bars during the test. The same load cells were used for both No. 14 and No. 18 bars. The nominal capacity of load cells was 600 kips. The load cells consisted of a steel pipe with two 2.5-in. thick steel plates on top and bottom of the pipe, as shown in Figure 2.23. The pipe was connected to the plates using a spring and eye bolt at the corner of each plate. The 2.5-in. thick plates were dimensioned so that test bars could be spaced at 6 in. on-center without interfering with each other. Four 350-ohm strain gauges were installed on the pipe at midheight in a full bridge, with two gauges orienting parallel and two gauges perpendicular to the loading direction. The gauges were alternated at 90° intervals around the pipe.



Figure 2.23 Load cell for No. 14 and No. 18 bars

2.3.6 Testing Procedure

A more detailed, step-by-step procedure for placement of specimens and the reaction frame for testing is provided in the report by Blessent et al. (2020). In summary, the concrete blocks were placed in position with respect to holes in the strong floor. The location of the blocks depended on

the bar size, since they would be placed below the bearing members, as shown in Figures 2.16 and 2.18 (the location of bearing members was a function of bar size, Figure 2.4). The location of bearing plates and contact points with the concrete blocks were marked on the specimen, which was then lifted and placed on the blocks. Hydrostone was used between the specimen and the steel plates on the blocks. The bearing plates were then seated and leveled on the specimen using hydrostone. The reaction frame assembly, consisting of the two bearing members, two columns, guides, hydraulic jacks, lower tension member (excluding the bottom set of channels), and four corner anchors, was lifted and placed on top of the specimen, so the bearing members were centered and aligned on the bearing plates. After placement, the reaction frame was secured in place by tightening the corner anchor rods to the strong floor using a washer and nut above and below the strong floor. The nuts attaching the anchors to the reaction frame were then loosened slightly to avoid applying load to the specimen through them.

The LVDT bearing plate attachments were then placed on each test bar. The built-up section was then lifted and placed across the 740-ton jacks, with the test bars passing through the designated openings. The 1-in. washer plates, load cells, 2.5-in. washer plates, and the couplers were placed on each test bar. The screws on the couplers were then tightened using an impact wrench in accordance with the manufacturer guidelines. For the No. 18 bars, final tightening was performed using a torque meter to ensure that every screw had reached the target torque. The bottom set of channels of the lower tension member (Bottom Lower Tension Member Channels in Figure 2.16) was lifted using a forklift so that the No. 14 threaded bars passed through the designated holes on the channels. Before the bottom tension member was placed on the back face of the specimen, hydrostone was used between the concrete and steel surface to ensure a level contact area. A nut was then screwed onto each of the No. 14 threaded bars to lock the bottom tension member in place. Hydraulic lines were connected to all four jacks. The lines were labeled, and same lines were used for each jack throughout all tests for consistency and ease of a possible troubleshooting. The assemblies with the LVDTs were clamped in place, as described earlier. The strain gauges, load cells, and LVDTs were connected to the DAQ.

Initially, a trial load equal to 5% of the calculated failure load was applied to check if the system and the apparatus were functioning properly. Once verified, the specimen was loaded in increments, also equal to 5% of the calculated failure load. Cracks were marked and labeled at loads equal to 20, 40, 50, 60, and 70% of the calculated failure load. After marking the cracks at

70% of the estimated failure load, the specimen was covered with a tarp as a safety measure, and then loaded to failure. Photographs were taken each time after the cracks were marked, and after the failure.

2.3.7 Summary of Test Program

Forty-two simulated beam-column joint specimens with No. 11, No. 14 and No. 18 bars were tested, 12 with hooked bars and 30 with headed bars. For the hooked bars, concrete compressive strengths ranged from 6,390 to 15,770 psi and bar stress at failure ranged from 87,300 to 130,600 psi. For the headed bars, concrete compressive strengths ranged from 5,310 to 16,210 psi. and bar stresses at failure ranged from 54,900 to 148,300 psi. Table 2.5 presents the test program and the main test parameters. Table 2.6 gives a summary of the test program and number of specimens tested with each bar.

Table 2.5 Test program and the main parameters for No. 11, No. 14, and No. 18 bar specimens

ID ^[1]	Bar size	<i>n</i>	<i>s</i> in.	<i>s/d_b</i>	Bar spacing ^[2]	<i>f'_c</i> ksi	<i>ℓ_{eh}</i> in.	<i>A_{tr}/A_{hs}</i> <i>A_{th}/A_{hs}</i>	<i>c_{so}</i> in.	L. C.
11-1	No. 11	2	14.1	10.0	Wide	16	18.5	0	3.5	B
11-2	No. 11	2	14.1	10.0	Wide	16	18.5	0.282	3.5	B
14-2	No. 14	2	18	10.6	Wide	15	20.5	0.267	3.5	A
14-3	No. 14	2	18	10.6	Wide	7	31.9	0	3.5	B
14-4	No. 14	2	18	10.6	Wide	7	31.9	0.267	3.5	A
14-15	No. 14	2	18	10.6	Wide	7	22.7	0	3.5	B
14-16	No. 14	2	18	10.6	Wide	7	22.7	0.178	3.5	A
14-16A ^[3]	No. 14	2	18	10.6	Wide	7	22.7	0.178	3.5	A
14-1A	No. 14	2	18	10.6	Wide	15	22.7	0	3.5	B
14-2A	No. 14	2	18	10.6	Wide	15	22.7	0.267	3.5	B
14-16B	No. 14	2	18	10.6	Wide	7	22.7	0.178	3.5	B
14-16C	No. 14	2	18	10.6	Wide	7	22.7	0.356	3.5	B
14-16D ^[4]	No. 14	2	18	10.6	Wide	7	22.7	0.827	3.5	A
14-16E ^[4]	No. 14	2	18	10.6	Wide	7	22.7	0.551	3.5	A
14-16F ^[5]	No. 14	2	18	10.6	Wide	7	22.7	0.551	3.5	A
14-17 ^{[5][6]}	No. 14	2	12	7.1	Close	7	22.7	0.551	6.5	A
14-5	No. 14	3	6	3.5	Close	7	22.7	0.178	3.5	B
14-6	No. 14	3	6	3.5	Close	7	22.7	0.276	3.5	B
14-7	No. 14	3	6	3.5	Close	7	31.9	0	3.5	B
14-8	No. 14	3	6	3.5	Close	7	31.9	0.276	3.5	B
14-9	No. 14	3	6	3.5	Close	12	22.7	0.276	3.5	B
14-10 ^[4]	No. 14	3	6	3.5	Close	7	22.7	0.551	3.5	A
H14-1	No. 14	2	18	10.6	Wide	15	26.6	0	3.5	A
H14-2	No. 14	2	18	10.6	Wide	15	26.6	0.267	3.5	A
H14-3	No. 14	2	18	10.6	Wide	7	35.8	0	3.5	A
H14-4	No. 14	2	18	10.6	Wide	7	35.8	0.267	3.5	A

H14-15	No. 14	2	18	10.6	Wide	7	26.6	0	3.5	A
H14-16	No. 14	2	18	10.6	Wide	7	26.6	0.178	3.5	A
H14-7	No. 14	3	6	3.5	Close	6	35.8	0	3.5	A
H14-8	No. 14	3	6	3.5	Close	6	35.8	0.276	3.5	A
18-1	No. 18	2	18	8.0	Wide	7	31.1	0.543	3.5	A
18-2	No. 18	2	18	8.0	Wide	15	27.8	0.543	3.5	A
18-3	No. 18	2	18	8.0	Wide	7	30.6	0.233	3.5	B
18-4	No. 18	2	18	8.0	Wide	7	30.6	0.465	3.5	B
18-5 ^[6]	No. 18	2	12	5.3	Close	7	30.9	0.543	6.5	A
18-6 ^[6]	No. 18	2	12	5.3	Close	15	27.8	0.543	6.5	A
18-7 ^{[4][6]}	No. 18	3	6	2.7	Close	7	30.9	0.543	6.5	A
18-8 ^{[5][6]}	No. 18	3	6	2.7	Close	7	27.8	0.543	6.5	A
H18-1	No. 18	2	18	8.0	Wide	16	28.6	0.233	3.5	A
H18-2	No. 18	2	18	8.0	Wide	16	28.6	0.465	3.5	A
H18-3	No. 18	2	18	8.0	Wide	7	37.8	0.233	3.5	A
H18-4	No. 18	2	18	8.0	Wide	7	37.8	0.465	3.5	A

- [1] Designations starting with “H” denote a hooked bar specimen
- [2] Widely-spaced bars: $s/d_b \geq 8.0$ (6.0 for hooks), Closely-spaced bars: $s/d_b < 8.0$ (6.0 for hooks)
- [3] Specimen had an additional No. 11 longitudinal bar on both sides, 2 in. from the bearing face on the head
- [4] Double overlapping No. 5 ties were used, refer to Figure 2.5
- [5] Double No. 5 ties were used
- [6] Specimen had an increased side cover of 6.5 in.
- n*** Number of bars
- s*** Center-to-center bar spacing
- f'_c*** Target concrete compressive strength
- ℓ_{eh}*** Nominal embedment length
- A_{tt}*** Total area of tie legs within $9.5d_b$ from the centerline of headed bars
- A_{th}*** Total area of tie legs within $9.5d_b$ from the centerline of hooked bars
- A_{hs}*** Total area of headed or hooked bars being developed
- c_{so}*** Side cover to the headed or hooked bar
- L. C.** Loading condition, refer to Section 2.3.2

Table 2.6 Summary of the test program and number of specimens

Bar size	Confining reinforcement	Number of headed bar specimens		Number of hooked bar specimens	
		Two heads	Three heads	Two hooks	Three hooks
No. 11	Without	1	0	0	0
	With	1	0	0	0
No. 14	Without	3	1	3	1
	With	11	5	3	1
No. 18	Without	0	0	0	0
	With	6	2	4	0

CHAPTER 3: TEST RESULTS

In this chapter, the general behavior of the simulated beam-column joint specimens with No. 14 and No. 18 hooked bars and the No. 11, No. 14, and No. 18 headed bars is discussed. Cracking patterns, failure modes, and stress/strain development in test bars and parallel ties in the joint region as observed during the tests are presented. Anchorage strengths of the 42 specimens tested are tabulated at the end of the chapter. The effects on anchorage strength of key parameters, including bar size and spacing, concrete compressive strength, development length, confining reinforcement in the joint region, and side cover are discussed in Chapter 4 and 5.

3.1 CRACKING PATTERNS

3.1.1 Hooked Bars

Cracks propagated in patterns that were similar to those observed for No. 5 through No. 11 hooked bars by Sperry et al. (2015b, 2017a). Examples are shown in Figures 3.1 and 3.2. Cracking initiated on the front face of the specimen (top of the specimen as tested) adjacent to the hooked bars (Figure 3.1a) and propagated towards the sides of the specimens (Figure 3.2a). As the force in the hooked bar increased, cracks on the sides of the specimens grew along the straight portion of the bars and additional cracks branched towards the upper and lower bearing members (Figure 3.2b and 3.2c). On the front face, the cracks continued to extend, radiating from the hooked bars (Figure 3.1b). At higher loads, the cracks on the sides of the specimens continued to propagate and branch towards the bearing members, resulting in a cone-shaped pattern (Figure 3.2d). As shown in Figure 3.2d, diagonal cracks extended through the joint to the lower bearing member, while the inclined cracks outside the joint reached the upper bearing member. On the front face, the cracks that radiated from the hooked bars connected to each other and portions of concrete were pulled out resulting in local damage to the concrete near the surface (Figure 3.1c).

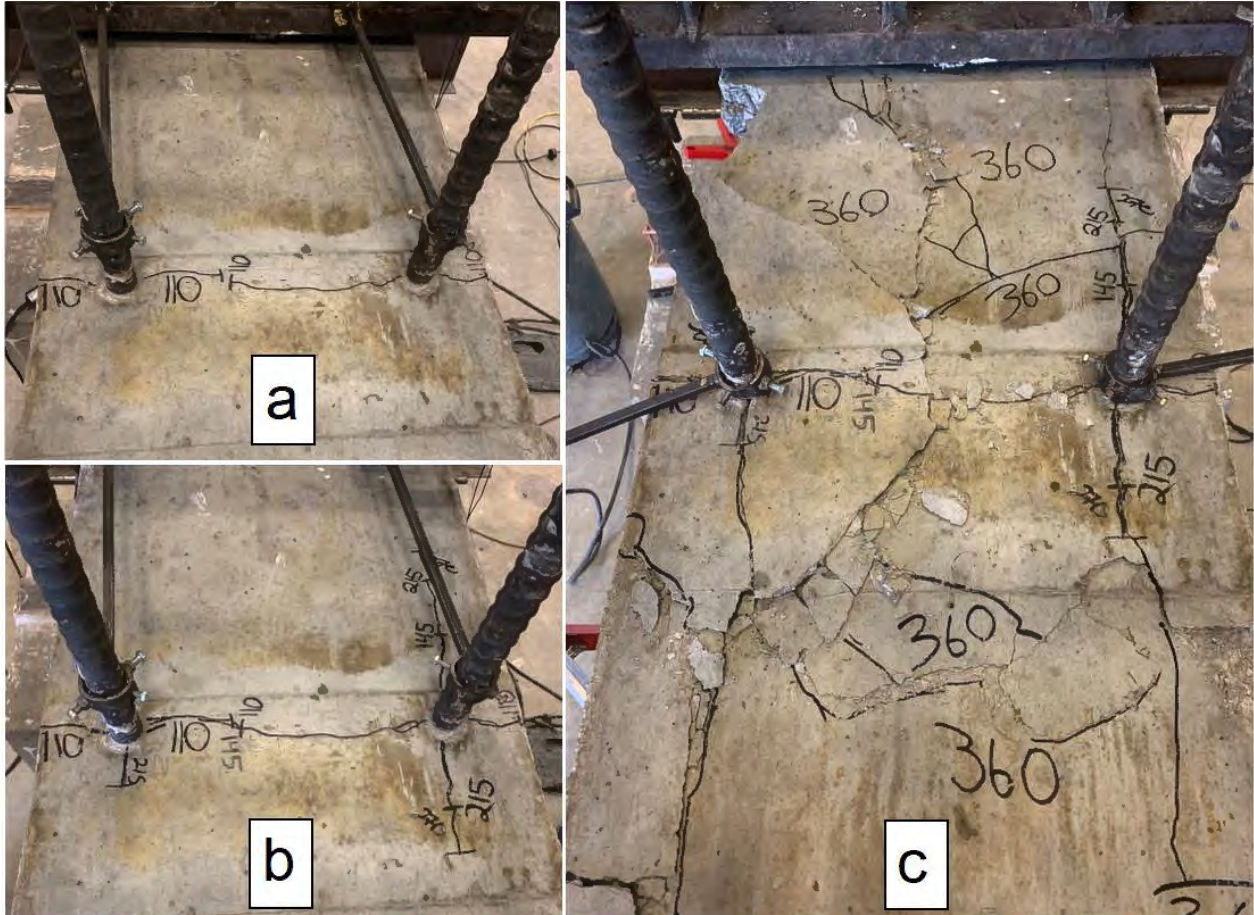


Figure 3.1 Example of cracking pattern in hooked bar specimens (front face, specimen H14-15): (a) Horizontal cracks likely initiating due to bar slip, (b) Cracks radiating from the hooked bars, and (c) Cracks radiated from the hooked bars connected to each other along with local concrete damage

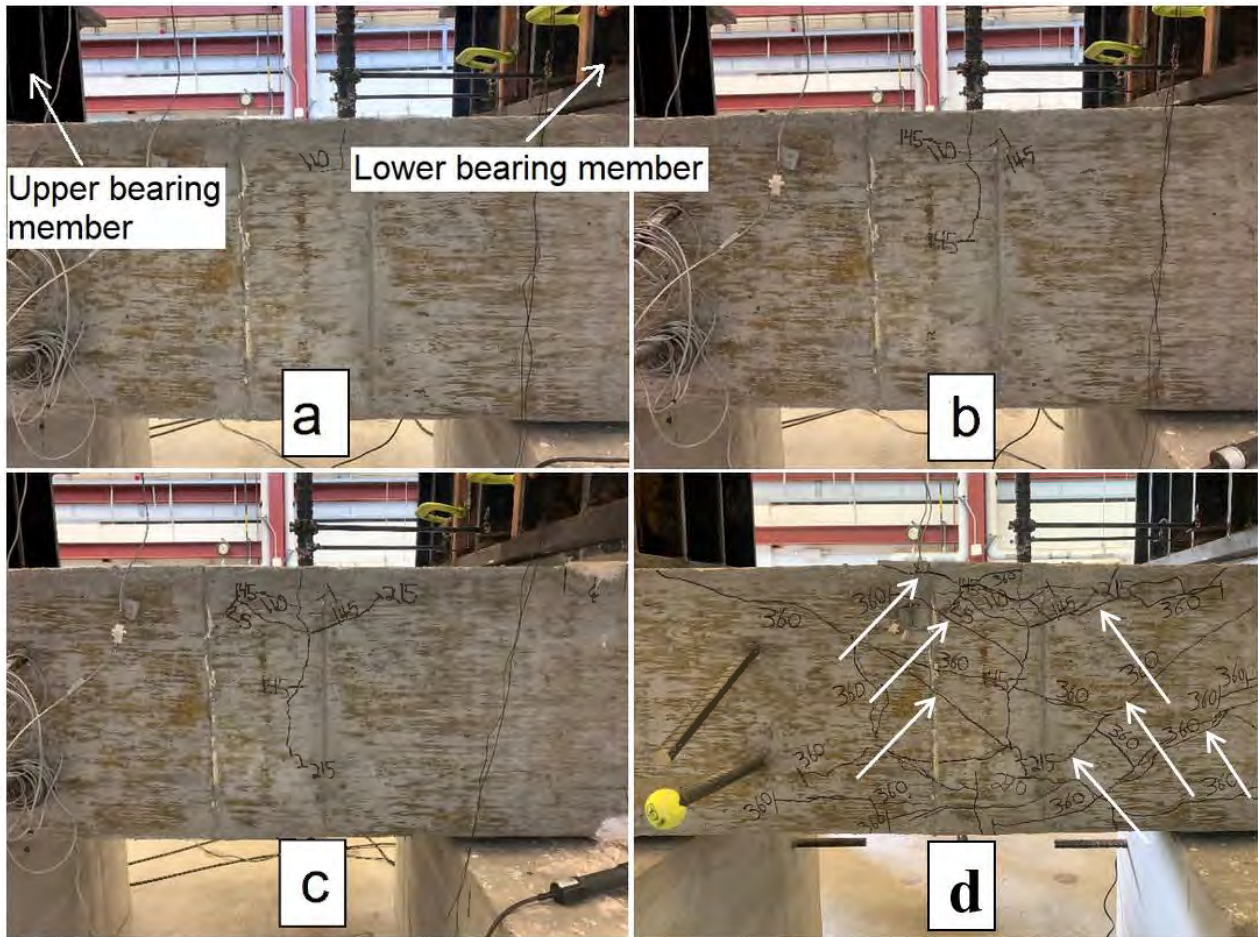


Figure 3.2 Example of cracking pattern in hooked bar specimens (side face, specimen H14-15): (a) Vertical crack likely initiating due to bar slip, (b) and (c) Cracks propagating and branching towards upper and lower bearing members, (d) Cone-shaped cracking pattern near failure (see arrows.)

3.1.2 Headed Bars

Headed bar specimens had cracking patterns similar to those observed for hooked bars. The side and top faces of specimen 18-3 are shown at the same load stages in Figures 3.3 and 3.4, illustrating the formation of cracks. Initially, a crack started to form on the front face adjacent to and between the headed bars (Figure 3.4a) and extended to the sides of the specimen, propagating along the bars (Figures 3.3a and 3.4a). This initial crack was likely due to the slip of the bars during the first stages of loading. As shown in Figure 3.4a, the cracks on the front face eventually radiated from the bars (Figure 3.4e) as the load increased. On the side faces, the crack in line with the bars continued to develop towards the head, while new cracks started to form, branching from this crack (Figure 3.3b). With an increase in load, a large diagonal crack appeared on the sides that extended

from the bearing face of the head to the edge of the nearest bearing member (compression region of the simulated beam) from one side of the joint to the other, as shown in Figure 3.3c. The formation of the first diagonal crack in the joint was often sudden and accompanied by a loud noise and a slight drop in the applied load. On the front face, more cracks parallel to the original crack between the bars formed across the column width above and below the level of headed bars (Figure 3.4b and 3.4c). Further increases in the load resulted in the formation of new diagonal cracks within the joint, and cracks branching towards upper and lower bearing members in a cone-shaped pattern (Figure 3.3d and 3.3e). The diagonal cracks in the joint usually extended parallel to the back face of the member towards the top of the column, passing close to the bearing face of the head (see dashed lines in Figures 3.3c-f). On the front face of the column, new cracks, primarily in the longitudinal direction, branched from the existing cracks that had formed across the column width, as shown in Figure 3.4d.

Near failure, the cracks grew wider, and the number of cone-shaped cracks on the sides branching towards bearing members increased (Figure 3.3f). The extension of diagonal cracks along the back face and towards the top of the column continued, and these cracks also extended diagonally towards the upper bearing member (bottom left corner of Figure 3.3f). On the front face of the specimen, the cracks branched further and connected to each other. The front face cracks extended towards the sides and connected to the cone-shaped cracks on both sides. The amount of cracking was mainly governed by the amount of confining reinforcement in the joint region, as specimens with parallel ties (or more parallel ties) generally underwent more deformation before failure and developed more cracks than specimens with no parallel ties or with a lower level of confinement, which failed in a more brittle fashion with fewer cracks at a lower force.

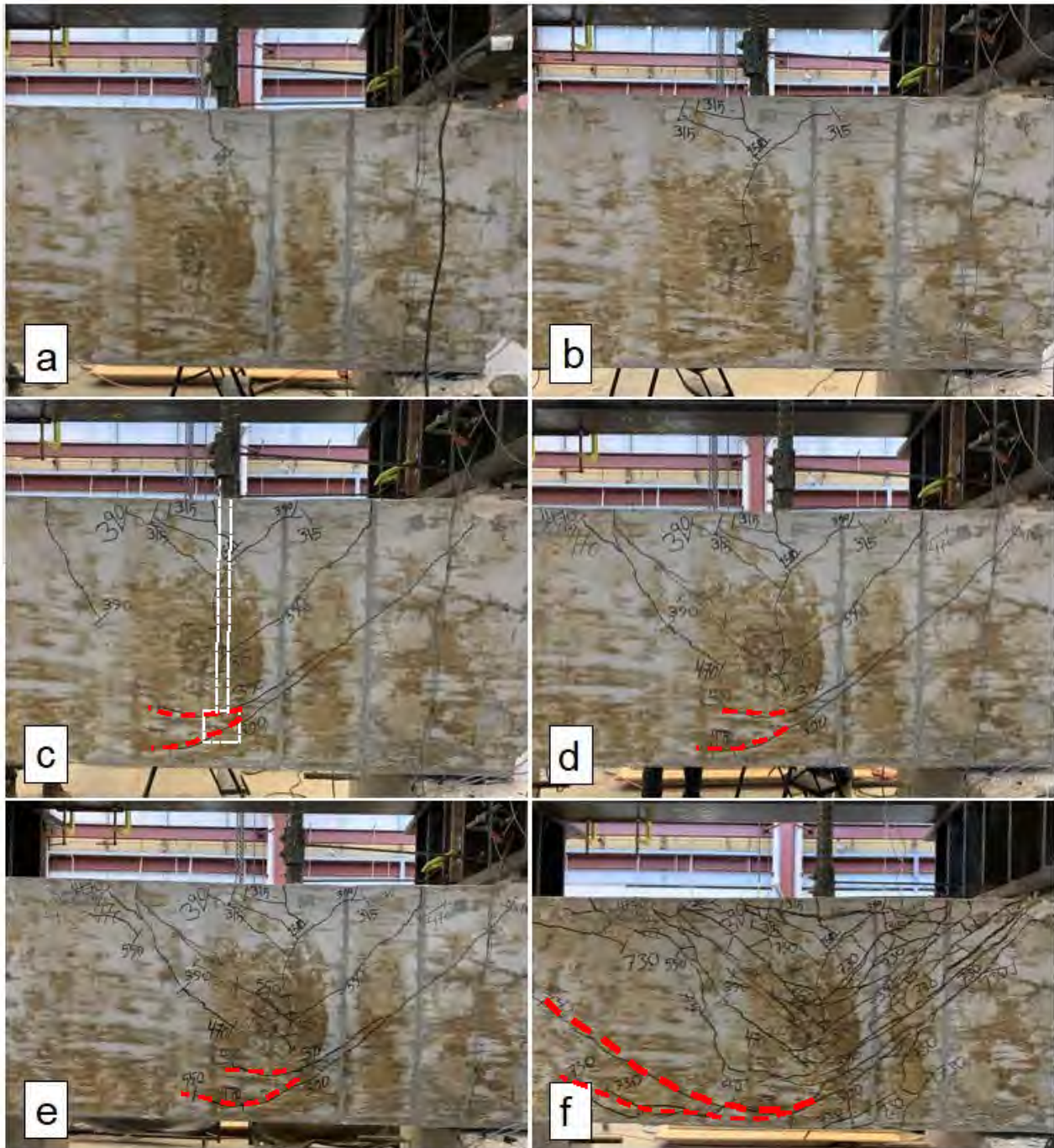


Figure 3.3 Example of cracking pattern in headed bar specimens (side face, specimen 18-3): (a) Vertical crack likely initiating due to bar slip, (b) Cracks branching towards bearing members, (c) First diagonal crack due to shear in joint, (d) and (e) Cracks propagating throughout the joint, (f) Cone-shaped cracking pattern after failure. (**Note:** Extension of diagonal cracks along the back face of the specimen towards the top of the column are marked by dashed lines.)

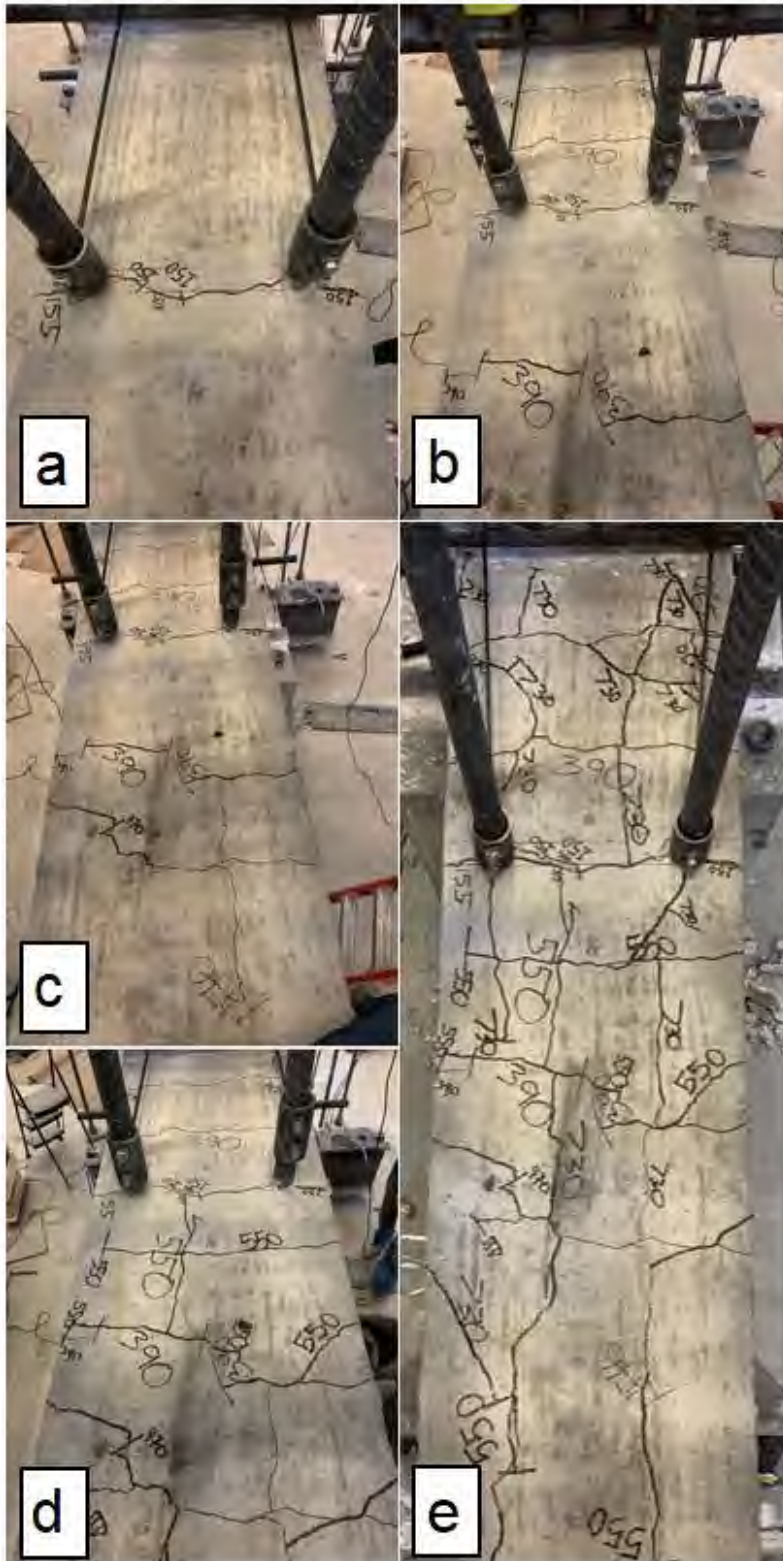


Figure 3.4 Example of cracking pattern in headed bar specimens (top face, specimen 18-3): (a) Crack between bars likely initiating due to bar slip, (b) Cracks branching towards bearing members, (c) First diagonal crack due to shear in joint, (d) and (e) Cracks propagating throughout the joint

3.2 FAILURE MODES

In this section, the different types of anchorage failure are discussed. For both hooked and headed bars, specimens showed two primary failure types, namely concrete breakout and side splitting. A few headed bar specimens failed in shear (not anchorage). In some specimens, a secondary failure mode was also observed.

3.2.1 Hooked Bars

As observed in previous research on No. 5 through No. 11 hooked bars (Sperry et al. 2015, Ajaam et al. 2017), two primary failure modes were observed in the specimens, concrete breakout and side splitting. A concrete breakout failure, accompanied by tail kickout, is shown in Figure 3.5. Concrete breakout, the only failure mode observed in seven out of the 12 specimens (four No. 14 bar and three No. 18 bar specimens), is characterized by a mass of concrete being pulled out along with the hooked bar from the front face of the specimen. As shown in Figure 3.5, the failure surface is cone-shaped, with spalling of concrete on the front face at failure. Side splitting is usually sudden and more explosive in nature than breakout failure and is marked by the side cover on the hooked bar separating from the column, as shown in Figure 3.6. Side splitting was observed as the only failure mode in three out of the 12 specimens (two No. 14 bar and one No. 18 bar specimen), while two specimens exhibited breakout on one hook and side splitting on the other.

The likelihood of a given failure mode depended on the amount of confinement in the joint. Three out of the four specimens without confining reinforcement in the joint region (all with No. 14 hooked bars) exhibited a breakout failure, while the other specimen without confining reinforcement had a breakout failure on one hook and a side-splitting failure on the other. Of the eight specimens with confining reinforcement, three (H14-4, H14-8, and H18-2) exhibited a side-splitting failure, four experienced a breakout failure, and one had a breakout failure on one hook and side-splitting failure on the other.

The effect of bar spacing on the failure mode was less clear. Of the two specimens with three closely-spaced bars, H14-7 (without confining reinforcement) exhibited a breakout failure, while the companion specimen H14-8 (with confining reinforcement) had a side-splitting failure. Of the ten specimens with widely spaced bars, six exhibited a breakout failure, two exhibited a side-splitting failure, and two (H14-2 and H14-3), experienced a breakout failure on one hook and side splitting on the other hook. In the latter case, it appeared that the bars acted independently

when widely spaced. Of the specimens with widely-spaced bars, in three No. 14 bar specimens and one No. 18 bar specimens, one hook failed first. After the initial failure, loading continued until the second hook failed. In these specimens, the maximum load on the second hook was noticeably higher than the load corresponding to the failure of the first hook. At the failure of the second hook, the load difference between the two bars ranged from 11.5 to 19 kips, corresponding to a bar stress of 5.1 to 8.4 ksi. The percentage difference between the bar stresses ranged from 4.8-9.6% of the average bar force at failure, f_s . The failure load for these specimens is reported as the average of the two bar loads, but the individual loads are reported in Appendix B2. In all other cases, the failure load is total applied peak load divided by the number of bars.

In two out of the four specimens without confining reinforcement in the joint region (H14-1 and H14-7), a secondary failure mode, tail kickout, was observed in conjunction with concrete breakout. Tail kickout occurs when the tail of the hooked bar pushes the concrete cover off the back of the column, causing the cover to spall and exposing the tail (Figure 3.5). The tendency for tail kickout in specimens without confining reinforcement in the joint region agrees with observations by Yasso et al. (2017, 2021) and Sperry et al. (2017a) for smaller bar sizes.



Figure 3.5 Side view of a concrete breakout failure in hooked bars with tail kickout (H14-7)



Figure 3.6 Side view of a side-splitting failure for hooked bars (H14-8)

3.2.2 Headed Bars

As observed for the hooked bar specimens, the two main anchorage failure types observed in headed bars were concrete breakout and side splitting, with the latter referred to as side-face blowout in some studies (Chun et al. 2017, Chun and Lee 2019, Sim and Chun 2022a, 2022b). The failure types generally matched those observed by Shao et al. (2016) and Ghimire et al. (2018) for No. 11 and smaller bars. Breakout or side-splitting failures were occasionally accompanied by a compression failure in the joint region along a line between the head and the lower bearing member. Four specimens (all with No. 14 bars) did not exhibit an anchorage failure. These specimens have been excluded from the analysis and are discussed later in this section.

The definitions of concrete breakout and side splitting for headed bars is similar to hooked bars. Breakout occurs when the concrete mass in front of the head separates from the front face of the column as the bar was being pulled out. Side splitting occurs when the movement of the head causes the concrete side cover around the head to spall and separate, usually blowing out in a sudden and explosive way, exposing the head.

Concrete breakout was the primary failure mode in six out of 20 No. 14 bar specimens and in two out of eight No. 18 specimens. Examples are shown in Figure 3.7. A cone-shaped failure

surface was observed in these specimens, characterized by diagonal cracks in the joint region extending beyond the joint, passing the location of the head and moving along the back face of the column in the form of splitting cracks (top and bottom images in Figure 3.7), or moving diagonally towards the upper bearing member (top image in Figure 3.7).

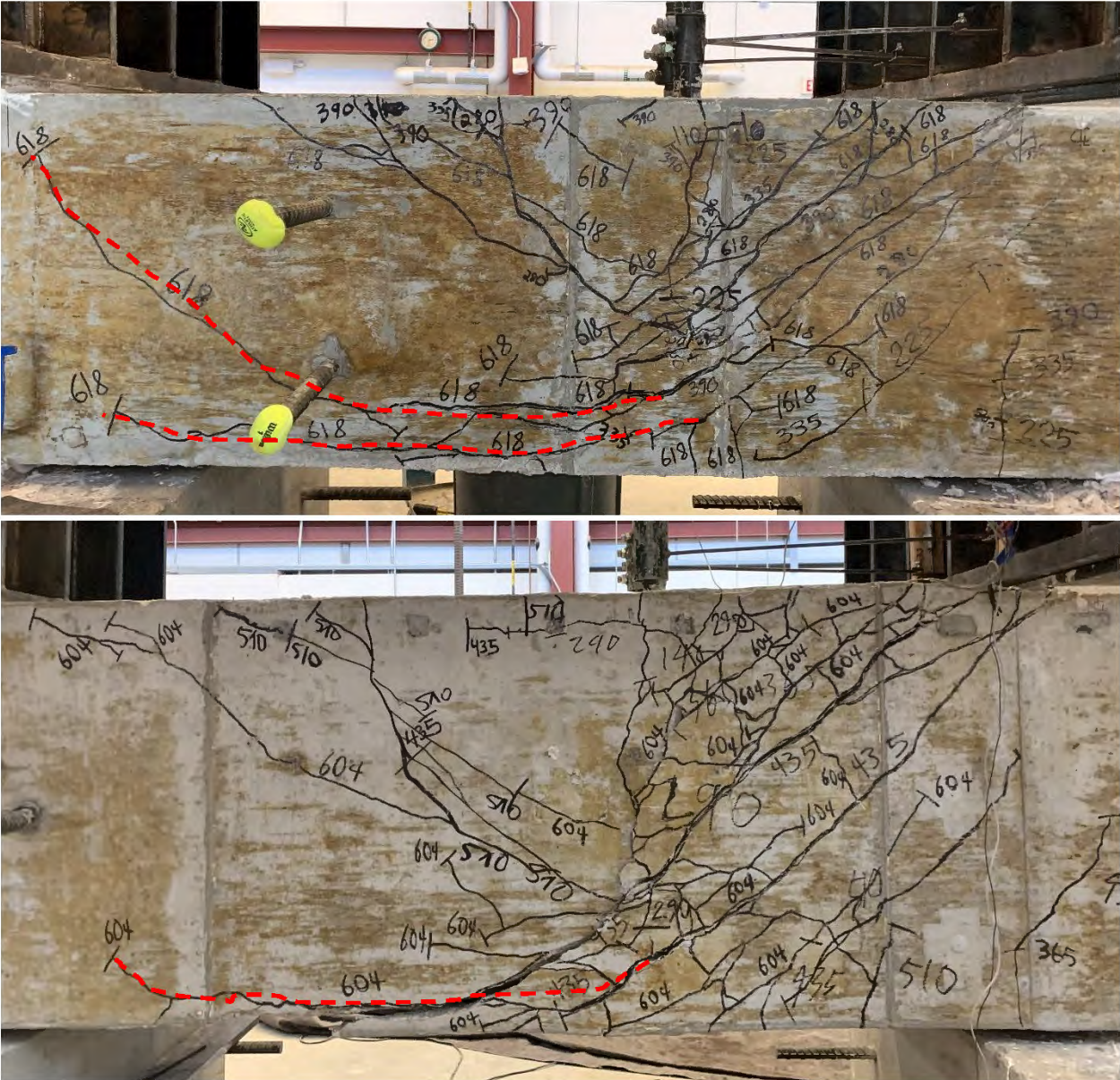


Figure 3.7 Primarily concrete breakout failure (top: specimen 14-10, bottom: specimen 18-5). (Note: Dashed lines highlight the cracks extending beyond the joint and along the back face of the column or towards the upper bearing member)

In one No. 11 bar specimen, six out of the 20 No. 14 bar specimens, and three out of the eight No. 18 bar specimens, failure was primarily due to side splitting, as shown in Figure 3.8. In specimens failing primarily due to side splitting, the cracks extending beyond the head along the

back face of the column and diagonally towards the top of the column (highlighted by dashed lines in Figures 3.3 and 3.7) did not form, a key difference between side splitting and concrete breakout failures. A failure primarily involving side-splitting was more likely to occur in specimens with a higher number of parallel ties in the joint region.

In one No. 11 bar specimen, four out of 20 No. 14 bar specimens, and three out of eight No. 18 bar specimens, the failure mode was a combination of concrete breakout and side splitting, as shown in Figure 3.9.

In some specimens, breakout or side splitting occurred along with a compression failure within the joint (from the bearing face of the head to the bearing member representing the compression region of the simulated beam, as shown in Figure 1.27). A compression failure, which was often explosive, was observed in five out of 20 No. 14 bar specimens and in four out of eight No. 18 bar specimens, including four out of the six specimens cast with high-strength concrete ($> 12,000$ psi), and was more likely to occur in specimens with a higher level of confining reinforcement in the joint region. An example of concrete breakout accompanied by compressive strut failure is shown in Figure 3.10.



Figure 3.8 Primarily side-splitting failure (left: specimen 14-3, right: specimen 18-4)



Figure 3.9 Combination of concrete breakout and side splitting (specimen 14-15)



Figure 3.10 Concrete breakout accompanied by side splitting and compression failure of concrete between bearing face of the head and lower bearing member (specimen 14-16B)

As described earlier, four headed bar specimens did not exhibit an anchorage failure but, rather, failed at a relatively low load with a diagonal crack between bearing face of the head and lower bearing member that was reminiscent of what might occur due to a shear failure and is referred to here as a “shear-like” failure (Figure 3.11). Three out of the four specimens had relatively low levels of confining reinforcement (two specimens with A_{tt}/A_{hs} of 0.178, namely 14-16 and 14-16A, and one with A_{tt}/A_{hs} of 0.267, specimen 14-2) and were tested under loading condition A (joint shear equal to 80% of the force applied to bars). The fourth specimen with a

shear-like failure, specimen 14-1A, contained no confining reinforcement and was tested under loading condition B (joint shear ~69% of the force applied to bars).

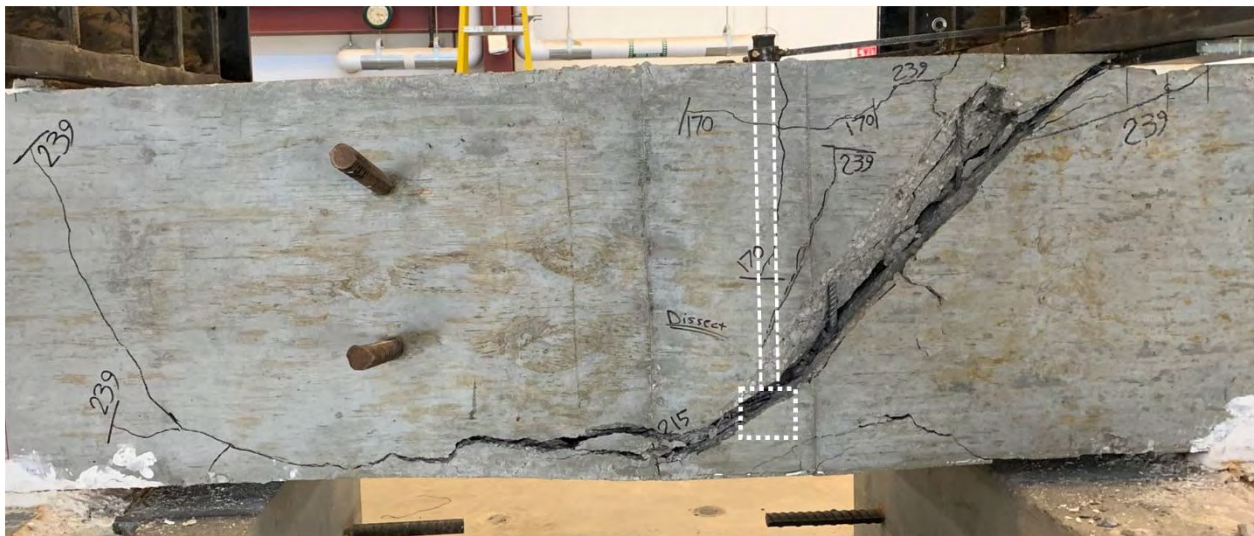


Figure 3.11 Shear-like failure in headed-bar specimen 14-16. (**Note:** The specimen shows no indication of a breakout or side-splitting failure.)

Shear-like failures occurred only in the headed bar specimens. The following characteristics were observed in these four specimens:

- The first diagonal crack in the joint region appeared at a force at or above 75% of the failure load with the specimen failing shortly after the formation of the crack.
- The diagonal crack extended beyond the joint, passing through the location of the head in the form of a splitting crack along the back face of the column.
- After formation of the diagonal crack, no more cone-shaped cracks, such as shown in Figures 3.2 and 3.3, formed.
- There was little to no damage on the front face of the columns around the headed bars.

The joint shear stress is worth analyzing for these four specimens. The shear force in the joint, V_J , depends on the loading condition, as discussed before. Under loading condition A, $V_J = 0.8T$, and under loading condition B, $V_J \approx 0.69T$. The joint shear stress is then V_J/bh , where b and h are column width and height, respectively. The joint shear stress is normalized with respect to $\sqrt{f_{cm}}$ for analysis. The values of $V_J/(bh\sqrt{f_{cm}})$ were 3.5, 3.5, 4.3, and 2.6 for specimens 14-2, 14-16, 14-16A, and 14-1A, respectively. These values are significantly lower than reflected in Table 15.4.2.3 of Chapter 15 in ACI 318-19 for a continuous column with a non-continuous beam that is not confined by transverse beams (which is the case in an external beam-column joint). For that

Failure type	No. 11	No. 14	No. 18	Total
CB ¹	0	6	2	8
SS ²	1	6	3	10
CB+SS ³	1	4	3	8
SF ⁴	0	4	0	4

Table 3.2 Summary of headed bar specimens with different failure types

Failure type	No. 14	No. 18	Total
CB ¹	4	3	7
SS ²	2	1	3
CB/SS ³	2	0	2
SF ⁴	0	0	0

Table 3.1 Summary of hooked bar specimens with different failure types

condition, Table 15.4.2.3 requires a nominal joint shear strength, V_n , to be $15bh\sqrt{f_{cm}}$, which is 3.5 to 5.7 times greater than obtained in the four specimens that exhibited a shear-like failure. This indicates that the shear-like failures were not strength-related and most likely the result of detailing issues. This point is further discussed in Section 5.5.1.

For two No. 14 headed bars specimens with widely-spaced bars (14-3 and 14-16D), one head failed first and loading continued until the failure of the second head. The load difference between the two bars was 26.2 and 29.1 kips, corresponding to a bar stress of 11.6 and 12.9 ksi, respectively. As in the similar hooked bar specimens, this difference in bar stress was less than 10% of the average bar stress at failure (8.6% and 10.0% in 14-3 and 14-16D, respectively). Although the widely-spaced bars failed independently, they were not treated as separate tests and the failure load was calculated as the average of the maximum load per bar. In all other specimens, the failure load is taken as the total peak load divided by the number of bars. The individual bar forces are reported in Appendix C2.

For specimens exhibiting an anchorage failure, no direct relationship was found between the type of failure and the anchorage strength. Tables 3.1 and 3.2 summarize the number of specimens for each failure type for, respectively, the hooked and headed bar specimens.

¹ Primarily concrete breakout
² Primarily side splitting
³ Combination of breakout and side splitting
⁴ Shear-like failure

3.3 STRAIN DEVELOPED IN REINFORCEMENT

In this section, the strain developed in the ties and the hooked and headed bars obtained from strain gauges during testing is discussed. As described in Section 2.2.5, strain gauges were mounted on the two parallel ties above the joint region (labeled S1 and S2) and on all ties within the joint region (labeled S3, S4, etc., in specimens with joint confining reinforcement). The gauges were installed at the center of each tie leg. Two strain gauges were mounted on one hooked or headed bar per specimen. On hooked bars, the first gauge was mounted just before the bend in the tail (labeled T1), and the second gauge 1 in. from the column front face (labeled T2). On headed bars, strain gauge T1 was mounted 1.5 in. from the bearing face of the head, and T2 was mounted 1 in. from the column front face. The strain gauge configuration is shown in Figure 2.14. Not all specimens provided good strain gauge readings due to damage to the gauges during concrete placement. The specimens selected for analysis in this section had all strain gauges working, providing good readings throughout the test.

3.3.1 Ties

In general, the strain development in the ties in specimens with confining reinforcement in the joint region was similar for hooked and headed bars. While the strain developed in each tie differed for each specimen, the overall load-strain curves showed similar patterns. The load-strain curves for the ties in hooked bar specimen H14-2 and headed bar specimen 14-6 are shown in Figure 3.12. Specimen H14-2 had two widely-spaced No. 14 hooked bars cast in high-strength concrete, with five No. 4 ties within the joint region. Specimen 14-6 had three closely-spaced headed bars cast in normal-strength concrete, with five No. 5 ties in the joint region.

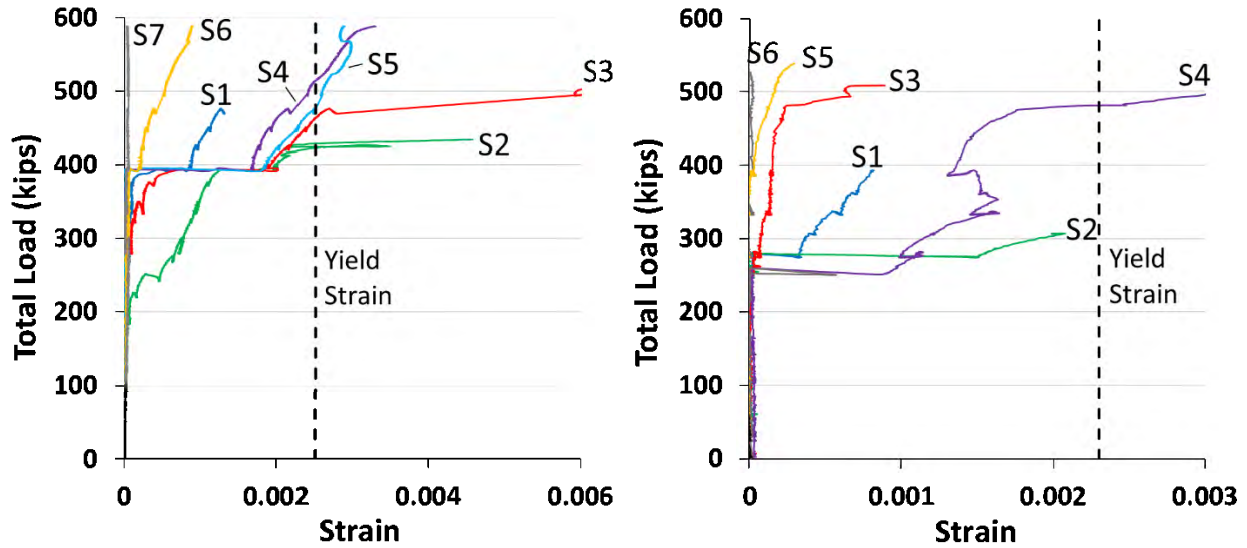


Figure 3.12 Examples of strain developed in parallel ties in hooked bar specimen H14-2 (left) and headed bar specimen 14-6 (right)

As shown in Figure 3.12, the strains developed in the ties for hooked and headed bar specimens were a function of their location. For hooked bar specimen H14-2, the ties just above and below the bars (S2 and S3, respectively) were the first ties to show a noticeable increase in strain. Up to about 200 kips, minimal strain developed in the ties. At a load close to 200 kips, S2 (the tie just above the hooked bars) started to show an increase in strain as the first diagonal crack appeared in the joint region. As the load increased to 350 kips, additional ties began to exhibit increases in strain as more diagonal cracks started to branch out from existing cracks above and below the joint. The increase in strain was generally more noticeable in ties closest to the hooked bars. The ties within the joint region (S3, S4, and S5) continued to undergo an increase in strain up to failure of the specimen. At a load of about 390 kips, a loud bang was heard. This marked the onset of a plateau in the load-strain curves of all ties, except for S7, the tie farthest from the hooked bars and closest to the bearing member at the base of the joint. While S6 (the second farthest tie from the bars) started to increase in strain at a load around 390 kips, S7 developed no significant strain during the test. The yield strength of the No. 4 ties was 72,700 psi, corresponding to a yield strain of 0.0025, as marked in Figure 3.12. In this specimen, four ties yielded, starting with S2 and followed by S3, S5, and S4. The peak load for specimen H14-2 was 587.8 kips. Figure 3.13 shows specimen H14-2 after failure along with the location of the ties and the corresponding strain gauges.

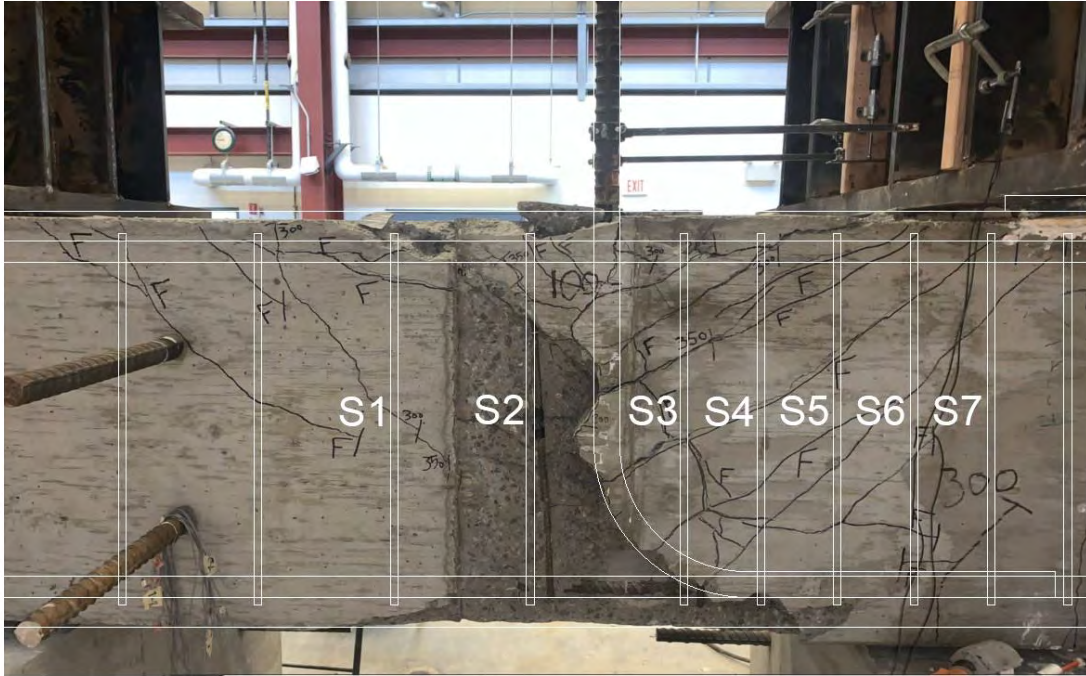


Figure 3.13 Specimens H14-2 at failure showing location of ties and strain gauges

As shown in Figure 3.12 for headed bar specimen 14-6, no strain development was observed up to a load of about 250 kips (only cracks in the plane of the headed bars, likely due to initial bar slip, had formed up to this point). At a load of about 255 kips, a loud pop was heard, coinciding with the formation of the first large diagonal crack in the joint, along with another diagonal crack above the joint. This was the onset of an increase in strain in all ties, except for the ties farthest from the headed bar, S5 and S6. At this point, the ties crossing the first diagonal cracks (S1, S2, S3, and S4, as shown in Figure 3.14 with the cracks marked at 280 kips) exhibited a sudden increase in strain, with S1, S2, and S4 almost immediately reaching a plateau in the load-strain curve. The noticeable increase in the strain in the ties arresting the first diagonal crack was observed in all specimens. The diagonal cracks passed close to the midheight of ties with strain gauges S2 and S4, which is likely the reason these gauges exhibited high strain. Strain gauge S2 indicated that the strain was close to yield at a load of 278 kips but provided no additional data at higher loads. S4 was the only tie in this specimen with an intact strain gage that yielded at a load close to failure. The tie just below the headed bars in the joint region, S3, did not have a plateau and continued showing a gradual increase in strain until a load of about 480 kips (failure load = 538.5 kips). Similar to hooked bar specimen H14-2, the ties farthest from the headed bars and closest to or in the compression region within the joint (S6 and S7) showed almost no strain development.



Figure 3.14 Parallel ties trapping the first diagonal cracks and their strain gauge labels in the headed bar specimen 14-6

These observations indicate that the ties closest to the hooked or headed bars were effective in arresting cracks and contributing to anchorage strength, as previously established by Sperry et al. (2015b) and Shao et al. (2016). In addition, by looking at the data for the specimens with strain gauges that provided readings throughout the test, the ties closest to the hooked or headed bars yielded in all cases (11 No. 14 headed bar specimens, all No. 18 headed bar specimens, 4 No. 14 hooked bar specimens, and 3 No. 18 hooked bar specimens). More specifically, the tie placed immediately below the bars (corresponding to strain gauge S3 in Figures 3.13 and 3.14) yielded in most cases, followed by the tie placed immediately above the bars (corresponding to strain gauge S2). In a few cases, ties corresponding to gauges S4 and S5 yielded as well. For the No. 18 bar specimens, it was generally observed that more ties yielded within the joint than for the No. 14 bar specimens, even those corresponding to strain gauges S6 and S7, indicating that larger bars are more likely to engage greater number of ties within the joint to arrest the large diagonal cracks.

3.3.2 Hooked Bars

As described in Section 2.2.5, two strain gauges were mounted on the hooked bars, T1 just before the bend in the tail of the bar and T2 at 1 in. from the front face of the column. The strain developed in hooked bars in the two locations generally followed a similar trend in all specimens. The load-strain behavior of hooked bars is plotted for specimens H14-2 and H14-15 in Figure 3.15.

The specimens had two widely-spaced No. 14 hooked bars. Specimen H14-2 had five No. 4 ties in the joint region, while H14-15 had none. It should be noted that, as shown in Figure 3.15, gauge T2 in specimen H14-15 stopped working at a load of about 150 kips. However, based on the similar trend observed in all specimens, it is fair to assume that the load-strain response of T2 followed the dashed line drawn.

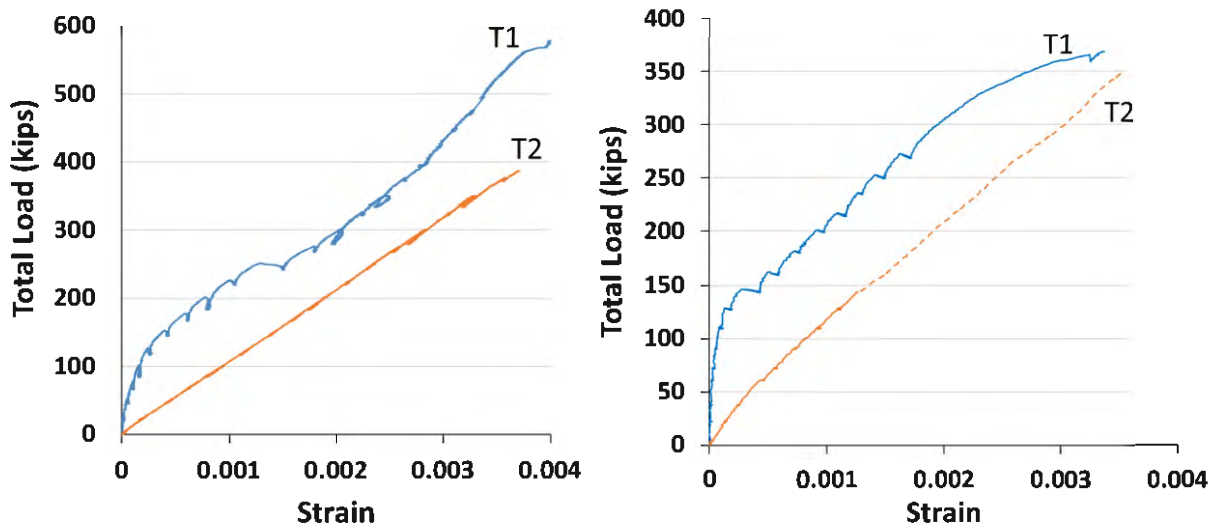


Figure 3.15 Strain developed in one hooked bar in specimens H14-2 (left) and H14-15 (right). (Note: T1 was mounted just before the bend in the tail, and T2 mounted 1 in. from the front face of the column)

As shown in Figure 3.15, the strain developed in the bar 1.5 in. from the column front face (T2) increased almost linearly during testing and was always higher than the strain at the bend (T1). The difference between the strains indirectly represents the force carried by bond along the straight portion of the bar. The strain at the bend increased slowly up to a load of about 100 kips for H14-2 and 150 kips for H14-15, corresponding to the first vertical cracks developing on the sides of the columns. The strain at the bend developed at a much faster rate as the load increased and once the cracks on the sides of the column reached the location of the bend. The strain at the bend continued to increase at a fast rate as the diagonal cracks appeared within the joint, indicating the increased contribution of the tail of the hook in carrying the load, holding the concrete in the joint together and providing anchorage. Due to increased damage on the front face of the column near failure, strain gauge T2 in specimen H14-2 failed at a load about 400 kips but gauge T1 remained functional until failure in both specimens.

3.3.3 Headed Bars

The strains developed in the headed bars (from gauges T1 and T2 as shown in Figure 2.14) are discussed in this section. Overall, the strain development in headed bars at both locations (1.5 in. from the bearing face of the head, T1, and 1 in. from the front face of the column, T2) followed a similar trend in all specimens regardless of bar size or confining reinforcement in the joint region. The load-strain curves for strain gauges T1 and T2 for specimens 14-16C and 18-8 are shown in Figure 3.16. Specimen 14-16C had two widely-spaced No. 14 bars with No. 4 ties in the joint region. Specimen 18-8 had three closely-spaced No. 18 bars with double overlapping No. 5 ties in the joint region.

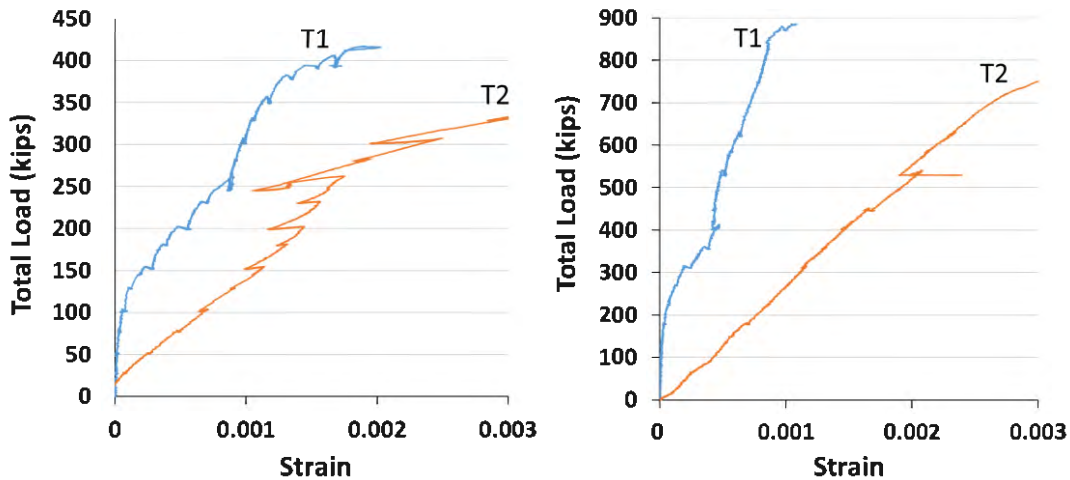


Figure 3.16 Strain developed in one headed bar in specimen 14-16C (left) and 18-8 (right) (Note: T1 was mounted 1.5 in. from the bearing face of the head, and T2 was mounted 1 in. from the column front face)

As shown in Figure 3.16, the strain in the bar 1 in. from the column front face (T2) started to increase almost as soon as the loading initiated and continued to develop throughout the test. At this point, a short crack started to form in the plane of the headed bars on the front face and extending on the sides of the column, likely due to initial bar slip. The strain in the bar 1.5 in. from the bearing face of the head (T1) remained near zero up to a load of about 100 kips in 14-16C and about 200 kips in 18-8. After the cracking initiated on the front face emanating from the bars, the strain near the head in both specimens increased at a faster rate as the vertical crack on the sides extended towards the location of the head. The first large diagonal cracks within and above the joint appeared at about 260 kips in specimen 14-16C and 400 kips in 18-8, accompanied by a small drop (~10 kips) in the load, as shown in Figure 3.16. After this point, the strain in the bar at both

locations continued to increase, at a slower rate near the head in both specimens and at a faster rate at the front face of the column in specimen 14-16C. The strain in the bar near the front face of the column always exceeded the strain near the head. The difference between the strain developed at the two locations provides an indication of the load transferred by the bond along the bar. This difference, however, is not a direct representation of load, since the bars were no longer on the linear portion of the stress-strain curve. The strain developed near the head increased much faster near failure, above 350 kips in 14-16C and 800 kips in 18-8, indicating the increased contribution of the head in carrying the applied force.

Looking at the available data for the headed bar specimens reveals that, at the initial stages of the loading (and in some cases up to about 50% of the failure load), the major portion of the applied force was carried by bond. As shown in Figure 3.16, the head would start to contribute in carrying the load after the initial cracking on the front face (Figure 3.4a) and continue to contribute, but would pick up load at a slower rate than it was by bond. The lower tensile stress near the head may have been due to the wedge of concrete forming on the head as the bar was being pulled out. If T1 had been mounted more than 1 in. from the head, a higher rate of increase in the strain may have resulted.

The difference observed between the contribution by bond and the head in carrying the forces in headed bar specimens seems to be a major distinction from the hooked bar specimens, comparing the plots in Figures 3.15 and 3.16. While both the hook and the head start to engage and provide anchorage after the start of cracking, the portion of the force carried by the hook increases with increasing load, while the portion of the load carried by bond remains nearly constant once cracking has occurred and may even drop off as the failure load is attained. In contrast, the contribution of the head increases at a slower rate than the contribution by bond up to failure based on the reading obtained for gauge locations used in this study.

3.4 ANCHORAGE STRENGTH

The anchorage strengths of the beam-column joint specimens measured in the tests are summarized in Tables 3.3 and 3.4 for the hooked and headed bars, respectively. The tables include the specimen ID (given in Table 2.5), specimen designation (described in Section 2.2.3), number of hooked or headed bars (n), center-to-center spacing between the bars in terms of bar diameter (s/d_b), measured concrete compressive strength (f_{cm}), average measured embedment length ($\ell_{eh,avg}$), ratio of effective confining reinforcement in the joint region (A_{th}/A_{hs} for headed bars or A_{th}/A_{hs} for

hooked bars; described in Figure 1.18), loading condition (discussed in Section 2.3.1), average peak load (T , total applied peak load divided by the number of bars), and failure mode (discussed in Section 3.2). Full details of the specimens are presented in Appendices B2 and C2. Analyses of the hooked and headed bar results are presented in Chapters 4 and 5, respectively.

Table 3.3 Summary of anchorage strength results for hooked bar specimens

ID ^[1]	Designation	n	s/d_b	f_{cm} psi	$\ell_{eh,avg}$ in.	A_{th}/A_{hs}	L. C.	T kips	Failure Mode ^[2]
H14-1	(2@10.6)14-15-i-3.5-2-26.6	2	10.6	12,980	27.0	0	A	240.0	CB
H14-2 ^[3]	(2@10.6)14-15-5#4-i-3.5-2-26.6	2	10.6	13,010	24.8	0.267	A	293.9	CB/SS
H14-3 ^[3]	(2@10.6)14-15-i-3.5-2-35.8	2	10.6	8,100	36.7	0	A	279.1	CB/SS
H14-4	(2@10.6)14-15-5#4-i-3.5-2-35.8	2	10.6	7,570	34.9	0.267	A	268.5*	SS
H14-15	(2@10.6)14-7-i-3.5-2-26.6	2	10.6	6,980	26.5	0	A	196.5*	CB
H14-16	(2@10.6)14-7-3#4-i-3.5-2-26.6	2	10.6	6,810	25.9	0.178	A	235.3*	CB
H14-7	(3@3.5)14-6-i-3.5-2-35.8	3	3.5	6,390	36.4	0	A	250.8	CB
H14-8	(3@3.5)14-6-5#4-i-3.5-2-35.8	3	3.5	6,650	36.6	0.276	A	298.2	SS
H18-1	(2@8.0)18-16-6#5-i-3.5-2-26.6	2	8.0	15,310	28.5	0.233	A	358.2	CB
H18-2	(2@8.0)18-16-12#5-i-3.5-2-26.6	2	8.0	15,770	27.0	0.465	A	445	SS
H18-3	(2@8.0)18-7-6#5-i-3.5-2-35.8	2	8.0	7,560	36.5	0.233	A	371.4	CB
H18-4	(2@8.0)18-7-12#5-i-3.5-2-35.8	2	8.0	7,610	36.4	0.465	A	427.9*	CB

- n Number of bars
 s Center-to-center bar spacing
 f_{cm} Measured concrete compressive strength
 $\ell_{eh,avg}$ Average measured embedment length
 A_{th} Total area of tie legs within $9.5d_b$ from the centerline of hooked bars larger than No' 8 – this differs from the definition in ACI 318-19
 A_{hs} Total area of headed or hooked bars being developed
L. C. Loading condition, refer to Section 2.3.2
 T Total applied peak load divided by the number of bars
^[1] The first number after “H” denotes the bar size
^[2] CB: Concrete breakout, SS: Side splitting
^[3] One bar had a breakout and the other bar had a side-splitting failure
* Bars failed independently, so T is the average of the maximum force on individual bar. Individual results in Appendix B2

Table 3.4 Summary of anchorage strength results for headed bar specimens

ID ^[1]	Designation	n	s/d_b	f_{cm} psi	$\ell_{eh,avg}$ in.	A_{tl}/A_{hs}	L. C.	T kips	Failure Mode ^[2]
11-1	(2@10)11-15-O4.5-i-3.5-3.5-18.25	2	10.0	16,210	18.5	0	B	163.0	CB+SS
11-2	(2@10)11-15-O4.5-7#3-i-3.5-3.5-18.25	2	10.0	15,850	18.5	0.282	B	221.0	SS
14-2	(2@10.6)14-15-B4.2-5#4-i-3.5-3.5-20.5	2	10.6	12,830	20.5	0.267	A	190.6	SF
14-3	(2@10.6)14-7-L4.2-i-3.5-3.5-31.9	2	10.6	8,510	31.8	0	B	303.0*	SS
14-4	(2@10.6)14-7-L4.2-5#4-i-3.5-3.5-31.9	2	10.6	7,700	32.0	0.267	A	333.6	SS
14-15	(2@10.6)14-7-L4.2-i-3.5-3.5-22.7	2	10.6	6,190	22.8	0	B	204.8	CB+SS
14-16	(2@10.6)14-7-L4.2-3#4-i-3.5-3.5-22.7	2	10.6	5,390	22.6	0.178	A	123.6	SF
14-16A ^[3]	(2@10.6)14-7-L4.2-3#4-i-3.5-3.5-22.7	2	10.6	8,350	22.4	0.178	A	186.0	SF
14-1A	(2@10.6)14-15-L4.2-i-3.5-3.5-22.7	2	10.6	12,030	22.4	0	B	160.0	SF
14-2A	(2@10.6)14-15-L4.2-5#4-i-3.5-3.5-22.7	2	10.6	13,750	23.0	0.267	B	248.1	CB
14-16B	(2@10.6)14-7-L4.2-3#4-i-3.5-3.5-22.7	2	10.6	7,500	22.1	0.178	B	191.7	CB+SS
14-16C	(2@10.6)14-7-L4.2-7#4-i-3.5-3.5-22.7	2	10.6	6,470	22.6	0.356	B	229.6	SS
14-16D ^[4]	(2@10.6)14-7-L4.2-10#5-i-3.5-3.5-22.7	2	10.6	6,900	22.9	0.827	A	289.8*	SS
14-16E ^[4]	(2@10.6)14-7-L4.2-6#5-i-3.5-3.5-22.7	2	10.6	6,170	22.4	0.551	A	218.6	SS
14-16F ^[5]	(2@10.6)14-7-L4.2-6#5-i-3.5-3.5-22.7	2	10.6	5,640	22.4	0.551	A	197.8	SS
14-17 ^{[5][6]}	(2@7.1)14-7-L4.2-6#5-i-6.5-3.5-22.7	2	7.1	6,540	22.4	0.551	A	206.7	CB
14-5	(3@3.5)14-7-L4.2-5#4-i-3.5-3.5-22.7	3	3.5	6,830	22.3	0.178	B	181.8	CB
14-6	(3@3.5)14-7-L4.2-5#5-i-3.5-3.5-22.7	3	3.5	6,890	22.4	0.276	B	179.5	CB
14-7	(3@3.5)14-7-L4.2-i-3.5-3.5-31.9	3	3.5	7,080	32.1	0	B	252.1	CB+SS
14-8	(3@3.5)14-7-L4.2-5#5-i-3.5-3.5-31.9	3	3.5	7,100	31.7	0.276	B	274.6	CB+SS
14-9	(3@3.5)14-12-L4.2-5#5-i-3.5-3.5-22.7	3	3.5	11,480	22.1	0.276	B	173.9	CB
14-10 ^[4]	(3@3.5)14-7-L4.2-10#5-i-3.5-3.5-22.7	3	3.5	6,820	22.3	0.551	A	206.6	CB
18-1	(2@8.0)18-7-L4.4-14#5-i-3.5-3.5-31.1	2	8.0	5,750	32.6	0.543	A	322.0	SS
18-2	(2@8.0)18-15-H4.4-14#5-i-3.5-3.5-27.8	2	8.0	11,770	28.4	0.543	A	406.6	CB+SS
18-3	(2@8.0)18-7-O4.3-6#5-i-3.5-3.5-30.6	2	8.0	6,540	30.9	0.233	B	366.5	CB
18-4	(2@8.0)18-7-O4.3-12#5-i-3.5-3.5-30.6	2	8.0	7,200	30.9	0.465	B	380.0	SS
18-5 ^[6]	(2@5.3)18-7-L4.4-14#5-i-6.5-3.5-31.1	2	5.3	5,310	32.5	0.543	A	300.8	CB
18-6 ^[6]	(2@5.3)18-15-H4.4-14#5-i-6.5-3.5-27.8	2	5.3	10,230	28.6	0.543	A	419.8	SS
18-7 ^{[4][6]}	(3@2.7)18-7-L4.4-20#5-i-6.5-3.5-31.1	3	2.7	5,890	32.1	0.543	A	252.1	CB+SS
18-8 ^{[5][6]}	(3@2.7)18-7-L4.4-20#5-i-6.5-3.5-31.1	3	2.7	6,380	32.3	0.543	A	295.3	CB+SS

- n Number of bars
 s Center-to-center bar spacing
 f_{cm} Measured concrete compressive strength
 $\ell_{eh,avg}$ Average measured embedment length
 A_{tl} Total area of tie legs within $9.5d_b$ from the centerline of headed bars larger than No' 8 – this differs from the definition in ACI 318-19
 A_{hs} Total area of headed or hooked bars being developed
L. C. Loading condition, refer to Section 2.3.2
 T Total applied peak load divided by the number of bars
^[1] The first number in ID denotes the bar size.
^[2] CB: Primarily concrete breakout, SS: Primarily side splitting, CB+SS: Combination of breakout and side splitting
^[3] Specimen had an additional No. 11 longitudinal bar on both sides, 2 in. from the bearing face on the head
^[4] Double overlapping No. 5 ties were used, refer to Figure 2.5
^[5] Double No. 5 ties were used
^[6] Specimen had an increased side cover of 6.5 in.
* Bars failed independently, so T is the average of the maximum force on individual bar. Individual results in Appendix C2

CHAPTER 4: ANALYSIS AND DISCUSSION: HOOKED BARS

In this chapter, the test results of the hooked bar specimens are analyzed. First, the results are compared with stresses based on the provisions in ACI 318-19 to show the limitations of the current Code. The results are then compared with the forces obtained using the descriptive equations proposed by Ajaam et al. (2017, 2018), Eq. (1.1) and (1.2). New descriptive equations are then developed based on a database that includes the No. 14 and No. 18 bar test results from this study. Finally, the effects on anchorage strength of key parameters, such as confining reinforcement, bar size and spacing, and strut angle are discussed.

4.1 COMPARISON OF TEST RESULTS WITH ACI 318-19

The provisions in ACI 318-19 for the development of hooked bars are discussed in detail in Section 1.3.1. ACI 318-19 gives no credit to confining reinforcement or wide spacing for hooked bars larger than No. 11 and requires that a modification factor of $\psi_r = 1.6$ be applied for No. 14 and No. 18 bars (even if confining reinforcement is provided or the center-to-center spacing of the bars is $\geq 6d_b$) when calculating the development length using Eq. (1.7). To compare the test results with stresses corresponding to the Code equation, Eq. (1.7), yield strength f_y is replaced by bar stress, $f_{s,ACI}$, f'_c is replaced by the measured compressive strength, f_{cm} (with an upper limit of 10,000 psi), and development length ℓ_{dh} is replaced by the measured embedment length, ℓ_{eh} , and the equation is solved for $f_{s,ACI}$. To better evaluate the ACI 318-19 provisions for No. 14 and No. 18 bars, the ψ_r factor is taken as it is for No. 11 and smaller bars ($= 1.0$ if $s \geq 6d_b$ or $A_{th,ACI}/A_{hs}^2 \geq 0.4$), rather than applying 1.6 for all No. 14 and No. 18 bar specimens, which will result in very high $f_s/f_{s,ACI}$ values for the large bars.

$$f_{s,ACI} = \frac{55\lambda\sqrt{f_{cm}}\ell_{eh}}{\psi_e\psi_r\psi_o\psi_c d_b^{1.5}} \quad (4.1)$$

where ψ_e is the coating factor, ψ_r is the confining reinforcement factor, ψ_o is the location factor, ψ_c is the concrete strength factor, and λ is the concrete density factor as shown in Table 1.3.

Table 4.1 presents the measured bar stress at failure, f_s , and the ratio $f_s/f_{s,ACI}$ for the specimens in this study. The table also presents the values of bar forces T , T_h , and the ratio T/T_h ,

² A_{th} is defined differently in ACI 318-19 than in the descriptive equations. Code ($A_{th,ACI}$): total cross-sectional area of confining reinforcement within $15d_b$ from the centerline of hooked bars. Descriptive equations (A_{th}): within $8d_b$ for No. 9 and smaller bars and $10d_b$ for larger bars.

where T_h is based on the descriptive equations developed by Ajaam et al. (2017, 2018), as described in the next section, along with specimen ID and key parameters (number and spacing of bars, concrete compressive strength, embedment length, and confining reinforcement).

Table 4.1 Comparison of No. 14 and No. 18 hooked bar test results with descriptive equations by Ajaam et al. (2018), Eq. (1.1) and (1.2), also Eq. (4.2) and (4.3), and ACI 318-19. Eq. (4.1)

ID ^[1]	n	s/d_b	f_{cm} psi	$\ell_{eh,avg}$ in.	A_{th}/A_{hs}	$A_{th,ACI}/A_{hs}$	ψ_r	T kips	T_h kips	T/T_h	f_s ksi	$f_{s,ACI}$ ksi	$f_s/f_{s,ACI}$
H14-1	2	10.6	12,980	27.0	0	0	1.0	240.0	219.2	1.09	106.7	106.7	1.58
H14-2	2	10.6	13,010	24.8	0.267	0.356	1.0	293.9	248.2	1.18	130.6	130.6	2.11
H14-3	2	10.6	8,100	36.7	0	0	1.0	279.1	266.0	1.05	124.0	124.0	1.50
H14-4	2	10.6	7,570	34.9	0.267	0.356	1.0	268.5	295.1	0.91	119.3	119.3	1.57
H14-5	2	10.6	6,980	26.5	0	0	1.0	196.5	178.9	1.10	87.3	87.3	1.58
H14-6	2	10.6	6,810	25.9	0.178	0.267	1.0	235.3	204.9	1.15	104.6	104.6	1.96
H14-7	3	3.5	6,390	36.4	0	0	1.6	250.8	181.3	1.38	111.5	111.5	2.45
H14-8	3	3.5	6,650	36.6	0.276	0.367	1.6	298.2	252.0	1.18	132.5	132.5	2.85
H18-1	2	8.0	15,310	28.5	0.233	0.388	1.0	358.2	371.6	0.96	89.6	89.6	1.94
H18-2	2	8.0	15,770	27.0	0.465	0.620	1.0	445.0	452.4	0.98	111.3	111.3	2.54
H18-3	2	8.0	7,560	36.5	0.233	0.388	1.0	371.4	388.8	0.96	92.9	92.9	1.80
H18-4	2	8.0	7,610	36.4	0.465	0.620	1.0	427.9	482.7	0.89	107.0	107.0	2.08
								Max	1.38			Max	2.85
								Min	0.89			Min	1.50
								Mean	1.07			Mean	2.00
								CoV	0.132			CoV	0.228

- n Number of bars
- s Center-to-center spacing of bars
- d_b Nominal bar diameter
- f_{cm} Measured concrete compressive strength
- $\ell_{eh,avg}$ Average measured embedment length
- A_{th} Total area of tie legs within $9.5d_b$ from the centerline of hooked bars
- $A_{th,ACI}$ Total area of tie legs within $15d_b$ from the centerline of hooked bars
- A_{hs} Total area of hooked bars being developed
- f_s Bar stress at failure
- T Average force per bar at failure
- T_h Calculated failure load using descriptive equations (Ajaam et al. 2017, 2018), Eq. (1.1) and (1.2)
- $f_{s,ACI}$ Bar stress calculated based on ACI 318-19 equation
- [1] The first number after “H” denotes the bar size

Table 4.1 shows that ACI 318-19 provides very conservative estimates of anchorage strength for No. 14 and No. 18 hooked bars, with values of $f_s/f_{s,ACI}$ ranging from 1.50 to 2.85 with a mean of 2.00, demonstrating that ACI 318-19 requires unnecessarily long embedment lengths for No. 14 and No. 18 hooked bars. These high numbers are in spite of using $\psi_r = 1.0$ when $s/d_b \geq 6$ or $A_{th,ACI}/A_{hs} \geq 0.4$ (and not 1.6 for all specimens as required by ACI 318-19 for No. 14 and No. 18 hooked bars). A degree of the conservative nature reflected in these comparisons is expected

because, unlike the descriptive equation, the Code equation has an embedded strength reduction factor. The strength reduction factor alone, however, would result in $f_s/f_{s,ACI}$ values averaging near 1.25, not 2.00. Separate from the strength reduction factor, a key reason that the provisions in ACI 318-19 are conservative is that ψ_r does not account for the combined effects of widely-spaced bars and confining reinforcement, while the descriptive equation does. When widely-spaced bars are used and confining reinforcement is provided, the required development length can be safely reduced. As will be shown in Chapter 6, the proposed design provisions for hooked bars provide a modified ψ_r factor that varies as a function of s/d_b and A_{th}/A_{hs} , resulting in values < 1.0 when confining reinforcement is provided. Here, the use of $\psi_r = 1.0$ is due solely to bar spacing for specimens H14-2, H14-4, H18-1, and H18-3. All four specimens also contained confining reinforcement, which adds to anchorage strength that is not acknowledged by the current Code. Only for two of the specimens, H18-2 and H18-4, is $\psi_r = 1.0$ used due to confining reinforcement because $A_{th,ACI} \geq 0.4$. The highest values of $f_s/f_{s,ACI}$ are obtained for specimens H14-7 and H14-8, because neither has $s/d_b \geq 6$ or $A_{th,ACI}/A_{hs} \geq 0.4$, requiring that $\psi_r = 1.6$ under ACI 318-19. Both, however, have $s/d_b = 3.5$, and H18-4 has $A_{th,ACI} = 0.367$ ($A_{th,ACI} = 0.367$ for H18-3), which justify values of ψ_r below 1.6.

The ratio of bar stress measured in the tests to the bar stress calculated based on the ACI 318-19 equation, $f_s/f_{s,ACI}$, is plotted versus the concrete compressive strength (f_{cm}) in Figure 4.1. As shown in the figure, ACI 318-19 is unrealistically conservative, independent of concrete compressive strength. Clearly, improvements could be made in these provisions.

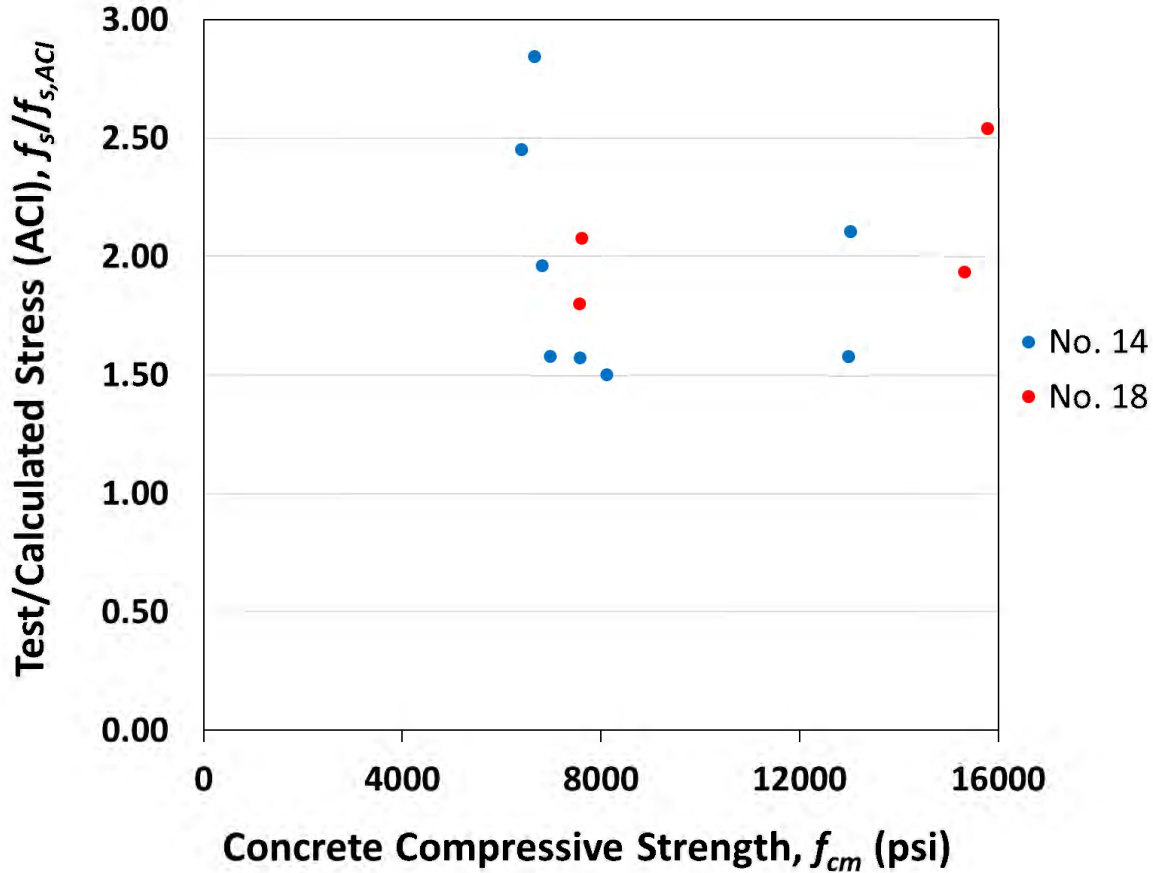


Figure 4.1 Ratio of test/calculated bar stress (ACI), $f_s/f_{s,ACI}$ versus concrete compressive strength f_{cm} for No. 14 and No. 18 hooked bar specimens (using values of ψ_r permitted for No. 11 and smaller bars, as shown in Table 4.1)

4.2 COMPARISON OF TEST RESULTS WITH DESCRIPTIVE EQUATIONS DEVELOPED BY AJAAM ET AL. (2017, 2018)

The descriptive equations to characterize the anchorage strength of hooked bars developed by Ajaam et al. (2017, 2018) based on test results for 245 beam-column joint specimens containing No. 5, No. 8, and No. 11 hooked bars without and with confining reinforcement are given in Eq. (1.1) and (1.2), respectively, and repeated here as Eq. (4.2) and (4.3).

$$T_h = 294 f_{cm}^{0.295} \ell_{eh}^{1.0845} d_b^{0.47} \left(0.0974 \frac{s}{d_b} + 0.391 \right) \quad (4.2)$$

where $\left(0.0974 \frac{s}{d_b} + 0.391 \right) \leq 1.0$.

$$T_h = \left(294 f_{cm}^{0.295} \ell_{eh}^{1.0845} d_b^{0.47} + 55,050 \left(\frac{A_{th}}{n} \right)^{1.0175} d_b^{0.73} \right) \left(0.0516 \frac{s}{d_b} + 0.6572 \right) \quad (4.3)$$

where $\left(0.0516 \frac{s}{d_b} + 0.6572 \right) \leq 1.0$.

and T_h is the anchorage strength of an individual hooked bar (lb); f_{cm} is the measured concrete compressive strength (psi); ℓ_{eh} is the embedment length of the hooked bar measured from the face of the column to the end of the hook (in.); d_b is the hooked bar diameter (in.); A_{hs} is the total area of the hooked bars (in.²); A_{th} is the effective confinement and defined as the area of confining reinforcement (in.²) within $8d_b$ from the top of the hooked bar for No. 8 bars and smaller or within $10d_b$ for No. 9 bars or larger; n is the number of hooked bars in the joint; and s is the center-to-center spacing between hooked bars. The specimens in this study were proportioned based on the descriptive equations.

To evaluate the applicability of Eq. (4.2) and (4.3) for No. 14 and No. 18 bars, the anchorage strengths measured in the tests, T (as reported in Table 3.4), are compared with the strengths calculated using the descriptive equations, T_h in Table 4.1. Table 4.2 summarizes the comparison of test results with Eq. (4.2) and (4.3), including the maximum, minimum, mean, standard deviation, and coefficient of variation. The specimens are categorized based on the presence of confining reinforcement in the joint region and bar size.

Table 4.2 Summary of test-to-calculated ratio for No. 14 and No. 18 hooked bars based on descriptive equations by Ajaam et a. (2017, 2018), Eq. (4.2) and (4.3)

	T/T_h				
	All	Without Confining Reinforcement	With Confining Reinforcement	No. 14	No. 18
No. of Specimens	12	4	8	8	4
Max	1.38	1.38	1.18	1.38	0.98
Min	0.89	1.05	0.89	0.91	0.89
Mean	1.07	1.16	1.03	1.13	0.95
STDEV	0.142	0.153	0.124	0.135	0.042
CoV	0.133	0.132	0.121	0.119	0.045

As shown in Table 4.2, the twelve hooked bar specimens had a mean test-to-calculated T/T_h ratio of 1.07 and a coefficient of variation of 0.133, with the values ranging from 0.89 to 1.38. The four specimens without confining reinforcement had a mean value of T/T_h of 1.16, higher than

the eight specimens with confining reinforcement with a mean value of T/T_h of 1.03. The mean value of T/T_h is 1.13 for the No. 14 bar specimens and 0.95 for the No. 18 bar specimens.

Student's t-test can be used to determine if the difference in the mean values is statistically significant. The type of t-test used in this study was homoscedastic (two-sample equal variance) with a two-tailed distribution. A threshold of 0.05 is used for the p value. Thus, if the p value is less than 0.05 the probability that the difference in to values occurred by chance is less than 5%. Values of p above 0.05 indicate the difference was not due to any meaningful difference in behavior.

Although the comparisons with Eq. (4.2) and (4.3) appear to be more conservative for the specimens without confining reinforcement than for the specimens with confining reinforcement (mean $T/T_h = 1.16$ and 1.03 , respectively), $p = 0.144$, indicating that the difference in the mean values is not statistically significant. In terms of bar size, however, the difference in the mean values of T/T_h for the No. 14 and No. 18 bar specimens, 1.13 and 0.95 , respectively, with $p = 0.026$.

4.3 NEW DESCRIPTIVE EQUATIONS

In this section, the descriptive equations developed for No. 11 and smaller hooked bars are updated by adding the No. 14 and 18 bar test results from this study to the database. Using the same procedure by Ajaam et al. (2017), an equation is first developed for specimens with widely-spaced bar (center-to-center spacing $\geq 6d_b$) without confining reinforcement using an iterative analysis resulting in $T/T_h = 1.00$. The effect of close bar spacing is then accounted for. The same procedure is then repeated for specimens with confining reinforcement. The database used by Ajaam et al. (2017, 2018) to develop the previous equations is used along with the results for the No. 14 and No. 18 bar specimens tested in this study. Eleven specimens with an effective beam depth to embedment length ratio (d_{eff}/ℓ_{eh} , as will be discussed in detail in Section 4.4.5) greater than 1.5 are removed from the analysis. Those include three No. 6 bar specimens by Ramirez and Russell (2008) and three No. 8 and five No. 11 bar specimens by Sperry et al. (2015b) and Ajaam (2017).

4.3.1 Widely-spaced Bars Without Confining Reinforcement

Developing a new descriptive equation starts with obtaining an expression for the 76 specimens with widely-spaced bars without confining reinforcement. The specimens include No. 7 hooked bars tested by Lee and Park (2010). The specimen details are presented in Table B.2 of

Section B3 (Specimens tested at the University of Kansas) and Table B.8 of Section B4 (Specimens tested in other studies) in Appendix B. The resulting expression is

$$T_c = 319 f_{cm}^{0.281} \ell_{eh}^{1.106} d_b^{0.430} \quad (4.4)$$

where T_c is the anchorage strength of hooked bars without confining reinforcement (lb), f_{cm} is concrete compressive strength on the day of test (psi), ℓ_{eh} is embedment length (in.), and d_b is bar diameter (in.). Compared with Eq. (4.2) developed by Ajaam et al. (2017, 2018), the constant has increased from 294 to 319, the power of f_{cm} has decreased from 0.295 to 0.281, the power of ℓ_{eh} has increased from 1.0845 to 1.106, and the power of d_b has decreased from 0.470 to 0.430. Figure 4.2 compares f_{cm} with T/T_c as a function of f_{cm} for the 76 specimens used to develop Eq. (4.4).

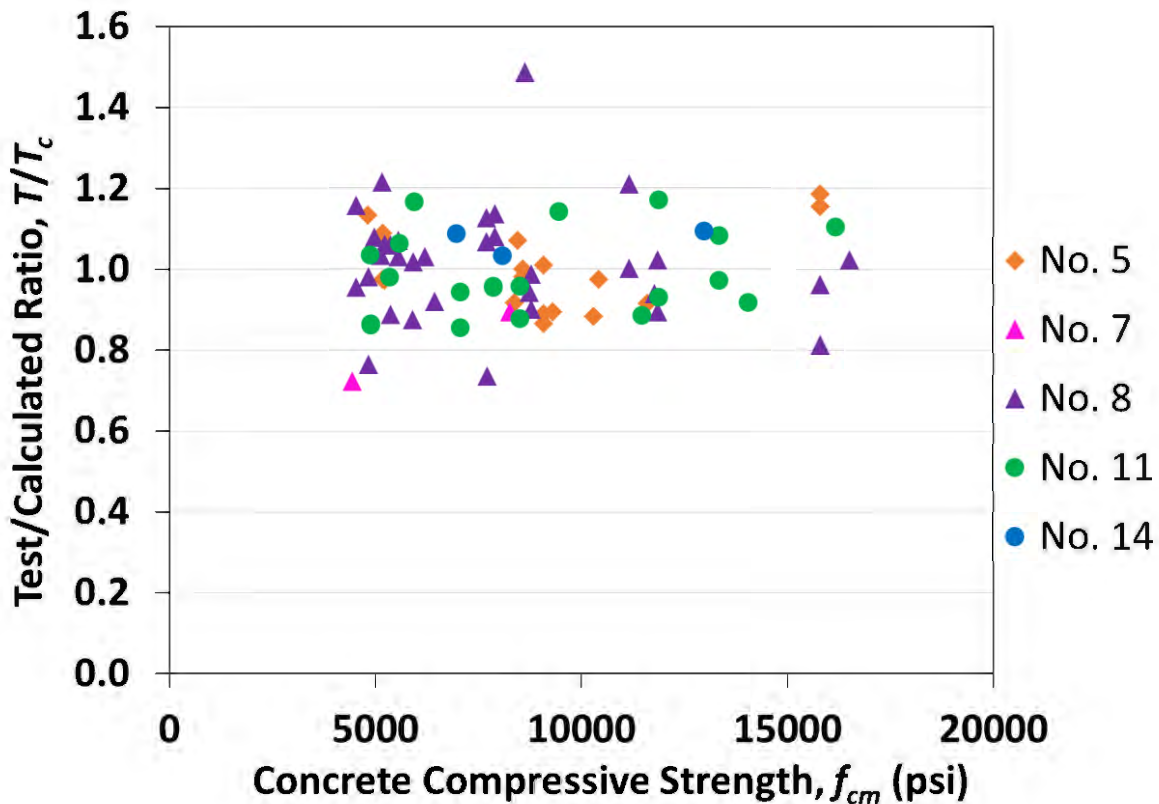


Figure 4.2 Ratio of test-to-calculated bar force at failure T/T_c versus concrete compressive strength for hooked bar specimens with widely-spaced bars (center-to-center spacing $\geq 6d_b$) without confining reinforcement

As shown in Figure 4.2, no noticeable trend is observed, indicating that the 0.281 power of f_{cm} captures the effect of concrete compressive strength. The statistical parameters for T/T_c are shown in Table 4.3, where T/T_c ranges from 0.72 to 1.49, with a mean of 1.00 and a coefficient of

variation of 0.122. Equation (4.4) is conservative for No. 14 bars with a mean of 1.07, but less so than Eq. (4.2) (mean = 1.13). At 0.81, the mean value of T/T_c are especially low for two No. 7 bar specimens tested by Lee and Park (2010).

Table 4.3 Statistical parameters of T/T_c ratio using Eq. (4.4) for hooked bar specimens with widely-spaced bars (center-to-center spacing $\geq 6d_b$) without confining reinforcement

Bar size	All	No. 5	No. 7	No. 8	No. 11	No. 14
No. of specimens	76	18	2	33	20	3
Max	1.49	1.19	0.89	1.49	1.17	1.09
Min	0.72	0.87	0.72	0.74	0.86	1.03
Mean	1.00	1.00	0.81	1.01	0.99	1.07
STDEV	0.122	0.099	0.120	0.141	0.103	0.027
CoV	0.122	0.099	0.149	0.139	0.105	0.025

4.3.2 Closely-spaced Bars Without Confining Reinforcement

For the 26 specimens with closely-spaced bars ($s/d_b < 6$, where s is the center-to-center spacing of hooked bars) without confining reinforcement, the values of T/T_c , with T_c based on Eq. (4.4), are plotted versus s/d_b in Figure 4.3. The specimens include two No. 7 bars by Hamad et al. (2003) and three No. 11 bars by Ramirez and Russell (2008). These specimens were tested as cantilevers, meaning the bottom of the columns were fixed and the only forces applied to specimens were tension on hooked bars and compression at the simulated beam. The specimens were retained for developing descriptive equations for consistency. Ajaam et al. (2017, 2018) also included six No. 7 bar specimens by Marques and Jirsa (1975), but those specimens are not used here due to their unrealistic geometry and proportions as well as yielding of the bars accompanied by relatively high bar slips, as discussed in detail in Section 4.5. The specimen details are presented in Table B.3 of Section B3 (Specimens tested at the University of Kansas) and Table B.8 of Section B4 (Specimens tested in other studies) in Appendix B.

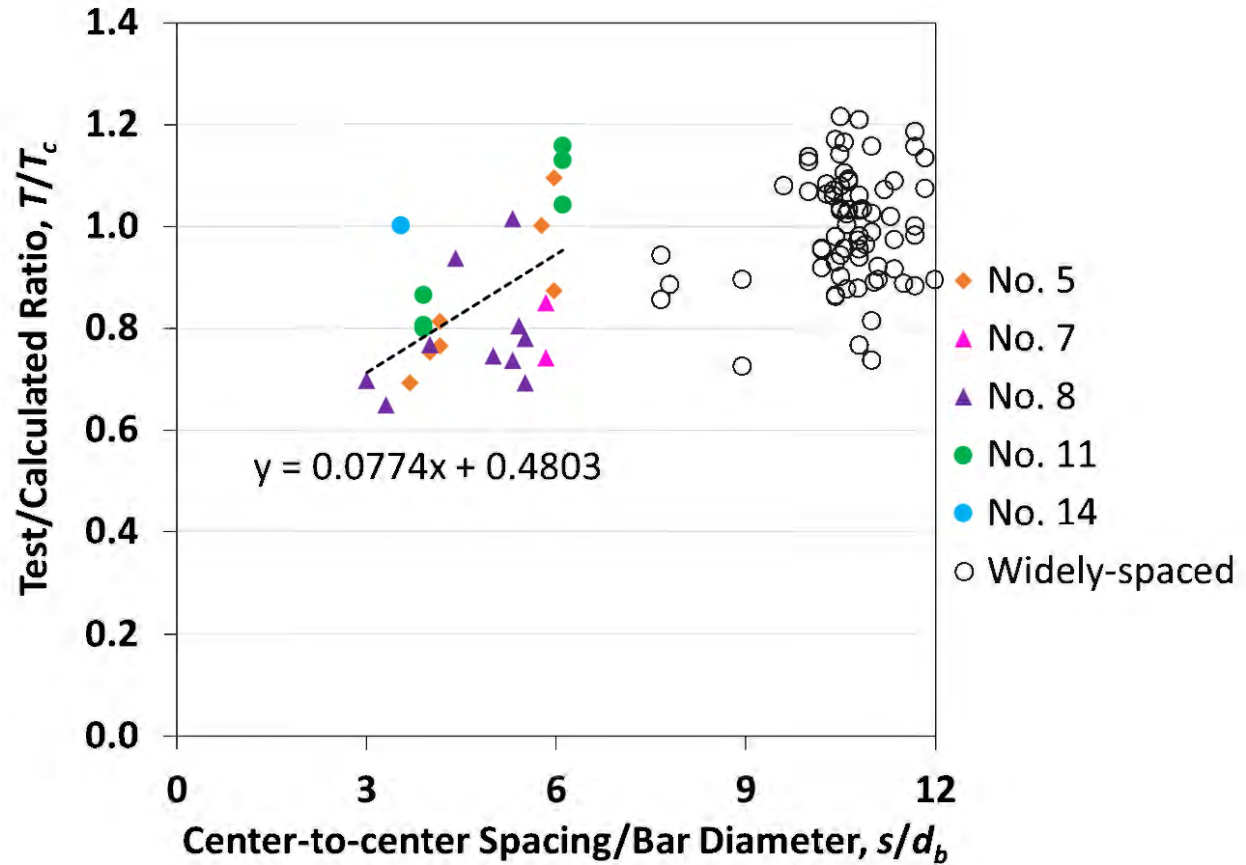


Figure 4.3 Test-to-calculated bar force at failure T/T_c versus ratio of center-to-center spacing to bar diameter s/d_b for widely- and closely-spaced hooked bars without confining reinforcement

As shown in Figure 4.3, the T/T_c ratio decreases with a decrease in s/d_b . T/T_c approaches 1.0 at $s/d_b = 6.0$. The linear trendline equation can be used as a multiplier to account for the effect of close bar spacing. When used in conjunction with Eq. (4.4), the equation for widely- and closely-spaced bars without confining reinforcement becomes

$$T_c = \left(319 f_{cm}^{0.281} \ell_{eh}^{1.106} d_b^{0.430} \right) \left(0.0774 \frac{s}{d_b} + 0.4803 \right) \quad (4.5)$$

where $\left(0.0774 \frac{s}{d_b} + 0.4803 \right) \leq 1.0$

It is worth noting that incorporating the effect of close bar spacing may actually be a convenient proxy for a bar group effect. For both hooked and headed bars, the majority of specimens with closely-spaced bars contain 3 or 4 bars, whereas all specimens with widely-spaced bars contain 2 bars. Therefore, what is considered to be the effect of close bar spacing on anchorage

strength, may be the effect of a greater total force on a member of fixed size. The center-to-center bar spacing, however, is a simple and safe proxy to take this effect into account.

The statistical parameters for the 26 specimens with closely-spaced bars and without confining reinforcement are shown in Table 4.4.

Table 4.4 Statistical parameters of T/T_c ratio using Eq. (4.5) for hooked bar specimens with closely-spaced ($s/d_b < 6d_b$) bars without confining reinforcement

Bar size	All	No. 5	No. 7	No. 8	No. 11	No. 14
No. of specimens	26	7	2	10	6	1
Max	1.33	1.16	0.91	1.14	1.22	1.33
Min	0.76	0.91	0.80	0.76	1.02	1.33
Mean	1.00	1.00	0.85	0.93	1.11	1.33
STDEV	0.141	0.092	0.083	0.126	0.079	0
CoV	0.141	0.092	0.097	0.135	0.071	0

As shown in Table 4.4 the T/T_c ratio ranged from 0.76 to 1.33 with a mean of 1.00 and a coefficient of variation of 0.141 for the specimens with closely-spaced bars and without confining reinforcement. The mean values range from 0.85 for No. 7 bars to 1.11 for No. 11 bars. T/T_c for the sole No. 14 bar is 1.33. T/T_c is plotted as a function of f_{cm} in Figure 4.4 for the 100 specimens without confining reinforcement. No visible trend is apparent, indicating that the effect of concrete compressive strength is adequately captured by Eq. (4.5). The statistical parameters of T/T_c ratio are presented in Table 4.5 for all specimens without confining reinforcement.

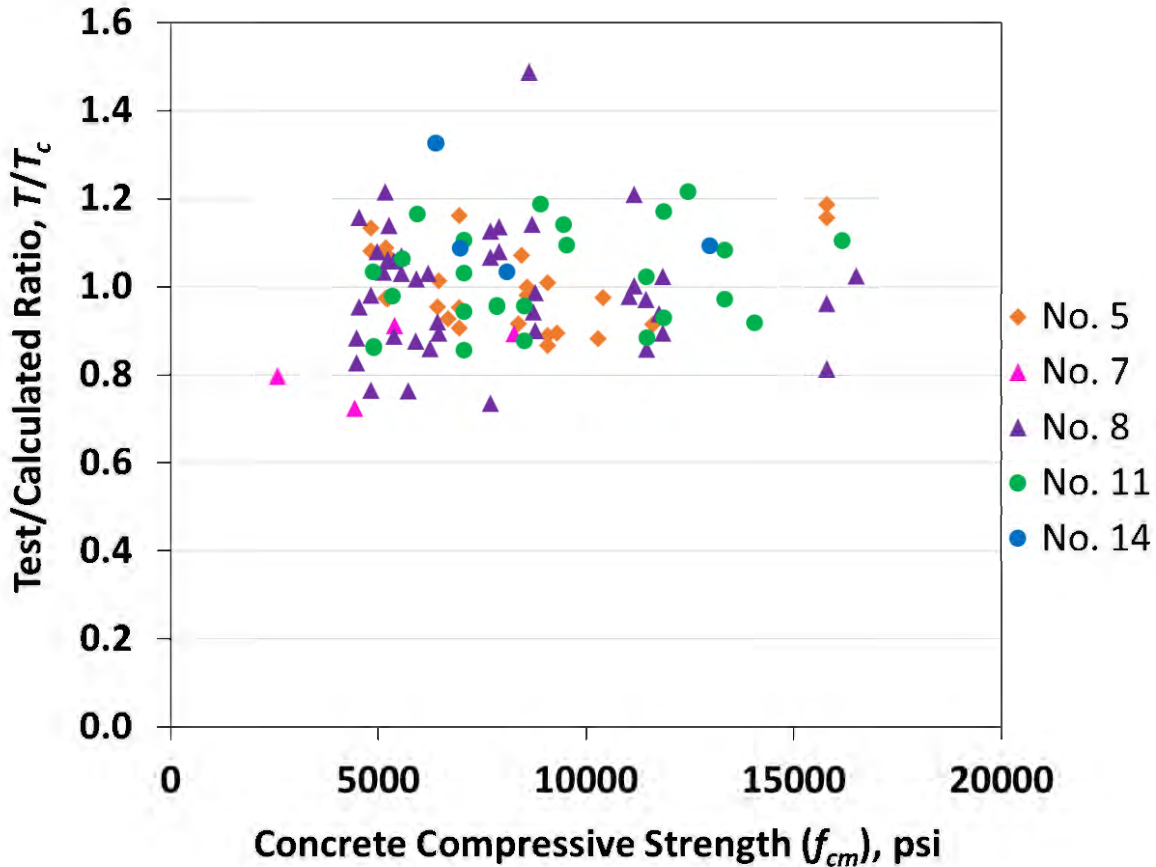


Figure 4.4 Ratio of test-to-calculated failure load T/T_c versus concrete compressive strength for hooked bar specimens having widely- and closely-spaced bars without confining reinforcement

Table 4.5 Statistical parameters of T/T_c ratio using Eq. (4.5) for hooked bar specimens with widely- and closely-spaced bars without confining reinforcement

Bar size	All	No. 5	No. 7	No. 8	No. 11	No. 14
No. of specimens	102	25	4	43	26	4
Max	1.49	1.19	0.89	1.49	1.22	1.33
Min	0.72	0.87	0.72	0.74	0.86	1.03
Mean	1.00	1.00	0.81	1.00	1.01	1.13
STDEV	0.128	0.095	0.120	0.141	0.110	0.131
CoV	0.128	0.095	0.149	0.142	0.109	0.115

As shown in Table 4.5, the 102 specimens without confining reinforcement had a mean T/T_c of 1.00, with individual values ranging from 0.72 to 1.49 with a coefficient of variation of 0.128. Based on bar size, the mean value of T/T_c ranges from 0.81 for the No. 7 bar specimens to 1.13 for the No. 14 bar specimens.

4.3.3 Widely-spaced Bars with Confining Reinforcement

The next step is developing an expression for the contribution of confining reinforcement. To begin, the same iterative analysis is performed for 54 specimens having widely-spaced bars with confining reinforcement (all tested at the University of Kansas as presented in detail in Table B.4 in Section B3 of Appendix B). The expression for the contribution of the confining steel, T_s , is added to the expression for the contribution of concrete, T_c , shown in Eq. (4.4), giving

$$T^h = T^c + T^s = 319 f_{cm}^{0.281} \rho_{1.106}^b d_b^{0.430} + 54,568 \left(\frac{A_h}{n} \right)^{0.693} d_b^n \quad (4.6)$$

where A_h is total cross-sectional area (in²) of tie legs within $8d_b$ from the top of the hooked bar for No. 8 bars and smaller or within $10d_b$ for No. 9 bars or larger, and n is the number of bars. Compared with the previous descriptive equation, Eq. (4.3), the constant in the T_s term has slightly decreased from 55,050 to 54,568, the power of A_h/n has decreased from 1.0175 to 1.0, and the power of d_b has decreased from 0.73 to 0.693. Figure 4.5 compares T/T_h calculated based on Eq. (4.6) with f_{cm} . As observed in the figure, Eq. (4.6) adequately captures the effect of concrete compressive strength, with no positive or negative trend in the data as a function of concrete compressive strength. Table 4.6 presents the statistical parameters of T/T_h for the specimens with widely-spaced bars and confining reinforcement.

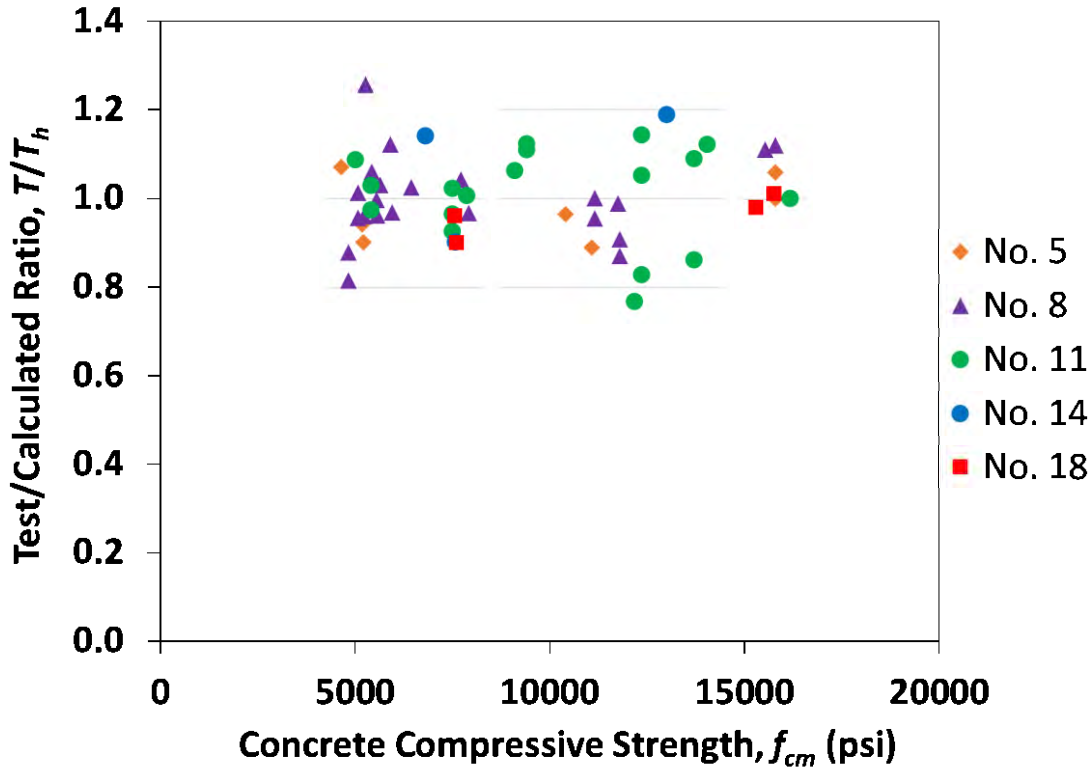


Figure 4.5 Ratio of test-to-calculated bar force at failure T/T_h versus concrete compressive strength for hooked bar specimens having widely-spaced ($s/d_b \geq 6d_b$) bars with confining reinforcement

Table 4.6 Statistical parameters of T/T_h ratio using Eq. (4.6) for hooked bar specimens with widely-spaced ($s/d_b \geq 6d_b$) bars with confining reinforcement

Bar size	All	No. 5	No. 8	No. 11	No. 14	No. 18
No. of specimens	54	7	22	18	3	4
Max	1.26	1.07	1.26	1.14	1.19	1.01
Min	0.77	0.89	0.82	0.77	0.90	0.90
Mean	1.00	0.98	1.00	1.01	1.08	0.96
STDEV	0.098	0.072	0.097	0.107	0.154	0.047
CoV	0.098	0.074	0.097	0.106	0.143	0.048

As shown in Table 4.6, T/T_h ranges from 0.77 to 1.26 with a mean of 1.00 and a coefficient of variation of 0.098. Based on bar size, the mean values of T/T_h range from a low of 0.96 for the No. 18 bar specimens to a high of 1.08 the No. 14 bar specimens.

4.3.4 Closely-spaced Bars with Confining Reinforcement

The last step in developing the new descriptive equations is to account for close bar spacing for specimens with confining reinforcement. The same approach used for specimens without confining reinforcement (Section 4.3.2) is followed. Figure 4.6 shows the plot of T/T_h versus s/d_b for 23 specimens having closely-spaced bars with confining reinforcement (all tested at the University of Kansas as presented in Table B.5 in Section B3 of Appendix B).

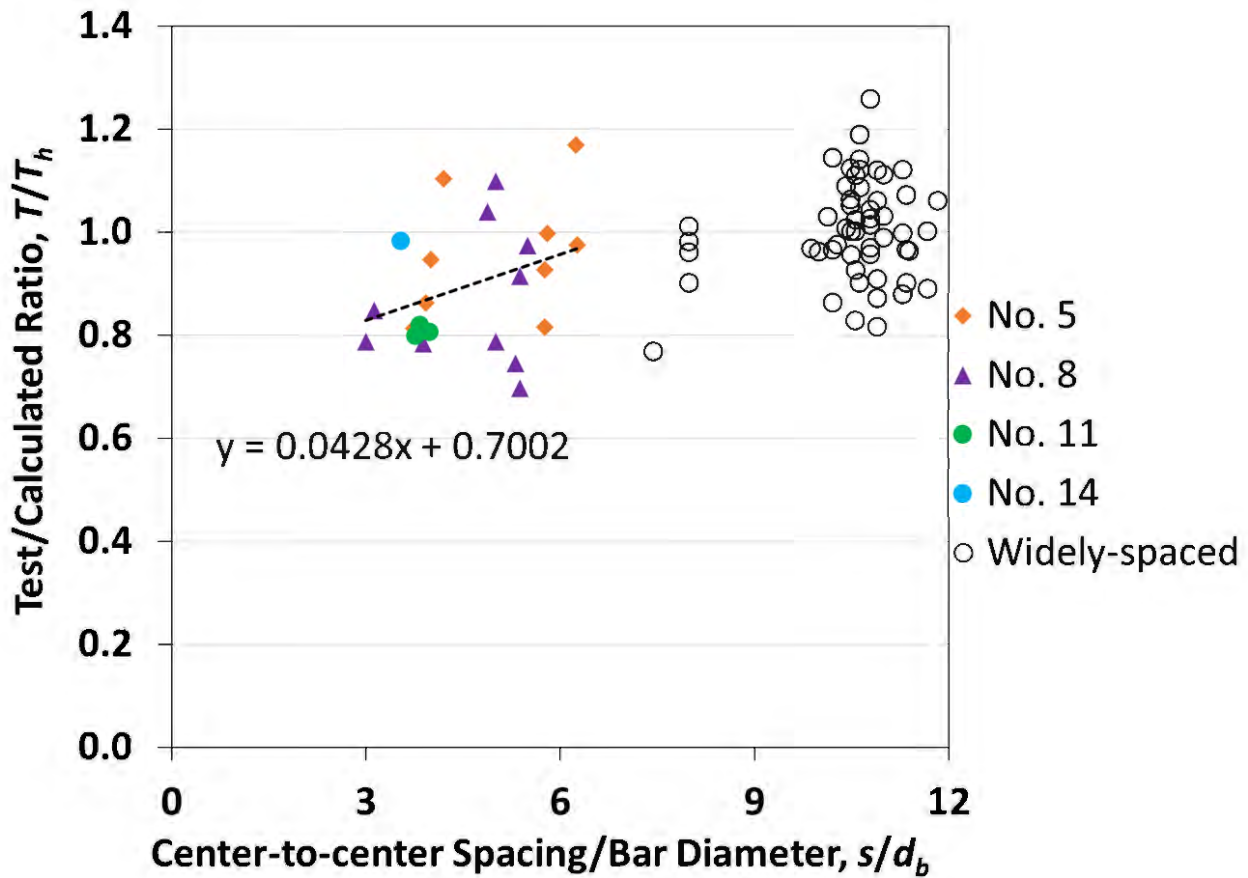


Figure 4.6 Test-to-calculated bar force at failure T/T_h versus ratio of center-to-center spacing to bar diameter s/d_b for widely- and closely-spaced hooked bars with confining reinforcement

As shown in Figure 4.6, the correlation between anchorage strength and bar spacing is not strong for hooked bars with confining reinforcement and is less significant than it is for specimens without confining reinforcement, indicating the adverse effects of having closely-spaced bars are less detrimental when confining reinforcement is used. The linear trendline equation given in Figure 4.6 is multiplied by Eq. (4.6) to give the final equation for specimens with confining reinforcement having widely- and closely spaced bars:

$$T_h = \left(319 f_{cm}^{0.281} \ell_{eh}^{1.106} d_b^{0.430} + 54,568 \left(\frac{A_{th}}{n} \right) d_b^{0.693} \right) \left(0.0428 \frac{s}{d_b} + 0.7002 \right) \quad (4.7)$$

where $\left(0.0428 \frac{s}{d_b} + 0.7002 \right) \leq 1.0$

The statistical parameters for T/T_h using Eq. (4.7) for specimens with closely-spaced bars and confining reinforcement are shown in Table 4.7. T/T_h ranges from 0.75 to 1.25 with a mean of 1.00 and a coefficient of variation of 0.130. Based on bar size, the mean value of T/T_h ranges from a low of 0.93 for the No. 11 bar specimens to a high of 1.04 for the No. 5 bar specimens. T/T_h equals 1.15 for the single No. 14 bar specimen.

Table 4.7 Statistical parameters of T/T_h ratio using Eq. (4.7) for hooked bar specimens with closely-spaced bars with confining reinforcement

Bar size	All	No. 5	No. 8	No. 11	No. 14
No. of specimens	23	9	10	3	1
Max	1.25	1.25	1.20	0.95	1.15
Min	0.75	0.86	0.75	0.93	1.15
Mean	1.00	1.04	0.97	0.93	1.15
STDEV	0.130	0.124	0.143	0.012	0
CoV	0.130	0.119	0.148	0.013	0

Table 4.8 presents the statistical parameters of T/T_h for all specimens with confining reinforcement. T/T_h ratio ranges from 0.75 to 1.26, with a mean of 1.00 and a coefficient of variation of 0.107. Based on bar size, the mean value of T/T_h ranges from a low of 0.99 for the No. 8 to a high of 1.10 for No. 14 bar specimens.

Table 4.8 Statistical parameters of T/T_h ratio using Eq. (4.7) for hooked bar specimens with widely- and closely-spaced bars with confining reinforcement

Bar size	All	No. 5	No. 8	No. 11	No. 14	No. 18
No. of specimens	77	16	32	21	4	4
Max	1.26	1.25	1.26	1.14	1.19	1.01
Min	0.75	0.86	0.75	0.77	0.90	0.90
Mean	1.00	1.01	0.99	1.00	1.10	0.96
STDEV	0.107	0.107	0.112	0.102	0.131	0.047
CoV	0.107	0.106	0.113	0.102	0.120	0.048

Figure 4.7 compares T/T_h with the concrete compressive strength for the specimens with confining reinforcement. Similar to Figure 4.5, no noticeable trend can be detected. Thus, the descriptive equations developed in this study represent the effect of concrete strength for all of the specimens in the database.

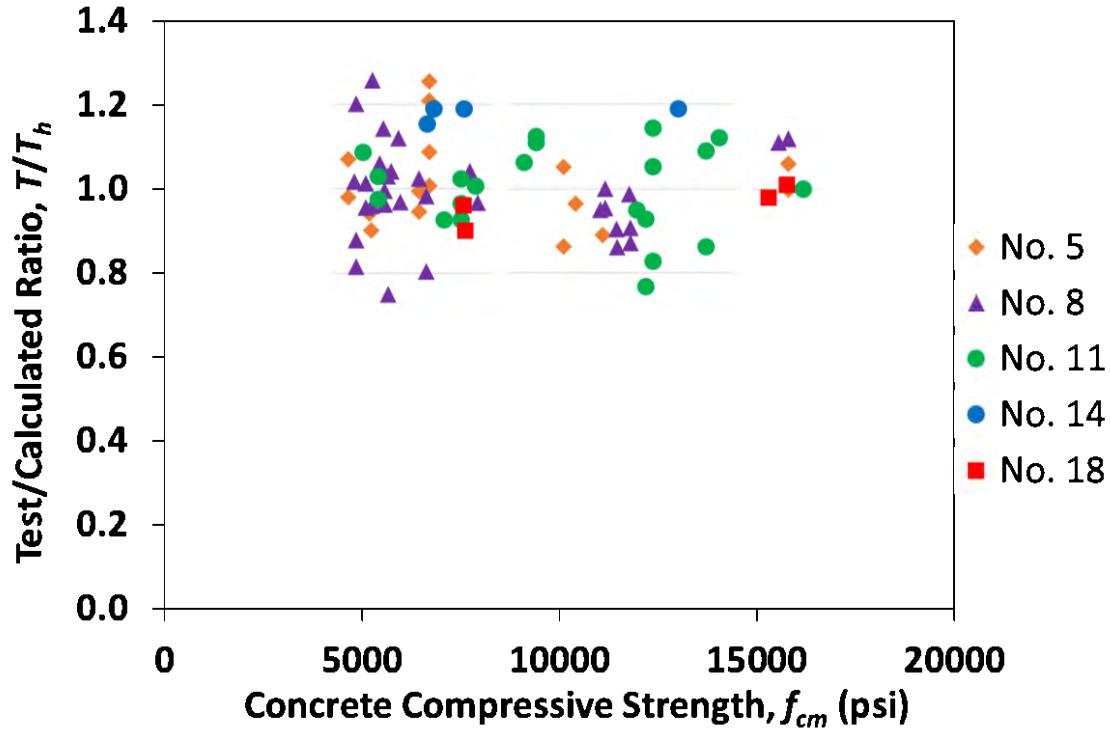


Figure 4.7 Ratio of test-to-calculated bar force at failure T/T_h versus concrete compressive strength for hooked bar specimens having widely- and closely-spaced bars with confining reinforcement

4.3.5 Summary

Table 4.9 presents the statistical parameters of T/T_h for all hooked bar specimens used to develop the descriptive equations.

Table 4.9 Statistical parameters of T/T_h ratio using Eq. (4.5) and (4.7) for all hooked bar specimens used to develop the descriptive equations

Bar size	All	No. 5	No. 7	No. 8	No. 11	No. 14	No. 18
No. of specimens	179	41	4	75	47	8	4
Max	1.49	1.25	0.89	1.49	1.22	1.33	1.01
Min	0.72	0.86	0.72	0.74	0.77	0.90	0.90
Mean	1.00	1.01	0.81	0.99	1.01	1.12	0.96
STDEV	0.117	0.099	0.098	0.129	0.106	0.123	0.047
CoV	0.117	0.099	0.122	0.130	0.105	0.110	0.048

As shown in Table 4.9, the test-to-calculated ratio T/T_h for all hooked bar specimens used to develop the new descriptive equations ranged from 0.72 to 1.49 with a mean of 1.00 and a coefficient of variation of 0.117. For No. 14 and No. 18 bars, the new equations provide improved coefficient of variation and mean compared with the equations developed previously for No. 11 and smaller bars by Ajaam et al. (2017, 2018), Eq. (4.2) and (4.3). Similar to Eqs. (4.2) and (4.3), the new equations are more conservative for No. 14 bars than No. 18 bars.

For the specimens in the database, the measured bar force at failure T is compared with the calculated failure load T_h in Figure 4.8. As shown in the figure, the best fit trendline for the specimens closely matches the dashed line representing $T = T_h$. The new descriptive equations are evaluated for No. 14 and No. 18 bars in Table 4.10.

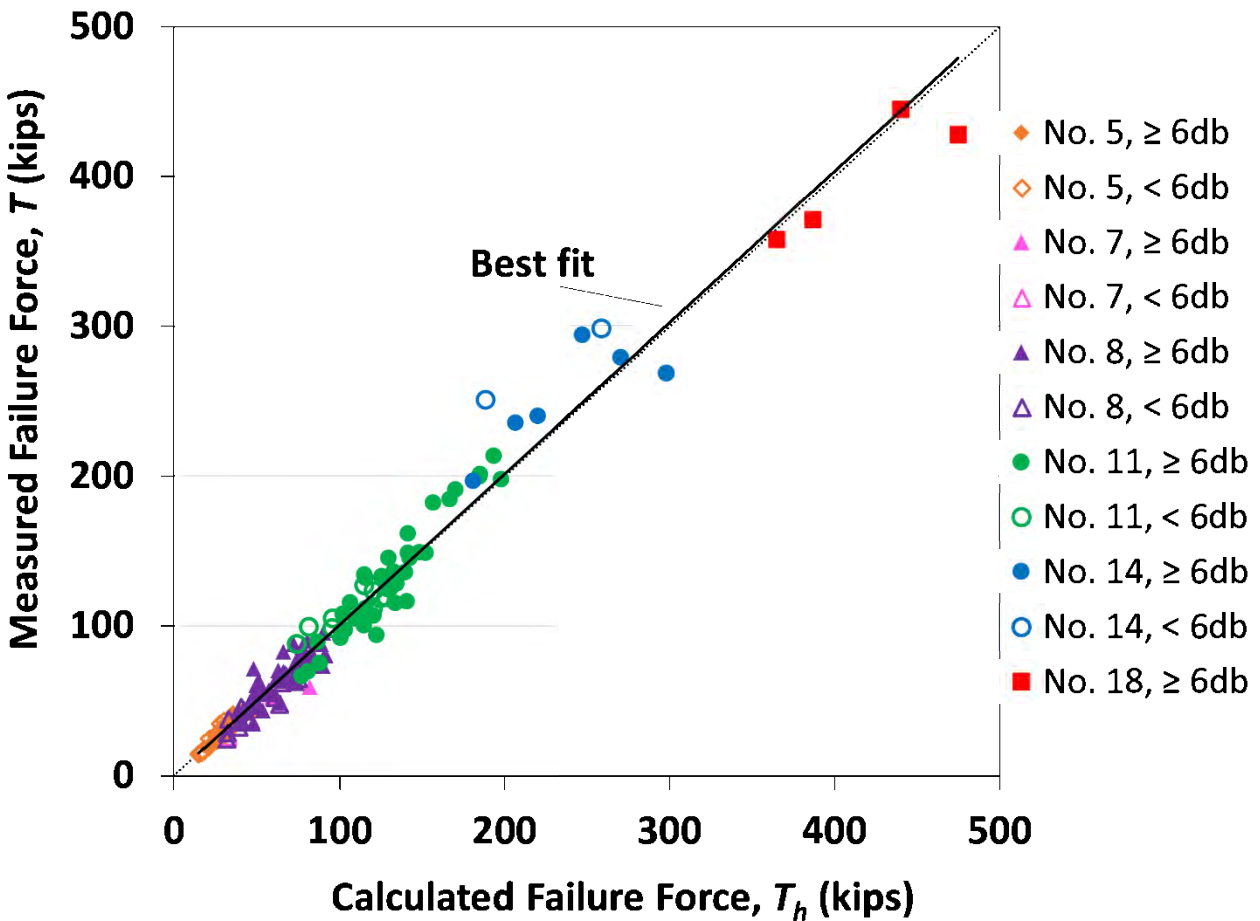


Figure 4.8 Measured versus calculated bar force at failure based on new descriptive equations for hooked bars, Eq. (4.5) and (4.7)

Table 4.10 Summary of test-to-calculated ratio T/T_h using Eq. (4.5) and (4.7) for No. 14 and No. 18 hooked bar specimens tested in this study

	T/T_h				
	All	Without Confining Reinforcement	With Confining Reinforcement	No. 14	No. 18
No. of Specimens	12	4	8	8	4
Max	1.33	1.33	1.19	1.33	1.01
Min	0.90	1.03	0.90	0.90	0.90
Mean	1.06	1.14	1.03	1.12	0.96
STDEV	0.127	0.133	0.116	0.124	0.047
CoV	0.119	0.117	0.112	0.111	0.048

As shown in Table 4.10, Eq. (4.5) and (4.7) are more conservative for No. 14 bars than No. 18 bars, with respective values of T/T_h of 1.12 and 0.96 for the No. 14 and No. 18 bar specimens, respectively, a difference that is statistically significant, with a p value of 0.042. Equations (4.5) and (4.7) give more conservative results, on average, for specimens without confining reinforcement than those with confining reinforcement, with respective mean T/T_h values of 1.14 and 1.03, similar to 1.16 and 1.03 obtained using Eq. (4.2) and (4.3). Overall, the new descriptive equations provide comparable results for No. 14 bars but are improved for No. 18 bars, compared with Eq. (4.2) and (4.3) developed for No. 11 and smaller bars. Compared with Eq. (4.2) and (4.3), the new equations have a lower overall coefficient of variation for No. 14 and No. 18 bar specimens (0.119 versus 0.133). Overall, Eq. (4.5) and (4.7) are appropriate for characterizing the anchorage strength of large hooked bars.

4.4 EVALUATING DESCRIPTIVE EQUATIONS

In this section, the descriptive equations are evaluated with respect to several key parameters, including bar location, confining reinforcement, bar spacing, strut angle, effective beam depth, and embedment length. In Section 4.5, the results for specimens not used to develop descriptive equations are investigated.

4.4.1 Bar Location

In accordance with Table 25.4.3.2 of ACI 318-19, the modification factor for bar location, ψ_o , is 1.0 for hooked bars terminating inside column longitudinal reinforcement (column core) with side cover normal to plane of hook ≥ 2.5 in., or with side cover normal to plane of hook $\geq 6d_b$. In all other cases, $\psi_o = 1.25$. These factors were adopted based on comparisons made by

Sperry et al. (2015b) and Ajaam et al. (2017, 2018) between 13 pairs of specimens with hooked bars placed outside versus inside the column core. The comparisons showed that specimens with hooked bars placed outside column core exhibited lower anchorage strength than the companion specimen with hooked bars inside the column core in 12 of 13 cases. $T_{outside}/T_{inside}$ ranged from 0.66 to 1.03 with an average of 0.85. The reduction in anchorage strength was then taken conservatively as 80% (therefore, $1/0.8 = 1.25$).

In this section, all of the specimens, not just paired specimens, tested by Sperry (2015b) and Ajaam et al. (2017) with hooked bars placed outside the column core are re-analyzed using the descriptive equations developed in this study, Eq. (4.5) and (4.7), to establish a more accurate bar location factor. Table 4.11 presents the key properties of these specimens along with their T/T_h ratio. Details of these specimens are presented in Table B.6 of Section B3 (specimens tested at the University of Kansas) of Appendix B.

Table 4.11 Test-to-calculated T/T_h ratio based on Eq. (4.5) and (4.7) for specimens with hooked bars placed outside column core (Ajaam et al. 2017)

Specimen ID	n	ℓ_{eh}	f_{cm}	d_b	s/d_b	A_{th}/A_{hs}	T	T_h	T/T_h
		in.	psi	in.			kips	kips	
5-5-90-0-o-1.5-2-5	2	5	4930	0.63	9.8	0	14.1	16.9	0.83
5-5-90-0-o-2.5-2-5	2	4.8	4930	0.63	9.2	0	19.3	16.2	1.19
5-5-90-0-o-1.5-2-6.5	2	6.2	5650	0.63	9.5	0	17.8	22.3	0.80
5-5-90-0-o-1.5-2-8	2	7.9	5650	0.63	9.5	0	22.8	29.2	0.78
5-5-90-0-o-2.5-2-8	2	9	5780	0.63	9.5	0	26.1	33.9	0.77
5-5-180-0-o-1.5-2-9.5	2	9.4	4420	0.63	9.2	0	29.5	33.0	0.89
5-5-180-0-o-2.5-2-9.5	2	9.5	4520	0.63	9.5	0	30.1	33.6	0.90
5-5-180-0-o-1.5-2-11.25	2	11.3	4520	0.63	9.5	0	32.4	40.8	0.80
5-5-180-2#3-o-2.5-2-9.5	2	9.2	4420	0.63	10.0	0.350	35.5	36.6	0.97
5-5-180-2#3-o-1.5-2-11.25	2	11.6	4420	0.63	10.0	0.350	43.1	46.0	0.94
5-5-180-2#3-o-1.5-2-9.5	2	8.8	4520	0.63	10.0	0.350	20.3	35.2	0.58
5-5-180-2#3-o-2.5-2-11.25	2	11.3	4520	0.63	10.0	0.350	42.3	45.1	0.94
5-5-90-5#3-o-1.5-2-5	2	5	5205	0.63	9.8	1.060	21.8	30.2	0.72
5-5-90-5#3-o-2.5-2-5	2	5.2	4930	0.63	10.0	1.060	22.5	30.7	0.73
5-5-90-5#3-o-1.5-2-8	2	7.9	5650	0.63	9.7	1.060	25.1	42.2	0.59
5-5-90-5#3-o-2.5-2-8	2	7.5	5650	0.63	9.8	1.060	24.9	40.6	0.61
5-5-90-5#3-o-1.5-2-6.5	2	6.5	5780	0.63	9.8	1.060	21.7	36.7	0.59
8-5-90-0-o-2.5-2-10a	2	10.4	5270	1	9.0	0	42.3	47.3	0.89
8-5-90-0-o-2.5-2-10b	2	9.8	5440	1	9.0	0	33.7	44.7	0.75
8-5-90-0-o-2.5-2-10c	2	10.6	5650	1	9.0	0	56.0	49.3	1.14
8-8-90-0-o-2.5-2-8	2	8.4	8740	1	8.0	0	33.0	43.1	0.77
8-8-90-0-o-3.5-2-8	2	7.8	8810	1	8.8	0	35.9	39.8	0.90
8-8-90-0-o-4-2-8	2	8.2	8630	1	8.8	0	37.5	41.8	0.90

8-5-90-5#3-o-2.5-2-10a	2	10.4	5270	1	9.1	0.420	54.3	65.4	0.83
8-5-90-5#3-o-2.5-2-10b	2	10.5	5440	1	9.1	0.420	65.6	66.4	0.99
8-5-90-5#3-o-2.5-2-10c	2	10.9	5650	1	9.1	0.420	57.7	69.0	0.84
8-8-90-5#3-o-2.5-2-8	2	8.5	8630	1	8.5	0.420	58.0	61.6	0.94
8-8-90-5#3-o-3.5-2-8	2	7.9	8810	1	8.7	0.420	55.0	58.5	0.94
8-8-90-5#3-o-4-2-8	2	8.3	8740	1	9.2	0.420	39.1	60.6	0.64
11-8-90-0-o-2.5-2-25	2	25.2	9460	1.41	8.6	0	174.7	172.2	1.01
11-8-90-0-o-2.5-2-17	2	16.6	9460	1.41	8.8	0	107.2	108.5	0.99
11-12-180-0-o-2.5-2-17	2	17.1	11800	1.41	8.5	0	83.5	119.3	0.70
11-12-90-0-o-2.5-2-17	2	16.9	11800	1.41	8.8	0	105.4	117.8	0.90
11-8-90-6#3-o-2.5-2-22	2	21.9	9120	1.41	8.5	0.210	170.2	168.6	1.01
11-8-90-6#3-o-2.5-2-16	2	16.2	9420	1.41	8.5	0.210	136.8	128.2	1.07
11-12-180-6#3-o-2.5-2-17	2	16.5	11800	1.41	8.5	0.210	113.1	137.4	0.82
11-12-90-6#3-o-2.5-2-17	2	16.4	11800	1.41	8.7	0.210	115.9	136.6	0.85
								Mean	0.85
								CoV	0.174

Based on the results shown in Table 4.11, the T/T_h ratio for the 37 specimens with hooked bars placed outside column core ranges from 0.58 to 1.19 with a mean of 0.85 and a coefficient of variation of 0.174. The average of 0.85 indicates that the bar location factor could be reduced to $1/0.85 = 1.17$. For simplification and for design purposes, a value of 1.15 is suggested.

Chun et al. (2017b) tested 26 specimens with No. 14 and No. 18 hooked bars, in which each specimen had two hooked bars placed outside column core. The specimens were designed to force a side-face blowout failure. All specimens had a high amount of confining reinforcement, with values of A_{th}/A_{hs} ranging from 0.44 to 0.88. In 20 of the specimens, the hooked bars were placed outside the confining ties, as shown in Figure 4.9.a, and were considered “unconfined” by Chun et al. (2017b). In the remaining 6 specimens, the confining ties were wrapped around the hooked bars, as shown in Figure 4.9.b; this configuration is the same as used by Sperry et al. (2015b) for hooked bars placed outside the column core, as shown in Figure 4.9.c.

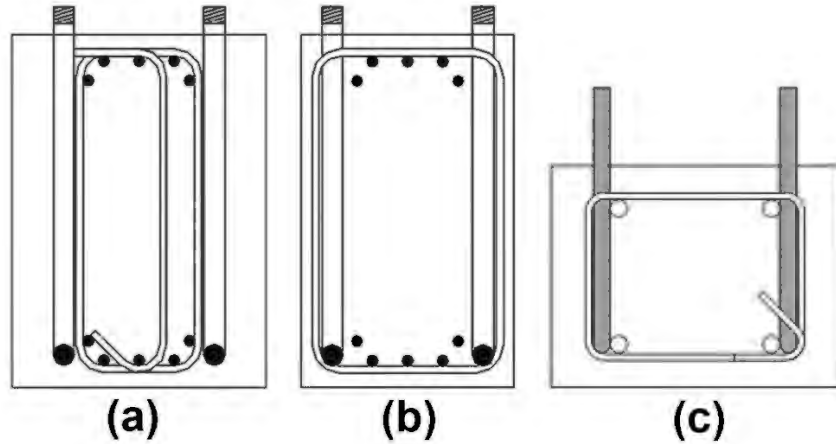


Figure 4.9 Confining reinforcement layouts in specimens with hooked bars placed outside the column core: (a) hooks outside the confining ties (Chun et al. 2017b), (b) hooks inside confining ties (Chun et al. 2017b), and (c) hooks inside confining ties (Sperry et al. 2015b)

Table 4.12 presents T/T_h based on Eq. (4.5) and (4.7) for the 26 specimens tested by Chun et al. (2017b). The specimens with hooks inside the confining ties are identified by Chun et al. as “confined” with a “C” at the end of the specimen ID. T/T_h is calculated for two cases. In the first case (second to last column), the confining reinforcement is counted as being effective and used to calculate T_h . In the second case (last column), the confining reinforcement is not counted for the specimens with hooks placed outside the confining ties (Figure 4.9a).

Table 4.12 Test-to-calculated ratio T/T_h based on Eq. (4.5) and (4.7) for specimens with No. 14 and No. 18 hooked bars placed outside column core by Chun et al. (2017b)

Specimen ID	n	ℓ_{eh}	f_{cm}	d_b	s/d_b	A_{th}/A_{hs}	T	T/T_h ^[2]	T/T_h ^[3]
		in.	psi	in.			kips		
D43-L10-C1-S42	2	16.9	6440	1.693	9.6	0.88	115.3	0.44	1.07
D43-L10-C1-S42-C ^[1]	2	16.9	6950	1.693	9.6	0.59	168.9	0.79	N/A
D43-L10-C1-S70	2	16.9	10010	1.693	9.6	0.88	123.2	0.44	1.01
D43-L10-C2-S42	2	16.9	7020	1.693	9.6	0.88	131.5	0.49	1.19
D43-L13-C1-S42	2	22.0	7020	1.693	9.6	0.88	144.9	0.48	0.98
D43-L13-C1-S42-C ^[1]	2	22.0	7020	1.693	9.6	0.59	170.7	0.68	N/A
D43-L13-C1-S70	2	22.0	10600	1.693	9.6	0.88	142.4	0.44	0.86
D43-L13-C2-S42	2	22.0	7020	1.693	9.6	0.88	154.5	0.51	1.05
D43-L16-C1-S42	2	27.1	7020	1.693	9.6	0.88	163.2	0.48	0.88
D43-L16-C1-S42-C ^[1]	2	27.1	7020	1.693	9.6	0.59	177.5	0.61	N/A
D43-L16-C1-S70	2	27.1	10010	1.693	9.6	0.88	172.7	0.48	0.84
D43-L16-C2-S42	2	27.1	7020	1.693	9.6	0.88	181.9	0.53	0.98
D43-L20-C1-S42	2	33.9	7020	1.693	9.6	0.88	172.0	0.44	0.72
D57-L10-C1-S42-a	2	22.6	5450	2.257	7.2	0.66	147.2	0.36	0.92
D57-L10-C1-S42-b	2	22.6	6150	2.257	7.2	0.66	150.4	0.36	0.91
D57-L10-C1-S42-C ^[1]	2	22.6	5450	2.257	7.2	0.44	223.2	0.68	N/A
D57-L10-C2-S42	2	22.6	5450	2.257	7.2	0.66	214.6	0.52	1.34

D57-L13-C1-S42-a	2	29.3	5450	2.257	7.2	0.66	236.4	0.51	1.11
D57-L13-C1-S42-b	2	29.3	6150	2.257	7.2	0.66	232.6	0.49	1.05
D57-L13-C1-S42-C ^[1]	2	29.3	5450	2.257	7.2	0.44	254.2	0.66	N/A
D57-L13-C2-S42	2	29.3	5450	2.257	7.2	0.66	273.4	0.59	1.28
D57-L16-C1-S42-a	2	36.1	5450	2.257	7.2	0.66	254.0	0.49	0.95
D57-L16-C1-S42-b	2	36.1	6150	2.257	7.2	0.66	284.0	0.53	1.02
D57-L16-C1-S42-C ^[1]	2	36.1	5450	2.257	7.2	0.44	279.6	0.64	N/A
D57-L16-C2-S42	2	36.1	6530	2.257	7.2	0.66	318.8	0.59	1.13
D57-L20-C1-S42	2	45.1	6530	2.257	7.2	0.66	328.4	0.53	0.91
							Max	0.79	1.34
							Min	0.36	0.61
							Mean	0.53	0.93
							CoV	0.192	0.210

^[1] Specimens with hooks placed inside the confining ties (Figure 4.9b)

^[2] Confining reinforcement counted towards anchorage strength

^[3] Confining reinforcement taken as not contributing to anchorage strength

As shown in Table 4.12, if the ties are taken as contributing to anchorage strength, T/T_h ranges from 0.36 to 0.89, with a mean of 0.53. The very low average indicates that confining reinforcement in specimens with hooks placed outside the confining ties (Figure 4.9.a) do not contribute to anchorage strength. If these specimens are treated as containing no confining reinforcement, the T/T_h ratio ranges from 0.61 to 1.34 with a mean of 0.93. Since the hooked bars were placed outside column core in all these specimens, a bar location factor of 1.17 should be applied, increasing the average T/T_h to 1.09, which is within the range of the coefficient of variation of the developed descriptive equations, Eq. (4.5) and (4.7).

For the six “confined” specimens (hooked bars inside confining ties, Figure 4.9.b), ties are counted towards anchorage strength and $A_{th}/A_{hs} = 0.4$ is used in calculating T_h , resulting in T/T_h ratio ranging from 0.72 to 0.92 with a mean of 0.79, after applying the bar location factor of 1.17. This indicates these specimens were weaker than similar specimens with respect to descriptive equations. For comparison, for the specimens by tested by Sperry et al. (2015b) and Ajaam et al. (2017) with a similar layout (shown in Figure 4.9c), T/T_h ranged from 0.68 to 1.25 with a mean of 0.96 after applying the bar location factor of 1.17. The lower T/T_h for specimens tested by Chun et al. (2017b) could be attributed to having a small concrete side cover, just $1d_b$ for No. 14 and No. 18 bars (to force a side-face blowout failure), whereas Ajaam et al. (2017) used 2.4 or $4d_b$ for No. 5 bars, 2.5 , 3.5 , or $4d_b$ for No. 8 bars, and $1.8d_b$ for No. 11 bars.

The justification for counting confining reinforcement towards anchorage strength when hooks are placed inside the confining ties (Figure 4.9.b and c) is that the tale of the hook is wrapped

by the column ties, thus mobilizing the outside longitudinal reinforcing bars when the hooked bars are being pulled out during the test. A direct design recommendation can be drawn from this observation; if the hooked bars are placed outside the column core and confining ties, the confining reinforcement should not be counted towards contributing to anchorage strength.

4.4.2 Confining Reinforcement

The effect of confining reinforcement on the anchorage strength of hooked bars is discussed in this section. Given the very limited number of specimens with No. 14 and No. 18 bars, earlier test results for No. 11 and smaller bars are also used in the analyses (Searle et al. 2014, Sperry et al. 2015a, 2015b, 2017a, 2017b, 2018, Yasso et al. 2017, Ajaam et al. 2017, 2018). The values of T/T_h based on new descriptive equations, Eq. (4.5) and (4.7), for specimens with confining reinforcement are compared with respect to A_{th}/A_{hs} in Figure 4.10. The details of these specimens are presented in Tables B.4 and B.5 of Section B3 in Appendix B.

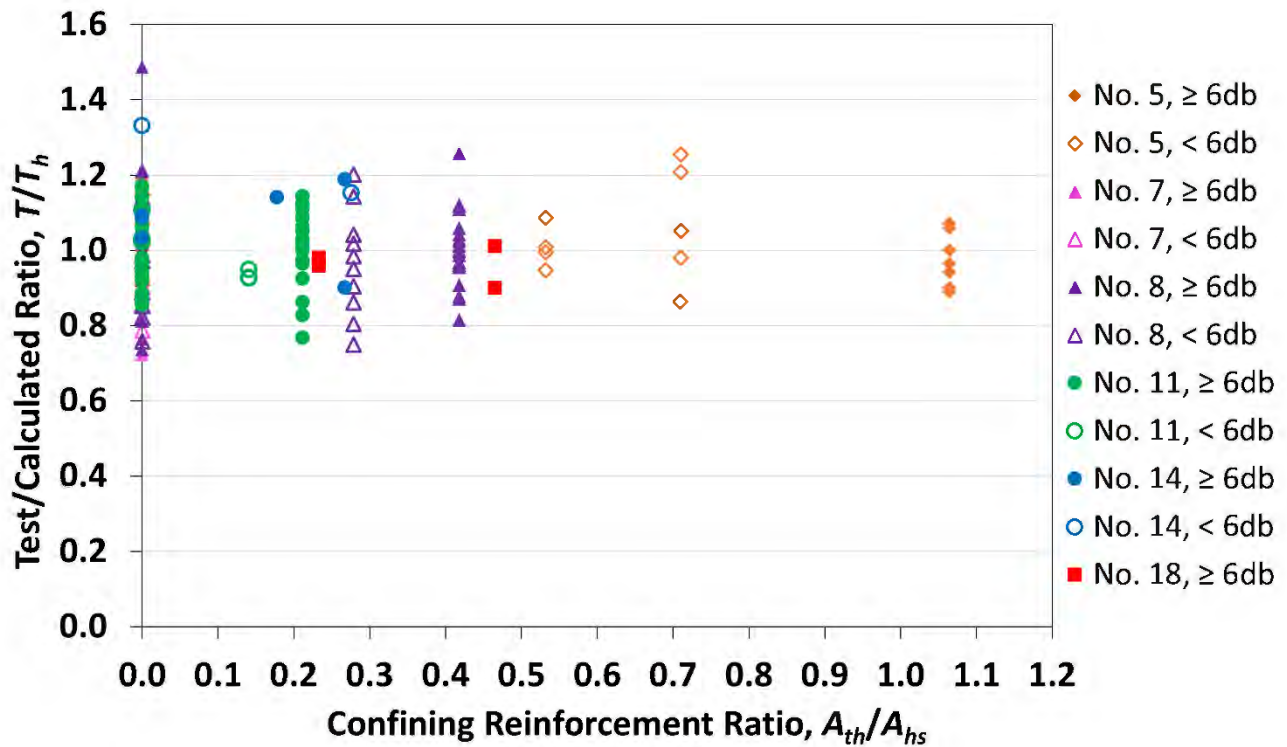


Figure 4.10 Test-to-calculated ratio T/T_h based on new descriptive equations, Eq. (4.5) and (4.7), for hooked bars versus confining reinforcement ratio A_{th}/A_{hs}

As shown in Figure 4.10, the A_{th}/A_{hs} ratio ranged from 0.14 to 1.06 for the specimens with confining reinforcement. The mean value of A_{th}/A_{hs} was 0.40 for all specimens. Values above 0.5 pertain solely to the No. 5 bars. No trend is evident, indicating the insensitivity of the descriptive

equations to the term A_{th}/n in Eq. (4.7). Since no bars larger than No. 8 had A_{th}/A_{hs} above 0.5, a cap on A_{th}/A_{hs} would be appropriate to consider for design purposes, as discussed in Chapter 6. Figure 4.10 also shows that, generally, the No. 14 and No. 18 bar specimens performed in a manner similar to the No. 11 and smaller bar specimens with comparable values of A_{th}/A_{hs} .

As discussed previously, the provisions in ACI 318-19 give no credit to confining reinforcement for hooked bars larger than No. 11, mainly due to a lack of test data on No. 14 and No. 18 bars. As shown in the test program for hooked bars (Table 2.5), the No. 14 and No. 18 hooked bar specimens were designed in pairs: one specimen without and the other specimen with confining reinforcement in the joint region, while keeping the dimensional properties, bar size, and bar spacing the same. The embedment lengths for each pair had close values (differing only within construction tolerances), with the exception of H14-1/H14-2, H14-3/H14-4, and H18-1/H18-2. Specimen H14-1 had a 2.2 in. longer embedment length than H14-2 (27.0 versus 24.8 in.), and specimen H14-3 had 1.8 in. longer embedment length than its companion H14-4 (36.7 versus 34.9 in.). Specimen H18-1 had a 1.5 in. longer embedment length than its companion H18-2 (28.5 in. versus 27.0 in.). The specimens in a pair were cast with the same concrete, but the measured concrete compressive strengths were slightly different due to different testing dates. Similarly, the No. 18 hooked bar specimens were also cast in pairs, with the second specimen in each pair having a higher quantity of confining reinforcement than the first.

Based on the results given in Table 4.1, providing confining reinforcement in the joint region contributes to the anchorage strength of No. 14 and No. 18 hooked bars. Comparing specimens without and with confining reinforcement in the joint region reveals that ties parallel to the straight portion of a hooked bar increase the anchorage strength for both widely-spaced ($s/d_b \geq 6$) and closely-spaced ($s/d_b < 6$) hooked bars. Figures 4.11 and 4.12 show bar charts displaying the anchorage strengths of the specimens in each pair of specimens for No. 14 and No. 18 hooked bars, respectively. The T/T_h ratios for each specimen are provided for comparison.

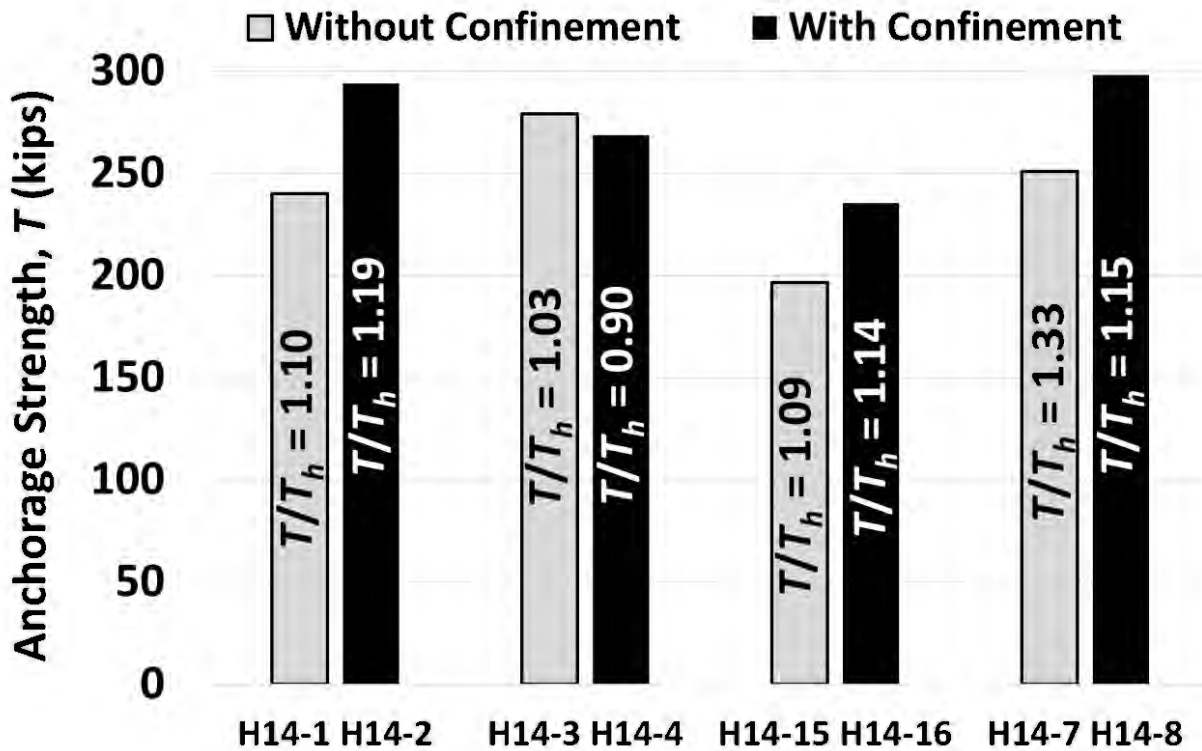


Figure 4.11 Comparing anchorage strength of No. 14 hooked bars for confining reinforcement. T/T_h ratios shown based on Eq. (4.5) and (4.7). Center-to-center spacing is $3.5d_b$ for specimens H14-7 and H14-8 (closely-spaced), and $10.6d_b$ for all other specimens (widely-spaced)

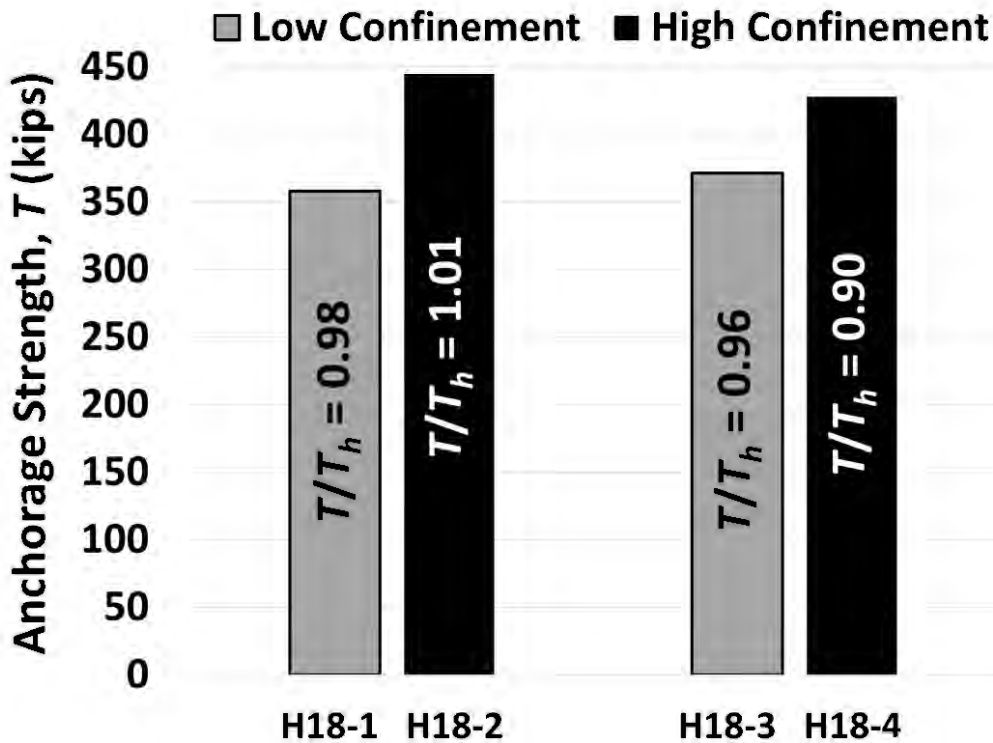


Figure 4.12 Comparing anchorage strength of No. 18 hooked bars for confining reinforcement. T/T_h ratios shown on top of each bar. Hooked bars have center-to-center spacing of $6d_b$.

As shown in Figures 4.11 and 4.12, the anchorage strength of the specimens with confining reinforcement or with the greater amount of confining reinforcement is higher than that of the companion specimen, with the exception of specimens H14-3 and H14-4, for which $T = 279.1$ kips and $T = 268.5$ kips, respectively. This might be attributed to the longer average embedment length in specimen H14-3 (36.7 in. compared with 34.9 in.) or to natural variability in test results. For the pair H14-1 and H14-2, the specimen with ties (H14-2) had a higher anchorage strength despite having a shorter average embedment length. Similarly, for the pair H18-1/H18-2, the specimen with a greater quantity of confining reinforcement (H18-2) had a higher anchorage strength than its companion despite having a shorter embedment length.

As discussed before, all hooked bar specimens were tested under loading condition A, in which the joint shear demand is equal to 80% of the load applied to the bars. All hooked bar specimens, even the four specimens without ties, carried the joint shear and exhibited an anchorage failure, whereas shear-like failures, as described in Section 3.2.2, were observed in headed bars under similar conditions, as will be discussed in Chapter 5. These observations reveal the distinct role of the tail of the hook in carrying the joint shear by preventing the inclined crack in the joint from propagating towards the back of the column.

Overall, the findings of this study indicate that the contribution by the ties in the joint region to the anchorage strength of hooked bars as large as No. 14 and No. 18 should be included in the ACI 318 Code.

4.4.3 Bar Spacing

As mentioned in Section 4.3.2, bar spacing is used as a useful proxy for a bar group effect on anchorage strength. In the database, bar spacing and number of bars are tied together, and it is not possible to separate the individual effects; therefore, the choice was made to continue using center-to-center bar spacing to represent the observed effect, done in previous studies, although the actual mechanism is not clear.

The relationship between spacing and the anchorage strength of hooked bars is discussed in Sections 4.3.2 and 4.3.4. The ratio of test-to-calculated failure load, T/T_h , is compared as a function of the center-to-center bar spacing normalized by bar diameter (s/d_b) in Figure 4.13.

As shown in Figure 4.13, no noticeable positive or negative trend can be observed for the data as a whole, indicating the match between the test results and the descriptive equation is not affected by s/d_b . It can also be observed that the results for No. 14 and No. 18 specimens fall within

the corresponding cluster of data points for both closely-spaced and widely spaced bars, suggesting that the relationship between bar spacing and anchorage strength as established for No. 11 and smaller bars is similar for larger bars. Of the specimens with closely-spaced bars, the highest T/T_h ratio belongs to the No. 14 bar specimen with three bars spaced at $3.5d_b$ on-center and no confining reinforcement (specimen H14-7).

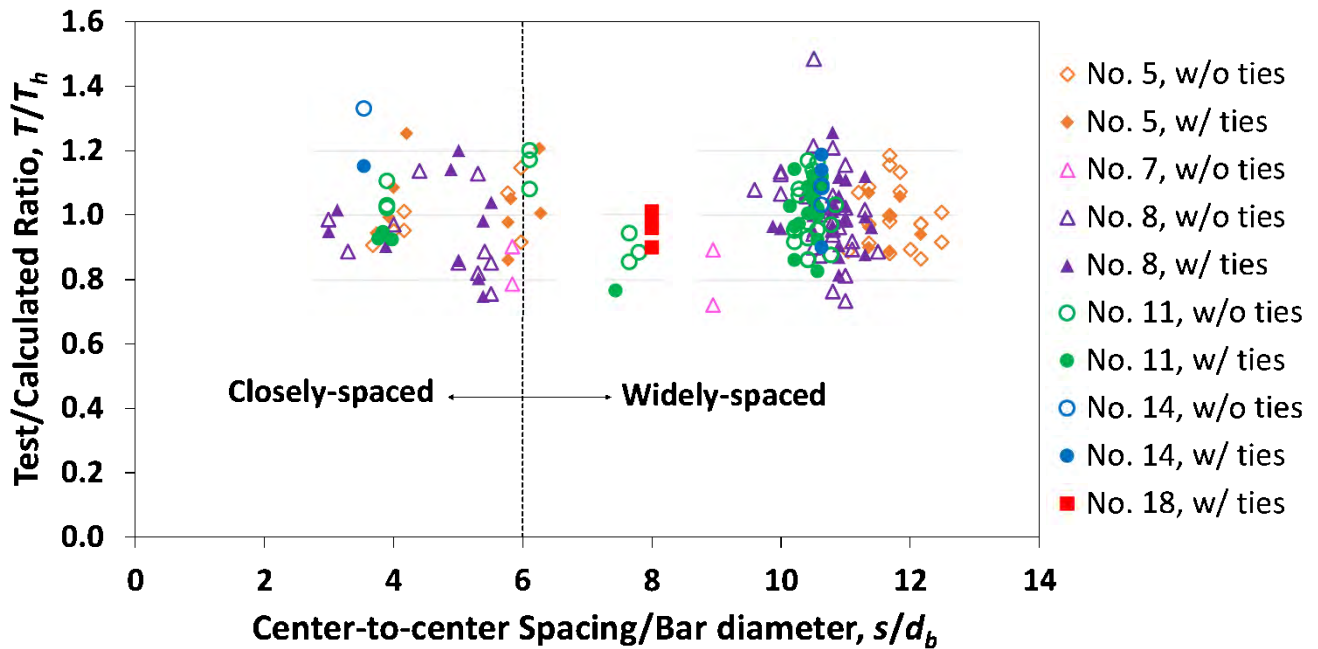


Figure 4.13 Test-to-calculated ratio T/T_h versus ratio of center-to-center spacing to bar diameter s/d_b based on Eq. (4.5) and (4.7), for hooked bar specimens used to develop the equations

4.4.4 Strut Angle

For hooked bars, the compression strut angle is defined as the angle from the centerline of the straight portion of the bar to an inclined line drawn between the intersection of the centerlines of the straight portion and tail of the hook and the center of the bearing plate simulating the compression zone of the imaginary beam, as shown in Figure 4.14. Among previous studies, Joh et al. (1993) and Coleman et al. (2023) investigated the influence of strut angle on anchorage strength. Joh et al. (1993) evaluated five specimens with the same column depth and proportions, but different embedment lengths, and observed that a decrease in strut angle θ resulted in an increase in anchorage strength. As shown in Figure 4.14, however, a decrease in θ will result from increasing the embedment length, which is, of course, expected to increase anchorage strength. This was also the case with the study by Coleman et al. (2023), as discussed later. A key point

often raised in a discussion of the effect of strut angle on anchorage strength of beam reinforcement in beam-column joints is the observed decrease in strength once the effective depth of a member exceeds $1.5\ell_{eh}$. This is discussed in Section 4.4.5. The results addressed in this section are for specimens in which the effective depth was less than or equal to $1.5\ell_{eh}$.

Any relationship between the strut angle and the test results for the specimens used in developing Eq. (4.5) and (4.7), including No. 14 and No. 18 bar specimens in this study (see Tables B.2 through B.5 in Section B3 in Appendix B) can be observed by comparing T/T_h versus θ for the specimens, as shown in Figure 4.15. The strut angle θ is calculated as the inverse tangent of the ratio x_{mid}/ℓ_{eh} , where x_{mid} is the distance from the center of the hooked bars to the center of the bearing plate representing the compression region of the simulated beam.

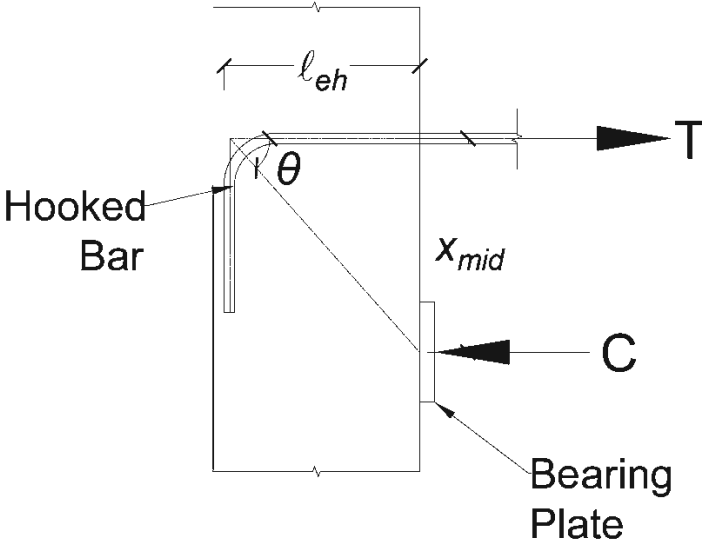


Figure 4.14 Definition of compression strut angle (θ) for hooked bars

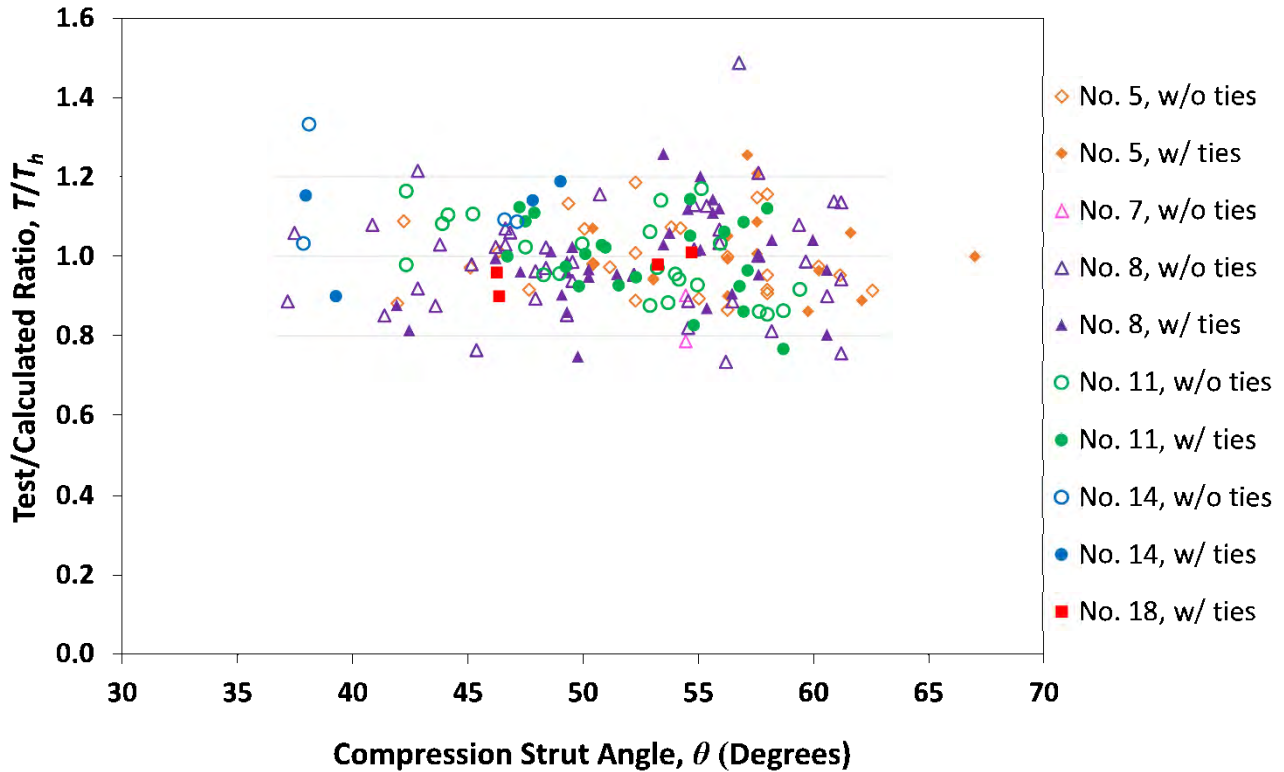


Figure 4.15 Test-to-calculated T/T_h ratio based on Eq. (4.5) and (4.7) versus compression strut angle θ for hooked bar specimens used to develop descriptive equations (not including specimens with $d_{eff}/\ell_{eh} > 1.5$)

As shown in Figure 4.15, there appears to be, at most, a weak negative trend, with T/T_h decreasing as the strut angle θ increases up to 60° , with a somewhat greater drop for the small number of specimens with $\theta > 60^\circ$, with 10 out of the 14 specimens in this range having $T/T_h < 1.0$. On the other hand, of the six specimens with a strut angle $\theta < 40^\circ$, four have $T/T_h > 1.0$, three of which are No. 14 bar specimens. The No. 14 and No. 18 bar specimens with $45^\circ < \theta < 55^\circ$ fall within the cloud of data points along with other bar sizes and do not exhibit a trend. Overall, Figure 4.15 indicates that descriptive equations are insensitive to strut angle.

The conclusion drawn here differs from that by Joh et al. (1993), as well as that in a recent study by Coleman et al. (2023), in which, like Joh et al., Coleman et al. also compared the strut angle θ with the bar stress at failure (f_{su}) normalized by concrete compressive strength (f_{cm}) to the 0.29 power, $f_{su} / f_{cm}^{0.29}$. The 0.29 power was chosen based on the descriptive equations developed by Sperry et al. (2015b). Coleman et al. (2023) observed a significant decrease in $f_{su} / f_{cm}^{0.29}$ with increase in θ and concluded that strut angle negatively affects the anchorage strength of hooked bars. Also, like Joh et al., however, Coleman et al. made a logical error, missing the point that the

increase in strut angle coincides with a decrease in the embedment length, as shown in Figure 4.16, where θ is plotted as a function of embedment length normalized by bar diameter, ℓ_{eh}/d_b , for specimens used to develop descriptive equations, Eq. (4.5) and (4.7). Bars of a given size are grouped together in the figure because each had a different value of x_{mid} .

Coleman et al. (2023) did make some comparisons for specimens with the same embedment length, but with increasing member depths, and made a similar observation. In that comparison, the reduction in anchorage strength with increasing strut angle only occurred for members with ratios of depth to embedment length over 1.5, a point that is discussed next in Section 4.4.5.

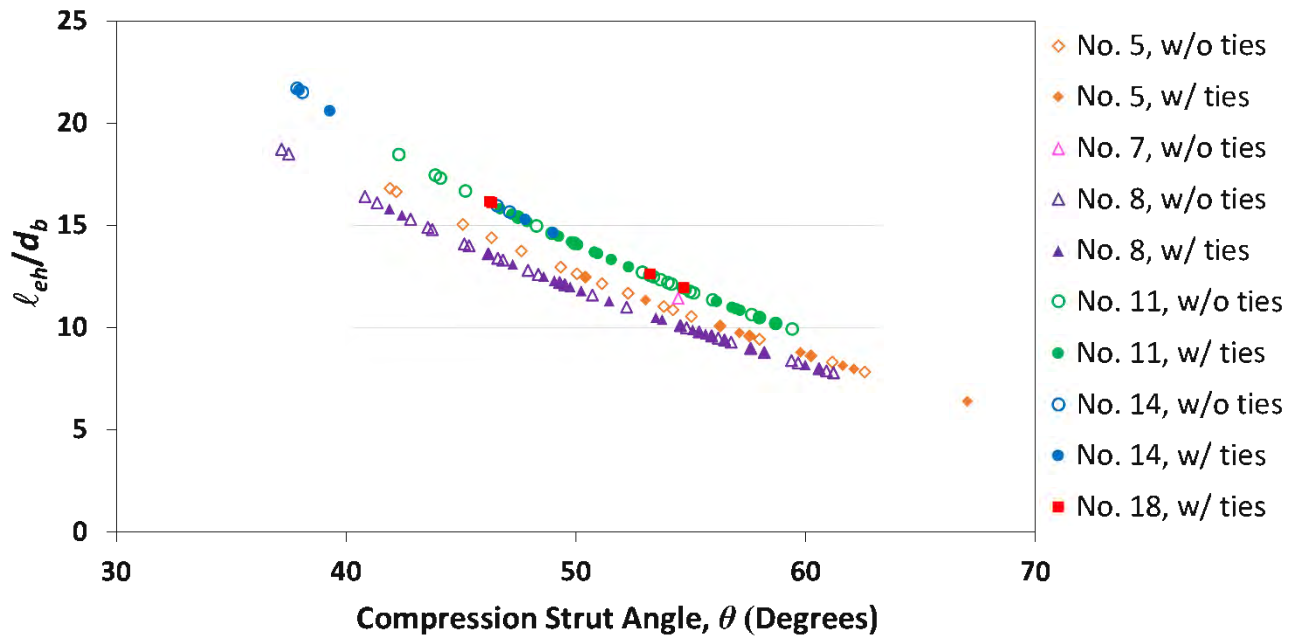


Figure 4.16 ℓ_{eh}/d_b versus compression strut angle θ for hooked bar specimens used to develop descriptive equations, Eq. (4.5) and (4.7)

4.4.5 Effective Beam Depth

The ratio of effective beam depth to embedment length, d_{eff}/ℓ_{eh} , is another parameter shown to affect the anchorage strength of hooked bars. For this analysis, the effective beam depth is defined in Figure 4.17 and is calculated as the sum of h_{cl} and c , where h_{cl} is the distance measured from the center of the hooked bars to the top edge of the bearing plate and c is the calculated neutral axis depth. c is calculated as a/β_1 , where a is the depth of equivalent rectangular compressive stress block and calculated as $nA_b f_s / 0.85 f_{cm} b$ per the flexural design procedure for reinforced concrete beams, $\beta_1 = 0.85 - 0.05((f_{cm} - 4000)/1000) \leq 0.65$ per Section 22.2.2.4.3 of ACI 318-19, and b is the

width of the specimen. Ajaam et al. (2017) showed that when $d_{eff}/\ell_{eh} > 1.5$ (deeper beam), specimens generally have a lower anchorage strength.

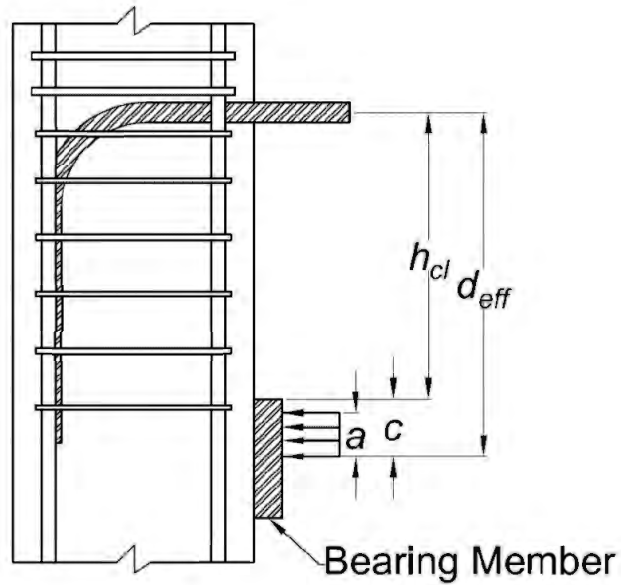


Figure 4.17 Effective beam depth d_{eff} for hooked bars (Ajaam et al. 2017)

Variations of T/T_h ratio with respect to d_{eff}/ℓ_{eh} for the hooked bar specimens used to develop descriptive equations, Eq. (4.5) and (4.7), are shown in Figure 4.18, plus specimens with $d_{eff}/\ell_{eh} > 1.5$ for comparison. Details of specimens with $d_{eff}/\ell_{eh} > 1.5$ are presented in Table B.7 in Section B3 of Appendix B.

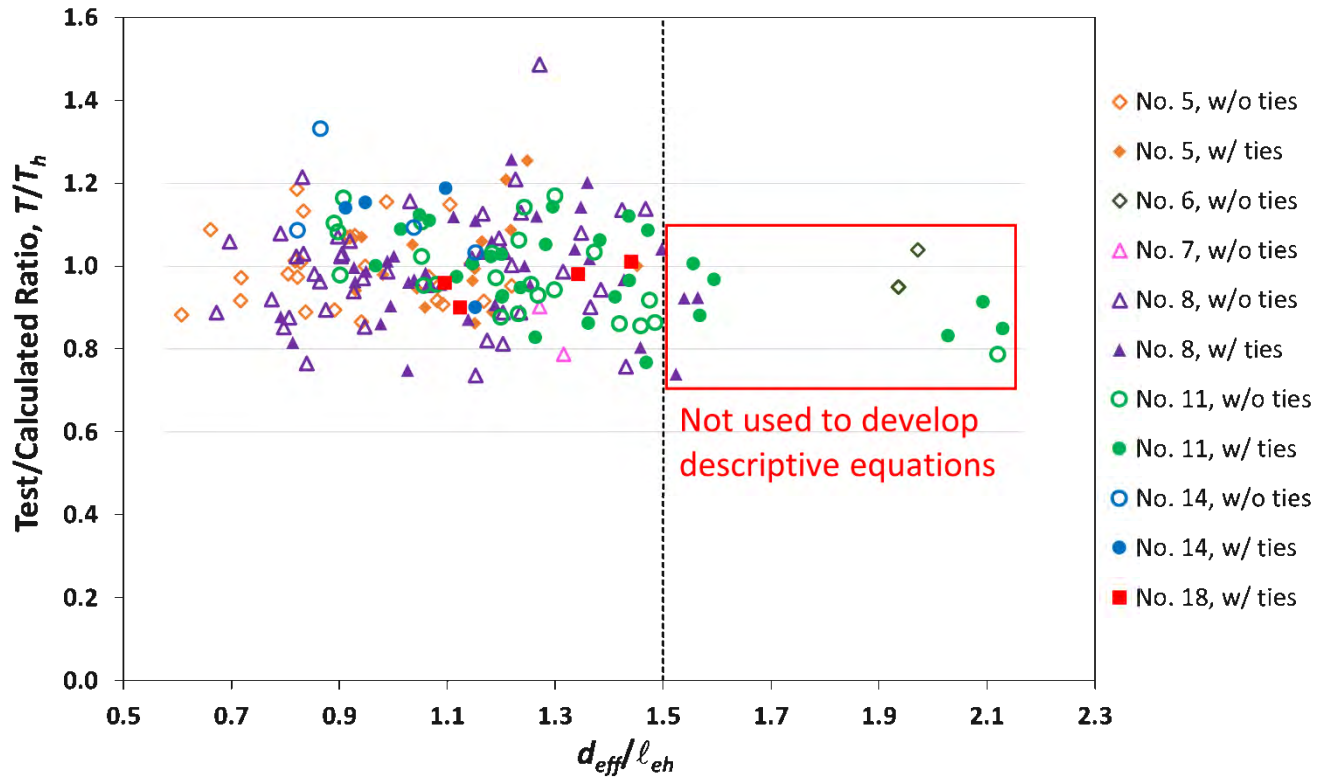


Figure 4.18 Test-to-calculated T/T_h ratio based on Eq. (4.5) and (4.7) versus effective beam depth to embedment length d_{eff}/l_{eh} ratio for hooked bar specimens used to develop descriptive equations plus specimens with $d_{eff}/l_{eh} > 1.5$

As shown in Figure 4.18, all but two specimens with $d_{eff}/l_{eh} > 1.5$ have a T/T_h ratio < 1.0 . No noticeable positive or negative trend, however, is observed for the rest of the specimens, including those with No. 14 and No. 18 hooked bars, indicating that anchorage strength of hooked bars, as represented by those in the database, is not affected by the d_{eff}/l_{eh} ratio when $d_{eff}/l_{eh} < 1.5$.

4.4.6 Embedment Length

Figure 4.19 compares T/T_h with the l_{eh}/d_b ratio for the specimens used to develop descriptive equations. The figure shows that, generally, there is a no noticeable trend in T/T_h with increasing l_{eh}/d_b . Of the specimens with the highest l_{eh}/d_b ratio, four had No. 14 bars with $l_{eh}/d_b > 20$, three of which had $T/T_h > 1.0$.

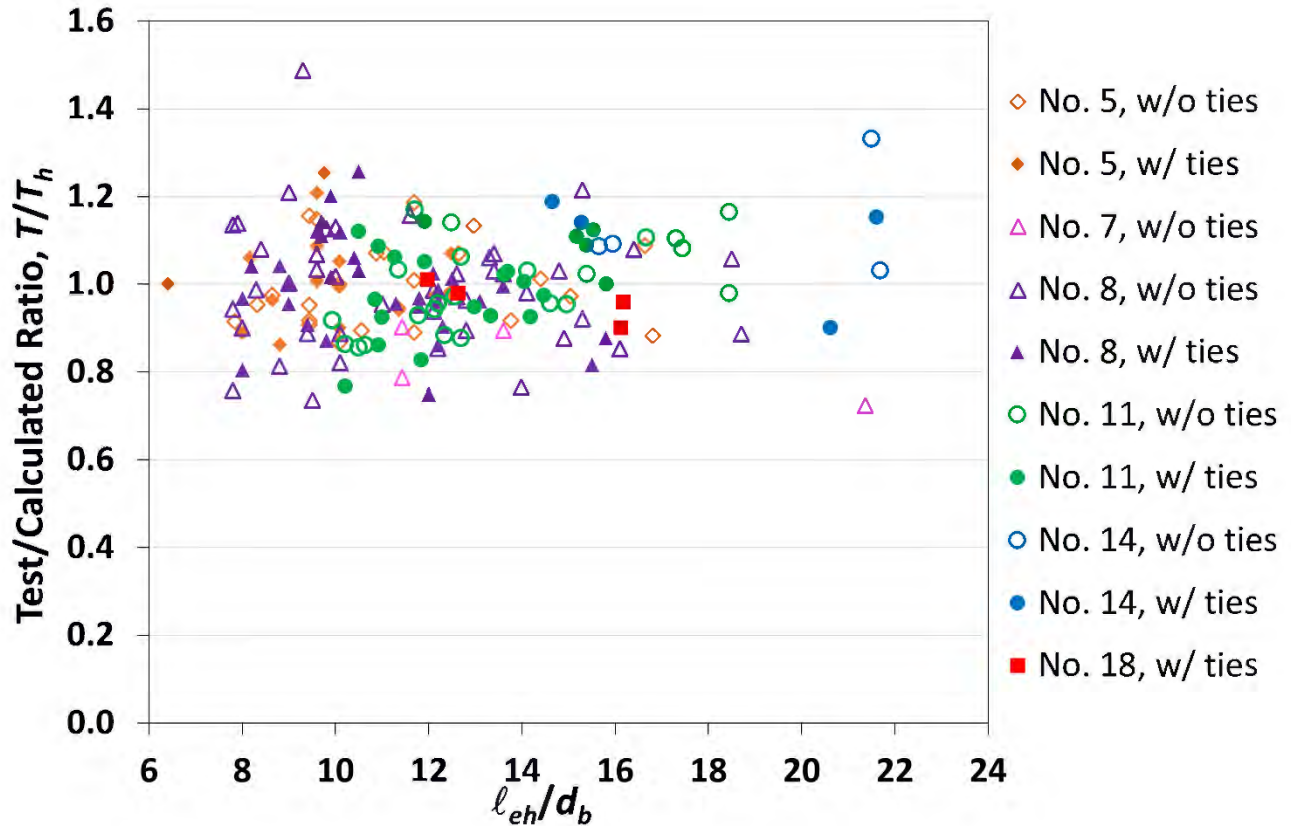


Figure 4.19 Test-to-calculated T/T_h ratio based on Eq. (4.5) and (4.7) versus embedment length to bar diameter ℓ_{eh}/d_b ratio for hooked bar specimens used to develop descriptive equations

4.5 SPECIMENS NOT USED TO DEVELOP DESCRIPTIVE EQUATIONS

In Section 4.3, Eq. (4.5) and (4.7) were developed to represent the anchorage strength of hooked bars by incorporating the results for No. 14 and No. 18 bar specimens in this study into the database used by Ajaam et al. (2017). The database included No. 11 bar and smaller hooked bar specimens tested at the University of Kansas (Searle et al. 2014, Sperry et al. 2015a, 2015b, 2017a, 2017b, 2018, Yasso et al. 2017, Ajaam et al. 2017, 2018) as well as two No. 7 bar specimens by Lee and Park (2010), two No. 7 bar specimens by Hamad et al. (1993), and three No. 11 bar specimens by Ramirez and Russell (2008). The details of these specimens are presented in Tables B.2 through B.5 in Section B3 (specimens tested at the University of Kansas) and Table B.8 in Section B4 (specimens tested in other studies) in Appendix B. As described in Section 4.3, three No. 6 bar specimens by Ramirez and Russell (2008) were originally included in the database but not used in this study because they had d_{eff}/ℓ_{eh} values > 1.5 . Those specimens are included in the analysis below.

In this section, the anchorage strengths based on the test results T for beam-column joint specimens tested in other studies and not used to develop descriptive equations are compared with those calculated using Eq. (4.5) and (4.7), T_h . The studies include those by Marques and Jirsa (1975), Pinc et al. (1977), Hamad et al. (1993), Ramirez and Russell (2008), and Lee and Park (2010). The specimens tested by Chun et al. (2017b) are covered in Section 4.4. The specimens tested by Marques and Jirsa (1975) (see Figure 1.3), discussed in detail later in this section, had narrow, short columns that reduced the force carried by the joint and an unrealistic reinforcement layout. The same is true of the specimens tested by Pinc et al. (1977). Some specimens tested by Hamad et al. (1993), Ramirez and Russell (2008), and Lee and Park (2010) were used by Ajaam et al. (2017) to develop the descriptive equations and were retained for that purpose in this study. The specimens tested by Hamad et al. (1993), Ramirez and Russell (2008), and Lee and Park (2010) that are discussed in this section were excluded for the same reasons they were excluded by Ajaam et al. (2017) when developing the descriptive equations: “because the number of the specimens was relatively small, 12 in total, and because of the inherent variability in the contribution of confining reinforcement to the anchorage strength of hooked bars as a result of the variations in test setup.” Table 4.13 shows a summary of these specimens, their key properties, and their T/T_h ratio based on Eq. (4.5) and (4.7). Full details of the specimens are presented in Table B.8 of Section B4 in Appendix B.

Table 4.13 Test-to-calculated T/T_h ratio based on Eq. (4.5) and (4.7) for specimens tested outside University of Kansas and not used to develop Eq. (4.5) and (4.7)

Study	Specimen ID	n	ℓ_{eh}	f_{cm}	d_b	s/d_b	A_{th}/A_{hs}	T	T_h	T/T_h
			in.	psi	in.			kips	kips	
Marques and Jirsa (1975)	J7-180-12-1-H	2	10.0	4350	0.875	6.1	0	36.6	38.8	0.94
	J7-180-15-1-H	2	13.0	4000	0.875	6.1	0	52.2	50.6	1.03
	J7-90-12-1-H	2	10.0	4150	0.875	6.1	0	37.2	38.3	0.97
	J7-90-15-1-H	2	13.0	4600	0.875	6.1	0	54.6	52.6	1.04
	J7-90-15-1-L	2	13.0	4800	0.875	6.1	0	58.2	53.3	1.09
	J7-90-15-1-M	2	13.0	5050	0.875	6.1	0	60.0	54.0	1.11
	J11-180-15-1-H	2	13.1	4400	1.41	3.4	0	70.2	50.1	1.40
	J11-90-12-1-H	2	10.1	4600	1.41	3.4	0	65.5	38.0	1.72
	J11-90-15-1-H	2	13.1	4900	1.41	3.4	0	74.9	50.6	1.48
	J11-90-15-1-L	2	13.1	4750	1.41	3.4	0	81.1	51.2	1.58
	J 7- 90 -15 -3a - H ^[1]	2	13.0	3750	0.875	6.1	0.367	58.8	53.8	1.09
	J 7- 90 -15 -3 - H ^[1]	2	13.0	4650	0.875	6.1	0.183	62.4	51.9	1.20
	J 11- 90 -15 -3a - L ^[1]	2	13.1	5000	1.41	3.4	0.282	107.6	72.5	1.48
	J 11- 90 -15 -3 - L ^[1]	2	13.1	4850	1.41	3.4	0.141	96.7	61.1	1.58

Pinc et al. (1977)	9-12	2	10.0	4700	1.13	4.5	0	47.0	36.6	1.28
	11-15	2	13.1	5400	1.41	3.4	0	78.0	47.6	1.64
	11-18	2	16.1	4700	1.41	3.4	0	90.5	57.5	1.57
Hamad et al. (1993)	11-90-U	2	13.0	2570	1.41	3.4	0	48.0	42.8	1.12
	11-90-U*	2	13.0	5400	1.41	3.4	0	75.0	52.7	1.42
	11-180-U-HS	2	13.0	7200	1.41	3.4	0	58.8	57.2	1.03
	11-90-U-HS	2	13.0	7200	1.41	3.4	0	73.8	57.2	1.29
	11-90-U-T6	2	13.0	3700	1.41	3.4	0.141	71.8	93.2	0.77
	7-180-U-T4	2	10.0	3900	0.88	6.1	0.183	34.6	32.2	1.08
	11-90-U-T4	2	13.0	4230	1.41	3.4	0.212	83.2	75.3	1.10
	7-90-U-SC ^[1]	2	10.0	4230	0.88	8.4	0	29.9	40.2	0.87
Ramirez and Russell (2008)	I-1 ^[2]	2	6.5	8910	0.75	12.3	0	30.0	28.8	1.04
	I-3 ^[2]	2	6.5	12460	0.75	12.3	0	30.0	31.7	0.95
	I-5 ^[2]	2	6.5	12850	0.75	12.3	0	30.5	31.9	0.95
	I-6	2	12.5	12850	1.41	6.1	0	114.0	86.4	1.32
	III-13	2	6.5	13980	0.75	12.3	0.500	41.3	42.6	0.97
	III-15	2	6.5	16350	0.75	12.3	0.500	38.5	44.0	0.87
	III-14	2	12.5	13980	1.41	6.1	0.212	105.0	111.3	0.94
	III-16	2	12.5	16500	1.41	6.1	0.212	120.0	115.5	1.04
Lee and Park (2010)	H3	2	15.0	4450	0.88	9.0	0.367	53.8	75.1	0.72
									Max	1.72
									Min	0.72
									Mean	1.18
									CoV	0.224

[1] Hooked bars outside column core, bar location factor of 1.17 applied to T/T_h

[2] Specimens had $d_{eff}/\ell_{eh} > 1.5$

The values of T/T_h for the specimens in Table 4.13 ranged from 0.72 to 1.72, with a mean of 1.18 and a coefficient of variation of 0.235. For the No. 7 and No. 11 bar specimens by Marques and Jirsa (1975), the mean T/T_h is 1.26. For the No. 9 and No. 11 bar specimens by Pinc et al. (1977), the mean T/T_h is 1.50. The mean T/T_h for the No. 7 and No. 11 bar specimens by Hamad et al. (1993) and No. 6 and No. 11 bar specimens by Ramirez and Russell (2008) are 1.12 and 0.98, respectively, both within the range of the coefficient of variation for Eq. (4.5) and (4.7), 12%.

The No. 7 bar specimens tested by Marques and Jirsa (1975) had a mean T/T_h value of 1.06. A careful look at the specimens tested by Marques and Jirsa (1975) reveals that, while the No. 7 bar specimens show a good match with the descriptive equations, the No. 11 bar specimens have

high T/T_h values with a mean of 1.54. The noticeable difference in the mean T/T_h values is despite the fact that the No. 7 bar specimens had the same specimen proportions and were tested in the same apparatus as the No. 11 bar specimens. For this reason, these specimens are investigated in more detail in terms of the test setup, specimen proportions, and applied forces.

The self-reacting system used to test specimens at the University of Kansas studies (Searle et al. 2014, Sperry et al. 2015a, 2015b, 2017a, 2017b, 2018, Yasso et al. 2017, Ajaam et al. 2017, 2018) was a modified version of the test apparatus used by Marques and Jirsa (1975). Both systems applied forces in a manner similar to loading condition B used in this study. The forces applied to specimens by the University of Kansas test setup and Marques and Jirsa (1975) are shown schematically in Figure 4.20.

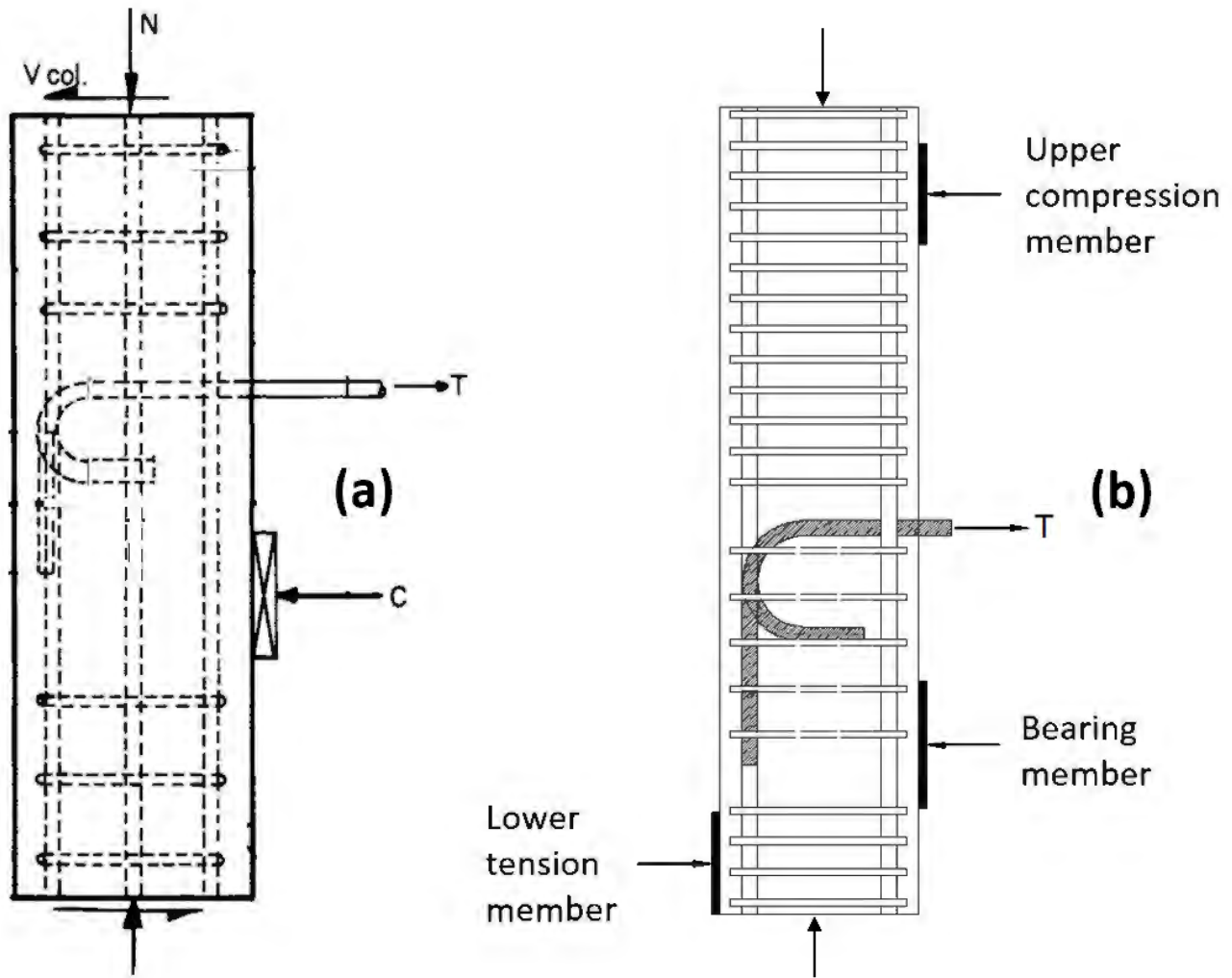


Figure 4.20 Schematic of the forces applied to specimens by (a) Marques and Jirsa (1975) and (b) University of Kansas studies (Searle et al. 2014, Sperry et al. 2015a, 2015b, 2017a, 2017b, 2018, Yasso et al. 2017, Ajaam et al. 2017, 2018) (**Note:** drawings are not to scale)

As shown in Figure 4.20, a bearing member was used to simulate the compression zone of the virtual beam in both studies. As shown on Figure 4.20b, two compressive reaction forces, one above and one below the joint region by the upper compression member and the lower tension member, respectively, counteracted the moment applied at the joint and prevented the specimen from rotating. In the schematic drawing provided by Marques and Jirsa (1975) and shown in Figure 4.20a, the two forces above and below the joint are represented by V_{col} . When describing the components of their test apparatus, however, Marques and Jirsa clearly state that “A horizontal reaction was provided at the top of the test column to balance the moment imposed by the simulated beam” but provide no information on how the force was applied at the bottom of the column, although the photo of the test setup shows something similar to a lower tension member with a tension rod at the bottom of the reaction frame. It is therefore fair to assume that the force at the bottom of the Marques and Jirsa (1975) specimens (below the joint) was provided solely by the stiffness of the test apparatus. For the tests in the University of Kansas studies, the compressive force at the bottom of the column was mobilized in the lower tension member (Peckover et al. 2013). In the latter case, that force was low due to the relative flexibility of tension tie used to provide that force (Searle et al. 2014, Sperry et al. 2015a, 2015b, 2017a, 2017b, 2018, Yasso et al. 2017, Ajaam et al. 2017, 2018). In this sense, the two test setups were similar.

The main difference between the approach taken by Marques and Jirsa and the studies at the University of Kansas, however, involves the specimen proportions. Marques and Jirsa (1975) used the same specimen proportions for No. 7 and No. 11 bar specimens, in which the distance from the center of the hooked bars to the center of the bearing member (x_{mid}) was 14.25 in. and the upper compression reaction was placed just $1.17x_{mid} = 16.75$ in. away from the hooked bars, as shown in Figure 4.21a. In addition to having the same proportions, the specimens also had the same geometry. All specimens were 12 in., had depths of 12 or 15 in., and had a height of 50 in. The specimen geometry and proportions used by Marques and Jirsa (1975) are not representative of those used in practice for reinforced concrete frames, although it was not unreasonable at the time for a study of the anchorage strength of hooked bars since the factors controlling the behavior of hooked bars were not known as well as they are now. The University of Kansas studies used specimens with more realistic proportions. The value of x_{mid} increased with the size of the hooked bar (9.44 in. for No. 5 bar, 14.44 in. for No. 8 bars, and 24.19 in. for No. 11 bars). Second, the upper compression member was placed farther away from the hooked bars than in Marques and

Jirsa (1975) specimens: $2.28x_{mid} = 21.56$ in. for No. 5 bars, $1.49x_{mid} = 21.56$ in. for No. 8 bars, and $1.97x_{mid} = 47.56$ in. for No. 11 bars. A total height of 54 in. was used for the No. 5 and No. 8 bar specimens and 96 in. for No. 11 bar specimens.

Figure 4.21 compares the specimen proportions and the resulting applied forces for the No. 11 bar specimens tested by Marques and Jirsa (1975) and at the University of Kansas (Searle et al. 2014, Sperry et al. 2015a, 2015b, 2017a, 2017b, 2018, Yasso et al. 2017, Ajaam et al. 2017, 2018). Because of its low value, the force in the lower tension member is neglected. As shown in the figure, a much higher portion of the total applied force T was shared with the upper region of the column in the No. 11 bar specimens by Marques and Jirsa (1975) ($0.46T$) than the University of Kansas specimens ($0.34T$). This means a much lower portion of T had to be carried within the joint in the Marques and Jirsa specimens than those tested at the University of Kansas ($0.54T$ versus $0.66T$)³. Thus, with the closer location of the upper compression member with respect to the hooked bars in the specimens tested by Marques and Jirsa specimens, the anchorage strength would be expected to be higher than if the geometry of the test specimens had been more realistic, such as that used in the specimens tested at the University of Kansas. This explains the higher strength of the No. 11 bar Marques and Jirsa specimens with respect to Eq. (4.5) and (4.7).

³ $0.695T$ and $0.60T$ for No. 5 and No 8 bar specimens, respectively, tested at the University of Kansas

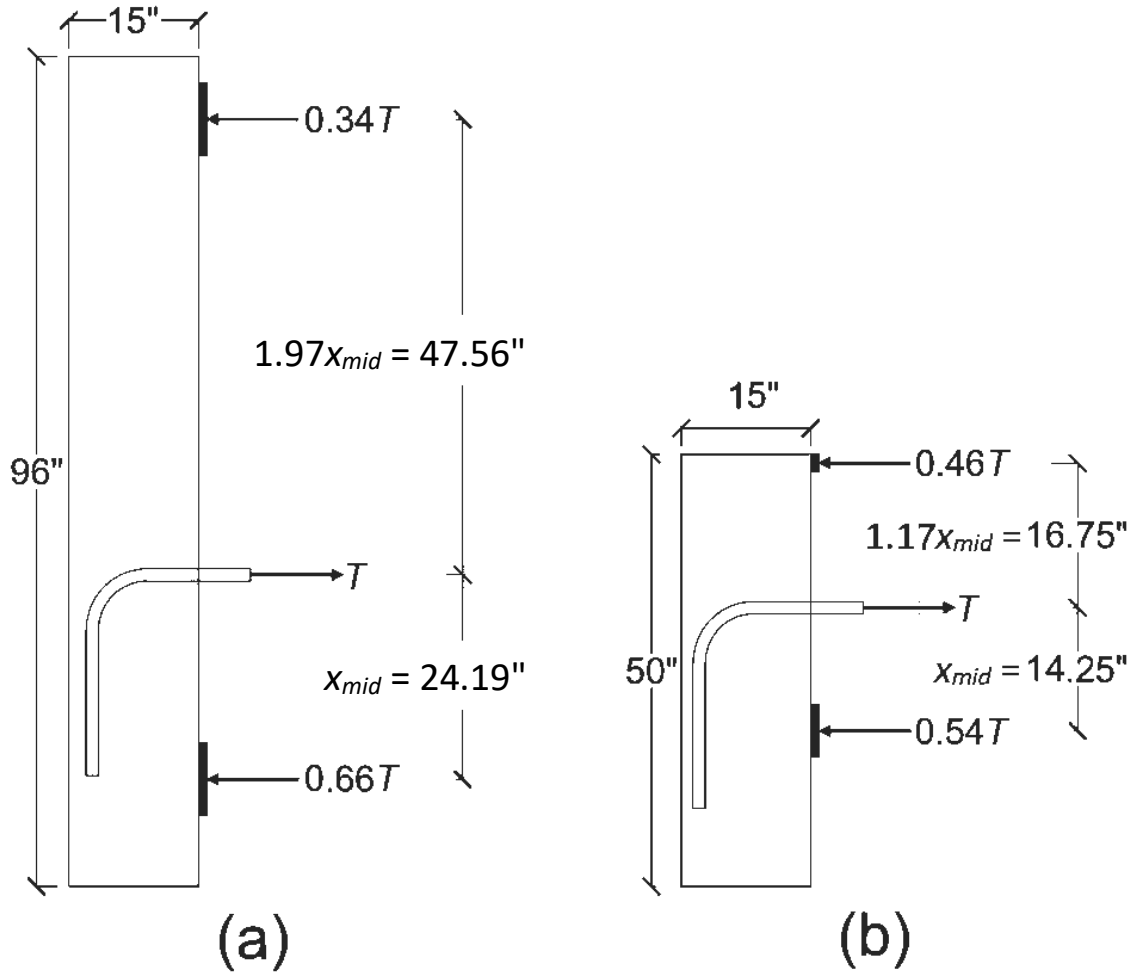


Figure 4.21 No. 11 hooked bar specimen proportions and applied forces: (a) University of Kansas (Searle et al. 2014, Sperry et al. 2015a, 2015b, 2017a, 2017b, 2018, Yasso et al. 2017, Ajaam et al. 2017, 2018), and (b) Marques and Jirsa (1975) (**Note:** T is the total applied force, and the force in the lower tension member is neglected)

The reasons for the higher strengths of the No. 11 bar specimens by Marques and Jirsa (1975) with respect to Eq. (4.5) and (4.7) also applies for the specimens tested by Pinc et al. (1977), as they used the same specimen proportions, with the exception that Pinc et al. used column depths between 12 and 24 in.

The question then arises as to why the No. 7 bar specimens tested by Marques and Jirsa (1975) had a mean T/T_h of just 1.05, despite having the same specimen proportions as the No. 11 bar specimens. The answer is found by looking at the bar stresses and approximate slip at failure reported for these specimens, as shown in Table 4.14.

Table 4.14 Bar stresses and slip at failure for No. 7 and No. 11 hooked bar specimens by Marques and Jirsa (1975) along with T/T_h based on descriptive equations, Eq. (4.5) and (4.7)

Specimen ID	Bar size	Slip	f_{su}	T	T_h	T/T_h
		in.	ksi	kips	kips	
J7-180-12-1-H	No. 7	0.07	61.0	36.6	38.8	0.94
J7-180-15-1-H	No. 7	0.15	87.0	52.2	50.6	1.03
J7-90-12-1-H	No. 7	0.08	62.0	37.2	38.3	0.97
J7-90-15-1-H	No. 7	0.15	91.0	54.6	52.6	1.04
J7-90-15-1-L	No. 7	0.21	97.0	58.2	53.3	1.09
J7-90-15-1-M	No. 7	0.18	100.0	60.0	54.0	1.11
J 7- 90 -15 -3a - H ^[1]	No. 7	0.22	98.0	58.8	50.1	1.40
J 7- 90 -15 -3 - H ^[1]	No. 7	0.21	104.0	62.4	38.0	1.72
J11-180-15-1-H	No. 11	0.05	45.0	70.2	50.6	1.48
J11-90-12-1-H	No. 11	0.04	42.0	65.5	51.2	1.58
J11-90-15-1-H	No. 11	0.06	48.0	74.9	53.8	1.09
J11-90-15-1-L	No. 11	0.06	52.0	81.1	51.9	1.20
J 11- 90 -15 -3a - L ^[1]	No. 11	0.06	69.0	107.6	72.5	1.48
J 11- 90 -15 -3 - L ^[1]	No. 11	0.09	62.0	96.7	61.1	1.58

^[1] Hooked bars outside column core, bar location factor of 1.17 applied to T/T_h

For the No. 11 bar specimens, the bar stress at failure ranged from 42 to 69 ksi with a mean of 53 ksi. The bars were Grade 60 and, although the actual yield stress is not reported by Marques and Jirsa (1975), it can be assumed to be about 69 ksi (Bournonville et al. 2004). This means that only one of the No. 11 bar specimens had bars that yielded (or were close to yield), while the other specimens had bar stresses at failure much below the yield stress. For the No. 7 bar specimens, however, the bar stresses ranged from 61 to 104 ksi, with a mean of 87.5 ksi, meaning that is likely that all but two of the No. 7 bar specimens had hooked bars that yielded prior to failure. This observation is further reinforced by the values of bar slip at failure. For the No. 7 bar specimens, slip ranged from 0.07 to 0.22 in., with a mean of 0.16 in., while for the No. 11 bar specimens, slip ranged from just 0.04 to 0.09, with a mean of 0.06 in. The prime mode of failure of the Marques and Jirsa specimens was side splitting, which would have been enhanced by the high slip of the No. 7 bars. The combined yielding and high slip are the likely reason for the lower values of T/T_h for the No. 7 bar specimens than for the No. 11 bar specimens.

CHAPTER 5: ANALYSIS AND DISCUSSION: HEADED BARS

In this chapter, the test results of the headed bar specimens are analyzed. The results are compared with stresses at anchorage failure based on the provisions in ACI 318-19 to evaluate the suitability of current Code provisions to large headed bars. The results are then compared with the forces at anchorage failure based on the descriptive equations proposed by Shao et al. (2016) and Ghimire et al. (2018, 2019a), Eq. (1.5) and (1.6). New descriptive equations developed to better represent the behavior of the larger bars are then presented and compared with the test database. After that, the effects on anchorage strength of key parameters, such as loading condition, contribution of parallel ties, bar size and spacing, bar placement within the cross-section, compression strut angle, and bar location are discussed.

5.1 COMPARISON OF TEST RESULTS WITH ACI 318-19

The provisions in ACI 318-19 for the development of headed bars are discussed in detail in Section 1.3.2. Under those provisions, No. 14 and No. 18 headed bars are not allowed, mainly due to a lack of experimental data. For No. 11 bars and smaller, the Code provides a binary choice of 1.0 or 1.6 for the parallel tie reinforcement modification factor, ψ_p . ψ_p equal to 1.0 can be applied only if $A_{tt,ACI} \geq 0.3A_{hs}$ or $s \geq 6d_b$, where $A_{tt,ACI}$ is the total cross-sectional area of ties or stirrups parallel to headed bars within $8d_b$ from the centerline of the headed bars and spaced no greater than $8d_b$ (as shown in Figure 1.26), A_{hs} is the total cross-sectional area of headed bars being developed, and s is the minimum center-to-center spacing of the headed bars. In all other cases, ψ_p is 1.6. To compare the test results with stresses corresponding to the Code equation, Eq. (1.10), yield strength f_y is replaced by bar stress, $f_{s,ACI}$, f'_c is replaced by the measured compressive strength, f_{cm} (with an upper limit of 10,000 psi), and the development length ℓ_{dh} is replaced by the measured embedment length, ℓ_{eh} . The equation is then solved for $f_{s,ACI}$:

$$f_{s,ACI} = \frac{75\sqrt{f_{cm}}\ell_{eh}}{\psi_e\psi_p\psi_o\psi_c d_b^{1.5}} \quad (5.1)$$

Using Eq. (5.1) and the modification factors for No. 11 and smaller bars, the ratios of bar stress measured in the tests to the bar stress calculated based on the Code equation, $f_s/f_{s,ACI}$, are presented in Table 5.1 and plotted versus the concrete compressive strength (f_{cm}) for the No. 14 and No. 18 headed bars in Figure 5.1. The four specimens that failed in shear (14-1A, 14-2, 14-16, 14-16A) are not included in the figure.

Table 5.1 Comparison of No. 14 and No. 18 headed bar test results with descriptive equations by Shao et al. (2016), Eq. (1.5) and (1.6), also (5.2) and (5.3), and ACI 318-19

ID ^[1]	n	s/d_b	f_{cm} psi	$\ell_{eh,avg}$ in.	A_{tt}/A_{hs}	$A_{tt,ACI}/A_{hs}$	L. C.	T kips	T_h kips	T/T_h ^[2]	f_s ksi	$f_{s,ACI}$ ksi	$f_s/f_{s,ACI}$
11-1	2	10.0	16,210	18.5	0	0	B	163.0	182.5	0.89	104.5	69.8	1.26
11-2	2	10.0	15,850	18.5	0.282	0.212	B	221.0	210.6	1.05	141.7	99.9	1.71
14-2*	2	10.6	12,830	20.5	0.267	0.178	A	190.6	250.6	0.76	84.7	95.6	1.21
14-3	2	10.6	8,510	31.8	0	0.000	B	303.0	290.6	1.04	134.7	61.1	1.35
14-4	2	10.6	7,700	32.0	0.267	0.178	A	333.6	332.1	1.00	148.3	58.9	1.55
14-15	2	10.6	6,190	22.8	0	0.000	B	204.8	191.1	1.07	91.0	69.7	1.49
14-16*	2	10.6	5,390	22.6	0.178	0.089	A	123.6	213.9	0.58	54.9	76.4	0.93
14-16A* ^[3]	2	10.6	8,350	22.4	0.178	0.089	A	186.0	233.0	0.80	82.7	78.3	1.19
14-1A*	2	10.6	12,030	22.4	0	0.000	B	160.0	220.1	0.73	71.1	65.2	0.93
14-2A	2	10.6	13,750	23.0	0.267	0.178	B	248.1	280.1	0.89	110.3	61.8	1.41
14-16B	2	10.6	7,500	22.1	0.178	0.089	B	191.7	225.1	0.85	85.2	64.7	1.31

14-16C	2	10.6	6,470	22.6	0.356	0.267	B	208.4	243.5	0.86	92.6	59.8	1.50
14-16D ^[4]	2	10.6	6,900	22.9	0.827	0.827	A	289.8	249.2	1.16	128.8	58.0	1.99
14-16E ^[4]	2	10.6	6,170	22.4	0.551	0.276	A	218.6	239.7	0.91	97.2	61.7	1.62
14-16F ^[5]	2	10.6	5,640	22.4	0.551	0.276	A	197.8	233.6	0.85	87.9	39.2	1.50
14-17 ^{[5][6]}	2	7.1	6,540	22.4	0.551	0.276	A	206.7	238.4	0.87	91.9	39.6	1.49
14-5	3	3.5	6,830	22.3	0.178	0.119	B	181.8	169.6	1.07	80.8	57.5	2.06
14-6	3	3.5	6,890	22.4	0.276	0.184	B	179.5	183.9	0.98	79.8	56.8	2.01
14-7	3	3.5	7,080	32.1	0	0.000	B	252.1	179.9	1.40	112.0	47.1	1.95
14-8	3	3.5	7,100	31.7	0.276	0.184	B	274.6	248.2	1.11	122.0	62.6	2.15
14-9	3	3.5	11,480	22.1	0.276	0.184	B	173.9	200.7	0.87	77.3	55.5	1.64
14-10 ^[4]	3	3.5	6,820	22.3	0.551	0.551	A	206.6	185.6	1.11	91.8	62.9	1.47
18-1	2	8.0	5,750	32.6	0.543	0.465	A	322.0	419.7	0.77	80.5	55.3	1.45
18-2	2	8.0	11,770	28.4	0.543	0.465	A	406.6	429.5	0.95	101.7	58.0	1.62
18-3	2	8.0	6,540	30.9	0.233	0.155	B	366.5	386.2	0.95	91.6	54.9	1.66
18-4	2	8.0	7,200	30.9	0.465	0.388	B	380.0	419.4	0.91	95.0	63.3	1.64
18-5 ^[6]	2	5.3	5,310	32.5	0.543	0.465	A	300.8	361.1	0.83	75.2	54.9	1.37
18-6 ^[6]	2	5.3	10,230	28.6	0.543	0.465	A	419.8	368.0	1.14	105.0	57.1	1.66
18-7 ^{[4][6]}	3	2.7	5,890	32.1	0.543	0.413	A	252.1	295.2	0.85	63.0	82.9	1.15
18-8 ^{[5][6]}	3	2.7	6,380	32.3	0.543	0.413	A	295.3	301.0	0.98	73.8	82.9	1.29

- n Number of bars
- s/d_b Center-to-center spacing of bars normalized by nominal bar diameter
- f_{cm} Measured concrete compressive strength
- $\ell_{eh,avg}$ Average measured embedment length
- A_{tt} Total area of tie legs within $9.5d_b$ from the centerline of headed bars (as defined in descriptive equation)
- $A_{tt,ACI}$ Total area of tie legs within $8.5d_b$ from the centerline of headed bars (as defined by ACI 318-19)
- A_{hs} Total area of headed bars being developed
- L. C. Loading condition, as defined in Section 2.3.2
- f_s Bar stress at failure
- $f_{s,ACI}$ Bar stress calculated based on ACI 318-19 equation (Eq. 5.1)
- T Average force per bar at failure
- T_h Anchorage strength of headed bars calculated using descriptive equations by Shao et al. (2016)
- [1] The first number in ID denotes the bar size
- [2] Maximum effective value for A_{tt}/A_{hs} of 0.3 applied for calculating T_h
- [3] Specimen had an additional No. 11 longitudinal bar on both sides, 2 in. from the bearing face of the head
- [4] Double overlapping No. 5 ties were used, refer to Figure 2.5
- [5] Double No. 5 ties were used
- [6] Specimen had a side cover of 6.5 in.
- * Specimen exhibited a shear-like failure (not anchorage)

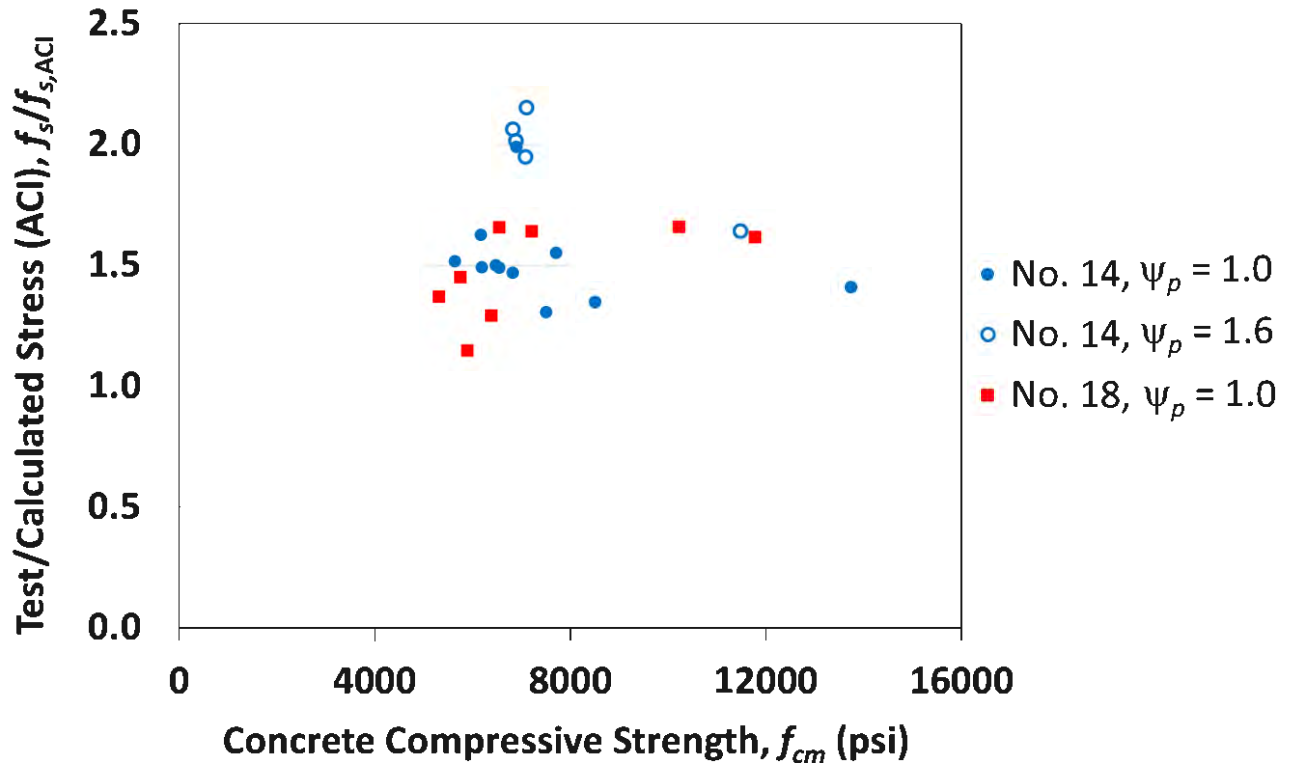


Figure 5.1 Ratio of test/calculated bar stress $f_s/f_{s,ACI}$ applying the ACI 318-19 provisions to No. 14 and No. 18 headed bar specimens versus concrete compressive strength f_{cm} , excluding specimens with shear-like failure

As shown in Table 5.1, $f_s/f_{s,ACI}$ for the four specimens that failed in shear ranged from 0.93 to 1.21 with an average of 1.07. For the rest of the specimens, the $f_s/f_{s,ACI}$ ratio ranged from 1.15 to 2.15, with an average of 1.59, as shown in Figure 5.1. This indicates that the current ACI equation would be very conservative if applied to No. 14 and No. 18 bars. There are several reasons for this conservatism. First, relative to descriptive equation the Code equation has an embedded strength reduction factor that results in $f_s/f_{s,ACI}$ values greater than T/T_h . This is reflected in the minimum $f_s/f_{s,ACI}$ value being 1.15 among specimens with an anchorage failure. Second, the current Code does not allow the ψ_p modification factor to be less than 1.0, whereas it would be appropriate to use in cases where bars are widely-spaced ($s \geq 6d_b$ based on Code and $\geq 8d_b$ based on descriptive equations) and parallel ties are provided, as will be shown when presenting the proposed design equation in Chapter 6. Despite applying $\psi_p = 1.0$ when $s \geq 6d_b$, $f_s/f_{s,ACI}$ for the specimens with widely-spaced bars ranges from 1.26 to 1.99, with an average of 1.53, indicating an overconservative estimation by the current Code provisions, even for specimens with bars spaced as wide as $10.6d_b$ with parallel ties, which could permit a shorter development length. Third, for

specimens for which ACI 318-19 requires that $\psi_p = 1.6$ to be applied, the Code is unnecessarily conservative, resulting in values of $f_s/f_{s,ACI}$ ranging from 1.64 to 2.15, with an average of 1.96. Four out of five specimens with $\psi_p = 1.6$ had parallel ties in the joint region (with $A_{tt,ACI}/A_{hs}$ values of 0.119 and 0.184), and as will be discussed in Section 5.5.2, providing parallel ties improves the anchorage strength even when $A_{tt,ACI} < 0.3A_{hs}$, a fact not recognized in ACI 318-19.

Overall, these observations show that the current Code provisions will have limitations that would cause an inaccurate representation of the effects of bar spacing and parallel tie reinforcement if extended to No. 14 and No. 18 headed bars. A modified approach is needed to provide alternative expressions for ψ_p , permitting the use of shorter development lengths (that is, ψ_p other than 1.6) under conditions where $s < 6d_b$ and $A_{tt,ACI} < 0.3A_{hs}$, and permitting ψ_p values < 1.0 when bars are widely-spaced and parallel ties are provided. These points are addressed in developing the design equation proposed in Chapter 6.

5.2 COMPARISON OF TEST RESULTS WITH DESCRIPTIVE EQUATIONS DEVELOPED BASED ON TESTS OF NO. 5 THROUGH NO. 11 HEADED BARS

In this section, the test results are compared with the descriptive equations developed by Shao et al. (2016) and Ghimire et al. (2018, 2019a, 2019b). As described in Section 1.2.2, the equations characterize the anchorage strength of headed bars based on 202 tests of simulated beam-column joint specimens with No. 5, No. 8, and No. 11 headed bars tested under a loading condition similar to that of loading condition B in this study. The descriptive equations are given below for headed bars without and with confining reinforcement in the joint region as Eq. (5.2) and (5.3), respectively:

$$T_h = 781 f_{cm}^{0.24} \ell_{eh}^{1.03} d_b^{0.35} \left(0.0836 \frac{s}{d_b} + 0.344 \right) \quad (5.2)$$

where $\left(0.0836 \frac{s}{d_b} + 0.344 \right) \leq 1.0$.

$$T_h = \left(781 f_{cm}^{0.24} \ell_{eh}^{1.03} d_b^{0.35} + 48,800 \frac{A_{tt}}{n} d_b^{0.88} \right) \left(0.0622 \frac{s}{d_b} + 0.5428 \right) \quad (5.3)$$

where $\left(0.0622 \frac{s}{d_b} + 0.5428 \right) \leq 1.0$ and $A_{tt} \leq 0.3A_{hs}$, T_h is the anchorage strength of an individual headed bar (lb); f_{cm} is the measured concrete compressive strength (psi); ℓ_{eh} is the embedment

length of the headed bar measured from the face of the column to the bearing face of the head (in.); d_b is the headed bar diameter (in.); A_{tt} is the area of confining reinforcement (in.²) within $8d_b$ from the top of the headed bar for No. 8 bars and smaller or within $10d_b$ for No. 9 bars or larger (Figure 1.18); A_{hs} is the total area of the headed bars (in.²) in a joint; n is the number of headed bars in the joint; and s is the center-to-center spacing between headed bars. The maximum value of A_{tt} in Eq. (5.3) is $0.3A_{hs}$ (Shao et al. 2016, Ghimire et al. 2018, 2019a, 2019b).

The specimens in this study were designed based on Eq. (5.2) and (5.3). To evaluate the applicability of the equations for the tests of No. 14 and No. 18 bars in this study, the anchorage strengths measured in the tests, T (reported in Table 3.4), are compared with the calculated strengths based on the descriptive equations, T_h . Table 5.1 presents the values of T , T_h , and the ratio of T/T_h for all specimens, along with specimen ID and key parameters (number and spacing of bars, concrete compressive strength, embedment length, confining reinforcement in the joint region, and loading condition).

Based on Table 5.1, the test-to-calculated ratio T/T_h varied among specimens with different properties. Among the No. 14 bar specimens with confining reinforcement, specimens 14-16B and 14-16F had the lowest T/T_h ratio (0.85). Specimen 14-16D with the highest amount of confining reinforcement ($A_{tt}/A_{hs} = 0.83$) had the highest T/T_h ratio (1.16). The test-to-calculated ratio T/T_h is below 1.0 for all but one No. 18 bar specimen. The specimens that failed in shear had the lowest T/T_h ratios, ranging from 0.58 to 0.80, with 14-16 with the lowest T/T_h ratio (0.58) among all specimens.

The test results can be compared with the descriptive equations based on specimen properties, including bar size, parallel ties, and loading condition. In the following comparisons, the four specimens exhibiting a shear-like failure (see Section 3.2.2) are excluded from analysis.

Table 5.2 summarizes the T/T_h values based on bar size and parallel ties for the No. 14 and No. 18 bar specimens, regardless of loading condition and excluding the specimens with a shear-like failure.

As shown in Table 5.2, the values of T/T_h range from 0.77 to 1.40, with a mean of 0.98 and a coefficient of variation of 0.147. The three specimens without parallel ties (all No. 14 bars) have a mean T/T_h ratio of 1.17, while those with parallel ties have a mean T/T_h ratio of 0.95, a statistically significant difference with a p value of 0.01. Based on bar size, the mean T/T_h is 1.00 for the No.

14 bar specimens and 0.92 for the No. 18 bar specimens (0.92), but the difference is not statistically significant ($p = 0.20$).

Table 5.2 Summary of test-to-calculated ratio T/T_h for No. 14 and No. 18 headed bars based on bar size and parallel ties with T_h based on Eq. (5.2) or (5.3), excluding specimens that failed in shear

	T/T_h				
	All	All - Without Parallel Ties	All - With Parallel Ties	All No. 14	All No. 18
No. of Specimens	24	3	21	16	8
Max	1.40	1.40	1.16	1.40	1.14
Min	0.77	1.04	0.77	0.85	0.77
Mean	0.98	1.17	0.95	1.00	0.92
STDEV	0.143	0.199	0.114	0.152	0.113
CoV	0.147	0.170	0.120	0.151	0.123

Table 5.3 summarizes the T/T_h values for the No. 14 and No. 18 headed bar specimens tested under loading condition A (joint shear equal to 80% of the applied load), excluding those with a shear-like failure. All specimens had parallel ties within the joint.

Table 5.3 Summary of test-to-calculated ratio T/T_h for No. 14 and No. 18 headed bars tested under loading condition A (all with parallel ties) with T_h based on Eq. (5.3), excluding specimens that failed in shear

	T/T_h – Loading Condition A		
	All	No. 14	No. 18
No. of Specimens	12	6	6
Max	1.16	1.16	1.14
Min	0.77	0.85	0.77
Mean	0.95	0.98	0.92
STDEV	0.131	0.132	0.133
CoV	0.137	0.134	0.145

As shown in Table 5.3, the headed bar specimens tested under loading condition A have test-to-calculated T/T_h ratios ranging from 0.77 to 1.16 with a mean of 0.95 and a coefficient of variation of 0.137. Under this loading condition, the mean T/T_h for No. 14 bars (0.98) is higher than that of No. 18 bars (0.92), but the difference is not statistically significant ($p = 0.42$).

Specimens with parallel ties and tested under loading condition B can be compared based on bar size, as shown in Table 5.4.

Table 5.4 Summary of test-to-calculated ratio T/T_h for No. 14 and No. 18 headed bars with parallel ties and tested under loading condition B with T_h based on Eq. (5.3)

	T/T_h ^[1] – Loading Condition B – with Parallel Ties		
	All	No. 14	No. 18
No. of Specimens	9	7	2
Max	1.11	1.11	0.95
Min	0.85	0.85	0.91
Mean	0.94	0.95	0.93
STDEV	0.094	0.107	0.030
COV	0.099	0.113	0.033

As shown in Table 5.4, the headed bar specimens with parallel ties and tested under loading condition B had T/T_h ratios ranging from 0.85 to 1.11, with a mean of 0.94 and a coefficient of variation of 0.099. Comparing based on bar size, the No. 14 bar specimens had a mean T/T_h of 0.95, slightly higher than that of No. 18 bars (0.93). This small difference is not statistically significant ($p = 0.83$).

The similarities in the mean values of T/T_h for the specimens with parallel ties tested under loading conditions A and B (0.95 and 0.94) indicate that in cases where confining reinforcement within a joint is adequate to prevent a shear-like failure, the differences in the two loading conditions did not affect anchorage strength.

The average force per bar at failure, T , for all No. 14 and No. 18 headed bar specimens (excluding those that failed in shear) is compared with that calculated using descriptive equations, T_h , in Figure 5.2.

As shown in Figure 5.2, the best fit trendline on all specimens starts slightly above $T = T_h$ for lower values of T and becomes less conservative as T increases, suggesting that it would be worthwhile to update the descriptive equations to more accurately represent the anchorage strength of headed bars larger than No. 11.

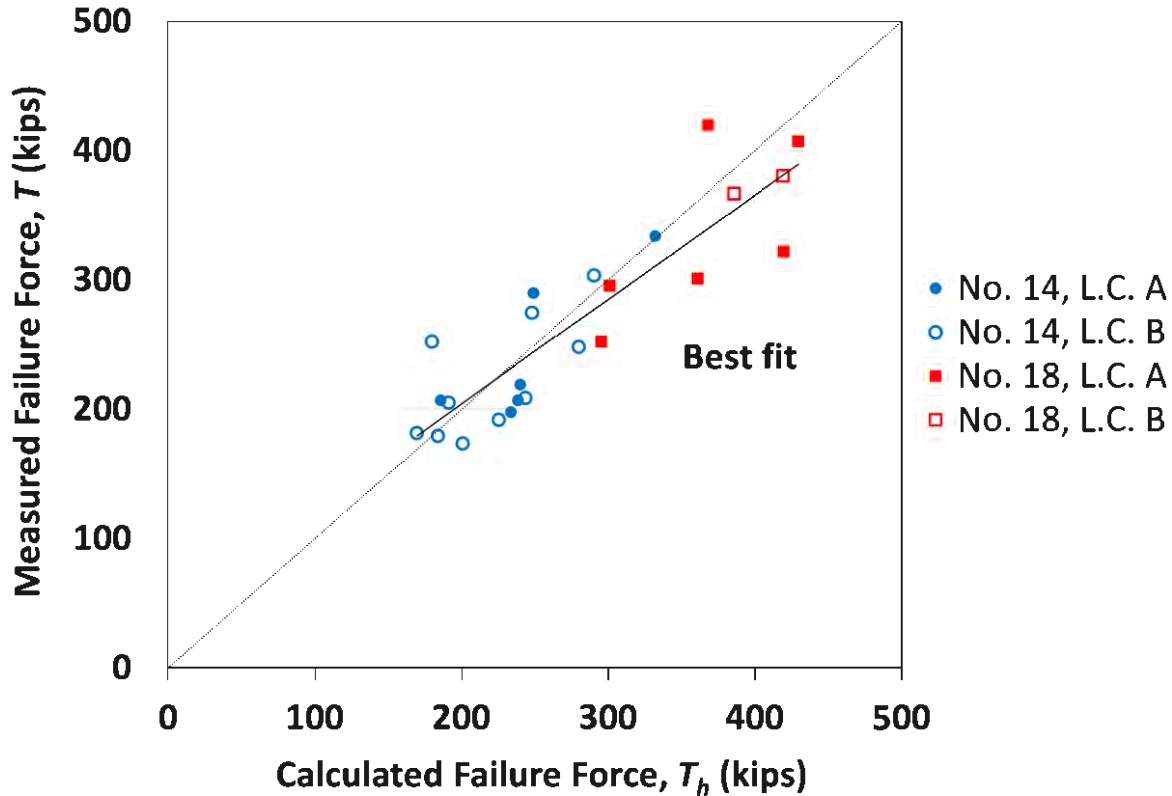


Figure 5.2 Test versus calculated force per bar at failure for No. 14 and No. 18 headed bar specimens based on descriptive equations by Shao et. al (2016)

5.3 NEW DESCRIPTIVE EQUATIONS

New descriptive equations were developed following the iterative analyses procedure used by Shao et al. (2016) for headed bars and Ajaam et al. (2017) for hooked bars. In summary, a base equation is first developed for specimens with widely-spaced bars without parallel ties. Using the same equation, an expression to account for close bar spacing is developed using specimens with closely-spaced bars without parallel ties. Next, the same base equation is used for specimens with widely-spaced bars with parallel ties to develop an expression representing the contribution of the parallel ties. Finally, the equation for widely-spaced bars with parallel tie is applied to specimens with closely-spaced bars and parallel ties to develop an expression for closely spaced bars. The new descriptive equations have the same format as Eq. (5.2) and (5.3). The iterative analysis is based on forcing the average T/T_h to be 1.00, in which T is the measured and T_h is the calculated failure load. The database used for analyses includes No. 5, No. 8, and No. 11 bar specimens tested by Shao et al. (2016) and the specimens tested in this study, excluding those that failed in shear.

5.3.1 Widely-spaced Bars Without Parallel Ties

The best-fit equation obtained using the iterative analysis for the 33 specimens with widely-spaced bars (center-to center bar spacing $\geq 8d_b$) without parallel ties is

$$T_c = 1296 f_{cm}^{0.207} \ell_{eh}^{0.941} d_b^{0.498} \quad (5.4)$$

where T_c is the anchorage strength of headed bars without parallel ties (lb), f_{cm} is concrete compressive strength (psi), ℓ_{eh} is embedment length (in.), and d_b is bar diameter (in.). Compared with Eq. (5.2), the constant increased from 768 to 1296, the power of f_{cm} decreased from 0.24 to 0.207, the power of ℓ_{eh} decreased from 1.03 to 0.941, and the power of d_b increased from 0.35 to 0.498. The T/T_c ratio is compared with f_{cm} in Figure 5.3.

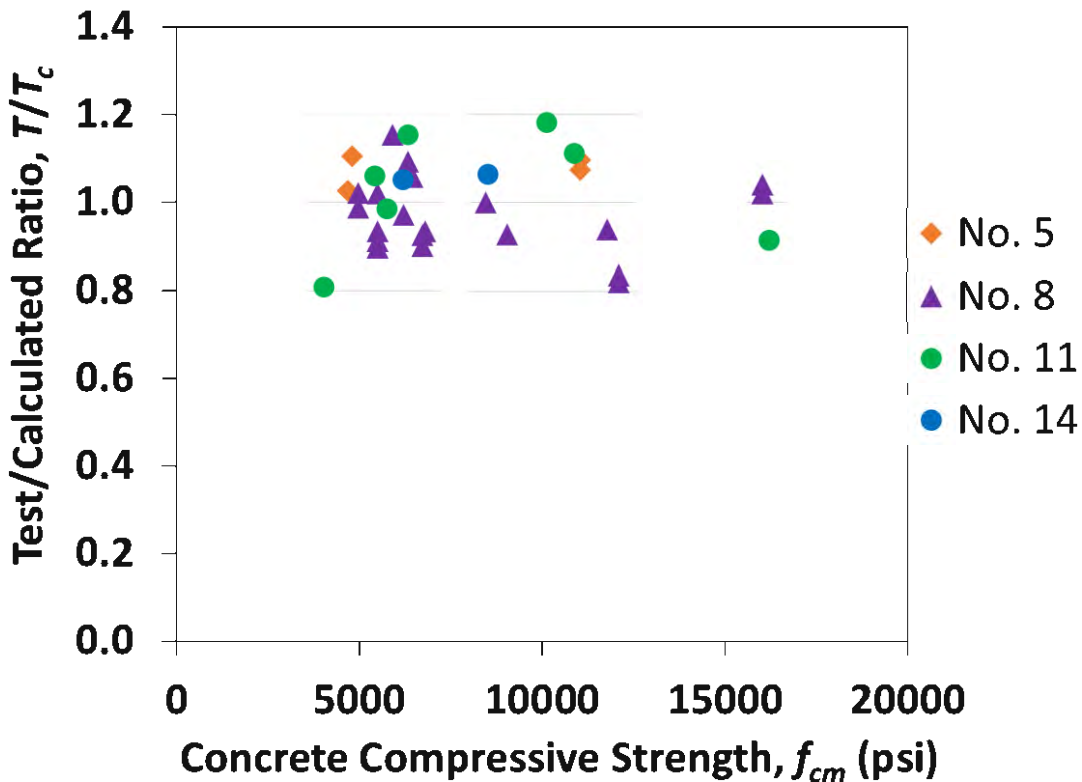


Figure 5.3 Ratio of test-to-calculated bar force at failure T/T_c , with T_c based on Eq. (5.4), versus concrete compressive strength for headed bar specimens with widely-spaced bars without parallel ties

As shown in Figure 5.3, there is no noticeable trend in T/T_c as function of f_{cm} indicating that the 0.207 power provides an adequate representation of the effect of concrete compressive strength on anchorage strength. Also, the distribution of T/T_c values indicates no noticeable bias towards bar size. The statistical parameters for the 33 specimens are presented in Table 5.5.

Table 5.5 Statistical parameters for T/T_c ratio for headed bar specimens with widely-spaced bars without parallel ties with T_c based on Eq. (5.4)

Bar size	All	No. 5	No. 8	No. 11	No. 14	No. 18
No. of specimens	33	4	20	7	2	0
Max	1.18	1.10	1.15	1.18	1.06	-
Min	0.81	1.03	0.82	0.81	1.05	-
Mean	1.00	1.07	0.97	1.03	1.06	-
STDEV	0.095	0.035	0.083	0.135	0.007	-
CoV	0.095	0.033	0.086	0.131	0.006	-

As shown in Table 5.5, the T/T_c ratio ranges from 0.81 to 1.18 with a mean of 1.00 and a coefficient of variation of 0.095 for the 33 headed bar specimens with widely-spaced bars and no parallel ties.

5.3.2 Closely-spaced Bars Without Parallel Ties

As discussed in Sections 4.3.2 and 4.4.3, center-to-center bar spacing is used as a proxy to represent the effects on anchorage strength for members with more than two widely spaced bars. Using Eq. (5.4), the effect of close bar spacing (center-to-center spacing $< 8d_b$) can be determined. To do so, the T/T_c is calculated for the 35 specimens with closely-spaced bars and no parallel ties. T/T_c versus s/d_b for these specimens is shown in Figure 5.4.

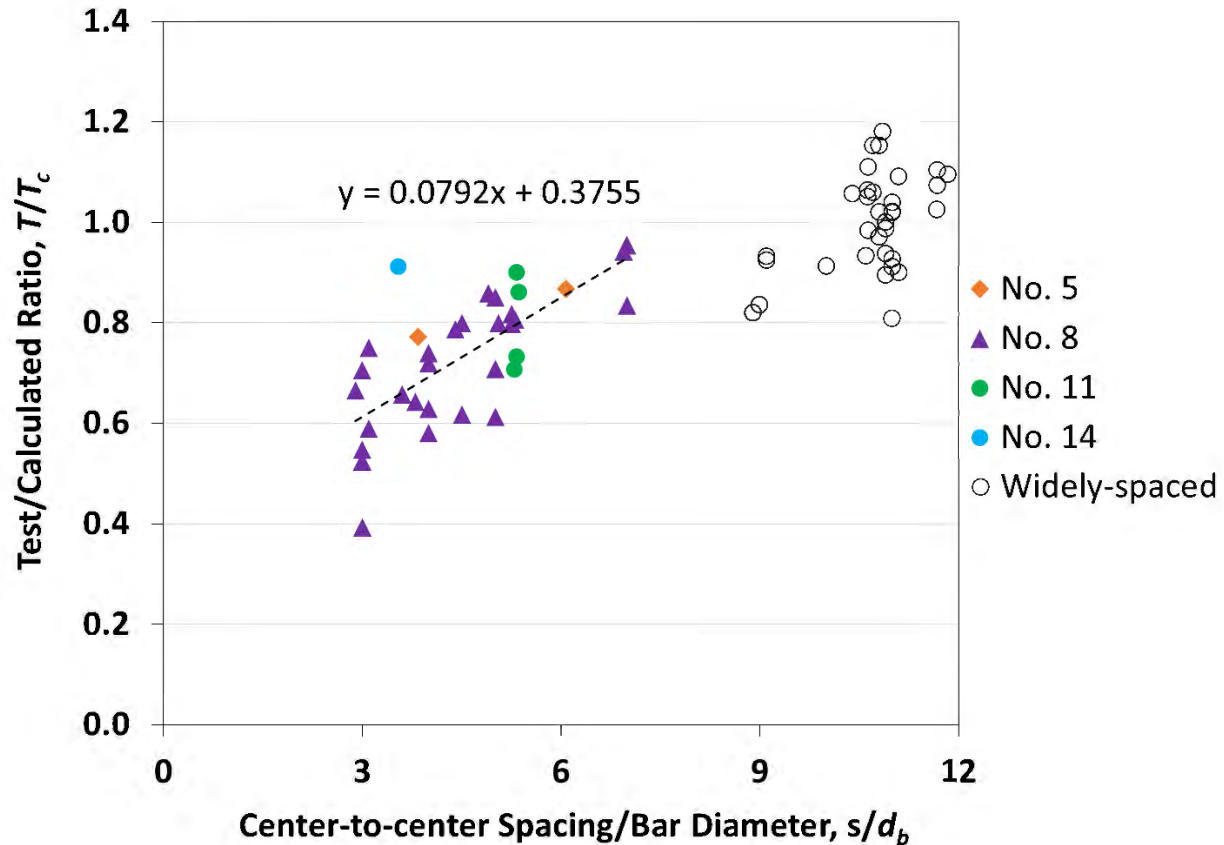


Figure 5.4 Test-to-calculated bar force at failure T/T_c versus ratio of center-to-center spacing to bar diameter s/d_b for widely- and closely-spaced headed bars without parallel ties with T_c based on Eq. (5.4)

As shown the figure, the T/T_c ratio (and therefore anchorage strength) decreases with a decrease in bar spacing. To account for the effect of bar spacing, the linear trendline equation shown in Figure 5.4 is combined with Eq. (5.4) to give

$$T_c = \left(1296 f_{cm}^{0.207} \ell_{eh}^{0.941} d_b^{0.498} \right) \left(0.0792 \frac{s}{d_b} + 0.3755 \right) \quad (5.5)$$

where $\left(0.0792 \frac{s}{d_b} + 0.3755 \right) \leq 1.0$, and s is the center-to-center spacing of the bars (in.). The statistical parameters for T/T_c for the 35 specimens with closely-spaced bars and no parallel ties are given in Table 5.6.

Table 5.6 Statistical parameters of T/T_c ratio for headed bar specimens with closely-spaced bars without parallel ties with T_c based on Eq. (5.5)

Bar size	All	No. 5	No. 8	No. 11	No. 14	No. 18
No. of specimens	35	2	28	4	1	0
Max	1.39	1.14	1.21	1.15	1.39	-
Min	0.64	1.01	0.64	0.89	1.39	-
Mean	1.00	1.07	0.98	1.01	1.39	-
STDEV	0.136	0.087	0.125	0.111	0	-
CoV	0.136	0.081	0.127	0.109	0	-

As shown in the table for the specimens with closely-spaced headed bars and no parallel ties, the T/T_c ratio ranges from 0.64 to 1.39, with a mean value of 1.00 and a coefficient of variation of 0.136. For all headed bar specimens without parallel ties, T/T_c is compared with the concrete compressive strength in Figure 5.5. The statistical parameters for T/T_c for the specimens without parallel ties are given in Table 5.7.

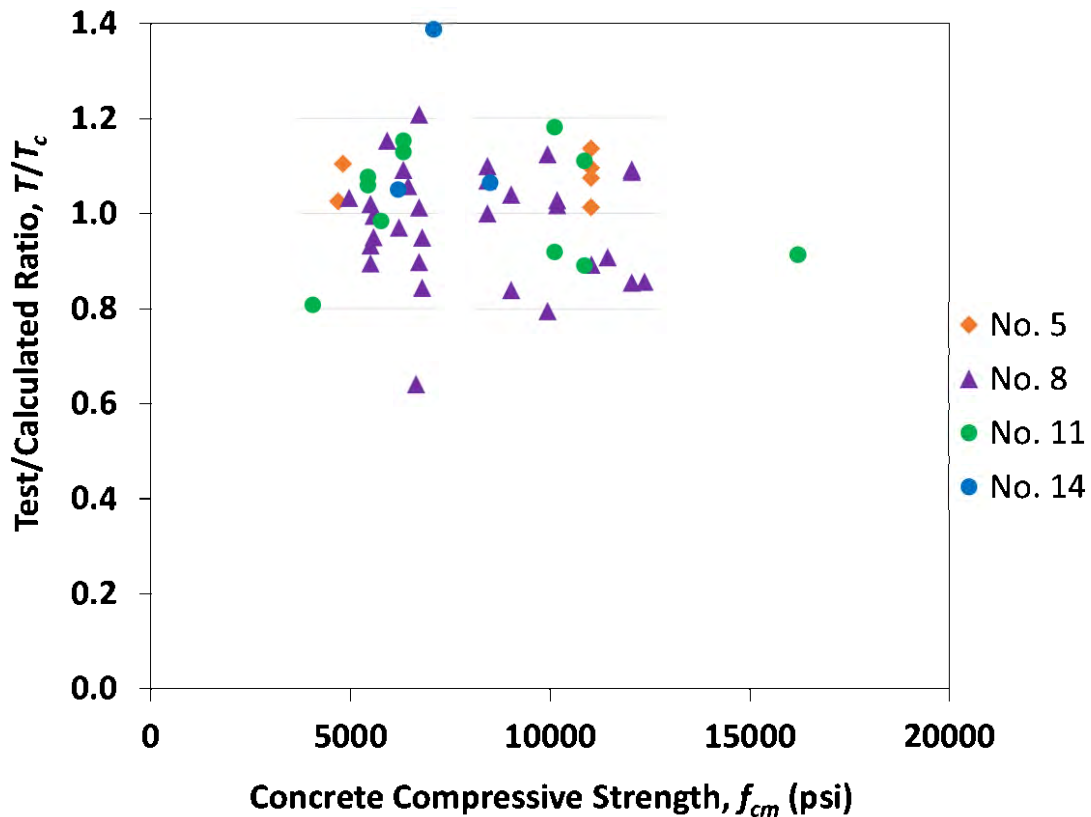


Figure 5.5 Ratio of test-to-calculated bar force at failure T/T_c , based on Eq. (5.5), versus concrete compressive strength for headed bar specimens with widely- and closely-spaced bars without parallel ties

As shown in Table 5.6 and Figure 5.5, the single specimen with three closely-spaced No. 14 bars, 14-7, had the highest T/T_h ratio of 1.39. If the close-bar spacing term in Eq. (5.5) is not applied, however, the T/T_c ratio is 0.91. This observation indicates that bar spacing might not be the controlling factor here, but as mentioned earlier, it can be safely used as a convenient representation of the effect of multiple bars anchored in a member.

Table 5.7 Statistical parameters of T/T_c , with T_c based on Eq. (5.5), for headed bar specimens with widely- and closely-spaced bars without parallel ties

Bar size	All	No. 5	No. 8	No. 11	No. 14	No. 18
No. of specimens	68	6	48	11	3	0
Max	1.39	1.14	1.21	1.18	1.39	-
Min	0.64	1.01	0.64	0.81	1.05	-
Mean	1.00	1.07	0.98	1.02	1.17	-
STDEV	0.119	0.048	0.109	0.124	0.191	-
CoV	0.119	0.044	0.111	0.121	0.164	-

As shown in Table 5.7, the 68 specimens without parallel ties have a T/T_c ratio ranging from 0.64 to 1.39 with a mean value of 1.00 and a coefficient of variation of 0.119.

5.3.3 Widely-Spaced Bars with Parallel Ties

The procedure to develop Eq. (5.4) was used for 55 specimens with widely-spaced bars with parallel ties to obtain an expression representing the contribution of ties to anchorage strength (T_s), assuming that Eq. (5.4) represents the contribution of concrete (T_c). In developing an expression for T_s , it is assumed that an effective area of parallel ties, A_{tt} contribute to anchorage strength. The definition of A_{tt} is retained from the previous research (Shao et al. 2016), that is, the total area of tie legs within $8d_b$ from the top of the headed bars for No. 3 through No. 8 bars and $10d_b$ for No. 11 and larger bars.

As stated earlier, Shao et al. (2016) limited A_{tt} to $0.3A_{hs}$, where A_{hs} is the total area of headed bars. The limit was chosen based on the range of A_{tt}/A_{hs} values tested (0.07 to 1.07, with an average of 0.3). If the No. 14 and No. 18 specimens are included, the average of A_{tt}/A_{hs} values increases to 0.33. If only the No. 14 and No. 18 bar specimens are considered, the average value of A_{tt}/A_{hs} is 0.42. Therefore, to better permit the effect of A_{tt}/A_{hs} to be evaluated for larger bars, the limit for A_{tt}

was chosen as $0.4A_{hs}$ for this study. As shown in the next few pages, the new limit provides a good match between calculated and measured failure loads.

For the 55 specimens with widely-spaced bars with parallel ties, the following equation is obtained using iterative analysis:

$$T_h = T_c + T_s = 1296 f_{cm}^{0.207} \ell_{eh}^{0.941} d_b^{0.498} + 49,402 \left(\frac{A_{tr}}{n} \right) d_b^{0.11} \text{ and } A_{tr} \leq 0.4A_{hs} \quad (5.6)$$

where n is the number of headed bars.

The noticeable difference between Eq. (5.6) and the equation developed by Shao et al. (2016), Eq. (5.3), is the reduction in the power of d_b in the expression for T_s from 0.88 to 0.11. This indicates a much lower effect of bar size on the contribution of parallel ties than previously obtained. The other difference is a very slight increase in the constant from 48,800 to 49,402.

The ratio T/T_h is compared with the concrete compressive strength for the 55 specimens used to develop Eq. (5.6) in Figure 5.6.

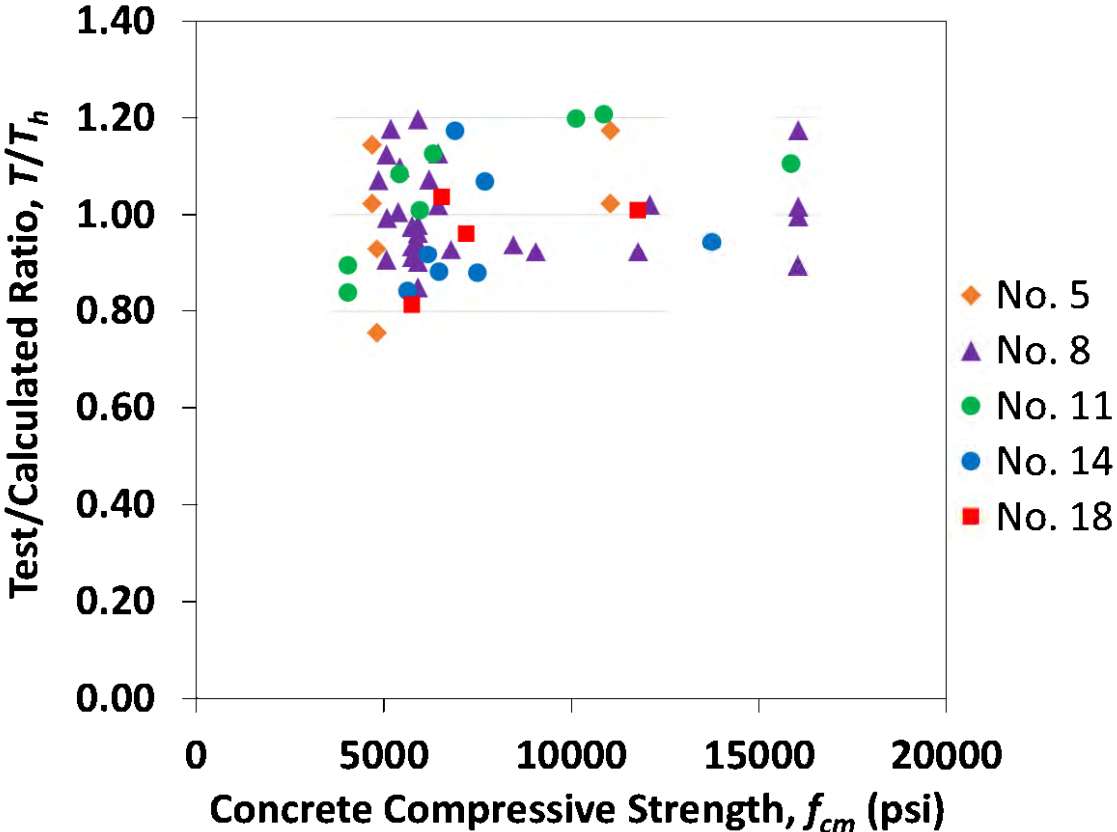


Figure 5.6 Ratio of test-to-calculated bar force at failure T/T_h versus concrete compressive strength for headed bar specimens with widely-spaced bars with parallel ties with T_h based on Eq. (5.6)

As shown in Figure 5.6, the data points show, perhaps, a slight positive trend, indicating a slight underestimation of the effect of concrete compressive strength by Eq. (5.6). The statistical parameters for T/T_h values for the specimens with widely-spaced bars and parallel ties are shown in Table 5.8. In this case, T/T_h ranges from 0.76 to 1.21, with an average of 1.00 and a coefficient of variation of 0.109.

Table 5.8 Statistical parameters of T/T_h ratio for headed bar specimens with widely-spaced bars with parallel ties with T_h based on Eq. (5.6)

Bar size	All	No. 5	No. 8	No. 11	No. 14	No. 18
No. of specimens	55	6	30	8	7	4
Max	1.21	1.17	1.20	1.21	1.17	1.04
Min	0.76	0.76	0.85	0.84	0.84	0.81
Mean	1.00	1.01	1.00	1.06	0.96	0.95
STDEV	0.109	0.153	0.093	0.135	0.111	0.086
CoV	0.109	0.151	0.093	0.127	0.116	0.091

5.3.4 Closely-Spaced Bars with Parallel Ties

As for the specimens without parallel ties, an expression to account for close bar spacing can be developed for specimens with parallel ties. To this end, T_h was calculated for 41 specimens with closely-spaced bars and parallel ties using Eq. (5.6), and the ratio T/T_h is plotted versus s/d_b in Figure 5.7.

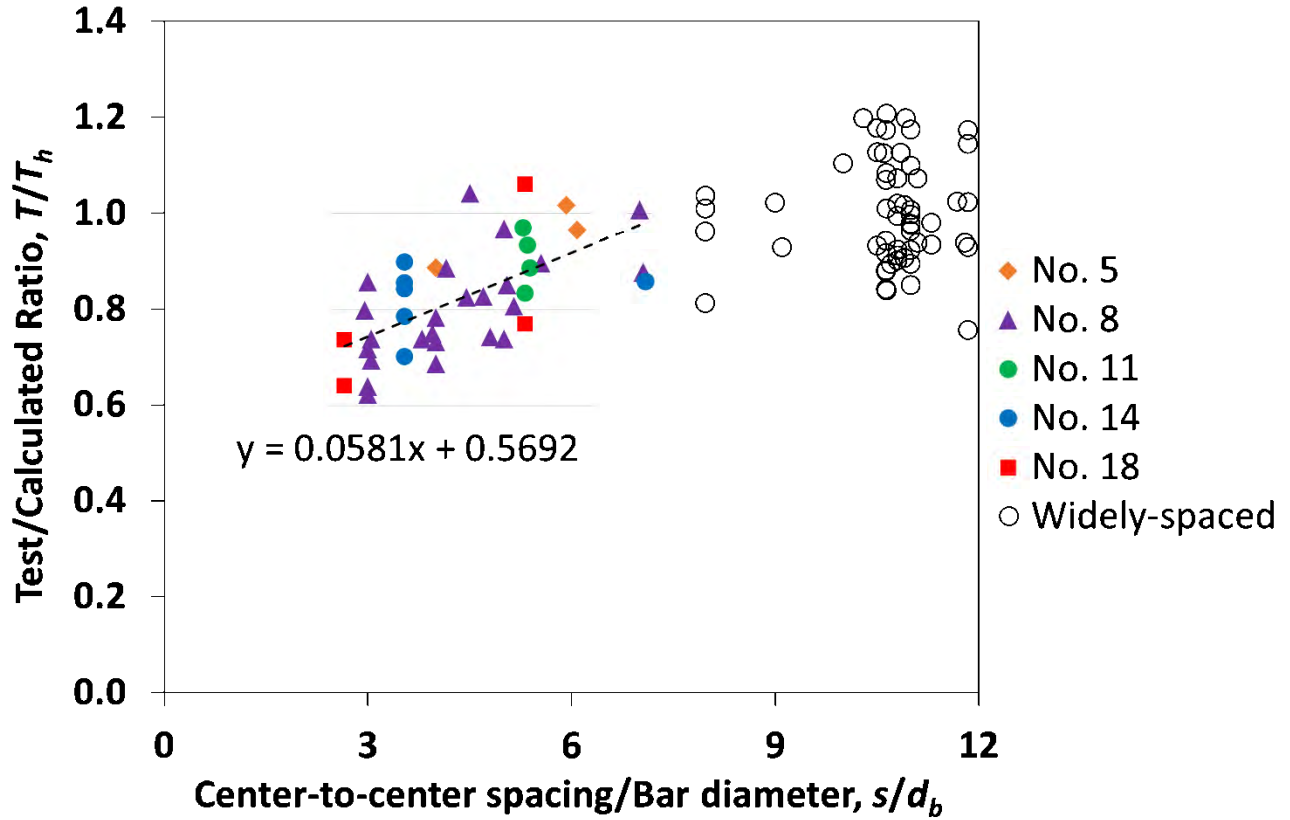


Figure 5.7 Test-to-calculated bar force at failure T/T_h versus ratio of center-to-center spacing to bar diameter s/d_b for widely- and closely-spaced headed bars with parallel ties with T_h based on Eq. (5.6)

As shown in Figure 5.7, and similar to specimens without parallel ties, the T/T_h ratio decreases as the spacing between bars decreases. Eq. (5.7) is multiplied by the equation given by the trendline to give

$$T_h = \left(1296 f_{cm}^{0.207} \ell_{ch}^{0.941} d_b^{0.498} + 49,402 \left(\frac{A_t}{n} \right) d_b^{0.11} \right) \left(0.0581 \frac{c_{ch}}{d_b} + 0.5692 \right) \quad (5.7)$$

where $\left(0.0581 \frac{c_{ch}}{d_b} + 0.5692 \right) \leq 1.0$ and $A_t \leq 0.4A_{hs}$. Table 5.9 shows the statistical parameters of T/T_h ratio for 41 specimens with closely-spaced bars with parallel ties.

Table 5.9 Statistical parameters of T/T_h ratio for headed bar specimens with closely-spaced bars with parallel ties with T_h based on Eq. (5.7)

Bar size	All	No. 5	No. 8	No. 11	No. 14	No. 18
No. of specimens	41	3	24	4	6	4
Max	1.25	1.11	1.25	1.11	1.16	1.21
Min	0.84	1.05	0.84	0.95	0.87	0.88
Mean	1.00	1.09	0.98	1.03	1.02	1.00
STDEV	0.104	0.037	0.104	0.068	0.114	0.155
CoV	0.104	0.034	0.106	0.066	0.112	0.155

As shown in Table 5.9, the headed bar specimens with closely-spaced bars and parallel ties the T/T_h ratios ranges from 0.84 to 1.25, with an average of 1.00 and coefficient of variation of 0.104. Using Eq. (5.7), the ratio of T/T_h for specimens with widely- and closely-spaced bars with parallel ties are plotted versus concrete compressive strength in Figure 5.8.

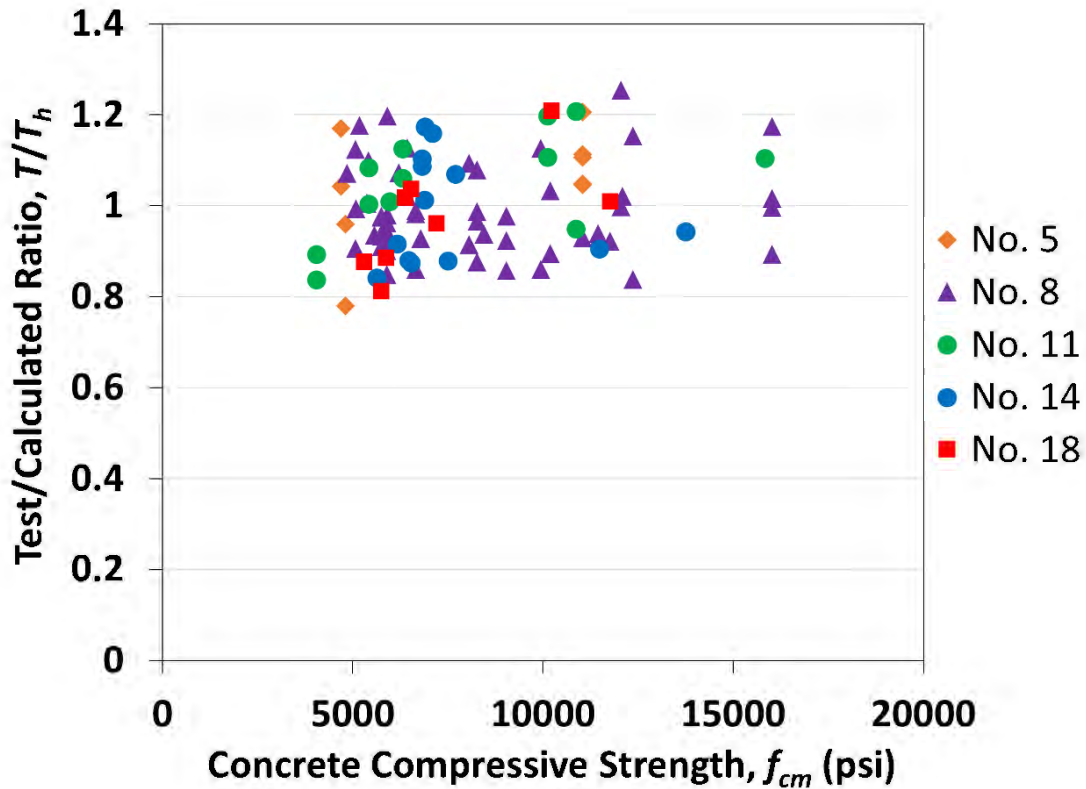


Figure 5.8 Ratio of test-to-calculated bar force at failure T/T_h versus concrete compressive strength for headed bar specimens with widely- and closely-spaced bars with parallel ties with T_h based on Eq. (5.7)

As shown in Figure 5.8, no trend is apparent with respect to concrete compressive strength. The statistical parameters of T/T_h are shown for all specimens with parallel ties in Table 5.10. As shown in table, T/T_h for specimens with parallel ties in the joint region range from 0.76 to 1.25 with an average of 1.00 and a coefficient of variation of 0.108.

Table 5.10 Statistical parameters of T/T_h ratio for headed bar specimens with widely- and closely-spaced bars with parallel ties with T_h based on Eq. (5.7)

Bar size	All	No. 5	No. 8	No. 11	No. 14	No. 18
No. of specimens	96	9	54	12	13	8
Max	1.25	1.17	1.25	1.21	1.17	1.21
Min	0.76	0.76	0.84	0.84	0.84	0.81
Mean	1.00	1.04	0.99	1.05	0.99	0.98
STDEV	0.108	0.128	0.097	0.114	0.117	0.123
CoV	0.108	0.124	0.098	0.109	0.119	0.126

5.3.5 Summary

Table 5.11 presents the statistical parameters of T/T_h for all headed bar specimens used to develop Eq. (5.5) and (5.7). As shown in the table, T/T_h averages of 1.00, with a coefficient of variation of 0.112. T/T_h values based on Eq. (5.5) and (5.7) for the No. 14 and No. 18 bar specimens tested in this study are summarized in Table 5.12 and further evaluated in the Section 5.4. The measured bar force at failure T is compared with the calculated failure load T_h based on Eq. (5.5) and (5.7) for the No. 14 and No. 18 bar specimens tested in this study in Figure 5.9. The best-fit line closely matches the $T = T_h$ dashed line. These comparisons indicate that Eq. (5.5) and (5.7), along with the new upper limit on A_{tt} of $0.4A_{hs}$, provide very good estimates of the anchorage strength of headed bars.

Table 5.11 Statistical parameters of T/T_h ratio for all headed bar specimens with T_h based on Eq. (5.5) or (5.7)

Bar size	All	No. 5	No. 8	No. 11	No. 14	No. 18
No. of specimens	164	15	102	23	16	8
Max	1.39	1.17	1.25	1.21	1.39	1.21
Min	0.64	0.76	0.64	0.81	0.84	0.81
Mean	1.00	1.05	0.98	1.03	1.02	0.98
STDEV	0.112	0.103	0.103	0.117	0.145	0.123
CoV	0.112	0.098	0.104	0.113	0.142	0.126

Table 5.12 Summary of T/T_h values for No. 14 and No. 18 headed bars specimens tested in this study based on the developed descriptive equations, Eq. (5.5) and (5.7)

ID	n	s/d_b	Bar spacing	f_{cm} psi	$\ell_{eh,avg}$ in.	A_H/A_{hs}	L. C.	T kips	T_h kips	T/T_h
14-2*	2	10.6	Wide	12,830	20.5	0.267	A	190.6	237.6	0.80
14-3	2	10.6	Wide	8,510	31.8	0	B	303.0	284.8	1.06
14-4	2	10.6	Wide	7,700	32.0	0.267	A	333.6	312.1	1.07
14-15	2	10.6	Wide	6,190	22.8	0	B	204.8	194.9	1.05
14-16*	2	10.6	Wide	5,390	22.6	0.178	A	123.6	208.8	0.59
14-16A*	2	10.6	Wide	8,350	22.4	0.178	A	186.0	225.0	0.83
14-1A*	2	10.6	Wide	12,030	22.4	0	B	160.0	184.7	0.87
14-2A	2	10.6	Wide	13,750	23.0	0.267	B	248.1	263.3	0.94
14-16B	2	10.6	Wide	7,500	22.1	0.178	B	191.7	218.2	0.88
14-16C	2	10.6	Wide	6,470	22.6	0.356	B	208.4	236.7	0.88
14-16D	2	10.6	Wide	6,900	22.9	0.827	A	289.8	247.1	1.17
14-16E	2	10.6	Wide	6,170	22.4	0.551	A	218.6	238.5	0.92
14-16F	2	10.6	Wide	5,640	22.4	0.551	A	197.8	235.0	0.84
14-17	2	7.1	Close	6,540	22.4	0.551	A	206.7	236.5	0.87
14-5	3	3.5	Close	6,830	22.3	0.178	B	181.8	167.2	1.09
14-6	3	3.5	Close	6,890	22.4	0.276	B	179.5	177.3	1.01
14-7	3	3.5	Close	7,080	32.1	0	B	252.1	181.6	1.39
14-8	3	3.5	Close	7,100	31.7	0.276	B	274.6	237.0	1.16
14-9	3	3.5	Close	11,480	22.1	0.276	B	173.9	192.2	0.90
14-10	3	3.5	Close	6,820	22.3	0.551	A	206.6	187.2	1.10
18-1	2	8.0	Wide	5,750	32.6	0.543	A	322.0	396.3	0.81
18-2	2	8.0	Wide	11,770	28.4	0.543	A	406.6	402.9	1.01
18-3	2	8.0	Wide	6,540	30.9	0.233	B	366.5	353.7	1.04
18-4	2	8.0	Wide	7,200	30.9	0.465	B	380.0	395.3	0.96
18-5	2	5.3	Close	5,310	32.5	0.543	A	300.8	343.1	0.88
18-6	2	5.3	Close	10,230	28.6	0.543	A	419.8	347.5	1.21
18-7	3	2.7	Close	5,890	32.1	0.543	A	252.1	284.8	0.89
18-8	3	2.7	Close	6,380	32.3	0.543	A	295.3	290.2	1.02

* Specimens failed in shear (not anchorage)

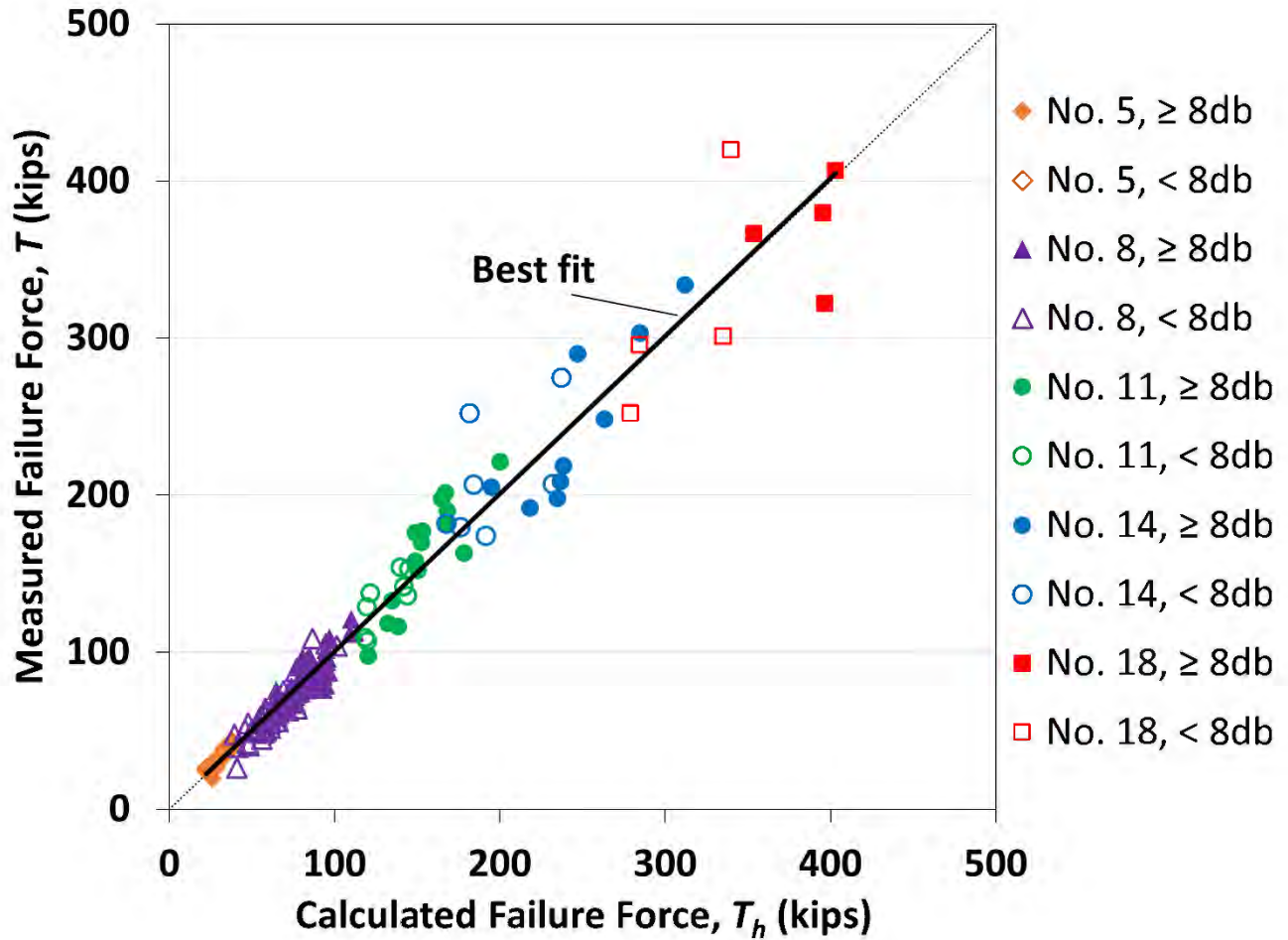


Figure 5.9 Measured versus calculated bar force at failure using new descriptive equations for all headed bar specimens, excluding those with a shear-like failure, with the calculated bar force, T_h , based on Eq. (5.5) or (5.7)

5.4 EVALUATING NEW DESCRIPTIVE EQUATIONS FOR NO. 14 AND NO. 18 BARS

In this section, the new descriptive equations, Eq. (5.5) and (5.7), are evaluated in more detail for the No. 14 and No. 18 bar specimens in this study. Table 5.13 summarizes the T/T_h values based on bar size and the presence of parallel ties for the No. 14 and No. 18 bar specimens, regardless of loading condition and excluding the specimens that failed in shear.

Table 5.13 Summary of test-to-calculated ratio T/T_h for No. 14 and No. 18 headed bars based on bar size and parallel ties, with T_h based on Eq. (5.5) or (5.7), excluding specimens that failed in shear

	T/T_h				
	All	All - Without Parallel Ties	All - With Parallel Ties	All No. 14	All No. 18
No. of Specimens	24	3	21	16	8
Max	1.39	1.39	1.21	1.39	1.21
Min	0.81	1.05	0.81	0.84	0.81
Mean	1.01	1.17	0.98	1.02	0.98
STDEV	0.137	0.191	0.117	0.145	0.123
CoV	0.136	0.164	0.119	0.142	0.126

As shown in Table 5.13, the T/T_h ratio, with T_h based on Eq. (5.5) or (5.7), has improved for No. 14 and No. 18 bar specimens, compared with the values based on the equations developed for No. 11 and smaller headed bars (given in Table 5.2). Most noticeably, the average T/T_h is now 0.98 for No. 18 bars compared with 0.92 based on Eq. (5.2) and (5.3). For all specimens with parallel ties, the new equations result in an average T/T_h of 0.98, compared with 0.95 based on Eq. (5.2) and (5.3). An overall improvement in the coefficient of variation is also observed. With Eq. (5.5) or (5.7), T/T_h for No. 14 and No. 18 bar specimens ranges from 0.81 to 1.39, with an average of 1.01 and a coefficient of variation of 0.136 (0.147 based on Eq. (5.2) and (5.3)).

Table 5.14 presents the new T/T_h values for No. 14 and No. 18 headed bar specimens with parallel ties and tested under loading condition A (joint shear equal to 80% of the applied load), excluding those with a shear-like failure.

Table 5.14 Summary of test-to-calculated ratio T/T_h for No. 14 and No. 18 headed bars tested under loading condition A (all with parallel ties) with T_h based on Eq. (5.7), excluding specimens that failed in shear

	T/T_h – Loading Condition A		
	All	No. 14	No. 18
No. of Specimens	12	6	6
Max	1.21	1.17	1.21
Min	0.81	0.84	0.81
Mean	0.98	1.00	0.97
STDEV	0.134	0.136	0.142
CoV	0.136	0.137	0.147

As shown in Table 5.14, T/T_h for the specimens with parallel ties and tested under loading condition A ranges from 0.81 to 1.21 with an average of 0.98 and a coefficient of variation of 0.136. These numbers show improvements compared with Eq. (5.3) (Table 5.3), most noticeably for No. 18 bars where the average T/T_h is now 0.97 compared with 0.92. The overall average is also improved, being 0.98 compared with 0.95 based on Eq. (5.3).

A similar summary is shown in Table 5.15 for specimens with parallel ties and tested under loading condition B.

Table 5.15 Summary of test-to-calculated ratio T/T_h for No. 14 and No. 18 headed bars with parallel ties and tested under loading condition B with T_h based on Eq. (5.7)

	T/T_h ^[1] – Loading Condition B – with Parallel Ties		
	All	No. 14	No. 18
No. of Specimens	9	7	2
Max	1.16	1.16	1.04
Min	0.88	0.88	0.96
Mean	0.98	0.98	1.00
STDEV	0.097	0.109	0.053
CoV	0.098	0.111	0.053

As shown in Table 5.15, T/T_h for the specimens with parallel ties and tested under loading condition B ranges from 0.88 to 1.16 with an average of 0.98 and a coefficient of variation of 0.098. A noticeable improvement in the average and coefficients of variation is, again, observed, compared with the values based on previous equations given in Table 5.4. The overall average increased from 0.94 to 0.98 for No. 14 bars and most noticeably from 0.93 to 1.00 for No. 18 bars.

Tables 5.14 and 5.15 show that the match of the test results provided by Eq. (5.7) is not affected by the loading condition, with the average T/T_h value of 0.98 for both cases.

The average force per bar at failure, T , for all No. 14 and No. 18 headed bar specimens (excluding those that failed in shear) is compared with that calculated using Eq. (5.5) or (5.7), T_h , in Figure 5.10. As shown in the figure, the best fit line is slightly above the dashed line representing $T = T_h$ for lower bar forces, indicating a slight overestimation of anchorage strength by Eq. (5.5) or (5.7), similar to what was observed based on Eq. (5.2) and (5.3) and shown in Figure 5.2. For higher bar forces, however, the best fit is slightly below the dashed line representing $T = T_h$, but much less so than observed in Figure 5.2 for Eq. (5.2) and (5.3). Overall, and compared with the

plot in Figure 5.2, Eq. (5.5) and (5.7) provide a more accurate representation of anchorage strength of the larger headed bars.

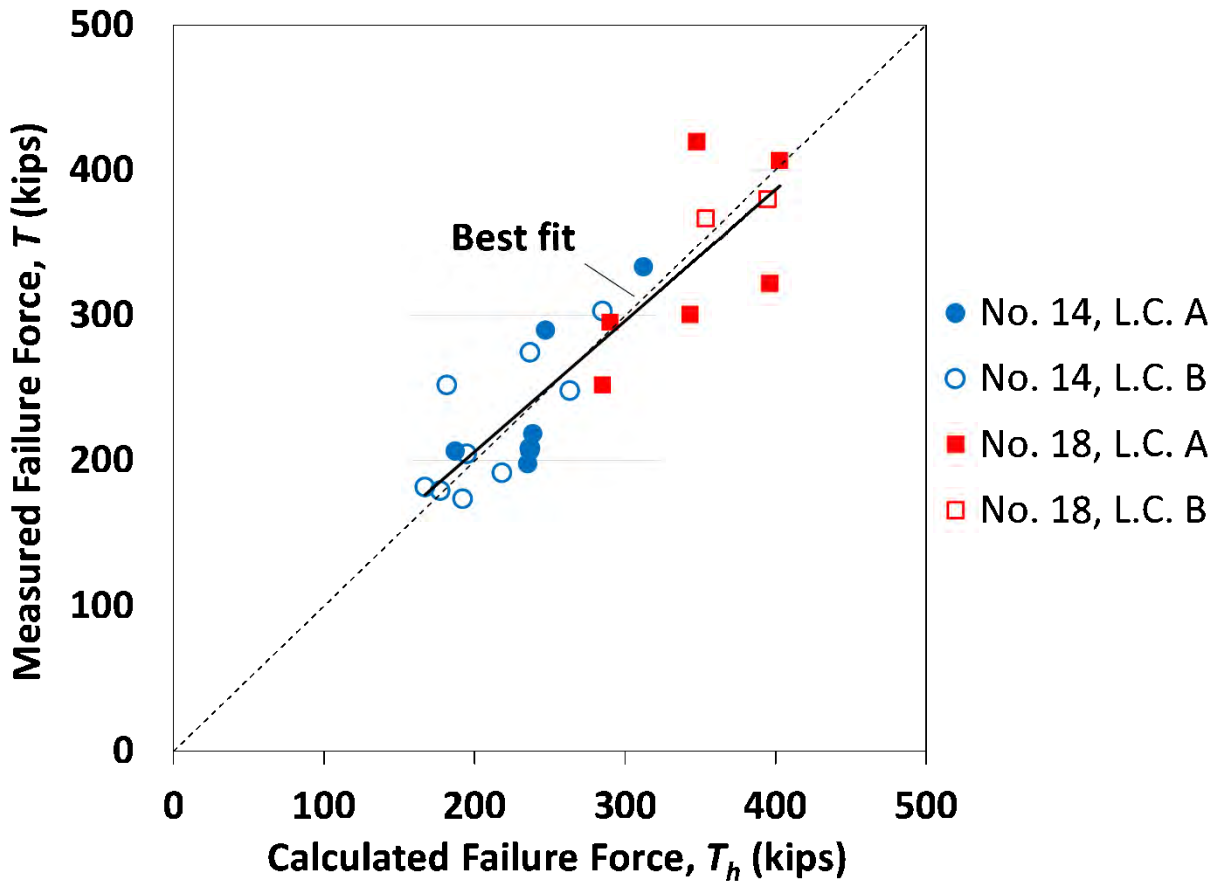


Figure 5.10 Measured versus calculated bar force at failure using new descriptive equations for No. 14 and No. 18 headed bar specimens, excluding those with a shear-like failure, with the calculated bar force, T_h , based on Eq. (5.5) or (5.7)

Values of T/T_h based on Eq. (5.5) and (5.7) are compared as a function of concrete compressive strength f_{cm} for the No. 14 and No. 18 headed bar specimens tested in this study, excluding those that failed in shear, in Figure 5.11. As shown in the figure, no noticeable trend is observed, indicating that the effect of concrete compressive strength on the anchorage strength of No. 14 and No. 18 headed bars is adequately captured by Eq. (5.5) and (5.7).

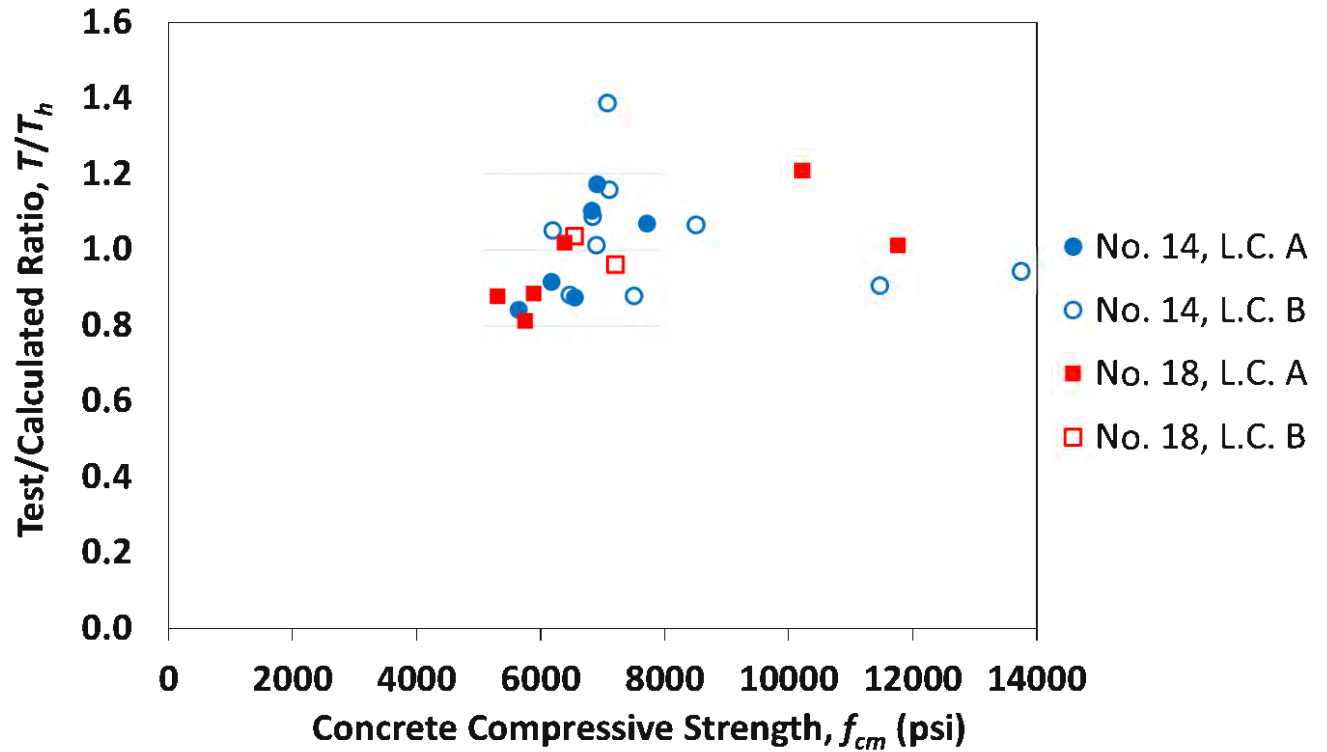


Figure 5.11 Ratio of test/calculated ratio T/T_h versus concrete compressive strength f_{cm} for No. 14 and No. 18 headed bar specimens, with the calculated bar force, T_h , based on Eq. (5.5) or (5.7)

Figure 5.12 shows T/T_h as a function of A_n/A_{hs} for the No. 14 and No. 18 specimens, excluding those that failed in shear.

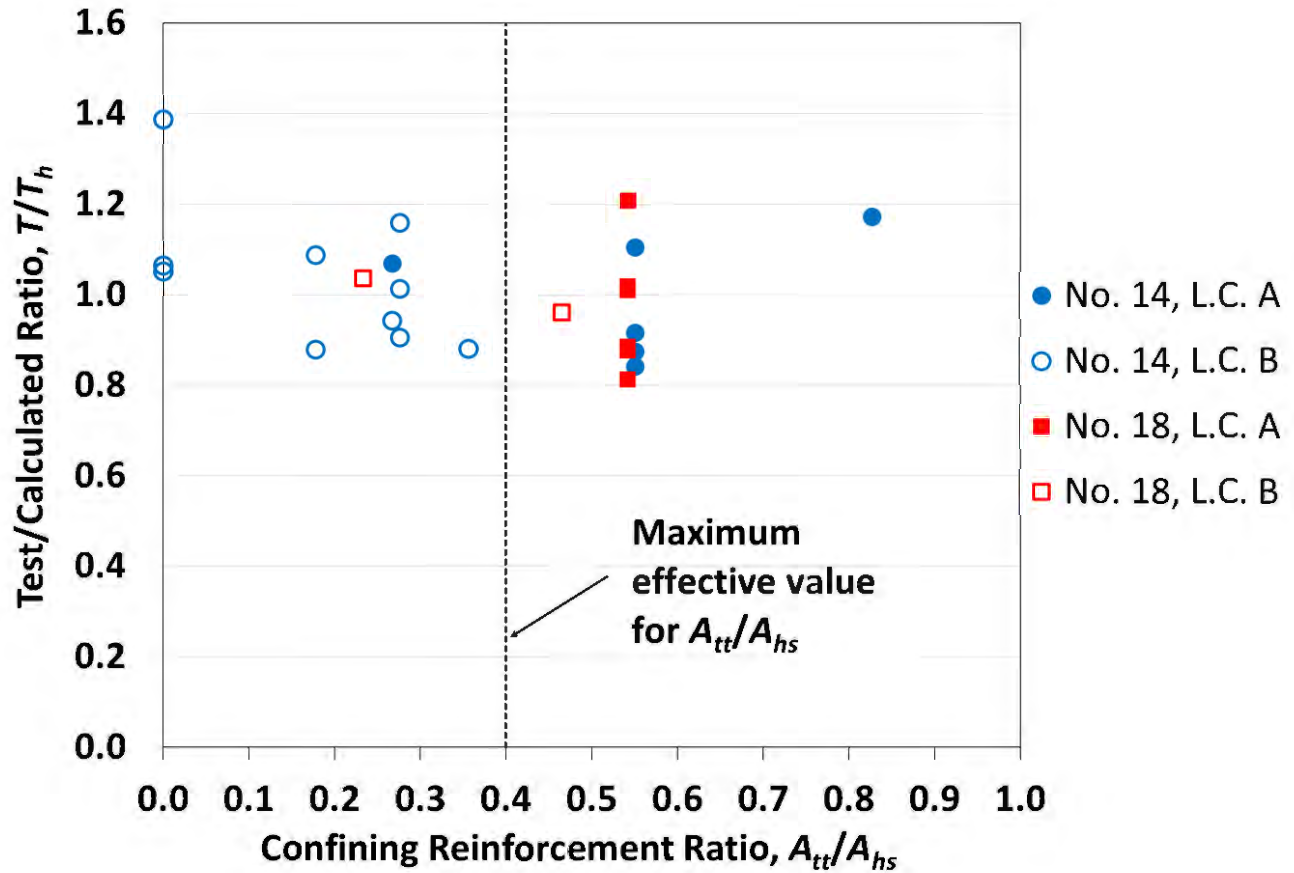


Figure 5.12 Ratio of test/calculated ratio T/T_h versus parallel tie reinforcement ratio A_{tt}/A_{hs} for No. 14 and No. 18 headed bar specimens, with the calculated bar force, T_h , based on Eq. (5.5) or (5.7)

As discussed in Section 5.3.3, the maximum effective limit for A_{tt}/A_{hs} was previously established as 0.3 (Shao et al. 2016, Ghimire et al. 2018, Ghimire et al. 2019a, 2019b). When applied with Eq. (5.7), it is increased to 0.4. A 0.4 limit on A_{tt}/A_{hs} means that values above 0.4 were not found to contribute to anchorage strength of headed bars. Figure 5.12 shows that T/T_h is largely independent of A_{tt}/A_{hs} with the upper limit of 0.4 in place for No. 14 and No. 18 headed bars.

A comparison between the test-to-calculated ratio T/T_h and the center-to-center bar spacing s normalized by bar diameter (d_b) is shown in Figure 5.13 for No. 14 and No. 18 headed bars. As shown in the figure, T/T_h for both loading conditions is largely independent of s/d_b .

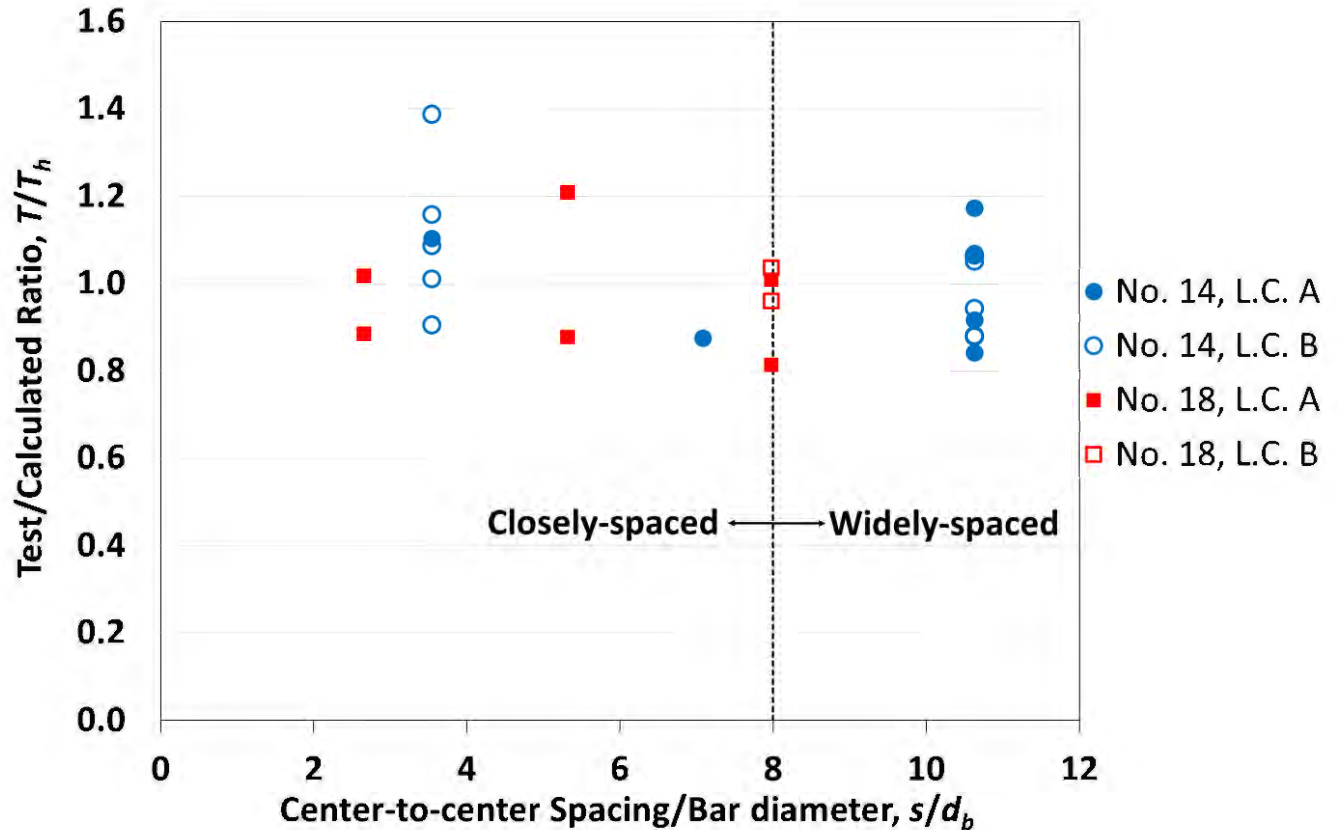


Figure 5.13 Ratio of test/calculated ratio T/T_h versus ratio of center-to-center spacing to bar diameter s/d_b for No. 14 and No. 18 headed bar specimens, with the calculated bar force, T_h , based on Eq. (5.5) or (5.7)

5.5 EFFECT OF TEST PARAMETERS

In this section, the effects of key test parameters in this study are discussed, including loading condition, confining reinforcement, bar size and spacing, side cover, and strut angle.

5.5.1 Loading Condition

As described in Section 2.3.1, two loading conditions were considered:

Loading Condition A – Beam located at column midheight between inflection points: In this loading condition, the column moment demands above and below the joint were equal, and the shear force within the joint region equals 80% of the force applied to the test bars. This loading condition simulates an exterior beam-column joint with the beam located at the midheight of the column.

Loading Condition B – Anchorage only: In this loading condition, the joint shear is equal to ~69% of applied force to the test bars.

The 11% difference in joint shear within the joint region between loading conditions A and B and the moment reversal present in loading condition A, appears to play a major role in the type of failure and anchorage strength of headed bars for joints without a minimum quantity of shear reinforcement parallel to the headed bars within the joint, as will be discussed in this section.

The first headed bar specimen tested under loading condition A was 14-2, which had two widely-spaced No. 14 bars (18 in. on-center or $10.6d_b$) cast with high-strength (15 ksi) concrete. The specimen had five No. 4 parallel ties in the joint region, three of which were within $9.5d_b$ of the centerline of the headed bars, resulting in an A_{tt}/A_{hs} ratio (based on the descriptive equations) of 0.267. The specimen exhibited a shear-like failure, as described in Section 3.2.2, and had a test-to-calculated ratio of just 0.76 based on Eq. (5.2) and (5.3), the descriptive equations developed by Shao et al. (2016) and Ghimire et al. (2018, 2019b), and 0.80 based on Eq. (5.5) and (5.7), the equations developed in this study. The next specimen exhibiting a shear-like failure under loading condition A was 14-16, with the same dimensions as 14-2 but cast with normal-strength concrete and with an A_{tt}/A_{hs} ratio of 0.178. Specimen 14-16 is shown in Figure 5.14a following failure. Figure 5.14b shows the specimen after dissection, in which the diagonal shear crack can be seen crossing the bearing face of the head towards the back of the column along the bottom face, extending through the width of the column. Specimen 14-16 had the lowest T/T_h ratio, 0.59, based on Eq. (5.7), among the specimens tested in this study.

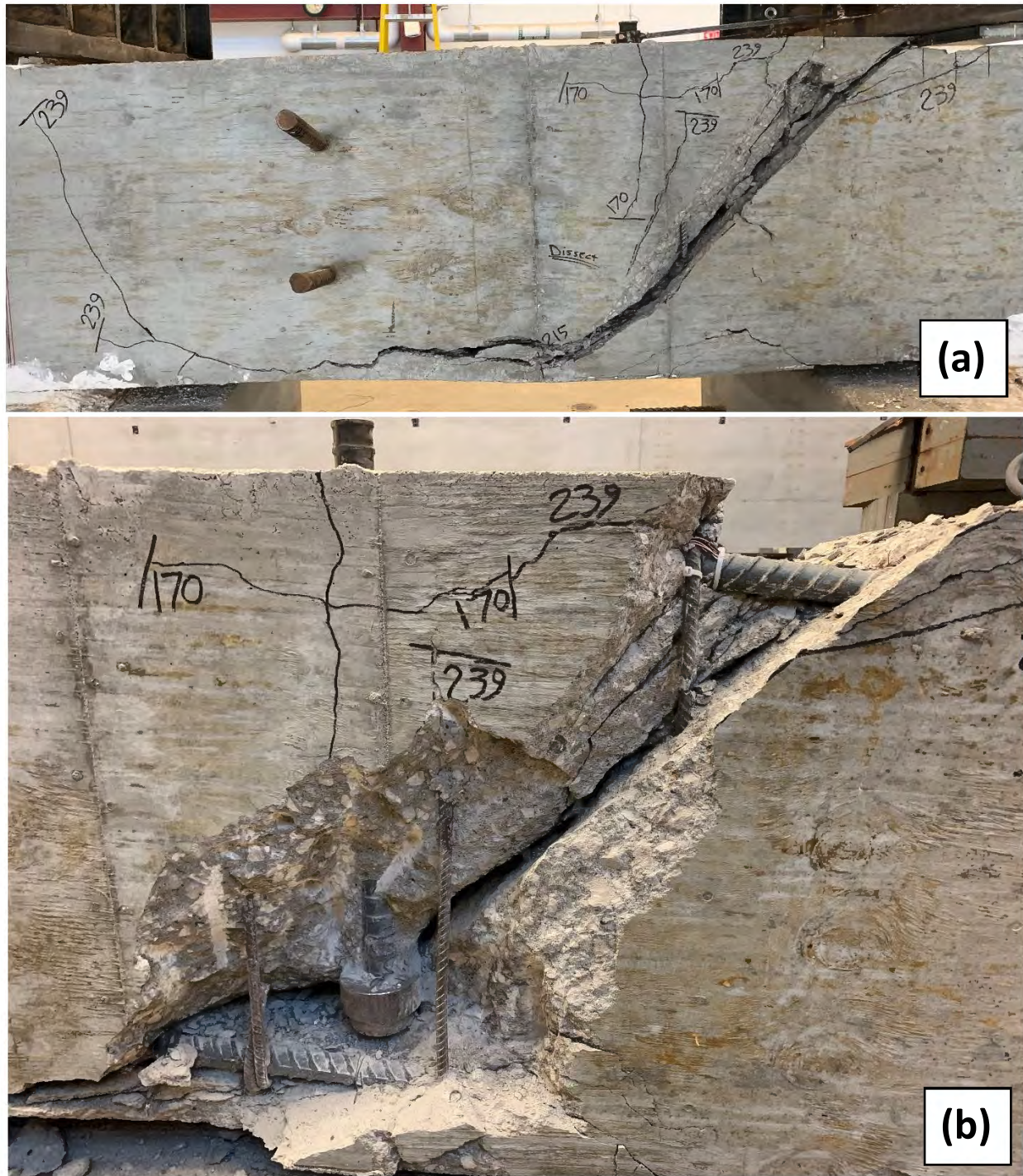


Figure 5.14 Shear-like failure observed in specimen 14-16 ($A_{tt}/A_{hs} = 0.178$) tested under loading condition A: (a) after failure and (b) after dissection

Because of the shear-like failures of specimens 14-2 and 14-16 under loading condition A, specimen 14-15, which had the same dimensions, number and spacing of headed and column bars and concrete strength as specimen 14-16, but without parallel ties, was tested under loading

condition B to reduce the shear demand in the joint region, remove the moment reversal, and promote an anchorage failure. Specimen 14-15 failed in anchorage with concrete breakout, as shown in Figure 5.15, with a test-to-calculated ratio T/T_h of 1.05 based on Eq. (5.5), illustrating the role of the loading condition on the anchorage strength of headed bars in a beam-column joint. At the time, the exact effect was not yet clear.



Figure 5.15 Anchorage failure observed in specimen 14-15 ($A_{tr}/A_{hs} = 0$) tested under loading condition B

Specimen 14-16 was then duplicated by a specimen designated as 14-16A with a modification to the longitudinal reinforcement. One additional No. 11 longitudinal bar was added on each side of the column, 2 in. from the bearing face of the headed bars, to help distribute the tensile force in the headed bars along the longitudinal bars, which serve as ties in the strut and tie model used to represent the member. The additional No. 11 bars are shown in Figure 5.16.



Figure 5.16 Additional No. 11 longitudinal bars in specimen 14-16A

Specimen 14-16A was tested under loading condition A. The specimen, however, again failed in shear, as did specimen 14-16, although the test-to-calculated ratio T/T_h increased from 0.59 to 0.83 based on Eq. (5.7). Specimen 14-16A following failure is shown in Figure 5.17.



Figure 5.17 Shear-like failure observed in specimen 14-16A ($A_{tr}/A_{hs} = 0.178$) tested under loading condition A

The final specimen in the study to exhibit a shear-like failure was 14-1A. It had two widely-spaced ($10.6d_b$ center-to-center) headed bars in high-strength concrete. The specimen had no parallel ties in the joint region and was tested under loading condition B to promote an anchorage failure. The specimen, however, failed in shear (shown in Figure 5.18) with a test-to-calculated ratio T/T_h of 0.87 based on Eq. (5.5).



Figure 5.18 Shear-like failure observed in specimen 14-1A ($A_{tt}/A_{hs} = 0$) tested under loading condition B

The companion specimen to 14-1A, designated as 14-2A, had properties similar to 14-1A, but with parallel ties in the joint region (A_{tt}/A_{hs} of 0.267). This specimen was also tested under loading condition B. The specimen failed in anchorage as shown in Figure 5.19, with an average test-to-calculated ratio T/T_h of 0.94 based on Eq. (5.7). Comparing the failure modes of specimens 14-1A and 14-2A revealed that the joint region must contain parallel ties to provide adequate shear strength when using large-diameter headed bars to preclude a shear-like failure.

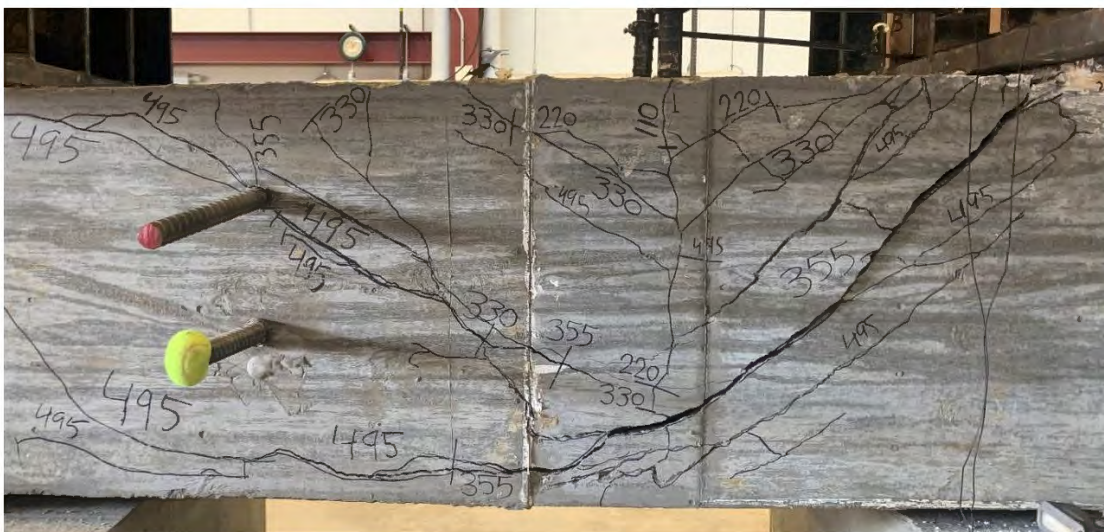


Figure 5.19 Anchorage failure observed in specimen 14-2A ($A_{tt}/A_{hs} = 0.267$) tested under loading condition B

The behavior of these headed bar specimens can be compared with that of hooked bar specimens. The first comparison can be made between headed bar specimen 14-2 and hooked bar specimen H14-2, both with ties as confining reinforcement ($A_{tt}/A_{hs} = A_{th}/A_{hs} = 0.267$, with A_{tt} and A_{th} defined in Sections 5.2 and 4.2, respectively) and both under loading condition A. Specimen 14-2 failed in shear while specimen H14-2 failed in anchorage. The next comparison is between specimen 14-16 and specimen H14-16 that had similar properties ($A_{tt}/A_{hs} = A_{th}/A_{hs} = 0.178$). Under loading condition A, Specimen 14-16 failed in shear, and specimen H14-16 failed in anchorage with a breakout failure. Finally, headed bar specimen 14-1A and hooked bar specimen H14-1 were similar but without parallel ties under loading condition A. Again, the headed bar specimen, 14-1A, failed in shear, while the hooked bar specimen, H14-1, failed in anchorage. These observations demonstrate the role played by the tail of hooks in carrying the joint shear by preventing the inclined crack from propagating towards the back of the column.

Two more duplicates of specimen 14-16 (designated as 14-16B and 14-16C) were tested under loading condition B (reduced joint shear demand). Specimen 14-16B had the same reinforcement as 14-16 ($A_{tt}/A_{hs} = 0.178$), while specimen 14-16C two times the quantity of confining reinforcement in the joint region ($A_{tt}/A_{hs} = 0.356$). Both specimens failed in anchorage with T/T_h value of 0.88, based on Eq. (5.7). The failure modes of the two specimens are shown in Figures 5.20 and 5.21.



Figure 5.20 Anchorage failure observed in specimen 14-16B ($A_{tt}/A_{hs} = 0.178$) tested under loading condition B



Figure 5.21 Anchorage failure observed in specimen 14-16C ($A_{tt}/A_{hs} = 0.356$) tested under loading condition B

To gain an improved understanding of the role of shear reinforcement within a beam-column joint on the anchorage strength of headed bars, another specimen with the same dimensions as 14-16 (designated as 14-16D) was tested under loading condition A. Using five double overlapping No. 5 ties, the number and spacing of ties were designed to carry the full shear within the joint (that is, treating the concrete contribution V_c as 0). The first tie was placed 2.5 in. from the center of the headed bar, with the balance placed 5 in. on center. Three of the five overlapping ties were located within $10d_b$ from the center of the bar, resulting in A_{tt}/A_{hs} of 0.827, the highest value used in this study. The double overlapping ties are shown in Figure 5.22. Specimen 14-16D failed in anchorage, as shown in Figure 5.23, with a T/T_h of 1.17 based on Eq. (5.7) with the $0.4A_{hs}$ limit on A_{tt} .

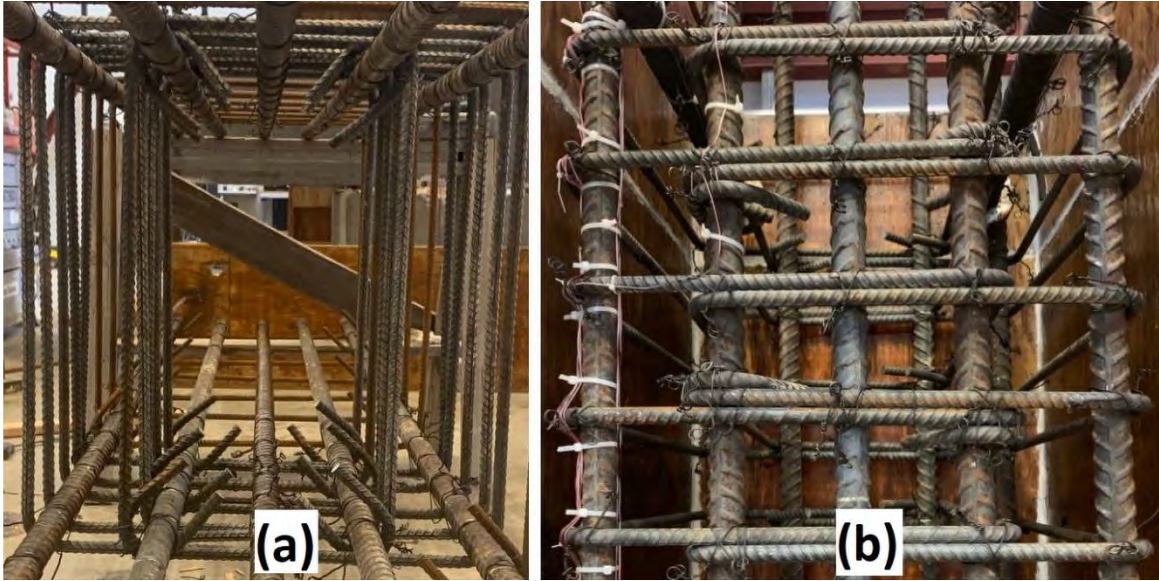


Figure 5.22 Double overlapping No. 5 ties in specimen 14-16D; (a) top view, (b) front view



Figure 5.23 Anchorage failure observed in specimen 14-16D ($A_{tr}/A_{hs} = 0.827$) tested under loading condition A (after removal of loose concrete)

Because specimen 14-16D was designed so that the entire joint shear would be carried by the ties within the joint, one question to be answered was whether less shear reinforcement proved to be adequate. To address this question, specimen 14-16E with two double overlapping No. 5 ties within $10d_b$ (8 legs total, $A_{tr}/A_{hs} = 0.551$) was tested under loading condition A. The specimen failed in anchorage, as shown in Figure 5.24, similar to 14-16D (Figure 5.23). T/T_h was 0.92 based on Eq. (5.7) applying the maximum effective value for A_{tr}/A_{hs} of 0.4. For comparison, using the

actual values of A_{tt}/A_{hs} of 0.827 for specimen 14-16D and 0.551 in specimen 14-16E result in respective values of T/T_h of 0.97 and 0.85.



Figure 5.24 Anchorage failure observed in specimen 14-16E ($A_{tt}/A_{hs} = 0.551$)

Based on the performance of specimens 14-16D and 14-16E, it is clear that, at least for larger headed bars, transverse reinforcement is needed within the joint to prevent a shear-like failure within an exterior beam-column joint with the beam located at the midheight of the column – loading simulated by loading condition A. In this study, the majority of No. 14 and No. 18 bar specimens with parallel ties that were tested under loading condition A and failed in anchorage (14-16E, 14-16F, 14-17, 14-10, 18-1, 18-2, 18-5, 18-6, 18-7, and 18-8) had A_{tt}/A_{hs} of 0.54 or 0.55 (14-16D had $A_{tt}/A_{hs} = 0.827$). These specimens included both widely- and closely-spaced bars and cast in both normal- and high-strength concrete. Since the ties in these specimens, with a wide range of properties, were effective in preventing a shear-like failure, it can be concluded that the minimum area of parallel ties (A_{tt}) needed for larger bars to address the joint shear demand is $0.5A_{hs}$. The single exception is specimen 14-4 with $A_{tt}/A_{hs} = 0.267$, the only specimen to fail in anchorage under loading condition A with $A_{tt}/A_{hs} < 0.5$. The only tests of beam-column joints containing No. 11 and smaller headed bars that failed in anchorage when loaded in a manner similar to condition A are those by Bashandy (1996) who tested 15 specimens, as discussed in more detail later in Section 5.6. All but one of the specimens had A_{tt}/A_{hs} values > 0.7 , with the majority having values as high as 1.0 or 2.0. Therefore, more study is warranted to investigate if parallel ties $< 0.5A_{hs}$ would be adequate to prevent a shear-like failure under loading condition A.

The 0.4 limit on the effective value of A_{tt}/A_{hs} , however, indicates that providing ties (A_{tt}) above $0.4A_{hs}$ does not add to the anchorage strength of headed bars. Thus, the addition of parallel ties to limit shear-like failures appears to be separate from their contribution to the anchorage strength of headed bars.

5.5.2 Parallel tie Reinforcement

Here, pairs of specimens with and without parallel ties are compared to investigate the effectiveness of ties when $A_{tt,ACI} < 0.3A_{hs}$, a case where the current Code gives no credit to parallel ties while the descriptive equations does. The contribution of middle legs (in specimens with double overlapping ties, as shown in Figure 5.22) is also investigated.

First, pairs of specimens are investigated in which one had parallel ties and the other did not. Figure 5.25 compares the anchorage strength of four pairs of specimens, 11-1 and 11-2, 14-3 and 14-4, 14-1A and 14-2A, and 14-7 and 14-8, where the first specimen in each pair did not contain parallel ties, while the second one did. All specimens with parallel ties had $A_{tt,ACI} < 0.3A_{hs}$.

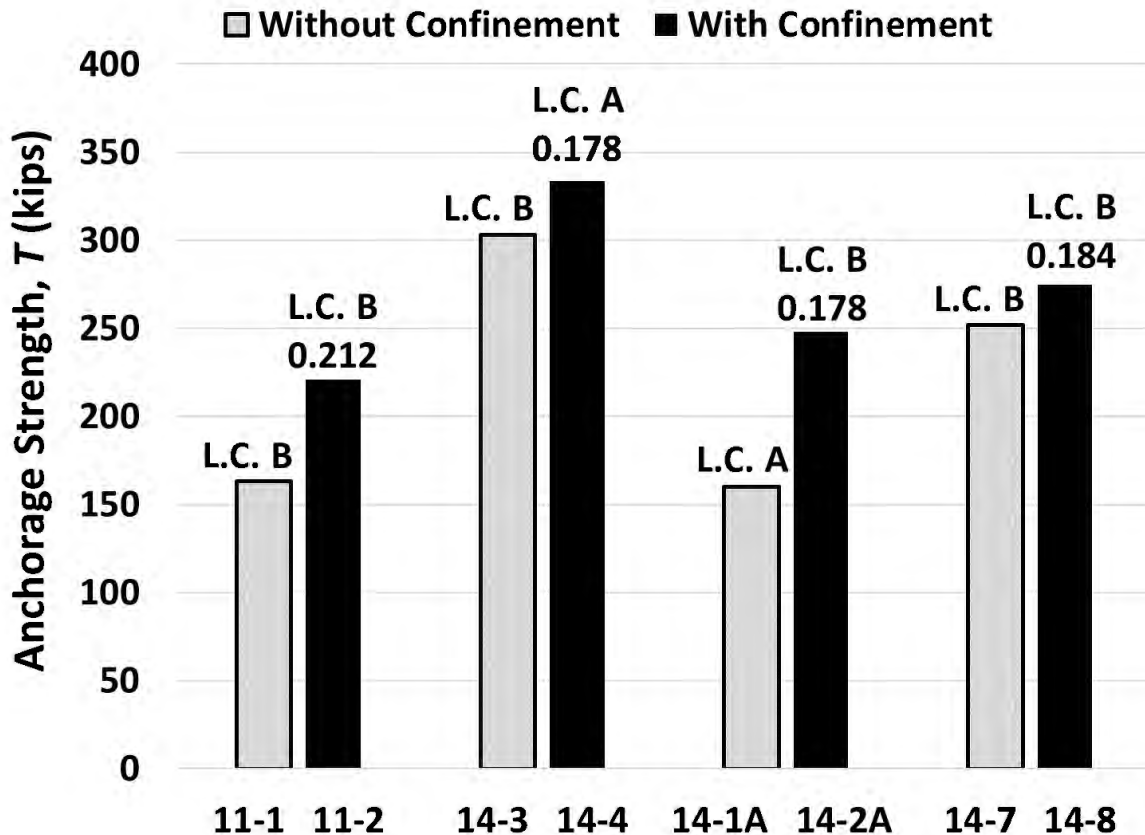


Figure 5.25 Comparing anchorage strength of headed bars with and without parallel ties (Note: L.C. = Loading Condition, and the number below L.C. denotes $A_{tt,ACI}/A_{hs}$)

As shown in Figure 5.25, providing ties in the joint region, even as low as $A_{tt,ACI}/A_{hs} = 0.178$, increased the anchorage strength in each case. These observations show that, as observed in earlier tests (Shao et al. 2016, Ghimire et al. 2018, 2019a, 2019b), and as would be predicted based on Eq. (5.7), providing ties within the joint region improves the anchorage strength of headed bars even when $A_{tt,ACI} < 0.3A_{hs}$, whereas the current Code does not allow taking advantage of such cases.

The contribution of middle legs to anchorage strength has also been investigated. To this end, two pairs of specimens are compared, namely 14-16E and 14-16F, and 18-7 and 18-8. Both specimens in each pair had the same size and spacing of ties and, therefore, the same A_{tt}/A_{hs} ratio. The only difference was that double overlapping ties were used (two external legs and two middle legs) in specimen 14-16E (similar to 14-16D, as shown in Figure 5.22) and specimen 18-8, while double ties (all four legs near the exterior) were used in specimen 14-16F (as shown in Figure 5.26) and specimen 18-7.

Specimens 14-16E and 14-16F had $A_{tt}/A_{hs} = 0.56$, were tested under loading condition A, and failed in anchorage as shown in Figure 5.27. The T/T_h ratios were 0.92 and 0.84 based on Eq. (5.7) for specimens 14-16E and 14-16F, respectively, meaning the specimen with middle legs had a 9.5% higher value of T/T_h .



Figure 5.26 Double No. 5 ties used in specimen 14-16F

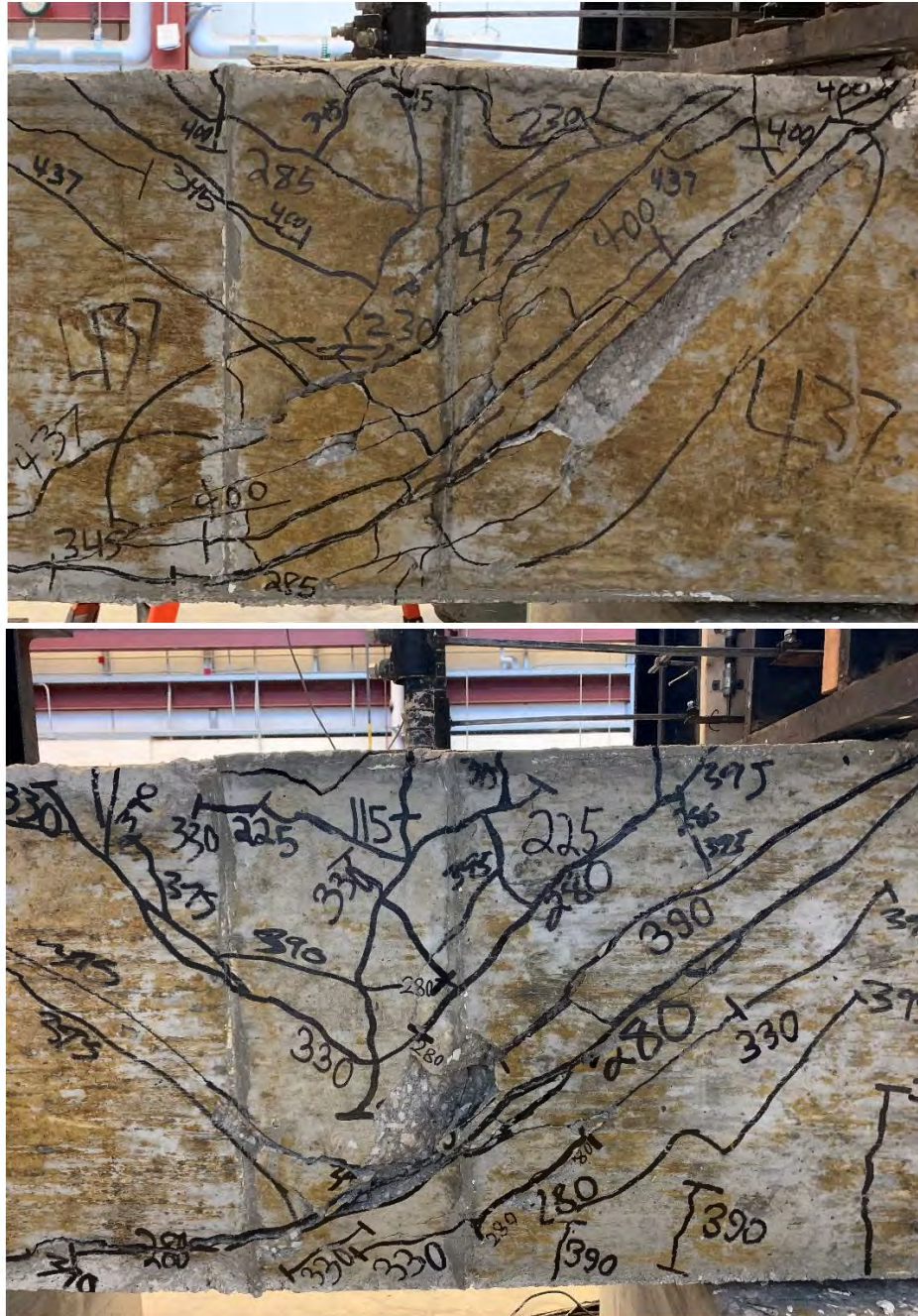


Figure 5.27 Comparing side splitting failure modes of specimens 14-16E with parallel ties with middle legs (top) and 14-16F with only external legs (bottom), both with $A_{tt}/A_{hs} = 0.551$

The contribution of middle legs to anchorage strength in the pair of No. 18 bar specimens (18-7 and 18-8) was more noticeable than the No. 14 bar specimens (14-16E and 14-16F). Both specimens had three closely-spaced No. 18 bars, with A_{tt}/A_{hs} of 0.54. Specimen 18-7 had double No. 5 ties, like specimen 16-16F, while specimen 18-8 had double overlapping ties, like specimen 14-16E. The T/T_h ratio based on Eq. (5.7) for specimen 18-8 (with middle legs) was 1.02, 14.6%

higher than that of specimen 18-7 (with external ties only), 0.89. The concrete compressive strength of specimen 18-8 was 490 psi higher than that of specimen 18-7, but based on descriptive equations, this difference should be responsible for only about 2% of the increase in anchorage strength. Therefore, the improvement in anchorage strength can be mainly attributed to the middle legs in specimen 18-8. These observations suggest that interior legs of parallel ties in the joint region contribute to anchorage strength of headed bars at least as well as exterior legs and that middle legs might be more effective in some cases.

5.5.3 Bar Spacing

Figure 5.28 presents comparisons between the anchorage strength of specimens based on bar spacing. The concrete compressive strength and A_{tt}/A_{hs} ratio were similar for each pair of specimens shown in the figure. Overall, anchorage strength for No. 14 and No. 18 headed bars correlates with bar spacing as observed for No. 11 and smaller bars, that is, individually, closely-spaced bars are weaker (lower anchorage strength) than widely-spaced bars. In general, the reduced area of the breakout surface in specimens with more closely-spaced bars can explain the differences in anchorage strength.

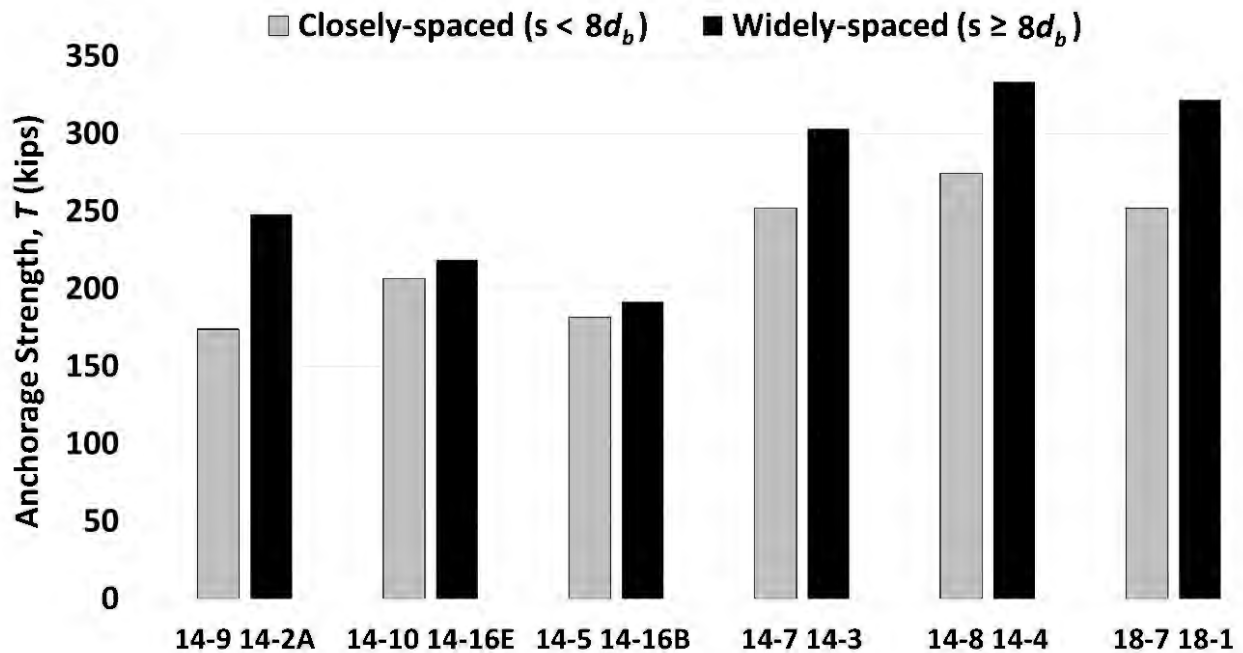


Figure 5.28 Comparing the anchorage strength (average force per bar at failure) of No. 14 and No. 18 headed bars based on bar spacing

5.5.4 Placement of Bars Within the Cross-section

The effect of placement of bars within the cross-section on the anchorage strength of headed bars is discussed in this section. The majority of specimens had a side cover to the bar of 3.5 in., similar to those tested by Shao et al. (2016). The low values of T/T_h for specimens 14-16E and 14-16F, 0.92 and 0.84, respectively, based on Eq. (5.5) and (5.7), combined with the side-splitting failure mode observed for both specimens, raised a question about the role of side cover in the anchorage strength. Both specimens had two widely-spaced headed bars, A_{tr}/A_{hs} of 0.551 and were tested under loading condition A. A third specimen, 14-17, was designed with the same properties and cross-sectional dimensions as specimen 14-16F, but with the two headed bars spaced at 12 in., which increased the side cover to the bar from 3.5 in. to 6.5 in. and the side cover to the head from 2.4 in. to 5.4 in. while reducing the center-to-center spacing from $10.6d_b$ to $7.1d_b$.

The combination of increased side cover and closer bar spacing seemed to have only a minimal effect on the anchorage strength, as the average test-to-calculated ratio T/T_h was 0.87, close to the value of 0.84 for 14-16F. Specimen 14-17, however, failed by concrete breakout, as shown in Figure 5.29, rather than the side splitting observed in specimens 14-16E and 14-16F (Figure 5.27).



Figure 5.29 Concrete breakout observed in specimen 14-17 ($A_{tr}/A_{hs} = 0.551$) with increased side cover to the bar and decreased bar spacing

The next comparison can be made between No. 18 bar specimens 18-1 and 18-5. The specimens had similar concrete strength, embedment length, and A_{tr}/A_{hs} (0.543) but different side cover to the bar and bar spacing. Specimen 18-1 had two bars spaced at 18 in. on-center ($8.0d_b$)

with a side cover to the bar of 3.5 in., while specimen 18-5 had two bars spaced at 12 in. on-center (5.3*d_b*), increasing the side cover to 6.5 in. The cover to the head was increased from 2.1 in. in specimen 18-1 to 5.1 in. in specimen 18-5. Both specimens were tested under loading condition A. The anchorage strength of specimen 18-1 ($T = 322.0$ kips) was 7% higher than that of specimen 18-5 ($T = 300.8$ kips), of which about 2% can be attributed to higher concrete compressive strength in 18-1 (5,750 versus 5,310 psi). T/T_h equals 0.81 and 0.88 for specimens 18-1 and 18-5, respectively. Similar to the previous comparison, however, increasing the side cover altered the failure mode from primarily side splitting (18-1) to primarily concrete breakout (18-5), as shown in Figure 5.30.

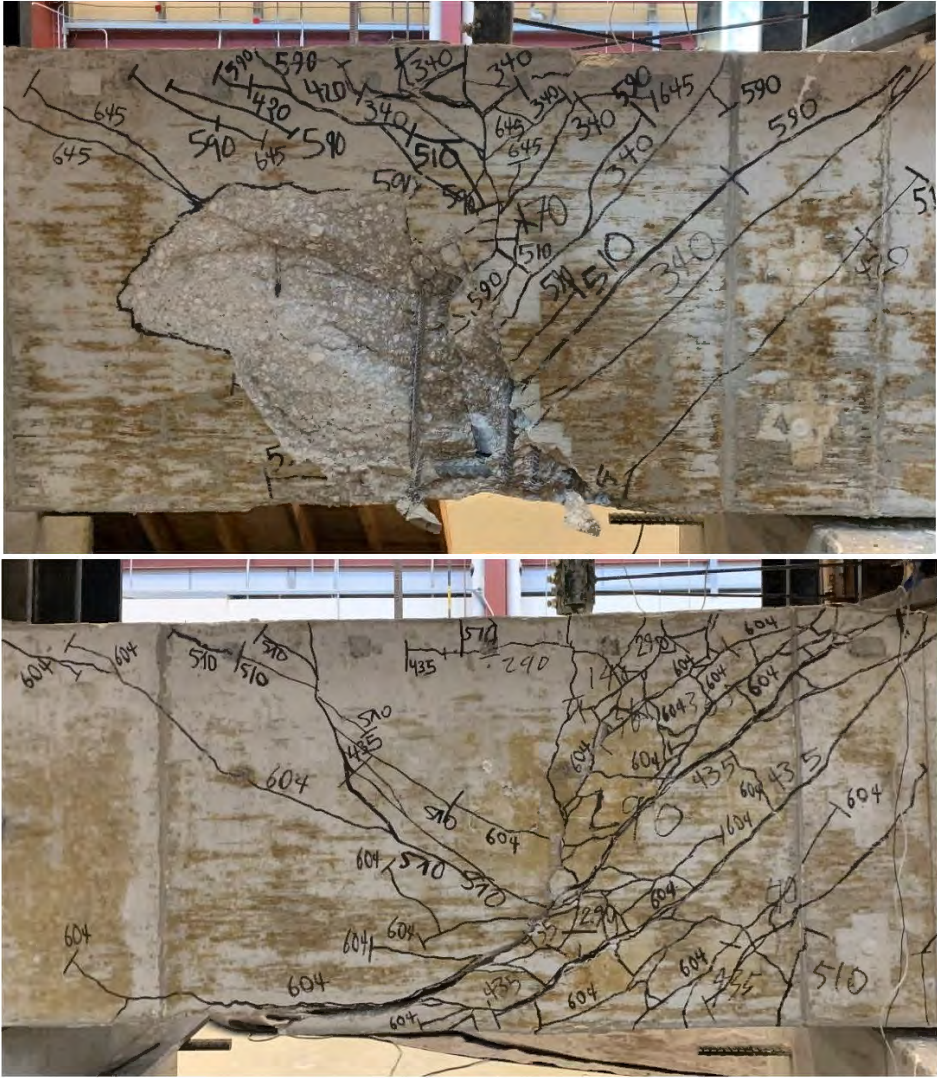


Figure 5.30 Comparing failure modes of specimen 18-1 with 3.5 in. side cover to the bar (top, side splitting) with specimen 18-5 with 6.5 in. side cover to the bar (bottom, concrete breakout), both with $A_{tt}/A_{hs} = 0.543$

The last pair of specimens to compare are 18-2 and 18-6. Both specimens contained high-strength concrete. The specimens had the same A_{tr}/A_{hs} (0.543) and were tested under loading condition A. The side cover to the bar and head in specimens 18-2 (3.5 and 2.1 in.) and 18-6 (6.5 and 5.1 in.) were the same as those in specimens 18-1 and 18-5, respectively. The anchorage strength of the specimen with increased side cover, 18-6 ($T = 419.8$ kips), was slightly higher (3.2%) than that of specimen 18-2 ($T = 406.6$ kips), despite having a lower concrete compressive strength (10,230 versus 11,770 psi). T/T_h was 1.01 and 1.21 for 18-2 and 18-6, respectively. The higher value of T/T_h for specimen 18-6 is due to the lower value of s/d_b compared with that of specimen 18-2, leading to a lower value of T_h . Figure 5.31 shows that the failure mode in specimen 18-2 was a combination of concrete breakout and side splitting, while that of specimen 18-6 appears to be side splitting (unlike previous specimens with increased side cover, 14-17 and 18-5) combined with an inclined crack through the column thickness.



Figure 5.31 Comparing failure modes of specimen 18-2 with 3.5 in. side cover to the bar (top) with specimen 18-6 with 6.5 in. side cover to the bar (bottom), both with $A_{tr}/A_{hs} = 0.543$

Overall, these observations indicate that the combined effects of increasing side cover to the bar (and thus, concrete cover to head) and decreasing bar spacing for joint with the same width did not have a major effect on the anchorage strength of No. 14 and No. 18 headed bars, but can change the failure type from side splitting to concrete breakout.

5.5.5 Compression Strut Angle

The compression strut angle is defined as the angle from the centerline of the headed bar to a line drawn between the centroid of the bearing face of the head and the center of the bearing plate simulating the compression zone of the imaginary beam, as shown in Figure 5.32. Based on the figure, the compression strut angle θ can be calculated as the inverse tangent (arctan) of x_{mid}/ℓ_{eh} . The effect of compression strut angle on the anchorage strength of hooked bars was discussed in Section 4.7, and its effect on the anchorage strength of headed bars is evaluated in this section.

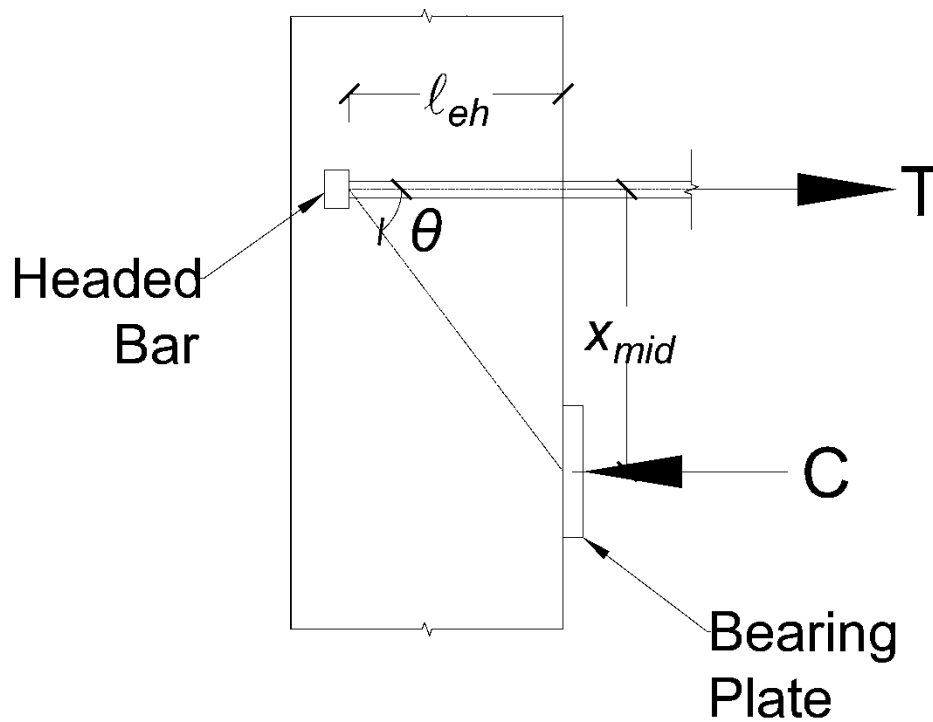


Figure 5.32 Compression strut angle (θ) for headed bars (x_{mid} is 28.56 and 38.15 in. for No. 14 and No. 18 bars, respectively, and ℓ_{eh} is the embedment length)

The values of T/T_h , with T_h based on Eq. (5.5) and (5.7), are plotted as a function of the strut angle θ for the No. 11 headed bar specimens tested by Shao et al. (2016) and Ghimire et al. (2018) and those tested in this study in Figure 5.33. Specimens with $d_{eff}/\ell_{eh} > 1.5$ are excluded from the figure, where d_{eff} is described in Section 2.3.3 and below.

As shown in Figure 5.33, no noticeable trend can be observed between T/T_h and θ with the exception of one of the specimens with the lowest (flattest) compression strut angles ($< 45^\circ$) that had a T/T_h ratio of 1.39. The rest of the specimens had values of T/T_h between 0.81 and 1.21. The insensitivity of the descriptive equations to strut angle for specimens with $d_{eff}/\ell_{eh} < 1.5$ matches the observation for hooked bars presented previously in Section 4.7 and Figure 4.15.

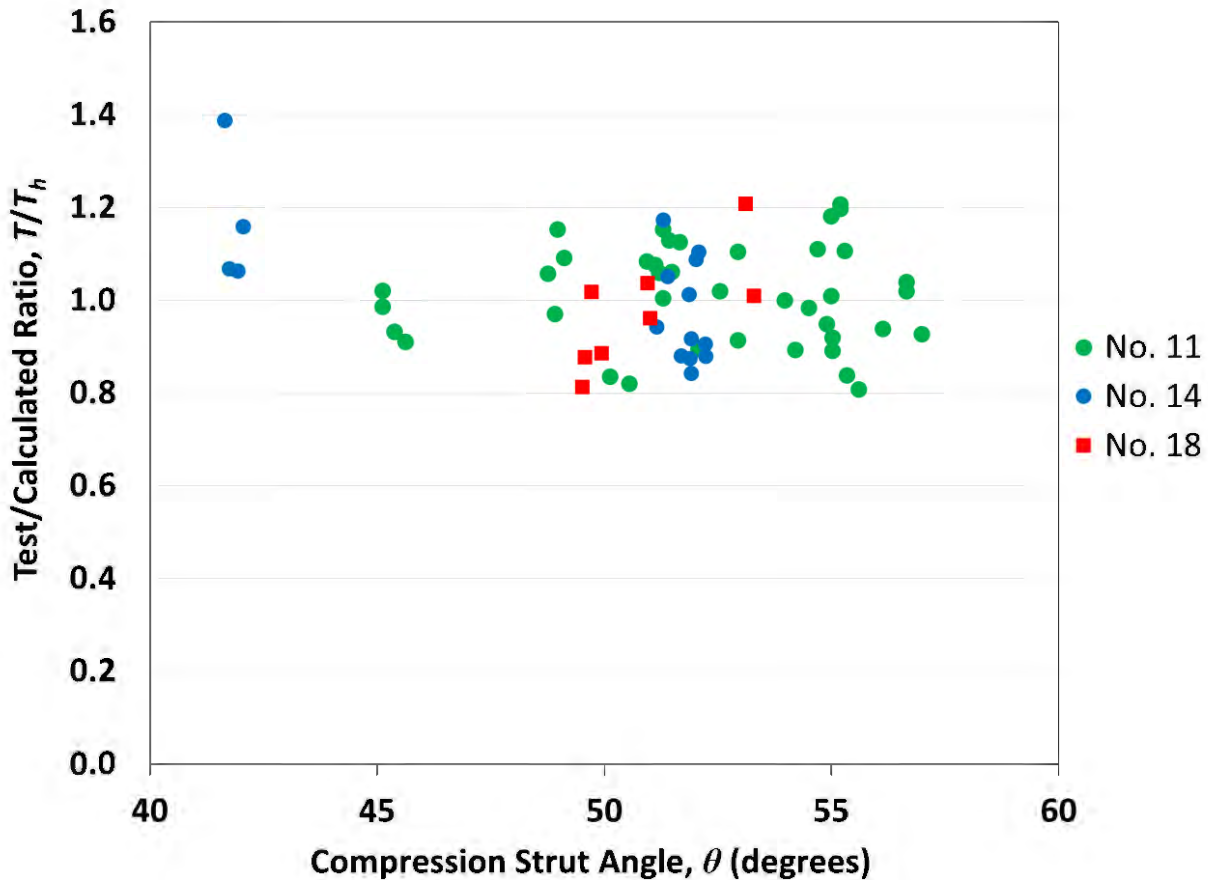


Figure 5.33 Comparison of strut angle θ versus test-to-calculated ratio T/T_h based on Eq. (5.5) and (5.7) for large (No. 11, No. 14, and No. 18) headed bars for specimens with $d_{eff}/\ell_{eh} < 1.5$

5.5.6 Effective Beam Depth

Another parameter closely related to the strut angle is ratio of the effective depth of the simulated beam to embedment length, d_{eff}/ℓ_{eh} . The approach used by Shao et al. (2016) to calculate d_{eff} is adopted here. The neutral axis of the beam is assumed to be represented by the top edge of the bearing plate, and the extreme compression fiber is assumed to be some distance c below that point. c is calculated as a/β_1 , where a is the depth of equivalent rectangular compressive stress block and calculated as $nA_{bf}s/0.85f_{cm}b$ per flexural design procedure for reinforced concrete

beams, $\beta_1 = 0.85 - 0.05((f_{cm} - 4000)/1000) \leq 0.65$ per Section 22.2.2.4.3 of ACI 318-19, and b is the width of the specimen. The effective depth of the beam, d_{eff} , is then calculated as the sum of h_{cl} and c as shown in Figure 5.34, where h_{cl} is the distance from the center of headed bars to the top edge of the bearing plate. Bearing plates with three different widths, 6, 9, and 12 in., were used. As described in Section 2.3.3, if the calculated value of c was < 6 in., the 6 in. plate was used. If $6 \text{ in.} < c \leq 9 \text{ in.}$, the 9 in. plate was used, and, for calculated value of $c > 9 \text{ in.}$, the 12 in. plate was used.

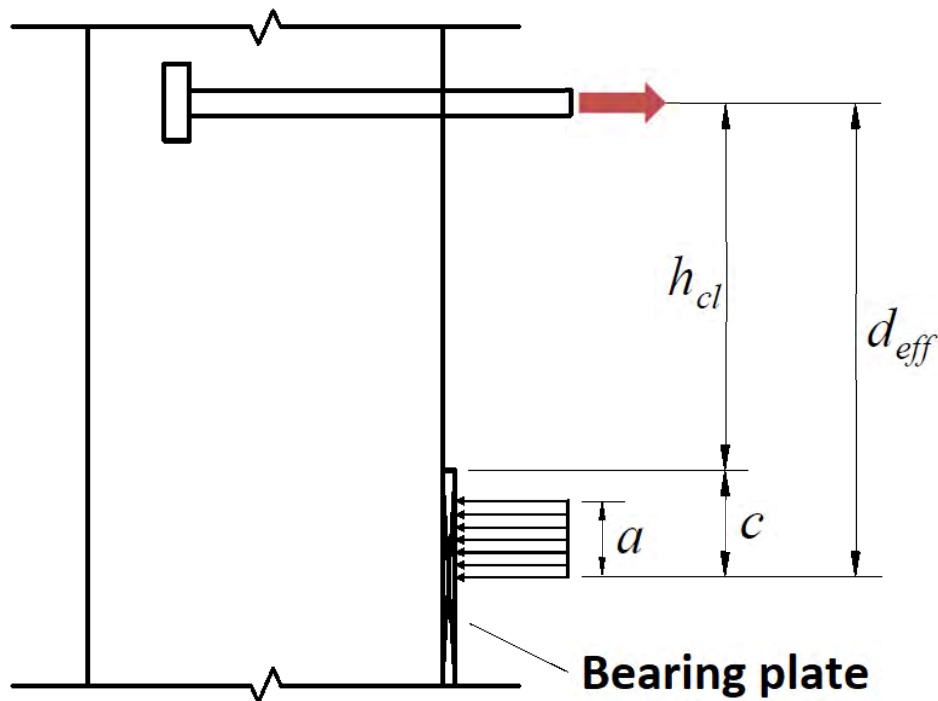


Figure 5.34 Effective beam depth d_{eff} for headed bars (Shao et al. 2016)

As established by Shao et al. (2016), specimens with $d_{eff}/\ell_{eh} > 1.5$ (that is, a deeper beam) generally have lower test-to-calculated T/T_h ratios and anchorage strengths than those with $d_{eff}/\ell_{eh} \leq 1.5$, which were used to develop descriptive equations. This point was considered in this study, with the specimens designed so that d_{eff}/ℓ_{eh} was below 1.5 to prevent possible lower anchorage strengths. As suggested in the commentary section of ACI 318-19, beam-column joints for which $d_{eff}/\ell_{eh} > 1.5$ should be provided with transverse reinforcement in the form of hoops or ties to “establish a load path in accordance with strut-and-tie modeling principles” (enable a strut-and-tie mechanism).

For the specimens shown in the previous plot (Figure 5.33), T/T_h is plotted as a function of the ratio of d_{eff}/ℓ_{eh} in Figure 5.35 below. As shown in the figure, no noticeable trend can be seen for T/T_h as function of d_{eff}/ℓ_{eh} for values of d_{eff}/ℓ_{eh} between 0.92 and 1.42 for No. 11 and larger bars. This observation is similar to that for hooked bars in Section 4.8.

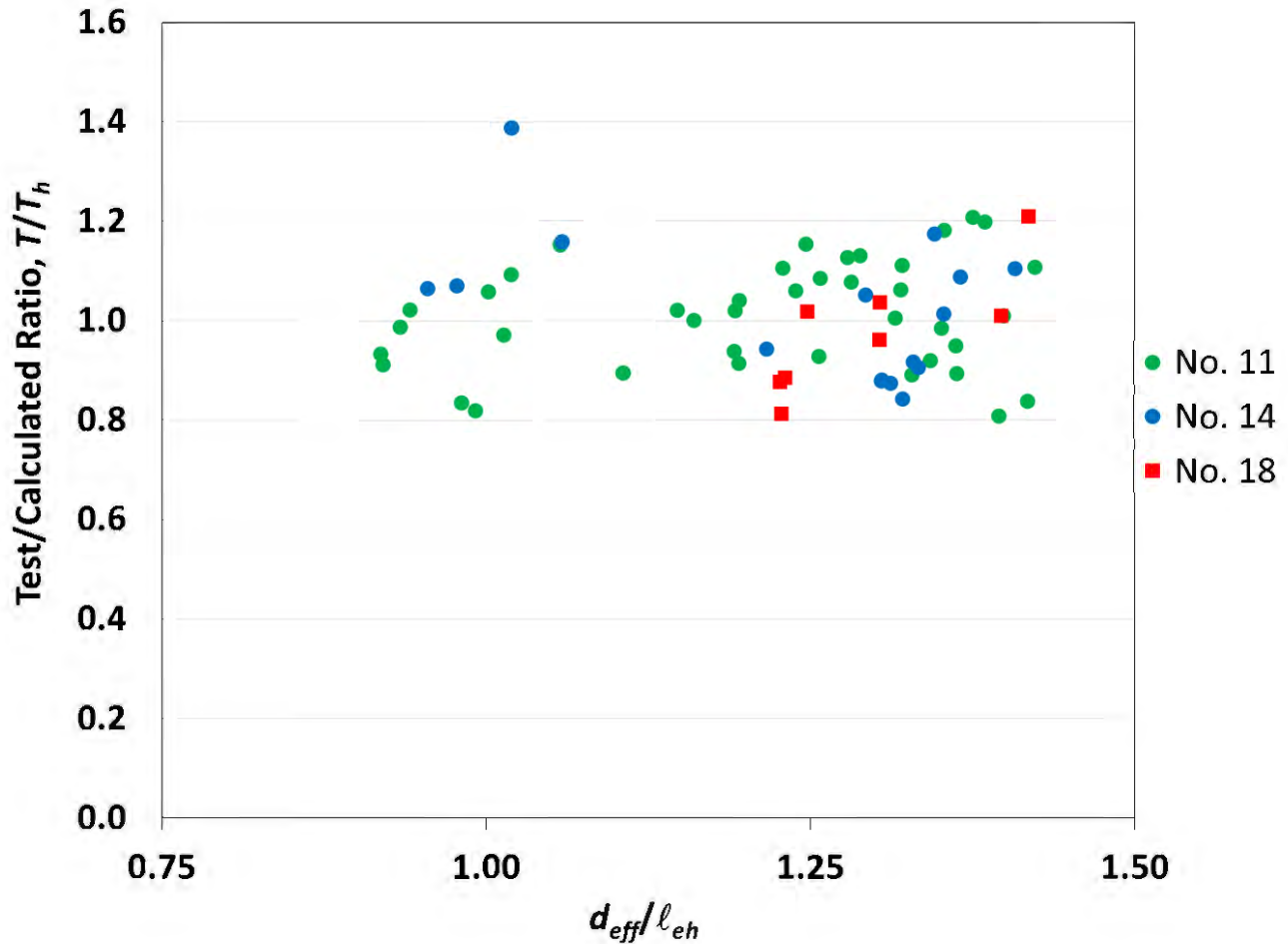


Figure 5.35 Comparison of d_{eff}/ℓ_{eh} versus test-to-calculated ratio T/T_h based on Eq. (5.5) and (5.7) for large (No. 11, No. 14, and No. 18) headed bars

5.5.7 Embedment Length

Figure 5.36 compares the values of T/T_h as a function of the ratio of embedment length to bar diameter ℓ_{eh}/d_b for the No. 11, No. 14, and No. 18 headed bar specimens used to develop Eq. (5.5) and (5.7). The majority of the specimens had ℓ_{eh}/d_b values ranging from 9.4 to 14.4. Four No. 14 bar specimens had the highest ℓ_{eh}/d_b values of 18.7-18.9, all of which had $T/T_h > 1.0$. As shown in the figure, no significant trend in T/T_h can be observed as ℓ_{eh}/d_b increases, indicating that the

accuracy of the descriptive equations developed in this study, Eq. (5.5) and (5.7), is generally not sensitive to the value of ℓ_{eh}/d_b .

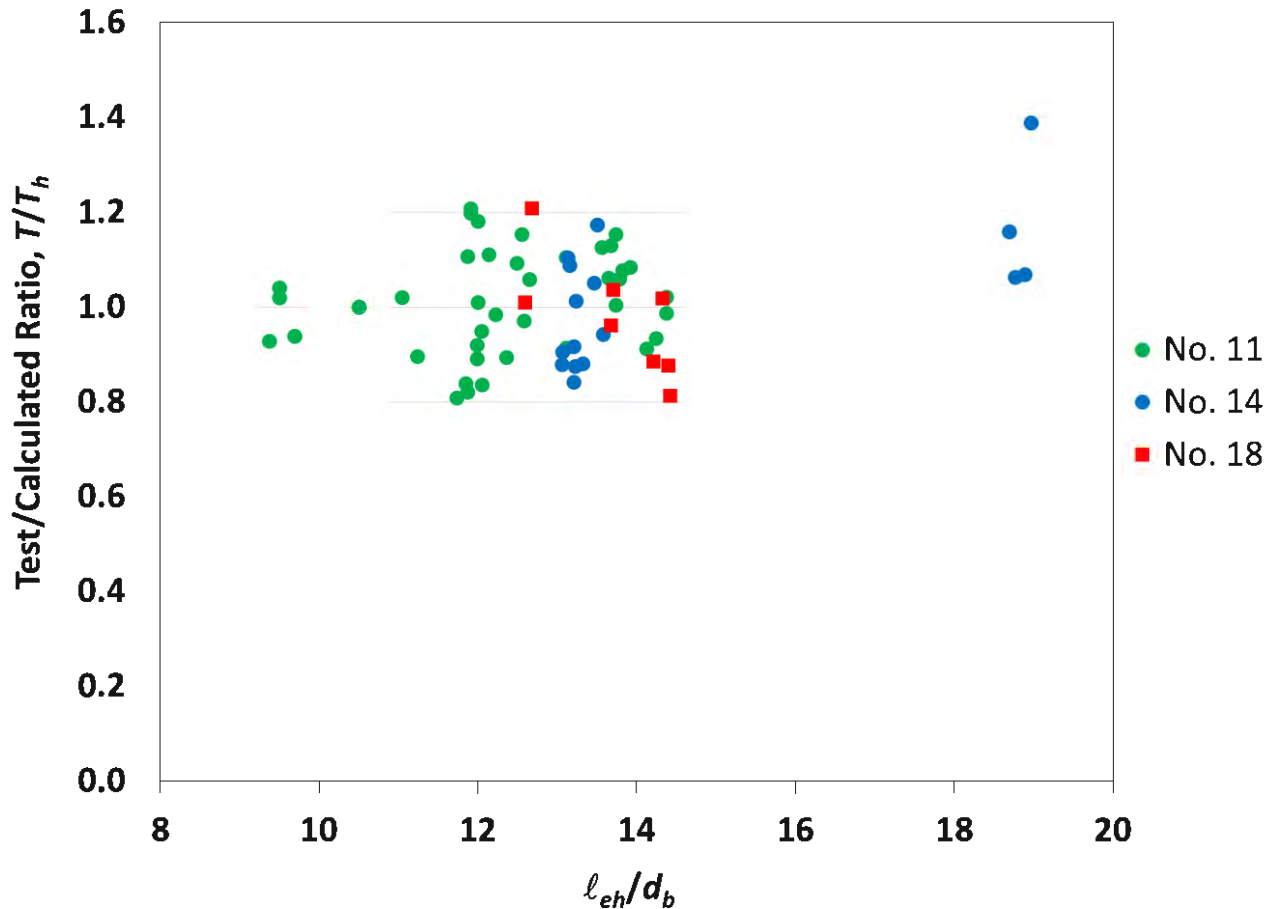


Figure 5.36 Comparison of ℓ_{eh}/d_b versus test-to-calculated ratio T/T_h for based on Eq. (5.5) and (5.7) for large (No. 11, No. 14, and No. 18) headed bars

5.5.8 Bar Location

The headed bar specimens tested at the University of Kansas, including this study, contained headed bars placed inside the column core (the area confined by the column longitudinal reinforcement, as shown in Figure 1.26). Sperry et al. (2015b) tested a limited number of hooked bar specimens with the hooked bars placed outside the column core and observed, generally, lower anchorage strengths (taken conservatively as 80%) compared with specimens with hooked bars placed inside the column core. For design purposes, Sperry et al. (2015b) suggested a bar location factor of 1.25 (1/0.8) to be applied to bars placed outside the column core, which was also adopted by Shao et al. (2016) for headed bars and eventually by the current ACI 318-19 provisions for both

hooked and headed bars. However, as the re-analysis of the hooked bar specimens in Section 4.4 showed, the bar location factor can be reasonably reduced to 1.17 (1.15 for design purposes).

To investigate the influence of bar location for headed bars and to verify the applicability of a reduced bar location factor of 1.17, specimens tested by Chun et al. (2017a) and Sim and Chun (2022a, 2022b) are used. As discussed in Section 1.2.2, these specimens were designed to force a side-blowout failure. The headed bars were placed outside the column core in all specimens. Each specimen had two headed bars in a single layer, except for those tested by Sim and Chun (2022a) where each specimen had four headed bars in two layers. The center-to-center spacing between the layers were used as s to calculate T_h for those specimens. The specimens were heavily reinforced in the joint region using double overlapping No. 5 ties providing A_{tt}/A_{hs} values between 1.01 and 1.37. The 0.4 cap on A_{tt}/A_{hs} , therefore, is applied to all specimens. The tests involve No. 14 and No. 18 (Chun et al. 2017a), No. 14 (Sim and Chun 2022a), and No. 7 and No. 10 (Sim and Chun 2022b) headed bars. The specimens were tested in a manner similar to loading condition B in this study, but with different specimen proportions, as discussed below.

In the majority of these specimens, the headed bars were placed outside the ties in addition to being placed outside the column core, as shown in Figure 5.37a, and were considered by the authors as “unconfined.” This configuration is similar to that used by Chun et al. (2017b) for No. 14 and No. 18 hooked bars, as shown in Figure 4.9a. As established in Section 4.4 for hooked bars, when bars are placed outside the column core and the confining reinforcement, ties should not be considered contributing to anchorage strength. Similarly, for the headed bar specimens in which the bars are outside the column core and parallel ties as in Figure 5.37a, A_{tt}/A_{hs} is taken as zero. In the rest of the specimens, the headed bars were wrapped by ties or hairpin transverse reinforcement, as shown in Figure 5.37b and 5.37c, respectively. For those specimens, the parallel ties were counted towards the anchorage strength. For eight specimens, the test was stopped after the headed bars yielded; those results are not considered in this analysis.

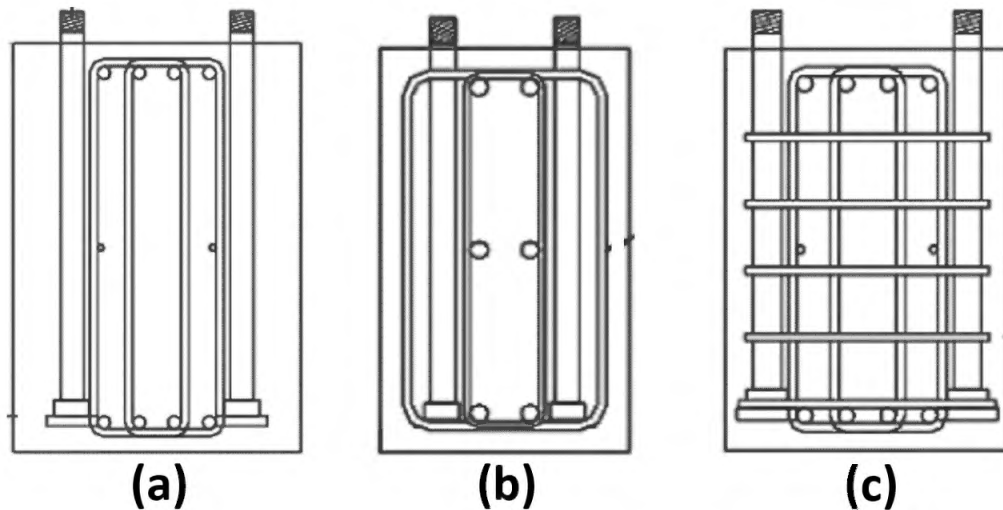


Figure 5.37 Parallel tie layouts in specimens with headed bars placed outside the column core tested by Chun et al. (2017) and Sim and Chun (2022a, 2022b): (a) heads outside parallel ties (“unconfined”), (b) heads inside parallel ties (“confined”), and (c) heads outside parallel ties but “confined” by hairpin transverse reinforcement

Table 5.15 summarizes the specimen details, including values of T/T_h based on two approaches. In approach one, parallel ties are counted for all specimens and no bar location factor is applied. In the second approach, parallel ties are not counted for specimens with bars outside the ties and a bar location factor of 1.17 is applied to all specimens.

Table 5.16 Details and test-to-calculated T/T_h ratios of the specimens tested by Chun et al. (2017) and Sim and Chun (2022a, 2022b) with headed bars outside column core

ID ^[1]	n	$\ell_{eh,avg}$ in.	f_{cm} psi	d_b in.	s/d_b	A_{tr}/A_{hs} ^[2]	T kips	T/T_h ^[3]	T/T_h ^[4]
D43-L7-C1-S42	2	11.9	6950	1.693	9.6	0.4	102.0	0.66	1.11
D43-L7-C1-S42-HP0.5	2	11.9	6950	1.693	9.6	0.4	136.0	0.88	1.03
D43-L7-C1-S70	2	11.9	9890	1.693	9.6	0.4	163.6	1.00	1.65
D43-L10-C1-S42	2	16.9	7570	1.693	9.6	0.4	142.7	0.71	1.09
D43-L10-C1-S42-HP0.5	2	16.9	7570	1.693	9.6	0.4	161.0	0.80	0.94
D43-L10-C1-S70	2	16.9	11,770	1.693	9.6	0.4	193.4	0.90	1.34
D43-L13-C1-S42	2	22.0	6640	1.693	5	0.4	155.0	0.76	1.23
D43-L13-C2-S42	2	22.0	6420	1.693	5	0.4	176.2	0.86	1.41
D43-L13-C1-S42-T1.5	2	22.0	5870	1.693	5	0.4	152.8	0.76	0.89
D43-L13-C2-S42-T1.5*	2	22.0	6060	1.693	5	0.4	210.2	1.04	1.22
D43-L16-C1-S42	2	27.1	6640	1.693	5	0.4	186.8	0.78	1.22
D43-L16-C2-S42*	2	27.1	6640	1.693	5	0.4	198.0	0.82	1.29
D43-L16-C1-S42-T1.5	2	27.1	6060	1.693	5	0.4	138.4	0.58	0.68
D43-L16-C2-S42-T1.5*	2	27.1	6420	1.693	5	0.4	205.0	0.86	1.00
D57-L7-C1-S42	2	15.8	7450	2.257	7.2	0.4	193.8	0.78	1.45
D57-L7-C1-S42-HP0.5	2	15.8	7450	2.257	7.2	0.4	246.0	0.99	1.16
D57-L7-C1-S70	2	15.8	11,150	2.257	7.2	0.4	230.0	0.87	1.58
D57-L10-C1-S42	2	22.6	7450	2.257	7.2	0.4	212.8	0.68	1.14

D57-L10-C1-S42-HP0.5	2	22.6	7450	2.257	7.2	0.4	274.2	0.87	1.02
D57-L10-C1-S70	2	22.6	11,150	2.257	7.2	0.4	258.0	0.77	1.27
D57-L13-C1-S42	2	29.3	5870	2.257	7.2	0.4	254.8	0.70	1.12
D57-L13-C1-S42-HP0.5*	2	29.3	5870	2.257	7.2	0.4	340.0	0.93	1.09
D57-L13-C1-S42-HP1.0a*	2	29.3	5870	2.257	7.2	0.4	340.0	0.93	1.09
D57-L13-C1-S42-HP1.0b*	2	29.3	5870	2.257	7.2	0.4	341.2	0.94	1.10
D57-L13-C2-S42	2	29.3	5870	2.257	7.2	0.4	319.2	0.88	1.40
D57-L16-C1-S42	2	36.1	6060	2.257	7.2	0.4	296.0	0.69	1.06
D57-L16-C2-S42*	2	36.1	6060	2.257	7.2	0.4	341.2	0.80	1.22
D43-L13-C1-42	4	22.0	6260	1.693	1**	0.4	88.9	0.60	1.21
D43-L13-C2-42	4	22.0	6260	1.693	2**	0.4	103.4	0.64	1.20
D43-L13-C2-70	4	22.0	12590	1.693	2**	0.4	143.2	0.79	1.44
D43-L13-C2-42-C	4	22.0	6260	1.693	2**	0.4	145.6	0.90	1.05
D43-L16-C1-42	4	27.1	6850	1.693	1**	0.4	114.6	0.65	1.26
D43-L16-C2-42	4	27.1	6850	1.693	2**	0.4	134.1	0.70	1.26
D43-L16-C2-70	4	27.1	11450	1.693	2**	0.4	156.2	0.74	1.31
D43-L16-C2-42-C*	4	27.1	6850	1.693	2**	0.4	164.3	0.85	1.00
D43-L20-C1-42	4	33.9	6260	1.693	1**	0.4	123.1	0.59	1.12
D43-L20-C2-42	4	33.9	6260	1.693	2**	0.4	135.6	0.60	1.05
D22-L6-C1	2	5.3	12020	0.875	13.5	0.4	41.4	0.79	1.20
D22-L6-C1.5	2	5.3	12020	0.875	13.5	0.4	33.7	0.65	0.98
D22-L6-C1-TR	2	5.3	12020	0.875	13.5	0.4	47.9	0.92	1.07
D22-L9-C1	2	7.9	12020	0.875	13.5	0.4	44.0	0.62	0.87
D32-L6-C1	2	7.6	12020	1.27	9.3	0.4	104.7	1.10	1.77
D32-L6-C1.5	2	7.6	12020	1.27	9.3	0.4	102.9	1.08	1.74
D32-L6-C1-TR	2	7.6	12020	1.27	9.3	0.4	91.3	0.96	1.13
D32-L9-C1	2	11.4	12020	1.27	9.3	0.4	92.6	0.73	1.07
D22-L6-C1	2	5.3	16680	0.875	13.5	0.4	38.7	0.70	1.05
D22-L6-C1.5	2	5.3	16680	0.875	13.5	0.4	31.5	0.57	0.85
D22-L6-C1-TR	2	5.3	16680	0.875	13.5	0.4	39.0	0.71	0.83
D22-L9-C1	2	7.9	16680	0.875	13.5	0.4	35.9	0.48	0.66
D32-L6-C1	2	7.6	16680	1.27	9.3	0.4	108.1	1.08	1.71
D32-L6-C1.5	2	7.6	16680	1.27	9.3	0.4	108.5	1.09	1.72
D32-L6-C1-TR	2	7.6	16680	1.27	9.3	0.4	101.5	1.02	1.19
D32-L9-C1	2	11.4	16680	1.27	9.3	0.4	103.2	0.77	1.12
							Mean:	0.79	1.19
							CoV:	0.199	0.223

n Number of headed bars

$\ell_{eh,avg}$ Measured embedment length

f_{cm} Measured concrete compressive strength

d_b Nominal diameter of the headed bar

s Center-to-center spacing of the bars

A_{tt} Total area of parallel ties within 8 or $10d_b$ from the top of the headed bar

A_{hs} Total area of headed bars

T Measured failure load

T_h Calculated failure load based on descriptive equations, Eq. (5.5) or (5.7)

[1] HP, C, and TR at the end of the designations denote a “confined” specimen per Figure 5.37b and 5.37c

[2] Cap of 0.4 applied to all specimens

[3] Parallel ties counted for all specimens and no bar location factor applied

[4] Parallel ties not counted for specimens with bars outside the ties, and bar location factor of 1.17 applied

* Headed bars yielded; specimens not included in calculation of Mean and CoV of T/T_h

** Center-to-center spacing between the two layers of headed bars was taken as s

As shown in Table 5.15, for the 45 specimens tested by Chun et al. (2017) and Sim and Chun (2022a, 2022b) in which headed bars did not yield, if the parallel ties are counted as contributing and no bar location being applied, T/T_h ranges from 0.48 to 1.10, with an average of 0.79 and coefficient of variation of 0.199. If the parallel ties are not counted towards anchorage strength for specimens with headed bars outside of the ties (“unconfined” per Figure 5.37a) and a bar location of 1.17 applied to all specimens, T/T_h ranges from 0.66 to 1.77, with an average of 1.19 and a coefficient of variation of 0.223. The average T/T_h of 1.19 is beyond the range of the coefficient of variation of descriptive equations (11.2%), indicating a generally conservative estimation of anchorage strength for these specimens for reasons discussed next.

This overall conservatism can be attributed to the specimen proportions used by Chun et al. (2017a) and Sim and Chun (2022a), shown in Figure 1.14. As shown in the figure, in specimens tested by Chun et al. (2017a), the distance from the center of the headed bar to the center of the bearing plate in the joint representing the compression region of the beam, x_{mid} , was $2/3$ of ℓ_{dt} , while the compressive reaction force above the joint was placed $1.0\ell_{dt}$ ($= 1.5x_{mid}$) from the center of the headed bars. For the specimens tested by Sim and Chun (2022a), x_{mid} equaled ℓ_{dt} and the compressive reaction force above the joint was placed $2/3\ell_{dt}$ ($= 0.67x_{mid}$) from the center of the headed bars. These specimen proportions resulted in forces within the joint of $0.6T$ and $0.4T$, respectively, in the specimens tested by Chun et al. (2017) and Sim and Chun (2022a). The geometry of their test specimens was clearly dissimilar to what would be expected in reinforced concrete frame structures. By way of comparison, the forces within the joints for the specimens tested in this study were $\sim 0.69T$ under loading condition B and $0.80T$ under loading condition A, both of which had realistic specimen geometries. The values of $0.6T$ and $0.4T$ indicate that lower forces were carried in the joint for these specimens compared with the specimens used to develop the descriptive equations in this study and by Shao et al. (2016) and Ghimire et al. (2018, 2019a, 2019b). It also means that a higher portion of the total applied force T was shared with the upper compression reaction. This is similar to the hooked bar specimens tested by Marques and Jirsa (1975) and Pinc et al. (1977) where in the force in the joint was just $0.54T$ (Figure 4.21b) and the resulting strength of the specimens was high compared to that calculated using the descriptive equations, as discussed in Section 4.9. Relatively high average T/T_h ratios are, thus, expected for headed bar specimens tested by Chun et al. (2017a) and Sim and Chun (2022a, 2022b).

Overall, the analysis presented in this Section indicates that applying a bar location factor of 1.17 (1.15 for design purposes) for headed bars placed outside the column core provides adequately safe results.

5.6 BEAM-COLUMN JOINT SPECIMENS NOT USED TO DEVELOP DESCRIPTIVE EQUATIONS

The descriptive equations in this study, Eq. (5.5) and (5.7), were developed based on No. 11 bar and smaller specimens tested by Shao et al. (2016) and No. 11 and larger bar specimens tested in this study, all at the University of Kansas. This section evaluates application of Eq. (5.5) and (5.7) to test results for beam-column joint specimens in other studies. The specimens include those by Bashandy (1996), Chun et al. (2009), Chun et al. (2017a), and Sim and Chun (2022a, 2022b). These four studies were described in Section 1.2.2. The study by Chun et al. (2009) is excluded because the specimens had a single headed bar, and, as discussed by Shao et al. (2016), the descriptive equations were developed based on the results from specimens with at least two headed bars and may not apply to single-bar specimens. As shown by Shao et al. (2016), most single-bar specimens tested by Chun et al. (2009) exhibited very low T/T_h values based on descriptive equations Eq. (5.2) and (5.3). The specimens tested by Chun et al. (2017a) and Sim and Chun (2022a, 2022b) were covered in the previous section. The specimens tested by Bashandy (1996) are therefore investigated here in more detail.

Bashandy (1996) tested 32 specimens, each containing two No. 8 or No. 11 headed bars, with and without parallel tie reinforcement. Specimens with parallel ties had A_{tt}/A_{hs} ratios ranging from 0.212 up to 2.025, with the majority having very high A_{tt}/A_{hs} (> 0.75). Also, all but two specimens had closely-spaced bars, with values of s/d_b of 4.6 or 5.0. The specimens were narrow, with a column width of 12 in., and depths of 12 or 15 in. Similar to the current study, two loading conditions were considered, comparable to loading conditions A and B (as defined in Section 2.3.1). In the first loading condition (comparable to loading condition A and is identified here as A'), the joint shear was almost the same as loading condition A (79.5% versus 80% of the total force applied to the headed bars for loading condition A). In the second loading condition (comparable to loading condition B and identified here as B'), the joint shear was ~66% of the force applied to the headed bars (comparable to ~69% in loading condition B in this study). Although the loading conditions used by Bashandy (1996) were similar to those in this study, the specimen proportions were different. As shown in Figure 5.38, the distance from the center of the

headed bars to the compression reaction above the joint, x_{top} , was almost the same in both studies – $2x_{mid}$ and $1.96x_{mid}$ for this study and Bashandy (1996), respectively. However, the compressive forces acting at the bottom of the specimen (equivalent to the force C_3 by the lower tension member in Figure 2.15) were placed closer to the joint region in Bashandy’s specimens than in this study. For Bashandy (1996), the distance from the center of the compression zone of the simulated beam to the compressive force at the bottom of the specimen, x_{bot} , was $1.18x_{mid}$, compared with $2x_{mid}$ in this study. As shown in Figure 5.38, despite the difference in x_{bot} , the shear force in the joint was still $0.8T$ in loading condition A’ (similar to loading condition A) since the force applied at the bottom of the specimen was chosen by Bashandy (1996) to equal $0.33T$.

Of the 32 specimens tested by Bashandy (1996), 19 were tested using loading condition A’ and 13 were tested using loading condition B’. Eleven of the specimens tested by Bashandy failed in shear, rather than anchorage and, hence, were not used by Bashandy in his analyses. Those specimens are also excluded from the comparisons provided here, as are three specimens in which the headed bars were anchored behind the column longitudinal bars leaving 18 specimens.

Bashandy (1996) used three different reinforcement configurations, shown schematically in Figure 5.39. In the first layout (specimens T10, T12, and T13), the headed bars were located outside the column core and the parallel ties (Figure 5.39a), similar to the layout used by Chun et al. (2017a) and shown in Figure 5.37a. The one distinction between the two is that, in Bashandy’s tests, the headed bars were in contact with column longitudinal bars and the parallel ties overlap with the headed bars, whereas in Chun et al.’s layout, the external legs of the ties were placed between the headed bars and column longitudinal bars. The headed bars had a side cover of 1.5 in. (equal to $1.1d_b$ for T10 and $1.5d_b$ for T12 and T13). For these three specimens, a bar location factor ψ_o of 1.17 is applied when calculating T/T_h using Eq. (5.5) and (5.7). In addition, as discussed in Sections 4.4 and 5.5.8, the ties are not taken as contributing to anchorage strength (that is, A_{ti}/A_{hs} should be taken as 0) when bars are placed outside the column core and confining ties. In the second layout, (specimens T14 and T25), the headed bars were placed inside the column core and parallel ties were wrapped around the column longitudinal bars (Figure 5.39b). For the rest of the specimens, both the headed bars and the parallel ties were placed inside the column longitudinal bars (Figure 5.39c). A side cover to the headed bars of 3 in. ($2.13d_b$ or $3d_b$) was used for the specimens shown in Figures 5.39b and c. The reinforcement layouts shown in Figure 5.39a and c are not common in practice, and along with the narrow column width, are not indicative of

reinforced concrete frames. For these reasons, the specimens tested by Bashandy (1996) were not used in developing the descriptive equations.

Table 5.17 presents the key specimen parameters along with the T/T_h ratios based on Eq. (5.5) and (5.7) for the 18 specimens considered for analysis.

Table 5.17 Test-to-calculated ratio T/T_h based on Eq. (5.5) and (5.7) for beam-column joint specimens tested by Bashandy (1996) (values converted from SI units)

Specimen ID	n	ℓ_{eh}	f_{cm}	d_b	s/d_b	A_n/A_{hs}^*	L. C.	T	T_h	T/T_h
		in.	psi	in.				kips	kips	
T9	2	11.0	5000	1.41	3.3	0.641	B'	76.4	89.6	0.85
T10**	2	12.5	5000	1.41	5.4	0.596	B'	60.9	77.8	0.92
T12**	2	9.8	5110	1	8.0	0.557	B'	40.0	65.1	0.72
T13**	2	12.8	5560	1	8.0	0.785	A'	61.4	85.1	0.84
T14	2	11.0	5400	1.41	3.3	0.212	A'	93.5	79.1	1.18
T16	2	14.0	5740	1.41	3.3	1.026	A'	95.8	108.5	0.88
T20	2	8.2	5110	1.41	3.3	1.026	A'	78.5	74.1	1.06
T21	2	8.3	5110	1	5.0	2.025	A'	49.0	61.4	0.80
T22	2	8.3	5110	1	5.0	2.025	A'	41.1	61.4	0.67
T23	2	11.2	4820	1.41	3.3	1.026	A'	68.8	90.1	0.76
T24	2	11.2	4690	1.41	3.3	1.026	A'	80.3	89.8	0.89
T25	2	11.0	4690	1.41	3.3	1.962	A'	95.8	88.7	1.08
T26	2	17.0	4550	1.41	3.3	1.026	A'	111.3	120.6	0.92
T27	2	8.0	4550	1.41	3.3	1.026	A'	44.5	71.8	0.62
T28	2	11.2	4830	1.41	3.3	1.026	A'	97.1	90.2	1.08
T29	2	11.0	4830	1.41	3.3	1.026	A'	86.6	89.1	0.97
T30	2	11.3	3210	1	5.0	2.025	A'	62.7	71.6	0.88
T32	2	8.0	4830	1	5.0	2.025	A'	48.6	59.4	0.82
									Mean:	0.89
									CoV:	0.168

* Cap of 0.4 applied to all specimens, except T10, T12, T13 (refer to next footnote)

** Headed bars were outside column core and side cover was 1.5 in. (half of other specimens), so bar location factor of 1.17 applied. Also, headed bars were outside parallel ties, therefore ties were not counted towards anchorage strength ($A_n/A_{hs} = 0$)

As shown in Table 5.17, T/T_h for the 18 specimens ranges from 0.62 to 1.18, with a mean of 0.89 and a coefficient of variation of 0.168. For the 15 specimens tested under loading condition A', T/T_h ranges from 0.62 to 1.18 with a mean of 0.90 and a coefficient of variation of 0.175. The mean values are within the range of the coefficients of variation of Eq. (5.5) and (5.7), 11.8%. The mean values of 0.89 or 0.90, however, indicate these specimens are relatively weak with respect to values calculated using the descriptive equations and thus, the majority of other specimens subjected to similar loading.

The low mean values of T/T_h also would seem to support the use of a limit on A_{tt}/A_{hs} , in this case 0.4, since 17 out of the 18 specimens had A_{tt}/A_{hs} values > 0.55 and 13 had values of 1.0 or 2.0. Clearly, all of parallel ties provided did not contribute to anchorage strength. Without applying the 0.4 limit on A_{tt}/A_{hs} (that is, assuming all ties contributed to anchorage strength), the mean T/T_h would drop to 0.65.

The last observation is that specimens T14 and T25, the only two specimens that, realistically, contained parallel ties wrapped around both the headed bars and column longitudinal reinforcement (Figure 5.39b), had the highest T/T_h values (1.18 and 1.08, respectively), suggesting that Eq. (5.5) and (5.7) are applicable to beam-column joints, as used in conventional practice.

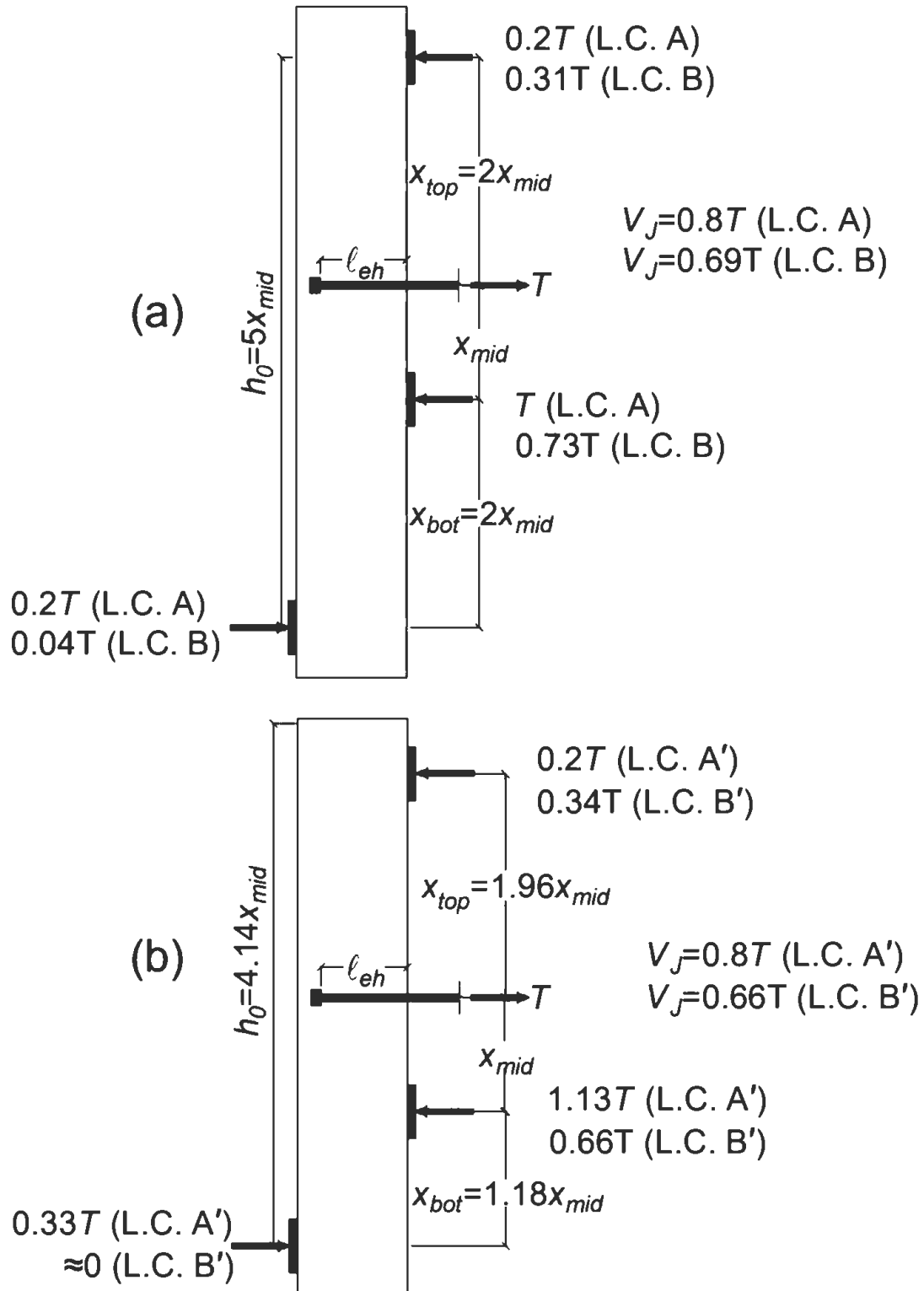


Figure 5.38 Specimen proportions and applied forces: (a) current study; (b) Bashandy 1996
(Note: the bottom drawing is not to scale, L.C. = Loading condition, V_J = Joint Shear)

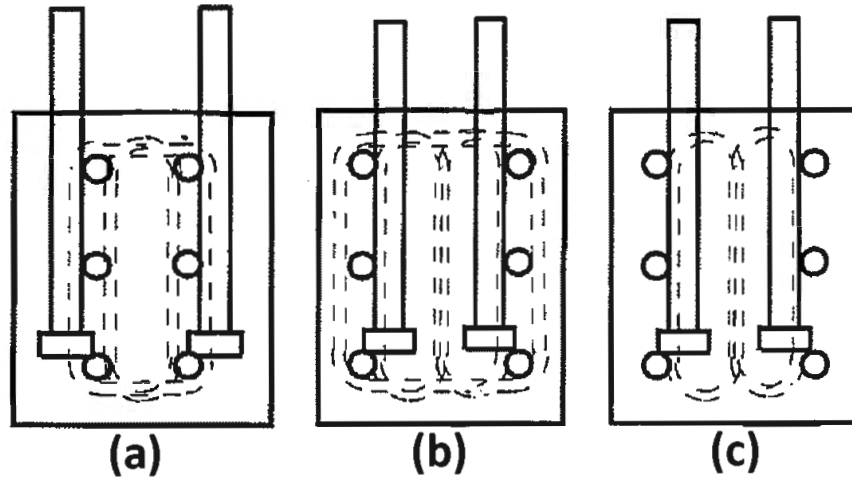


Figure 5.39 Schematic of the reinforcement layouts used by Bashandy (1996): (a) Headed bars outside the column core and parallel ties (specimens T10, T12, and T13); (b) Headed bars inside the column core and parallel ties (specimens T14 and T25); and (c) Headed bars inside column core but ties were not wrapped around column longitudinal bars (rest of the specimens)

CHAPTER 6: DESIGN APPROACH

In the previous chapters, the test results for hooked and headed bar beam-column joints containing No. 11, No. 14, and No. 18 bars were presented and discussed. Previous descriptive equations to characterize anchorage strength developed for No. 11 and smaller bars were evaluated for No. 14 and No. 18 bars. New descriptive equations were then developed to represent the anchorage strength of bars as large as No. 18. In this chapter, new design provisions are proposed for hooked and headed bars, including new equations to calculate development length. The proposed design equations are based on simplified versions of the new descriptive equations, Eq. (4.5) and (4.7) for hooked and Eq. (5.5) and Eq. (5.7) for headed bars to include the effects of bar spacing and confining/parallel tie reinforcement. The procedure is discussed in the next sections, and the proposed design equations are evaluated for the hooked and headed bar beam-column joint database.

6.1 HOOKED BARS

6.1.1 Simplified Descriptive Equations

Simplifying the descriptive equations is accomplished by rounding the powers of different variables (such as f_{cm} and d_b) to numbers suitable for a design equation and finding new constants so that the mean test-to-calculated ratio T/T_h is 1.0. The procedure used by Ajaam et al. (2017) is followed to simplify the descriptive equations, which starts with the base equation for widely-spaced (center-to-center spacing $\geq 6d_b$) hooked bars without confining reinforcement, as shown in Eq. (4.4) and repeated here.

$$T_c = 319 f_{cm}^{0.281} \ell_{eh}^{1.106} d_b^{0.430} \quad (6.1)$$

where T_c is the anchorage strength of hooked bars without confining reinforcement (lb), f_{cm} is concrete compressive strength (psi), ℓ_{eh} is embedment length (in.), and d_b is bar diameter (in.). Rounding the powers of f_{cm} , ℓ_{eh} , and d_b to 0.25, 1.0, and 0.5, respectively, a new constant is then found using the same iterative analysis used to derive Eq. (6.1).

$$T_c = 551 f_{cm}^{0.25} \ell_{eh} d_b^{0.5} \quad (6.2)$$

A new expression for the effect of close bar spacing is found by plotting center-to-center spacing/ d_b versus T/T_c using Eq. (6.2), as shown in Figure 6.1.

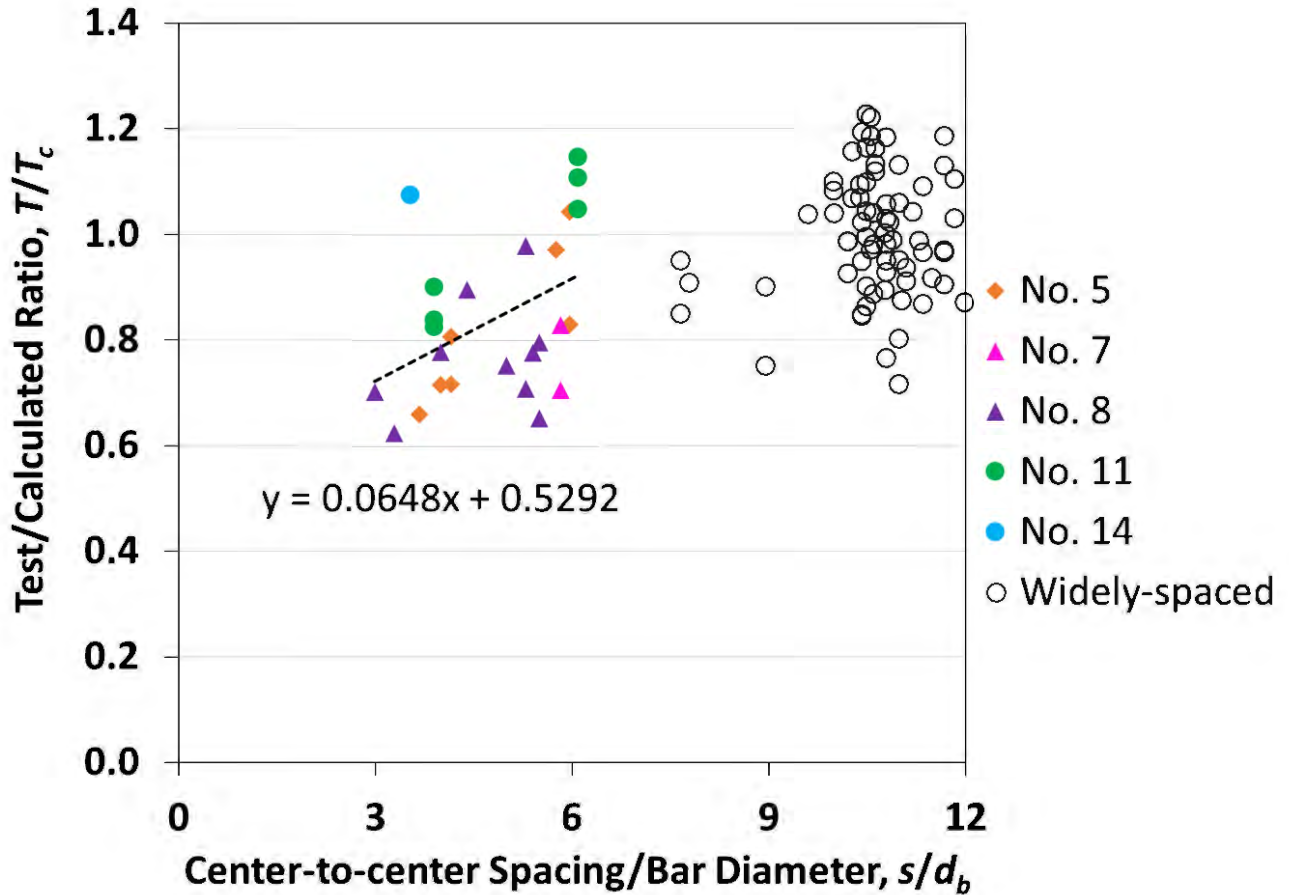


Figure 6.1 Test-to-calculated bar force at failure T/T_c based on simplified Eq. (6.2) versus ratio of center-to-center spacing to bar diameter s/d_b for widely- and closely-spaced hooked bars without confining reinforcement used to develop descriptive equations, Eq. (4.5) and (4.7)

Using the trendline equation given in Figure 6.1, the simplified descriptive equation for widely- and closely-spaced hooked bars without confining reinforcement becomes:

$$T_c = \left(551 f_{cm}^{0.25} \ell_{ch} d_b^{0.5} \right) \left(0.0648 \frac{s}{d_b} + 0.5292 \right) \quad (6.3)$$

where $\left(0.0648 \frac{s}{d_b} + 0.5292 \right) \leq 1.0$.

The plot of T/T_c based on Eq. (6.3) versus concrete compressive strength is shown in Figure 6.2, where no noticeable trend can be seen in T/T_c as a function of f_{cm} . The statistical parameters of T/T_c for specimens without confining reinforcement are given in Table 6.1.

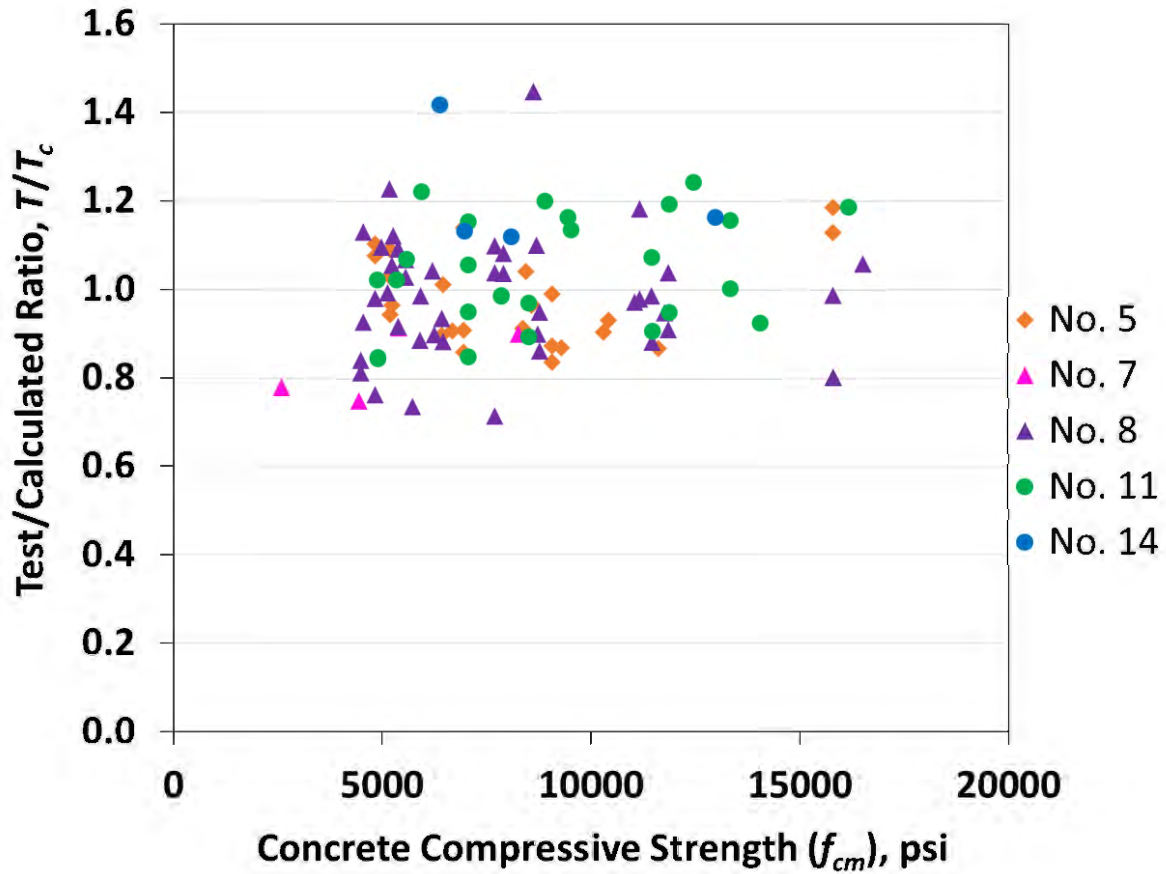


Figure 6.2 Ratio of test-to-calculated bar force at failure T/T_c based on simplified descriptive equation Eq. (6.3) versus concrete compressive strength f_{cm} for hooked bar specimens with widely- and closely-spaced bars without confining reinforcement used to develop descriptive equations, Eq. (4.5) and (4.7)

Table 6.1 Statistical parameters of T/T_c ratio using Eq. (6.3) for hooked bar specimens with widely- and closely-spaced bars without confining reinforcement

Bar size	All	No. 5	No. 7	No. 8	No. 11	No. 14
No. of specimens	102	25	4	43	26	4
Max	1.45	1.18	0.90	1.45	1.24	1.42
Min	0.72	0.84	0.75	0.72	0.84	1.12
Mean	1.00	0.98	0.83	0.99	1.04	1.21
STDEV	0.135	0.099	0.106	0.137	0.125	0.141
CoV	0.135	0.102	0.129	0.139	0.120	0.117

As shown in Table 6.1, T/T_c ranges from 0.72 to 1.45, with a mean of 1.00 and a coefficient of variation of 0.135. The lowest mean is for No. 7 bars (0.83) and the highest is for No. 14 bars

(1.21). The next step involves developing a simplified the equation for specimens with confining reinforcement. The original equation (4.6) is

$$T_h = T_c + T_s = 319 f_{cm}^{0.281} \ell_{eh}^{1.106} d_b^{0.430} + 54,568 \left(\frac{A_{th}}{n} \right) d_b^{0.693} \quad (6.4)$$

where A_{th} is the total cross-sectional area (in.²) of tie legs within $8d_b$ from the top of the hooked bar for No. 8 bars and smaller or within $10d_b$ for No. 9 bars or larger, and n is the number of hooked bars. The power of d_b in the steel contribution term, T_s , is rounded to 0.75 and the simplified equation becomes

$$T_h = 551 f_{cm}^{0.25} \ell_{eh} d_b^{0.5} + 54,067 \left(\frac{A_{th}}{n} \right) d_b^{0.75} \quad (6.5)$$

Figure 6.3 shows the plot of T/T_h using Eq. (6.5) versus ratio of bar spacing to bar diameter s/d_b .

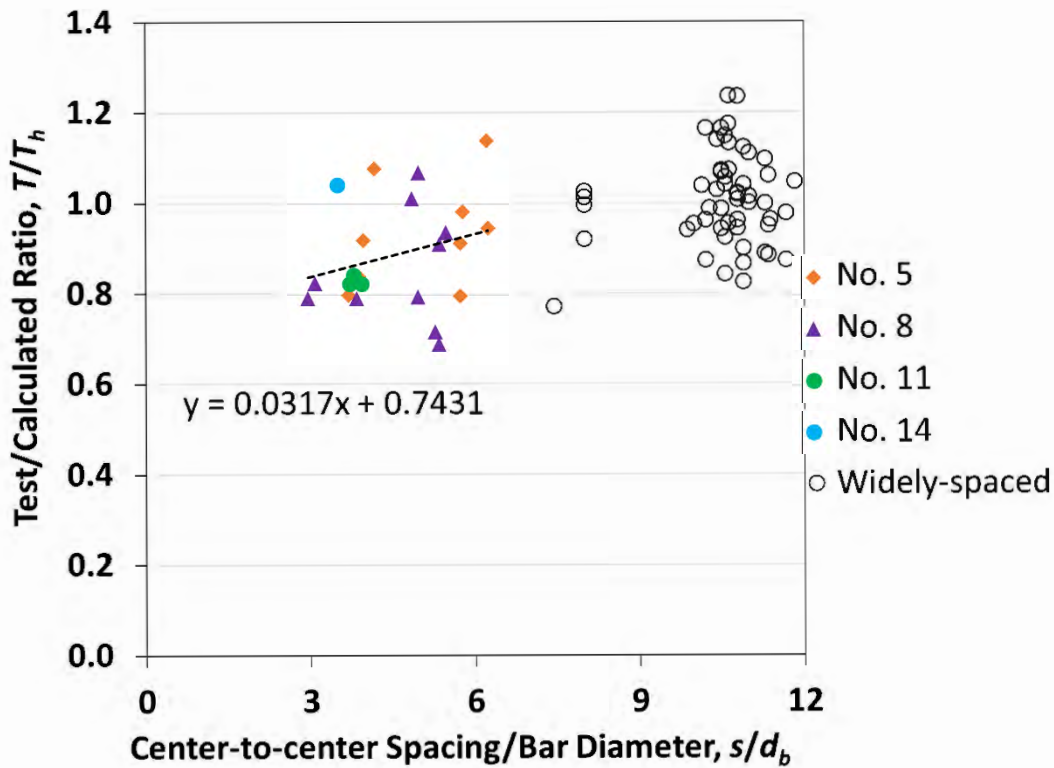


Figure 6.3 Test-to-calculated bar force at failure T/T_h based on simplified Eq. (6.5) versus ratio of center-to-center spacing to bar diameter s/d_b for widely- and closely-spaced hooked bars with confining reinforcement used to develop descriptive equations, Eq. (4.5) and (4.7)

The trendline equation given in Figure 6.3 is used as the expression to account for close bar spacing, giving a simplified descriptive equation for bars with confining reinforcement.

$$T_h = \left(551 f_{cm}^{0.25} \ell_{ch} d_b^{0.5} + 54,067 \left(\frac{A_{th}}{n} \right) d_b^{0.75} \right) \left(0.0317 \frac{s}{d_b} + 0.7431 \right) \quad (6.6)$$

where $\left(0.0317 \frac{s}{d_b} + 0.7431 \right) \leq 1.0$.

Figure 6.4 shows the variation of T/T_h using Eq. (6.6) with concrete compressive strength.

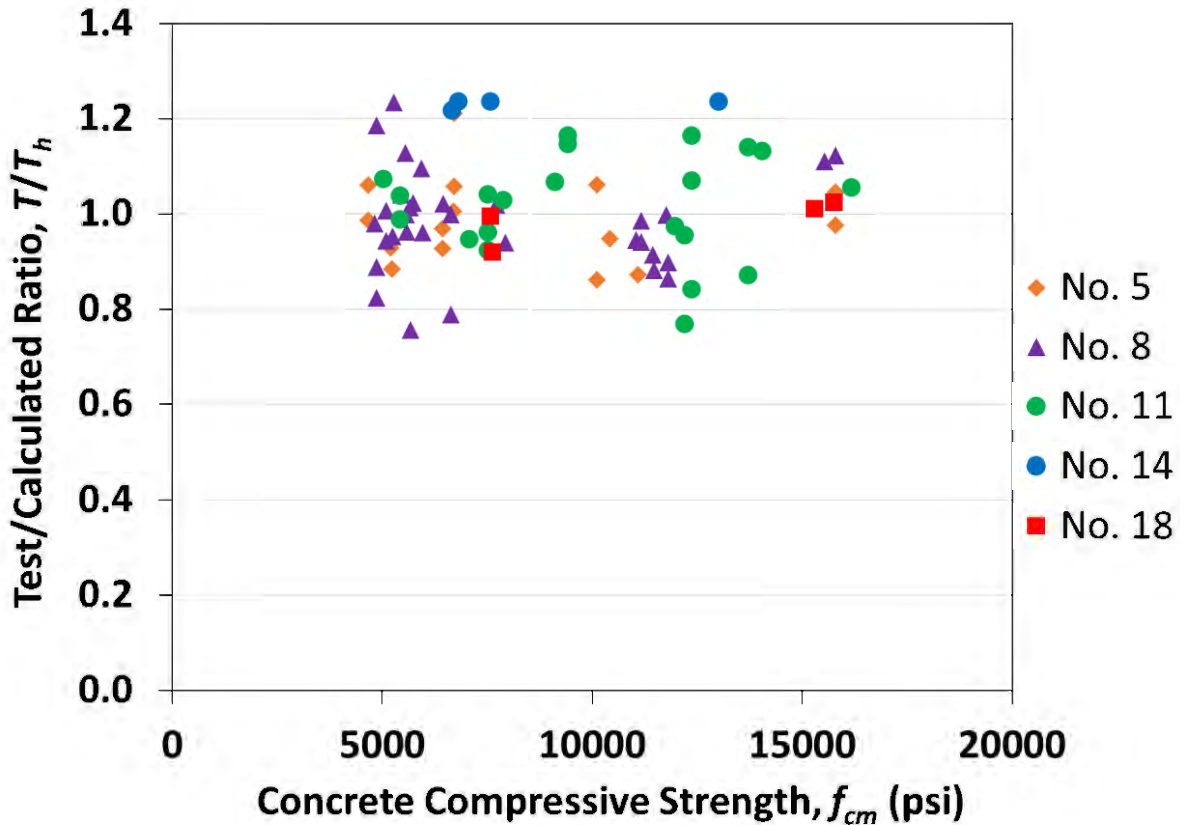


Figure 6.4 Ratio of test-to-calculated bar force at failure T/T_c based on simplified Eq. (6.6) versus concrete compressive strength for hooked bars with widely- and closely-spaced bars with confining reinforcement used to develop descriptive equations, Eq. (4.5) and (4.6)

As shown in Figure 6.4, Eq. (6.6) captures the effect of concrete compressive strength, as no trend is visible on the data points as a function of concrete compressive strength. Table 6.2 presents the statistical parameters for specimens with confining reinforcement. As shown in the table, the specimens with confining reinforcement had a mean T/T_h of 1.00 and a coefficient of variation of 0.110. The statistical parameters of T/T_h are given in Table 6.3 for the hooked bar specimens used to develop the simplified descriptive equations.

Table 6.2 Statistical parameters of T/T_h using Eq. (6.6) for hooked bar specimens with widely- and closely-spaced bars with confining reinforcement used to develop descriptive equations Eq. (4.5) and (4.7)

Bar size	All	No. 5	No. 8	No. 11	No. 14	No. 18
No. of specimens	77	16	32	21	4	4
Max	1.23	1.23	1.23	1.16	1.23	1.02
Min	0.76	0.86	0.76	0.77	0.95	0.92
Mean	1.00	1.00	0.98	1.02	1.14	0.99
STDEV	0.110	0.107	0.106	0.108	0.130	0.047
CoV	0.110	0.107	0.108	0.107	0.113	0.047

Table 6.3 Statistical parameters of T/T_h ratio using Eq. (6.3) and (6.6) for hooked bar specimens used to develop descriptive equations Eq. (4.5) and (4.7)

Bar size	All	No. 5	No. 7	No. 8	No. 11	No. 14	No. 18
No. of specimens	179	41	4	75	47	8	4
Max	1.45	1.23	0.90	1.45	1.24	1.42	1.02
Min	0.72	0.84	0.75	0.72	0.77	0.95	0.92
Mean	1.00	0.99	0.83	0.98	1.03	1.18	0.99
STDEV	0.125	0.102	0.087	0.124	0.117	0.130	0.047
CoV	0.124	0.103	0.105	0.126	0.114	0.110	0.047

As shown in Table 6.3, the simplified equations for hooked bars result in values of T/T_h that range from 0.72 to 1.45, with a mean of 1.00 and a coefficient of variation of 0.124. The next step, converting the simplified descriptive equations to a design equation for the development length of hooked bars, is described in the next section.

6.1.2 Design Equation for Development Length

To derive a design equation for development length, the simplified descriptive equation for widely-spaced hooked bars without confining reinforcement, Eq. (6.2), is considered. In Eq. (6.2), T_c is replaced by $A_b f_y$, with $A_b = \pi d_b^2/4$. The equation is then solved for ℓ_{eh} to become:

$$\ell_{eh} = 0.0014 \frac{f_s \Psi_{cr}}{f_{cm}^{0.25}} d_b^{1.5} \quad (6.9)$$

where $\psi_{cr} = 1 - \frac{54,067}{f_s} \frac{A_{th}}{A_{hs}} d_b^{0.75}$ and is the modification factor for the contribution of confining reinforcement on the anchorage strength, f_s is the bar stress at failure (psi), A_{th} is the total area of tie legs within $8d_b$ from the top of the hooked bars for No. 3 through No. 8 bars and $10d_b$ for No. 11 and larger bars (in.²), A_{hs} is the total area of hooked bars (in.²), d_b is the bar diameter (in.), and f_{cm} is the measured concrete compressive strength (psi). For design, embedment length ℓ_{eh} is replaced by development length ℓ_{dt} , bar stress at failure f_s by yield strength f_y , and measured concrete strength f_{cm} by target compressive strength f'_c , resulting in

$$\ell_{dt} = 0.0014 \frac{f_y \psi_{cr}}{f_{cm}^{0.25}} d_b^{1.5} \quad (6.10)$$

where $\psi_{cr} = 1 - \frac{54,067}{f_y} \frac{A_{th}}{A_{hs}} d_b^{0.75}$, as defined earlier. Since ψ_{cr} decreases with increasing A_{th}/A_{hs} , an upper limit should be selected for A_{th}/A_{hs} . As discussed in Section 4.4 following Figure 4.9, the A_{th}/A_{hs} ratio ranges from 0.14 to 1.06 in specimens with confining reinforcement, with a mean of 0.40 among all specimens. All specimens had $A_{th}/A_{hs} \leq 0.40$, except for No. 5 bar specimens and two No. 18 bar specimens. Therefore, an upper limit of 0.4 on A_{th}/A_{hs} is selected. To evaluate this upper limit, the statistical parameters for T/T_h based on Eq. (6.8) with applying the 0.4 limit of A_{th}/A_{hs} is presented in Table 6.4.

Table 6.4 Statistical parameters of T/T_h ratio using Eq. (6.8) with applying $A_{th}/A_{hs} \leq 0.4$ for hooked bar specimens with widely- and closely-spaced bars with confining reinforcement used to develop descriptive equations Eq. (4.5) and (4.7)

Bar size	All	No. 5	No. 8	No. 11	No. 14	No. 18
No. of specimens	77	16	32	21	4	4
Max	1.39	1.39	1.25	1.16	1.23	1.09
Min	0.76	0.97	0.76	0.77	0.95	0.97
Mean	1.04	1.17	0.99	1.02	1.14	1.02
STDEV	0.133	0.134	0.108	0.108	0.130	0.050
CoV	0.127	0.115	0.109	0.107	0.113	0.049

Comparing the results shown in Table 6.4 with those in Table 6.3 shows that applying the 0.4 upper limit on A_{th}/A_{hs} had the greatest effect on the No. 5 bar specimens, as expected, increasing

the mean T/T_h for those specimens from 1.00 to 1.17. For No. 18 bar specimens, the mean T/T_h increased slightly from 0.99 to 1.02.

As described in Section 4.1, A_{th} is defined differently in the ACI 318 Code than in the descriptive equations. In the Code, A_{th} is the total area of confining reinforcement within $15d_b$ from the centerline of hooked bars. The notation designated in Section 4.1, Table 4.1 for A_{th} within $15d_b$, $A_{th,ACI}$, is used in the following sections. The 0.4 limit on $A_{th,ACI}$ is retained from ACI 318-19.

6.1.2.1 Modification Factor for Confining Reinforcement and Bar Spacing

As described in Section 1.3.1 and as shown in Table 1.3, the current provisions in ACI 318-19 for hooked bars do not provide flexibility for designers because the factor ψ_r , which is based on confining reinforcement and bar spacing, is limited to a binary choice between 1.0 (if specific requirements for confining reinforcement or bars spacing are met) and 1.6 (all other cases). Modifying the provisions for ψ_r to allow the use of a function or functions of $A_{th,ACI}/A_{hs}$ and s/d_b to account for confining reinforcement and spacing of the hooked bars in cases other than those that meet the specific conditions included in ACI 318-19 would provide designers with more avenues for calculating ψ_r and ultimately allow the use of shorter development lengths.

As a first step, a single expression can be developed for ψ_r based on the combined effects of bar spacing and confining reinforcement. The linear trendline equations for T/T_h versus s/d_b in Figures 6.1 and 6.3 based on the simplified descriptive equations for hooked bar specimens without and with confining reinforcement, respectively are used to start. For $s/d_b = 2$, T/T_h is 0.66 and 0.81 for hooked bars without and with confining reinforcement, respectively, which can be conservatively taken as 0.60 and 0.75, and for simplicity, T/T_h is taken as 1 for $s/d_b = 6$. Using the value of 0.60, a linear equation for hooked bars without confining reinforcement becomes

$$\psi_{r1} = 2 - \frac{1}{6} \frac{s}{d_b} \quad (6.11)$$

For bars with confining reinforcement, the resulting linear equation is multiplied by the expression for the effect of confining reinforcement, ψ_{cr} , given following Eq. (6.10), to give

$$\psi_{r2} = \left(\frac{3}{2} - \frac{1}{12} \frac{s}{d_b} \right) \left(1 - \frac{54,067}{f_y} \frac{A_{th,ACI}}{A_{hs}} d_b^{0.75} \right) \quad (6.12)$$

which is a best-fit for all values of $A_{th,ACI}/A_{hs}$ for specimens with confining reinforcement. To find a single expression for ψ_r , the expressions developed above, ψ_{r1} and ψ_{r2} , need to be combined. To

do so, a bilinear interpolation analysis can be performed to find the constants A, B, C, and D in an expression of the general form

$$\psi_r = A + B \frac{A_{th,ACI}}{A_{hs}} + C \frac{s}{d_b} + D \frac{A_{th,ACI}}{A_{hs}} \frac{s}{d_b} \quad (6.13)$$

which would be form obtained if the two terms in Eq. (6.12) are multiplied. To perform the bilinear interpolation analysis, values for ψ_r need to be generated. Each value of ψ_r is called an observation. For the case of $A_{th,ACI}/A_{hs} = 0$, Eq. (6.11) is used, producing five observations for integer values of s/d_b from 2 to 6 in Eq. (6.11).

For $A_{th,ACI}/A_{hs} \neq 0$, Eq. (6.12) is used. Using five values for s/d_b (2, 3, 4, 5, 6), four values for $A_{th,ACI}/A_{hs}$ (0.1, 0.2, 0.3, and 0.4), three values for f_y (60,000, 80,000, 100,000 psi), and five values for d_b (0.625, 1, 1.41, 1.693, 2.257 corresponding respectively to No. 5, No. 8, No. 11, No. 14, No. 18), generates 300 observations (values of ψ_r) using Eq. (6.12).

Since five values for s/d_b and four values for $A_{th,ACI}/A_{hs}$ are used, there are 20 combinations of $(\frac{A_{th,ACI}}{A_{hs}}, \frac{s}{d_b}, \frac{A_{th,ACI}}{A_{hs}} \frac{s}{d_b})$. For each combination of s/d_b and $A_{th,ACI}/A_{hs}$, there are 15 different values of ψ_r based on the integer values of f_y and d_b . These 15 different ψ_r values are averaged for each combination of $(\frac{A_{th,ACI}}{A_{hs}}, \frac{s}{d_b}, \frac{A_{th,ACI}}{A_{hs}} \frac{s}{d_b})$ to give a single value of ψ_r .

The four constants in Eq. (6.13) can be found by performing an Ordinary Least Squares (OLS) regression analysis (in this case, using the “Data Analysis” tool in Excel) on the final 25 observations (5 generated using Eq. (6.11) for specimens without confining reinforcement and 20 using Eq. (6.13) for specimens with confining reinforcement). The OLS method minimizes the sum of the squares of the residuals. A residual is the difference between the values of the dependent variable, in this case the ψ_r values obtained using Eq. (6.11) and (6.12), and corresponding values based on Eq. (6.13). Since 25 observations were used, there are 25 residual values used to establish the four constants. The values obtained for A, B, C, and D from this analysis are 1.8, -2.34, -0.13, and 0.24, respectively. The constants A and C are changed to 2 and -0.167 (-1/6), respectively, to match Eq. (6.1). The constants B and D were rounded to -2.5 and 0.25, respectively. The final expression for ψ_r then is:

$$\psi_r = 2 - 2.5 \frac{A_{th,ACI}}{A_{hs}} - \frac{1}{6} \frac{s}{d_b} + \frac{1}{4} \frac{A_{th,ACI}}{A_{hs}} \frac{s}{d_b}$$

$$\geq 0.9 \text{ for No. 11 and smaller bars and}$$

$$\geq 0.7 \text{ for No. 14 and No. 18 bars}$$
(6.14)

where $2 \leq \frac{s}{d_b} \leq 6$ and $\frac{A_{th,ACI}}{A_{hs}} \leq 0.4$. The cap of 0.4 on $A_{th,ACI}/A_{hs}$ is retained from ACI 318-19

since values higher than 0.4 do not result in increased anchorage strength and would, thus, result in an unconservative designs, as explained below.

Although ψ_r varies from 0.86 to 1.67 for $s/d_b = 2$ and from 0.6 to 1.0 for $s/d_b = 6$, depending on the amount of confining reinforcement, Eq. (6.14) contains limits on the minimum values of ψ_r of 0.9 for No. 11 and smaller hooked bars and 0.7 for No. 14 and No. 18 hooked bars to avoid very high calculated anchorage strengths with respect to the test results and to ensure that no more than 5% of all specimens have a test-to-calculated ratio less than 1.0 when used in a design expression for development length (discussed in Section 6.1.2.4). ψ_r is permitted to be as low as 0.7 for No. 14 and No. 18 bars since, as shown in Eq. (4.7), the effect of confining reinforcement increases as the hooked bar size increases. The effect is less significant for smaller bars, but is high enough that it is worth taking advantage of for the larger bars.

The approach used to find ψ_r is similar to that used by Ajaam et al. (2017) to develop a modification factor for confining reinforcement and bar spacing. Instead of using bilinear interpolation to find a single expression for ψ_r , Ajaam et al. (2017) provided six values for ψ_r for two confinement levels, none and $A_{th}/A_{hs} > 0.2$; two bar spacings, $s = 2d_b$ and $s > 6d_b$; and two values of f_y , 60,000 and 120,000 psi, as shown in Table 1.2; allowing linear interpolation to obtain intermediate values.

Because ACI Committee 318 has chosen not to adopt an expression similar to Eq. (6.14) in the past, a conservative simplification of the ψ_r expression is worthy of consideration that consists of two terms each for No. 11 and smaller bars and for No. 14 and No. 18 bars: one expressed as a function of s/d_b for $A_{th,ACI}/A_{hs} = 0$ and one expressed as a function of $A_{th,ACI}/A_{hs}$ for $s/d_b = 2$. Using $s/d_b = 2$ in Eq. (6.14) gives $\psi_r = 5/3 - 2A_{th,ACI}/A_{hs}$. For simplicity, $5/3$ is rounded to 1.6. To take advantage of the increasing effect of confining reinforcement on anchorage strength with increasing hooked bar size the expression is changed to $\psi_r = 5/3 - 3A_{th,ACI}/A_{hs}$ for No. 14 and

No. 18 bars. Also, the minimum value for ψ_r for No. 14 and No. 18 bars is increased from 0.7 to 0.8 to avoid high calculated anchorage strengths. The final form of simplified expressions is

$$\begin{aligned}\psi_r &= \min \left\{ 2 - \frac{1}{6} \frac{s}{d_b}, 1.6 - 2 \frac{A_{th,ACI}}{A_{hs}} \right\} \geq 0.9 \text{ for No. 11 and smaller} \\ \psi_r &= \min \left\{ 2 - \frac{1}{6} \frac{s}{d_b}, 1.6 - 3 \frac{A_{th,ACI}}{A_{hs}} \right\} \geq 0.8 \text{ for No. 14 and No. 18}\end{aligned}\tag{6.15}$$

As shown in Section 4.4.1, if the hooked bars are placed outside the column core and confining ties, the confining reinforcement should not be counted towards contributing to anchorage strength, meaning $A_{th,ACI}/A_{hs}$ should equal 0 when calculating ψ_r .

6.1.2.2 Modification Factor for Bar Coating and Concrete Density

The values currently provided for the modification factors for coated bars and lightweight concrete, ψ_e and λ , are retained. Per Table 25.4.3.2 of ACI 318-19, for epoxy-coated or zinc and epoxy dual-coated bars, $\psi_e = 1.2$, and for uncoated or zinc-coated bars, $\psi_e = 1.0$. $\lambda = 0.75$ is applied when using lightweight concrete and $\lambda = 0.1.0$ when using normalweight concrete.

6.1.2.3 Modification Factor for Bar Location

The provisions in ACI 318-19 include a bar location factor $\psi_o = 1.0$ for hooked bars terminating inside the column core with a side cover to the bar of at least 2.5 in., or terminating in supporting members with a side cover of at least $6d_b$, and $\psi_o = 1.25$ for other cases. The value 1.25 is based on the observations by Sperry et al. (2015a) and Ajaam et al. (2017) that, in general, specimens with hooked bars placed outside the column core had a lower anchorage strength than those with bars inside column core. Therefore, conservatively, a strength modification factor of 0.8 was suggested, and later retained by Shao et al. (2016) for headed bars ($1/0.8 = 1.25$).

The re-analysis of the specimens with hooked bars placed outside column core in Section 4.4.1 has shown, however, that a bar location factor of 1.17 would be more appropriate based on the mean test-to-calculated T/T_h ratio of 0.85 for those specimens based on descriptive equations. For design purposes, a bar location factor of 1.15 is suggested.

6.1.2.4 Strength-Reduction Factor and Final Design Equation

Now that all the modification factors are in hand, a strength-reduction factor, ϕ , needs to be incorporated into Eq. (6.10) to limit the probability of failure, as shown in Eq. (6.16).

$$\ell_{dh} = \frac{0.0014}{\phi} \frac{f_y \Psi_e \Psi_r \Psi_o}{f_c^{0.25}} d_b^{1.5} \quad (6.16)$$

The criterion for selecting the value for ϕ is that 5% or less of beam-column test specimens have a test-to-calculated ratio of below 1.0. Using $\phi = 0.79$ results in 4.0% of the specimens used to develop the descriptive equations having a test-to-calculated ratio of below 1.0. Imbedding $\phi = 0.79$ within the design equation (as is traditionally applied in ACI 318) and using $0.0014/0.79 = 1/570$, the design equation for development of hooked bars is

$$\ell_{dh} = \frac{f_y \Psi_e \Psi_r \Psi_o}{570 \lambda f_c^{0.25}} d_b^{1.5} \quad (6.17)$$

Eq. (6.17) is similar in format to that proposed by Ajaam et al. (2018). Equation (6.17) has advantages compared with the equation in Section 25.4.3.1 of ACI 318-19. First, the expressions developed for confining reinforcement and bar spacing factor, Ψ_r , provides design flexibility compared to the limited choice between 1.0 and 1.6 in ACI 318-19. Second, using $f_c^{0.25}$ provides a better representation of the contribution of concrete compressive strength and eliminates the need for a concrete strength modification factor (ψ_c in Table 25.4.3.2 of ACI 318-19), and, thus, simplifies the design process. Third, the bar location factor Ψ_o is reduced from 1.25 to 1.15. These advantages can result in shorter development lengths. In addition, given the range of concrete compressive strength (up to 16,200 psi) and bar stress at failure (up to 144,000 psi) available in the database used to develop Eq. (6.17), the proposed design equation is applicable to bars for specified yield strengths up to 120,000 psi and concrete strengths up to 16,000 psi.

A summary of the modification factors incorporated into Eq. (6.17) is given in Table 6.5.

Table 6.5 Modification factors for the proposed design equation for development of hooked bars

Modification Factor	Condition	Value ^{[1][2][3][4]}
Concrete Density, λ	Lightweight concrete	0.75
	Normalweight concrete	1.0
Epoxy coating, ψ_e	Epoxy- or zinc and epoxy dual-coated bars	1.2
	Uncoated or zinc-coated (galvanized) bars	1.0
Confining reinforcement and bar spacing, ψ_r ^{[5][6]}	For No. 11 and smaller bars	$2 - 2.5 \frac{A_{th,ACI}}{A_{hs}} - \frac{1}{6} \frac{s}{d_b} + \frac{1}{4} \frac{A_{th,ACI}}{A_{hs}} \frac{s}{d_b} \geq 0.9$ <p style="text-align: center;">or, smaller of</p> $\left\{ 2 - \frac{1}{6} \frac{s}{d_b} \text{ and } 1.6 - 2 \frac{A_{th,ACI}}{A_{hs}} \right\} \geq 0.9$
	For No. 14 and No. 18 bars	$2 - 2.5 \frac{A_{th,ACI}}{A_{hs}} - \frac{1}{6} \frac{s}{d_b} + \frac{1}{4} \frac{A_{th,ACI}}{A_{hs}} \frac{s}{d_b} \geq 0.7$ <p style="text-align: center;">or, smaller of</p> $\left\{ 2 - \frac{1}{6} \frac{s}{d_b} \text{ and } 1.6 - 3 \frac{A_{th,ACI}}{A_{hs}} \right\} \geq 0.8$
Bar location, ψ_o	(1) Bars terminating inside column core with a minimum side cover to bar of 2.5 in., or (2) Bars terminating in supporting members with a side cover of at least $6d_b$	1.0
	Other	1.15

^[1] $A_{th,ACI}$: Total cross-sectional area of tie legs within $15d_b$ from the centerline of the hooked bars, in.²

^[2] A_{hs} : Total cross-sectional area of the hooked bars being developed, in.²

^[3] s : Minimum center-to-center spacing of hooked bars, in.

^[4] d_b : Nominal diameter of hooked bar, in.

^[5] When calculating ψ_r , $A_{th,ACI}/A_{hs}$ shall not exceed 0.4 and s/d_b shall not exceed 6

^[6] When bars are placed outside both the column core and the confining ties, $A_{th,ACI}/A_{hs} = 0$ when calculating ψ_r

6.1.3 Evaluating Proposed Design Equation

In this section, the proposed design equation for development length of hooked bars, Eq. (6.17), is compared with the results in the beam-column joint database. The database includes the beam-column joint tests at the University of Kansas by Searle et al. (2014), Sperry et al. (2015a, 2015b, 2017a, 2017b, 2018), Yasso et al. (2017), Ajaam et al. (2017, 2018), plus tests available in the literature including those by Marques and Jirsa (1975), Pinc et al (1977), Hamad et al. (1993), Ramirez and Russell (2008), Lee and Park (2010), and Chun et al. (2017b). Details of the University of Kansas specimens are provided in Tables B2 through B5 in Section B3 of Appendix B, and the other specimens are presented in Table B8 in Section B4.

For the comparison, the bar stress at failure measured in the test, f_{su} , is compared with the bar stress calculated based on Eq. (6.17), $f_{s,calc}$. To find $f_{s,calc}$, Eq. (6.17) is solved for yield strength, f_y , which is replaced by $f_{s,calc}$, specified concrete compressive strength f'_c is replaced by the measured concrete strength f_{cm} , and development length ℓ_{dh} is replaced by measured embedment length ℓ_{eh} . The resulting equation is

$$f_{s,calc} = \frac{570\lambda\ell_{eh}f_{cm}^{0.25}}{\Psi_e\Psi_r\Psi_o d_b^{1.5}} \quad (6.18)$$

6.1.3.1 University of Kansas Database

The design equation is first compared with the tests results in the database available in Ajaam et al. (2017, 2018), presented in detail in Tables B2 to B5 in Section B3 of Appendix B. The database, with a total of 251 specimens, is an extended version of the one with 185 specimens used to develop the descriptive equations, Eq. (4.5) and (4.7). The database includes No. 5, No. 8, and No. 11 hooked bar specimens tested at the University of Kansas by Searle et al. (2014), Sperry et al. (2015a, 2015b, 2017a, 2017b, 2018), Yasso et al. (2017), Ajaam et al. (2017, 2018), No. 14 and No. 18 bars tested in this study, plus three No. 6 and three No. 11 bar specimens by Ramirez and Russell (2008), two No. 7 bar specimens by Lee and Park (2010), six No. 7 bar specimens by Marques and Jirsa (1975), and two No. 7 bar specimens by Hamad et al. (1993).

The statistical parameters of $f_{s,calc}/f_{su}$ using the full expression for ψ_r , Eq. (6.14), are presented for specimens without confining reinforcement in Table 6.6.

Table 6.6 Statistical parameters of test-to-calculated bar stress at failure $f_{su}/f_{s,calc}$ for hooked bar specimens without confining reinforcement, based on the proposed design equation, Eq. (6.17), and the full expression for ψ_r , Eq. (6.14)

	All	$s \geq 6d_b$					$2d_b \leq s < 6d_b$				
		No. 5	No. 7	No. 8	No. 11	No. 14	No. 5	No. 7	No. 8	No. 11	No. 14
Number of specimens	108	18	2	33	20	3	7	8	10	6	1
Max	1.87	1.44	1.12	1.77	1.50	1.43	1.29	1.32	1.39	1.50	1.87
Min	0.87	1.02	0.94	0.88	1.04	1.38	1.01	0.91	0.87	1.29	1.87
Mean	1.23	1.19	1.03	1.23	1.24	1.40	1.17	1.16	1.14	1.39	1.87
STDEV	0.167	0.121	0.132	0.168	0.149	0.022	0.097	0.138	0.172	0.068	0.0
CoV	0.136	0.102	0.129	0.136	0.120	0.016	0.082	0.120	0.151	0.049	0.0
No. with $f_{su}/f_{s,calc} < 1.0$	7	0	1	3	0	0	0	1	2	0	0

As shown in Table 6.6, $f_{s,calc}/f_{su}$ using the full expression for ψ_r for hooked bar specimens without confining reinforcement ranges from 0.87 to 1.87 with a mean of 1.23 and a coefficient of variation of 0.136. The design equation is least conservative for the two No. 7 bar specimens with widely-spaced bars (Lee and Park 2010), and most conservative for the single No. 14 bar test specimen with closely-spaced bars, which appears to be an outlier, with a $f_{su}/f_{s,calc} = 1.87$. This specimen was tested only to be compared to its companion specimen with confining reinforcement. Otherwise, using multiple closely-spaced No. 14 hooked bars without confining reinforcement in practice is highly unlikely.

The statistical parameters of $f_{s,calc}/f_{su}$ using the simplified expressions for ψ_r , Eq. (6.15), are presented for specimens without confining reinforcement in Table 6.7.

Table 6.7 Statistical parameters of test-to-calculated bar stress at failure $f_{su}/f_{s,calc}$ for hooked bar specimens without confining reinforcement, based on the proposed design equation, Eq. (6.17) and the simplified expressions for ψ_r , Eq. (6.15)

	All	$s \geq 6d_b$					$2d_b \leq s < 6d_b$				
		No. 5	No. 7	No. 8	No. 11	No. 14	No. 5	No. 7	No. 8	No. 11	No. 14
Number of specimens	108	18	2	33	20	3	7	8	10	6	1
Max	1.87	1.44	1.12	1.77	1.50	1.43	1.29	1.32	1.39	1.50	1.87
Min	0.87	1.02	0.94	0.88	1.04	1.38	1.01	0.91	0.87	1.29	1.87
Mean	1.23	1.19	1.03	1.23	1.24	1.40	1.17	1.16	1.14	1.39	1.87
STDEV	0.167	0.121	0.132	0.168	0.149	0.022	0.097	0.138	0.172	0.068	0
CoV	0.136	0.102	0.129	0.136	0.120	0.016	0.082	0.120	0.151	0.049	0
No. with $f_{su}/f_{s,calc} < 1.0$	7	0	1	3	0	0	0	1	2	0	0

As shown in Table 6.7, the results obtained using the simplified expressions for ψ_r are identical to those obtained using the full expression for ψ_r (Table 6.6).

The statistical parameters of $f_{s,calc}/f_{su}$ using the full expression for ψ_r , Eq. (6.14), are presented for specimens with confining reinforcement in Table 6.8. As shown in the table, the hooked bar specimens with confining reinforcement had values of $f_{s,calc}/f_{su}$ ranging from 0.89 to 1.85, with a mean of 1.29 and a coefficient of variation of 0.147. The specimens with widely-spaced bars have higher mean values.

Table 6.8 Statistical parameters of test-to-calculated bar stress at failure $f_{su}/f_{s,calc}$ for hooked bar specimens with confining reinforcement, based on the proposed design equation, Eq. (6.17) and the full expression for ψ_r , Eq. (6.14)

	All	$s \geq 6d_b$					$2d_b \leq s < 6d_b$			
		No. 5	No. 8	No. 11	No. 14	No. 18	No. 5	No. 8	No. 11	No. 14
Number of specimens	143	24	49	26	3	4	11	20	5	1
Max	1.85	1.76	1.85	1.55	1.33	1.52	1.69	1.48	1.33	1.27
Min	0.89	1.03	1.08	1.05	0.99	1.13	0.91	0.89	1.04	1.27
Mean	1.29	1.37	1.34	1.32	1.20	1.28	1.26	1.14	1.16	1.27
STDEV	0.190	0.227	0.157	0.146	0.180	0.177	0.242	0.179	0.145	0
COV	0.147	0.166	0.117	0.110	0.151	0.138	0.192	0.156	0.125	0
No. with $f_{su}/f_{s,calc} < 1.0$	6	0	0	0	1	0	2	3	0	0

The statistical parameters of $f_{s,calc}/f_{su}$ using the simplified expressions for ψ_r , Eq. (6.15), are presented for specimens with confining reinforcement in Table 6.9. Using the simplified expressions for ψ_r results in values of $f_{s,calc}/f_{su}$ ranging from 0.91 to 1.85, matching the range for the full expression for ψ_r , a higher overall mean value of $f_{s,calc}/f_{su}$, 1.35 versus 1.29, and a lower coefficient of variation, 0.134. As a result of using simplified expressions, No. 8 through No. 18 bar specimens with $s \geq 6d_b$ have noticeably higher mean values of $f_{s,calc}/f_{su}$.

Table 6.9 Statistical parameters of test-to-calculated bar stress at failure $f_{su}/f_{s,calc}$ for hooked bar specimens with confining reinforcement, based on the proposed design equation, Eq. (6.17) and the simplified expressions for ψ_r , Eq. (6.15)

	All	$s \geq 6d_b$					$2d_b \leq s < 6d_b$			
		No. 5	No. 8	No. 11	No. 14	No. 18	No. 5	No. 8	No. 11	No. 14
Number of specimens	143	24	49	26	3	4	11	20	5	1
Max	1.85	1.76	1.85	1.55	1.52	1.74	1.69	1.56	1.48	1.24
Min	0.91	1.03	1.09	1.05	1.13	1.29	0.91	0.92	1.18	1.24
Mean	1.35	1.37	1.41	1.36	1.34	1.47	1.26	1.23	1.30	1.24
STDEV	0.181	0.227	0.144	0.126	0.198	0.203	0.242	0.178	0.158	0.0
COV	0.134	0.166	0.102	0.093	0.147	0.138	0.192	0.144	0.121	0.0
No. with $f_{su}/f_{s,calc} < 1.0$	3	0	0	0	0	0	2	1	0	0

The statistical parameters of $f_{su}/f_{s,calc}$ using the full expression for ψ_r are presented in Table 6.10 for the hooked bar specimens, without and with confining reinforcement, used to develop descriptive equations Eq. (4.5) and (4.7).

Table 6.10 Statistical parameters of test-to-calculated bar stress at failure $f_{su}/f_{s,calc}$ for hooked bar specimens, without and with confining reinforcement, used to develop descriptive equations Eq. (4.5) and (4.7), based on the proposed design equation Eq. (6.17) and using the full expression for ψ_r , Eq. (6.14)

Bar size	All	No. 5	No. 7	No. 8	No. 11	No. 14	No. 18
No. of specimens	251	60	10	112	57	8	4
Max	1.87	1.76	1.32	1.85	1.55	1.87	1.52
Min	0.87	0.91	0.91	0.87	1.04	0.99	1.13
Mean	1.26	1.27	1.13	1.25	1.29	1.36	1.28
STDEV	0.184	0.205	0.140	0.183	0.151	0.244	0.177
COV	0.145	0.161	0.124	0.146	0.118	0.179	0.138
No. with $f_{su}/f_{s,calc} < 1.0$	13	2	2	8	0	1	0

As shown in Table 6.10, for the 251 hooked bar specimens for comparison, $f_{su}/f_{s,calc}$ based on the proposed design equation and using the full expression for ψ_r ranges from 0.87 to 1.87 with a mean of 1.26 and a coefficient of variation of 0.145. The mean $f_{su}/f_{s,calc}$ is the highest for No. 14 bars, in part due to the two specimens with closely-spaced bars as mentioned previously. A total of 13 specimens (5.2% of all specimens) had $f_{su}/f_{s,calc} < 1.0$.

A similar table can be presented for the case of using the simplified expressions for ψ_r , as shown below. As shown in Table 6.11, the simplified expressions for ψ_r result in a higher overall mean (1.30 versus 1.27), the same coefficient of variation, and a higher overall mean for No. 14 and No. 18 bars (1.42 and 1.47 versus 1.36 and 1.28, respectively). Ten specimens (4.0 % of all specimens) have $f_{su}/f_{s,calc} < 1.0$.

Table 6.11 Statistical parameters of test-to-calculated bar stress at failure $f_{su}/f_{s,calc}$ for hooked bar specimens, without and with confining reinforcement, used to develop descriptive equations Eq. (4.5) and (4.7), based on the proposed design equation Eq. (6.17) and using the simplified expressions for ψ_r , Eq. (6.15)

Bar size	All	No. 5	No. 7	No. 8	No. 11	No. 14	No. 18
No. of specimens	251	60	10	112	57	8	4
Max	1.76	1.32	1.85	1.55	1.87	1.74	1.76
Min	0.91	0.91	0.87	1.04	1.13	1.29	0.91
Mean	1.27	1.13	1.30	1.32	1.42	1.47	1.27
STDEV	0.205	0.140	0.186	0.143	0.217	0.203	0.205
COV	0.161	0.124	0.143	0.108	0.153	0.138	0.161
No. with $f_{su}/f_{s,calc} < 1.0$	10	2	2	6	0	0	0

6.1.3.2 Marques and Jirsa (1975)

Table 6.12 presents the comparisons of the No. 7 and No. 11 specimens tested by Marques and Jirsa (1975) with the proposed design equation.

As shown in Table 6.12, $f_{su}/f_{s,calc}$ for the specimens tested by Marques and Jirsa (1975) using the full expression for ψ_r ranges from 1.09 to 2.12, with a mean of 1.54 and a coefficient of variation of 0.227. Using the simplified expressions for ψ_r results in comparable values for $f_{su}/f_{s,calc}$, with a slightly higher mean of 1.56. The relatively higher overall mean obtained here is mainly due to the No. 11 bar specimens, which also had high T/T_h ratios based on descriptive equation. As discussed in Section 4.5, the specimens carried a much lower portion of the total applied force within the joint due to the close spacing between the upper compression member and the hooked bars, resulting in higher anchorage strength than if the geometry of the test specimens had been more realistic, such as the specimens tested at the University of Kansas. If only the No. 7 bars are considered, the mean is 1.27 using both full and simplified expressions for ψ_r , which is consistent with the values reported for the University of Kansas database. Although the specimen geometry was the same as that of the No. 11 bar specimens, the No. 7 bar specimens did not have high anchorage strengths or T/T_h ratios, likely due to bars yielding and high bar slip prior to failure, as explained in Section 4.5.

Table 6.12 Comparison of hooked bar specimens tested by Marques and Jirsa (1975) versus the proposed design equation, Eq. (6.17) using full and simplified expressions for ψ_r

Specimen ID	n	ℓ_{eh} in.	f_{cm} psi	d_b in.	s/d_b	$\frac{A_{th,ACI}}{A_{hs}}$	$\psi_r^{[1]}$	$\psi_r^{[2]}$	f_{su} ksi	$f_{su}/f_{s,calc}^{[1]}$	$f_{su}/f_{s,calc}^{[2]}$
J7-180-12-1-H	2	10.0	4350	0.88	6.1	0	1.00	1.00	61.0	1.09	1.09
J7-180-15-1-H	2	13.0	4000	0.88	6.1	0	1.00	1.00	87.0	1.22	1.22
J7-90-12-1-H	2	10.0	4150	0.88	6.1	0	1.00	1.00	62.0	1.12	1.12
J7-90-15-1-H	2	13.0	4600	0.88	6.1	0	1.00	1.00	91.0	1.23	1.23
J7-90-15-1-L	2	13.0	4800	0.88	6.1	0	1.00	1.00	97.0	1.30	1.30
J7-90-15-1-M	2	13.0	5050	0.88	6.1	0	1.00	1.00	100.0	1.32	1.32
J11-180-15-1-H	2	13.1	4400	1.41	3.4	0	1.43	1.43	45.0	1.77	1.77
J11-90-12-1-H	2	10.1	4600	1.41	3.4	0	1.43	1.43	42.0	2.12	2.12
J11-90-15-1-H	2	13.1	4900	1.41	3.4	0	1.43	1.43	48.0	1.84	1.84
J11-90-15-1-L	2	13.1	4750	1.41	3.4	0	1.43	1.43	52.0	2.01	2.01
J7-90-15-3a-H	2	13.0	3750	0.875	6.1	0.917	0.90	0.90	98.0	1.43	1.43
J7-90-1-3-H	2	13.0	4650	0.875	6.1	0.367	0.90	0.90	104.0	1.44	1.44
J11-90-15-3a-L	2	13.1	5000	1.41	3.4	0.564	0.90	0.90	69.0	1.90	1.90
J11-90-15-3-L	2	13.1	4850	1.41	3.4	0.282	0.90	1.04	62.0	1.72	1.98
									Mean	1.54	1.56
									CoV	0.227	0.235

^[1] Using the full expression for ψ_r , Eq. (6.14)

^[2] Using the simplified expressions for ψ_r , Eq. (6.15)

6.1.3.3 Pinc et al. (1977)

Table 6.13 presents the comparisons of the three No. 9 and No. 11 specimens tested by Pinc et al. (1977) with the proposed design equation.

As shown for the tests by Marques and Jirsa (1975) in Table 6.12, the proposed design equation provides very conservative results for the specimens tested by Pinc et al. (1977), with a mean $f_{su}/f_{s,calc}$ ratio of 1.73 using both full and simplified expressions for ψ_r . These specimens also had high T/T_h ratios based on descriptive equations, similar to and for the same reason as No. 11 bar specimens by Marques and Jirsa (1975), as discussed in the previous section and Section 4.5.

Table 6.13 Comparison of hooked bar specimens tested by Pinc et al. (1977) versus the proposed design equation, Eq. (6.17)

Specimen ID	n	ℓ_{eh}	f_{cm}	d_b	s/d_b	$\frac{A_{th,ACI}}{A_{hs}}$	$\Psi_r^{[1]}$	$\Psi_r^{[2]}$	f_{su}	$f_{su}/f_{s,calc}^{[1]}$	$f_{su}/f_{s,calc}^{[2]}$
		in.	psi	in.					ksi		
9-12	2	10.0	4700	1.130	4.5	0	1.24	1.24	47.0	1.49	1.49
11-15	2	13.1	5400	1.41	3.4	0	1.43	1.43	50.0	1.87	1.87
11-18	2	16.1	4700	1.41	3.4	0	1.43	1.43	58.0	1.83	1.83
									Mean	1.73	1.73
									CoV	0.122	0.122

^[1] Using the full expression for Ψ_r , Eq. (6.14)

^[2] Using the simplified expressions for Ψ_r , Eq. (6.15)

6.1.3.4 Hamad et al. (1993)

Hamad et al. (1993) tested both coated and uncoated hooked bars specimens. Table 6.14 presents the comparisons with the proposed design equation for four No. 7 and four No. 11 specimens with uncoated bars tested by Hamad et al. (1993).

Table 6.14 Comparison of hooked bar specimens tested by Hamad et al. (1993) versus the proposed design equation, Eq. (6.17)

Specimen ID	n	ℓ_{eh}	f_{cm}	d_b	s/d_b	$\frac{A_{th,ACI}}{A_{hs}}$	$\Psi_r^{[1]}$	$\Psi_r^{[2]}$	f_{su}	$f_{su}/f_{s,calc}^{[1]}$	$f_{su}/f_{s,calc}^{[2]}$
		in.	psi	in.					ksi		
7-90-U	2	10.0	2570	0.88	6.1	0	1.00	1.00	43.3	0.88	0.88
7-90-U*	2	10.0	5400	0.88	6.1	0	1.00	1.00	61.2	1.03	1.03
11-90-U	2	13.0	2570	1.41	3.4	0	1.43	1.30	30.8	1.40	1.27
11-90-U*	2	13.0	5400	1.41	3.4	0	1.43	1.30	48.1	1.81	1.65
11-180-U-HS	2	13.0	7200	1.41	3.4	0	1.43	1.30	37.7	1.32	1.20
11-90-U-HS	2	13.0	7200	1.41	3.4	0	1.43	1.30	47.3	1.66	1.51
11-90-U-T6	2	13.0	3700	1.41	3.4	0.212	1.00	1.09	46.0	1.34	1.45
7-180-U-T4	2	10.0	3900	0.88	6.1	0.550	0.90	0.90	57.7	0.95	0.95
11-90-U-T4	2	13.0	4230	1.41	3.4	0.353	0.90	0.95	53.3	1.34	1.42
7-90-U-SC ^[3]	2	10.0	4230	0.88	8.4	0	1.00	1.00	49.9	1.03	1.03
									Mean	1.26	1.30
									CoV	0.241	0.245

^[1] Using the full expression for Ψ_r , Eq. (6.14)

^[2] Using the simplified expressions for Ψ_r , Eq. (6.15)

^[3] Hooked bars outside column core, bar location Ψ_r of 1.15 applied

As shown in Table 6.14, $f_{su}/f_{s,calc}$ ratio for these specimens ranges from 0.88 to 1.81, with a mean of 1.26 and a coefficient of variation of 0.241 using the full expression for Ψ_r , and higher mean (1.30) using the simplified expressions. The mean values are consistent with those reported for the University of Kansas database.

6.1.3.5 Ramirez and Russell (2008)

Table 6.15 presents the comparisons of the No. 6 and No. 11 specimens tested by Ramirez and Russell (2008) with the proposed design equation.

Table 6.15 Comparison of hooked bar specimens tested by Ramirez and Russell (2008) versus the proposed design equation, Eq. (6.17)

Specimen ID	n	ℓ_{eh}	f_{cm}	d_b	s/d_b	$\frac{A_{th,ACI}}{A_{hs}}$	$\psi_r^{[1]}$	$\psi_r^{[2]}$	f_{su}	$f_{su}/f_{s,calc}^{[1]}$	$f_{su}/f_{s,calc}^{[2]}$
		in.	psi	in.		ksi					
I-1	2	6.5	8910	0.75	12.3	0	1.00	1.00	68.2	1.23	1.23
I-3	2	6.5	12460	0.75	12.3	0	1.00	1.00	68.2	1.13	1.13
I-5	2	6.5	12850	0.75	12.3	0	1.00	1.00	69.3	1.14	1.14
I-2	2	12.5	8910	1.41	6.1	0	1.00	1.00	56.4	1.36	1.36
I-2'	2	15.5	9540	1.41	6.1	0	1.00	1.00	67.3	1.29	1.29
I-4	2	12.5	12460	1.41	6.1	0	1.00	1.00	63.5	1.41	1.41
I-6	2	12.5	12850	1.41	6.1	0	1.00	1.00	73.1	1.61	1.61
III-13	2	6.5	13980	0.75	12.3	1.000	0.90	0.90	93.9	1.36	1.36
III-15	2	6.5	16350	0.75	12.3	1.000	0.90	0.90	87.5	1.22	1.22
III-14	2	12.5	13980	1.41	6.1	0.282	0.90	1.00	67.3	1.31	1.45
III-16	2	12.5	16500	1.41	6.1	0.282	0.90	1.00	76.9	1.44	1.59
									Mean	1.32	1.35
									CoV	0.107	0.122

^[1] Using the full expression for ψ_r , Eq. (6.14)

^[2] Using the simplified expressions for ψ_r , Eq. (6.15)

As shown in Table 6.15, for the 11 specimens tested by Ramirez and Russell (2008), the $f_{su}/f_{s,calc}$ ratio ranges from 1.13 and 1.61 with a mean of 1.32 and a coefficient of variation of 0.107 using the full expression for ψ_r , and a slightly higher mean and coefficient of variation using the simplified expressions (1.35 and 0.122, respectively). These numbers are similar to the mean and coefficient of variation values reported for the University of Kansas database in Section 6.1.3.1.

6.1.3.6 Lee and Park (2010)

Table 6.16 presents the comparisons of the three No. 7 specimens tested by Lee and Park (2010) with the proposed design equation. As shown in the table, the three specimens tested by Lee and Park (2010) had a mean $f_{su}/f_{s,calc}$ ratio of 1.00 using both the full and simplified expressions for ψ_r , the lowest among all studies reported.

Table 6.16 Comparison of hooked bar specimens tested by Lee and Park (2010) versus the proposed design equation, Eq. (6.17)

Specimen ID	n	ℓ_{eh}	f_{cm}	d_b	s/d_b	$\frac{A_{th,ACI}}{A_{hs}}$	$\psi_r^{[1]}$	$\psi_r^{[2]}$	f_{su}	$f_{su}/f_{s,calc}^{[1]}$	$f_{su}/f_{s,calc}^{[2]}$
		in.	psi	in.					ksi		
H1	2	18.7	4450	0.88	9.0	0	1.00	1.00	98.7	0.94	0.93
H2	2	11.9	8270	0.88	9.0	0	1.00	1.00	88.0	1.12	1.12
H3	2	15.0	4450	0.88	9.0	0.733	0.90	0.90	89.6	0.95	0.95
									Mean	1.00	1.00
									CoV	0.121	0.102

^[1] Using the full expression for ψ_r , Eq. (6.14)

^[2] Using the simplified expressions for ψ_r , Eq. (6.15)

6.1.3.7 Chun et al. (2017b)

Table 6.17 presents the comparisons with the proposed design equation for the 26 No. 14 and No. 18 bar specimens tested by Chun et al. (2017). As discussed in Chapter 1, these specimens were designed to force a side-blowout failure. The hooked bars were placed outside the column core in all these specimens, therefore $\psi_o = 1.15$ applies. Also, the majority of specimens had a unconventional reinforcement layout with the hooked bars outside the confining ties, as described in Section 4.4.1 and Figure 4.9a. Therefore, although all specimens had $A_{th}/A_{hs} > 0.6$, ties are not counted for the specimens with hooks outside the ties.

Table 6.17 Comparison of hooked bar specimens tested by Chun et al. (2017b) versus the proposed design equation, Eq. (6.17)

Specimen ID ^[1]	n	ℓ_{eh}	f_{cm}	d_b	s/d_b	$\frac{A_{th,ACI}}{A_{hs}}$	$\psi_r^{[2]}$	$\psi_r^{[3]}$	f_{su}	$f_{su}/f_{s,calc}^{[2]}$	$f_{su}/f_{s,calc}^{[3]}$
		in.	psi	in.					ksi		
D43-L10-C1-S42*	2	16.9	6440	1.693	9.6	0	1.00	1.00	51.3	1.50	1.50
D43-L10-C1-S42-C**	2	16.9	6950	1.693	9.6	1.173	0.70	0.80	75.1	1.51	1.73
D43-L10-C1-S70*	2	16.9	10010	1.693	9.6	0	1.00	1.00	54.8	1.44	1.44
D43-L10-C2-S42*	2	16.9	7020	1.693	9.6	0	1.00	1.00	58.5	1.68	1.68
D43-L13-C1-S42*	2	22.0	7020	1.693	9.6	0	1.00	1.00	64.4	1.42	1.42
D43-L13-C1-S42-C**	2	22.0	7020	1.693	9.6	0.978	0.70	0.80	75.9	1.17	1.34
D43-L13-C1-S70*	2	22.0	10600	1.693	9.6	0	1.00	1.00	63.3	1.26	1.26
D43-L13-C2-S42*	2	22.0	7020	1.693	9.6	0	1.00	1.00	68.7	1.51	1.51
D43-L16-C1-S42*	2	27.1	7020	1.693	9.6	0	1.00	1.00	72.6	1.30	1.30
D43-L16-C1-S42-C**	2	27.1	7020	1.693	9.6	0.978	0.70	0.80	78.9	0.99	1.13
D43-L16-C1-S70*	2	27.1	10010	1.693	9.6	0	1.00	1.00	76.8	1.26	1.26
D43-L16-C2-S42*	2	27.1	7020	1.693	9.6	0	1.00	1.00	80.9	1.45	1.45
D43-L20-C1-S42*	2	33.9	7020	1.693	9.6	0	1.00	1.00	76.5	1.10	1.10
D57-L10-C1-S42-a*	2	22.6	5450	2.257	7.2	0	1.00	1.00	36.8	1.30	1.30
D57-L10-C1-S42-b*	2	22.6	6150	2.257	7.2	0	1.00	1.00	37.6	1.29	1.29
D57-L10-C1-S42-C**	2	22.6	5450	2.257	7.2	0.660	0.70	0.80	55.8	1.38	1.57

D57-L10-C2-S42*	2	22.6	5450	2.257	7.2	0	1.00	1.00	53.7	1.89	1.89
D57-L13-C1-S42-a*	2	29.3	5450	2.257	7.2	0	1.00	1.00	59.1	1.60	1.60
D57-L13-C1-S42-b*	2	29.3	6150	2.257	7.2	0	1.00	1.00	58.2	1.53	1.53
D57-L13-C1-S42-C**	2	29.3	5450	2.257	7.2	0.660	0.70	0.80	63.6	1.21	1.38
D57-L13-C2-S42*	2	29.3	5450	2.257	7.2	0	1.00	1.00	68.4	1.85	1.85
D57-L16-C1-S42-a	2	36.1	5450	2.257	7.2	0	1.00	1.00	63.5	1.40	1.40
D57-L16-C1-S42-b*	2	36.1	6150	2.257	7.2	0	1.00	1.00	71.0	1.52	1.52
D57-L16-C1-S42-C**	2	36.1	5450	2.257	7.2	0.660	0.70	0.80	69.9	1.08	1.23
D57-L16-C2-S42*	2	36.1	6530	2.257	7.2	0	1.00	1.00	79.7	1.68	1.68
D57-L20-C1-S42*	2	45.1	6530	2.257	7.2	0	1.00	1.00	82.1	1.38	1.38
									Mean	1.41	1.45
									CoV	0.158	0.141

* Specimens with hooks placed outside the confining ties (Figure 4.9.a), ties not counted towards ψ_r ($A_{th}/A_{hs} = 0$)

** Specimens with hooks placed inside the confining ties (Figure 4.9.b), ties counted towards ψ_r

[1] Bar location factor ψ_o of 1.15 applied to all specimens

[2] Using the full expression for ψ_r , Eq. (6.14)

[3] Using the simplified expressions for ψ_r , Eq. (6.15)

As shown in Table 6.17, the $f_{su}/f_{s,calc}$ ratio using both the full expressions for ψ_r ranges from 0.99 to 1.89 with a mean of 1.41 and a coefficient of variation of 0.158 for the No. 14 and No. 18 bar specimens tested by Chun et al. (2017b). A higher mean of 1.45 is obtained using the simplified expression for ψ_r . These values are similar to the mean values obtained for No. 14 and No. 18 bar specimens tested in this study (1.42 and 1.47, respectively, as given in Table 6.11).

A summary of the statistical parameters of $f_{su}/f_{s,calc}$ ratio for specimens tested outside the University of Kansas using the full expression for ψ_r is presented in Table 6.18.

Table 6.18 Statistical parameters of $f_{su}/f_{s,calc}$ for hooked bar specimens tested outside University of Kansas, based on the proposed design equation Eq. (6.17) and using the full expression for ψ_r , Eq. (6.14)

Bar size	All	No. 6	No. 7	No. 9	No. 11	No. 14	No. 18
No. of specimens	71	5	17	1	22	13	13
Max	2.12	1.36	1.44	1.49	2.12	1.68	1.89
Min	0.88	1.13	0.88	1.49	1.20	0.99	1.08
Mean	1.39	1.22	1.16	1.49	1.59	1.35	1.47
STDEV	0.275	0.093	0.180	N/A	0.273	0.194	0.242
COV	0.198	0.076	0.155	N/A	0.172	0.143	0.164
No. with $f_{su}/f_{s,calc} < 1.0$	4	0	3	0	0	1	0

As shown in Table 6.18, for the 70 hooked bar specimens tested outside the University of Kansas, $f_{su}/f_{s,calc}$ using the full expression for ψ_r ranges from 0.88 to 2.12 with a mean of 1.40 and a coefficient of variation of 0.195. Using the simplified expressions for ψ_r give similar results, with a slightly higher overall mean and lower coefficient of variation (1.42 and 0.195, respectively), and a higher mean No. 11 through No. 18 bar specimens (1.63, 1.39, and 1.51 for No. 11, No. 14, and No. 18 bar specimens, respectively). The proposed design equation performs adequately, in line with the values previously reported for comparisons with the University of Kansas database. The exception, the mean of 1.60 for the No. 11 bar specimens, which is due to the specimens tested by Marques and Jirsa (1975) and Pinc et al. (1977). As discussed before, those specimens had relatively high anchorage strength because of the use of specimens with a geometry not representing that in reinforced concrete frame structures for which a reduced load was carried within the joint, resulting in a higher anchorage strength.

6.2 HEADED BARS

6.2.1 Simplified Descriptive Equations

To simplify the descriptive equations, the approach used by Sperry et al. (2015b) for hooked bars and Shao et al. (2016) for headed bars is followed. The specimens used are the same as those used to develop the descriptive equations, Eq. (5.5) and (5.7), presented in detail in Tables C2 to C5 in Section C3 of Appendix C. The process starts with the descriptive equation for widely-spaced headed bars (center-to-center spacing $\geq 8d_b$) without parallel ties, Eq. (5.4), and repeated here.

$$T_c = 1296 f_{cm}^{0.207} \ell_{eh}^{0.941} d_b^{0.498} \quad (6.18)$$

where T_c is the anchorage strength of headed bars without parallel ties (lb), f_{cm} is concrete compressive strength (psi), ℓ_{eh} is embedment length (in.), and d_b is bar diameter (in.). To simplify the equation, the powers of f_{cm} , ℓ_{eh} , and d_b is increased to 0.25, 1.0, and 0.5, respectively. Then, using the same iterative analysis described in Section 5.3, a new constant is found so that the mean test-to-calculated ratio T/T_c equals 1.0, giving

$$T_c = 764 f_{cm}^{0.25} \ell_{eh} d_b^{0.5} \quad (6.19)$$

To account for the effect of close bar spacing (center-to-center spacing $< 8d_b$), the procedure used in Section 5.3.2 is followed and the values of T/T_c are plotted versus s/d_b , as shown in Figure 6.5, with T_c being calculated based on Eq. (6.19).

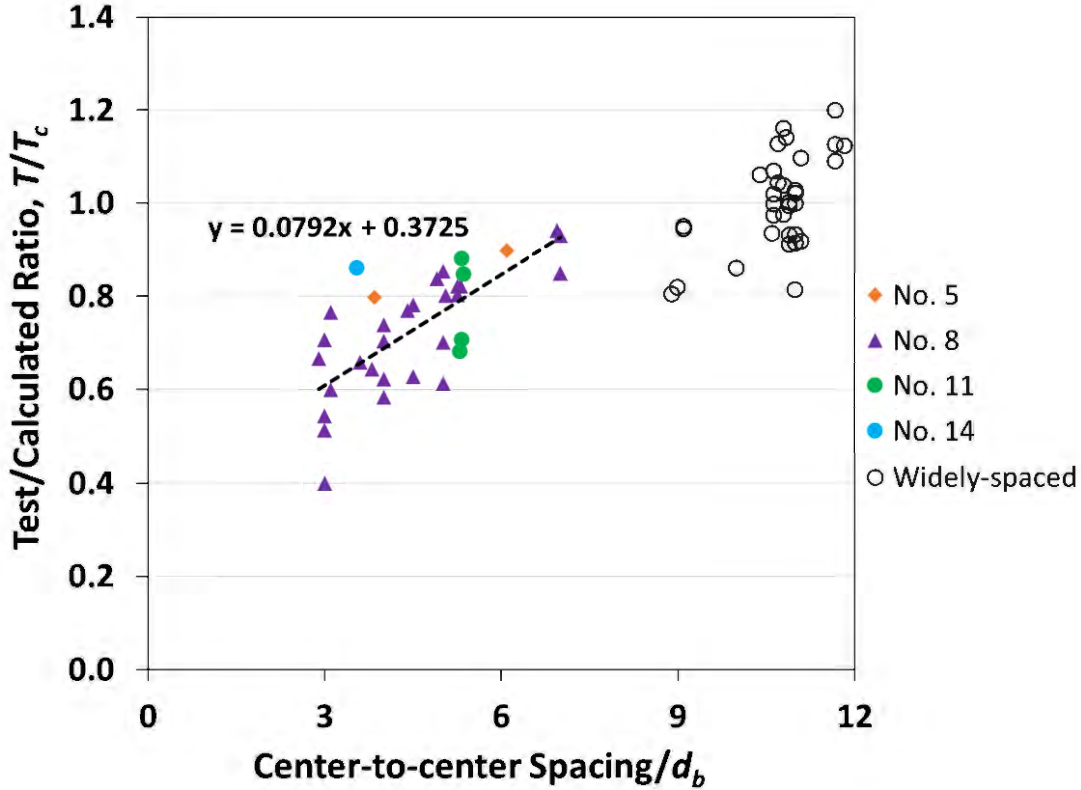


Figure 6.5 Test-to-calculated bar force at failure T/T_c based on Eq. (6.19) versus ratio of center-to-center spacing to bar diameter s/d_b for widely- and closely-spaced headed bars without parallel ties

Using the linear trendline equation shown in Figure 6.5, the simplified descriptive equation for widely- and closely-spaced headed bars without parallel ties becomes

$$T_h = \left(764 f_{cm}^{0.25} \ell_{eh} d_b^{0.5} \right) \left(0.0792 \frac{s}{d_b} + 0.3725 \right) \quad (6.20)$$

where $\left(0.0792 \frac{s}{d_b} + 0.3725 \right) \leq 1.0$, s is the center-to-center spacing of the bars (in.). The statistical parameters of T/T_c for all specimens without parallel ties are given in Table 6.19.

Table 6.19 Statistical parameters of T/T_c ratio based on simplified descriptive equation, Eq. (6.20), for headed bar specimens with widely- and closely-spaced bars without parallel ties used to develop descriptive equations, Eq. (5.5) and (5.7)

Bar size	All	No. 5	No. 8	No. 11	No. 14	No. 18
No. of specimens	68	6	48	11	3	0
Max	1.32	1.20	1.24	1.14	1.32	-
Min	0.66	1.05	0.66	0.81	1.00	-
Mean	1.00	1.13	0.98	1.00	1.11	-
STDEV	0.118	0.055	0.109	0.120	0.179	-
CoV	0.118	0.048	0.112	0.121	0.161	-

As shown in Table 6.19, the mean value of T/T_c for headed bar specimens without parallel ties using simplified descriptive equations is 1.00, with a coefficient of variation of 0.118. The T/T_c ratios are compared as a function of concrete compressive strength in Figure 6.6.

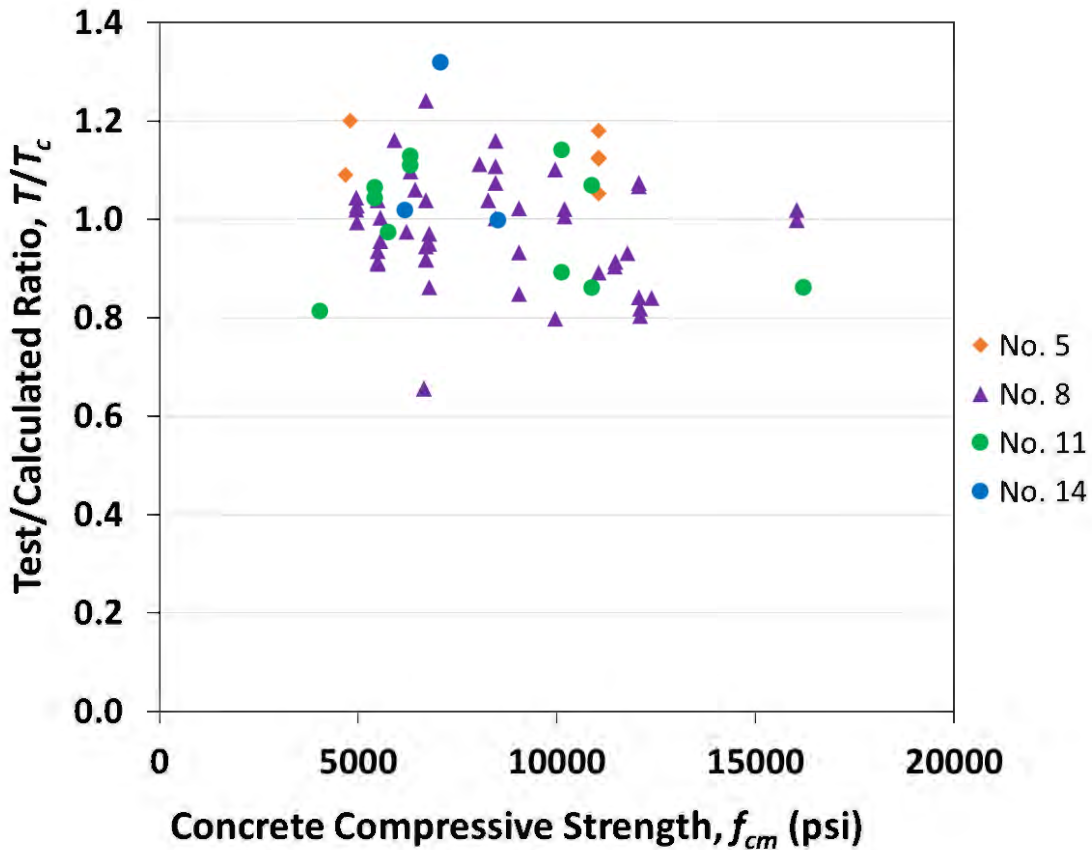


Figure 6.6 Ratio of test-to-calculated bar force at failure T/T_c based on simplified descriptive equation, Eq. (6.20), versus concrete compressive strength f_{cm} for headed bar specimens with widely- and closely-spaced bars without parallel ties used to develop descriptive equations, Eq. (5.5) and (5.7)

As shown in Figure 6.6, T/T_c decreases slightly as the concrete compressive strength increases, due to the small overestimation of the effect of concrete strength by the 0.25 power used in Eq. (6.20) compared with 0.207 in the original descriptive equation, Eq. (6.18).

The original descriptive equation for specimens with parallel ties is given below:

$$T_h = T_c + T_s = 1296 f_{cm}^{0.207} \ell_{eh}^{0.941} d_b^{0.498} + 49,402 \left(\frac{A_t}{n} \right) d_b^{0.11} \quad (6.21)$$

where A_t is the total area of tie legs within $8d_b$ from the top of the headed bars for No. 3 through No. 8 bars and $10d_b$ for No. 11 and larger bars, and n is the number of bars. The first term in Eq. (6.21), T_c , is already simplified and given in Eq. (6.19). Using Eq. (6.19), the second term in Eq. (6.21), T_s , can be simplified by changing the power of d_b to 0.1 and finding a new constant to replace 49,402 so that the mean T/T_h in specimens with widely-spaced bars with parallel ties is 1.0. The resulting equation is given below in Eq. (6.22).

$$T_h = 764 f_{cm}^{0.25} \ell_{eh} d_b^{0.5} + 41,150 \left(\frac{A_t}{n} \right) d_b^{0.1} \quad (6.22)$$

Using Eq. (6.22), T/T_h versus s/d_b for specimens with parallel ties with both widely- and closely-spaced bars and parallel ties is shown in Figure 6.7.

To account for the effect of close bar spacing, the linear trendline equation shown in Figure 6.8 is multiplied by Eq. (6.22) to give Eq. (6.23):

$$T_h = \left(764 f_{cm}^{0.25} \ell_{eh} d_b^{0.5} + 41,150 \left(\frac{A_t}{n} \right) d_b^{0.1} \right) \left(0.0559 \frac{s}{d_b} + 0.5743 \right) \quad (6.23)$$

where $\left(0.0559 \frac{s}{d_b} + 0.5743 \right) \leq 1.0$.

The statistical parameters of T/T_h for all specimens with parallel ties are given in Table 6.20.

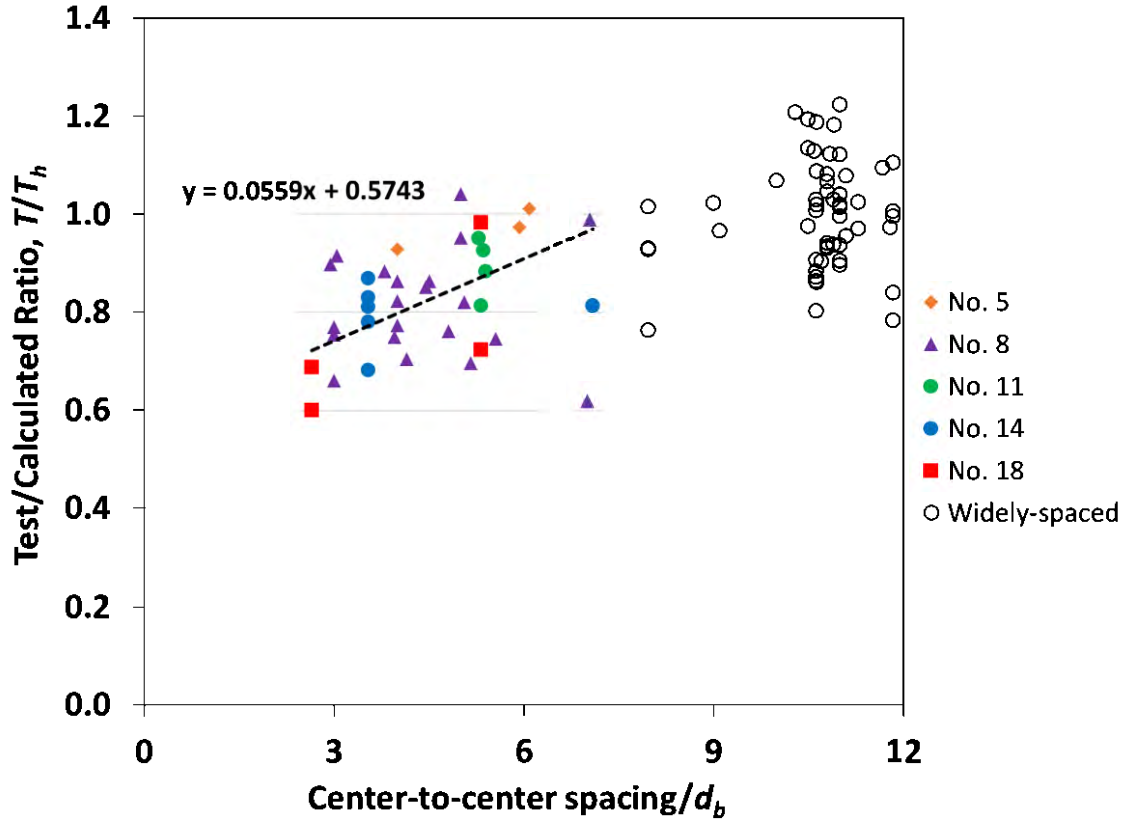


Figure 6.7 Test-to-calculated bar force at failure T/T_h based on Eq. (6.22) versus ratio of center-to-center spacing to bar diameter s/d_b for widely- and closely-spaced headed bars with parallel ties used to develop descriptive equations, Eq. (5.5) and (5.7)

Table 6.20 Statistical parameters of T/T_h ratio based on simplified descriptive equation, Eq. (6.23), for headed bar specimens with widely- and closely-spaced bars with parallel ties used to develop descriptive equations, Eq. (5.5) and (5.7)

Bar size	All	No. 5	No. 8	No. 11	No. 14	No. 18
No. of specimens	96	9	54	12	13	8
Max	1.26	1.16	1.26	1.19	1.12	1.13
Min	0.76	0.78	0.83	0.86	0.80	0.76
Mean	1.00	1.02	1.01	1.04	0.95	0.92
STDEV	0.106	0.129	0.095	0.104	0.103	0.116
CoV	0.106	0.127	0.094	0.099	0.109	0.126

As shown in Table 6.20, the test-to-calculated ratio T/T_h using the simplified descriptive equations for specimens with parallel ties ranges from 0.76 to 1.26, with a mean value of 1.00 and a coefficient of variation of 0.106. The variation of T/T_h using Eq. (6.23) versus concrete compressive strength can be evaluated, as plotted in Figure 6.8.

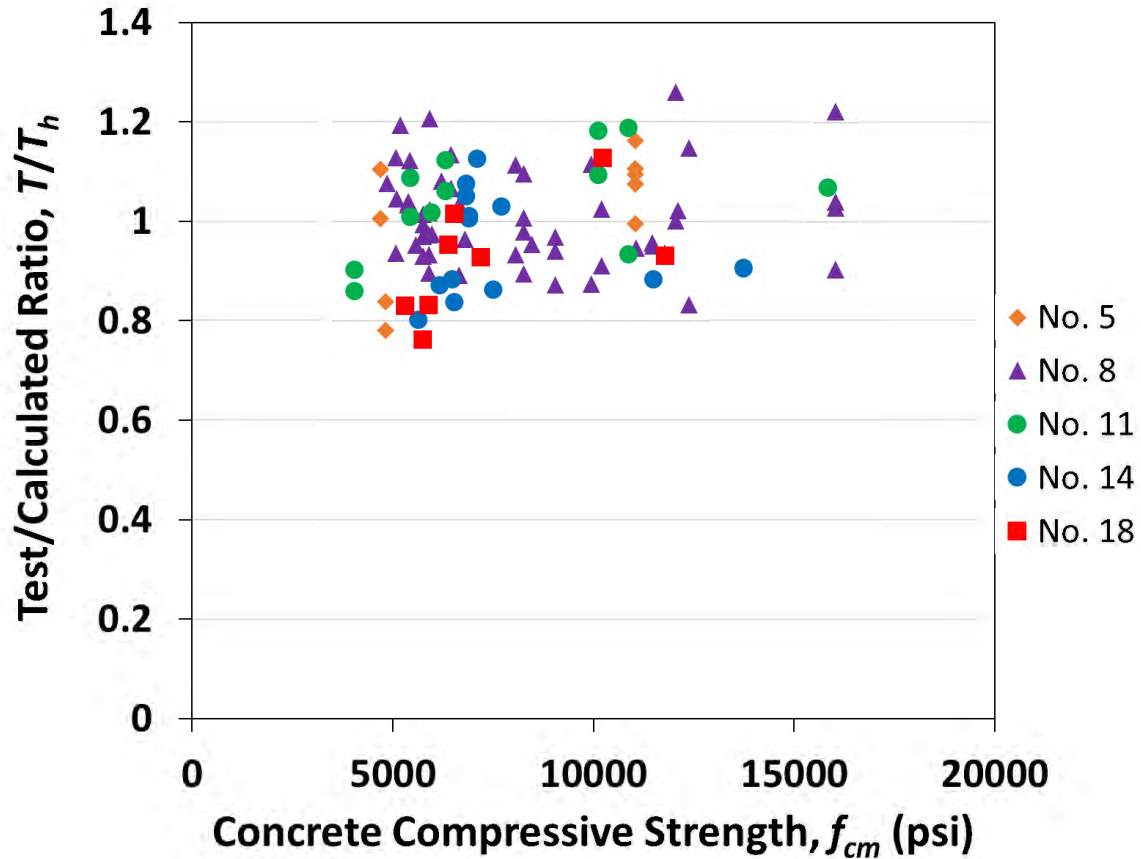


Figure 6.8 Ratio of test-to-calculated bar force at failure T/T_h based on simplified descriptive equation, Eq. (6.23), versus concrete compressive strength f_{cm} for headed bar specimens with widely- and closely-spaced bars with parallel ties used to develop descriptive equations, Eq. (5.5) and (5.7)

Figure 6.8 shows a very slight positive trend of T/T_c with respect to concrete compressive strength, but overall the 0.25 power for f_{cm} in Eq. (6.6) adequately captures the effect of concrete compressive strength.

In summary, the simplified descriptive equations are presented in Eq. (6.20) and (6.23) for headed bar specimens without and with parallel ties, respectively. For all 164 headed bar specimens, the statistical parameters of T/T_h using Eq. (6.20) and (6.23) are tabulated in Table 6.21.

Table 6.21 Statistical parameters of T/T_h ratio based on simplified descriptive equation, Eq. (6.20) and (6.23), for all headed bar specimens used to develop descriptive equations, Eq. (5.5) and (5.7)

Bar size	All	No. 5	No. 8	No. 11	No. 14	No. 18
No. of specimens	164	15	102	23	16	8
Max	1.32	1.20	1.26	1.19	1.32	1.13
Min	0.66	0.78	0.66	0.81	0.80	0.76
Mean	1.00	1.06	1.00	1.02	0.98	0.92
STDEV	0.111	0.117	0.103	0.112	0.131	0.116
CoV	0.111	0.110	0.103	0.110	0.133	0.126

As presented in Table 6.21, the simplified descriptive equations result in a mean value of T/T_h of 1.00 for all headed bar specimens, with a coefficient of variation of 0.111. For the No. 18 bar specimens, the mean dropped to 0.92 in simplified equations, similar to the mean obtained using the descriptive equations by Shao et al. (2016). The procedure for converting the simplified equations to a design equation for development length is discussed next.

6.2.2 Design Equation for Development Length

The simplified descriptive equations developed in the previous section can be used to derive a design expression for development length. To start, the equation for widely-spaced bars without parallel ties, Eq. (6.19), is solved for embedment length, ℓ_{eh} and T_h is replaced by $A_b f_s = \pi f_s d_b^2 / 4$. The resulting expression is

$$\ell_{eh} = 0.001 \frac{f_s \Psi_{pr}}{f_{cm}^{0.25}} d_b^{1.5} \quad (6.24)$$

where $\Psi_{pr} = 1 - \frac{41,150}{f_s} \frac{A_{tt}}{A_{hs}} d_b^{0.1}$ is the modification factor for the contribution of parallel tie reinforcement on the anchorage strength, f_s is the bar stress at failure (psi), A_{tt} is the total area of tie legs within $8d_b$ from the top of the headed bars for No. 3 through No. 8 bars and $10d_b$ for No. 11 and larger bars (in.^2), A_{hs} is the total area of headed bars (in.^2), d_b is the bar diameter (in.), and f_{cm} is the measured concrete compressive strength (psi).

To be used for design, Eq. (6.24) is modified by replacing embedment length ℓ_{eh} by development length ℓ_{dt} , bar stress at failure f_s by yield strength f_y , and measured concrete strength f_{cm} by the specified compressive strength f'_c . The resulting equation is:

$$\ell_{dt} = 0.001 \frac{f_y \Psi_{pr}}{f_c^{0.25}} d_b^{1.5} \quad (6.25)$$

where $\Psi_{pr} = 1 - \frac{41,150}{f_y} \frac{A_{tt}}{A_{hs}} d_b^{0.1}$ accounts for the effect of parallel ties. As discussed in Section 5.3.3, an upper limit of 0.4 on A_{tt}/A_{hs} was chosen when developing the new descriptive equations for headed bars and was shown to provide reasonable calculated failure loads. Therefore, the same upper limit is retained and used here for the proposed design equation.

6.2.2.1 Modification Factor for Parallel Tie Reinforcement and Bar Spacing

In this section, an expression is developed to account for the contribution of parallel tie reinforcement and the effect of bar spacing. As discussed in Chapter 1, as for hooked bars, the design provisions for headed bars in ACI 318-19 limit the flexibility in design by providing a binary choice between 1.0 and 1.6 for the parallel tie reinforcement factor, Ψ_p . If $A_{tt}/A_{hs} \geq 0.3$ or $s \geq 6d_b$ per ACI 318-19 Table 25.4.4.3 are met, Ψ_p is 1.0, otherwise, it jumps to 1.6. This means that designers cannot take advantage of the intermediate values of A_{tt}/A_{hs} and s/d_b . Developing an alternative expression for Ψ_p that varies as a function of A_{tt}/A_{hs} and s/d_b will result in shorter development lengths in cases where one of the two requirements on parallel ties or headed bar are not satisfied.

The effect of bar spacing can be accounted for using descriptive equations for headed bars without and with parallel ties. For headed bars without parallel ties, the linear trendline equation in Figure 6.5 reveals that for $s/d_b = 2$, the T/T_h is 0.53 which, conservatively, can be taken as 0.5. Similarly, for specimens with parallel ties and as shown in Figure 6.7, T/T_h is 0.69 for $s/d_b = 2$, where T_h is the strength for widely-space bars, which is taken conservatively as 0.6. Taking T/T_h as 1.0 when $s/d_b = 8$ for both cases and using linear interpolation, the effects of bar spacing and parallel ties for headed bars without and with parallel tie reinforcement can be expressed, respectively as

$$\Psi_{p1} = \left(\frac{7}{3} - \frac{1}{6} \frac{s}{d_b} \right) \quad (6.26)$$

$$\Psi_{p2} = \left(\frac{17}{9} - \frac{1}{9} \frac{s}{d_b} \right) \left(1 - \frac{41,150}{f_y} \frac{A_{tt}}{A_{hs}} d_b^{0.1} \right) \quad (6.27)$$

For headed bars with parallel ties, the bar spacing expression is multiplied by the parallel tie expression, ψ_{pr} , given in Eq. (6.10). To simplify design, and as used for hooked bars, a single expression for ψ_p as a function of A_{tt}/A_{hs} and s/d_b is needed. The general form of the expression is

$$\psi_p = A + B \frac{A_{tt}}{A_{hs}} + C \frac{s}{d_b} + D \frac{A_{tt}}{A_{hs}} \frac{s}{d_b} \quad (6.28)$$

To find the constants A, B, C, and D, a bilinear interpolation needs to be conducted. The procedure is the same as what used to develop an expression for confining reinforcement and bar spacing factor for hooked bars, ψ_r , as described in detail in Section 6.2.1. The only difference is the range of values used for s/d_b , which is 3 to 8 here for headed bars, rather than 2 to 6. The lower bound for s/d_b was chosen to be 3, the minimum value currently permitted in ACI 318-19. The coefficients A, B, and C and the intercept D are found through performing regression analysis using the “Data Analysis” tool in Excel. The resulting expression for ψ_p is

$$\begin{aligned} \psi_p &= 2 - 2.5 \frac{A_{tt}}{A_{hs}} - \frac{1}{8} \frac{s}{d_b} + \frac{1}{6} \frac{A_{tt}}{A_{hs}} \frac{s}{d_b} \\ &\geq 0.85 \text{ for No. 11 and smaller bars and} \\ &\geq 0.95 \text{ for No. 14 and No. 18 bars} \end{aligned} \quad (6.29)$$

where $3 \leq \frac{s}{d_b} \leq 8$ and $\frac{A_{tt}}{A_{hs}} \leq 0.4$. The values of ψ_p obtained using Eq. (6.29) are limited to 0.85 for No. 11 and smaller and 0.95 for No. 14 and No. 18 bars to avoid overprediction of anchorage strength and to ensure that no more than 5% of specimens have a test-to-calculated ratio < 1.0 . The expression for ψ_p has the same form as the expression for ψ_r for hooked bars, but with a difference in constants and the limit for No. 14 and No. 18 bars. For hooked bars, the limit was chosen as 0.7, whereas here the limit is 0.95. For $s/d_b = 3$, ψ_p varies from 0.85 or 0.95 to 1.625 depending on the ratio of the area of the parallel ties to the area of the headed bars A_{tt}/A_{hs} . Similarly, when bars are widely-spaced ($s/d_b \geq 8.0$), ψ_p ranges from 0.85 or 0.95 to 1.0.

Alternatively, and since an expression in a form similar to Eq. (6.29) has not been considered simple enough by ACI Committee 318, a conservative simplification of the ψ_p expression is worthy of consideration that consists of two terms based Eq. (6.15) for the cases of $A_{tt}/A_{hs} = 0$ and $s/d_b = 3$, respectively.

$$\psi_p = \min \left\{ 2 - \frac{1}{8} \frac{s}{d_b}, 1.6 - 2 \frac{A_{tr}}{A_{hs}} \right\}$$

$$\geq 0.85 \text{ for No. 11 and smaller bars and}$$

$$\geq 0.95 \text{ for No. 14 and No. 18 bars}$$
(6.30)

Although A_{tr} cannot exceed $0.4A_{hs}$ when calculating ψ_p using either the full or simplified expression, as demonstrated in Section 5.5.1, No. 14 and No. 18 headed bars need at least $0.5A_{hs}$ to address the joint shear demand and prevent a shear failure in cases in beam-column joints. Also, as established in Section 5.5.8, when headed bars are placed outside the column core and the parallel ties, ties should not be counted as contributing to anchorage strength. In such cases, $A_{tr}/A_{hs} = 0$ when calculating ψ_p .

6.2.2.2 *Modification Factor for Bar Coating*

For the modification factor for coated bars, ψ_e , given in Table 25.4.4.3 of ACI 318-19 are retained. For epoxy-coated or zinc and epoxy dual-coated bars, $\psi_e = 1.2$. For uncoated or zinc-coated bars, $\psi_e = 1.0$.

6.2.2.3 *Modification Factor for Bar Location*

In Table 25.4.4.3 of ACI 318-19, for headed bars terminating inside the column core with a side cover to the bar of at least 2.5 in., or terminating in supporting members with a side cover of at least $6d_b$, $\psi_o = 1.0$. In all other cases, $\psi_o = 1.25$. The value of 1.25 is based on the observations by Sperry et al. (2015a) that, in general, specimens with hooked bars placed outside the column core had a lower anchorage strength than those with bars inside column core. Therefore, conservatively, a strength modification factor of 0.8 was suggested, and later retained by Shao et al. (2016) for headed bars ($1/0.8 = 1.25$).

However, as the re-analysis of the hooked bar specimens in Section 4.4.1 and later analysis of the headed bar specimens tested by Chun et al. (2017a) and Sim and Chun (2022a, 2022b) in Section 5.5.8 reveal, the bar location factor can safely be reduced to 1.15 for headed as well as bars. Therefore, the value of 1.15 is used here as well.

6.2.2.4 Strength-Reduction Factor

Incorporating the three modification factors, ψ_e , ψ_p , and ψ_o , to represent the effects of bar coating, parallel tie reinforcement and bar spacing, and bar location into Eq. (6.10), along with strength-reduction factor ϕ gives

$$\ell_{dt} = \frac{0.001}{\phi} \frac{f_y \psi_e \psi_p \psi_o}{f_c^{0.25}} d_b^{1.5} \quad (6.30)$$

In this study, the value of ϕ is selected so that 5% or less of all beam-column test specimens used to develop the descriptive equations, Eq. (5.5) and (5.7), have a test-to-calculated ratio of below 1.0. An analysis of the data using Eq. (6.30) shows that a value of $\phi = 0.78$ results in 3.05% of the specimens having a test-to-calculated ratio < 1.0 . For developing reinforcement, the strength-reduction factor has, by tradition, been incorporated in the expression for ℓ_{dt} . Doing so for Eq. (6.30) and recognizing that $0.001/0.78 = 1/780$ gives

$$\ell_{dt} = \frac{f_y \psi_e \psi_p \psi_o}{780 f_c^{0.25}} d_b^{1.5} \quad (6.31)$$

The format of Eq. (6.31) is similar to those previously proposed at the University of Kansas (Shao et al. 2016, Ghimire et al. 2018, Ghimire et al. 2019b). Compared with the design equation in Section 25.4.4.2 of ACI 318-19, Eq. (6.31) provides more flexibility for designers as the binary choice of 1.0 and 1.6 for the parallel tie and bar spacing factor, ψ_p , is replaced by an expression that varies as a function of A_{tt}/A_{hs} and s/d_b . Also, with the proposed equation, the modification factor for concrete strength (ψ_c in ACI 318-19) is no longer needed, as $f_c^{0.25}$ provides a good representation of the contribution of concrete compressive strength to anchorage of headed bars and is applicable up to 16,000 psi, as later discussed further in Section 6.3.1. Finally, given the range of bar stresses at failure (up to 150,000 psi) available in the database used to develop Eq. (6.31), the proposed design equation can be applied to high-strength headed bars with specified yield strengths up to 120,000 psi. Table 6.22 summarizes the modification factors and their values incorporated in the proposed design equation.

Table 6.22 Modification factors for the proposed design equation for development of headed bars, Eq. (6.31)

Modification Factor	Condition	Value ^{[1][2][3][4]}
---------------------	-----------	-------------------------------

Epoxy coating, ψ_e	Epoxy- or zinc and epoxy dual-coated bars	1.2
	Uncoated or zinc-coated (galvanized) bars	1.0
Parallel tie reinforcement and bar spacing, ψ_p ^{[5][6]}	For No. 11 and smaller bars	$2 - 2.5 \frac{A_{tt}}{A_{hs}} - \frac{1}{8} \frac{s}{d_b} + \frac{1}{6} \frac{A_{tt}}{A_{hs}} \frac{s}{d_b} \geq 0.85$ <p style="text-align: center;">or, smaller of</p> $\left\{ 2 - \frac{1}{8} \frac{s}{d_b}, 1.6 - 2 \frac{A_{tt}}{A_{hs}} \right\} \geq 0.85$
	For No. 14 and No. 18 bars ^[7]	$2 - 2.5 \frac{A_{tt}}{A_{hs}} - \frac{1}{8} \frac{s}{d_b} + \frac{1}{6} \frac{A_{tt}}{A_{hs}} \frac{s}{d_b} \geq 0.95$ <p style="text-align: center;">or, smaller of</p> $\left\{ 2 - \frac{1}{8} \frac{s}{d_b}, 1.6 - 2 \frac{A_{tt}}{A_{hs}} \right\} \geq 0.95$
Bar location, ψ_o	(1) Bars terminating inside column core with a minimum side cover to bar of 2.5 in., or (2) Bars terminating in supporting members with a side cover of at least $6d_b$	1.0
	Other	1.15

^[1] A_{tt} : Total cross-sectional area of tie legs within $8d_b$ from the top of the headed bars for No. 3 through No. 8 bars and $10d_b$ for No. 11 and larger bars, in.²

^[2] A_{hs} : Total cross-sectional area of the headed bars being developed, in.²

^[3] s : Minimum center-to-center spacing of headed bars, in.

^[4] d_b : Nominal diameter of headed bar, in.

^[5] When calculating ψ_p , A_{tt}/A_{hs} shall not exceed 0.4 and s/d_b shall not exceed 8

^[6] When bars are placed outside both the column core and the parallel ties, $A_{tt}/A_{hs} = 0$ when calculating ψ_p

^[7] Larger bars need at least $A_{tt} = 0.5A_{hs}$ to address the joint shear demand and prevent a shear failure

6.2.3 Evaluating Proposed Design Equation

In this section, the proposed design equation for the development length of headed bars, Eq. (6.31), is compared with the results in the beam-column joint database. The database includes the beam-column joint tests at the University of Kansas by Shao et al. (2016), plus tests available in literature including Bashandy (1996) at the University of Texas at Austin and Chun et al. (2017), Chun and Lee (2019), and Sim and Chun (2022a, 2022b) at South Korea. For the comparison, the

bar stress at failure measured in the test, f_{su} , is compared with the bar stress calculated based on Eq. (6.16), $f_{s,calc}$. To find $f_{s,calc}$, Eq. (6.16) is solved for yield strength, f_y , which is replaced by $f_{s,calc}$, specified concrete compressive strength f'_c is replaced by the measured concrete strength f_{cm} , and development length ℓ_{dt} is replaced by measured embedment length ℓ_{eh} . The resulting equation is

$$f_{s,calc} = \frac{780 \ell_{eh} f_{cm}^{0.25}}{\Psi_e \Psi_p \Psi_o d_b^{1.5}} \quad (6.32)$$

6.2.3.1 University of Kansas Database

In this section, the stresses calculated based on the proposed design equation, Eq. (6.32), are compared with the results for specimens tested at the University of Kansas, including No. 5, No. 8, and No. 11 headed bars tested by Shao et al. (2016) and the specimens with No. 11, No. 14, and No. 18 bars from the current study. The specimen details are presented in Tables C2 to C5 in Section C3 of Appendix C.

Table 6.23 presents the statistical parameters of $f_{su}/f_{s,calc}$ ratio based on the proposed design provisions for specimens without parallel ties, using the full expression for Ψ_p . The same results are obtained if the simplified expressions for Ψ_p is used since for $A_{tt}/A_{hs} = 0$, both the full and simplified expressions are governed solely by s/d_b . As shown in the table, for specimens without parallel tie reinforcement, the test-to-calculated $f_{su}/f_{s,calc}$ ranges from 0.81 to 1.67, with a mean of 1.26 and a coefficient of variation of 0.121. For No. 5 bars, the proposed equation is more conservative than for No. 8 and larger bars. The single specimen with three closely-spaced No. 14 bars has a noticeably higher $f_{su}/f_{s,calc}$ ratio of 1.67 than the other specimens, and is likely an outlier, similar to its companion specimen with hooked bars.

Table 6.23 Statistical parameters of test-to-calculated bar stress at failure $f_{su}/f_{s,calc}$ based on the proposed design equation Eq. (6.32) and using the full expression for Ψ_p , Eq. (6.29) for headed bar specimens without parallel tie used to develop descriptive equations, Eq. (5.5) and (5.7)

All	$s \geq 8d_b$					$3d_b \leq s < 8d_b$				
	No. 5	No. 8	No. 11	No. 14	No. 18	No. 5	No. 8	No. 11	No. 14	No. 18

Number of specimens	68	4	20	7	2	0	2	28	4	1	0
Max	1.67	1.48	1.44	1.42	1.27	-	1.50	1.53	1.47	1.67	-
Min	0.81	1.35	1.00	1.02	1.25	-	1.38	0.81	1.14	1.67	-
Mean	1.26	1.40	1.20	1.25	1.26	-	1.44	1.26	1.30	1.67	-
STDEV	0.153	0.057	0.106	0.159	0.013	-	0.086	0.164	0.163	0	-
CoV	0.121	0.041	0.088	0.127	0.010	-	0.060	0.131	0.126	0	-
No. with $f_{su}/f_{s,calc} < 1.0$	2	0	1	0	0	0	0	1	0	0	0

Table 6.24 presents the statistical parameters of $f_{su}/f_{s,calc}$ for specimens with parallel tie reinforcement using the full expression for ψ_p .

Table 6.24 Statistical parameters of test-to-calculated bar stress at failure $f_{su}/f_{s,calc}$ based on the proposed design equation Eq. (6.32) and using the full expression for ψ_p , Eq. (6.29) for headed bar specimens with parallel tie used to develop descriptive equations, Eq. (5.5) and (5.7)

	All	$s \geq 8d_b$					$3d_b \leq s < 8d_b$				
		No. 5	No. 8	No. 11	No. 14	No. 18	No. 5	No. 8	No. 11	No. 14	No. 18
Number of specimens	96	6	30	8	7	4	3	24	4	6	4
Max	1.66	1.56	1.65	1.37	1.66	1.42	1.44	1.52	1.40	1.37	1.51
Min	0.93	1.08	1.02	1.02	1.11	1.17	1.21	0.99	1.19	0.98	0.93
Mean	1.26	1.36	1.28	1.23	1.29	1.33	1.32	1.22	1.31	1.19	1.15
STDEV	0.162	0.170	0.174	0.129	0.164	0.094	0.116	0.157	0.090	0.128	0.249
COV	0.128	0.125	0.136	0.105	0.127	0.071	0.088	0.129	0.069	0.107	0.216
No. with $f_{su}/f_{s,calc} < 1.0$	3	0	0	0	0	0	0	1	0	1	1

As shown in Table 6.24, for specimens with parallel ties, $f_{su}/f_{s,calc}$ ranges from 0.93 to 1.66, with a mean of 1.26 and a coefficient of variation of 0.128. The mean obtained here is the same as that for specimens without parallel ties, indicating a consistent margin of safety provided by the proposed design equation. The design equation is the most conservative for widely spaced No. 5 bars and the least conservative for closely spaced ($3d_b \leq s < 8d_b$) No. 18 bars. A similar table is presented for the case of using the simplified expressions for ψ_p , as shown below.

Table 6.25 Statistical parameters of test-to-calculated bar stress at failure $f_{su}/f_{s,calc}$ based on the proposed design equation Eq. (6.32) and using the simplified expressions for ψ_p , Eq. (6.30) for headed bar specimens with parallel tie used to develop descriptive equations, Eq. (5.5) and (5.7)

	All	$s \geq 8d_b$					$3d_b \leq s < 8d_b$				
		No. 5	No. 8	No. 11	No. 14	No. 18	No. 5	No. 8	No. 11	No. 14	No. 18
Number of specimens	96	6	30	8	7	4	3	24	4	6	4
Max	1.67	1.56	1.65	1.62	1.66	1.44	1.53	1.67	1.66	1.40	1.51
Min	0.93	1.13	1.16	1.17	1.17	1.17	1.30	0.97	1.42	1.00	0.93
Mean	1.33	1.39	1.33	1.43	1.32	1.35	1.45	1.30	1.56	1.21	1.15
STDEV	0.170	0.152	0.133	0.170	0.154	0.105	0.130	0.181	0.105	0.131	0.249
COV	0.127	0.109	0.101	0.119	0.117	0.078	0.089	0.139	0.067	0.108	0.216
No. with $f_{su}/f_{s,calc} < 1.0$	3	0	0	0	0	0	0	1	0	1	1

As shown in Table 6.25 and as expected, using the simplified expressions for ψ_p results in a higher mean for $f_{su}/f_{s,calc}$ (1.33 compared to 1.26 using the full expression for ψ_p), more noticeable for No. 11 and smaller bars.

The statistical parameters of $f_{su}/f_{s,calc}$ using the full expression for ψ_p are presented in Table 6.26 for all headed bar specimens tested at the University of Kansas.

Table 6.26 Statistical parameters of test-to-calculated bar stress at failure $f_{su}/f_{s,calc}$ based on the proposed design equation Eq. (6.32) and using the full expression for ψ_p , Eq. (6.29) for all headed bar specimens used to develop descriptive equations, Eq. (5.5) and (5.7)

Bar size	All	No. 5	No. 8	No. 11	No. 14	No. 18
No. of specimens	164	15	102	23	16	8
Max	1.67	1.56	1.65	1.47	1.67	1.51
Min	0.81	1.08	0.81	1.02	0.98	0.93
Mean	1.26	1.37	1.24	1.26	1.27	1.24
STDEV	0.158	0.122	0.156	0.134	0.178	0.203
COV	0.125	0.089	0.126	0.106	0.139	0.163
No. with $f_{su}/f_{s,calc} < 1.0$	5	0	3	0	1	1

For all 164 headed bar specimens in the University of Kansas database (Section C3 in Appendix C), the test-to-calculated ratio $f_{su}/f_{s,calc}$ based on the proposed design equation using the full expression for ψ_p ranges from 0.81 to 1.67, with a mean of 1.26 and a coefficient of variation

of 0.125. Only five specimens (3.05% of all specimens) had $f_{su}/f_{s,calc} < 1.0$. A similar table is shown below for the case of using the simplified expressions for ψ_p .

Table 6.27 Statistical parameters of test-to-calculated bar stress at failure $f_{su}/f_{s,calc}$ based on the proposed design equation Eq. (6.32) and using the full expression for ψ_p , Eq. (6.30) for all headed bar specimens used to develop descriptive equations, Eq. (5.5) and (5.7)

Bar size	All	No. 5	No. 8	No. 11	No. 14	No. 18
No. of specimens	164	15	102	23	16	8
Max	1.67	1.56	1.67	1.66	1.67	1.51
Min	0.81	1.13	0.81	1.02	1.00	0.93
Mean	1.30	1.41	1.28	1.38	1.29	1.25
STDEV	0.166	0.112	0.155	0.186	0.173	0.211
COV	0.127	0.080	0.121	0.135	0.134	0.168
No. with $f_{su}/f_{s,calc} < 1.0$	5	0	3	0	1	1

As shown in Table 6.27, using the simplified expressions for ψ_p results in a higher mean $f_{su}/f_{s,calc}$ ratio than when the full expression for ψ_p is used (1.31 versus 1.26), more noticeably for No. 5 and No. 11 bars than for the other bar sizes.

6.2.3.2 Bashandy (1996)

To further evaluate the proposed design provisions, results from the beam-column joint specimens tested in other studies available in literature can be compared against Eq. (6.32). In Section 1.2.2, beam-column specimens tested by Bashandy (1996), Chun et al. (2009), and Chun et al. (2017a), Chun and Lee (2019), Sim and Chun (2022a, 2022b) were presented. The study by Chun et al. (2009) is excluded because the specimens had a single headed bar, as previously described in Section 5.6. The specimens tested by Sim and Chun (2022a) are also excluded because the specimens had two layers of headed bars with s/d_b of either 1 or 2, which is less than 3 and therefore the proposed design equation is not applicable.

The specimens tested by Bashandy (1996) are described in Section 5.6. Table 6.28 presents the key specimen parameters along with the bar stresses at failure f_{su} and the bar stresses based on Eq. (6.32), $f_{s,calc}$. As shown in the table, the values of $f_{su}/f_{s,calc}$ for the 18 specimens shown ranges from 0.79 to 1.64, with a mean of 1.05 and a coefficient of variation of 0.199 using the full expression for ψ_p . The results are almost the same using the simplified expressions for ψ_p . As discussed in Section 5.6, the majority of these specimens used unconventional reinforcement

layouts in which parallel ties did not enclose the headed bars (Figure 5.39a and c) and were relatively weak with respect to values calculated using the descriptive equations, as reflected also here in the relatively low mean values of $f_{su}/f_{s,calc}$ of 1.05 shown in Table 6.28.

Table 6.28 Comparison of beam-column joint test results by Bashandy (1996) versus the proposed design equation Eq. (6.32) (values converted from SI units)

Specimen ID	n	ℓ_{eh}	f_{cm}	d_b	s/d _b	A _{th} /A _{hs} *	$\psi_p^{[1]}$	$\psi_p^{[2]}$	L. C.	f_{su}	f _{su} /f _{s,calc} ^[1]	f _{su} /f _{s,calc} ^[2]	
		in.	psi	in.						ksi			
T9	2	11.0	5000	1.41	3.3	0.641	0.85	0.85	B'	49.0	0.96	0.96	
T10**	2	12.5	5000	1.41	5.4	0.596	1.33	1.33	B'	39.1	1.21	1.21	
T12**	2	9.8	5110	1	8.0	0.557	1.00	1.00	B'	50.7	0.90	0.90	
T13**	2	12.8	5560	1	8.0	0.785	1.00	1.00	A'	77.7	1.03	1.03	
T14	2	11.0	5400	1.41	3.3	0.212	1.18	1.20	A'	59.9	1.60	1.64	
T16	2	14.0	5740	1.41	3.3	1.026	0.85	0.85	A'	61.4	0.92	0.92	
T20	2	8.2	5110	1.41	3.3	1.026	0.85	0.85	A'	50.3	1.32	1.32	
T21	2	8.3	5110	1	5.0	2.025	0.85	0.85	A'	62.0	0.96	0.96	
T22	2	8.3	5110	1	5.0	2.025	0.85	0.85	A'	52.1	0.81	0.81	
T23	2	11.2	4820	1.41	3.3	1.026	0.85	0.85	A'	44.1	0.86	0.86	
T24	2	11.2	4690	1.41	3.3	1.026	0.85	0.85	A'	51.4	1.01	1.01	
T25	2	11.0	4690	1.41	3.3	1.962	0.85	0.85	A'	61.4	1.23	1.23	
T26	2	17.0	4550	1.41	3.3	1.026	0.85	0.85	A'	71.3	0.93	0.93	
T27	2	8.0	4550	1.41	3.3	1.026	0.85	0.85	A'	28.5	0.79	0.79	
T28	2	11.2	4830	1.41	3.3	1.026	0.85	0.85	A'	62.3	1.21	1.21	
T29	2	11.0	4830	1.41	3.3	1.026	0.85	0.85	A'	55.5	1.10	1.10	
T30	2	11.3	3210	1	5.0	2.025	0.85	0.85	A'	79.4	1.02	1.02	
T32	2	8.0	4830	1	5.0	2.025	0.85	0.85	A'	61.5	1.00	1.00	
											Mean	1.05	1.05
											CoV	0.194	0.199

^[1] Using the full expression for ψ_p , Eq. (6.29)

^[2] Using the simplified expressions for ψ_p , Eq. (6.30)

* Cap of 0.4 applied to all specimens, except T10, T12, T13 (refer to next footnote)

** Headed bars were outside column core and side cover was 1.5 in. (half of other specimens), so bar location factor of 1.15 applied. Also, headed bars were outside parallel ties (Figure 5.39.a), therefore ties were not counted towards ψ_p ($A_{th}/A_{hs} = 0$)

6.2.3.3 Chun et al. (2017a) and Chun and Lee (2019)

Table 6.29 presents the comparisons with the proposed design equation for the 27 No. 14 and No. 18 bar specimens tested by Chun et al. (2017a) and Chun and Lee (2019). As described in Section 5.5.8, these specimens were designed to force a side-blowout failure. The headed bars were placed outside the column core; therefore, $\psi_o = 1.15$ applies. All specimens had $A_{th}/A_{hs} > 0.4$, but the majority had headed bars were placed outside the parallel ties, as described in Section 5.5.8 and shown in Figure 5.37a. For those specimens, the ties are not used when calculating ψ_p . In

seven specimens, headed bars yielded. Those specimens are reported in Table 6.29 but excluded from the analysis. For this and the following study in Section 6.2.3.4, the same results are obtained using full or simplified expressions for ψ_p since all specimens have A_{th}/A_{hs} values of either 0 or 0.4, therefore the expressions are either only a function of s/d_b , or a cap of 0.85 or 0.95 applies.

Table 6.29 Comparison of headed bar specimens tested by Chun et al. (2017a) and Chun and Lee (2019) versus the proposed design equation, Eq. (6.32)

Specimen ID ^{[1][2]}	<i>n</i>	<i>l_{eh}</i>	<i>f_{cm}</i>	<i>d_b</i>	<i>s/d_b</i>	<i>A_{th}/A_{hs}</i> ^[3]	ψ_p ^[4]	<i>f_{su}</i>	<i>f_{su}/f_{s,calc}</i> ^[4]
		in.	psi	in.				ksi	
D43-L7-C1-S42	2	11.9	6950	1.693	9.6	0.4	1.00	45.4	1.36
D43-L7-C1-S42-HP0.5	2	11.9	6950	1.693	9.6	0.4	0.95	60.5	1.72
D43-L7-C1-S70	2	11.9	9890	1.693	9.6	0.4	1.00	72.7	2.00
D43-L10-C1-S42	2	16.9	7570	1.693	9.6	0.4	1.00	63.4	1.30
D43-L10-C1-S42-HP0.5	2	16.9	7570	1.693	9.6	0.4	0.95	71.6	1.40
gD43-L10-C1-S70	2	16.9	11770	1.693	9.6	0.4	1.00	86.0	1.58
D43-L13-C1-S42	2	22.0	6640	1.693	5.0	0.4	1.38	68.9	1.55
D43-L13-C2-S42	2	22.0	6420	1.693	5.0	0.4	1.38	78.3	1.77
D43-L13-C1-S42-T1.5	2	22.0	5870	1.693	5.0	0.4	0.95	67.9	1.09
D43-L13-C2-S42-T1.5*	2	22.0	6060	1.693	5.0	0.4	0.95	93.4	1.48
D43-L16-C1-S42	2	27.1	6640	1.693	5.0	0.4	1.38	83.0	1.52
D43-L16-C2-S42*	2	27.1	6640	1.693	5.0	0.4	1.38	88.0	1.61
D43-L16-C1-S42-T1.5	2	27.1	6060	1.693	5.0	0.4	0.95	61.5	0.79
D43-L16-C2-S42-T1.5*	2	27.1	6420	1.693	5.0	0.4	0.95	91.1	1.16
D57-L7-C1-S42	2	15.8	7450	2.257	7.2	0.4	1.10	48.5	1.82
D57-L7-C1-S42-HP0.5	2	15.8	7450	2.257	7.2	0.4	0.95	61.5	1.99
D57-L7-C1-S70	2	15.8	11150	2.257	7.2	0.4	1.10	57.5	1.95
D57-L10-C1-S42	2	22.6	7,450	2.257	7.2	0.4	1.10	53.2	1.40
D57-L10-C1-S42-HP0.5	2	22.6	7450	2.257	7.2	0.4	0.95	68.6	1.55
D57-L10-C1-S70	2	22.6	11150	2.257	7.2	0.4	1.10	64.5	1.53
D57-L13-C1-S42	2	29.3	5,870	2.257	7.2	0.4	1.10	63.7	1.36
D57-L13-C1-S42-HP0.5*	2	29.3	5870	2.257	7.2	0.4	0.95	85.0	1.57
D57-L13-C1-S42-HP1.0a*	2	29.3	5870	2.257	7.2	0.4	0.95	85.0	1.57
D57-L13-C1-S42-HP1.0b*	2	29.3	5870	2.257	7.2	0.4	0.95	85.3	1.58
D57-L13-C2-S42	2	29.3	5870	2.257	7.2	0.4	1.10	79.8	1.71
D57-L16-C1-S42	2	36.1	6060	2.257	7.2	0.4	1.10	74.0	1.28
D57-L16-C2-S42*	2	36.1	6060	2.257	7.2	0.4	1.10	85.3	1.47
								Mean	1.53
								CoV	0.199

^[1] HP and C at the end of the designations denote a “confined” specimen per Figure 5.37b and 5.37c, thus parallel ties counted towards ψ_p . For all other specimens (Figure 5.37a), $A_{th}/A_{hs} = 0$ when calculating ψ_p .

^[2] Bar location factor $\psi_o = 1.15$ applied to all specimens

^[3] Cap of 0.4 applied to all specimens

^[4] Using both the full and simplified expressions for ψ_p , Eq. (6.29) and (6.30)

* Headed bars yielded, specimens excluded from the analysis

As shown in Table 6.29, for the 20 specimens tested by Chun et al. (2017) and Chun and Lee (2019) for which the headed bars did not yield, $f_{su}/f_{s,calc}$ ranges from 0.79 to 2.00, with a mean of 1.53 and a coefficient of variation of 0.199 using both full and simplified expressions for ψ_p . As discussed in Section 5.5.8, these specimens also had a relatively high mean value of T/T_h based on descriptive equations, Eq. (5.5) and (5.7). The high values of T/T_h were primarily due to the specimen proportions, which results in relatively low force within the joint, similar to the No. 11 hooked bars tested by Marques and Jirsa (1975) and Pinc et al. (1977), as described in Section 4.5. The geometry of these specimens is dissimilar to what would be expected in reinforced concrete frame structures.

6.2.3.4 Sim and Chun (2022b)

Table 6.30 presents the comparisons of the 16 No. 7 and No. 10 specimens tested by Sim and Chun (2022b) with the proposed design equation. These specimens were also designed to force a side-blowout failure. The headed bars were placed outside the column core in all these specimens; therefore $\psi_o = 1.15$. Also, all specimens had $A_{th}/A_{hs} > 0.4$. The parallel ties are counted towards ψ_p only for specimens where ties were wrapped around the headed bars (Figure 5.37b), as discussed in Section 5.5.8.

As shown in Table 6.30 for the specimens tested by Sim and Chun (2022b), $f_{su}/f_{s,calc}$ ranges from 0.81 to 2.18, with a mean of 1.50 and a coefficient of variation of 0.287. The relatively high mean is similar to the one obtained for Chun et al. (2017a), mainly due to using unconventional specimen proportions and geometry that results in a relatively low force carried by the joint.

Table 6.30 Comparison of headed bar specimens tested by Sim and Chun (2022b) versus the proposed design equation, Eq. (6.32)

Specimen ID ^{[1][2]}	n	ℓ_{eh}	f_{cm}	d_b	s/d_b	A_{th}/A_{hs} ^[3]	ψ_p ^[4]	f_{su}	$f_{su}/f_{s,calc}$ ^[4]
		in.	psi	in.				ksi	

D22-L6-C1	2	5.3	12020	0.875	13.5	0.4	1.00	69.0	1.51
D22-L6-C1.5	2	5.3	12020	0.875	13.5	0.4	1.00	56.2	1.23
D22-L6-C1-TR	2	5.3	12020	0.875	13.5	0.4	0.85	79.8	1.49
D22-L9-C1	2	7.9	12020	0.875	13.5	0.4	1.00	73.4	1.07
D32-L6-C1	2	7.6	12020	1.27	9.3	0.4	1.00	82.5	2.18
D32-L6-C1.5	2	7.6	12020	1.27	9.3	0.4	1.00	81.0	2.14
D32-L6-C1-TR	2	7.6	12020	1.27	9.3	0.4	0.85	71.9	1.62
D32-L9-C1	2	11.4	12020	1.27	9.3	0.4	1.00	73.0	1.29
D22-L6-C1	2	5.3	16680	0.875	13.5	0.4	1.00	64.5	1.31
D22-L6-C1.5	2	5.3	16680	0.875	13.5	0.4	1.00	52.4	1.06
D22-L6-C1-TR	2	5.3	16680	0.875	13.5	0.4	0.85	65.0	1.12
D22-L9-C1	2	7.9	16680	0.875	13.5	0.4	1.00	59.8	0.81
D32-L6-C1	2	7.6	16680	1.27	9.3	0.4	1.00	85.1	2.07
D32-L6-C1.5	2	7.6	16680	1.27	9.3	0.4	1.00	85.4	2.08
D32-L6-C1-TR	2	7.6	16680	1.27	9.3	0.4	0.85	79.9	1.66
D32-L9-C1	2	11.4	16680	1.27	9.3	0.4	1.00	81.3	1.32
								Mean	1.50
								CoV	0.287

^[1] TR at the end of the designations denote a “confined” specimen per Figure 5.37b and 5.37c, therefore parallel ties counted towards ψ_p . For all other specimens (Figure 5.37a), $A_t/A_{hs} = 0$ when calculating ψ_p .

^[2] Bar location factor $\psi_o = 1.15$ applied to all specimens

^[3] Cap of 0.4 applied to all specimens

^[4] Using both the full and simplified expressions for ψ_p , Eq. (6.29) and (6.30)

* Headed bars yielded, specimens excluded from the analysis

A summary of the statistical parameters of $f_{su}/f_{s,calc}$ for the specimens described in this chapter that were tested outside the University of Kansas is presented in Table 6.32. As shown in the table, for the 54 specimens tested outside the University of Kansas, $f_{su}/f_{s,calc}$ ranges from 0.79 to 2.18 with a mean of 1.36 and a coefficient of variation of 0.283. Almost the same results are obtained using the simplified expressions for ψ_p (very slightly higher overall coefficient of variation of 0.284, and slightly higher coefficient of variation of 0.216 for No. 11 bar specimens). The relatively high mean values obtained for No. 10, No. 14, and No. 18 bars are due mainly to the specimen proportions and geometry used by Chun et al. (2017a) and Sim and Chun (2022b) that results in lower forces in the joint and do not represent usual reinforced concrete structures. The relatively low mean values seen for No. 8 and No. 11 bars (responsible for 8 out of 10 specimens with $f_{su}/f_{s,calc} < 1.0$) are primarily due to the unconventional reinforcement layouts used by Bashandy (1996) that results in low anchorage strengths.

Table 6.31 Statistical parameters of $f_{su}/f_{s,calc}$ for all headed bar specimens tested outside University of Kansas (Bashandy 1996, Chun et al 2017a, Chun and Lee 2019, Sim and Chun 2022b) based on the proposed design equation Eq. (6.32), excluding specimens with shear failure and those with headed bars that yielded

As a result of the original proposal modifications, the development length provisions for hooked and headed bars provide a decreased margin of safety for concretes with compressive strengths near 10,000 psi; they are, also, slightly more complex than necessary due to the addition of the concrete strength factor ψ_c . This decreased margin of safety can be illustrated by comparing the ACI 318-19 provisions with the best-fit expression upon which the provisions are based. The

of $f'_c = 10,000$ psi, corresponding to the maximum permitted value on $\sqrt{f'_c}$ of 100 psi. application of the design equations. As adopted, the equations in ACI 318-19 have an upper limit strengths. The original proposal included an upper compressive strength of 16,000 psi for strength concretes, while limiting the potential for low anchorage strengths at higher compressive with the principle goal of preventing excessively long development lengths for lower compressive $f'_c/15,000+0.6$) was included in the development length expressions for values of $f'_c \leq 6,000$ psi, difference between the square root and the quarter power, a concrete strength factor ($\psi_c =$ (Sperry et al. 2015b, Ajam 2017, Shao et al. 2016, and Ghimire et al. 2018). To account for the 2019 edition of the Code, rather than incorporating the more accurate $f_{0.25}^c$ as originally proposed compressive strength $\sqrt{f'_c}$ for both hooked and headed bar design equations when finalizing the As discussed in Section 1.3.1, ACI Committee 318 chose to stay with the square root of

6.3.1 Concrete Compressive Strength

In this section, the proposed design provisions for hooked and headed bars are compared with the provisions in ACI 318-19.

6.3 COMPARISONS WITH ACI 318-19

[1] Using the full expression for ψ_p , Eq. (6.29)

Bar size	All ^[1]	No. 7	No. 8	No. 10	No. 11	No. 14	No. 18
No. of specimens	54	8	6	8	12	11	9
Max	2.18	1.51	1.03	2.18	1.60	2.00	1.99
Min	0.79	0.81	0.81	1.29	0.79	0.79	1.28
Mean	1.36	1.20	0.95	1.79	1.10	1.46	1.62
STDEV	0.386	0.237	0.086	0.371	0.231	0.332	0.259
COV	0.283	0.197	0.090	0.207	0.211	0.227	0.160
No. with $f_{sw}/f_{s,calc} < 1.0$	10	1	3	0	5	1	0

expression for development length in ACI 318-19 is:

$$\ell_{dt} = \left(\frac{f_y \Psi_e \Psi_p \Psi_o \Psi_c}{75 \sqrt{f'_c}} \right) d_b^{1.5} \quad (6.33)$$

where $\sqrt{f'_c}$ may not exceed 100 psi.

For uncoated, headed bars in a beam-column joint with side cover to bar ≥ 2.5 in., and center-to-center bar spacing $s \geq 6d_b$ or $A_{tt}/A_{hs} \geq 0.3$, $\Psi_e = \Psi_p = \Psi_o = 1.0$. Now, replacing f_y with $f_{s,calc}$, f'_c with f_{cm} , and ℓ_{dt} with ℓ_{eh} , and solving for the bar stress gives:

$$f_{s,calc} = \frac{75 \ell_{eh} \sqrt{f'_c}}{\Psi_c d_b^{1.5}} \quad (6.34)$$

where $\Psi_c = f'_c/15,000 + 0.6$. Under the same conditions for bar spacing and parallel ties, the proposed design equation gives $\Psi_p = 1.25$ for No. 11 and smaller bars.

The experimentally-based descriptive expression for the headed bar stress at failure $f_{s,Descriptive}$ for these conditions with $s = 6d_b$ and $A_{tt}/A_{hs} = 0$ based on Eq. (5.5) is

$$f_{s,Descriptive} = \frac{1650 \ell_{eh}^{0.941} f_{cm}^{0.207}}{d_b^{1.502}} \quad (6.35)$$

where ℓ_{eh} is the embedded length of the headed bar and f_{cm} is the actual concrete compressive strength. The mean and coefficient of variation for the descriptive equation are, respectively, 1.00, and 0.112. Equation (6.35) is valid up to 16,000 psi. Figure 6.9 shows the ratio $f_{s,Descriptive}/f_{s,calc}$ for No. 8 bars for a given ℓ_{eh} of 15 in. as a function of concrete compressive strength for both the proposed and ACI 318-19 design equations, Eq. (6.32) and (6.34), respectively.

As shown in Figure 6.9, the ratio $f_{s,Descriptive}/f_{s,calc}$ based on the ACI 318-19 equation, Eq. (6.34), reaches a peak of approximately 1.25 for concrete with a compressive strength of 6,000 psi and then drops to a low point of approximately 1.07 at a compressive strength of 10,000 psi, corresponding to the upper limit for $\sqrt{f'_c}$ of 100 psi. Because $\sqrt{f'_c}$ for use in design is limited to a maximum of 100, the ratio $f_{s,Descriptive}/f_{s,calc}$ increases as the compressive strength increases above 10,000 psi to 1.18 at 16,000 psi. Similar variations in safety margin occur for hooked bars. Figure 6.9 also shows $f_{s,Descriptive}/f_{s,calc}$ as a function of f'_c for the proposed expression, Eq. (6.32) with $s = 6d_b$ and $A_{tt}/A_{hs} = 0$, indicating that the proposed equation provides a more uniform margin of safety.

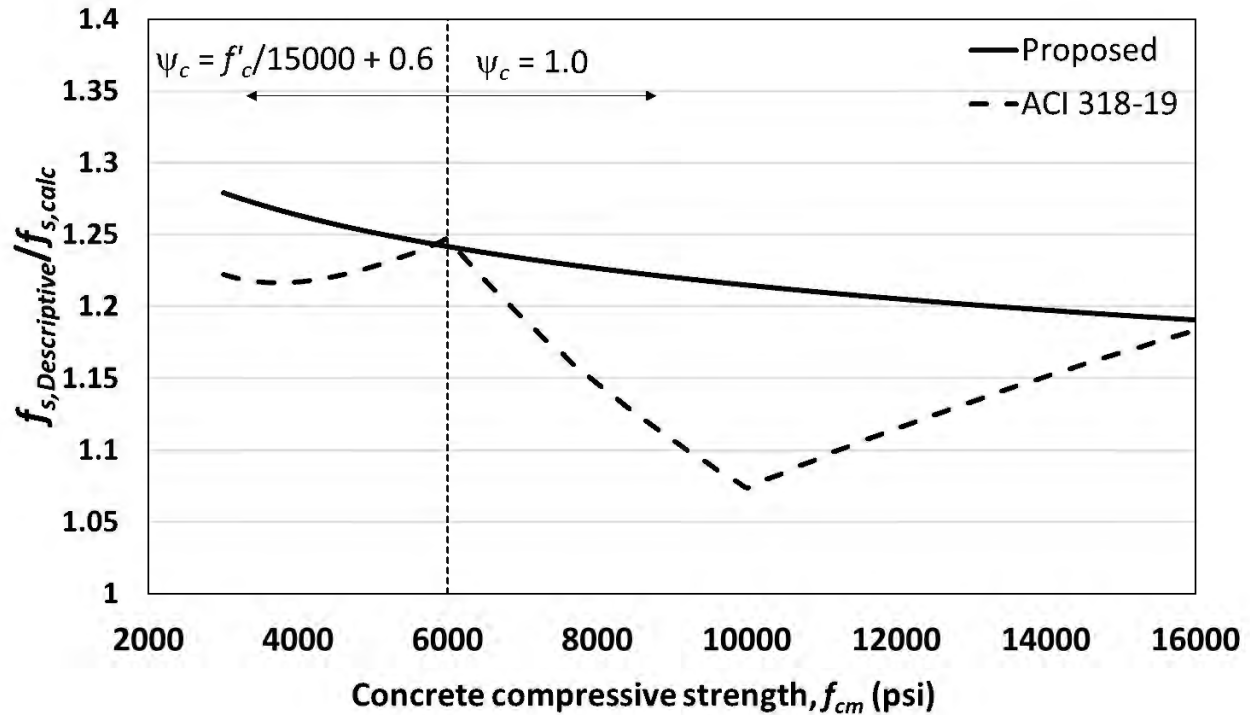


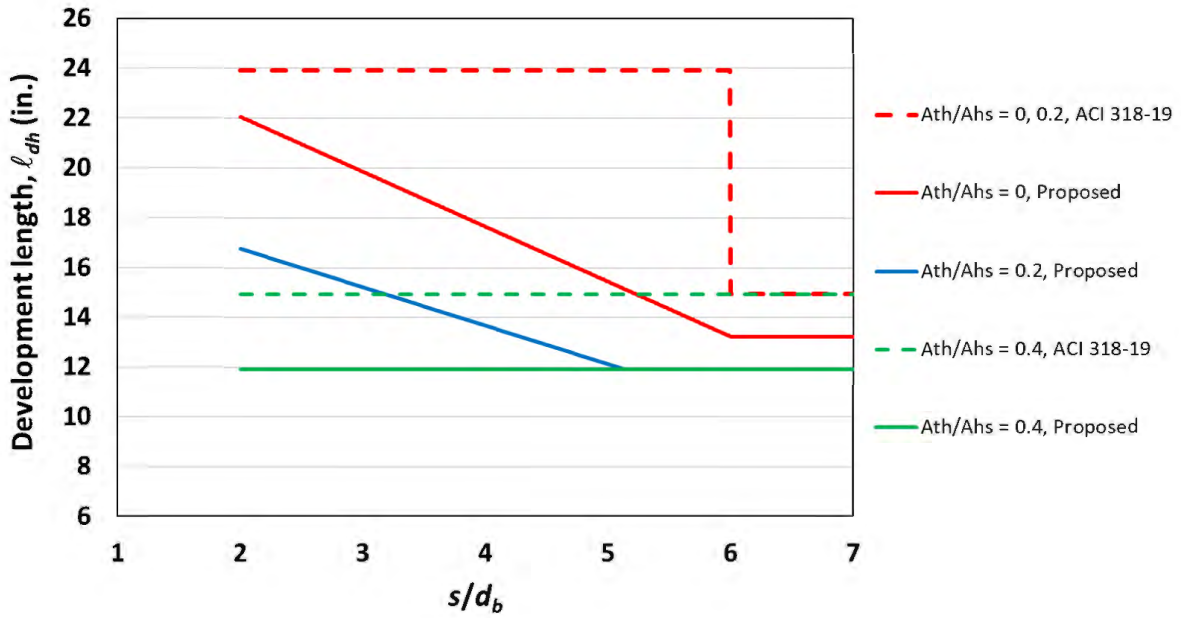
Figure 6.9 Ratio $f_{s,Descriptive}/f_{s,calc}$ versus concrete compressive strength f_{cm} for No. 8 bars headed bars with $s = 6d_b$ and $A_{tr}/A_{hs} = 0$ for ACI 318-19 and proposed design provisions

6.3.2 Required Development Length

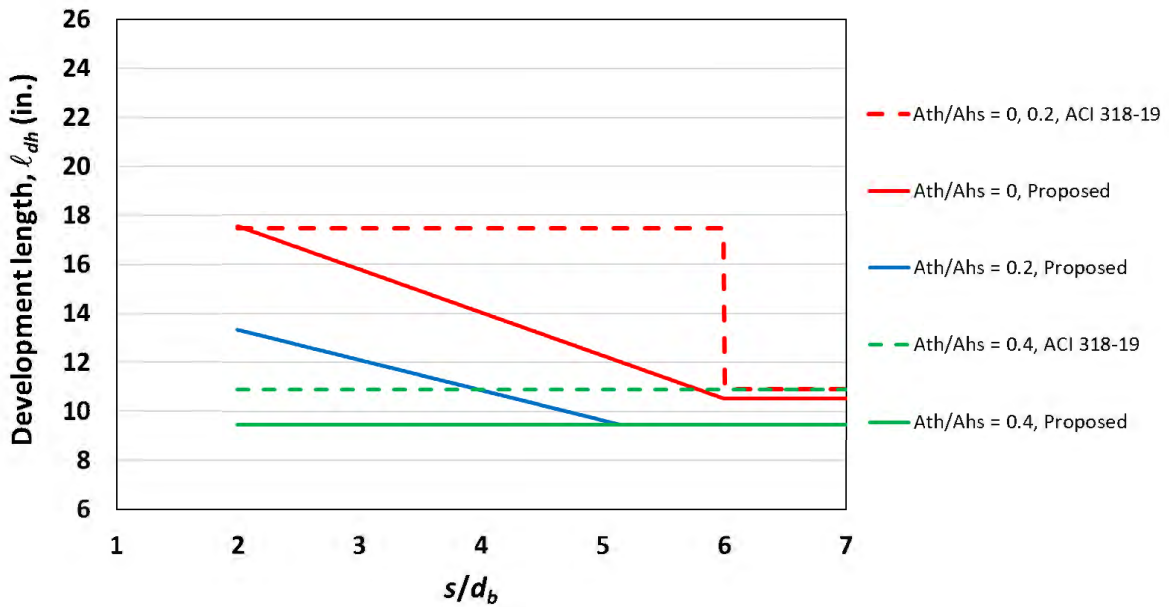
The effects of the provisions for ψ_r and ψ_p in ACI 318-19 are illustrated in Figures 6.10 and 6.11 for hooked bars, and 6.12, and 6.13 for headed bars, which show the required development lengths for No. 8 bars in beam-column joints with at least 2.5 in. of side cover on the exterior bars in normalweight concrete. The figures also show the required development lengths based on the proposed provisions, using the full (Figures 6.10 and 6.12) and simplified (Figures 6.11 and 6.13) expressions for ψ_r and ψ_p .

As discussed before, ACI 318-19 adopted a binary choice, 1.0 or 1.6, on the confining reinforcement and parallel-tie reinforcement factors, ψ_r and ψ_p , in place of factors that vary as a function of bar spacing and the level of confinement. The factor 1.0 is applied only if the confining reinforcement equals or exceeds a specific value ($A_{tr,ACI} \geq 0.4A_{hs}$ and $A_{tr} \geq 0.3A_{hs}$ for hooked and headed bars, respectively) or the center-to-center spacing between the bars, s , exceeds $6d_b$. Intermediate values of ψ_r or ψ_p in cases where the spacing and confining reinforcement do not meet one of the requirements are not permitted by ACI 318-19, resulting in higher values of ℓ_{dh} and ℓ_{dt} than needed to develop f_y . Intermediate values of ψ_r and ψ_p are permitted by the proposed

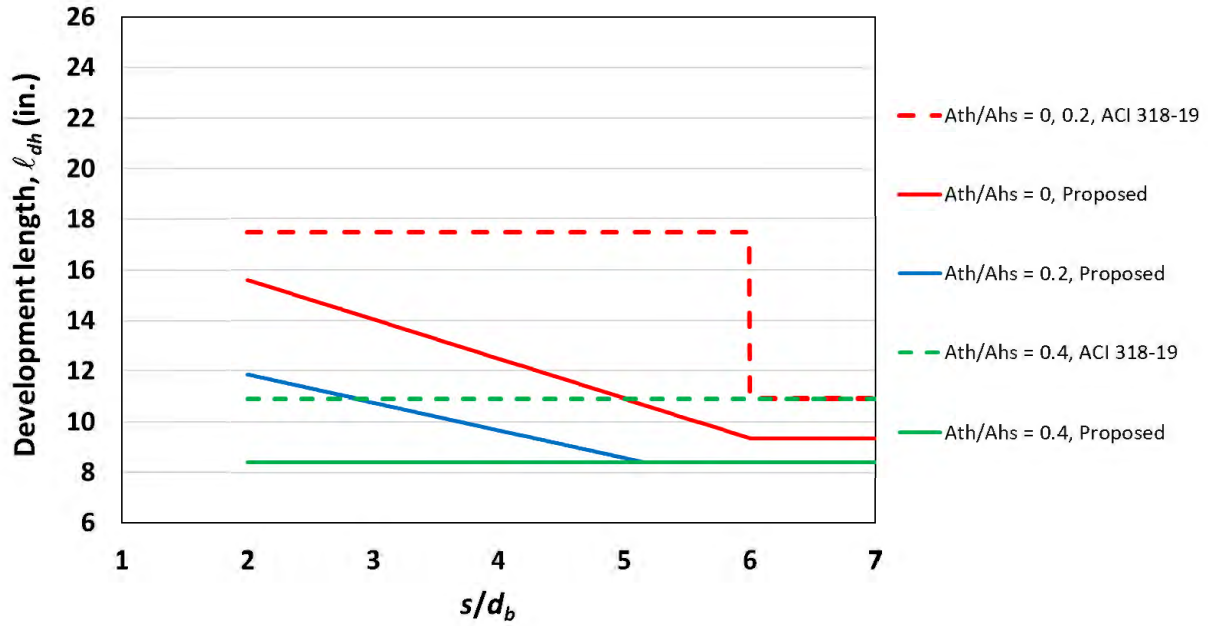
expressions, as given respectively in Eqs. (6.14) or (6.15) for hooked and (6.29) or (6.30) for headed bars.



(a)

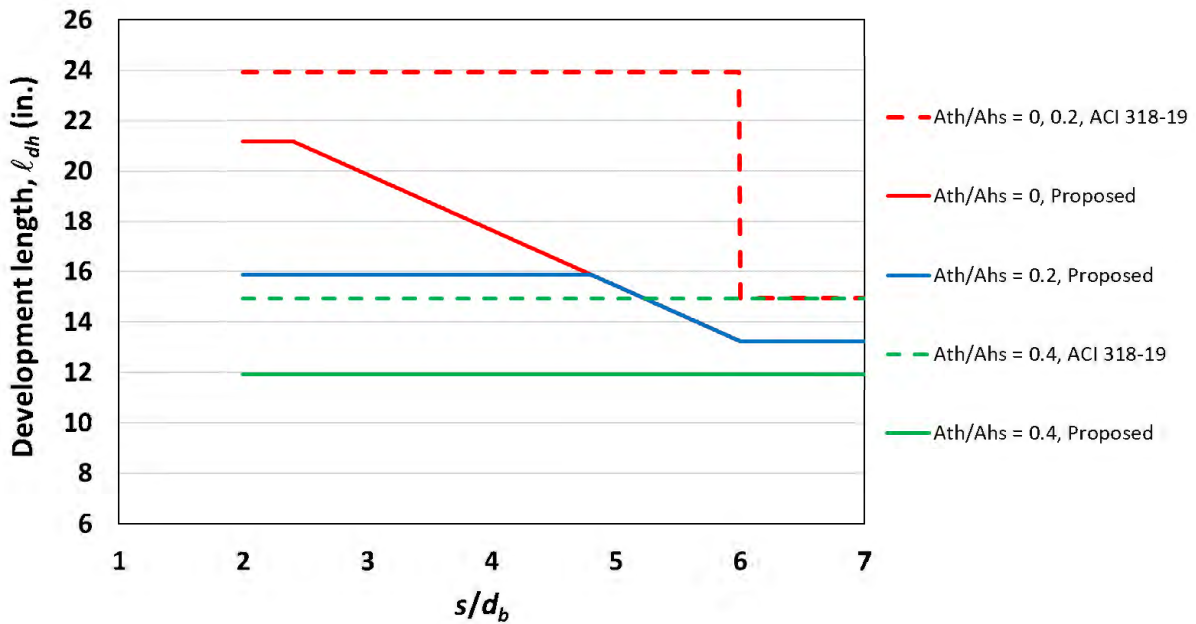


(b)

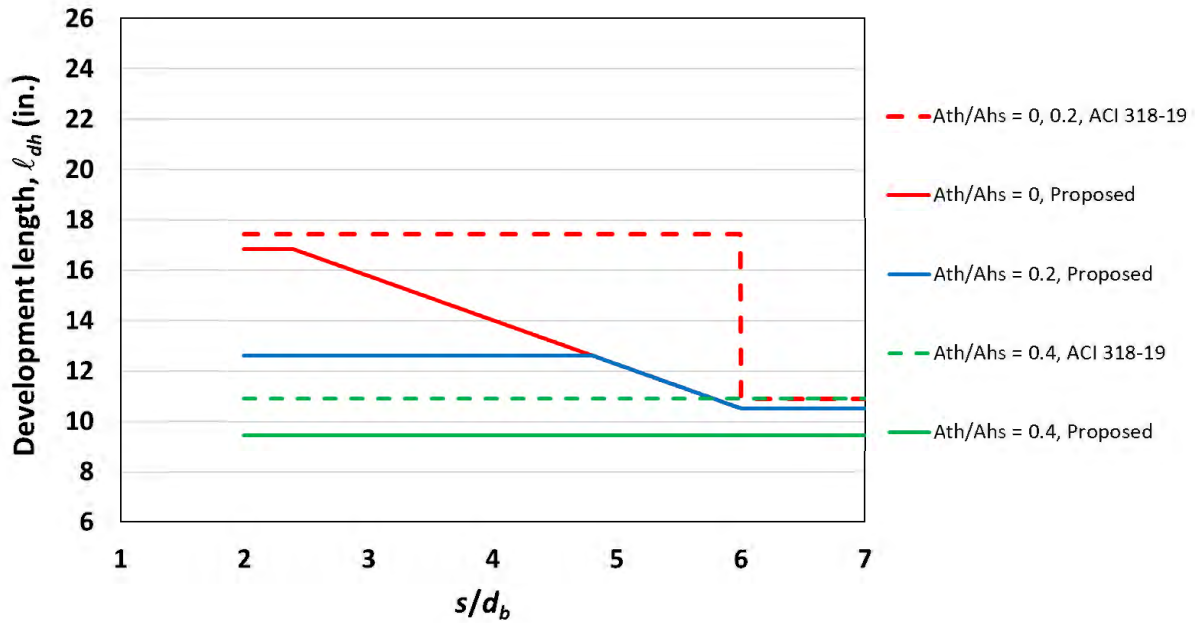


(c)

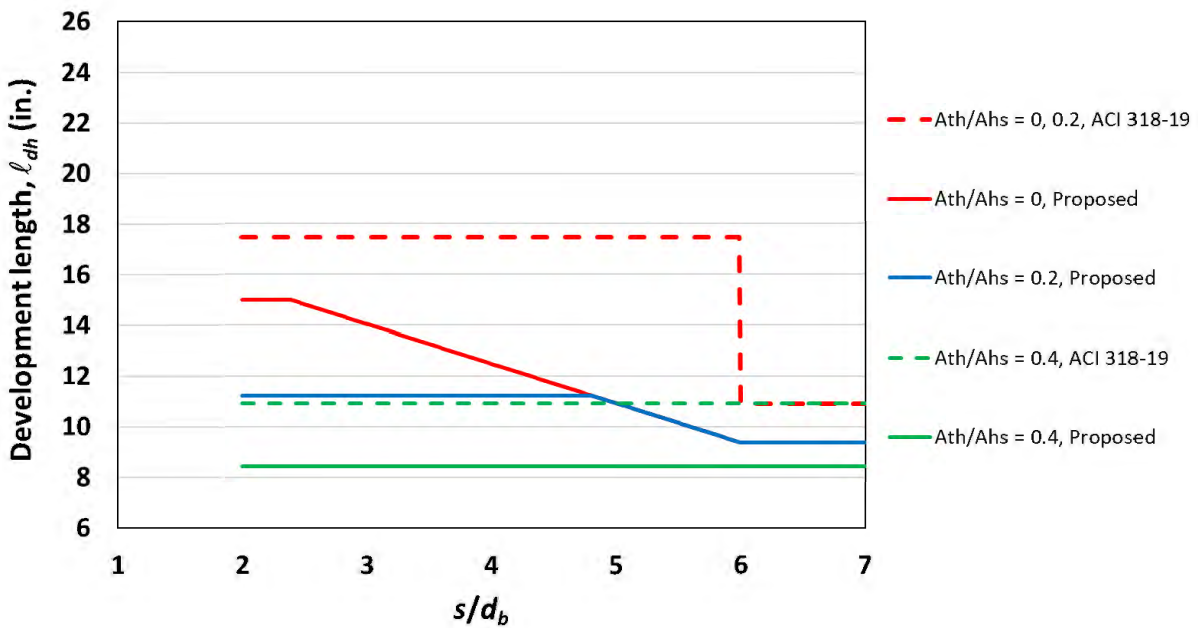
Figure 6.10 Required development lengths of No. 8 hooked bars for $f'_c =$ (a) 4000 psi, (b) 10,000 psi, and (c) 16,000 psi as a function of s/d_b and A_{th}/A_{hs} based on based on ACI 318-19 and the proposed provisions using the full expression for ψ_r , Eq. (6.14)



(a)

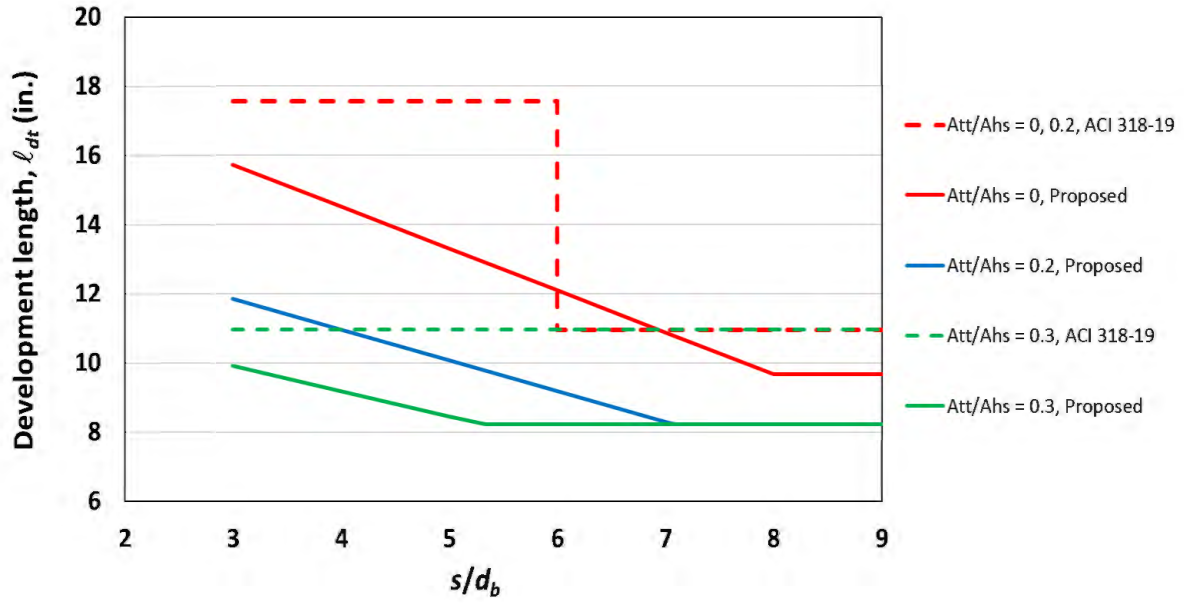


(b)

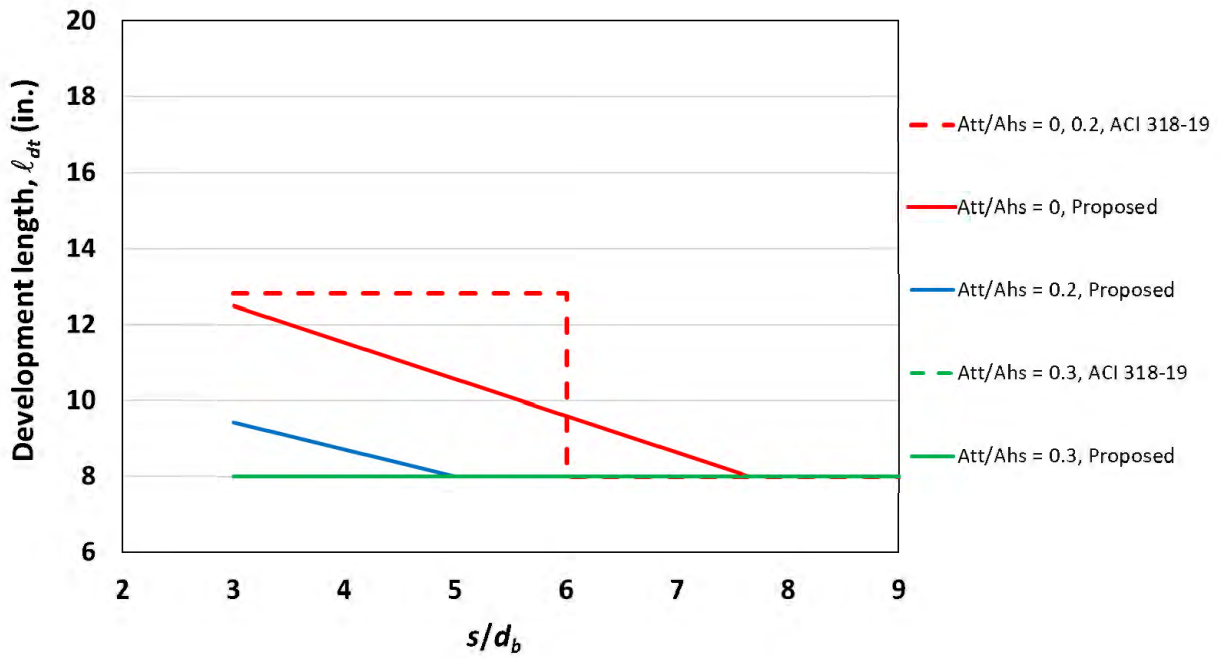


(c)

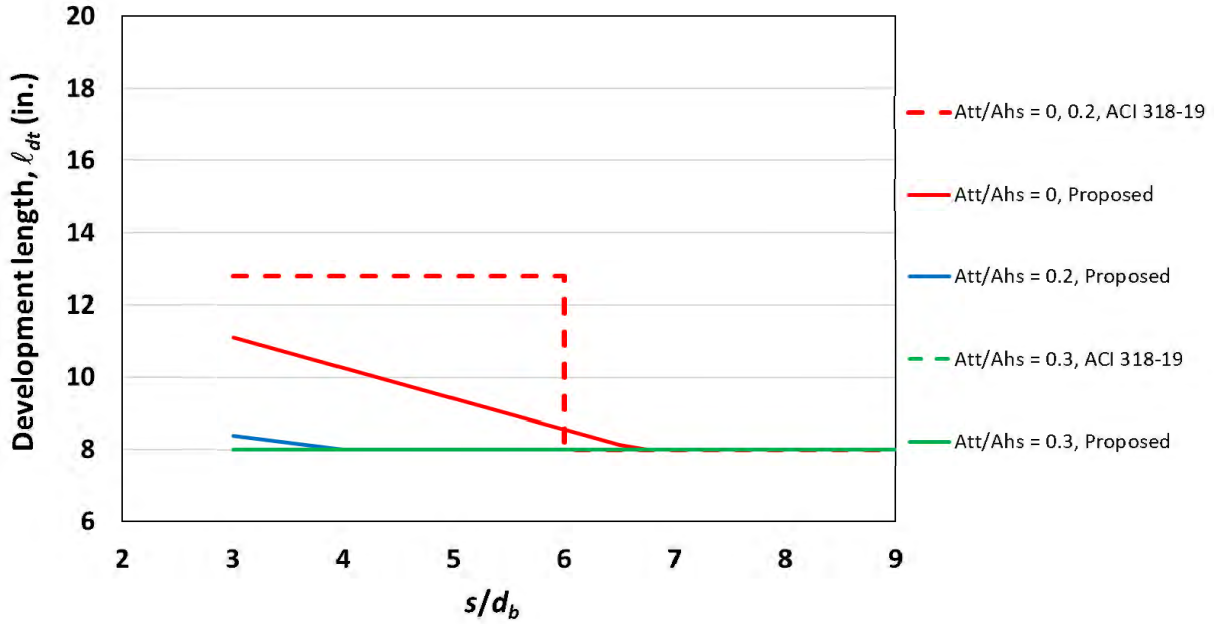
Figure 6.11 Required development lengths of No. 8 hooked bars for $f'_c =$ (a) 4000 psi, (b) 10,000 psi, and (c) 16,000 psi as a function of s/d_b and A_{th}/A_{hs} based on ACI 318-19 and the proposed provisions using the simplified expressions for ψ_r , Eq. (6.15)



(a)

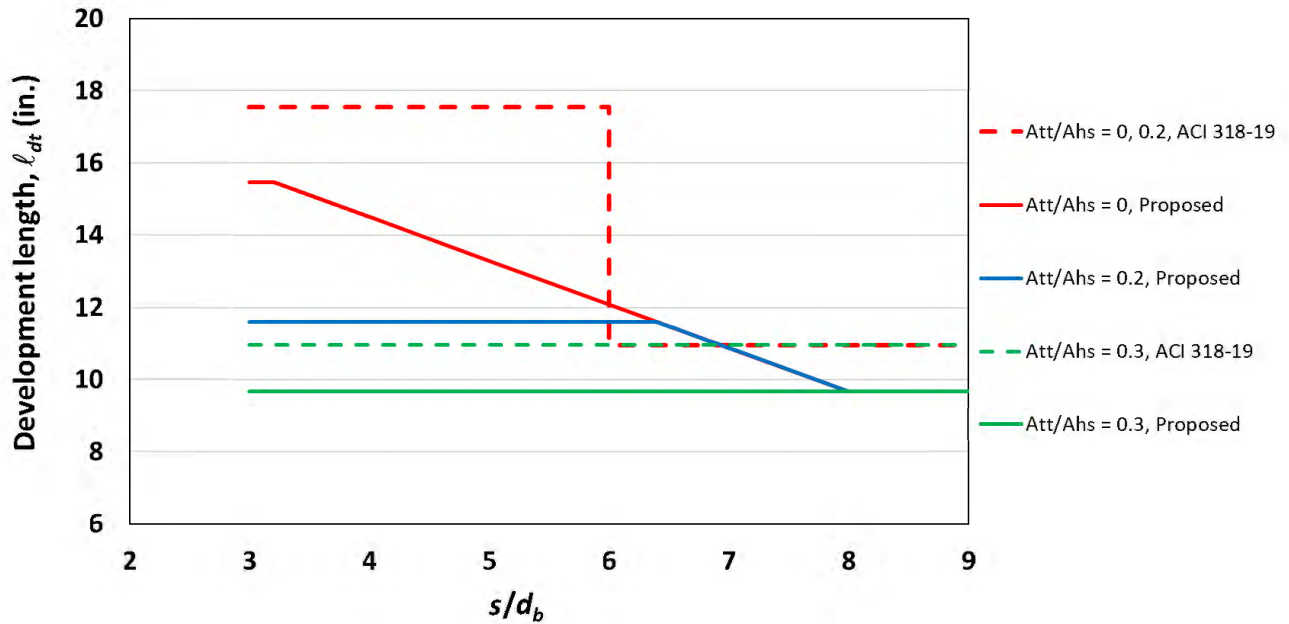


(b)

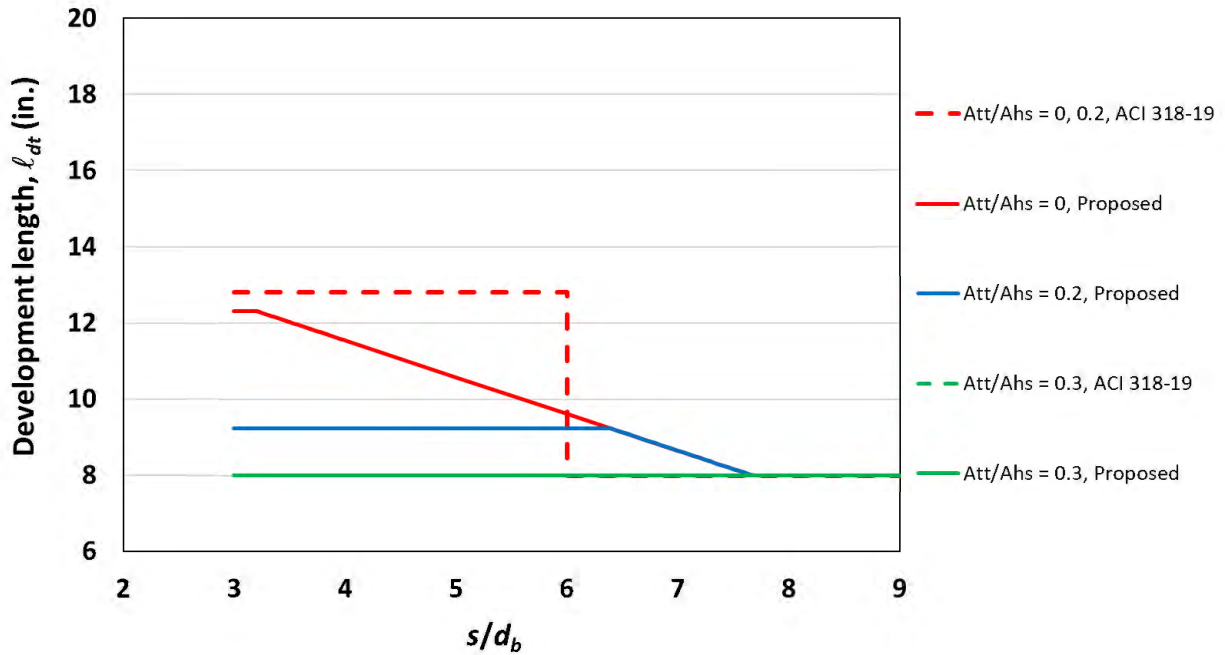


(c)

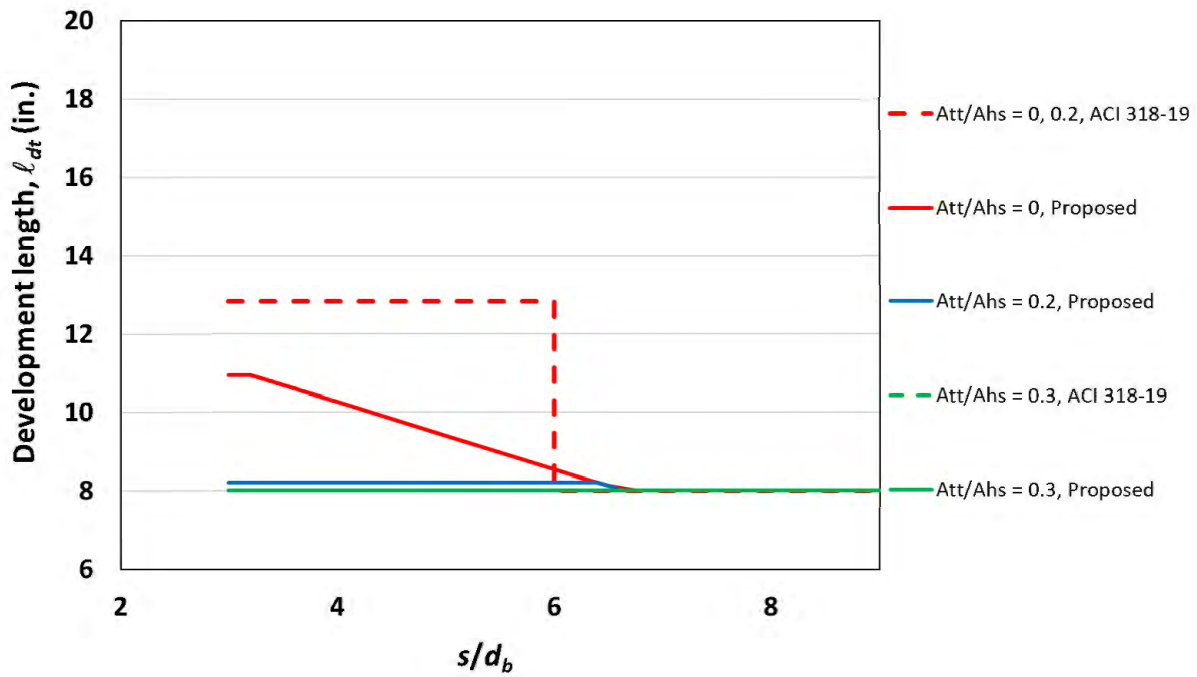
Figure 6.12 Required development lengths of No. 8 headed bars for $f'_c =$ (a) 4000 psi, (b) 10,000 psi, and (c) 16,000 psi as a function of s/d_b and A_t/A_{hs} based on ACI 318-19 and the proposed provisions using the full expression for ψ_p , Eq. (6.29)



(a)



(b)



(c)

Figure 6.13 Required development lengths of No. 8 headed bars for $f'_c =$ (a) 4000 psi, (b) 10,000 psi, and (c) 16,000 psi as a function of s/d_b and A_{tt}/A_{hs} based on ACI 318-19 and the proposed provisions using the simplified expressions for ψ_p , Eq. (6.30)

As shown in Figures 6.10 to 6.13, for both hooked and headed bars, the proposed provisions result in shorter development lengths than those required by ACI 318-19 for most values of A_{th}/A_{hs} or A_{tt}/A_{hs} and s/d_b , for both the full and simplified expressions for ψ_r and ψ_p . The differences between the development lengths based on the proposed provisions and those based on ACI 318-19 are greatest for lower concrete compressive strengths and in cases where ACI 318-19 gives no credit for intermediate values of A_{th}/A_{hs} or A_{tt}/A_{hs} and s/d_b , a prime example being the case where $A_{th}/A_{hs} = 0.2$ and $s/d_b < 6$ for hooked bars, as shown Figures 6.10a and 6.11a.

CHAPTER 7: SUMMARY, CONCLUSIONS, AND FUTURE WORK

7.1 SUMMARY

This research continues a series of studies of the anchorage and development of high-strength reinforcing bars with standard hooks and heads (Searle et al. 2014, Sperry et al. 2015a, 2015b, 2017a, 2017b, 2018, Yasso et al. 2017, Ajaam et al. 2017, 2018, Shao et al. Al 2016, Ghimire et al. 2018, 2019a, 2019b) to expand the available data to include bars larger than No. 11 (No. 14 and No. 18). Forty-two large-scale simulated beam-column joint specimens containing No. 11, No. 14 and No. 18 hooked and headed bars were tested. Of the 42 specimens, 12 contained hooked bars and 30 contained headed bars. The effects of bar size, bar spacing, bar location, embedment length, confining transverse reinforcement in the joint region, placement of bars within the cross-section, concrete compressive strength, compression strut angle, and effective beam depth on anchorage strength were investigated.

Two loading conditions were used. In loading condition A, the joint shear was 80% of the total applied force to the bars, simulating the forces in an exterior beam-column joint with the beam located at the midheight of the column. The joint shear was reduced to ~69% of the total applied force in loading condition B. Loading condition A also had a moment reversal within the joint (with equal and opposite column moments acting on opposing joint faces), whereas loading condition B did not. All hooked bar specimens and 15 headed bar specimens were tested under loading condition A, while the other 15 headed bar specimens tested using loading condition B.

Of the 12 specimens containing hooked bars, eight contained No. 14 and four contained No. 18 bars. The No. 14 bar specimens included six with two widely-spaced bars (center-to-center spacing $s \geq 6d_b$) and two with three closely-spaced bars ($s < 6d_b$), where d_b = hooked or headed bar diameter. All four No. 18 bar specimens had two widely-spaced bars. Bar spacing ranged from $3.5d_b$ to $10.6d_b$. The hooked bar specimens had concrete compressive strengths ranging from 6,390 to 15,770 psi and bar stresses at failure ranging from 87,300 to 130,600 psi. Four No. 14 bar specimens had no confining reinforcement in the joint region. The remaining hooked bar specimens had ties in the joint region A_{th} ranging from $0.178A_{hs}$ to $0.465A_{hs}$, where A_{th} is the total cross-sectional area of tie legs within $8d_b$ from the top of the hooked bar for No. 8 bars and smaller or within $10d_b$ for No. 9 bars or larger, and A_{hs} is the total area of the hooked bars being developed. All specimens had a side cover to the bar of 3.5 in.

The 30 specimens containing headed bars included two with No. 11, 20 with No. 14, and eight with No. 18 bars. Of the 20 specimens with No. 14 bars, 13 had two widely-spaced (center-to-center spacing $\geq 8d_b$) bars, one had two closely-spaced bars (center-to-center spacing $< 8d_b$), and six had three closely-spaced bars. Of the eight specimens with No. 18 headed bars, four had two widely-spaced bars, two had two closely-spaced bars, and two had three closely-spaced bars. Concrete compressive strength ranged from 5,310 to 16,210 psi, and bar stresses at failure ranged from 54,900 to 148,300 psi. The center-to-center bar spacing ranged from $2.7d_b$ to $10.6d_b$. Headed bars from different manufacturers were used with net bearing areas between 4.2 and 4.4 times the bars area. The majority of the specimens contained parallel ties within the joint, with the total area of tie legs within $10d_b$ from the top of headed bars ranging from $0.178A_{hs}$ to $0.827A_{hs}$, where A_t is the total cross-sectional area of tie legs within $8d_b$ from the top of the headed bar for No. 8 bars and smaller or within $10d_b$ for No. 9 bars or larger, and A_{hs} is the total area of the headed bars being developed. Most specimens had a side cover to the bar of 3.5 in. One No. 14 specimen and four No. 18 specimens had a side cover of 6.5 in.

Test results are compared with the current provisions for the development length of hooked and headed bars in Chapter 25 of ACI 318-19 Building Code. Descriptive equations to characterize anchorage strength of hooked and headed bars developed previously for No. 11 and smaller bars are evaluated. New descriptive equations are developed to more accurately represent the anchorage strength for bars as large as No. 18. The equations are compared with the test results available in the literature. New design provisions for development length are developed for hooked and headed bars and evaluated with respect to test results and the provisions of ACI 318-19.

7.2 CONCLUSIONS

The following conclusions are based on the observations and analyses described in this report:

1. ACI 318-19 is unnecessarily conservative for No. 14 and No. 18 hooked and headed bars, independent of concrete compressive strength.
2. The bar location factor ψ_o of 1.25 in ACI 318-19, applied to hooked and headed bars terminating inside column longitudinal reinforcement (column core) with side cover < 2.5 in. or bars with side cover $< 6d_b$, can be safely reduced to 1.15 for design.

3. For both hooked and headed bars, confining reinforcement does not contribute to anchorage strength when bars are placed outside both the column core and the confining reinforcement.
4. The descriptive equations for hooked and headed bars developed in this study accurately account for concrete compressive strength, confining reinforcement, and bar spacing. The ability of the equations to accurately represent anchorage strength is insensitive to variations in compression strut angle and effective beam depth in cases where the ratio of effective beam depth to embedment length < 1.5 .
5. Specimens with widely-spaced No. 14 and 18 bars had higher anchorage strengths than those with closely-spaced bars in most but not all cases similar to the observations for No. 11 and smaller bars.
6. Although not reflected in the current Code provisions, providing confining reinforcement in the joint region, even when $A_{th,ACI}^4 < 0.4A_{hs}$, contributes to anchorage strength of No. 14 and No. 18 hooked bars.
7. Under loading condition A, all hooked bar specimens, even the four specimens without confining reinforcement, carried the joint shear and exhibited an anchorage failure, whereas shear-like failures were observed in some headed bar specimens under similar conditions. These observations reveal the distinct role of the tail of the hook in resisting the propagation of joint shear cracks to the back of the joint, thereby allowing the joints with hooked bars to carry more shear.
8. The contribution of confining reinforcement to anchorage strength increases with hooked bar size. The contribution is high enough for No. 14 and No. 18 hooked bars as to warrant special treatment in design.
9. Compared with the descriptive equations developed for No. 11 headed bars and smaller, the power of headed bar diameter, d_b , in the expression for contribution of parallel ties (T_s) is reduced from 0.88 to 0.11 in the new equations, indicating a much lower effect of bar size on the contribution of parallel ties than previously obtained.
10. Loading condition and joint shear demand play a major role for headed bars. The difference in joint shear between 0.80 and 0.69 times the force in the headed bar under loading conditions A and B, respectively, combined with differences in the column

⁴ Total area of tie legs within $15d_b$ from the centerline of hooked bars, based on ACI 318-19.

moment distributions, are key factors in the type of failure and anchorage strength of headed bars for joints without a minimum quantity of shear reinforcement parallel within the joint.

11. The minimum area of parallel ties (A_{tt}) needed for larger bars to address the joint shear demand is $0.5A_{hs}$. More study is warranted to investigate if parallel ties providing values below $0.5A_{hs}$ would be adequate to prevent a shear-like failure under loading condition A.
12. For headed bars, the upper limit on A_{tt}/A_{hs} is increased to 0.4 for both the descriptive equations and design purposes. The limit was previously 0.3 based on No. 11 and smaller bar tests.
13. The upper limit of 0.4 on A_{tt}/A_{hs} indicates that providing ties (A_{tt}) above $0.4A_{hs}$ does not add to the anchorage strength of headed bars. Thus, the contribution of parallel ties to joint shear strength appears to be separate from their contribution to the anchorage strength.
14. Providing parallel ties within the joint region improves the anchorage strength of headed bars even when $A_{tt,ACI}^5 < 0.3A_{hs}$ (not reflected in ACI 318-19).
15. The interior legs of parallel ties within joints contribute to the anchorage strength of headed bars at least as well as exterior legs.
16. Increasing side cover to the bar (and thus, concrete cover to head) did not have a major effect on the anchorage strength of No. 14 and No. 18 headed bars, but changed the failure type from side splitting to concrete breakout.
17. The proposed design equations for hooked and headed bars are applicable to concrete with compressive strengths up to 16,000 psi, steel with yield strengths up to 120,000 psi, and bars up to No. 18.
18. Similar to earlier findings established for No. 11 and smaller hooked and headed bars, the effect on anchorage strength of concrete compressive strength is best represented by the 0.25 power for design purposes.
19. The proposed modification factors for confining reinforcement (expressed as A_{th}/A_{hs} or A_{tt}/A_{hs}) and bar spacing (expressed as s/d_b), in the form of a single expression or simplified expressions that address the effects of confining reinforcement and bar

⁵ Total area of tie legs within $8d_b$ from the centerline of headed bars, based on ACI 318-19.

spacing independently, provide more flexibility for designers, enabling them with more avenues to take advantage of a range of values for A_{th}/A_{hs} or A_{tt}/A_{hs} and s/d_b and ultimately use a shorter development length as they would using the current provisions.

7.3 FUTURE WORK

This study included only a limited number of specimens with No. 14 and No. 18 hooked bars under loading condition A. For example, no specimens had closely-spaced No. 18 hooked bars or more than a single layer of No. 14 or No. 18 bars. Expanding the scope of the test parameters would provide a better understanding of the anchorage strength of large bars. It would, also, be worthwhile to test No. 11 and smaller hooked bar specimens under loading condition A since, other than the tests on No. 14 and No. 18 bars in this study, no data are available on hooked bars under monotonic loading in a configuration matching that found in most beam-column joints.

More study is needed of headed bars in beam-column joints under loading condition A with different bar sizes and quantities of parallel ties to establish the minimum area of parallel ties needed to address the joint shear demand and prevent a shear-like failure. In addition, the effects of concrete side cover to the bar for larger headed bars can be further investigated by testing specimens with the same bar spacing but different side cover. Both the current Code and the proposed design provisions only permit anchoring headed bars in normalweight concrete because no tests have been performed on headed bars in lightweight concrete. Therefore, tests using different size headed bars cast in lightweight concrete are recommended.

For both hooked and headed bars, it is not clear if bar spacing is the best parameter to address the effects on anchorage strength of groups of closely-spaced bars. A broader range of specimen configurations would be useful to answer this question.

REFERENCES

ACI Committee 318, 2014. "Building Code Requirements for Structural Concrete (ACI 318-14) and Commentary," (ACI 318R-14), American Concrete Institute, Farmington Hills, Michigan, 520 pp.

ACI Committee 318, 2019. "Building Code Requirements for Structural Concrete (ACI 318-19) and Commentary," (ACI 318R-19), American Concrete Institute, Farmington Hills, Michigan, 625 pp.

Ajaam, A., Yasso, S., Darwin, D., O'Reilly, M., and Sperry, J., 2018. "Anchorage Strength of Closely-Spaced Hooked Bars," *ACI Structural Journal*, Vol. 115, No. 4, July-Aug., pp. 1143-1152.

Ajaam, A., Darwin, D., and O'Reilly, M., 2017. "Anchorage Strength of Reinforcing Bars with Standard Hooks," *SM Report No. 125*, University of Kansas Center for Research, Inc., Lawrence, KS, Apr., 372 pp.

ASTM A970, 2016. "Standard Specification for Headed Steel Bars for Concrete Reinforcement," (ASTM A970/A970M-16), ASTM International, West Conshohocken, Pennsylvania, 9 pp.

ASTM A970, 2018. "Standard Specification for Headed Steel Bars for Concrete Reinforcement," (ASTM A970/A970M-18), ASTM International, West Conshohocken, Pennsylvania, 10 pp.

Bashandy, T. R., 1996. "Application of Headed Bars in Concrete Members," *PhD dissertation*, University of Texas at Austin, Dec., 303 pp.

Blessent, M., Darwin, D., Lepage, A., Lequesne, R.D., and O'Reilly, M., 2020. "Anchorage of Large High-Strength Reinforcing Bars with Standard Hooks and Heads: Initial Tests," *SL Report 20-3*, University of Kansas Center for Research, Inc., Lawrence, KS, Feb., 40 pp.

Bournonville, M., Dahnke, J., and Darwin, D., 2004. "Statistical Analysis of the Mechanical Properties and Weight of Reinforcing Bars," *SL Report 04-1*, The University of Kansas Center for Research, Inc., Lawrence, Kansas, Dec., 194 pp.

Chun, S.-C., 2015, "Lap Splice Tests Using High-Strength Headed Bars of 550 MPa (80 ksi) Yield Strength," *ACI Structural Journal*, Vol. 112, No. 6, Nov.-Dec., pp. 679-688.

Chun, S.-C., B.-S. Lee. 2019. “Components of Side-Face Blowout Strengths of Headed Bars in Exterior Beam-Column Joints.” *ACI Structural Journal*. Vol. 116, No. 3, Mar., pp 159–170.

Chun, S.-C., Choi C.-S., and Jung H.-S., 2017a. “Side-face blowout failure of large-diameter high-strength headed bars in beam–column joints.” *ACI Structural Journal*. Vol. 114, No. 1, Jan.-Feb., pp 161–172.

Chun, S.-C., Bae M.-S., and Lee B.-S., 2017b. “Side-Face Blowout Strength of 43 and 57 mm (No. 14 and No. 18) Hooked Bars in Beam-Column Joints.” *ACI Structural Journal*. Vol. 114, No. 5, Sep.-Oct., pp 1227–1238.

Chun, S.-C., Oh, B., Lee, S.-H., and Naito, C. J., 2009. “Anchorage Strength and Behavior of Headed Bars in Exterior Beam-Column Joints,” *ACI Structural Journal*, Vol. 120, No. 3, May, pp. 579-590.

Coleman, Z., Jacques, E., and Roberts-Wollmann, C., 2023. “Effect of Beam Depth on Anchorage Strength of Hooked and Headed Bars” *ACI Structural Journal*, Vol. 106, No. 5, Sep.-Oct., pp. 197-206.

DeVries, R. A., 1996. “Anchorage of Headed Reinforcement in Concrete,” *PhD dissertation*, University of Texas at Austin, Dec., 294 pp.

Ghimire, K. P., Shao, Y., Darwin, D., and O’Reilly, M., 2019a. “Conventional and High-Strength Headed Bars – Part 1: Anchorage Tests,” *ACI Structural Journal*, Vol. 116, No. 4, May, pp. 255-264.

Ghimire, K. P., Shao, Y., Darwin, D., and O’Reilly, M., 2019b. “Conventional and High-Strength Headed Bars – Part 2: Data Analysis,” *ACI Structural Journal*, Vol. 116, No. 4, May, pp. 265-272.

Ghimire, K., Darwin, D., and O’Reilly, M., 2018. “Anchorage of Headed Reinforcing Bars in Concrete,” *SM Report No. 127*, University of Kansas Center for Research, Inc., Lawrence, KS, Jan., 278 pp.

Hamad, B. S.; Jirsa, J. O.; and de Paolo, N. I., 1993. “Anchorage Strength of Epoxy-Coated Hooked Bars,” *ACI Structural Journal*, V. 90, No. 2, Mar.-Apr., pp. 210-217.

Joh, O., Goto, Y., and Shibata, T. 1995. “Anchorage of Beam Bars with 90-Degree Bend in Reinforced Concrete Beam-Column Joints,” *ACI Special Publication*, Vol. 157, Oct., pp. 97-116.

Joh, O. and Shibata, T. 1996. "Anchorage of Beam Bars with 90-Degree Bend in Reinforced Concrete Beam-Column Joints," *Eleventh World Conference Earthquake Engineering*, No. 1196, Elsevier Science Ltd., 8 pp.

Kang, T. H.-K., Ha, S.-S., and Choi, D.-U., 2010. "Bar Pullout Tests and Seismic Tests of Small-Headed Bars in Beam-Column Joints," *ACI Structural Journal*, Vol. 107, No. 1, Jan.-Feb., pp. 32-42.

Lee, J., and Park, H., 2010. "Bending - Applicability Study of Ultra-Bar (SD 600) and Ultra-Bar for Rebar Stirrups and Ties (SD 500 and 600) for Compression Rebar," [Translated from Korean] Korea Concrete Institute, Aug., 504 pp.

Marques, J. L., and Jirsa, J. O., 1975. "A Study of Hooked Bar Anchorages in Beam-Column Joints," *ACI Journal, Proceedings* Vol. 72, No. 5, May-Jun., pp. 198-209.

Nazzal, L. A., Darwin, D., and O'Reilly, M., 2023. "Anchorage of High-Strength Reinforcing Bars in Concrete," *SM Report No. 150*, University of Kansas Center for Research, Inc., Lawrence, KS, Jan., 300 pp.

Peckover, J. and Darwin, D., 2013. "Anchorage of High-Strength Reinforcing Bars with Standard Hooks: Initial Tests," *SL Report 13-1*, The University of Kansas Center for Research, Inc., Lawrence, Kansas, Jan., 55 pp.

Pinc, R. L., Watkins, M. D., and Jirsa, J. O., 1977. "The Strength of Hooked Bar Anchorages in Beam-Column Joints," *CESRL Report No. 77-3*, Department of Civil Engineering-Structures Research Laboratory, University of Texas, Austin, Texas, 67 pp.

Ramirez, J. and Russell, B. 2008. "Transfer, Development, and Splice Length for Standard/Reinforcement in High-strength Concrete," Washington, D.C.: Transportation Research Board, National Research Council, pp. 99-120.

Searle, N., DeRubeis, M., Darwin, D., Matamoros, A. B., O'Reilly, M., and Feldman, L., 2014. "Anchorage of High-Strength Reinforcing Bars with Standard Hooks - Initial Tests," *SM Report No. 108*, University of Kansas Center for Research, Inc., Lawrence, KS, Feb., 120 pp.

Shao, Y., Darwin, D., O'Reilly, M., Lequesne, R.D., Ghimire, K., Hano, Muna, 2016. "Anchorage of Conventional and High-Strength Headed Reinforcing Bars," *SM Report No. 117*, University of Kansas Center for Research, Inc., Lawrence, KS, Aug., 234 pp.

Sim, H.-J., and Chun, S.-C. 2022a. “Side-Face Blowout Strength of Two-Layer Headed Bars Embedded in Exterior Beam-Column Joints.” *ACI Structural Journal*. Vol. 119, No. 2, Mar., pp 221–231.

Sim, H.-J., and Chun, S.-C. 2022b. “Side-Face Blowout Failure of Headed Bars in High-Strength Concrete.” *ACI Structural Journal*. Vol. 119, No. 5, Sep., pp 221–231.

Sperry, J., Darwin, D., O'Reilly, M., Lequesne, R. D., Yasso, S., Matamoros, A., Feldman, L. R., and Lepage, A., 2017b. “Conventional and High-Strength Hooked Bars - Part 2: Data Analysis,” *ACI Structural Journal*, Vol. 114, No. 1, Jan.-Feb., pp. 267-314.

Sperry, J., Al-Yasso, S., Searle, N., DeRubeis, M., Darwin, D., O'Reilly, M., Matamoros, A. B., Feldman, L., Lepage, A., Lequesne, R., and Ajaam, A., 2015a. “Anchorage of High-Strength Reinforcing Bars with Standard Hooks,” *SM Report No. 111*, University of Kansas Center for Research, Inc., Lawrence, KS, June, 266 pp.

Sperry, J., Darwin, D., O'Reilly, M., Lepage, A., Lequesne, R., Matamoros, A., Feldman, L., Yasso, S., Searle, N., DeRubeis, M., and Ajaam, A., 2018. “Conventional and High-Strength Hooked Bars: Detailing Effects,” *ACI Structural Journal*, Vol. 115, No. 1, Jan.-Feb., pp. 247-257.

Sperry, J., Darwin, D., O'Reilly, M., and Lequesne, R., 2015b. “Anchorage Strength of Conventional and High-Strength Hooked Bars in Concrete,” *SM Report No. 115*, University of Kansas Center for Research, Inc., Lawrence, KS, Dec., 281 pp.

Sperry, J., Yasso, S., Searle, N., DeRubies, M., Darwin, D., O'Reilly, M., Matamoros, A., Feldman, L.R., Lepage, A., Lequesne, R.D., and Ajaam, A., 2017a. “Conventional and High-Strength Hooked Bars - Part 1: Anchorage Tests,” *ACI Structural Journal*, Vol. 114, No. 1, Jan.-Feb., pp. 255-342.

Thompson, M. K., Jirsa, J. O., and Breen, J. E., 2006a. “CCT Nodes Anchored by Headed Bars-Part 2: Capacity of Nodes,” *ACI Structural Journal*, Vol. 103, No. 1, Jan.-Feb., pp. 65-73.

Thompson, M. K., Ledesma, A., Jirsa, J. O., and Breen, J. E., 2006b. “Lap Splices Anchored by Headed Bars,” *ACI Structural Journal*, Vol. 103, No. 2, Mar.-Apr., pp. 271-279.

Thompson, M. K., Ziehl, M. J., Jirsa, J. O., and Breen, J. E., 2005. “CCT Nodes Anchored by Headed Bars-Part 1: Behavior of Nodes,” *ACI Structural Journal*, Vol. 102, No. 6, Nov.-Dec., pp. 808-815.

Wright, J. L., and McCabe, S. L., 1997. “The Development Length and Anchorage Behavior of Headed Reinforcing Bars,” *SM Report* No. 44, University of Kansas Center for Research, Inc., Lawrence, Kansas, Sep., 147 pp.

Yasso, S., Darwin, D., and O'Reilly, M., 2017. “Anchorage Strength of Standard Hooked Bars in Simulated Exterior Beam-Column Joints,” *SM Report* No. 124, University of Kansas Center for Research, Inc., Lawrence, KS, Apr., 330 pp.

Yasso, S., Darwin, D., and O'Reilly, M. O., 2021 “Effects of Concrete Tail Cover and Tail Kickout on Anchorage Strength of 90-Degree Hooks,” *ACI Structural Journal*, Vol. 118, No. 6, Nov., pp. 227-236.

APPENDIX A: NOTATION

a	Depth of equivalent rectangular compressive stress block, in.
A_b	Cross-sectional area of an individual hooked or headed bar, in. ²
A_{brg}	Net bearing area of the head calculated as the gross head area minus maximum area of the obstruction adjacent to the head; net bearing area of the head calculated as gross head area minus bar area if no obstruction is present or the obstruction, in. ²
A_{hs}	Total cross-sectional area of hooked or headed bars being developed (nA_b), in. ²
A_{tp}	Cross-sectional area of a single leg of parallel ties within the joint region for headed bars, in. ²
A_{tr}	Cross-sectional area of a single leg of confining reinforcement within the joint region for hooked bars, in. ²
A_{th}	Total cross-sectional area of effective confining reinforcement ($n_{tl}A_{tr}$) for hooked bars being developed within $8d_b$ from top of the hooked bars for No. 3 through No. 8 bars or within $10d_b$ for No. 9 bars and larger, in. ²
$A_{th,ACI}$	Total cross-sectional area of effective confining reinforcement for hooked bars being developed within $15d_b$ from centerline of hooked bars, per ACI 318-19, in. ²
A_{tt}	Total cross-sectional area of effective parallel ties ($n_{tl}A_{tp}$) for headed bars being developed within $8d_b$ from top of the headed bars for No. 3 through No. 8 bars or within $10d_b$ for No. 9 bars and larger, in. ²
$A_{tt,ACI}$	Total cross-sectional area of effective parallel ties for headed bars being developed within $8d_b$ from centerline of headed bars, per ACI 318-19, in. ²
b	Width of column, in.
b_{BP}	Width of the bearing plate, in.
c	Depth of neutral axis from the extreme compression fiber, in.
c_{bc}	Clear cover from the back of the head to the back of the column, in.
c_{bh}	Clear cover from the back of the hook to the back of the column, in.
c_o	Clear side cover to the head, in.
c_{so}	Clear side cover to the hooked or headed bar, in.
d	Distance from the centroid of the tension bar to the extreme compression fiber of the beam, in.
d_b	Nominal diameter of bar, in.
d_{eff}	Effective depth of the simulated beam, in.
d_{to}	Nominal diameter of ties outside the joint region, in.
d_{tp}	Nominal diameter of parallel ties within the joint region for headed bars, in.
d_{tr}	Nominal diameter of confining reinforcement within the joint region for hooked bars, in.
f'_c	Specified or target concrete compressive strength, psi
f_{cm}	Measured concrete compressive strength, psi

f_s, f_{su}	Stress in the hooked or headed bar at failure, ksi
$f_{s,ACI}$	Calculated stress in the hooked or headed bar per ACI 318-19, ksi
$f_{s,max}$	Maximum stress in individual hooked or headed bar, ksi
$f_{s,calc}$	Calculated stress in the hooked or headed bar, ksi
f_y	Measured yield strength of the hooked or headed bar, ksi
h	Depth of column, in.
h_o	Total height of column, in.
h_{cl}	Distance between the center of hooked or headed bar to the top of the bearing plate or bearing member in the joint region, in.
K_{tr}	Confining reinforcement index per ACI 318-19
ℓ_{dh}	Development length in tension of deformed bar or deformed wire with a standard hook, measured from outside end of hook, point of tangency, toward critical section, in.
ℓ_{dt}	Development length in tension of headed deformed bar, measured from the critical section to the bearing face of the head, in.
ℓ_{eh}	Embedment length measured from the bearing face of the head to the front face of the specimen for headed bars and embedment length of a standard hook measured from the outside of the hook to the front face of the specimen for hooked bars, in.
$\ell_{eh,avg}$	Average embedment length of hooked or headed bars, in.
n	Number of hooked or headed bars loaded simultaneously in tension, in.
n_{tl}	Number of tie legs within $10d_b$ from top of hooked or headed bars
n_{tp}	Number of parallel ties (single, double overlapping, or double) within $10d_b$ from top of headed bars
n_{tr}	Number of single confining reinforcement ties within $10d_b$ from top of hooked bars
N_{tp}	Number of parallel ties (single, double overlapping, or double) within the joint region for headed bars
N_{tr}	Number of single confining reinforcement ties within the joint region for hooked bars
s	Center-to-center spacing of hooked or headed bars (previously c_{ch}), in.
T	Average load on a hooked or headed bar at failure, pounds, kips
T_c	Anchorage strength of a hooked or headed bar without confining reinforcement ties; contribution of concrete to anchorage strength of a hooked or headed bar, pounds, kips
T_h	Anchorage strength of a hooked or headed bar using descriptive equations, pounds, kips
T_{ind}	Peak load on individual hooked or headed bar at failure, kips
T_{max}	Maximum load on individual hooked or headed bar, kips
T_s	Contribution of steel confining reinforcement ties to anchorage strength of a hooked or headed bar, pounds, kips
T_{total}	Sum of loads on hooked or headed bars at failure, kips
V_J	Shear force in the joint, kips
w/c	Water-to-cement ratio by weight

x_{bot}	Height measured from the center of the test bar to the center of the lower tension member, in.
x_{mid}	Height measured from the center of the test bar to the center of the bearing member in the joint, in.
x_{top}	Height measured from the center of the test bar to the center of the upper bearing member, in.
β_1	Factor relating depth of equivalent rectangular compressive stress block to neutral axis depth
Δ_{ind}	Measured displacement of individual hooked or headed bar at failure, relative to the front face of the column, in.
Δ_{max}	Maximum displacement of individual hooked or headed bar relative to the front face of the column, in.
ϕ	Strength-reduction factor
ψ_c	Factor used to modify development length based on concrete compressive strength
ψ_{cr}	Factor used to modify development length based on confining reinforcement for hooked bars
ψ_e	Factor used to modify development length based on reinforcement coating
ψ_o	Factor used to modify development length based on bar location within member
ψ_p	Factor used to modify development length based on parallel ties and bar spacing for headed bars
ψ_{p1}	Factor used to modify development length based on bar spacing for headed bars without parallel ties
ψ_{p2}	Factor used to modify development length based on bar spacing and parallel ties for headed bars with parallel ties
ψ_{pr}	Factor used to modify development length based on parallel ties for headed bars
ψ_r	Factor used to modify development length based on confining reinforcement and bar spacing for hooked bars
ψ_{r1}	Factor used to modify development length based on bar spacing for hooked bars without confining reinforcement
ψ_{r2}	Factor used to modify development length based on bar spacing and confining reinforcement for hooked bars with confining reinforcement
θ	Compression strut angle, degrees
λ	Modification factor to reflect the reduced mechanical properties of lightweight concrete relative to normalweight concrete of the same compressive strength

Acronym list

ACI	American Concrete Institute
ASTM	American Society of Testing and Materials - International
BSG	Bulk Specific Gravity (Oven Dry)
BSG (SSD)	Bulk Specific Gravity (Saturated Surface Dry)
CCT	Compression-Compression-Tension
CoV	Coefficient of Variation
HA	Class of head satisfying head dimension requirements detailed in ASTM A970
L. C.	Loading Condition as described in Section 2.3.1
MAX	Maximum
MIN	Minimum
SG	Specific Gravity
SN	Specimen Number
SSD	Saturated Surface Dry
STDEV	Standard Deviation

Failure Types

CB	Concrete breakout
SS	Side splitting
SF	Shear failure

APPENDIX B: HOOKED BAR BEAM-COLUMN JOINT SPECIMENS

Appendix B presents the details of the hooked bar specimens. Appendix B1 presents specimen drawings and reinforcement layouts for No. 14 and No. 18 bars tested in this study. Appendix B2 presents detailed properties and test results for the No. 14 and No. 18 bar specimens of this study. Appendix B3 presents specimens tested at the University of Kansas, including those used to develop descriptive equations, Eq. (4.5) and (4.7). The specimens include No. 5, No. 8, and No. 11 bar specimens by Searle et al. (2014), Sperry et al. (2015a, 2015b, 2017a, 2017b, 2018), Yasso et al. (2017), Ajaam et al. (2017, 2018), and No. 14 and No. 18 bars tested in this study. Appendix B4 presents the specimens tested outside the University of Kansas, a few of which were used to develop descriptive equations, including those by Marques and Jirsa (1975), Pinc et al (1977), Hamad et al. (193), Ramirez and Russel (2008), Lee and Park (2010), and Chun et al. (2017b). In each section, specimens not used to develop descriptive equations are identified.

B.1 DRAWINGS AND REINFORCEMENT LAYOUTS FOR NO. 14 AND NO. 18 BAR SPECIMENS TESTED IN CURRENT STUDY

This section presents elevation and cross-sectional drawings of the No. 14 and No. 18 bar specimens tested in this study, showing the details of the reinforcement layouts. In the cross-sectional drawings, confining reinforcement is omitted for clarity.

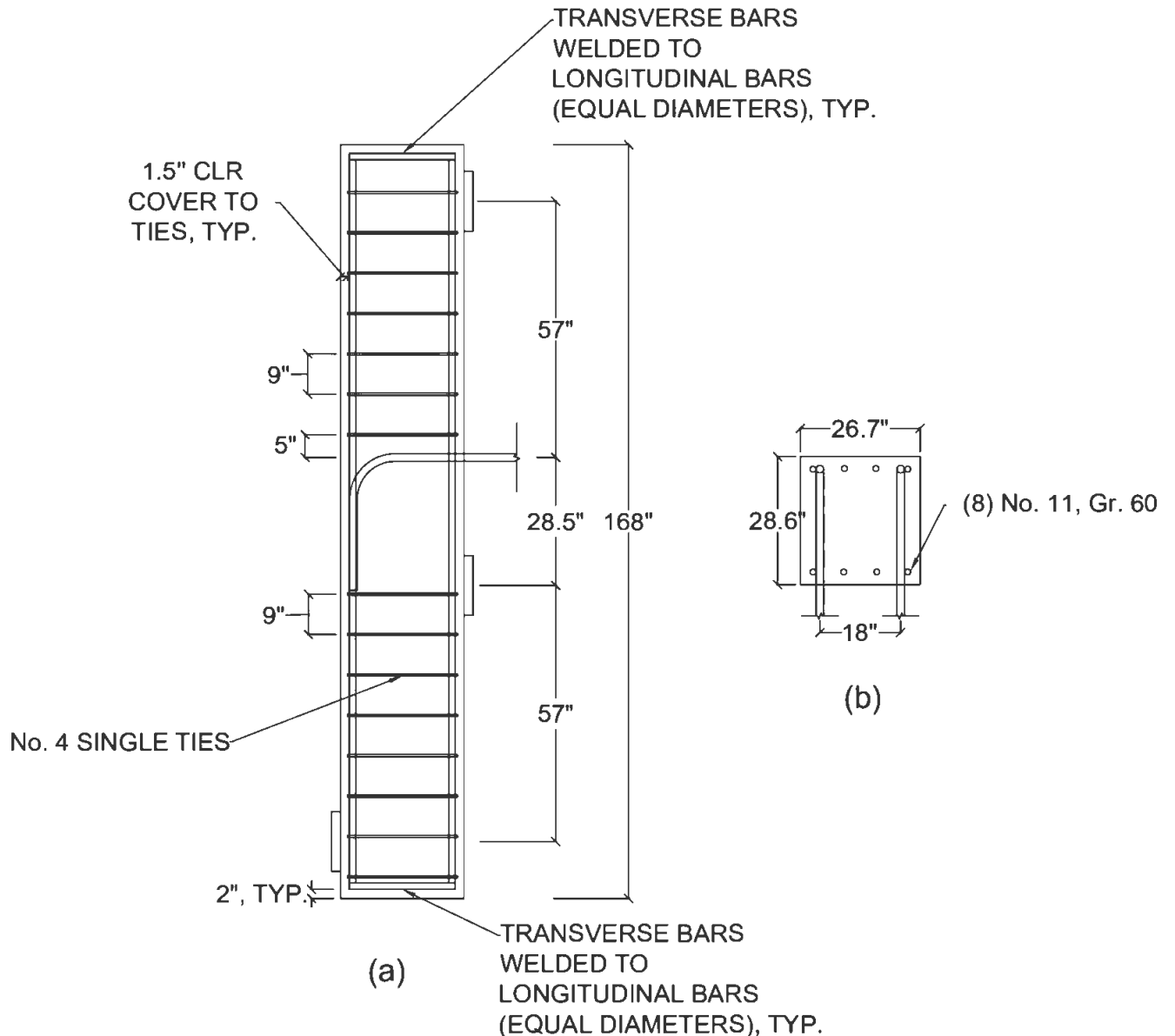


Figure B.1 Details of reinforcement layout for No. 14 hooked bar specimen H14-1: (a) elevation, (b) cross-section

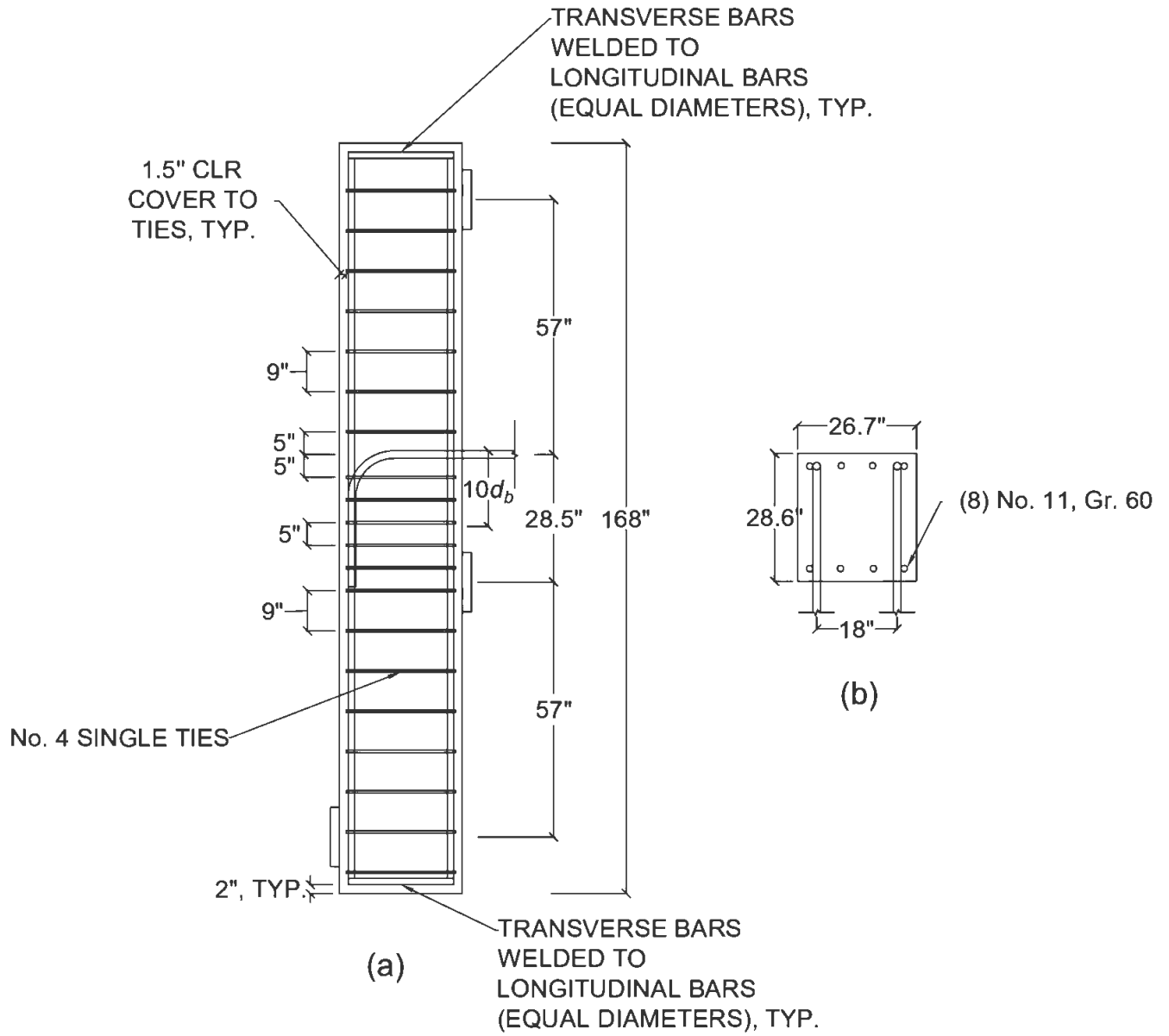


Figure B.2 Details of reinforcement layout for No. 14 hooked bar specimen H14-2: (a) elevation, (b) cross-section

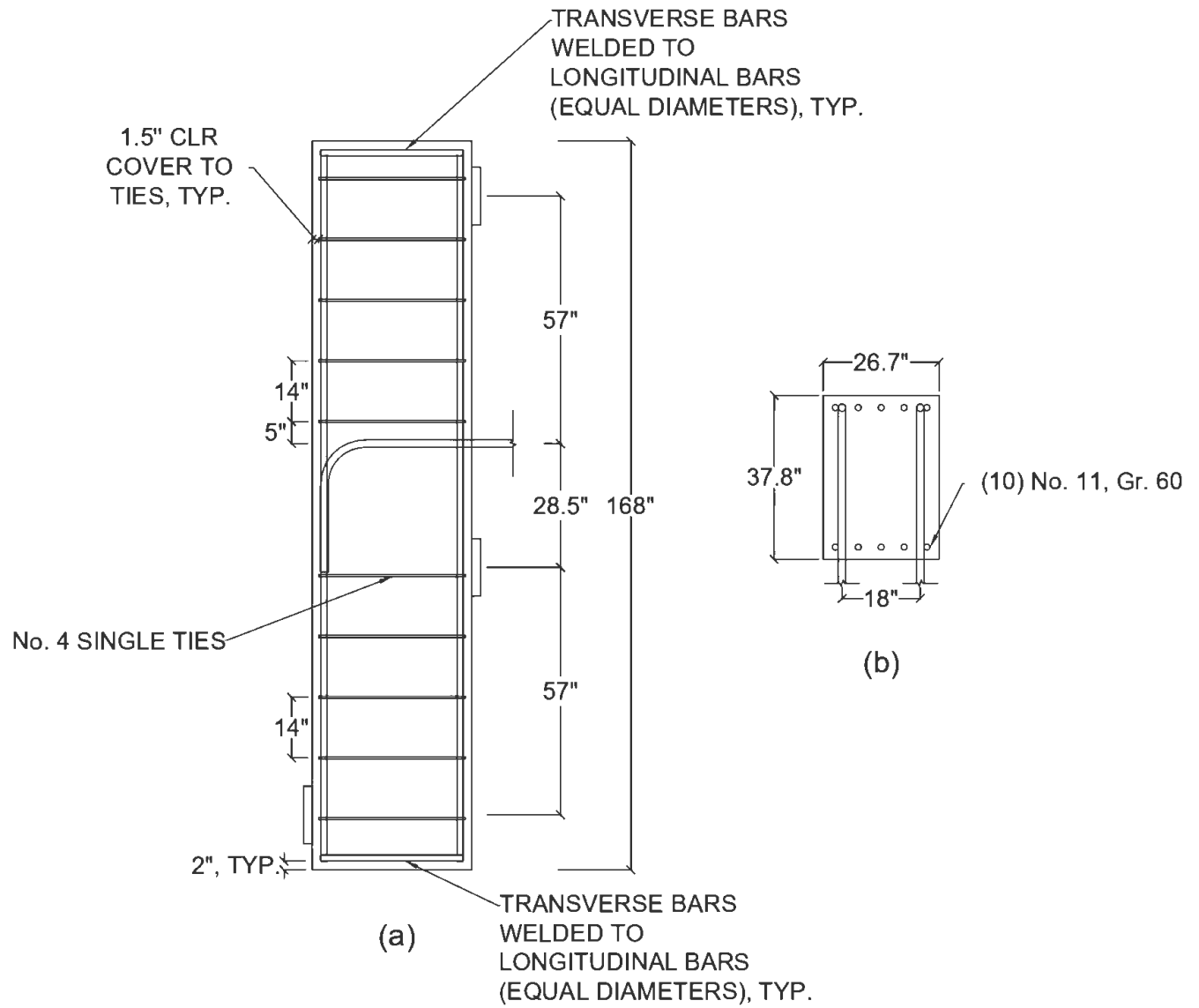


Figure B.3 Details of reinforcement layout for No. 14 hooked bar specimen H14-3: (a) elevation, (b) cross-section

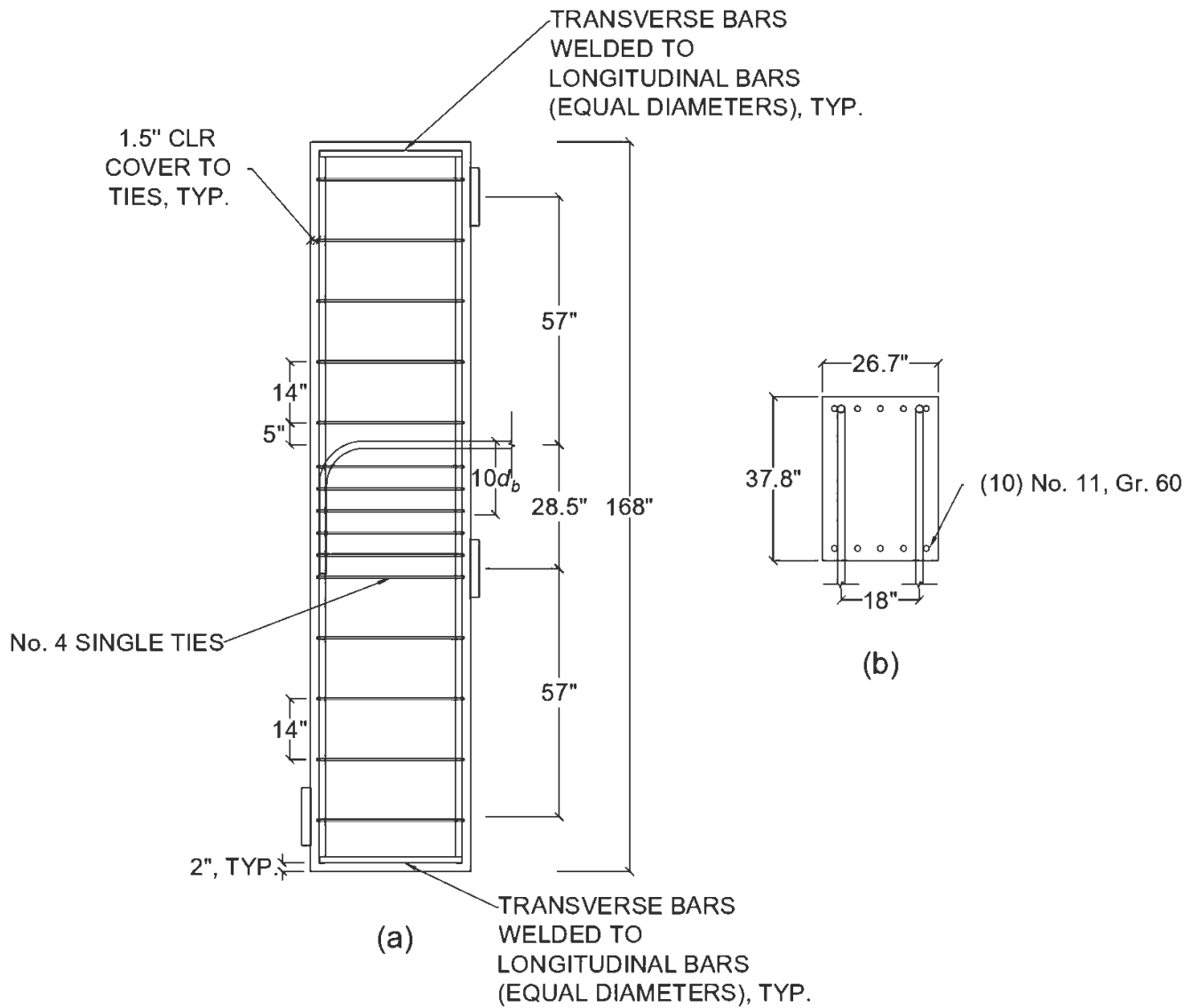


Figure B.4 Details of reinforcement layout for No. 14 hooked bar specimen H14-3: (a) elevation, (b) cross-section

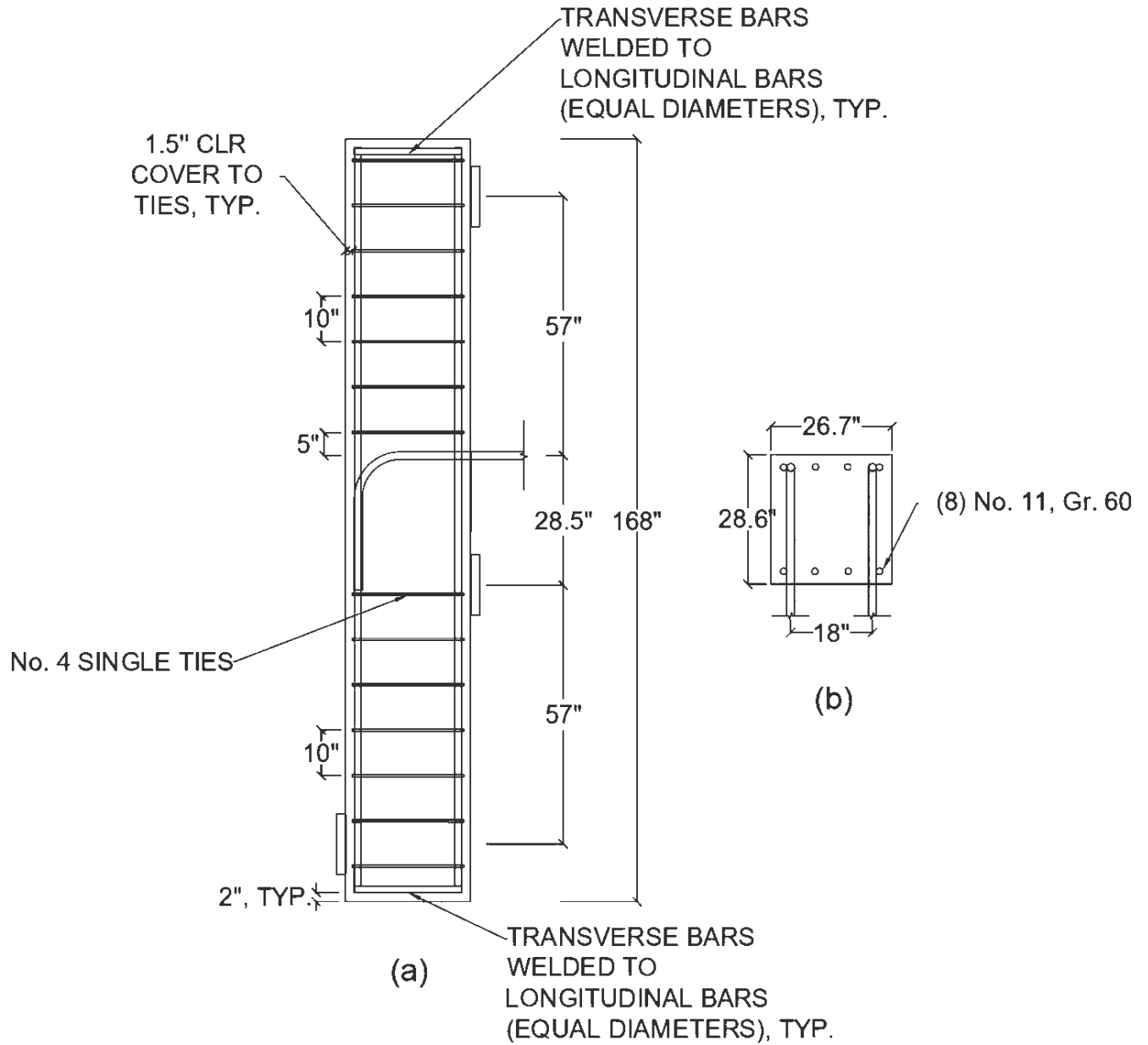


Figure B.5 Details of reinforcement layout for No. 14 hooked bar specimen H14-15: (a) elevation, (b) cross-section

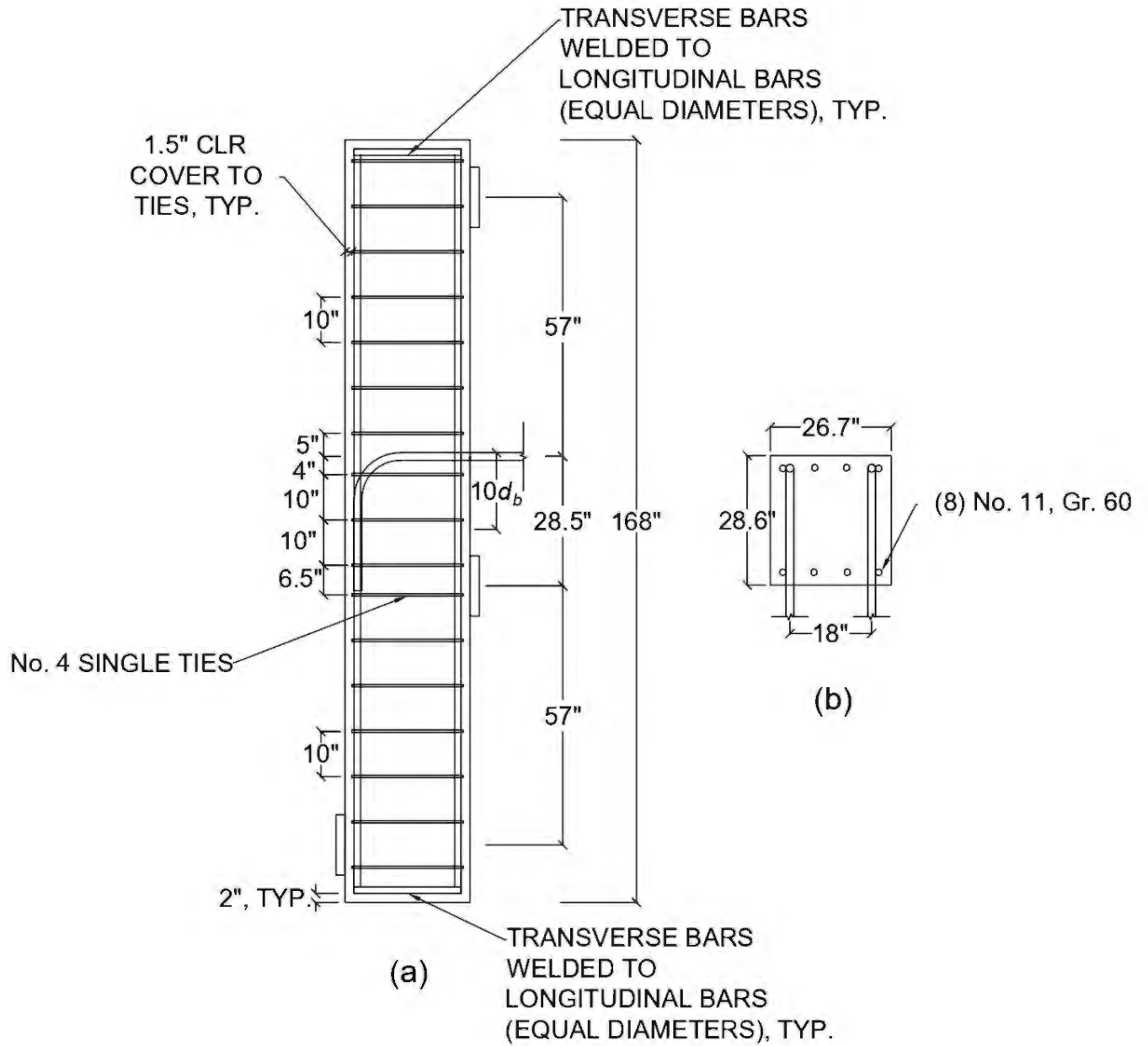


Figure B.6 Details of reinforcement layout for No. 14 hooked bar specimen H14-16: (a) elevation, (b) cross-section

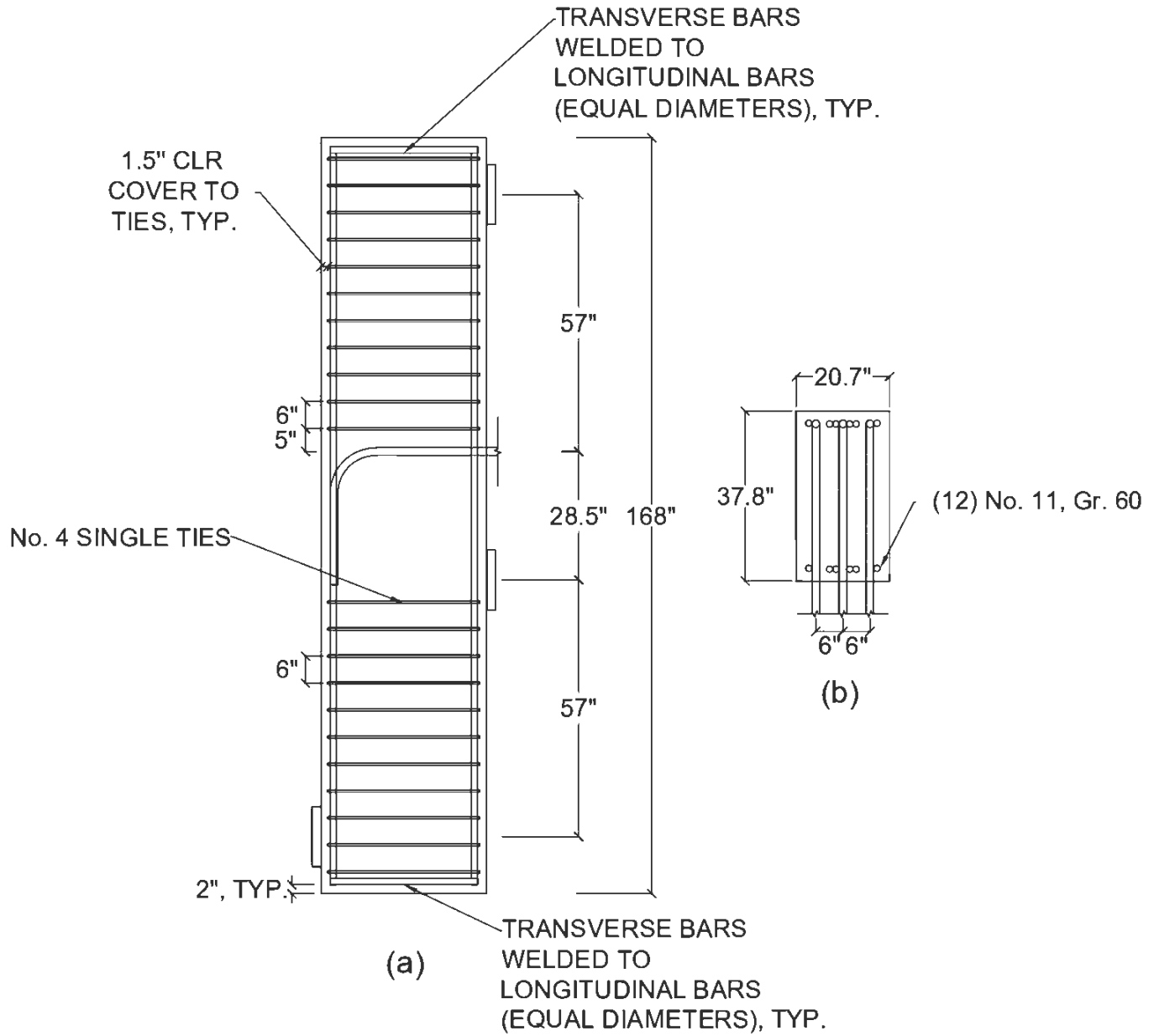


Figure B.7 Details of reinforcement layout for No. 14 hooked bar specimen H14-7: (a) elevation, (b) cross-section

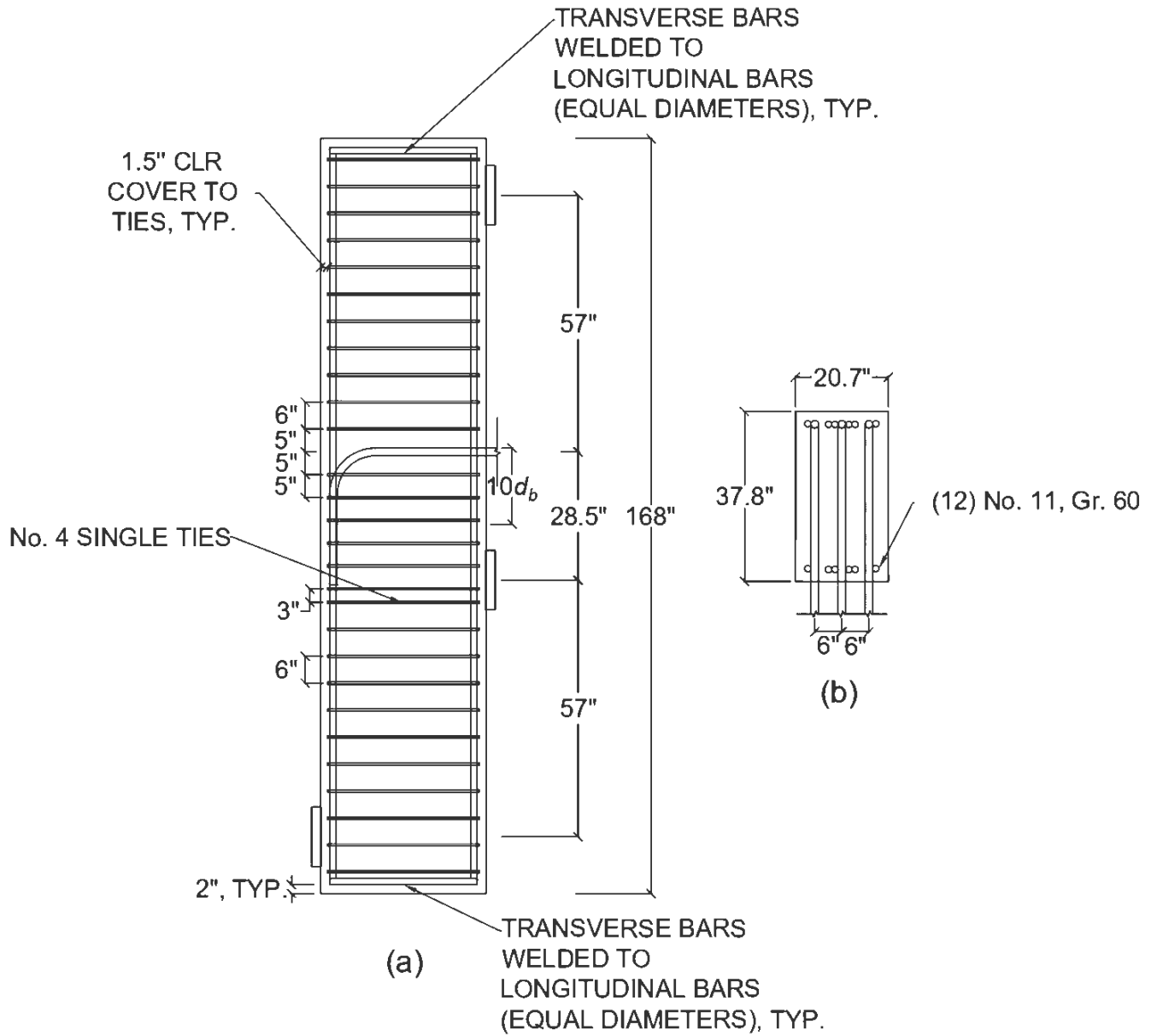


Figure B.8 Details of reinforcement layout for No. 14 hooked bar specimen H14-8: (a) elevation, (b) cross-section

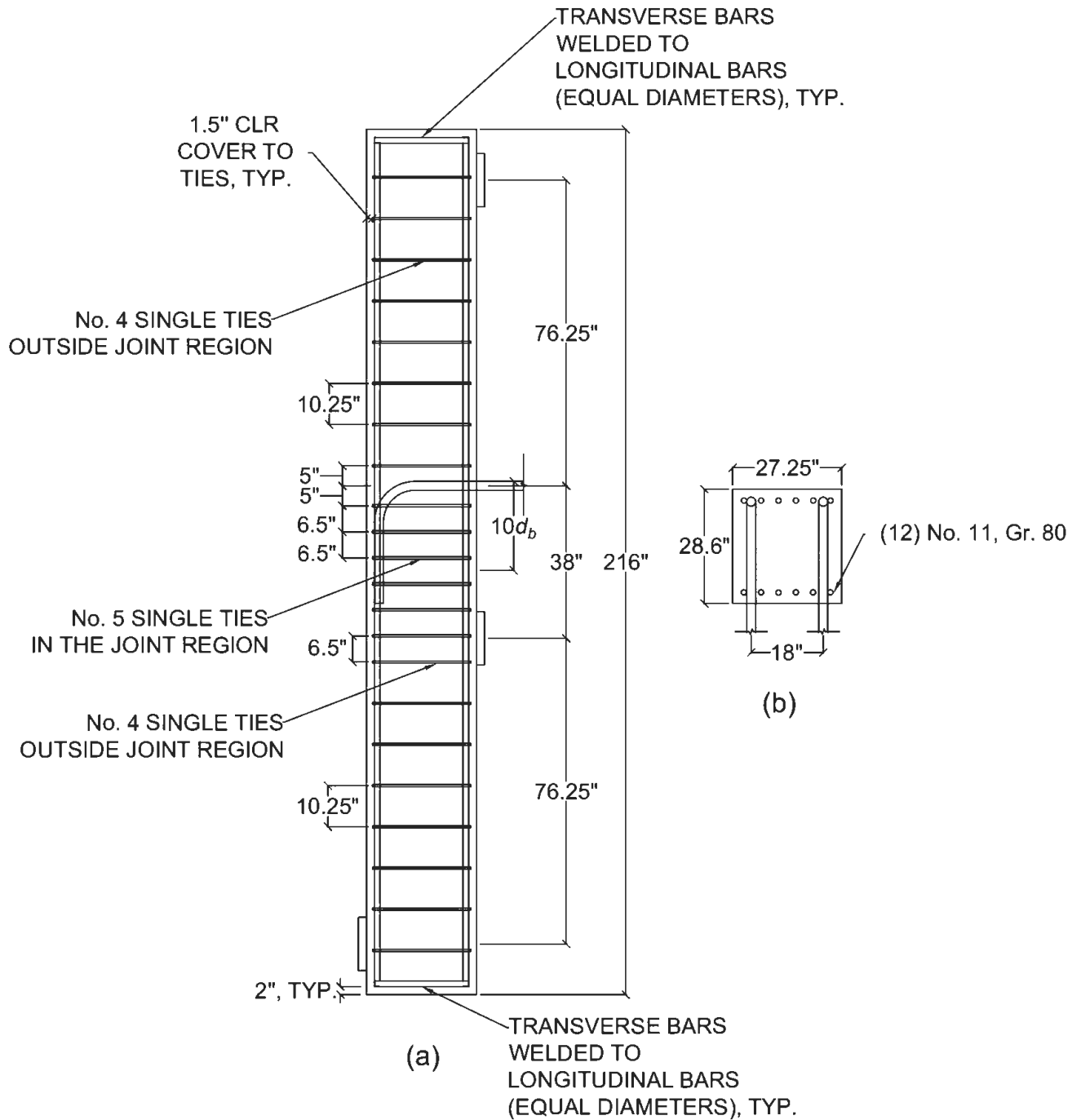


Figure B.9 Details of reinforcement layout for No. 18 hooked bar specimen H18-1: (a) elevation, (b) cross-section

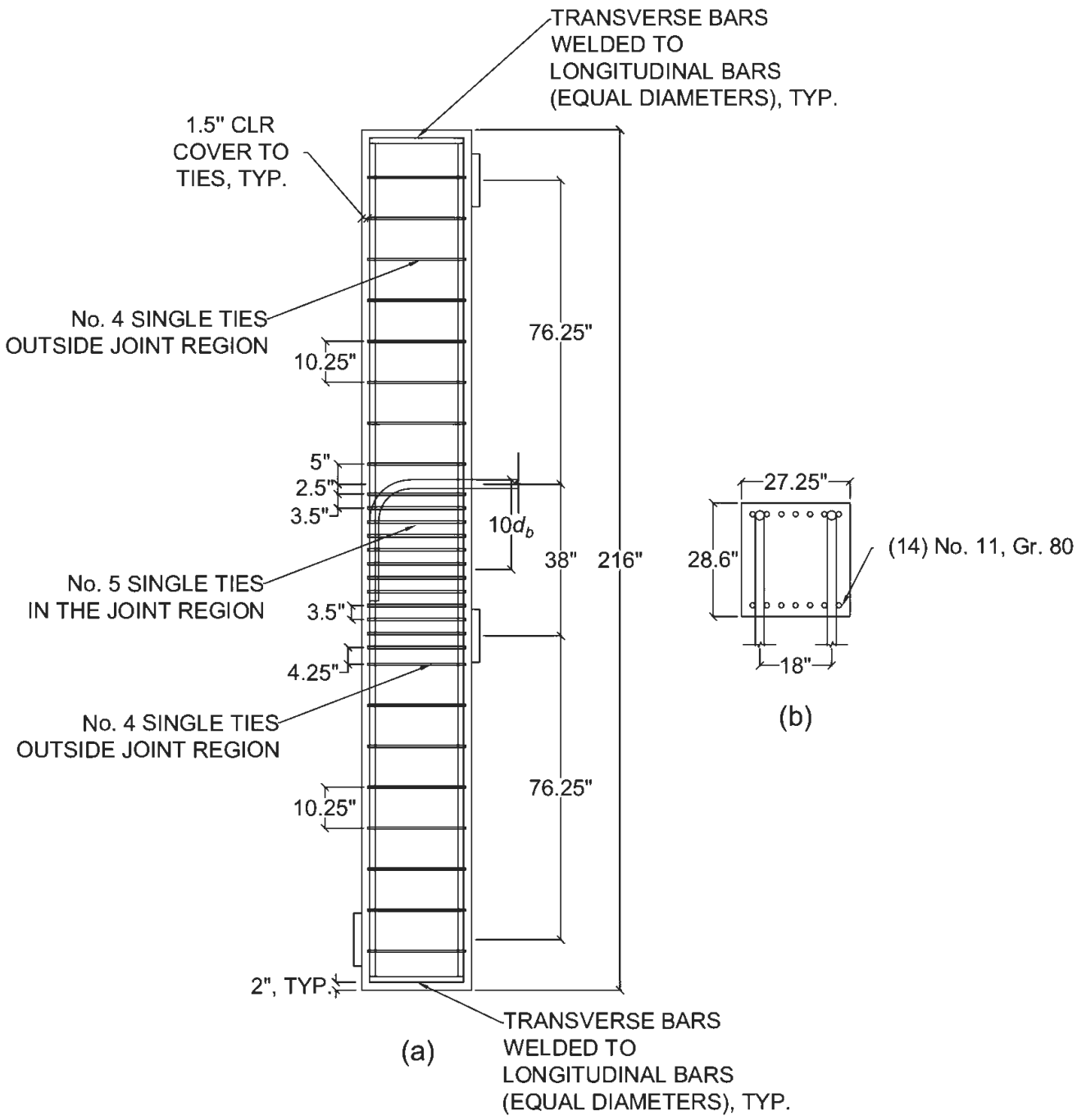


Figure B.10 Details of reinforcement layout for No. 18 hooked bar specimen H18-2: (a) elevation, (b) cross-section

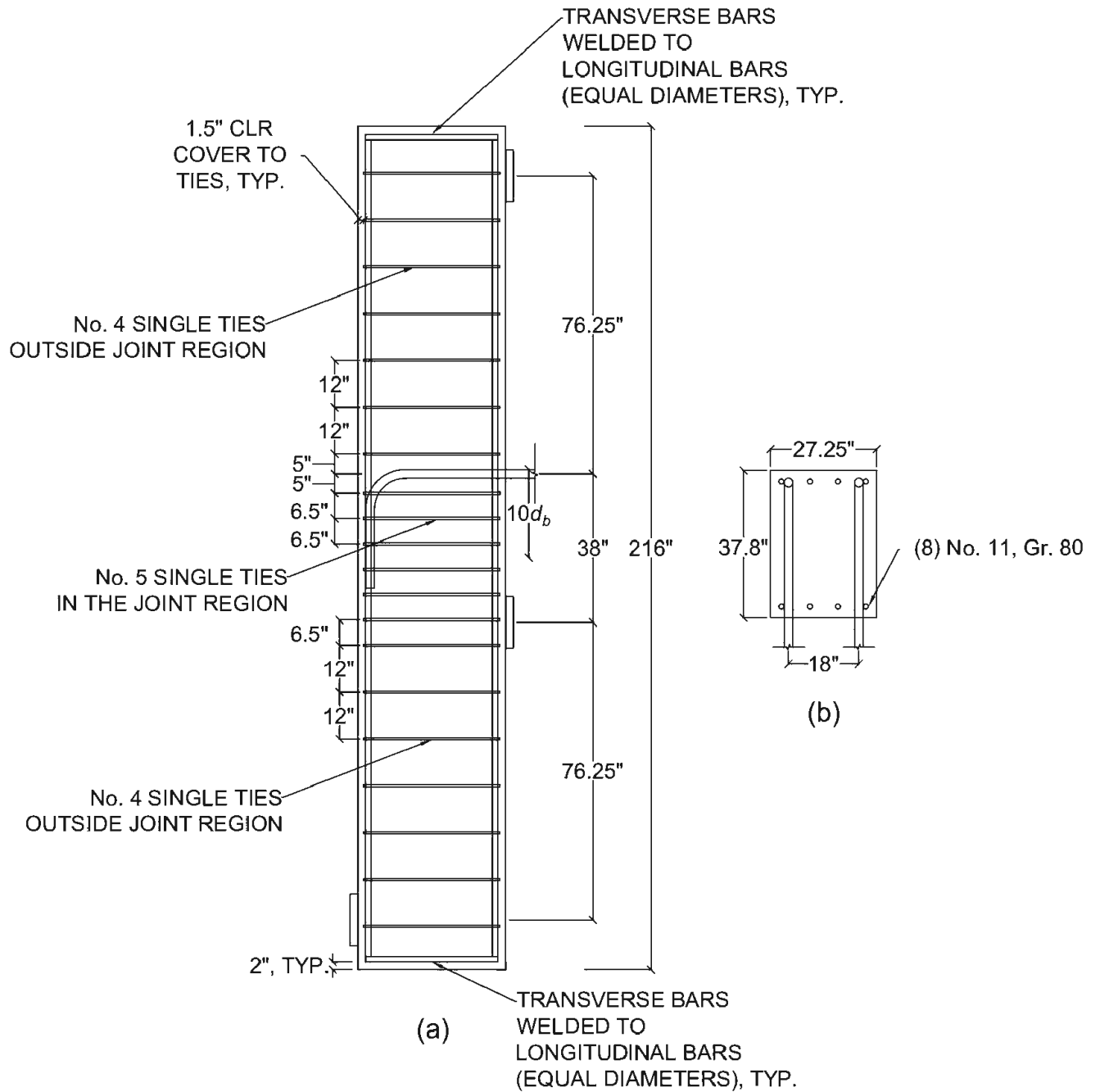


Figure B.11 Details of reinforcement layout for No. 18 hooked bar specimen H18-3: (a) elevation, (b) cross-section

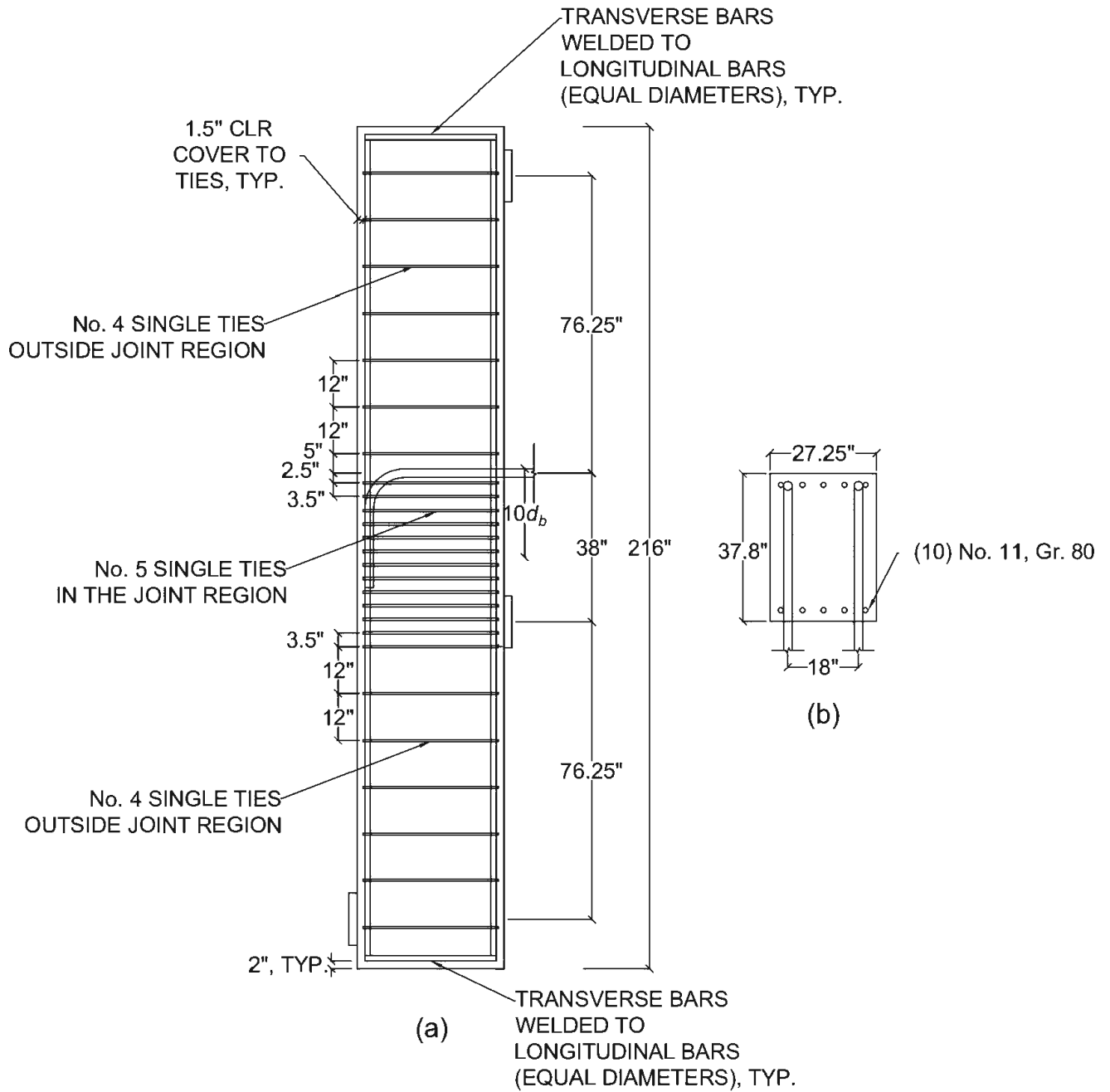


Figure B.12 Details of reinforcement layout for No. 18 hooked bar specimen H18-4: (a) elevation, (b) cross-section

B.2 DETAILED PROPERTIES AND TEST RESULTS FOR NO. 14 AND NO. 18 BAR SPECIMENS TESTED IN CURRENT STUDY

Table B.1 Detailed properties and test results for No. 14 and No. 18 bar specimens tested in current study

ID	Designation	n	Hook	ℓ_{eh}	$\ell_{eh,avg}$	f_{cm}	Age	d_b	A_b
				in.	in.	psi	Days	in.	in. ²
H14-1	(2@10.6)14-15-i-3.5-2-26.6	2	A	27.3	27.0	12,980	77	1.693	2.25
			B	26.8					
H14-2	(2@10.6)14-15-5#4-i-3.5-2-26.6	2	A	24.5	24.8	13,010	88	1.693	2.25
			B	25.0					
H14-3	(2@10.6)14-15-i-3.5-2-35.8	2	A	36.8	36.7	8,100	49	1.693	2.25
			B	36.6					
H14-4	(2@10.6)14-15-5#4-i-3.5-2-35.8	2	A	34.9	34.9	7,570	53	1.693	2.25
			B	35.0					
H14-15	(2@10.6)14-7-i-3.5-2-26.6	2	A	26.5	26.5	6,980	38	1.693	2.25
			B	26.3					
H14-16	(2@10.6)14-7-3#4-i-3.5-2-26.6	2	A	26.0	25.9	6,810	44	1.693	2.25
			B	25.8					
H14-7	(3@3.5)14-6-i-3.5-2-35.8	3	A	36.5	36.4	6,390	27	1.693	2.25
			B	36.5					
			C	36.3					
H14-8	(3@3.5)14-6-5#4-i-3.5-2-35.8	3	A	36.3	36.6	6,650	33	1.693	2.25
			B	37.5					
			C	36.0					
H18-1	(2@8.0)18-16-6#5-i-3.5-2-26.6	2	A	28.5	28.5	15,310	41	2.257	4.00
			B	28.5					
H18-2	(2@8.0)18-16-12#5-i-3.5-2-26.6	2	A	28.5	27.0	15,770	46	2.257	4.00
			B	25.5					
H18-3	(2@8.0)18-7-6#5-i-3.5-2-35.8	2	A	36.5	36.5	7,560	85	2.257	4.00
			B	36.5					
H18-4	(2@8.0)18-7-12#5-i-3.5-2-35.8	2	A	36.4	36.4	7,610	113	2.257	4.00
			B	36.4					

Table B.1 Cont. Detailed properties and test results for No. 14 and No. 18 bar specimens tested in current study

ID	b	h	h_{cl}	b_{BP}	d_{eff}	d_{eff}/ℓ_{eh}	θ	c_{so}	c_{bh}	s	s/d_b	Bar spacing
	in.	in.	in.	in.	in.		°	in.	in.	in.		
H14-1	26.7	28.6	25.5	6	28.05	1.04	46.6	3.5	2.0	18	10.6	Wide
H14-2	26.7	28.6	25.5	6	28.60	1.15	49.0	3.5	2.0	18	10.6	Wide
H14-3	26.7	37.8	25.5	6	30.21	0.82	37.9	3.5	2.0	18	10.6	Wide
H14-4	26.7	37.8	25.5	6	30.19	0.87	39.3	3.5	2.0	18	10.6	Wide
H14-15	26.7	28.6	25.5	6	29.08	1.10	47.1	3.5	2.0	18	10.6	Wide
H14-16	26.7	28.6	25.5	6	29.83	1.15	47.8	3.5	2.0	18	10.6	Wide
H14-7	20.7	37.8	24.0	9	33.20	0.91	38.1	3.5	2.0	6	3.5	Close
H14-8	20.7	37.8	24.0	9	34.70	0.95	37.9	3.5	2.0	6	3.5	Close
H18-1	27.25	28.6	35.2	6	38.26	1.34	53.2	3.5	2.0	18	8.0	Wide
H18-2	27.25	28.6	35.2	6	38.90	1.44	54.7	3.5	2.0	18	8.0	Wide
H18-3	27.25	37.8	33.7	9	39.96	1.09	46.3	3.5	2.0	18	8.0	Wide
H18-4	27.25	37.8	33.7	9	40.90	1.12	46.3	3.5	2.0	18	8.0	Wide

Table B.1 Cont. Detailed properties and test results for No. 14 and No. 18 bar specimens tested in current study

ID	d_{to}	N_{tr}	n_{tr}	n_d	d_{tr}	A_{tr}	A_{th}	A_{hs}	A_{tr}/A_{hs}	L. C.
	in.				in.	in. ²	in. ²	in. ²		
H14-1	0.5	0	0	0	0.5	0.2	0	4.50	0	A
H14-2	0.5	5	3	6	0.5	0.2	1.2	4.50	0.267	A
H14-3	0.5	0	0	0	0	0	0	4.50	0	A
H14-4	0.5	5	3	6	0.5	0.2	1.2	4.50	0.267	A
H14-15	0.5	0	0	0	0	0	0	4.50	0	A
H14-16	0.5	3	2	4	0.5	0.2	0.8	4.50	0.178	A
H14-7	0.5	0	0	0	0	0	0	6.75	0	A
H14-8	0.5	5	3	6	0.625	0.31	1.86	6.75	0.276	A
H18-1	0.5	6	3	6	0.625	0.31	1.86	8.00	0.233	A
H18-2	0.5	12	6	12	0.625	0.31	3.72	8.00	0.465	A
H18-3	0.5	6	3	6	0.625	0.31	1.86	8.00	0.233	A
H18-4	0.5	12	6	12	0.625	0.31	3.72	8.00	0.465	A

Table B.1 Cont. Detailed properties and test results for No. 14 and No. 18 bar specimens tested in current study

ID	Δ_{max}	Δ_{ind}	T_{max}	$f_{s,max}$	T_{ind}	T_{total}	T	f_{su}	Failure Type
	in.	in.	kips	ksi	kips	kips	kips	ksi	
H14-1	0.52	0.27	250.1	111.2	244.2	480.0	240.0	106.7	CB
	1.53	0.02	236.3	105.0	235.8				
H14-2	0.41	0.41	296.4	131.8	296.1	587.8	293.9	130.6	CB/SS
	0.02	0.02	292.2	129.9	291.8				
H14-3	0.11	0.02	289.1	128.5	280	558.2	279.1	124.0	CB/SS
	1.39	0.26	278.8	123.9	278.3				
H14-4*	0.72	0.13	259.7	115.4	259.3	537.0	268.5	119.3	SS
	0.95	0.02	277.7	123.4	246.2				
H14-15*	0.66	0.08	206.0	91.6	181.7	393.0	196.5	87.3	CB
	0.15	0.15	187.1	83.1	186.8				
H14-16*	0.18	0.08	229.5	102.0	229.4	470.6	235.3	104.6	CB
	1.36	0.07	241.0	107.1	203				
H14-7	0.97	0.07	251.7	111.9	251.7	752.4	250.8	111.5	CB
	0.14	0.00	250.4	111.3	250.4				
	1.17	0.28	250.3	111.2	250.3				
H14-8	1.72	0.31	314.6	139.8	297.1	894.6	298.2	132.5	SS
	0.48	0.28	329.5	146.4	301.1				
	1.60	0.12	296.7	131.9	296.4				
H18-1	0.32	0.11	357.6	89.4	356.8	716.4	358.2	89.6	CB
	1.26	0.24	375.9	94.0	359.5				
H18-2	1.61	0.22	444.9	111.2	444.6	890.0	445.0	111.3	SS
	0.67	0.37	445.3	111.3	445.3				
H18-3	0.47	0.35	370.5	92.6	370.5	742.8	371.4	92.9	CB
	0.80	0.36	372.4	93.1	372.4				
H18-4*	0.41	0.37	437.7	109.4	417.2	855.8	427.9	107.0	CB
	0.46	0.18	418.6	104.7	418.1				

* Bars failed independently, so T is the average of the maximum force on individual bar

B.3 SPECIMENS TESTED AT THE UNIVERSITY OF KANSAS

This section presents the specimens tested at the University of Kansas, including No. 5, No. 8, and No. 11 bar specimens tested by Searle et al. (2014), Sperry et al. (2015a, 2015b, 2017a, 2017b, 2018), Yasso et al. (2017), Ajaam et al. (2017, 2018), and No. 14 and No. 18 bar specimens tested in this study. Specimens are tabulated in six categories: widely-spaced bars without confining reinforcement (Table B2), closely-spaced bars without confining reinforcement (Table B3), widely-spaced bars with confining reinforcement (Table B4), closely-spaced bars with confining reinforcement (Table B5), specimens with bars outside column core (Table B6), and specimens with $d_{eff}/\ell_{eh} > 1.5$ (Table B7). In each category, specimens not used to develop descriptive equations, Eq. (4.5) and (4.7), are identified, if any.

Table B.2 Detailed properties and test results for hooked bar specimens having widely-spaced bars without confining reinforcement tested at the University of Kansas

SN	ID	b	h	$\ell_{eh,avg}$	f_{cm}	d_b	A_b	s	s/db
		in.	in.	in.	psi	in.	in. ²	in.	
1	5-5-90-0-i-2.5-2-8	13.0	10.1	8.1	4830	0.625	0.31	7.4	11.8
2	5-5-90-0-i-2.5-2-10	12.7	11.4	9.4	5230	0.625	0.31	7.1	11.4
3	5-5-90-0-i-2.5-2-7	13.0	8.9	6.9	5190	0.625	0.31	7.4	11.8
4	5-8-90-0-i-2.5-2-6	12.6	8.8	6.8	8450	0.625	0.31	7.0	11.2
5	5-8-90-0-i-2.5-2-6(1)	13.2	8.3	6.3	9080	0.625	0.31	7.6	12.2
6	5-8-90-0-i-2.5-2-8	12.9	9.8	7.8	8580	0.625	0.31	7.3	11.7
7	5-12-90-0-i-2.5-2-10	12.9	12.5	10.5	10290	0.625	0.31	7.3	11.7
8	5-12-90-0-i-2.5-2-5	12.7	6.9	4.9	11600	0.625	0.31	7.1	11.4
9	5-15-90-0-i-2.5-2-5.5	12.9	7.9	5.9	15800	0.625	0.31	7.3	11.7
10	5-15-90-0-i-2.5-2-7.5	12.9	9.3	7.3	15800	0.625	0.31	7.3	11.7
11	5-5-90-0-i-3.5-2-10	14.7	12.4	10.4	5190	0.625	0.31	7.1	11.4
12	5-5-90-0-i-3.5-2-7	15.2	9.6	7.6	5190	0.625	0.31	7.6	12.2
13	5-8-90-0-i-3.5-2-6	14.9	8.3	6.3	8580	0.625	0.31	7.3	11.7
14	5-8-90-0-i-3.5-2-6(1)	15.1	8.6	6.6	9300	0.625	0.31	7.5	12.0
15	5-8-90-0-i-3.5-2-8	15.4	10.6	8.6	8380	0.625	0.31	7.8	12.5
16	5-12-90-0-i-3.5-2-5	15.2	7.4	5.4	10410	0.625	0.31	7.6	12.2
17	5-8-180-0-i-2.5-2-7	12.5	9.3	7.3	9080	0.625	0.31	6.9	11.0
18	5-8-180-0-i-3.5-2-7	15.4	9.3	7.3	9080	0.625	0.31	7.8	12.5

Table B.2 Cont. Detailed properties and test results for hooked bar specimens having widely-spaced bars without confining reinforcement tested at the University of Kansas

SN	n	A_{th}	A_{hs}	A_{th}/A_{hs}	h_{cl}	x_{mid}	d_{eff}	d_{eff}/ℓ_{eh}	θ
		in. ²	in. ²		in.	in.	in.		°
1	2	0	0.62	0	5.25	9.44	6.75	0.83	49.4
2	2	0	0.62	0	5.25	9.44	6.76	0.72	45.1
3	2	0	0.62	0	5.25	9.44	6.41	0.93	53.8
4	2	0	0.62	0	5.25	9.44	6.25	0.92	54.2
5	2	0	0.62	0	5.25	9.44	5.93	0.94	56.3
6	2	0	0.62	0	5.25	9.44	6.28	0.81	50.4
7	2	0	0.62	0	5.25	9.44	6.38	0.61	41.9
8	2	0	0.62	0	5.25	9.44	5.72	1.17	62.6
9	2	0	0.62	0	5.25	9.44	5.83	0.99	58.0
10	2	0	0.62	0	5.25	9.44	6.00	0.82	52.3
11	2	0	0.62	0	5.25	9.44	6.88	0.66	42.2
12	2	0	0.62	0	5.25	9.44	6.25	0.82	51.2
13	2	0	0.62	0	5.25	9.44	5.97	0.95	56.3
14	2	0	0.62	0	5.25	9.44	5.88	0.89	55.0
15	2	0	0.62	0	5.25	9.44	6.17	0.72	47.7
16	2	0	0.62	0	5.25	9.44	5.76	1.07	60.2
17	2	0	0.62	0	5.25	9.44	6.11	0.84	52.3
18	2	0	0.62	0	5.25	9.44	6.04	0.83	52.3

Table B.2 Cont. Detailed properties and test results for hooked bar specimens having widely-spaced bars without confining reinforcement tested at the University of Kansas

SN	T	T_h ^[1]	T/T_h	f_{su}	$f_{su}/f_{s,calc}$ ^[2]	$f_{su}/f_{s,calc}$ ^[3]
	lb	lb		ksi		
1	32448	28627	1.13	104.7	1.34	1.34
2	33583	34515	0.97	108.3	1.17	1.17
3	26265	24463	1.07	84.7	1.25	1.25
4	29570	27604	1.07	95.4	1.27	1.27
5	22425	25885	0.87	72.3	1.02	1.02
6	31673	32267	0.98	102.2	1.18	1.18
7	41657	47180	0.88	134.4	1.10	1.10
8	19220	20998	0.92	62.0	1.06	1.06
9	32511	28126	1.16	104.9	1.37	1.37
10	42221	35598	1.19	136.2	1.44	1.44
11	41927	38517	1.09	135.2	1.33	1.33
12	26516	27223	0.97	85.5	1.15	1.15
13	25475	25476	1.00	82.2	1.17	1.17
14	24541	27436	0.89	79.2	1.06	1.06
15	32745	35710	0.92	105.6	1.11	1.11
16	22121	22680	0.98	71.4	1.13	1.13
17	27108	30467	0.89	87.4	1.06	1.06
18	30754	30467	1.01	99.2	1.21	1.21

^[1] Based on descriptive equations, Eq. (4.5) and (4.7)

^[2] Based on design equation, Eq. (6.18), using full expression for ψ_r , Eq. (6.14)

^[3] Based on design equation, Eq. (6.18), using simplified expression for ψ_r , Eq. (6.15)

Table B.2 Cont. Detailed properties and test results for hooked bar specimens having widely-spaced bars without confining reinforcement tested at the University of Kansas

SN	ID	<i>b</i>	<i>h</i>	$\ell_{eh,avg}$	f_{cm}	d_b	A_b	<i>s</i>	s/d_b
		in.	in.	in.	psi	in.	in. ²	in.	
19	8-5-90-0-i-2.5-2-16	16.5	18.4	16.4	4980	1	0.79	10.5	10.5
20	8-5-90-0-i-2.5-2-9.5	16.5	11.6	9.6	5140	1	0.79	10.5	10.5
21	8-5-90-0-i-2.5-2-12.5	16.8	15.3	13.3	5240	1	0.79	10.8	10.8
22	8-5-90-0-i-2.5-2-18	17.5	20.7	18.7	5380	1	0.79	11.5	11.5
23	8-5-90-0-i-2.5-2-13	16.8	15.4	13.4	5560	1	0.79	10.8	10.8
24	8-5-90-0-i-2.5-2-15(1)	16.6	16.9	14.9	5910	1	0.79	10.6	10.6
25	8-5-90-0-i-2.5-2-15	16.5	16.8	14.8	6210	1	0.79	10.5	10.5
26	8-5-90-0-i-2.5-2-10	17.3	12.0	10.0	5920	1	0.79	11.3	11.3
27	8-8-90-0-i-2.5-2-8	15.6	10.4	8.4	7910	1	0.79	9.6	9.6
28	8-8-90-0-i-2.5-2-10	16.0	11.6	9.6	7700	1	0.79	10.0	10.0
29	8-8-90-0-i-2.5-2-8(1)	16.5	10.0	8.0	8780	1	0.79	10.5	10.5
30	8-8-90-0-i-2.5-2-9	17.0	11.5	9.5	7710	1	0.79	11.0	11.0
31	8-12-90-0-i-2.5-2-9	16.6	11.0	9.0	11160	1	0.79	10.6	10.6
32	8-12-90-0-i-2.5-2-12.5	17.1	14.8	12.8	11850	1	0.79	11.1	11.1
33	8-12-90-0-i-2.5-2-12	16.8	14.1	12.1	11760	1	0.79	10.8	10.8
34	8-15-90-0-i-2.5-2-8.5	17.0	10.8	8.8	15800	1	0.79	11.0	11.0
35	8-15-90-0-i-2.5-2-13	16.9	14.8	12.8	15800	1	0.79	10.9	10.9
36	8-5-90-0-i-3.5-2-18	18.4	20.5	18.5	5380	1	0.79	10.4	10.4
37	8-5-90-0-i-3.5-2-13	18.4	15.4	13.4	5560	1	0.79	10.4	10.4
38	8-5-90-0-i-3.5-2-15(2)	18.5	17.3	15.3	5180	1	0.79	10.5	10.5
39	8-5-90-0-i-3.5-2-15(1)	19.1	17.3	15.3	6440	1	0.79	11.1	11.1
40	8-8-90-0-i-3.5-2-8(1)	18.0	9.8	7.8	7910	1	0.79	10.0	10.0
41	8-8-90-0-i-3.5-2-10	18.0	11.8	9.8	7700	1	0.79	10.0	10.0
42	8-8-90-0-i-3.5-2-8(2)	19.0	10.3	8.3	8780	1	0.79	11.0	11.0
43	8-12-90-0-i-3.5-2-9	18.8	11.0	9.0	11160	1	0.79	10.8	10.8
44	8-8-90-0-i-4-2-8	19.5	9.8	7.8	8740	1	0.79	10.5	10.5
45	8-5-180-0-i-2.5-2-11	16.8	13.0	11.0	4550	1	0.79	10.8	10.8
46	8-5-180-0-i-2.5-2-14	16.8	16.0	14.0	4840	1	0.79	10.8	10.8

Table B.2 Cont. Detailed properties and test results for hooked bar specimens having widely-spaced bars without confining reinforcement tested at the University of Kansas

SN	n	A_{th}	A_{hs}	A_{th}/A_{hs}	h_{cl}	x_{mid}	d_{eff}	d_{eff}/ℓ_{eh}	θ
		in. ²	in. ²		in.	in.	in.		°
19	2	0	1.58	0	10.00	14.19	12.98	0.79	40.9
20	2	0	1.58	0	10.00	14.19	11.56	1.20	55.9
21	2	0	1.58	0	10.00	14.19	12.23	0.92	46.8
22	2	0	1.58	0	10.00	14.19	12.59	0.67	37.2
23	2	0	1.58	0	10.00	14.19	12.14	0.91	46.6
24	2	0	1.58	0	10.00	14.19	12.03	0.81	43.6
25	2	0	1.58	0	10.00	14.19	12.34	0.83	43.8
26	2	0	1.58	0	10.00	14.19	11.45	1.15	54.8
27	2	0	1.58	0	10.00	14.19	11.32	1.35	59.4
28	2	0	1.58	0	10.00	14.19	11.48	1.20	55.9
29	2	0	1.58	0	10.00	14.19	10.92	1.37	60.6
30	2	0	1.58	0	10.00	14.19	10.95	1.15	56.2
31	2	0	1.58	0	10.00	14.19	10.98	1.22	57.6
32	2	0	1.58	0	10.00	14.19	11.2	0.87	47.9
33	2	0	1.58	0	10.00	14.19	11.21	0.93	49.5
34	2	0	1.58	0	10.00	14.19	10.59	1.20	58.2
35	2	0	1.58	0	10.00	14.19	11.06	0.86	47.9
36	2	0	1.58	0	10.00	14.19	12.9	0.70	37.5
37	2	0	1.58	0	10.00	14.19	12.03	0.90	46.6
38	2	0	1.58	0	10.00	14.19	12.72	0.83	42.8
39	2	0	1.58	0	10.00	14.19	11.86	0.77	42.8
40	2	0	1.58	0	10.00	14.19	11.11	1.42	61.2
41	2	0	1.58	0	10.00	14.19	11.42	1.17	55.4
42	2	0	1.58	0	10.00	14.19	10.91	1.31	59.7
43	2	0	1.58	0	10.00	14.19	11.04	1.23	57.6
44	2	0	1.58	0	10.00	14.19	10.8	1.38	61.2
45	2	0	1.58	0	10.00	14.19	11.73	1.07	52.2
46	2	0	1.58	0	10.00	14.19	11.76	0.84	45.4

Table B.2 Cont. Detailed properties and test results for hooked bar specimens having widely-spaced bars without confining reinforcement tested at the University of Kansas

SN	T	T_h ^[1]	T/T_h	f_{su}	$f_{su}/f_{s,calc}$ ^[2]	$f_{su}/f_{s,calc}$ ^[3]
	lb	lb		ksi		
19	83239	77119	1.08	105.4	1.34	1.34
20	44485	43023	1.03	56.3	1.22	1.22
21	65819	62044	1.06	83.3	1.29	1.29
22	80881	91128	0.89	102.4	1.12	1.12
23	65539	63611	1.03	83.0	1.26	1.26
24	63767	72772	0.88	80.7	1.08	1.08
25	75478	73243	1.03	95.5	1.28	1.28
26	47681	46834	1.02	60.4	1.21	1.21
27	45243	41893	1.08	57.3	1.27	1.27
28	51455	48197	1.07	65.1	1.27	1.27
29	36821	40872	0.90	46.6	1.06	1.06
30	35100	47659	0.74	44.4	0.88	0.88
31	49923	49807	1.00	63.2	1.20	1.20
32	66937	74791	0.89	84.7	1.11	1.11
33	65879	70129	0.94	83.4	1.16	1.16
34	43575	53569	0.81	55.2	0.98	0.98
35	78120	81087	0.96	98.9	1.21	1.21
36	95372	90050	1.06	120.7	1.34	1.34
37	68099	63611	1.07	86.2	1.31	1.31
38	87709	72211	1.21	111.0	1.50	1.50
39	70651	76766	0.92	89.4	1.14	1.14
40	43845	38595	1.14	55.5	1.32	1.32
41	55567	49309	1.13	70.3	1.34	1.34
42	42034	42571	0.99	53.2	1.16	1.16
43	60238	49807	1.21	76.3	1.45	1.45
44	37431	39692	0.94	47.4	1.10	1.10
45	46143	48332	0.95	58.4	1.13	1.13
46	49152	64218	0.77	62.2	0.93	0.93

^[1] Based on descriptive equations, Eq. (4.5) and (4.7)

^[2] Based on design equation, Eq. (6.18), using full expression for ψ_r , Eq. (6.14)

^[3] Based on design equation, Eq. (6.18), using simplified expression for ψ_r , Eq. (6.15)

Table B.2 Cont. Detailed properties and test results for hooked bar specimens having widely-spaced bars without confining reinforcement tested at the University of Kansas

SN	ID	<i>b</i>	<i>h</i>	$\ell_{eh,avg}$	f_{cm}	d_b	A_b	<i>s</i>	<i>s/d_b</i>
		in.	in.	in.	psi	in.	in. ²	in.	
47	8-8-180-0-i-2.5-2-11.5	16.5	11.3	9.3	8630	1	0.79	10.5	10.5
48	8-12-180-0-i-2.5-2-12.5	16.6	14.6	12.6	11850	1	0.79	10.6	10.6
49	8-5-180-0-i-3.5-2-11	19.0	13.6	11.6	4550	1	0.79	11.0	11.0
50	8-5-180-0-i-3.5-2-14	18.8	16.1	14.1	4840	1	0.79	10.8	10.8
51	8-15-180-0-i-2.5-2-13.5	17.0	15.6	13.6	16510	1	0.79	11.0	11.0
52	11-5-90-0-i-2.5-2-14	21.1	16.4	14.4	4910	1.41	1.56	14.7	10.4
53	11-5-90-0-i-2.5-2-26	21.1	28.0	26.0	5360	1.41	1.56	14.7	10.4
54	11-5-90-0-i-2.5-2-16	21.7	18.0	16.0	4890	1.41	1.56	15.3	10.9
55	(2@7.5) 11-8-90-0-i-2.5-2-15	17.2	16.8	14.8	7070	1.41	1.56	10.8	7.7
56	(2@7.5) 11-8-90-0-i-2.5-2-18	17.2	19.1	17.1	7070	1.41	1.56	10.8	7.7
57	11-8-90-0-i-2.5-2-17	21.2	19.6	17.6	9460	1.41	1.56	14.8	10.5
58	11-8-90-0-i-2.5-2-21	20.8	22.6	20.6	7870	1.41	1.56	14.4	10.2
59	11-8-90-0-i-2.5-2-17	21.3	19.2	17.2	8520	1.41	1.56	14.9	10.6
60	(2@7.5) 11-12-90-0-i-2.5-2-17	17.4	19.4	17.4	11476	1.41	1.56	11.0	7.8
61	11-12-90-0-i-2.5-2-17	21.1	18.5	16.5	11880	1.41	1.56	14.7	10.4
62	11-12-90-0-i-2.5-2-17.5	21.6	19.7	17.7	13330	1.41	1.56	15.2	10.8
63	11-12-90-0-i-2.5-2-25	20.9	26.6	24.6	13330	1.41	1.56	14.5	10.3
64	11-15-90-0-i-2.5-2-24	21.3	26.4	24.4	16180	1.41	1.56	14.9	10.6
65	11-15-90-0-i-2.5-2-15	20.8	16.0	14.0	14050	1.41	1.56	14.4	10.2
66	11-5-90-0-i-3.5-2-17	22.9	19.9	17.9	5600	1.41	1.56	14.5	10.3
67	11-5-90-0-i-3.5-2-14	23.1	17.0	15.0	4910	1.41	1.56	14.7	10.4
68	11-5-90-0-i-3.5-2-26	23.3	28.0	26.0	5960	1.41	1.56	14.9	10.6
69	11-8-180-0-i-2.5-2-21	20.8	23.1	21.1	7870	1.41	1.56	14.4	10.2
70	11-8-180-0-i-2.5-2-17	21.6	19.9	17.9	8520	1.41	1.56	15.2	10.8
71	11-12-180-0-i-2.5-2-17	21.1	18.6	16.6	11880	1.41	1.56	14.7	10.4
72	H14-1	26.7	28.6	27.0	12980	1.693	2.25	18.0	10.6
73	H14-3	26.7	37.8	36.7	8100	1.693	2.25	18.0	10.6
74	H14-15	26.7	28.6	26.5	6980	1.693	2.25	18.0	10.6

Table B.2 Cont. Detailed properties and test results for hooked bar specimens having widely-spaced bars without confining reinforcement tested at the University of Kansas

SN	n	A_{th}	A_{hs}	A_{th}/A_{hs}	h_{cl}	x_{mid}	d_{eff}	d_{eff}/ℓ_{eh}	θ
		in. ²	in. ²		in.	in.	in.		°
47	2	0	1.58	0	10.00	14.19	11.82	1.27	56.8
48	2	0	1.58	0	10.00	14.19	11.38	0.90	48.4
49	2	0	1.58	0	10.00	14.19	11.96	1.03	50.7
50	2	0	1.58	0	10.00	14.19	12.03	0.85	45.2
51	2	0	1.58	0	10.00	14.19	11.16	0.82	46.2
52	2	0	3.12	0	19.50	23.69	21.38	1.48	58.7
53	2	0	3.12	0	19.50	23.69	23.45	0.90	42.3
54	2	0	3.12	0	19.50	23.69	21.96	1.37	56.0
55	2	0	3.12	0	19.50	23.69	21.59	1.46	58.0
56	2	0	3.12	0	19.50	23.69	22.2	1.30	54.2
57	2	0	3.12	0	19.50	23.69	21.88	1.24	53.4
58	2	0	3.12	0	19.50	23.69	22.24	1.08	49.0
59	2	0	3.12	0	19.50	23.69	21.59	1.26	54.0
60	2	0	3.12	0	19.50	23.69	21.43	1.23	53.7
61	2	0	3.12	0	19.50	23.69	21.44	1.30	55.1
62	2	0	3.12	0	19.50	23.69	21.07	1.19	53.2
63	2	0	3.12	0	19.50	23.69	22.09	0.90	43.9
64	2	0	3.12	0	19.50	23.69	21.74	0.89	44.2
65	2	0	3.12	0	19.50	23.69	20.64	1.47	59.4
66	2	0	3.12	0	19.50	23.69	22.08	1.23	52.9
67	2	0	3.12	0	19.50	23.69	21.29	1.42	57.7
68	2	0	3.12	0	19.50	23.69	23.6	0.91	42.3
69	2	0	3.12	0	19.50	23.69	22.3	1.06	48.3
70	2	0	3.12	0	19.50	23.69	21.47	1.20	52.9
71	2	0	3.12	0	19.50	23.69	21.05	1.27	55.0
72	2	0	4.5	0	25.5	28.54	28.05	1.04	46.6
73	2	0	4.5	0	25.5	28.54	30.21	0.82	37.9
74	2	0	4.5	0	25.5	28.54	29.08	1.10	47.1

Table B.2 Cont. Detailed properties and test results for hooked bar specimens having widely-spaced bars without confining reinforcement tested at the University of Kansas

SN	T	T_h ^[1]	T/T_h	f_{su}	$f_{su}/f_{s,calc}$ ^[2]	$f_{su}/f_{s,calc}$ ^[3]
	lb	lb		ksi		
47	71484	48048	1.49	90.5	1.77	1.77
48	75208	73500	1.02	95.2	1.27	1.27
49	59292	51257	1.16	75.1	1.38	1.38
50	63504	64725	0.98	80.4	1.20	1.20
51	89916	87790	1.02	113.8	1.30	1.30
52	66590	77100	0.86	42.7	1.04	1.04
53	148727	151937	0.98	95.3	1.26	1.26
54	89396	86533	1.03	57.3	1.26	1.26
55	75313	88045	0.86	48.3	1.04	1.04
56	97379	103303	0.94	62.4	1.17	1.17
57	132055	115743	1.14	84.7	1.43	1.43
58	125126	130818	0.96	80.2	1.21	1.21
59	104779	109566	0.96	67.2	1.19	1.19
60	106718	120663	0.88	68.4	1.12	1.12
61	134371	114888	1.17	86.1	1.47	1.47
62	124622	128251	0.97	79.9	1.23	1.23
63	199743	184601	1.08	128.0	1.42	1.42
64	213265	193176	1.10	136.7	1.46	1.46
65	92168	100415	0.92	59.1	1.14	1.14
66	108122	101775	1.06	69.3	1.31	1.31
67	69514	80662	0.86	44.6	1.04	1.04
68	182254	156535	1.16	116.8	1.50	1.50
69	128123	134336	0.95	82.1	1.21	1.21
70	100453	114510	0.88	64.4	1.10	1.10
71	107461	115659	0.93	68.9	1.17	1.17
72	240000	219708	1.09	106.7	1.43	1.43
73	279100	270268	1.03	124.0	1.38	1.38
74	196500	180788	1.09	87.3	1.39	1.39

^[1] Based on descriptive equations, Eq. (4.5) and (4.7)

^[2] Based on design equation, Eq. (6.18), using full expression for ψ_r , Eq. (6.14)

^[3] Based on design equation, Eq. (6.18), using simplified expression for ψ_r , Eq. (6.15)

Table B.3 Detailed properties and test results for hooked bar specimens having closely-spaced bars without confining reinforcement tested at the University of Kansas

SN	ID	<i>b</i>	<i>h</i>	$\ell_{eh,avg}$	f_{cm}	d_b	A_b	<i>s</i>	<i>s/d_b</i>
		in.	in.	in.	psi	in.	in. ²	in.	
75	(3) 5-5-90-0-i-2.5-2-8	12.8	9.9	7.9	4830	0.625	0.31	3.6	5.8
76	(4@4) 5-5-90-0-i-2.5-2-6	13.4	7.2	5.2	6430	0.625	0.31	2.6	4.2
77	(4@4) 5-5-90-0-i-2.5-2-10	13.4	11.0	9.0	6470	0.625	0.31	2.6	4.2
78	(4@4) 5-8-90-0-i-2.5-2-6	12.5	7.9	5.9	6950	0.625	0.31	2.3	3.7
79	(3@4) 5-8-90-0-i-2.5-2-6	10.6	7.9	5.9	6950	0.625	0.31	2.5	4.0
80	(4@6) 5-8-90-0-i-2.5-2-6	17.0	7.9	5.9	6693	0.625	0.31	3.8	6.1
81	(3@6) 5-8-90-0-i-2.5-2-6	13.2	8.0	6.0	6950	0.625	0.31	3.8	6.1
82	(3@5.5) 8-5-90-0-i-2.5-2-16	17.0	18.1	16.1	6255	1	0.79	5.5	5.5
83	(3@5.5) 8-5-90-0-i-2.5-2-10	16.8	11.4	9.4	6461	1	0.79	5.4	5.4
84	(3@5.5) 8-5-90-0-i-2.5-2-8	17.0	9.8	7.8	5730	1	0.79	5.5	5.5
85	(3@3) 8-5-90-0-i-2.5-2-10	12.6	12.1	10.1	4490	1	0.79	3.3	3.3
86	(3@5) 8-5-90-0-i-2.5-2-10	16.6	12.1	10.1	4490	1	0.79	5.3	5.3
87	(3@5.5) 8-8-90-0-i-2.5-2-8	14.8	9.9	7.9	8700	1	0.79	4.4	4.4
88	(3@3) 8-12-90-0-i-2.5-2-12	12.0	14.1	12.1	11040	1	0.79	3.0	3.0
89	(3@4) 8-12-90-0-i-2.5-2-12	14.0	14.6	12.6	11440	1	0.79	4.0	4.0
90	(3@5) 8-12-90-0-i-2.5-2-12	16.0	14.2	12.2	11460	1	0.79	5.0	5.0
91	(3@5) 8-5-180-0-i-2.5-2-10	16.6	12.0	10.0	5260	1	0.79	5.3	5.3
92	(3@3.75) 11-8-90-0-i-2.5-2-20	17.4	21.9	19.9	7070	1.41	1.56	5.5	3.9
93	(3@3.75) 11-8-90-0-i-2.5-2-24	17.4	25.5	23.5	7070	1.41	1.56	5.5	3.9
94	(3@3.75) 11-12-90-0-i-2.5-2-22	17.4	23.7	21.7	11460	1.41	1.56	5.5	3.9
95	H14-7	20.7	37.8	36.4	6390	1.693	2.25	6.0	3.5

Table B.3 Cont. Detailed properties and test results for hooked bar specimens having closely-spaced bars without confining reinforcement tested at the University of Kansas

SN	n	A_{th}	A_{hs}	A_{th}/A_{hs}	h_{cl}	x_{mid}	d_{eff}	d_{eff}/ℓ_{eh}	θ
		in. ²	in. ²		in.	in.	in.		°
75	3	0	0.93	0	5.25	9.44	7.21	0.91	50.1
76	4	0	1.24	0	5.25	9.44	6.34	1.22	61.1
77	4	0	1.24	0	5.25	9.44	7.37	0.82	46.4
78	4	0	1.24	0	5.25	9.44	6.44	1.09	58.0
79	3	0	0.93	0	5.25	9.44	6.39	1.08	58.0
80	4	0	1.24	0	5.25	9.44	6.36	1.08	58.0
81	3	0	0.93	0	5.25	9.44	6.61	1.10	57.6
82	3	0	2.37	0	10.00	14.19	12.83	0.80	41.4
83	3	0	2.37	0	10.00	14.19	11.61	1.24	56.5
84	3	0	2.37	0	10.00	14.19	11.16	1.43	61.2
85	3	0	2.37	0	10.00	14.19	12.15	1.20	54.6
86	3	0	2.37	0	10.00	14.19	11.85	1.17	54.6
87	3	0	2.37	0	10.00	14.19	11.59	1.47	60.9
88	3	0	2.37	0	10.00	14.19	11.97	0.99	49.5
89	3	0	2.37	0	10.00	14.19	11.89	0.94	48.4
90	3	0	2.37	0	10.00	14.19	11.55	0.95	49.3
91	3	0	2.37	0	10.00	14.19	12.36	1.24	54.8
92	3	0	4.68	0	19.50	23.69	23.55	1.18	50.0
93	3	0	4.68	0	19.50	23.69	24.73	1.05	45.2
94	3	0	4.68	0	19.50	23.69	22.85	1.05	47.5
95	3	0	6.75	0	24.00	28.54	33.20	0.91	38.1

Table B.3 Cont. Detailed properties and test results for hooked bar specimens having closely-spaced bars without confining reinforcement tested at the University of Kansas

SN	T	T_h ^[1]	T/T_h	f_{su}	$f_{su}/f_{s,calc}$ ^[2]	$f_{su}/f_{s,calc}$ ^[3]
	lb	lb		ksi		
75	27869	25789	1.08	89.9	1.23	1.23
76	14542	15243	0.95	46.9	1.14	1.14
77	28402	28016	1.01	91.6	1.29	1.29
78	15479	17086	0.91	49.9	1.11	1.11
79	16805	17639	0.95	54.2	1.16	1.16
80	19303	21008	0.92	62.3	1.01	1.01
81	24886	21633	1.15	80.3	1.27	1.27
82	62798	72985	0.86	79.5	1.06	1.06
83	36054	40262	0.90	45.6	1.05	1.05
84	24411	31939	0.76	30.9	0.87	0.87
85	28480	32234	0.88	36.1	1.11	1.11
86	32300	39016	0.83	40.9	0.97	0.97
87	37670	33002	1.14	47.7	1.39	1.39
88	48039	49088	0.98	60.8	1.29	1.29
89	55822	57486	0.97	70.7	1.27	1.27
90	52352	60935	0.86	66.3	1.07	1.07
91	45930	40344	1.14	58.1	1.34	1.34
92	98488	95566	1.03	63.1	1.37	1.37
93	126976	114868	1.11	81.4	1.50	1.50
94	123180	120461	1.02	79.0	1.39	1.39
95	250800	189076	1.33	111.5	1.87	1.87

^[1] Based on descriptive equations, Eq. (4.5) and (4.7)

^[2] Based on design equation, Eq. (6.18), using full expression for ψ_r , Eq. (6.14)

^[3] Based on design equation, Eq. (6.18), using simplified expression for ψ_r , Eq. (6.15)

Table B.4 Detailed properties and test results for hooked bar specimens having widely-spaced bars with confining reinforcement tested at the University of Kansas

SN	ID	<i>b</i>	<i>h</i>	$\ell_{eh,avg}$	f_{cm}	d_b	A_b	<i>s</i>	<i>s/d_b</i>
		in.	in.	in.	psi	in.	in. ²	in.	
96	5-5-90-5#3-i-2.5-2-8	12.7	9.8	7.8	4660	0.625	0.31	7.1	11.4
97	5-5-90-5#3-i-2.5-2-7	12.7	8.3	6.3	5230	0.625	0.31	7.1	11.4
98	5-12-90-5#3-i-2.5-2-5	12.7	7.4	5.4	10410	0.625	0.31	7.1	11.4
99	5-15-90-5#3-i-2.5-2-4	12.9	6.0	4.0	15800	0.625	0.31	7.3	11.7
100	5-15-90-5#3-i-2.5-2-5	13.0	7.1	5.1	15800	0.625	0.31	7.4	11.8
101	5-5-90-5#3-i-3.5-2-7	13.2	9.1	7.1	5190	0.625	0.31	7.6	12.2
102	5-12-90-5#3-i-3.5-2-5	12.9	7.0	5.0	11090	0.625	0.31	7.3	11.7
103*	5-5-90-2#3-i-2.5-2-8	12.9	9.8	7.8	5860	0.625	0.31	7.3	11.7
104*	5-5-90-2#3-i-2.5-2-6	12.9	7.9	5.9	5800	0.625	0.31	7.3	11.7
105*	5-8-90-2#3-i-2.5-2-6	12.4	8.0	6.0	8580	0.625	0.31	6.8	10.9
106*	5-8-90-2#3-i-2.5-2-8	12.7	10.4	8.4	8380	0.625	0.31	7.1	11.4
107*	5-12-90-2#3-i-2.5-2-5	12.7	7.8	5.8	11090	0.625	0.31	7.1	11.4
108*	5-15-90-2#3-i-2.5-2-6	12.9	8.4	6.4	15800	0.625	0.31	7.3	11.7
109*	5-15-90-2#3-i-2.5-2-4	13.0	5.8	3.8	15800	0.625	0.31	7.4	11.8
110*	5-5-90-2#3-i-3.5-2-6	14.7	7.9	5.9	5230	0.625	0.31	7.1	11.4
111*	5-5-90-2#3-i-3.5-2-8	15.0	9.7	7.7	5190	0.625	0.31	7.4	11.8
112*	5-8-90-2#3-i-3.5-2-6	14.6	8.3	6.3	8580	0.625	0.31	7.0	11.2
113*	5-8-90-2#3-i-3.5-2-8	14.9	9.1	7.1	8710	0.625	0.31	7.3	11.7
114*	5-12-90-2#3-i-3.5-2-5	14.9	7.4	5.4	10410	0.625	0.31	7.3	11.7
115*	5-5-180-2#3-i-2.5-2-8	13.1	10.0	8.0	5670	0.625	0.31	7.5	12.0
116*	5-5-180-2#3-i-2.5-2-6	12.9	7.6	5.6	5860	0.625	0.31	7.3	11.7
117*	5-8-180-2#3-i-2.5-2-7	12.6	9.1	7.1	9080	0.625	0.31	7.0	11.2
118*	5-8-180-2#3-i-3.5-2-7	15.2	8.8	6.8	9080	0.625	0.31	7.6	12.2
119*	(3@10) 5-5-90-2#3-i-2.5-2-7	18.4	9.0	7.0	5950	0.625	0.31	6.4	10.2
120	8-5-90-5#3-i-2.5-2-10b	16.9	12.4	10.4	5440	1	0.79	10.9	10.9
121	8-5-90-5#3-i-2.5-2-10c	17.0	12.5	10.5	5650	1	0.79	11	11.0
122	8-5-90-5#3-i-2.5-2-15	16.9	17.5	15.5	4850	1	0.79	10.9	10.9
123	8-5-90-5#3-i-2.5-2-13	17.3	15.6	13.6	5560	1	0.79	11.3	11.3
124	8-5-90-5#3-i-2.5-2-12(1)	16.8	13.3	11.3	5090	1	0.79	10.8	10.8
125	8-5-90-5#3-i-2.5-2-12	16.8	13.8	11.8	5960	1	0.79	10.8	10.8
126	8-5-90-5#3-i-2.5-2-12(2)	16.0	14.2	12.2	5240	1	0.79	10	10.0
127	8-5-90-5#3-i-2.5-2-10a	16.8	12.5	10.5	5270	1	0.79	10.8	10.8
128	8-5-90-5#3-i-2.5-2-10	17.3	11.6	9.6	5920	1	0.79	11.3	11.3
129	8-8-90-5#3-i-2.5-2-9	16.8	10.8	8.8	7710	1	0.79	10.8	10.8

* Specimens not used to develop descriptive equations, Eq. (4.5) and (4.7)

Table B.4 Cont. Detailed properties and test results for hooked bar specimens having widely-spaced bars with confining reinforcement tested at the University of Kansas

SN	n	A_{th}	A_{hs}	A_{th}/A_{hs}	$A_{th,ACI}/A_{hs}$	h_{cl}	x_{mid}	d_{eff}	d_{eff}/ℓ_{eh}	θ
		in. ²	in. ²			in.	in.	in.		°
96	2	0.66	0.62	1.065	1.774	5.25	9.44	7.34	0.94	50.4
97	2	0.66	0.62	1.065	1.774	5.25	9.44	6.67	1.06	56.3
98	2	0.66	0.62	1.065	1.774	5.25	9.44	6.19	1.15	60.2
99	2	0.66	0.62	1.065	1.774	5.25	9.44	5.81	1.45	67.0
100	2	0.66	0.62	1.065	1.774	5.25	9.44	5.94	1.16	61.6
101	2	0.66	0.62	1.065	1.774	5.25	9.44	6.81	0.96	53.0
102	2	0.66	0.62	1.065	1.774	5.25	9.44	6.02	1.20	62.1
103*	2	0.22	0.62	0.355	0.710	5.25	9.44	6.77	0.87	50.4
104*	2	0.22	0.62	0.355	0.710	5.25	9.44	6.47	1.10	58.0
105*	2	0.22	0.62	0.355	0.710	5.25	9.44	6.29	1.05	57.6
106*	2	0.22	0.62	0.355	0.710	5.25	9.44	6.61	0.79	48.3
107*	2	0.22	0.62	0.355	0.710	5.25	9.44	5.87	1.01	58.4
108*	2	0.22	0.62	0.355	0.710	5.25	9.44	6.01	0.94	55.9
109*	2	0.22	0.62	0.355	0.710	5.25	9.44	5.58	1.47	68.1
110*	2	0.22	0.62	0.355	0.710	5.25	9.44	6.07	1.03	58.0
111*	2	0.22	0.62	0.355	0.710	5.25	9.44	6.95	0.90	50.8
112*	2	0.22	0.62	0.355	0.710	5.25	9.44	6.12	0.97	56.3
113*	2	0.22	0.62	0.355	0.710	5.25	9.44	6.05	0.85	53.0
114*	2	0.22	0.62	0.355	0.710	5.25	9.44	5.91	1.09	60.2
115*	2	0.22	0.62	0.355	0.710	5.25	9.44	6.66	0.83	49.7
116*	2	0.22	0.62	0.355	0.710	5.25	9.44	6.35	1.13	59.3
117*	2	0.22	0.62	0.355	0.710	5.25	9.44	6.17	0.87	53.0
118*	2	0.22	0.62	0.355	0.710	5.25	9.44	6.06	0.89	54.2
119*	3	0.22	0.93	0.237	0.473	5.25	9.44	6.59	0.94	53.4
120	2	0.66	1.58	0.418	0.696	10.00	14.19	12.29	1.18	53.8
121	2	0.66	1.58	0.418	0.696	10.00	14.19	12.20	1.16	53.5
122	2	0.66	1.58	0.418	0.696	10.00	14.19	12.61	0.81	42.5
123	2	0.66	1.58	0.418	0.696	10.00	14.19	12.61	0.93	46.2
124	2	0.66	1.58	0.418	0.696	10.00	14.19	12.30	1.09	51.5
125	2	0.66	1.58	0.418	0.696	10.00	14.19	12.25	1.04	50.2
126	2	0.66	1.58	0.418	0.696	10.00	14.19	12.55	1.03	49.3
127	2	0.66	1.58	0.418	0.696	10.00	14.19	12.80	1.22	53.5
128	2	0.66	1.58	0.418	0.696	10.00	14.19	12.14	1.26	55.9
129	2	0.66	1.58	0.418	0.696	10.00	14.19	11.76	1.34	58.2

* Specimens not used to develop descriptive equations, Eq. (4.5) and (4.7)

Table B.4 Cont. Detailed properties and test results for hooked bar specimens having widely-spaced bars with confining reinforcement tested at the University of Kansas

SN	T	T_h ^[1]	T/T_h	f_{su}	$f_{su}/f_{s,calc}$ ^[2]	$f_{su}/f_{s,calc}$ ^[3]
	lb	lb		ksi		
96	43030	40185	1.07	138.8	1.68	1.68
97	31696	35172	0.90	102.2	1.49	1.49
98	34420	35684	0.96	111.0	1.59	1.59
99	31318	31300	1.00	101.0	1.76	1.76
100	39156	36942	1.06	126.3	1.72	1.72
101	36025	38252	0.94	116.2	1.50	1.50
102	30441	34207	0.89	98.2	1.49	1.49
103*	37154	33323	1.11	119.9	1.37	1.37
104*	29444	25559	1.15	95.0	1.44	1.44
105*	30638	28472	1.08	98.8	1.34	1.34
106*	40168	39127	1.03	129.6	1.26	1.26
107*	24348	29321	0.83	78.5	1.03	1.03
108*	42638	35110	1.21	137.5	1.50	1.50
109*	18667	21621	0.86	60.2	1.10	1.10
110*	21093	24951	0.85	68.0	1.06	1.06
111*	44665	31954	1.40	144.1	1.72	1.72
112*	30035	29811	1.01	96.9	1.25	1.25
113*	28656	33536	0.85	92.4	1.05	1.05
114*	28364	27015	1.05	91.5	1.31	1.31
115*	34078	33872	1.01	109.9	1.24	1.24
116*	26728	24426	1.09	86.2	1.37	1.37
117*	29230	33880	0.86	94.3	1.06	1.06
118*	30931	32502	0.95	99.8	1.17	1.17
119*	31296	28718	1.09	101.0	1.28	1.28
120	69715	65770	1.06	88.2	1.56	1.56
121	68837	66795	1.03	87.1	1.51	1.51
122	73377	89921	0.82	92.9	1.13	1.13
123	82376	82669	1.00	104.3	1.40	1.40
124	66363	69394	0.96	84.0	1.39	1.39
125	72000	74359	0.97	91.1	1.39	1.39
126	71470	74399	0.96	90.5	1.38	1.38
127	82800	65849	1.26	104.8	1.85	1.85
128	70356	62773	1.12	89.1	1.67	1.67
129	64397	61797	1.04	81.5	1.56	1.56

* Specimens not used to develop descriptive equations, Eq. (4.5) and (4.7)

^[1] Based on descriptive equations, Eq. (4.5) and (4.7)

^[2] Based on design equation, Eq. (6.18), using full expression for ψ_r , Eq. (6.14)

^[3] Based on design equation, Eq. (6.18), using simplified expression for ψ_r , Eq. (6.15)

Table B.4 Cont. Detailed properties and test results for hooked bar specimens having widely-spaced bars with confining reinforcement tested at the University of Kansas

SN	ID	<i>b</i>	<i>h</i>	$\ell_{eh,avg}$	f_{cm}	d_b	A_b	<i>s</i>	<i>s/d_b</i>
		in.	in.	in.	psi	in.	in. ²	in.	
130	8-12-90-5#3-i-2.5-2-9	16.5	11.0	9	11160	1	0.79	10.5	10.5
131	8-12-90-5#3-i-3.5-2-9	18.5	11.0	9	11160	1	0.79	10.5	10.5
132	8-12-90-5#3-i-2.5-2-10	16.9	11.4	9.4	11800	1	0.79	10.9	10.9
133	8-12-90-5#3-i-2.5-2-12	17.0	14.2	12.2	11760	1	0.79	11	11.0
134	8-15-90-5#3-i-2.5-2-10	16.9	12.1	10.1	15800	1	0.79	10.9	10.9
135	8-5-90-5#3-i-3.5-2-15	19.3	17.8	15.8	4850	1	0.79	11.3	11.3
136	8-5-90-5#3-i-3.5-2-13	19.4	15.1	13.1	5570	1	0.79	11.4	11.4
137	8-5-90-5#3-i-3.5-2-12(1)	18.8	14.5	12.5	5090	1	0.79	10.8	10.8
138	8-5-90-5#3-i-3.5-2-12	18.8	14.1	12.1	6440	1	0.79	10.8	10.8
139	8-12-180-5#3-i-2.5-2-10	16.9	11.8	9.8	11800	1	0.79	10.9	10.9
140	8-15-180-5#3-i-2.5-2-9.5	17.0	11.7	9.7	15550	1	0.79	11	11.0
141	8-8-90-5#3-i-3.5-2-8	17.9	10.0	8	7910	1	0.79	9.88	9.9
142*	8-5-90-2#3-i-2.5-2-16	16.5	17.4	15.4	4810	1	0.79	10.5	10.5
143*	8-5-90-2#3-i-2.5-2-9.5	17.0	11.1	9.1	5140	1	0.79	11	11.0
144*	8-5-90-2#3-i-2.5-2-12.5	16.5	14.0	12	5240	1	0.79	10.5	10.5
145*	8-5-90-2#3-i-2.5-2-8.5	16.1	11.3	9.3	5240	1	0.79	10.1	10.1
146*	8-5-90-2#3-i-2.5-2-14	16.3	15.8	13.8	5450	1	0.79	10.3	10.3
147*	8-5-90-2#3-i-2.5-2-10	17.3	12.1	10.1	5920	1	0.79	11.3	11.3
148*	8-8-90-2#3-i-2.5-2-8	16.0	10.3	8.3	7700	1	0.79	10	10.0
149*	8-8-90-2#3-i-2.5-2-10	15.5	11.7	9.7	8990	1	0.79	9.5	9.5
150*	8-12-90-2#3-i-2.5-2-9	16.5	11.0	9	11160	1	0.79	10.5	10.5
151*	8-12-90-2#3-i-2.5-2-11	16.5	12.9	10.9	12010	1	0.79	10.5	10.5
152*	8-15-90-2#3-i-2.5-2-11	17.0	13.0	11	15800	1	0.79	11	11.0
153*	8-5-90-2#3-i-3.5-2-17	17.1	19.3	17.3	5570	1	0.79	11.1	11.1
154*	8-5-90-2#3-i-3.5-2-13	19.3	15.6	13.6	5560	1	0.79	11.3	11.3
155*	8-8-90-2#3-i-3.5-2-8	17.5	10.1	8.1	8290	1	0.79	9.5	9.5
156*	8-8-90-2#3-i-3.5-2-10	17.5	10.8	8.8	8990	1	0.79	9.5	9.5
157*	8-12-90-2#3-i-3.5-2-9	18.6	11.0	9	11160	1	0.79	10.6	10.6
158*	8-5-180-2#3-i-2.5-2-11	16.5	12.6	10.6	4550	1	0.79	10.5	10.5
159*	8-5-180-2#3-i-2.5-2-14	16.8	15.8	13.8	4870	1	0.79	10.8	10.8
160*	8-8-180-2#3-i-2.5-2-11.5	17.0	12.4	10.4	8810	1	0.79	11	11.0
161*	8-12-180-2#3-i-2.5-2-11	16.6	12.8	10.8	12010	1	0.79	10.6	10.6
162*	8-5-180-2#3-i-3.5-2-11	18.8	12.4	10.4	4300	1	0.79	10.8	10.8
163*	8-5-180-2#3-i-3.5-2-14	18.8	15.6	13.6	4870	1	0.79	10.8	10.8

* Specimens not used to develop descriptive equations, Eq. (4.5) and (4.7)

Table B.4 Cont. Detailed properties and test results for hooked bar specimens having widely-spaced bars with confining reinforcement tested at the University of Kansas

SN	n	A_{th}	A_{hs}	A_{th}/A_{hs}	$A_{th,ACI}/A_{hs}$	h_{cl}	x_{mid}	d_{eff}	d_{eff}/ℓ_{ch}	θ
		in. ²	in. ²			in.	in.	in.		°
130	2	0.66	1.58	0.418	0.696	10	14.19	11.27	1.25	57.6
131	2	0.66	1.58	0.418	0.696	10	14.19	11.19	1.24	57.6
132	2	0.66	1.58	0.418	0.696	10	14.19	11.17	1.19	56.5
133	2	0.66	1.58	0.418	0.696	10	14.19	11.59	0.95	49.3
134	2	0.66	1.58	0.418	0.696	10	14.19	11.22	1.11	54.6
135	2	0.66	1.58	0.418	0.696	10	14.19	12.50	0.79	41.9
136	2	0.66	1.58	0.418	0.696	10	14.19	12.18	0.93	47.3
137	2	0.66	1.58	0.418	0.696	10	14.19	12.36	0.99	48.6
138	2	0.66	1.58	0.418	0.696	10	14.19	12.11	1.00	49.5
139	2	0.66	1.58	0.418	0.696	10	14.19	11.16	1.14	55.4
140	2	0.66	1.58	0.418	0.696	10	14.19	11.18	1.15	55.6
141	2	0.66	1.58	0.418	0.696	10	14.19	11.42	1.43	60.6
142*	2	0.66	1.58	0.418	0.278	10	14.19	12.92	0.84	42.7
143*	2	0.66	1.58	0.418	0.278	10	14.19	11.82	1.30	57.3
144*	2	0.22	1.58	0.139	0.278	10	14.19	12.49	1.04	49.8
145*	2	0.22	1.58	0.139	0.278	10	14.19	11.79	1.27	56.8
146*	2	0.22	1.58	0.139	0.278	10	14.19	12.62	0.91	45.8
147*	2	0.22	1.58	0.139	0.278	10	14.19	11.71	1.16	54.6
148*	2	0.22	1.58	0.139	0.278	10	14.19	11.37	1.37	59.7
149*	2	0.22	1.58	0.139	0.278	10	14.19	11.59	1.19	55.6
150*	2	0.22	1.58	0.139	0.278	10	14.19	11.20	1.24	57.6
151*	2	0.22	1.58	0.139	0.278	10	14.19	11.25	1.03	52.5
152*	2	0.22	1.58	0.139	0.278	10	14.19	11.12	1.01	52.2
153*	2	0.22	1.58	0.139	0.278	10	14.19	12.88	0.74	39.4
154*	2	0.22	1.58	0.139	0.278	10	14.19	12.28	0.90	46.2
155*	2	0.22	1.58	0.139	0.278	10	14.19	11.22	1.38	60.3
156*	2	0.22	1.58	0.139	0.278	10	14.19	11.24	1.28	58.2
157*	2	0.22	1.58	0.139	0.278	10	14.19	10.87	1.21	57.6
158*	2	0.22	1.58	0.139	0.278	10	14.19	12.30	1.16	53.2
159*	2	0.22	1.58	0.139	0.278	10	14.19	12.72	0.92	45.8
160*	2	0.22	1.58	0.139	0.278	10	14.19	11.41	1.10	53.8
161*	2	0.22	1.58	0.139	0.278	10	14.19	11.17	1.03	52.7
162*	2	0.22	1.58	0.139	0.278	10	14.19	11.95	1.15	53.8
163*	2	0.22	1.58	0.139	0.278	10	14.19	12.02	0.88	46.2

* Specimens not used to develop descriptive equations, Eq. (4.5) and (4.7)

Table B.4 Cont. Detailed properties and test results for hooked bar specimens having widely-spaced bars with confining reinforcement tested at the University of Kansas

SN	<i>T</i>	<i>T_h</i> ^[1]	<i>T/T_h</i>	<i>f_{su}</i>	<i>f_{su}/f_{s,calc}</i> ^[2]	<i>f_{su}/f_{s,calc}</i> ^[3]
	lb	lb		ksi		
130	64753	67814	0.95	82.0	1.40	1.40
131	67830	67814	1.00	85.9	1.47	1.47
132	64530	71094	0.91	81.7	1.32	1.32
133	87711	88778	0.99	111.0	1.38	1.38
134	90003	80398	1.12	113.9	1.59	1.59
135	80341	91463	0.88	101.7	1.22	1.22
136	77069	80076	0.96	97.6	1.36	1.36
137	76431	75465	1.01	96.7	1.45	1.45
138	79150	77221	1.02	100.2	1.46	1.46
139	64107	73599	0.87	81.1	1.25	1.25
140	85951	77403	1.11	108.8	1.59	1.59
141	55810	57699	0.97	70.6	1.48	1.48
142*	79629	89242	0.89	100.8	1.24	1.38
143*	53621	58558	0.92	67.9	1.39	1.55
144*	72067	61372	1.17	91.2	1.41	1.57
145*	50561	47766	1.06	64.0	1.28	1.42
146*	76964	71349	1.08	97.4	1.30	1.44
147*	56203	53354	1.05	71.1	1.27	1.41
148*	47876	47032	1.02	60.6	1.23	1.37
149*	61024	56923	1.07	77.2	1.29	1.43
150*	61013	55809	1.09	77.2	1.32	1.46
151*	68683	68849	1.00	86.9	1.20	1.34
152*	83320	74572	1.12	105.5	1.35	1.50
153*	89914	90432	0.99	113.8	1.20	1.34
154*	80360	70664	1.14	101.7	1.37	1.52
155*	48773	46777	1.04	61.7	1.26	1.40
156*	53885	51723	1.04	68.2	1.26	1.40
157*	49777	55809	0.89	63.0	1.08	1.19
158*	60235	52394	1.15	76.2	1.38	1.54
159*	76279	69316	1.10	96.6	1.32	1.47
160*	58171	60693	0.96	73.6	1.15	1.28
161*	64655	68211	0.95	81.8	1.14	1.27
162*	55869	50711	1.10	70.7	1.33	1.47
163*	63467	68301	0.93	80.3	1.12	1.24

* Specimens not used to develop descriptive equations, Eq. (4.5) and (4.7)

[1] Based on descriptive equations, Eq. (4.5) and (4.7)

[2] Based on design equation, Eq. (6.18), using full expression for ψ_r , Eq. (6.14)

[3] Based on design equation, Eq. (6.18), using simplified expression for ψ_r , Eq. (6.15)

Table B.4 Cont. Detailed properties and test results for hooked bar specimens having widely-spaced bars with confining reinforcement tested at the University of Kansas

SN	ID	<i>b</i>	<i>h</i>	$\ell_{eh,avg}$	f_{cm}	d_b	A_b	<i>s</i>	s/d_b
		in.	in.	in.	psi	in.	in. ²	in.	
164*	8-15-180-2#3-i-2.5-2-11	16.8	13.1	11.1	15550	1	0.79	10.8	10.8
165*	8-12-90-5#3vr-i-2.5-2-10	16.8	12.2	10.2	11800	1	0.79	10.8	10.8
166*	8-12-90-4#3vr-i-2.5-2-10	16.0	12.4	10.4	11850	1	0.79	10	10.0
167*	8-12-180-5#3vr-i-2.5-2-10	16.8	12.8	10.8	11800	1	0.79	10.8	10.8
168*	8-12-180-4#3vr-i-2.5-2-10	16.8	12.3	10.3	11850	1	0.79	10.8	10.8
169	11-5-90-6#3-i-2.5-2-20	20.7	21.3	19.3	5420	1.41	1.56	14.3	10.1
170	11-5-90-6#3-i-2.5-2-16	21.4	17.4	15.4	5030	1.41	1.56	15	10.6
171	11-8-90-6#3-i-2.5-2-16	21.2	17.9	15.9	9120	1.41	1.56	14.8	10.5
172	11-8-90-6#3-i-2.5-2-22	21.3	23.4	21.4	9420	1.41	1.56	14.9	10.6
173	11-8-90-6#3-i-2.5-2-22	21.2	23.9	21.9	9420	1.41	1.56	14.8	10.5
174	11-8-90-6#3-i-2.5-2-15	21.3	17.5	15.5	7500	1.41	1.56	14.9	10.6
175	11-8-90-6#3-i-2.5-2-19	21.3	21.2	19.2	7500	1.41	1.56	14.9	10.6
176	11-12-90-6#3-i-2.5-2-17	20.8	18.8	16.8	12370	1.41	1.56	14.4	10.2
177	11-12-90-6#3-i-2.5-2-16	20.8	17.4	15.4	13710	1.41	1.56	14.4	10.2
178	11-12-90-6#3-i-2.5-2-22	21.1	23.7	21.7	13710	1.41	1.56	14.7	10.4
179	11-15-90-6#3-i-2.5-2-22	21.3	24.3	22.3	16180	1.41	1.56	14.9	10.6
180	11-15-90-6#3-i-2.5-2-15	21.4	16.8	14.8	14045	1.41	1.56	15	10.6
181	11-5-90-6#3-i-3.5-2-20	22.9	22.4	20.4	5420	1.41	1.56	14.5	10.3
182	11-8-180-6#3-i-2.5-2-15	20.8	17.3	15.3	7500	1.41	1.56	14.4	10.2
183	11-8-180-6#3-i-2.5-2-19	21.1	21.8	19.8	7870	1.41	1.56	14.7	10.4
184	(2@7.5) 11-12-180-6#3-i-2.5-2-14	16.9	16.4	14.4	12190	1.41	1.56	10.5	7.4
185	11-12-180-6#3-i-2.5-2-17	21.3	18.7	16.7	12370	1.41	1.56	14.9	10.6
186	11-12-180-6#3-i-2.5-2-17	21.2	18.8	16.8	12370	1.41	1.56	14.8	10.5
187*	11-5-90-2#3-i-2.5-2-17	21.2	19.6	17.6	5600	1.41	1.56	14.8	10.5
188*	(2@7.5) 11-8-90-2#3-i-2.5-2-17a	17.2	18.4	16.4	7070	1.41	1.56	10.8	7.7
189*	(2@7.5) 11-12-90-2#3-i-2.5-2-16a	16.9	17.3	15.3	11850	1.41	1.56	10.5	7.4
190*	11-12-90-2#3-i-2.5-2-17.5	21.1	19.8	17.8	13710	1.41	1.56	14.7	10.4
191*	11-15-90-2#3-i-2.5-2-23	20.8	25.5	23.5	16180	1.41	1.56	14.4	10.2
192*	11-15-90-2#3-i-2.5-2-15	21.4	16.1	14.1	14045	1.41	1.56	15	10.6
193*	11-5-90-2#3-i-3.5-2-17	23.2	19.6	17.6	7070	1.41	1.56	14.8	10.5
194*	(2@7.5) 11-8-90-6#3-i-2.5-2-15a	17.2	16.0	14	7070	1.41	1.56	10.8	7.7

* Specimens not used to develop descriptive equations, Eq. (4.5) and (4.7)

Table B.4 Cont. Detailed properties and test results for hooked bar specimens having widely-spaced bars with confining reinforcement tested at the University of Kansas

SN	n	A_{th}	A_{hs}	A_{th}/A_{hs}	$A_{th,ACI}/A_{hs}$	h_{cl}	x_{mid}	d_{eff}	d_{eff}/ℓ_{eh}	θ
		in. ²	in. ²			in.	in.	in.		°
164*	2	0.22	1.58	0.139	0.278	10	14.19	11.09	1.00	52.0
165*	2	0.66	1.58	0.418	0.696	10	14.19	11.10	1.09	54.3
166*	2	0.66	1.58	0.418	0.557	10	14.19	11.13	1.07	53.8
167*	2	0.22	1.58	0.139	0.696	10	14.19	11.24	1.04	52.7
168*	2	0.22	1.58	0.139	0.557	10	14.19	11.26	1.09	54.0
169	2	0.66	3.12	0.212	0.423	19.5	23.69	23.17	1.20	50.8
170	2	0.66	3.12	0.212	0.423	19.5	23.69	22.66	1.47	57.0
171	2	0.66	3.12	0.212	0.423	19.5	23.69	21.99	1.38	56.1
172	2	0.66	3.12	0.212	0.423	19.5	23.69	22.83	1.07	47.9
173	2	0.66	3.12	0.212	0.423	19.5	23.69	22.96	1.05	47.2
174	2	0.66	3.12	0.212	0.423	19.5	23.69	21.86	1.41	56.8
175	2	0.66	3.12	0.212	0.423	19.5	23.69	22.67	1.18	51.0
176	2	0.66	3.12	0.212	0.423	19.5	23.69	21.77	1.30	54.7
177	2	0.66	3.12	0.212	0.423	19.5	23.69	20.96	1.36	57.0
178	2	0.66	3.12	0.212	0.423	19.5	23.69	22.02	1.01	47.5
179	2	0.66	3.12	0.212	0.423	19.5	23.69	21.58	0.97	46.7
180	2	0.66	3.12	0.212	0.423	19.5	23.69	21.25	1.44	58.0
181	2	0.66	3.12	0.212	0.423	19.5	23.69	22.80	1.12	49.3
182	2	0.66	3.12	0.212	0.423	19.5	23.69	21.99	1.44	57.1
183	2	0.66	3.12	0.212	0.423	19.5	23.69	22.71	1.15	50.1
184	2	0.66	3.12	0.212	0.423	19.5	23.69	21.15	1.47	58.7
185	2	0.66	3.12	0.212	0.423	19.5	23.69	21.10	1.26	54.8
186	2	0.66	3.12	0.212	0.423	19.5	23.69	21.55	1.28	54.7
187*	2	0.22	3.12	0.071	0.141	19.5	23.69	22.09	1.26	53.4
188*	2	0.22	3.12	0.071	0.141	19.5	23.69	22.44	1.37	55.3
189*	2	0.22	3.12	0.071	0.141	19.5	23.69	21.46	1.40	57.1
190*	2	0.22	3.12	0.071	0.141	19.5	23.69	21.13	1.19	53.1
191*	2	0.22	3.12	0.071	0.141	19.5	23.69	21.75	0.93	45.2
192*	2	0.22	3.12	0.071	0.141	19.5	23.69	20.89	1.48	59.2
193*	2	0.22	3.12	0.071	0.141	19.5	23.69	21.76	1.24	53.4
194*	2	0.66	3.12	0.212	0.423	19.5	23.69	22.45	1.60	59.4

* Specimens not used to develop descriptive equations, Eq. (4.5) and (4.7)

Table B.4 Cont. Detailed properties and test results for hooked bar specimens having widely-spaced bars with confining reinforcement tested at the University of Kansas

SN	T	T_h ^[1]	T/T_h	f_{su}	$f_{su}/f_{s,calc}$ ^[2]	$f_{su}/f_{s,calc}$ ^[3]
	lb	lb		ksi		
164*	78922	74953	1.05	99.9	1.27	1.41
165*	60219	76115	0.79	76.2	1.13	1.13
166*	59241	77448	0.76	75.0	1.09	1.09
167*	67780	67904	1.00	85.8	1.20	1.20
168*	69188	64811	1.07	87.6	1.29	1.29
169	136272	132453	1.03	87.4	1.39	1.39
170	115623	106456	1.09	74.1	1.51	1.51
171	132986	125227	1.06	85.2	1.45	1.45
172	184569	166365	1.11	118.3	1.48	1.48
173	191042	170080	1.12	122.5	1.50	1.50
174	108312	117059	0.93	69.4	1.27	1.27
175	145430	142238	1.02	93.2	1.38	1.38
176	161648	141386	1.14	103.6	1.55	1.55
177	115197	133663	0.86	73.8	1.17	1.17
178	201189	184800	1.09	129.0	1.45	1.45
179	197809	197713	1.00	126.8	1.33	1.33
180	145267	129618	1.12	93.1	1.53	1.53
181	135821	139385	0.97	87.1	1.31	1.31
182	111678	115715	0.97	71.6	1.33	1.33
183	149000	148055	1.01	95.5	1.35	1.35
184	93955	122388	0.77	60.2	1.05	1.05
185	116371	140606	0.83	74.6	1.12	1.12
186	148678	141386	1.05	95.3	1.42	1.42
187*	100695	107505	0.94	64.5	1.12	1.25
188*	106031	106250	1.00	68.0	1.19	1.33
189*	108718	113221	0.96	69.7	1.15	1.28
190*	130389	137692	0.95	83.6	1.15	1.27
191*	209575	192923	1.09	134.3	1.34	1.49
192*	115189	108814	1.06	73.8	1.27	1.41
193*	109644	114265	0.96	70.3	1.15	1.28
194*	106190	105641	1.01	68.1	1.40	1.40

* Specimens not used to develop descriptive equations, Eq. (4.5) and (4.7)

[1] Based on descriptive equations, Eq. (4.5) and (4.7)

[2] Based on design equation, Eq. (6.18), using full expression for ψ_r , Eq. (6.14)

[3] Based on design equation, Eq. (6.18), using simplified expression for ψ_r , Eq. (6.15)

Table B.4 Cont. Detailed properties and test results for hooked bar specimens having widely-spaced bars with confining reinforcement tested at the University of Kansas

SN	ID	<i>b</i>	<i>h</i>	$\ell_{eh,avg}$	f_{cm}	d_b	A_b	<i>s</i>	s/d_b
		in.	in.	in.	psi	in.	in. ²	in.	
195	H14-2	26.7	28.6	24.8	13010	1.693	2.25	18	10.6
196	H14-4	26.7	37.8	34.9	7570	1.693	2.25	18	10.6
197	H14-16	26.7	28.6	25.9	6810	1.693	2.25	18	10.6
198	H18-1	27.25	28.6	28.5	15310	2.25	4	18	8.0
199	H18-2	27.25	28.6	27.0	15770	2.25	4	18	8.0
200	H18-3	27.25	37.8	36.5	7560	2.25	4	18	8.0
201	H18-4	27.25	37.8	36.4	7610	2.25	4	18	8.0

Table B.4 Cont. Detailed properties and test results for hooked bar specimens having widely-spaced bars with confining reinforcement tested at the University of Kansas

SN	<i>n</i>	A_{th}	A_{hs}	A_{th}/A_{hs}	$A_{th,ACI}/A_{hs}$	h_{cl}	x_{mid}	d_{eff}	d_{eff}/ℓ_{eh}	θ
		in. ²	in. ²			in.	in.	in.		°
195	2	1.20	4.5	0.267	0.356	25.5	28.54	28.60	1.15	49.0
196	2	1.20	4.5	0.267	0.356	25.5	28.54	30.19	0.87	39.3
197	2	0.80	4.5	0.178	0.267	25.5	28.54	29.83	1.15	47.8
198	2	1.86	8	0.233	0.388	35.15	38.15	38.26	1.34	53.2
199	2	3.72	8	0.465	0.620	35.15	38.15	38.90	1.44	54.7
200	2	1.86	8	0.233	0.388	33.65	38.15	39.96	1.09	46.3
201	2	3.72	8	0.465	0.620	33.65	38.15	40.90	1.12	46.4

Table B.4 Cont. Detailed properties and test results for hooked bar specimens having widely-spaced bars with confining reinforcement tested at the University of Kansas

SN	<i>T</i>	T_h ^[1]	T/T_h	f_{su}	$f_{su}/f_{s,calc}$ ^[2]	$f_{su}/f_{s,calc}$ ^[3]
	lb	lb		ksi		
195	293900	247326	1.19	130.6	1.33	1.52
196	268500	298033	0.90	119.3	0.99	1.13
197	235300	206333	1.14	104.6	1.26	1.38
198	358200	365269	0.98	89.6	1.17	1.34
199	445000	440211	1.01	111.3	1.52	1.74
200	371400	386914	0.96	92.9	1.13	1.29
201	427900	475138	0.90	107.0	1.31	1.49

^[1] Based on descriptive equations, Eq. (4.5) and (4.7)

^[2] Based on design equation, Eq. (6.18), using full expression for ψ_r , Eq. (6.14)

^[3] Based on design equation, Eq. (6.18), using simplified expression for ψ_r , Eq. (6.15)

Table B.5 Detailed properties and test results for hooked bar specimens having closely-spaced bars with confining reinforcement tested at the University of Kansas

SN	ID	<i>b</i>	<i>h</i>	$\ell_{eh,avg}$	<i>f_{cm}</i>	<i>d_b</i>	<i>A_b</i>	<i>s</i>	<i>s/d_b</i>
		in.	in.	in.	psi	in.	in. ²	in.	
202	(3@6) 5-8-90-5#3-i-2.5-2-6.25	12.8	7.5	5.5	10110	0.625	0.31	3.6	5.8
203	(3@4) 5-8-90-5#3-i-2.5-2-6	10.9	8.1	6.1	6700	0.625	0.31	2.6	4.2
204	(3@6) 5-8-90-5#3-i-2.5-2-6	13.4	8.0	6.0	6700	0.625	0.31	3.9	6.2
205	(3) 5-5-90-5#3-i-2.5-2-8	12.8	9.8	7.8	4660	0.625	0.31	3.6	5.8
206	(4@4) 5-5-90-5#3-i-2.5-2-7	12.6	9.1	7.1	6430	0.625	0.31	2.3	3.7
207	(4@4) 5-5-90-5#3-i-2.5-2-6	13.0	8.3	6.3	6430	0.625	0.31	2.5	3.9
208	(4@4) 5-8-90-5#3-i-2.5-2-6	13.1	8.0	6.0	6700	0.625	0.31	2.5	4.0
209	(4@6) 5-8-90-5#3-i-2.5-2-6	17.4	8.0	6.0	6690	0.625	0.31	3.9	6.3
210	(3@6) 5-8-90-5#3-i-3.5-2-6.25	12.9	8.3	6.3	10110	0.625	0.31	3.6	5.8
211*	(4@4) 5-5-90-2#3-i-2.5-2-6	13.1	8.3	6.3	6430	0.625	0.31	2.5	4.0
212*	(4@4) 5-5-90-2#3-i-2.5-2-8	13.1	10.0	8.0	6430	0.625	0.31	2.5	4.0
213	(3@5.5) 8-5-90-5#3-i-2.5-2-8	16.6	10.0	8	6620	1	0.79	5.3	5.3
214	(3@5.5) 8-5-90-5#3-i-2.5-2-12	16.8	14.2	12.2	6620	1	0.79	5.4	5.4
215	(3@5.5) 8-5-90-5#3-i-2.5-2-12(1)	16.8	14.0	12	5660	1	0.79	5.4	5.4
216	(3@5.5) 8-5-90-5#3-i-2.5-2-8(2)	17.0	10.2	8.2	5730	1	0.79	5.5	5.5
217	(3@3) 8-5-90-5#3-i-2.5-2-10	12.3	11.9	9.9	4810	1	0.79	3.1	3.1
218	(3@5) 8-5-90-5#3-i-2.5-2-10	16.0	11.9	9.9	4850	1	0.79	5.0	5.0
219	(3@3) 8-12-90-5#3-i-2.5-2-12	12.0	13.8	11.8	11040	1	0.79	3.0	3.0
220	(3@4) 8-12-90-5#3-i-2.5-2-12	13.8	14.3	12.3	11440	1	0.79	3.9	3.9

* Specimens not used to develop descriptive equations, Eq. (4.5) and (4.7)

Table B.5 Cont. Detailed properties and test results for hooked bar specimens having closely-spaced bars with confining reinforcement tested at the University of Kansas

SN	n	A_{th}	A_{hs}	A_{th}/A_{hs}	$A_{th,ACI}/A_{hs}$	h_{cl}	x_{mid}	d_{eff}	d_{eff}/ℓ_{eh}	θ
		in. ²	in. ²			in.	in.	in.		°
202	3	0.66	0.93	0.710	1.183	5.25	9.44	6.33	1.15	59.8
203	3	0.66	0.93	0.710	1.183	5.25	9.44	7.61	1.25	57.1
204	3	0.66	0.93	0.710	1.183	5.25	9.44	7.25	1.21	57.6
205	3	0.66	0.93	0.710	1.183	5.25	9.44	7.65	0.98	50.4
206	4	0.66	1.24	0.532	0.887	5.25	9.44	7.41	1.04	53.0
207	4	0.66	1.24	0.532	0.887	5.25	9.44	7.25	1.15	56.3
208	4	0.66	1.24	0.532	0.887	5.25	9.44	7.31	1.22	57.6
209	4	0.66	1.24	0.532	0.887	5.25	9.44	6.85	1.14	57.6
210	3	0.66	0.93	0.710	1.183	5.25	9.44	6.72	1.07	56.3
211*	4	0.22	1.24	0.177	0.355	5.25	9.44	6.89	1.09	56.3
212*	4	0.22	1.24	0.177	0.355	5.25	9.44	7.24	0.91	49.7
213	3	0.66	2.37	0.278	0.464	10	14.19	11.66	1.46	60.6
214	3	0.66	2.37	0.278	0.464	10	14.19	12.92	1.06	49.3
215	3	0.66	2.37	0.278	0.464	10	14.19	12.32	1.03	49.8
216	3	0.66	2.37	0.278	0.464	10	14.19	12.28	1.50	60.0
217	3	0.66	2.37	0.278	0.464	10	14.19	13.50	1.36	55.1
218	3	0.66	2.37	0.278	0.464	10	14.19	13.45	1.36	55.1
219	3	0.66	2.37	0.278	0.464	10	14.19	12.55	1.06	50.2
220	3	0.66	2.37	0.278	0.464	10	14.19	12.24	1.00	49.1

* Specimens not used to develop descriptive equations, Eq. (4.5) and (4.7)

Table B.5 Cont. Detailed properties and test results for hooked bar specimens having closely-spaced bars with confining reinforcement tested at the University of Kansas

SN	T	T_h ^[1]	T/T_h	f_{su}	$f_{su}/f_{s,calc}$ ^[2]	$f_{su}/f_{s,calc}$ ^[3]
	lb	lb		ksi		
202	25830	29941	0.86	83.3	1.18	1.18
203	34889	27808	1.25	112.5	1.59	1.59
204	36448	30166	1.21	117.6	1.69	1.69
205	33260	33941	0.98	107.3	1.30	1.30
206	27114	28656	0.95	87.5	1.07	1.07
207	25898	26045	0.99	83.5	1.16	1.16
208	27493	25287	1.09	88.7	1.27	1.27
209	28300	28090	1.01	91.3	1.31	1.31
210	35268	33525	1.05	113.8	1.41	1.41
211*	21405	22360	0.96	69.0	0.95	0.95
212*	26017	28553	0.91	83.9	0.91	0.91
213	37126	46151	0.80	47.0	1.03	1.03
214	66094	67203	0.98	83.7	1.20	1.20
215	47851	63818	0.75	60.6	0.92	0.92
216	47994	46091	1.04	60.8	1.34	1.34
217	47276	46460	1.02	59.8	1.15	1.15
218	61305	51010	1.20	77.6	1.48	1.48
219	62206	65470	0.95	78.7	1.03	1.03
220	64940	71784	0.90	82.2	1.02	1.02

* Specimens not used to develop descriptive equations, Eq. (4.5) and (4.7)

^[1] Based on descriptive equations, Eq. (4.5) and (4.7)

^[2] Based on design equation, Eq. (6.18), using full expression for ψ_r , Eq. (6.14)

^[3] Based on design equation, Eq. (6.18), using simplified expression for ψ_r , Eq. (6.15)

Table B.5 Cont. Detailed properties and test results for hooked bar specimens having closely-spaced bars with confining reinforcement tested at the University of Kansas

SN	ID	<i>b</i>	<i>h</i>	$\ell_{eh,avg}$	f_{cm}	d_b	A_b	s	s/d_b
		in.	in.	in.	psi	in.	in. ²	in.	
221	(3@5) 8-12-90-5#3-i-2.5-2-12	16.0	14.2	12.2	11460	1	0.79	5.0	5.0
222	(3@5) 8-5-180-5#3-i-2.5-2-10	15.8	11.7	9.7	5540	1	0.79	4.9	4.9
223*	(2@3) 8-5-90-2#3-i-2.5-2-10	9.3	12.3	10.3	4760	1	0.79	3.3	3.3
224*	(2@5) 8-5-90-2#3-i-2.5-2-10	10.9	11.8	9.8	4760	1	0.79	4.9	4.9
225*	(2@3) 8-5-90-5#3-i-2.5-2-10	9.0	12.3	10.3	4805	1	0.79	3	3.0
226*	(2@5) 8-5-90-5#3-i-2.5-2-10	11.3	11.7	9.7	4805	1	0.79	5.3	5.3
227*	(3@5.5) 8-5-90-2#3-i-2.5-2-14	17.0	16.4	14.4	6460	1	0.79	5.5	5.5
228*	(3@5.5) 8-5-90-2#3-i-2.5-2-8.5	16.6	11.1	9.1	6460	1	0.79	5.3	5.3
229*	(3@5.5) 8-5-90-2#3-i-2.5-2-14(1)	16.6	16.9	14.9	5450	1	0.79	5.3	5.3
230*	(3@5.5) 8-5-90-2#3-i-2.5-2-8.5(1)	16.6	10.2	8.2	5450	1	0.79	5.3	5.3
231*	(3@5) 8-5-90-2#3-i-2.5-2-10	15.8	12.5	10.5	4760	1	0.79	4.9	4.9
232*	(3@5) 8-5-180-2#3-i-2.5-2-10	16.4	11.7	9.7	5400	1	0.79	5.2	5.2
233	(3@3.75) 11-8-90-6#3-i-2.5-2-21	17.6	22.0	20	7070	1.41	1.56	5.6	4.0
234	(3@3.75) 11-12-90-6#3-i-2.5-2-19	17.2	20.3	18.3	11960	1.41	1.56	5.4	3.8
235	(3@3.75) 11-12-180-6#3-i-2.5-2-19	17.0	20.8	18.8	12190	1.41	1.56	5.3	3.8
236*	(3@3.75) 11-8-90-2#3-i-2.5-2-23	17.4	24.0	22	7070	1.41	1.56	5.5	3.9
237*	(3@3.75) 11-12-90-2#3-i-2.5-2-21	17.4	23.0	21	11850	1.41	1.56	5.5	3.9
238	H14-8	20.7	37.8	36.6	6650	1.693	2.25	6	3.5

* Specimens not used to develop descriptive equations, Eq. (4.5) and (4.7)

Table B.5 Cont. Detailed properties and test results for hooked bar specimens having closely-spaced bars with confining reinforcement tested at the University of Kansas

SN	<i>n</i>	<i>A_{th}</i>	<i>A_{hs}</i>	<i>A_{th}/A_{hs}</i>	<i>A_{th,ACI}/A_{hs}</i>	<i>h_{cl}</i>	<i>x_{mid}</i>	<i>d_{eff}</i>	<i>d_{eff}/ℓ_{eh}</i>	<i>θ</i>
		in. ²	in. ²			in.	in.	in.		°
221	3	0.66	2.37	0.278	0.464	10	14.19	11.92	0.98	49.3
222	3	0.66	2.37	0.278	0.464	10	14.19	13.07	1.35	55.6
223*	2	0.22	1.58	0.139	0.278	10	14.19	13.06	1.27	54.0
224*	2	0.44	1.58	0.278	0.278	10	14.19	12.71	1.30	55.4
225*	2	0.66	1.58	0.418	0.696	10	14.19	13.89	1.35	54.0
226*	2	0.66	1.58	0.418	0.696	10	14.19	12.99	1.34	55.6
227*	3	0.22	2.37	0.093	0.186	10	14.19	12.53	0.87	44.6
228*	3	0.22	2.37	0.093	0.186	10	14.19	11.85	1.30	57.3
229*	3	0.22	2.37	0.093	0.186	10	14.19	13.28	0.89	43.6
230*	3	0.22	2.37	0.093	0.186	10	14.19	11.62	1.42	60.0
231*	3	0.22	2.37	0.093	0.186	10	14.19	12.58	1.20	53.5
232*	3	0.22	2.37	0.093	0.186	10	14.19	12.63	1.30	55.6
233	3	0.66	4.68	0.141	0.282	19.5	23.69	24.02	1.20	49.8
234	3	0.66	4.68	0.141	0.282	19.5	23.69	22.62	1.24	52.3
235	3	0.66	4.68	0.141	0.282	19.5	23.69	22.61	1.20	51.6
236*	3	0.22	4.68	0.047	0.094	19.5	23.69	24.30	1.10	47.1
237*	3	0.22	4.68	0.047	0.094	19.5	23.69	22.86	1.09	48.4
238	3	1.86	6.75	0.276	0.367	24.0	28.54	34.70	0.95	38.0

* Specimens not used to develop descriptive equations, Eq. (4.5) and (4.7)

Table B.5 Cont. Detailed properties and test results for hooked bar specimens having closely-spaced bars with confining reinforcement tested at the University of Kansas

SN	T	T_h ^[1]	T/T_h	f_{su}	$f_{su}/f_{s,calc}$ ^[2]	$f_{su}/f_{s,calc}$ ^[3]
	lb	lb		ksi		
221	64761	75205	0.86	82.0	1.03	1.03
222	58669	51317	1.14	74.3	1.40	1.40
223*	46810	43348	1.08	59.3	1.20	1.27
224*	48515	50120	0.97	61.4	1.19	1.38
225*	57922	52734	1.10	73.3	1.35	1.35
226*	55960	56281	0.99	70.8	1.38	1.38
227*	57261	70966	0.81	72.5	0.89	1.07
228*	40885	43795	0.93	51.8	1.00	1.24
229*	65336	69653	0.94	82.7	1.02	1.27
230*	32368	37767	0.86	41.0	0.92	1.14
231*	44668	45946	0.97	56.5	1.08	1.35
232*	51501	44411	1.16	65.2	1.25	1.56
233	111288	120200	0.93	71.3	1.04	1.18
234	118300	124742	0.95	75.8	1.08	1.21
235	119045	128284	0.93	76.3	1.06	1.18
236*	119045	122782	0.97	74.7	1.31	1.47
237*	119045	134402	0.89	81.9	1.33	1.48
238	298200	258627	1.15	132.5	1.27	1.24

* Specimens not used to develop descriptive equations, Eq. (4.5) and (4.7)

[2] Based on design equation, Eq. (6.18), using full expression for ψ_r , Eq. (6.14)

[3] Based on design equation, Eq. (6.18), using simplified expression for ψ_r , Eq. (6.15)

Table B.6 Detailed properties and test results for hooked bar specimens with bars placed outside column longitudinal reinforcement (column core) tested at the University of Kansas

SN*	ID	<i>b</i>	<i>h</i>	$\ell_{eh,avg}$	f_{cm}	d_b	A_b	<i>s</i>	s/d_b
		in.	in.	in.	psi	in.	in. ²	in.	
239	5-5-90-0-o-1.5-2-5	9.8	7.0	5.0	4930	0.63	0.31	6.2	9.8
240	5-5-90-0-o-2.5-2-5	11.4	6.8	4.8	4930	0.63	0.31	5.8	9.2
241	5-5-90-0-o-1.5-2-6.5	9.6	8.2	6.2	5650	0.63	0.31	6.0	9.5
242	5-5-90-0-o-1.5-2-8	9.6	9.9	7.9	5650	0.63	0.31	6.0	9.5
243	5-5-90-0-o-2.5-2-8	11.6	11.0	9.0	5780	0.63	0.31	6.0	9.5
244	5-5-180-0-o-1.5-2-9.5	9.4	11.4	9.4	4420	0.63	0.31	5.8	9.2
245	5-5-180-0-o-2.5-2-9.5	11.6	11.5	9.5	4520	0.63	0.31	6.0	9.5
246	5-5-180-0-o-1.5-2-11.25	9.6	13.3	11.3	4520	0.63	0.31	6.0	9.5
247	5-5-180-2#3-o-2.5-2-9.5	11.9	11.2	9.2	4420	0.63	0.31	6.3	10.0
248	5-5-180-2#3-o-1.5-2-11.25	9.9	13.6	11.6	4420	0.63	0.31	6.3	10.0
249	5-5-180-2#3-o-1.5-2-9.5	9.9	10.8	8.8	4520	0.63	0.31	6.3	10.0
250	5-5-180-2#3-o-2.5-2-11.25	11.9	13.3	11.3	4520	0.63	0.31	6.3	10.0
251	5-5-90-5#3-o-1.5-2-5	9.8	7.0	5.0	5205	0.63	0.31	6.2	9.8
252	5-5-90-5#3-o-2.5-2-5	11.9	7.2	5.2	4930	0.63	0.31	6.3	10.0
253	5-5-90-5#3-o-1.5-2-8	9.7	9.9	7.9	5650	0.63	0.31	6.1	9.7
254	5-5-90-5#3-o-2.5-2-8	11.8	9.5	7.5	5650	0.63	0.31	6.2	9.8
255	5-5-90-5#3-o-1.5-2-6.5	9.8	8.5	6.5	5780	0.63	0.31	6.2	9.8

* No specimen used in developing descriptive equations, Eq. (4.5) and (4.7)

Table B.6 Cont. Detailed properties and test results for hooked bar specimens with bars placed outside column longitudinal reinforcement (column core) tested at the University of Kansas

SN*	<i>n</i>	<i>A_{th}</i>	<i>A_{hs}</i>	<i>A_{th}</i> / <i>A_{hs}</i>	<i>A_{th,ACT}</i> / <i>A_{hs}</i>	<i>h_{ct}</i>	<i>x_{mid}</i>	<i>d_{eff}</i>	<i>d_{eff}</i> / <i>ℓ_{eh}</i>	<i>θ</i>
		in. ²	in. ²			in.	in.	in.		°
239	2	0	0.62	0	0	5.25	9.44	6.10	1.22	62.1
240	2	0	0.62	0	0	5.25	9.44	6.25	1.30	63.0
241	2	0	0.62	0	0	5.25	9.44	6.25	1.01	56.7
242	2	0	0.62	0	0	5.25	9.44	6.54	0.83	50.1
243	2	0	0.62	0	0	5.25	9.44	6.45	0.72	46.4
244	2	0	0.62	0	0	5.25	9.44	7.26	0.77	45.1
245	2	0	0.62	0	0	5.25	9.44	6.89	0.72	44.8
246	2	0	0.62	0	0	5.25	9.44	7.38	0.65	39.9
247	2	0.22	0.62	0.350	0.583	5.25	9.44	7.16	0.78	45.7
248	2	0.22	0.62	0.350	0.583	5.25	9.44	8.04	0.69	39.1
249	2	0.22	0.62	0.350	0.583	5.25	9.44	6.54	0.74	47.0
250	2	0.22	0.62	0.350	0.583	5.25	9.44	7.49	0.66	39.9
251	2	0.66	0.62	1.060	1.767	5.25	9.44	6.52	1.30	62.1
252	2	0.66	0.62	1.060	1.767	5.25	9.44	6.37	1.23	61.1
253	2	0.66	0.62	1.060	1.767	5.25	9.44	6.65	0.84	50.1
254	2	0.66	0.62	1.060	1.767	5.25	9.44	6.39	0.85	51.5
255	2	0.66	0.62	1.060	1.767	5.25	9.44	6.43	0.99	55.4

* No specimen used in developing descriptive equations, Eq. (4.5) and (4.7)

Table B.6 Cont. Detailed properties and test results for hooked bar specimens with bars placed outside column longitudinal reinforcement (column core) tested at the University of Kansas

SN*	T	T_h ^[1]	T/T_h ^[2]	f_{su}	$f_{su}/f_{s,calc}$ ^[3]	$f_{su}/f_{s,calc}$ ^[4]
	lb	lb		ksi		
239	14100	16942	0.97	45.5	1.10	1.10
240	19300	16194	1.39	62.3	1.56	1.56
241	17800	22333	0.93	57.4	1.08	1.08
242	22800	29200	0.91	73.5	1.08	1.08
243	26100	33947	0.90	84.2	1.08	1.08
244	29500	33034	1.04	95.2	1.25	1.25
245	30100	33634	1.05	97.1	1.26	1.26
246	32400	40752	0.93	104.5	1.14	1.14
247	35500	36556	1.14	114.5	1.39	1.39
248	43100	45987	1.10	139.0	1.33	1.33
249	20300	35202	0.67	65.5	0.82	0.82
250	42300	45051	1.10	136.5	1.34	1.34
251	21800	30222	0.84	70.3	1.50	1.50
252	22500	30713	0.86	72.6	1.51	1.51
253	25100	42221	0.70	81.0	1.07	1.07
254	24900	40589	0.72	80.3	1.12	1.12
255	21700	36703	0.69	70.0	1.12	1.12

* No specimen used in developing descriptive equations, Eq. (4.5) and (4.7)

[1] Based on descriptive equations, Eq. (4.5) and (4.7)

[2] Bar location factor of 1.17 applied

[3] Based on design equation, Eq. (6.18), using full expression for ψ_r , Eq. (6.14)

[4] Based on design equation, Eq. (6.18), using simplified expression for ψ_r , Eq. (6.15)

Table B.6 Cont. Detailed properties and test results for hooked bar specimens with bars placed outside column longitudinal reinforcement (column core) tested at the University of Kansas

SN*	ID	<i>b</i>	<i>h</i>	$\ell_{eh,avg}$	f_{cm}	d_b	A_b	<i>s</i>	s/d_b
		in.	in.	in.	psi	in.	in. ²	in.	
256	8-5-90-0-o-2.5-2-10a	15.0	12.4	10.4	5270	1	0.79	9.0	9.0
257	8-5-90-0-o-2.5-2-10b	15.0	11.8	9.8	5440	1	0.79	9.0	9.0
258	8-5-90-0-o-2.5-2-10c	15.0	12.6	10.6	5650	1	0.79	9.0	9.0
259	8-8-90-0-o-2.5-2-8	14.0	10.4	8.4	8740	1	0.79	8.0	8.0
260	8-8-90-0-o-3.5-2-8	16.8	9.8	7.8	8810	1	0.79	8.8	8.8
261	8-8-90-0-o-4-2-8	17.8	10.2	8.2	8630	1	0.79	8.8	8.8
262	8-5-90-5#3-o-2.5-2-10a	15.1	12.4	10.4	5270	1	0.79	9.1	9.1
263	8-5-90-5#3-o-2.5-2-10b	15.1	12.5	10.5	5440	1	0.79	9.1	9.1
264	8-5-90-5#3-o-2.5-2-10c	15.1	12.9	10.9	5650	1	0.79	9.1	9.1
265	8-8-90-5#3-o-2.5-2-8	14.5	10.5	8.5	8630	1	0.79	8.5	8.5
266	8-8-90-5#3-o-3.5-2-8	16.7	9.9	7.9	8810	1	0.79	8.7	8.7
267	8-8-90-5#3-o-4-2-8	18.2	10.3	8.3	8740	1	0.79	9.2	9.2
268	11-8-90-0-o-2.5-2-25	18.5	27.2	25.2	9460	1.41	1.56	12.1	8.6
269	11-8-90-0-o-2.5-2-17	18.8	18.6	16.6	9460	1.41	1.56	12.4	8.8
270	11-12-180-0-o-2.5-2-17	18.4	19.1	17.1	11800	1.41	1.56	12.0	8.5
271	11-12-90-0-o-2.5-2-17	18.8	18.9	16.9	11800	1.41	1.56	12.4	8.8
272	11-8-90-6#3-o-2.5-2-22	18.4	23.9	21.9	9120	1.41	1.56	12.0	8.5
273	11-8-90-6#3-o-2.5-2-16	18.4	18.2	16.2	9420	1.41	1.56	12.0	8.5
274	11-12-180-6#3-o-2.5-2-17	18.4	18.5	16.5	11800	1.41	1.56	12.0	8.5
275	11-12-90-6#3-o-2.5-2-17	18.7	18.4	16.4	11800	1.41	1.56	12.3	8.7

* No specimen used in developing descriptive equations, Eq. (4.5) and (4.7)

Table B.6 Cont. Detailed properties and test results for hooked bar specimens with bars placed outside column longitudinal reinforcement (column core) tested at the University of Kansas

SN*	<i>n</i>	<i>A_{th}</i>	<i>A_{hs}</i>	<i>A_{th}/A_{hs}</i>	<i>A_{th,ACI}/A_{hs}</i>	<i>h_{cl}</i>	<i>x_{mid}</i>	<i>d_{eff}</i>	<i>d_{eff}/ℓ_{eh}</i>	<i>θ</i>
		in. ²	in. ²			in.	in.	in.		°
256	2	0	1.58	0	0	10.00	14.19	11.60	1.12	53.8
257	2	0	1.58	0	0	10.00	14.19	11.25	1.15	55.4
258	2	0	1.58	0	0	10.00	14.19	12.03	1.13	53.2
259	2	0	1.58	0	0	10.00	14.19	10.98	1.31	59.4
260	2	0	1.58	0	0	10.00	14.19	10.88	1.39	61.2
261	2	0	1.58	0	0	10.00	14.19	10.88	1.33	60.0
262	2	0.66	1.58	0.420	0.700	10.00	14.19	12.04	1.16	53.8
263	2	0.66	1.58	0.420	0.700	10.00	14.19	12.42	1.18	53.5
264	2	0.66	1.58	0.420	0.700	10.00	14.19	12.07	1.11	52.5
265	2	0.66	1.58	0.420	0.700	10.00	14.19	11.68	1.37	59.1
266	2	0.66	1.58	0.420	0.700	10.00	14.19	11.35	1.44	60.9
267	2	0.66	1.58	0.420	0.700	10.00	14.19	10.89	1.31	59.7
268	2	0	3.12	0	0	19.50	23.69	23.11	0.92	43.2
269	2	0	3.12	0	0	19.50	23.69	21.68	1.31	55.0
270	2	0	3.12	0	0	19.50	23.69	20.89	1.22	54.2
271	2	0	3.12	0	0	19.50	23.69	21.22	1.26	54.5
272	2	0.66	3.12	0.210	0.350	19.50	23.69	23.17	1.06	47.2
273	2	0.66	3.12	0.210	0.350	19.50	23.69	22.36	1.38	55.6
274	2	0.66	3.12	0.210	0.350	19.50	23.69	21.39	1.30	55.1
275	2	0.66	3.12	0.210	0.350	19.50	23.69	21.40	1.31	55.3

* No specimen used in developing descriptive equations, Eq. (4.5) and (4.7)

Table B.6 Cont. Detailed properties and test results for hooked bar specimens with bars placed outside column longitudinal reinforcement (column core) tested at the University of Kansas

SN*	T	T_h ^[1]	T/T_h ^[2]	f_{su}	$f_{su}/f_{s,calc}$ ^[3]	$f_{su}/f_{s,calc}$ ^[4]
	lb	lb		ksi		
256	42300	47338	1.05	53.5	1.22	1.22
257	33700	44723	0.88	42.7	1.02	1.02
258	56000	49301	1.33	70.9	1.56	1.56
259	33000	43084	0.90	41.8	1.04	1.04
260	35900	39781	1.06	45.4	1.21	1.21
261	37500	41801	1.05	47.5	1.21	1.21
262	54300	65444	0.97	68.7	1.41	1.41
263	65600	66376	1.16	83.0	1.67	1.67
264	57700	68953	0.98	73.0	1.40	1.40
265	58000	61602	1.10	73.4	1.63	1.63
266	55000	58452	1.10	69.6	1.65	1.65
267	39100	60622	0.75	49.5	1.12	1.12
268	174700	172174	1.19	112.0	1.52	1.52
269	107200	108489	1.16	68.7	1.42	1.42
270	83500	119293	0.82	53.5	1.01	1.01
271	105400	117750	1.05	67.6	1.30	1.30
272	170200	168581	1.18	109.1	1.55	1.55
273	136800	128155	1.25	87.7	1.67	1.67
274	113100	137350	0.96	72.5	1.28	1.28
275	115900	136582	0.99	74.3	1.32	1.32

* No specimen used in developing descriptive equations, Eq. (4.5) and (4.7)

^[1] Based on descriptive equations, Eq. (4.5) and (4.7)

^[2] Bar location factor of 1.17 applied

^[3] Based on design equation, Eq. (6.18), using full expression for ψ_r , Eq. (6.14)

^[4] Based on design equation, Eq. (6.18), using simplified expression for ψ_r , Eq. (6.15)

Table B.7 Detailed properties and test results for hooked bar specimens with effective beam depth to embedment ratio $d_{eff}/\ell_{eh} > 1.5$ tested at the University of Kansas

SN*	ID	<i>b</i>	<i>h</i>	$\ell_{eh,avg}$	f_{cm}	d_b	A_b	<i>s</i>	s/d_b
		in.	in.	in.	psi	in.	in. ²	in.	
276	8-5-90-5#3-i-2.5-2-8	16.0	9.6	7.6	5240	1	0.79	10	10.0
277	8-8-90-5#3-i-2.5-2-8	15.5	9.3	7.3	8290	1	0.79	9.5	9.5
278	(3@5.5) 8-5-90-5#3-i-2.5-2-8(1)	16.2	9.6	7.6	5660	1	0.79	5.1	5.1
279	11-15-90-0-i-2.5-2-10	20.9	11.5	9.5	14050	1.41	1.56	15.0	10.6
280	11-5-90-2#3-i-2.5-2-14	21.1	15.6	13.6	4910	1.41	1.56	14.7	10.4
281	11-15-90-2#3-i-2.5-2-10	21.2	12.0	10.0	14045	1.41	1.56	14.8	10.5
282	11-5-90-2#3-i-3.5-2-14	23.1	15.9	13.9	4910	1.41	1.56	14.7	10.4
283	(2@7.5) 11-12-90-6#3-i-2.5-2-14a	16.9	15.6	13.6	11960	1.41	1.56	10.5	7.4
284	11-15-90-6#3-i-2.5-2-10a	21.2	11.8	9.8	14045	1.41	1.56	14.8	10.5
285	11-15-90-6#3-i-2.5-2-10b	20.8	11.6	9.6	14050	1.41	1.56	14.4	10.2

* No specimen used in developing descriptive equations, Eq. (4.5) and (4.7)

Table B.7 Cont. Detailed properties and test results for hooked bar specimens with effective beam depth to embedment ratio $d_{eff}/\ell_{eh} > 1.5$ tested at the University of Kansas

SN*	<i>n</i>	A_{th}	A_{hs}	A_{th}/A_{hs}	$A_{th,ACI}/A_{hs}$	h_{cl}	x_{mid}	d_{eff}	d_{eff}/ℓ_{eh}	θ
		in. ²	in. ²			in.	in.	in.		°
276	2	0.66	1.58	0.418	0.696	10.00	14.19	11.69	1.54	61.8
277	2	0.66	1.58	0.418	0.696	10.00	14.19	11.42	1.56	62.8
278	3	0.66	2.37	0.278	0.464	10.00	14.19	11.57	1.52	61.8
279	2	0	3.12	0	0	19.5	23.69	20.13	2.12	68.1
280	2	0.22	3.12	0.071	0.118	19.5	23.69	21.68	1.59	60.1
281	2	0.22	3.12	0.071	0.118	19.5	23.69	20.28	2.03	67.1
282	2	0.22	3.12	0.071	0.118	19.5	23.69	21.62	1.56	59.6
283	2	0.66	3.12	0.212	0.353	19.5	23.69	21.33	1.57	60.1
284	2	0.66	3.12	0.212	0.353	19.5	23.69	20.50	2.09	67.5
285	2	0.66	3.12	0.212	0.353	19.5	23.69	20.44	2.13	67.9

* No specimen used in developing descriptive equations, Eq. (4.5) and (4.7)

Table B.7 Cont. Detailed properties and test results for hooked bar specimens with effective beam depth to embedment ratio $d_{eff}/\ell_{eh} > 1.5$ tested at the University of Kansas

SN*	T	T_h ^[1]	T/T_h	f_{su}	$f_{su}f_{s,calc}$ ^[2]	$f_{su}f_{s,calc}$ ^[3]
	lb	lb		ksi		
276	47478	51412	0.92	60.1	1.47	1.47
277	50266	54351	0.92	63.6	1.44	1.44
278	31369	42379	0.74	39.7	0.95	0.95
279	51481	65385	0.79	33.0	0.94	0.94
280	77422	79990	0.97	49.6	1.15	1.28
281	63940	76811	0.83	41.0	1.00	1.11
282	82275	81759	1.01	52.7	1.20	1.33
283	102038	115789	0.88	65.4	1.22	1.22
284	82681	90512	0.91	53.0	1.31	1.31
285	75579	88993	0.85	48.4	1.23	1.23

* No specimen used in developing descriptive equations, Eq. (4.5) and (4.7)

^[1] Based on descriptive equations, Eq. (4.5) and (4.7)

^[2] Based on design equation, Eq. (6.18), using full expression for ψ_r , Eq. (6.14)

^[3] Based on design equation, Eq. (6.18), using simplified expression for ψ_r , Eq. (6.15)

B.4 SPECIMENS TESTED IN OTHER STUDIES

This section presents the specimens tested outside the University of Kansas, including those by Marques and Jirsa (1975), Pinc et al (1977), Hamad et al. (1993), Ramirez and Russel (2008), Lee and Park (2010), and Chun et al. (2017b), as tabulated in Table B.8. A few of these specimens were used in developing the descriptive equations, Eq. (4.5) and (4.7), which are identified here.

Table B.8 Detailed properties and test results for hooked bar specimens tested outside the University of Kansas

Study	SN	ID	<i>b</i>	<i>h</i>	$\ell_{eh,avg}$	f_{cm}	d_b	A_b	<i>s</i>	s/d_b
			in.	in.	in.	psi	in.	in. ²	in.	
Marques and Jirsa (1975)	286	J7-180-12-1-H	12.0	12.0	10.0	4350	0.875	0.6	5.3	6.1
	287	J7-180-15-1-H	12.0	15.0	13.0	4000	0.875	0.6	5.3	6.1
	288	J7-90-12-1-H	12.0	12.0	10.0	4150	0.875	0.6	5.3	6.1
	289	J7-90-15-1-H	12.0	15.0	13.0	4600	0.875	0.6	5.3	6.1
	290	J7-90-15-1-L	12.0	15.0	13.0	4800	0.875	0.6	5.3	6.1
	291	J7-90-15-1-M	12.0	15.0	13.0	5050	0.875	0.6	5.3	6.1
	292	J11-180-15-1-H	12.0	15.0	13.1	4400	1.41	1.56	4.8	3.4
	293	J11-90-12-1-H	12.0	12.0	10.1	4600	1.41	1.56	4.8	3.4
	294	J11-90-15-1-H	12.0	15.0	13.1	4900	1.41	1.56	4.8	3.4
	295	J11-90-15-1-L	12.0	15.0	13.1	4750	1.41	1.56	4.8	3.4
	296	J7-90-15-3a-H	12.0	15.0	13.0	3750	0.875	0.6	5.3	6.1
	297	J7-90-15-3-H	12.0	15.0	13.0	4650	0.875	0.6	5.3	6.1
	298	J11-90-15-3a-L	12.0	15.0	13.1	5000	1.41	1.56	4.8	3.4
	299	J11-90-15-3-L	12.0	15.0	13.1	4850	1.41	1.56	4.8	3.4
Pinc et al. (1977)	300	9-12	12.0	12.0	10.0	4700	1.13	1	5.1	4.5
	301	11-15	12.0	15.0	13.1	5400	1.41	1.56	4.8	3.4
	302	11-18	12.0	18.0	16.1	4700	1.41	1.56	4.8	3.4

Table B.8 Cont. Detailed properties and test results for hooked bar specimens tested outside the University of Kansas

Study	SN	<i>n</i>	A_{th}	A_{hs}	A_{th}/A_{hs}	$A_{th,ACI}/A_{hs}$	h_{cl}	x_{mid}	d_{eff}	d_{eff}/ℓ_{eh}	θ
			in. ²	in. ²			in.	in.	in.		°
Marques and Jirsa (1975)	286	2	0	1.20	0	0	11.25	14.25	13.48	1.35	55.4
	287	2	0	1.20	0	0	11.25	14.25	14.51	1.12	48.1
	288	2	0	1.20	0	0	11.25	14.25	13.59	1.36	55.4
	289	2	0	1.20	0	0	11.25	14.25	14.34	1.10	48.1
	290	2	0	1.20	0	0	11.25	14.25	14.44	1.11	48.1
	29	2	0	1.20	0	0	11.25	14.25	14.42	1.11	48.1
	292	2	0	3.12	0	0	11.25	14.25	15.02	1.15	47.4
	293	2	0	3.12	0	0	11.25	14.25	14.66	1.45	54.7
	294	2	0	3.12	0	0	11.25	14.25	14.97	1.14	47.4
	295	2	0	3.12	0	0	11.25	14.25	15.37	1.17	47.4
	296	2	0.44	1.20	0.367	0.917	11.25	14.25	14.81	1.14	47.6
	297	2	0.22	1.20	0.183	0.367	11.25	14.25	14.47	1.11	47.6
	298	2	0.88	3.12	0.282	0.564	11.25	14.25	16.53	1.26	47.4
	299	2	0.44	3.12	0.141	0.282	11.25	14.25	16.09	1.23	47.4
Pinc et al. (1977)	300	2	0	2.00	0	0	11.25	14.25	13.66	1.37	54.9
	301	2	0	3.12	0	0	11.25	14.25	14.88	1.14	47.4
	302	2	0	3.12	0	0	11.25	14.25	15.88	0.99	41.5

Table B.8 Cont. Detailed properties and test results for hooked bar specimens tested outside the University of Kansas

Study	SN	T	T_h ^[1]	T/T_h	f_{su}	$f_{su}/f_{s,calc}$ ^[2]	$f_{su}/f_{s,calc}$ ^[3]
		lb	lb		ksi		
Marques and Jirsa (1975)	286	36600	39236	0.93	61.0	1.08	1.08
	287	52200	51230	1.02	87.0	1.21	1.21
	288	37200	38721	0.96	62.0	1.11	1.11
	289	54600	53281	1.02	91.0	1.22	1.22
	290	58200	53922	1.08	97.0	1.29	1.29
	291	60000	54697	1.10	100.0	1.31	1.31
	292	70200	49787	1.41	45.0	1.78	1.78
	293	65520	37873	1.73	42.0	2.13	2.13
	294	74880	50255	1.49	48.0	1.84	1.84
	295	81120	51019	1.59	52.0	2.01	2.01
	296	58800	53945	1.09	98.0	1.24	1.24
	297	62400	52000	1.20	104.0	1.25	1.25
	298	107640	72730	1.48	69.0	1.66	1.66
299	96720	61215	1.58	62.0	1.61	1.73	
Pinc et al. (1977)	300	47000	36719	1.28	47.0	1.50	1.50
	301	78000	46988	1.66	50.0	1.87	1.87
	302	90480	56906	1.59	58.0	1.83	1.83

^[1] Based on descriptive equations, Eq. (4.5) and (4.7)

^[2] Based on design equation, Eq. (6.18), using the full expression for ψ_r , Eq. (6.14)

^[3] Based on design equation, Eq. (6.18), using the simplified expression for ψ_r , Eq. (6.15)

Table B.8 Cont. Detailed properties and test results for hooked bar specimens tested outside the University of Kansas

Study	SN	ID	<i>b</i>	<i>h</i>	$\ell_{eh,avg}$	f_{cm}	d_b	A_b	<i>s</i>	s/d_b
			in.	in.	in.	psi	in.	in. ²	in.	
Hamad et al. (1993)	303*	7-90-U	12.0	12.0	10	2570	0.875	0.6	5.3	6.1
	304*	7-90-U'	12.0	12.0	10	5400	0.875	0.6	5.3	6.1
	305	11-90-U	12.0	15.0	13	2570	1.41	1.56	4.8	3.4
	306	11-90-U'	12.0	15.0	13	5400	1.41	1.56	4.8	3.4
	307	11-180-U-HS	12.0	15.0	13	7200	1.41	1.56	4.8	3.4
	308	11-90-U-HS	12.0	15.0	13	7200	1.41	1.56	4.8	3.4
	309	11-90-U-T6	12.0	15.0	13	3700	1.41	1.56	4.8	3.4
	310	7-180-U-T4	12.0	12.0	10	3900	0.875	0.6	5.3	6.1
	311	11-90-U-T4	12.0	15.0	13	4230	1.41	1.56	4.8	3.4
	312	7-90-U-SC**	12.0	12.0	10	4230	0.875	0.6	7.4	8.4
Ramirez and Russel (2008)	313	I-1	15.0	9.0	6.5	8910	0.75	0.44	9.2	12.3
	314	I-3	15.0	9.0	6.5	12460	0.75	0.44	9.2	12.3
	315	I-5	15.0	9.0	6.5	12850	0.75	0.44	9.2	12.3
	316*	I-2	15.0	15.0	12.5	8910	1.41	1.56	8.6	6.1
	317*	I-2'	15.0	18.0	15.5	9540	1.41	1.56	8.6	6.1
	318*	I-4	15.0	15.0	12.5	12460	1.41	1.56	8.6	6.1
	319	I-6	15.0	15.0	12.5	12850	1.41	1.56	8.6	6.1
	320	III-13	15.0	9.0	6.5	13980	0.75	0.44	9.2	12.3
	321	III-15	15.0	9.0	6.5	16350	0.75	0.44	9.2	12.3
	322	III-14	15.0	15.0	12.5	13980	1.41	1.56	8.6	6.1
	323	III-16	15.0	15.0	12.5	16500	1.41	1.56	8.6	6.1
Lee and Park (2010)	324*	H1	14.6	20.7	18.7	4450	0.875	0.6	7.9	9.0
	325*	H2	14.6	13.9	11.9	8270	0.875	0.6	7.9	9.0
	326	H3	14.6	17.0	15.0	4450	0.875	0.6	7.9	9.0

* Specimens used in developing descriptive equations, Eq. (4.5) and (4.7)

** Bars outside column core

Table B.8 Cont. Detailed properties and test results for hooked bar specimens tested outside the University of Kansas

Study	SN	n	A_{th}	A_{hs}	A_{th}/A_{hs}	$A_{th,ACI}/A_{hs}$	h_{cl}	x_{mid}	d_{eff}	d_{eff}/ℓ_{eh}	θ
			in. ²	in. ²			in.	in.	in.		°
Hamad et al. (1993)	303*	2	0	1.20	0	0	12.00	15.00	14.15	1.42	56.3
	304*	2	0	1.20	0	0	12.00	15.00	13.71	1.37	56.3
	305	2	0	3.12	0	0	12.00	15.00	15.98	1.23	49.1
	306	2	0	3.12	0	0	12.00	15.00	15.49	1.19	49.1
	307	2	0	3.12	0	0	12.00	15.00	14.32	1.10	49.1
	308	2	0	3.12	0	0	12.00	15.00	14.91	1.15	49.1
	309	2	0.44	3.12	0.141	0.141	12.00	15.00	16.40	1.26	49.1
	310	2	0.22	1.20	0.183	0.183	12.00	15.00	14.04	1.40	56.3
	311	2	0.66	3.12	0.212	0.212	12.00	15.00	16.60	1.28	49.1
	312	2	0	1.20	0	0	12.00	15.00	13.66	1.37	56.3
Ramirez and Russel (2008)	313	2	0	0.88	0	0	12.00	15.00	12.81	1.97	66.6
	314	2	0	0.88	0	0	12.00	15.00	12.58	1.94	66.6
	315	2	0	0.88	0	0	12.00	15.00	12.57	1.93	66.6
	316*	2	0	3.12	0	0	12.00	15.00	14.38	1.15	50.2
	317*	2	0	3.12	0	0	12.00	15.00	14.66	0.95	44.1
	318*	2	0	3.12	0	0	12.00	15.00	13.92	1.11	50.2
	319	2	0	3.12	0	0	12.00	15.00	14.14	1.13	50.2
	320	2	0.44	0.88	0.5	0.5	12.00	15.00	12.71	1.96	66.6
	321	2	0.44	0.88	0.5	0.5	12.00	15.00	12.57	1.93	66.6
	322	2	0.66	3.12	0.212	0.212	12.00	15.00	13.81	1.10	50.2
	323	2	0.66	3.12	0.212	0.212	12.00	15.00	13.75	1.10	50.2
Lee and Park (2010)	324*	2	0	1.2	0	0	**	**			
	325*	2	0	1.2	0	0	**	**			
	326	2	0.44	1.2	0.367	0.367	**	**			

* Specimens used in developing descriptive equations, Eq. (4.5) and (4.7)

** Information not provided

Table B.8 Cont. Detailed properties and test results for hooked bar specimens tested outside the University of Kansas

Study	SN	T	T_h ^[1]	T/T_h	f_{su}	$f_{su}/f_{s,calc}$ ^[2]	$f_{su}/f_{s,calc}$ ^[3]
		lb	lb		ksi		
Hamad et al. (1993)	303*	25980	32994	0.79	43.3	0.87	0.87
	304*	36720	40662	0.90	61.2	1.03	1.03
	305	48048	42520	1.13	30.8	1.40	1.40
	306	75036	52473	1.43	48.1	1.82	1.82
	307	58812	57099	1.03	37.7	1.33	1.33
	308	73788	56760	1.30	47.3	1.66	1.66
	309	71760	92000	0.78	46.0	1.44	1.57
	310	34620	32056	1.08	57.7	0.94	0.94
	311	83148	74239	1.12	53.3	1.34	1.34
	312	29940	40237	0.87**	49.9	1.02	1.02
Ramirez and Russel (2008)	313	30008	28854	1.04	68.2	1.23	1.23
	314	30008	31587	0.95	68.2	1.13	1.13
	315	30492	32097	0.95	69.3	1.14	1.14
	316*	87984	75072	1.17	56.4	1.36	1.36
	317*	104988	97097	1.08	67.3	1.29	1.29
	318*	99060	82471	1.20	63.5	1.41	1.41
	319	114036	86391	1.32	73.1	1.61	1.61
	320	41316	42159	0.98	93.9	1.36	1.36
	321	38500	43750	0.88	87.5	1.22	1.22
	322	104988	110514	0.95	67.3	1.31	1.45
	323	119964	114251	1.05	76.9	1.43	1.59
Lee and Park (2010)	324*	59220	81795	0.72	98.7	0.93	0.93
	325*	52800	59034	0.89	88.0	1.11	1.11
	326	53760	74667	0.72	89.6	0.95	0.95

* Specimens used in developing descriptive equations, Eq. (4.5) and (4.7)

** Bar location factor of 1.17 applied

[1] Based on descriptive equations, Eq. (4.5) and (4.7)

[2] Based on design equation, Eq. (6.18), using the simplified expression for ψ_r , Eq. (6.14)

[3] Based on design equation, Eq. (6.18), using the simplified expression for ψ_r , Eq. (6.15)

Table B.8 Cont. Detailed properties and test results for hooked bar specimens tested outside the University of Kansas

Study	SN	ID	<i>b</i>	<i>h</i>	$\ell_{eh,avg}$	<i>f_{cm}</i>	<i>d_b</i>	<i>A_b</i>	<i>s</i>	<i>s/d_b</i>
			in.	in.	in.	psi	in.	in. ²	in.	
Chun et al. (2017b)*	327	D43-L10-C1-S42	21.1	18.9	16.9	6440	1.693	2.25	16.3	9.6
	328	D43-L10-C1-S42-C	21.1	18.9	16.9	6950	1.693	2.25	16.3	9.6
	329	D43-L10-C1-S70	21.1	18.9	16.9	10010	1.693	2.25	16.3	9.6
	330	D43-L10-C2-S42	24.5	18.9	16.9	7020	1.693	2.25	16.3	9.6
	331	D43-L13-C1-S42	21.1	24.0	22	7020	1.693	2.25	16.3	9.6
	332	D43-L13-C1-S42-C	21.1	24.0	22	7020	1.693	2.25	16.3	9.6
	333	D43-L13-C1-S70	21.1	24.0	22	10600	1.693	2.25	16.3	9.6
	334	D43-L13-C2-S42	24.5	24.0	22	7020	1.693	2.25	16.3	9.6
	335	D43-L16-C1-S42	21.1	29.1	27.1	7020	1.693	2.25	16.3	9.6
	336	D43-L16-C1-S42-C	21.1	29.1	27.1	7020	1.693	2.25	16.3	9.6
	337	D43-L16-C1-S70	21.1	29.1	27.1	10010	1.693	2.25	16.3	9.6
	338	D43-L16-C2-S42	24.5	29.1	27.1	7020	1.693	2.25	16.3	9.6
	339	D43-L20-C1-S42	21.1	36.5	33.9	7020	1.693	2.25	16.3	9.6
	340	D57-L10-C1-S42-a	22.2	24.4	22.6	5450	2.257	4	16.3	7.2
	341	D57-L10-C1-S42-b	22.2	24.4	22.6	6150	2.257	4	16.3	7.2
	342	D57-L10-C1-S42-C	22.2	24.4	22.6	5450	2.257	4	16.3	7.2
	343	D57-L10-C2-S42	26.7	24.4	22.6	5450	2.257	4	16.3	7.2
	344	D57-L13-C1-S42-a	22.2	31.5	29.3	5450	2.257	4	16.3	7.2
	345	D57-L13-C1-S42-b	22.2	31.5	29.3	6150	2.257	4	16.3	7.2
	346	D57-L13-C1-S42-C	22.2	31.5	29.3	5450	2.257	4	16.3	7.2
	347	D57-L13-C2-S42	26.7	31.5	29.3	5450	2.257	4	16.3	7.2
	348	D57-L16-C1-S42-a	22.2	38.3	36.1	5450	2.257	4	16.3	7.2
	349	D57-L16-C1-S42-b	22.2	38.3	36.1	6150	2.257	4	16.3	7.2
350	D57-L16-C1-S42-C	22.2	38.3	36.1	5450	2.257	4	16.3	7.2	
351	D57-L16-C2-S42	26.7	38.3	36.1	6530	2.257	4	16.3	7.2	
352	D57-L20-C1-S42	22.2	47.2	45.1	6530	2.257	4	16.3	7.2	

* Bars outside column core in all specimens. Bars outside confining ties in specimens without “-C” at the end of their designation, therefore $A_{th}/A_{hs} = 0$ when calculating ψ_r .

Table B.8 Cont. Detailed properties and test results for hooked bar specimens tested outside the University of Kansas

Study	SN	n	A_{th}	A_{hs}	A_{th}/A_{hs}	$A_{th,ACI}/A_{hs}$	h_{cl}	x_{mid}	d_{eff}	d_{eff}/ℓ_{eh}	θ
			in. ²	in. ²			in.	in.	in.		°
Chun et al. (2017b)	327	2	3.96	4.5	0.88	0.196	8.74	11.3	11.48	0.68	33.7
	328	2	2.66	4.5	0.59	1.173	8.74	11.3	12.60	0.75	33.7
	329	2	3.96	4.5	0.88	0.196	8.74	11.3	10.85	0.64	33.7
	330	2	3.96	4.5	0.88	0.196	8.74	11.3	11.31	0.67	33.7
	331	2	3.96	4.5	0.88	0.196	11.82	14.7	15.12	0.69	33.7
	332	2	2.66	4.5	0.59	0.978	11.82	14.7	15.70	0.71	33.7
	333	2	3.96	4.5	0.88	0.196	12.12	14.7	14.43	0.66	33.7
	334	2	3.96	4.5	0.88	0.196	11.82	14.7	14.85	0.68	33.7
	335	2	3.96	4.5	0.88	0.196	14.71	18.1	18.42	0.68	33.7
	336	2	2.66	4.5	0.59	0.978	14.71	18.1	18.74	0.69	33.7
	337	2	3.96	4.5	0.88	0.196	15.21	18.1	18.17	0.67	33.7
	338	2	3.96	4.5	0.88	0.196	14.71	18.1	18.27	0.67	33.7
	339	2	3.96	4.5	0.88	0.196	18.82	22.6	22.74	0.67	33.7
	340	2	5.28	8	0.66	0.083	11.30	15.1	14.97	0.66	33.7
	341	2	5.28	8	0.66	0.083	11.30	15.1	14.78	0.65	33.7
	342	2	3.52	8	0.44	0.660	11.30	15.1	16.87	0.75	33.7
	343	2	5.28	8	0.66	0.083	11.70	15.1	16.16	0.71	33.7
	344	2	5.28	8	0.66	0.083	15.36	19.5	21.27	0.73	33.7
	345	2	5.28	8	0.66	0.083	15.36	19.5	20.76	0.71	33.7
	346	2	3.52	8	0.44	0.660	15.36	19.5	21.72	0.74	33.7
347	2	5.28	8	0.66	0.083	15.36	19.5	21.04	0.72	33.7	
348	2	5.28	8	0.66	0.083	19.37	24.1	25.72	0.71	33.7	
349	2	5.28	8	0.66	0.083	19.37	24.1	25.96	0.72	33.7	
350	2	3.52	8	0.44	0.660	19.37	24.1	26.36	0.73	33.7	
351	2	5.28	8	0.66	0.083	19.37	24.1	25.31	0.70	33.7	
352	2	5.28	8	0.66	0.083	24.79	30.1	32.15	0.71	33.7	

Table B.8 Cont. Detailed properties and test results for hooked bar specimens tested outside the University of Kansas

Study	SN	T	T_h ^[1]	T/T_h	f_{su}	$f_{su}/f_{s,calc}$ ^[2]	$f_{su}/f_{s,calc}$ ^[3]
		lb	lb		ksi		
Chun et al. (2017b)	327	115425	92200	1.25	51.3	1.51	1.51
	328	168975	182814	0.92	75.1	1.51	1.73
	329	123300	104341	1.18	54.8	1.44	1.44
	330	131625	94538	1.39	58.5	1.68	1.68
	331	144900	126374	1.15	64.4	1.42	1.42
	332	170775	214649	0.80	75.9	1.17	1.34
	333	142425	141547	1.01	63.3	1.26	1.26
	334	154575	125824	1.23	68.7	1.52	1.52
	335	163350	158654	1.03	72.6	1.30	1.30
	336	177525	248739	0.71	78.9	0.99	1.13
	337	172800	175824	0.98	76.8	1.26	1.26
	338	182025	158752	1.15	80.9	1.45	1.45
	339	172125	204327	0.84	76.5	1.10	1.10
	340	147200	136752	1.08	36.8	1.30	1.30
	341	150400	141260	1.06	37.6	1.29	1.29
	342	223200	280543	0.80	55.8	1.38	1.57
	343	214800	137007	1.57	53.7	1.89	1.89
	344	236400	182028	1.30	59.1	1.61	1.61
	345	232800	189499	1.23	58.2	1.53	1.53
	346	254400	329448	0.77	63.6	1.21	1.38
	347	273600	182692	1.50	68.4	1.86	1.86
	348	254000	228520	1.11	63.5	1.40	1.40
349	284000	237976	1.19	71.0	1.52	1.52	
350	279600	373397	0.75	69.9	1.08	1.23	
351	318800	241132	1.32	79.7	1.68	1.68	
352	328400	308444	1.06	82.1	1.39	1.39	

^[1] Based on descriptive equations, Eq. (4.5) and (4.7)

^[2] Based on design equation, Eq. (6.18), using the simplified expression for ψ_r , Eq. (6.14)

^[3] Based on design equation, Eq. (6.18), using the simplified expression for ψ_r , Eq. (6.15)

APPENDIX C: HEADED BAR BEAM-COLUMN JOINT SPECIMENS

Appendix C presents the details of the headed bar specimens. Appendix C1 presents specimen drawings and reinforcement layouts for No. 14 and No. 18 bars tested in this study. Appendix C2 presents detailed properties and test results for the No. 14 and No. 18 bar specimens of this study. Appendix C3 presents specimens tested at the University of Kansas used to develop descriptive equations, Eq. (5.5) and (5.7), including No. 5, No. 8, and No. 11 bar specimens by Shao et al. (2016), and No. 14 and No. 18 bars tested in this study. Appendix C4 presents the specimens tested outside the University of Kansas, including those by Bashandy (1996), Chun et al. (2017a), and Sim and Chun (2022a, 2022b), none of which were used to develop descriptive equations.

C.1 DRAWINGS AND REINFORCEMENT LAYOUTS FOR NO. 14 AND NO. 18 BAR SPECIMENS TESTED IN CURRENT STUDY

This section presents elevation and cross-sectional drawings of the No. 14 and No. 18 bar specimens tested in this study, showing the details of the reinforcement layouts. In the cross-sectional drawings, confining reinforcement is omitted for clarity.

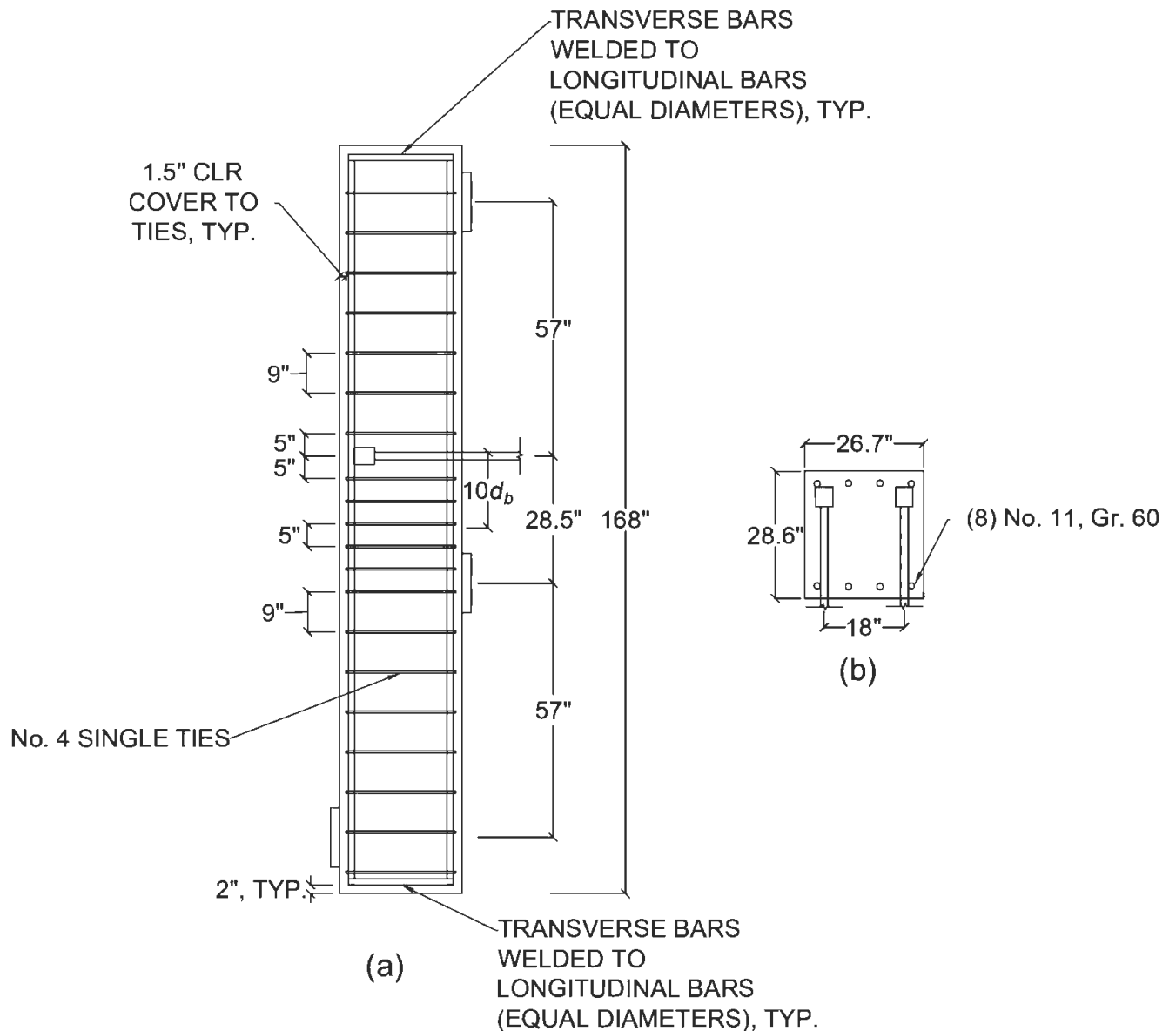


Figure C.1 Details of reinforcement layout for No. 14 headed bar specimen 14-2: (a) elevation, (b) cross-section

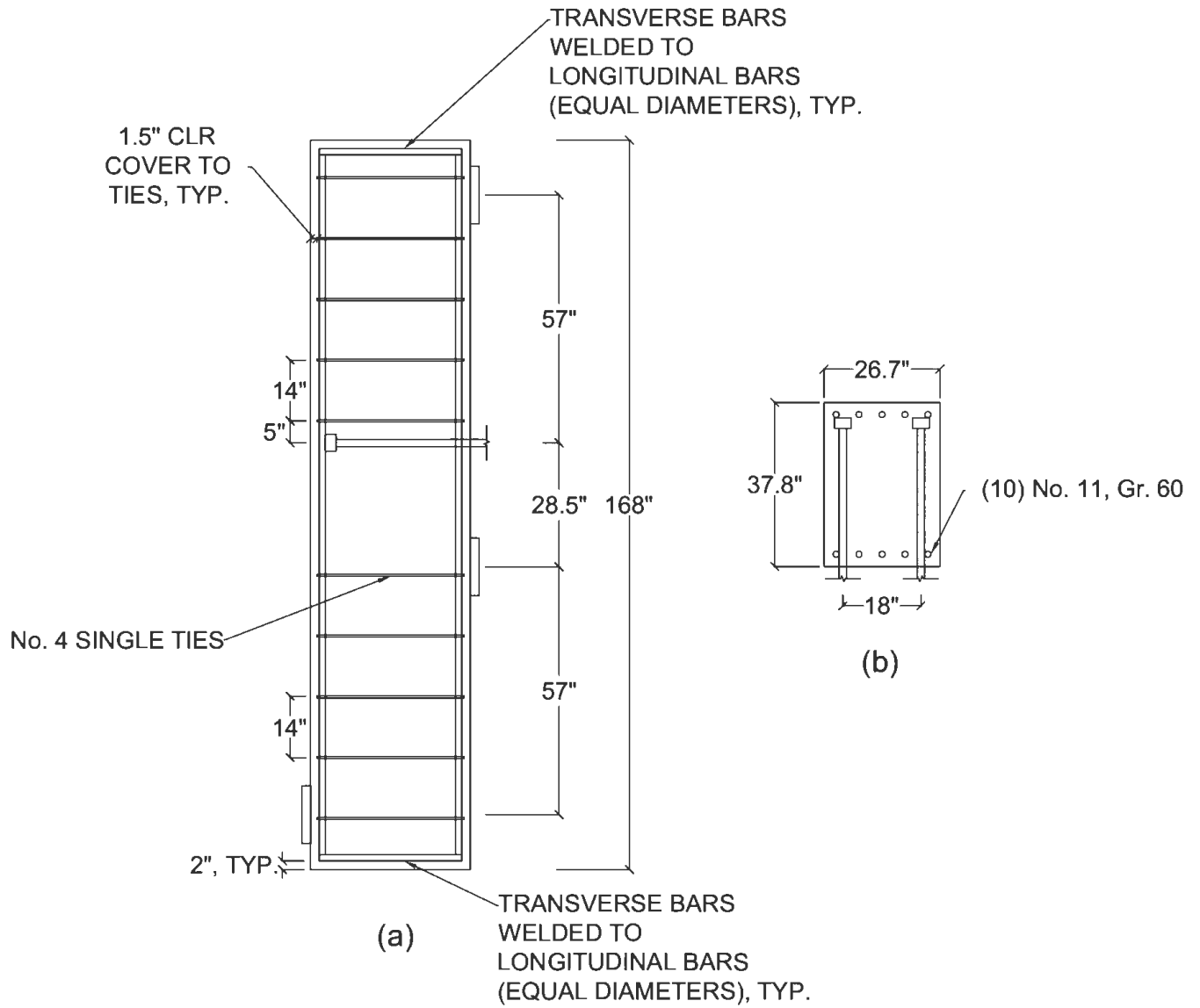


Figure C.2 Details of reinforcement layout for No. 14 headed bar specimen 14-3: (a) elevation, (b) cross-section

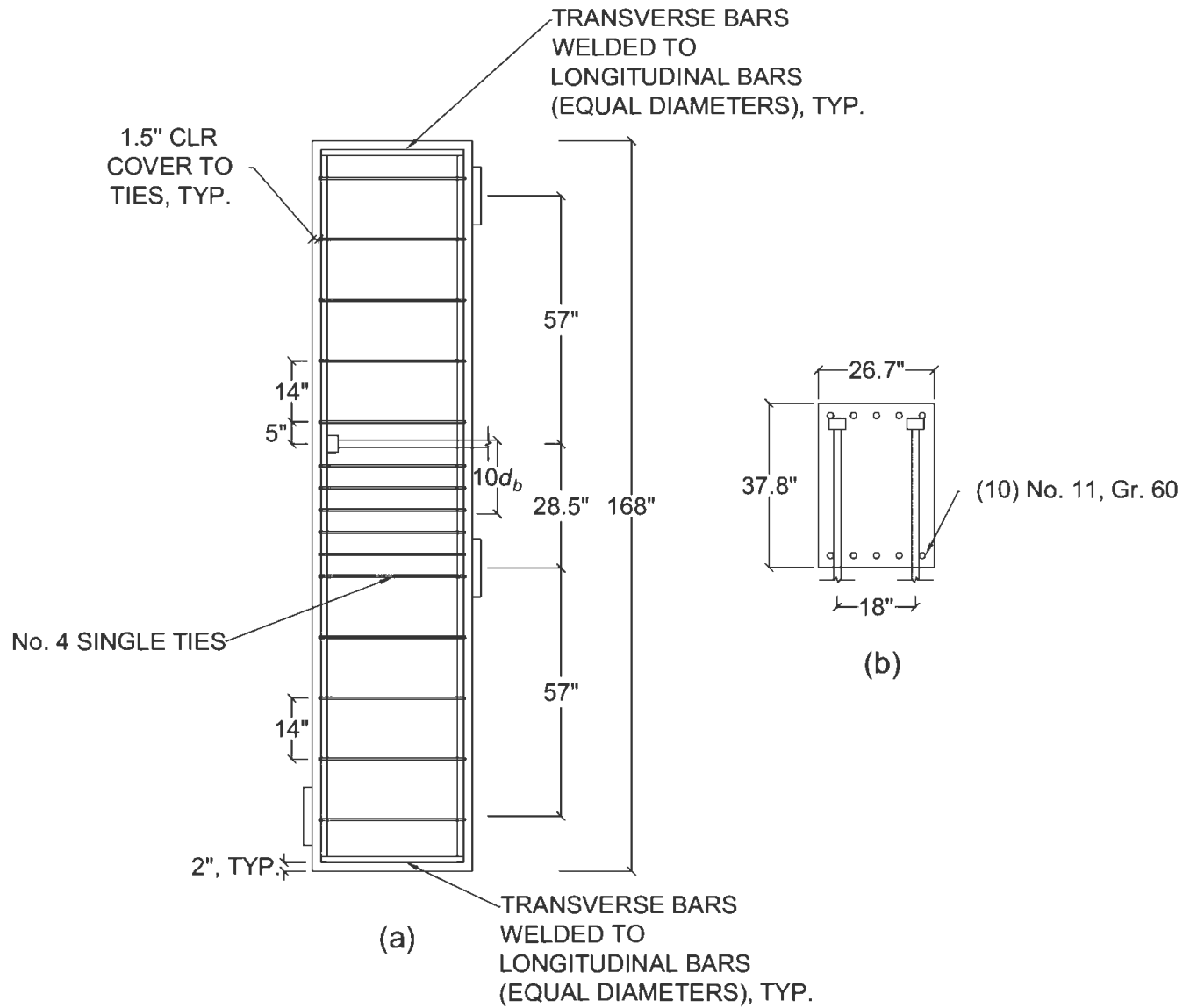


Figure C.3 Details of reinforcement layout for No. 14 headed bar specimen 14-4: (a) elevation, (b) cross-section

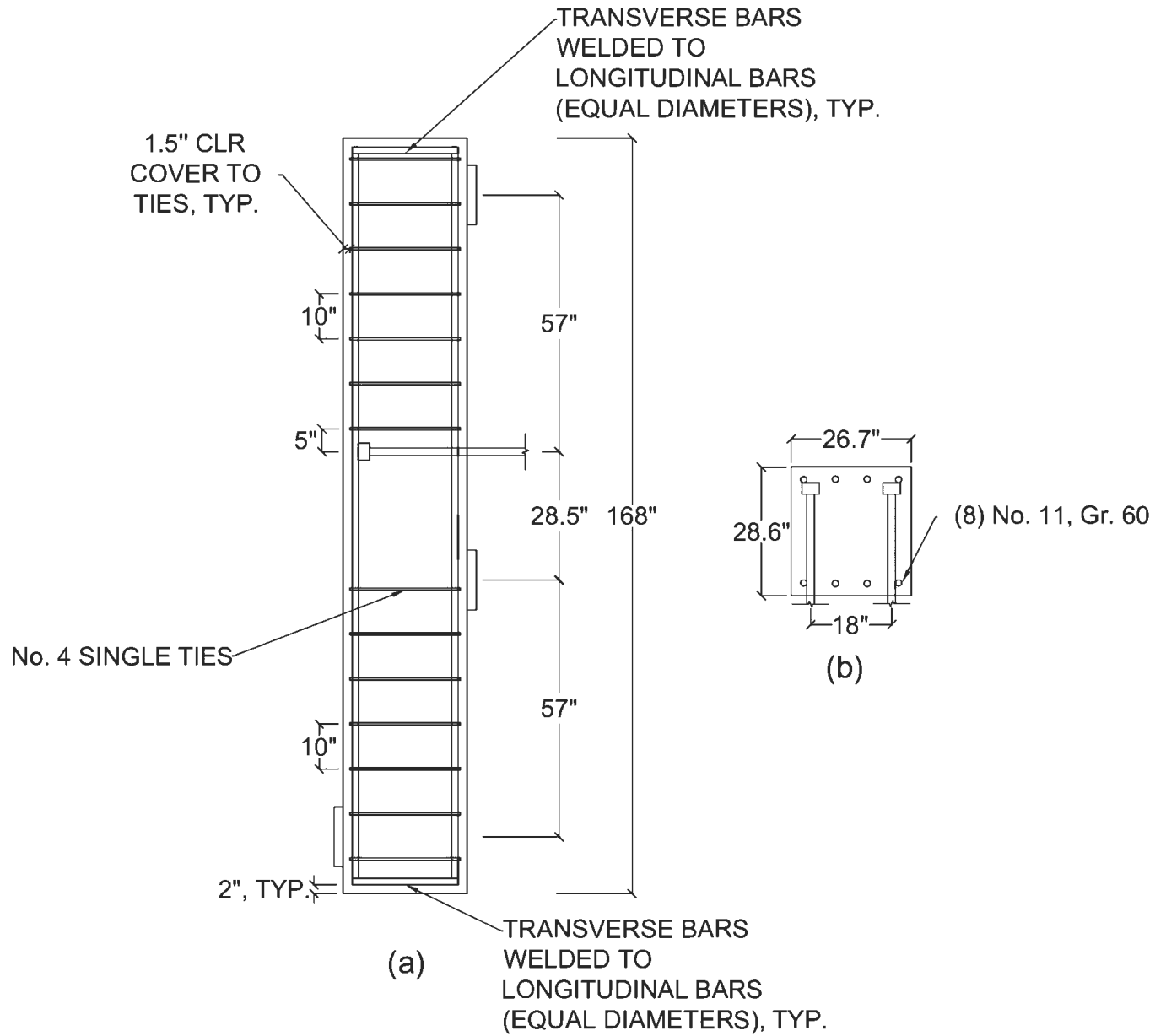


Figure C.4 Details of reinforcement layout for No. 14 headed bar specimen 14-15: (a) elevation, (b) cross-section

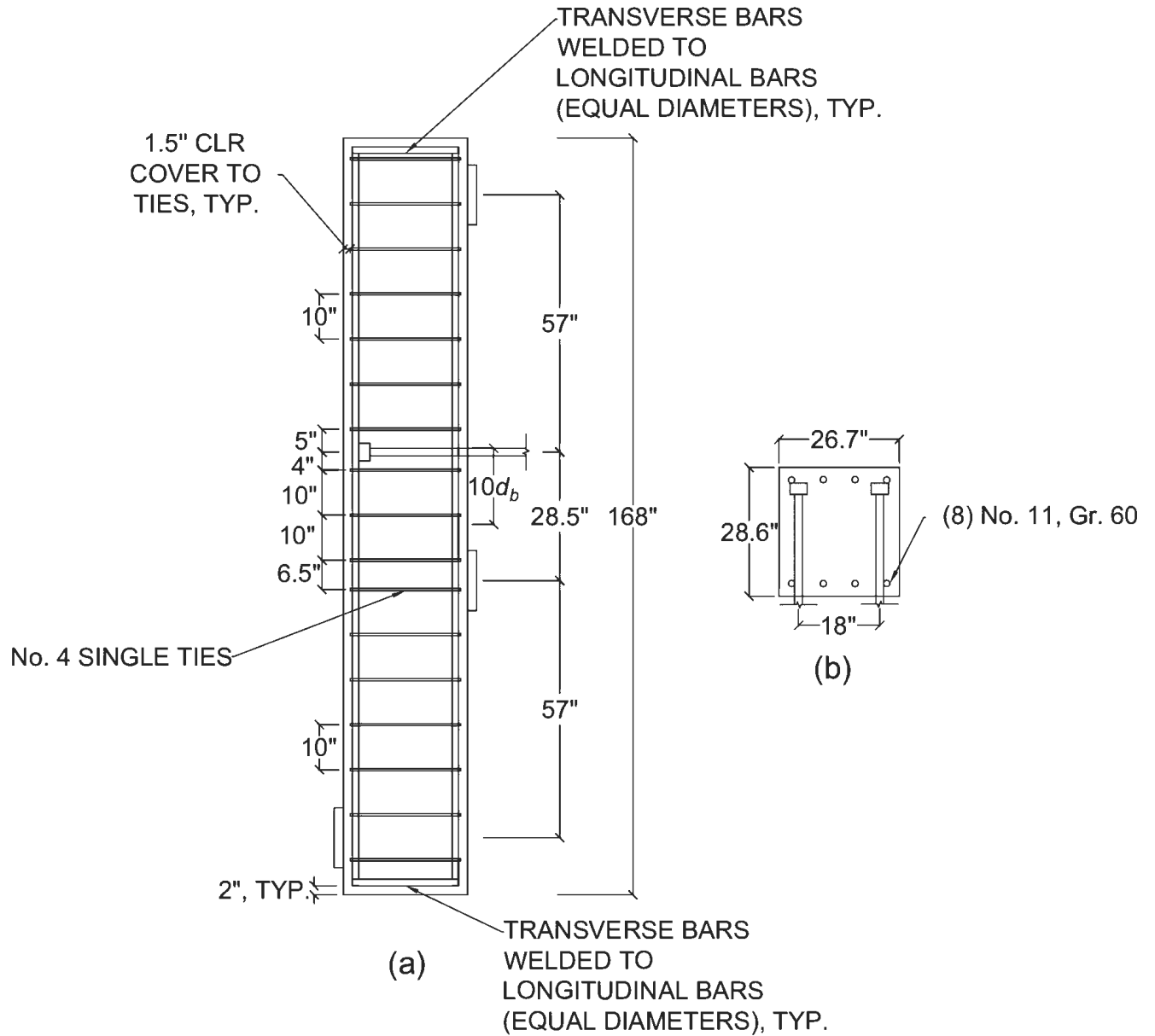


Figure C.5 Details of reinforcement layout for No. 14 headed bar specimen 14-16: (a) elevation, (b) cross-section

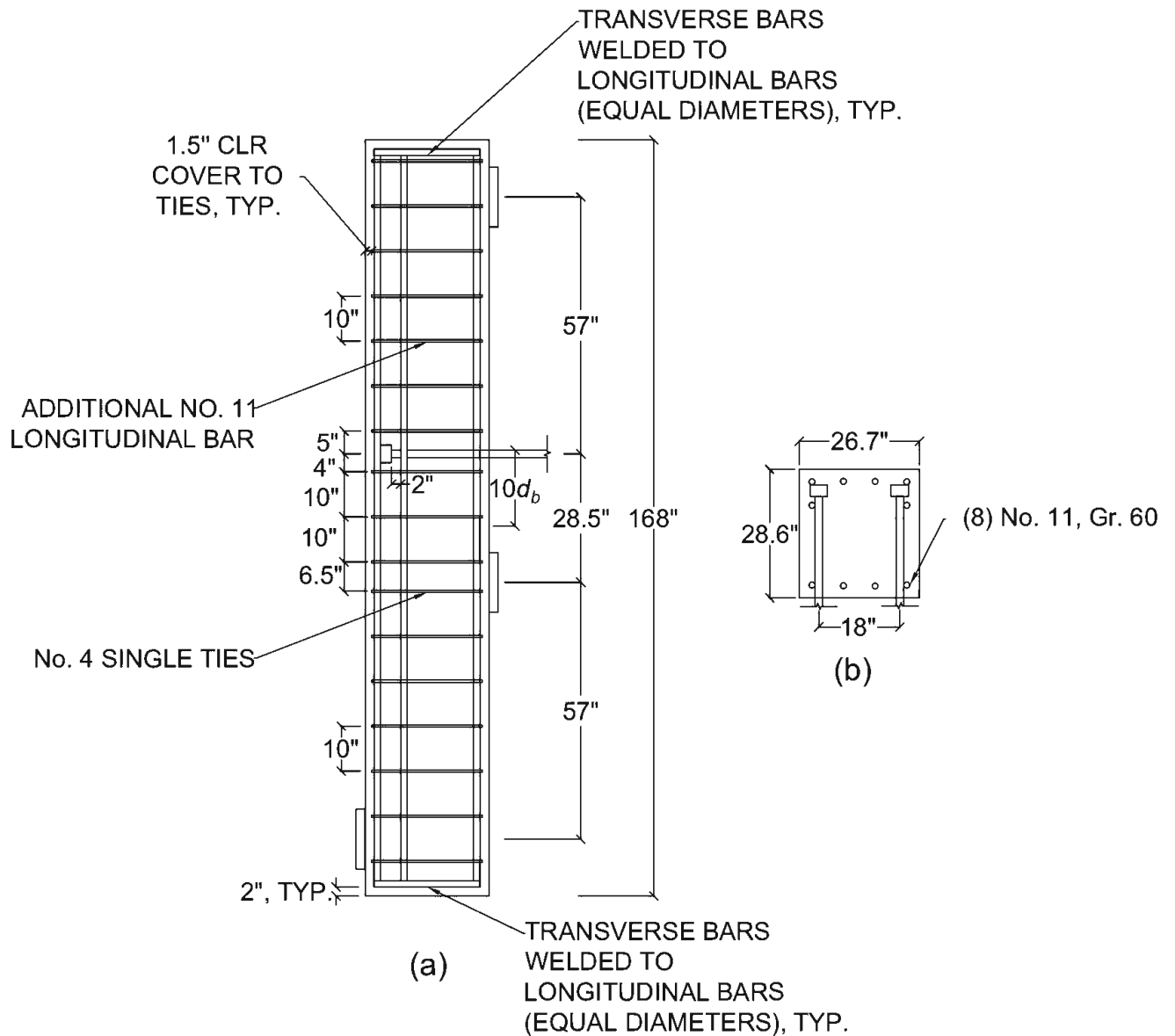


Figure C.6 Details of reinforcement layout for No. 14 headed bar specimen 14-16A: (a) elevation, (b) cross-section

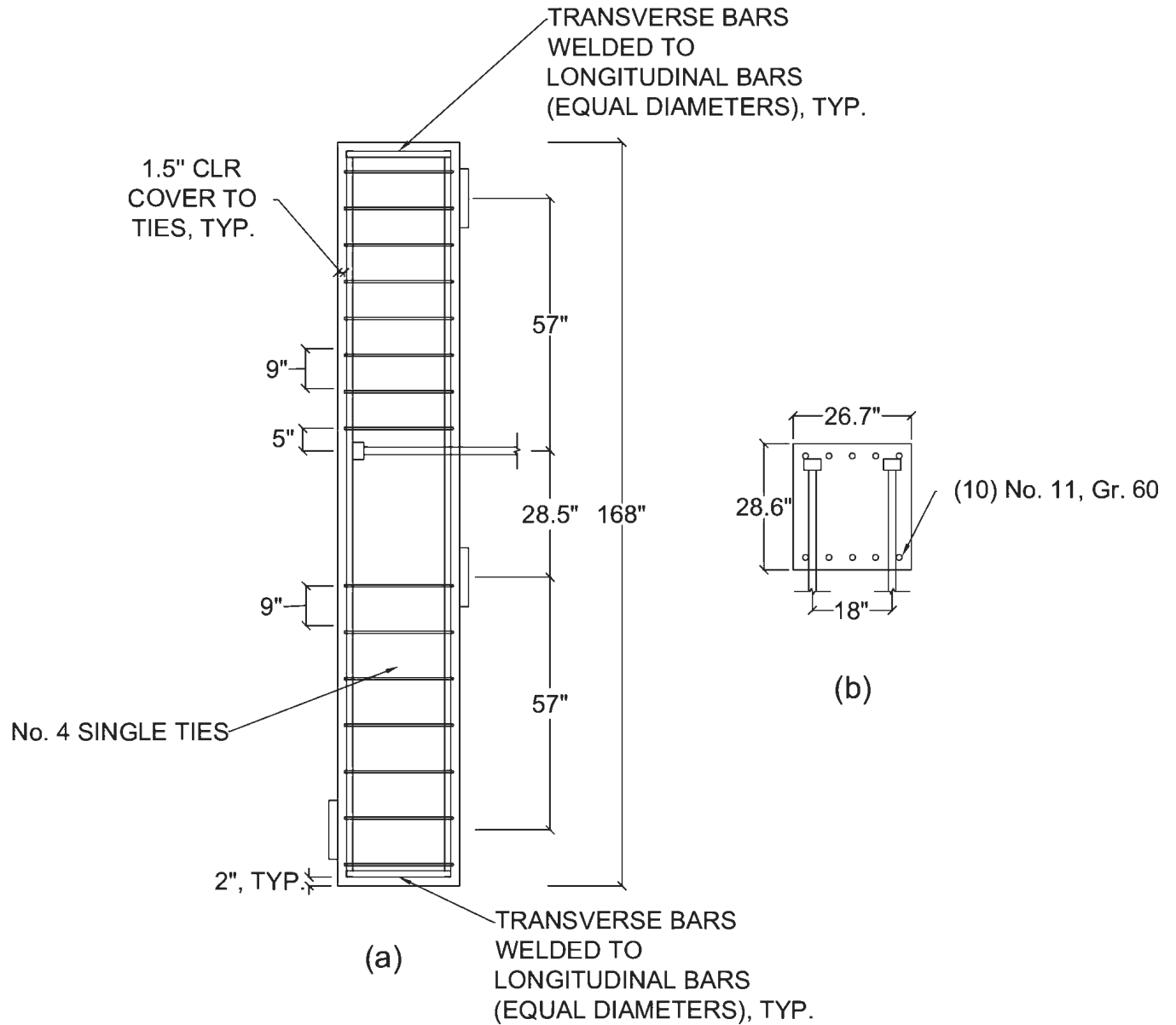


Figure C.7 Details of reinforcement layout for No. 14 headed bar specimen 14-1A: (a) elevation, (b) cross-section

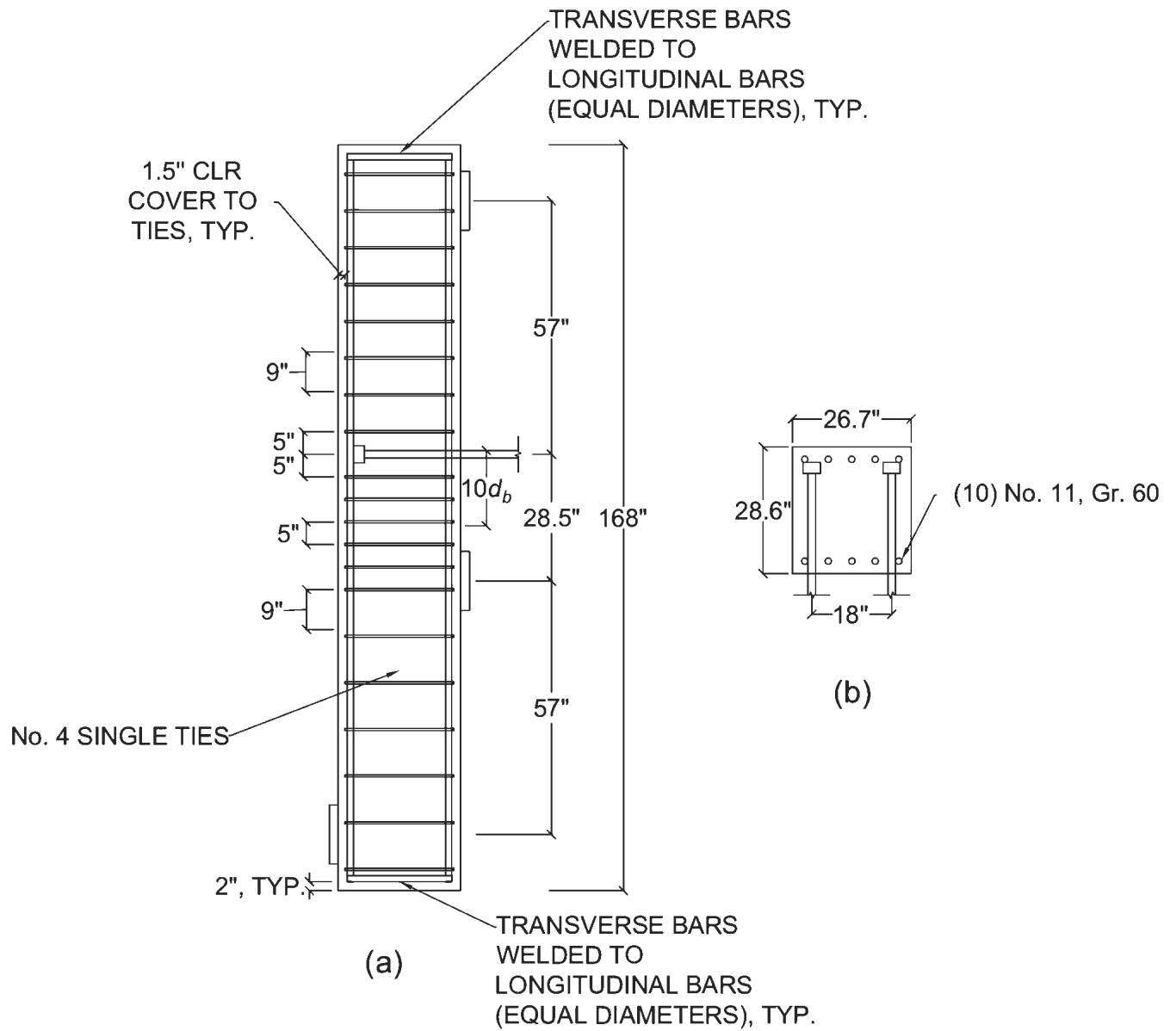


Figure C.8 Details of reinforcement layout for No. 14 headed bar specimen 14-2A: (a) elevation, (b) cross-section

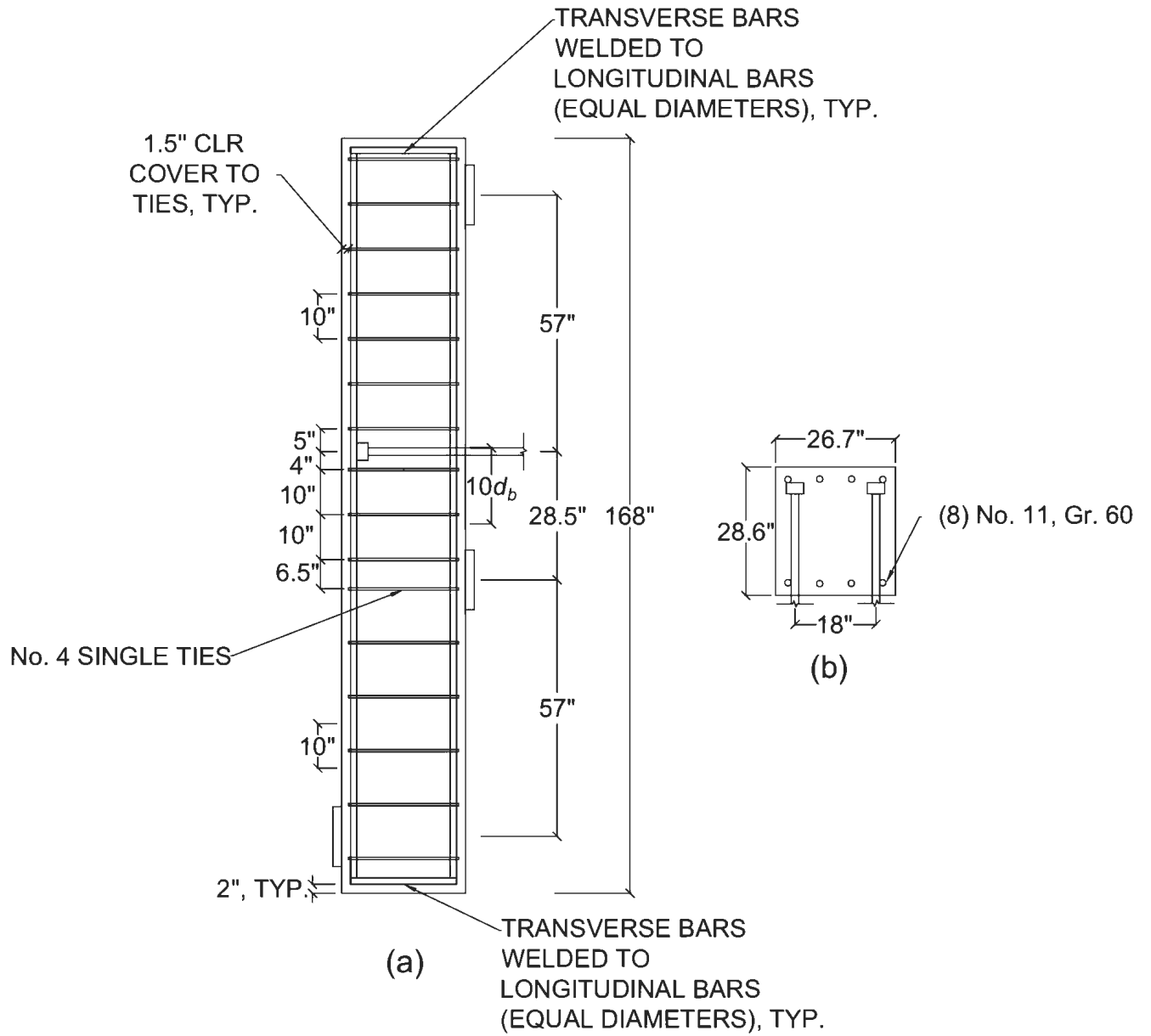


Figure C.9 Details of reinforcement layout for No. 14 headed bar specimen 14-16B: (a) elevation, (b) cross-section

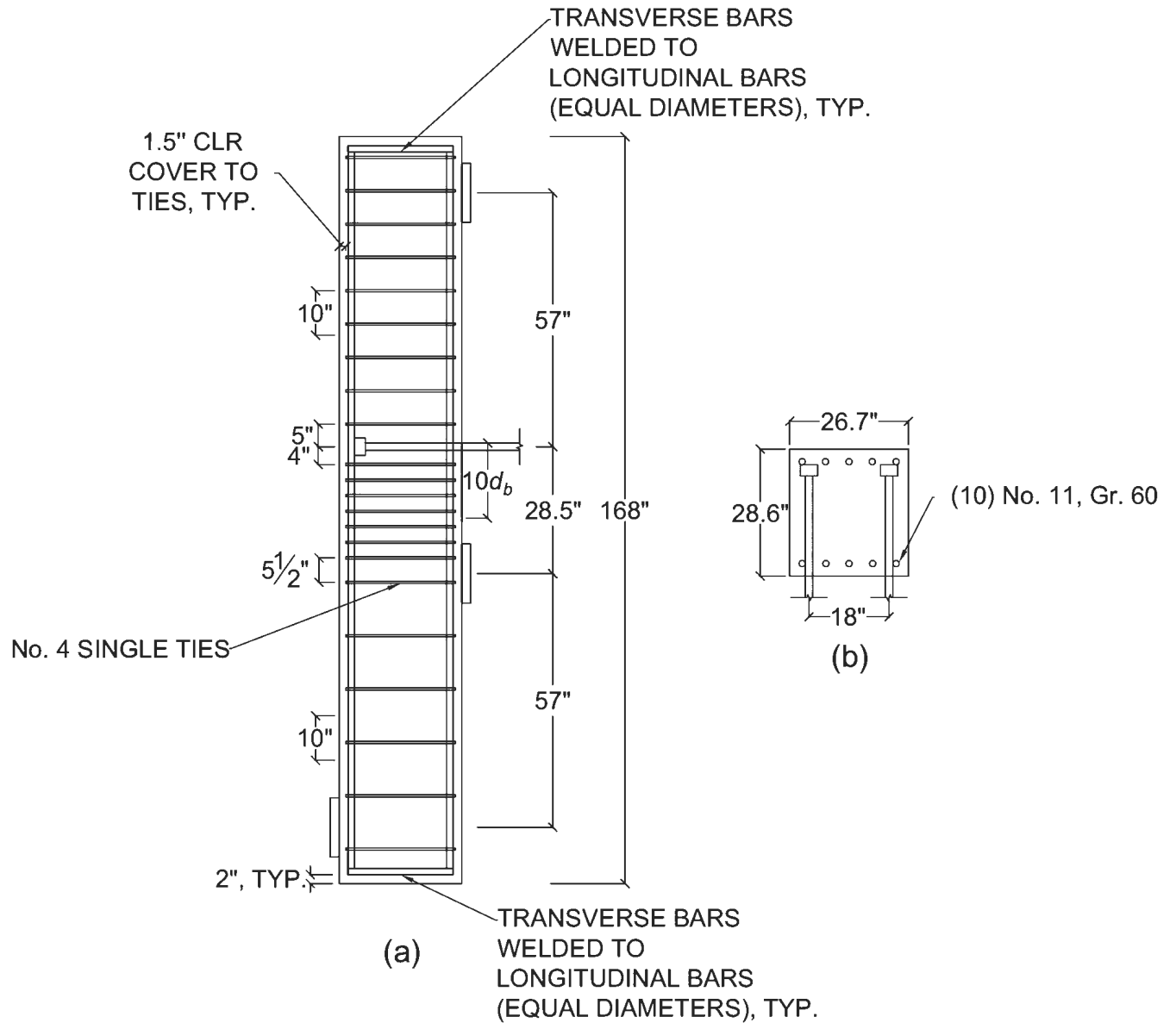


Figure C.10 Details of reinforcement layout for No. 14 headed bar specimen 14-16C: (a) elevation, (b) cross-section

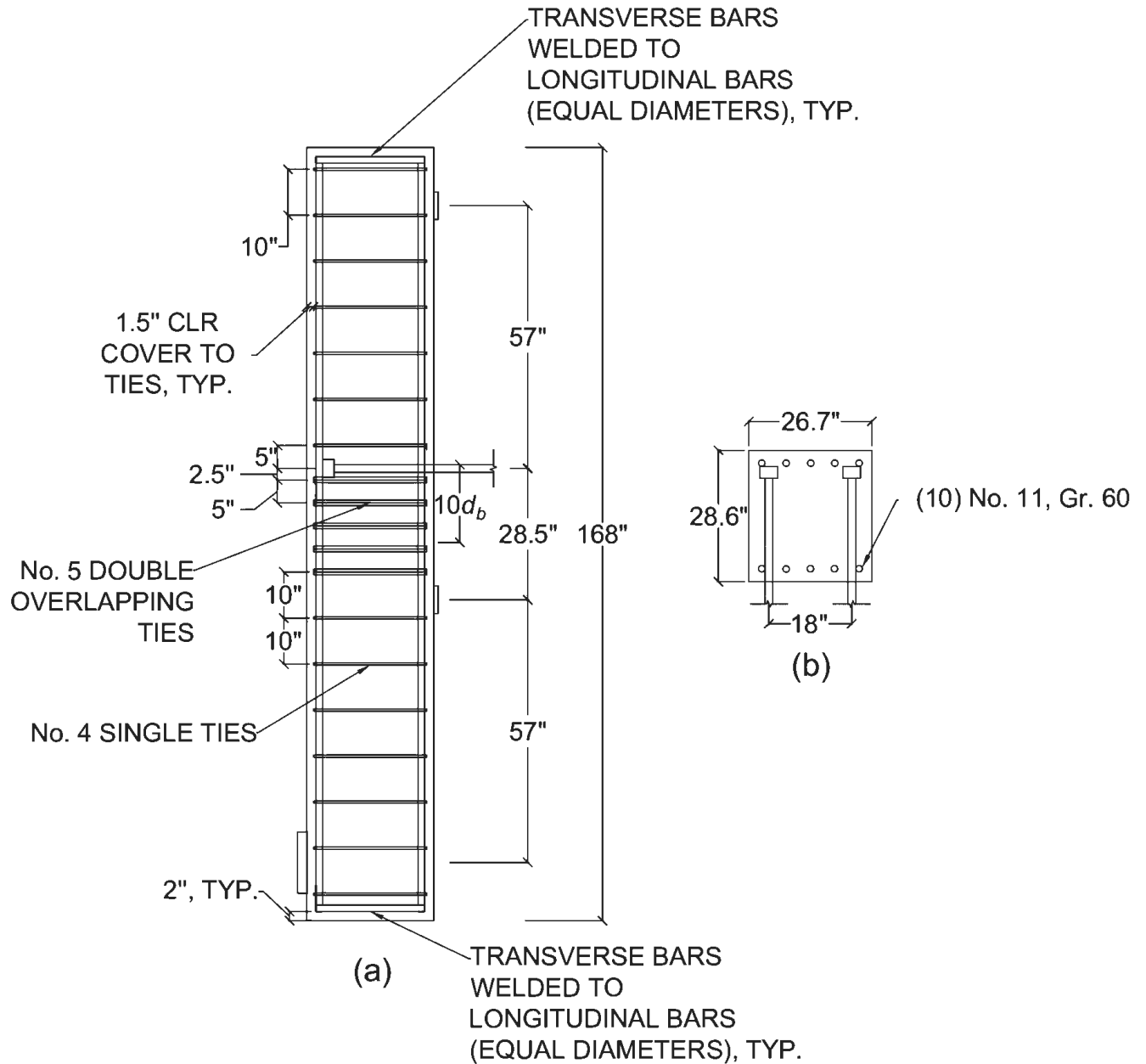


Figure C.11 Details of reinforcement layout for No. 14 headed bar specimen 14-16D: (a) elevation, (b) cross-section

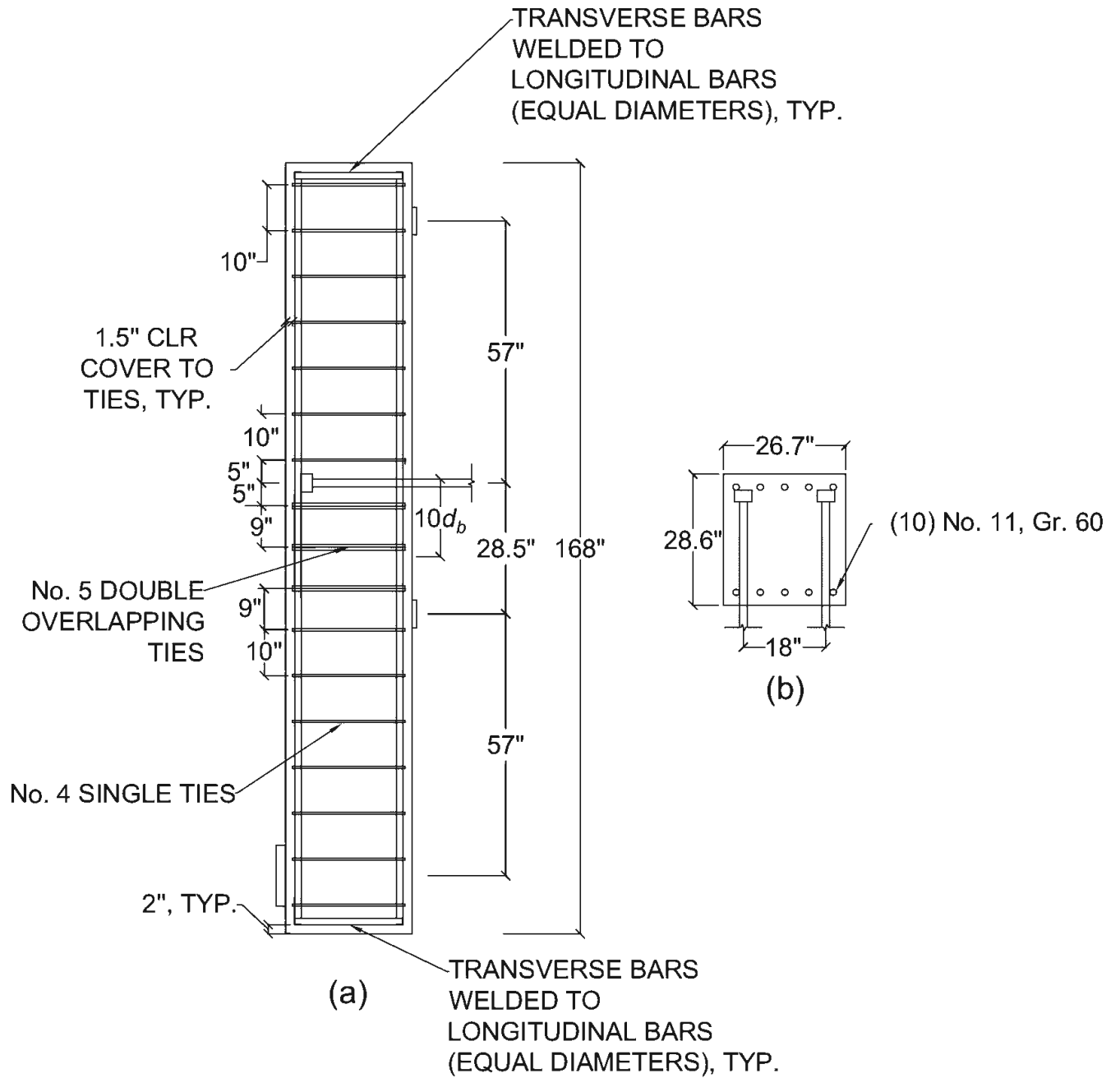


Figure C.12 Details of reinforcement layout for No. 14 headed bar specimen 14-16E: (a) elevation, (b) cross-section

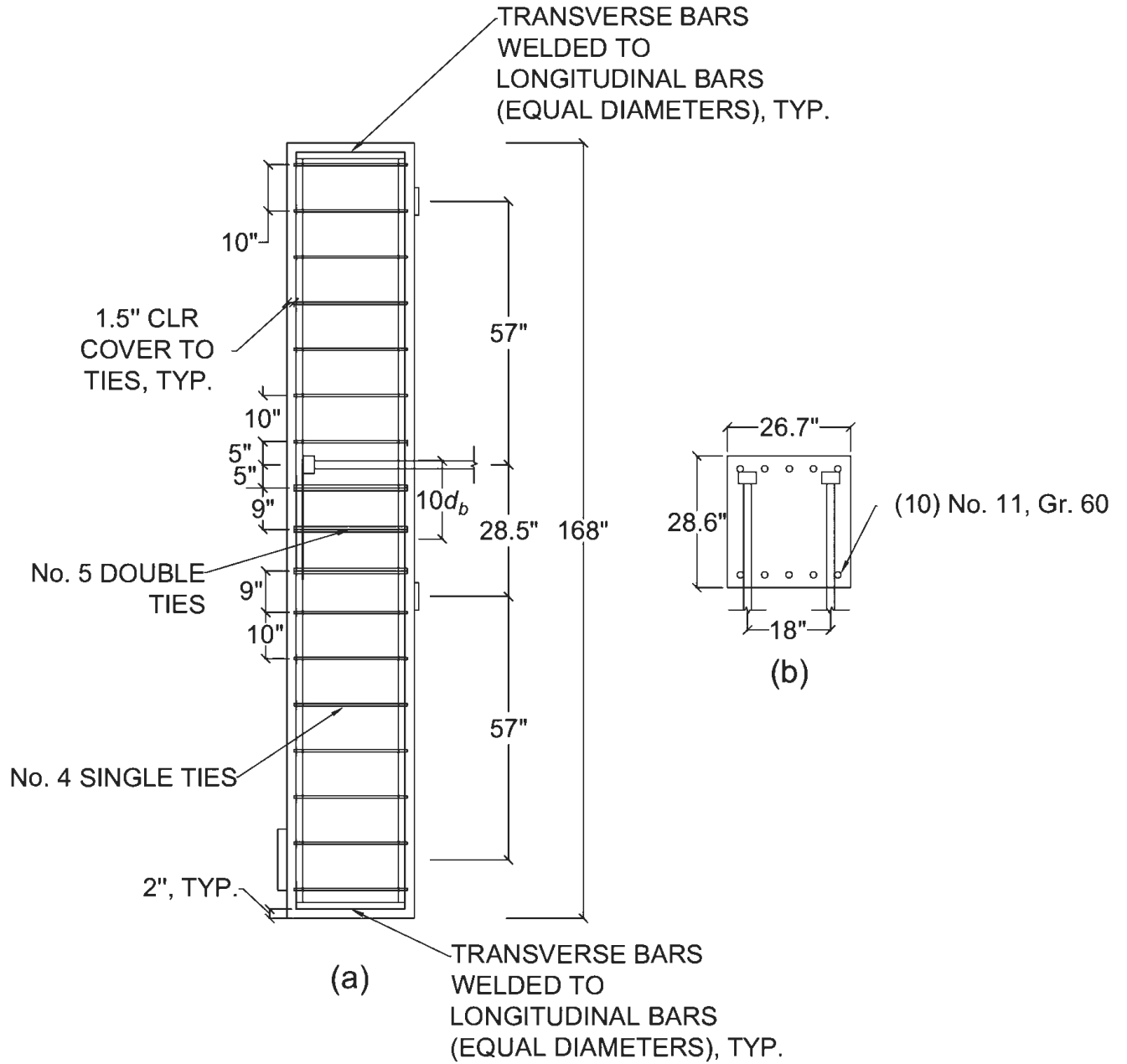


Figure C.13 Details of reinforcement layout for No. 14 headed bar specimen 14-16F: (a) elevation, (b) cross-section

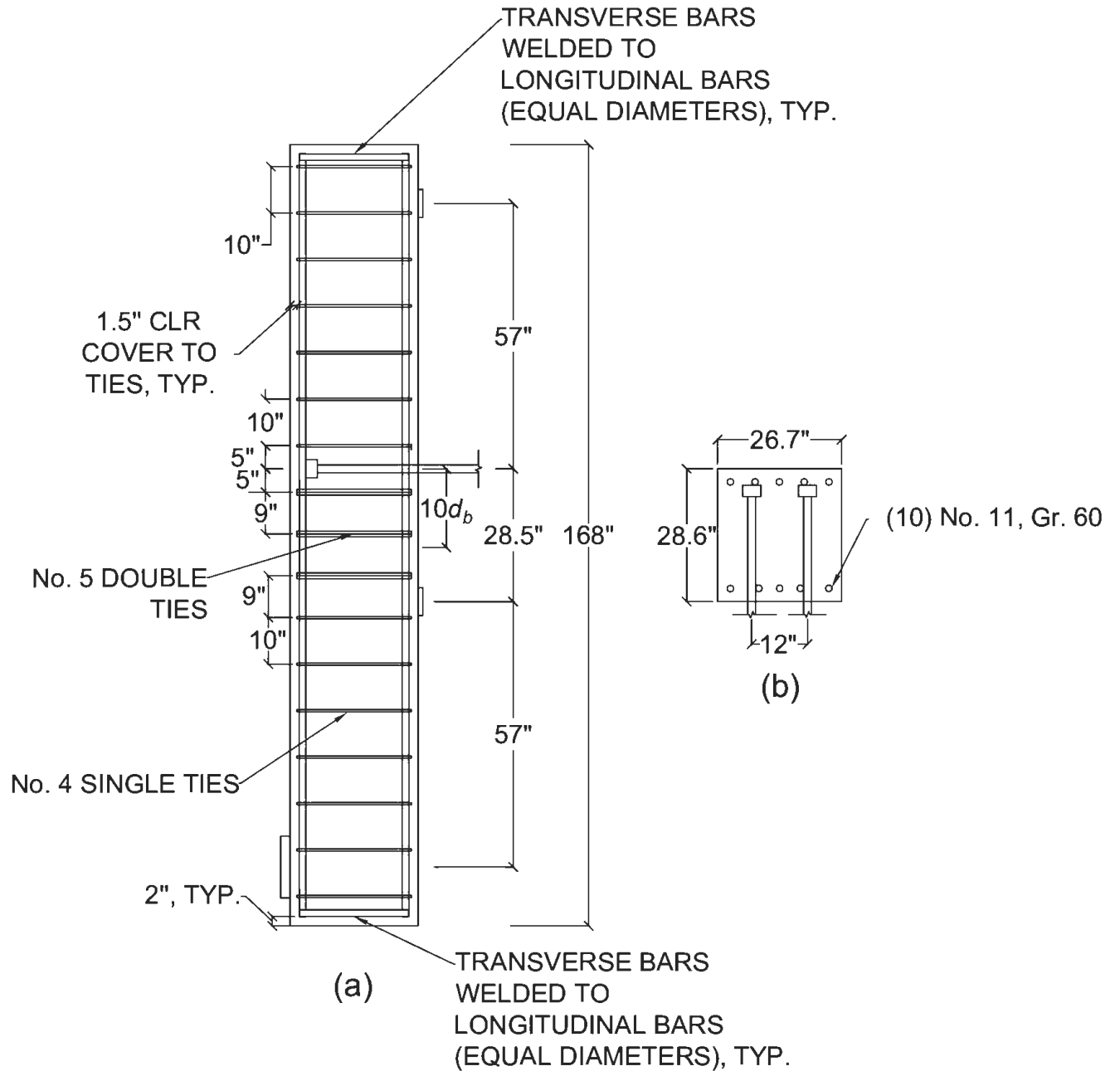


Figure C.14 Details of reinforcement layout for No. 14 headed bar specimen 14-17: (a) elevation, (b) cross-section

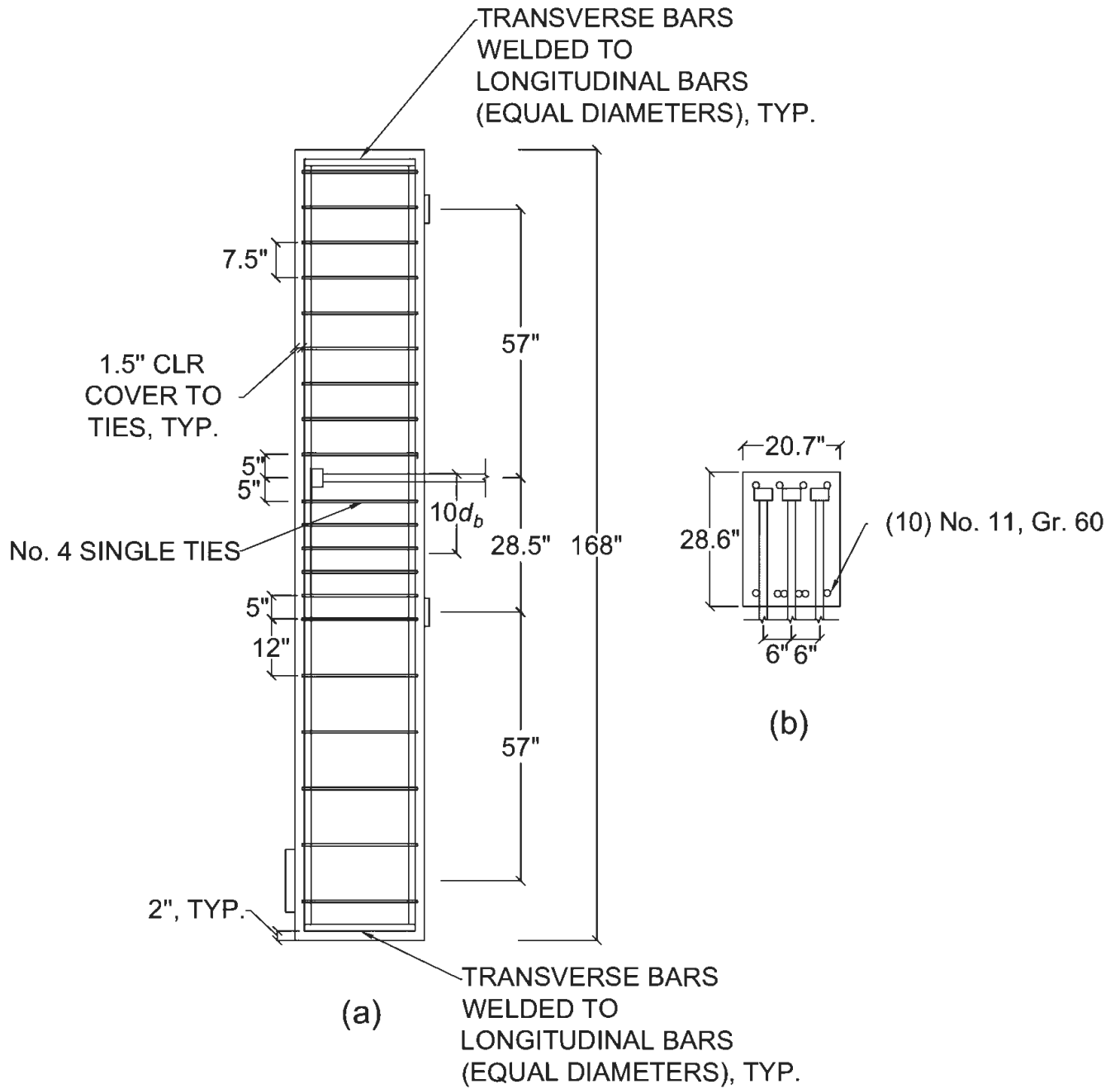


Figure C.15 Details of reinforcement layout for No. 14 headed bar specimen 14-5: (a) elevation, (b) cross-section

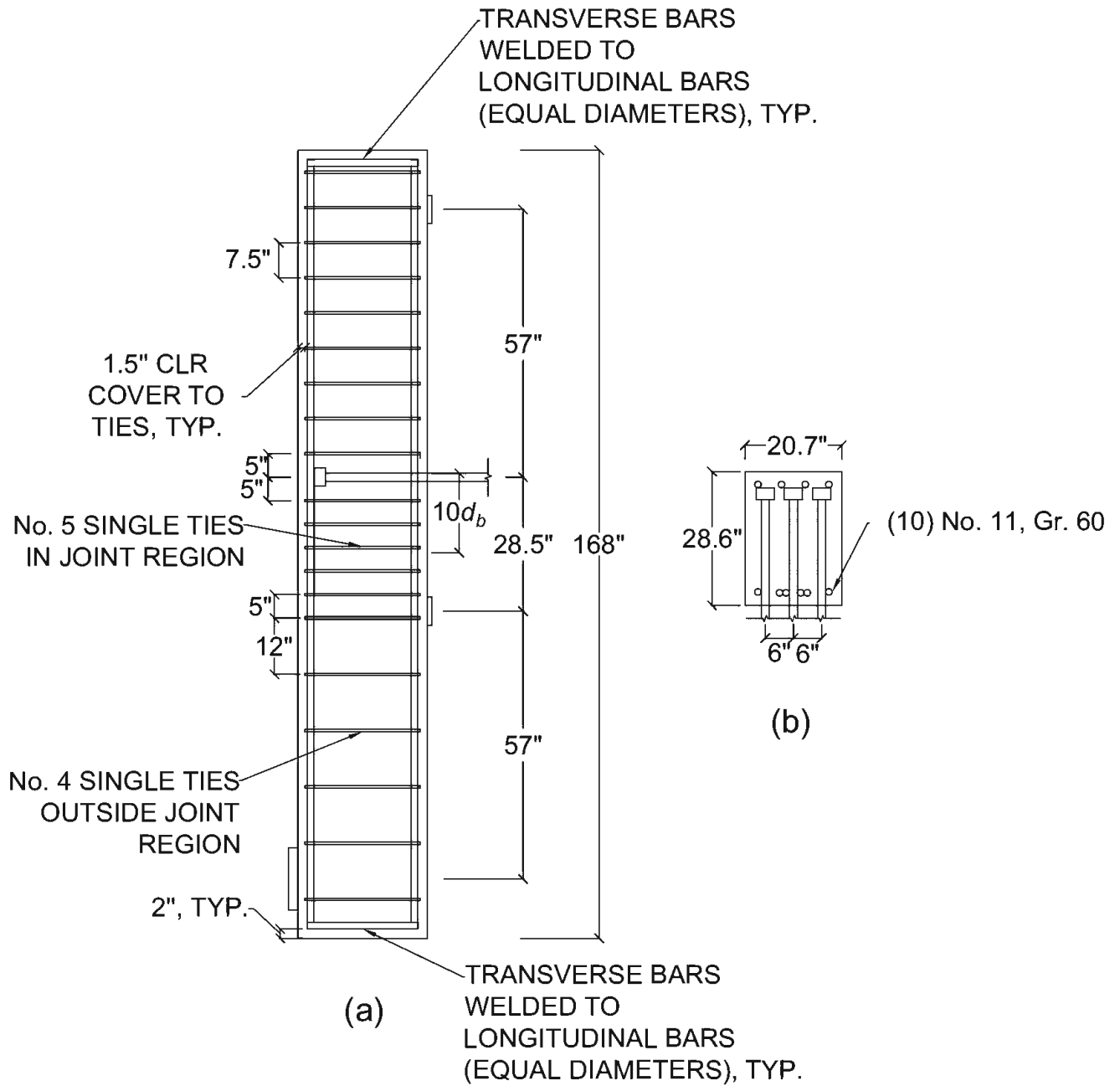


Figure C.16 Details of reinforcement layout for No. 14 headed bar specimen 14-6: (a) elevation, (b) cross-section

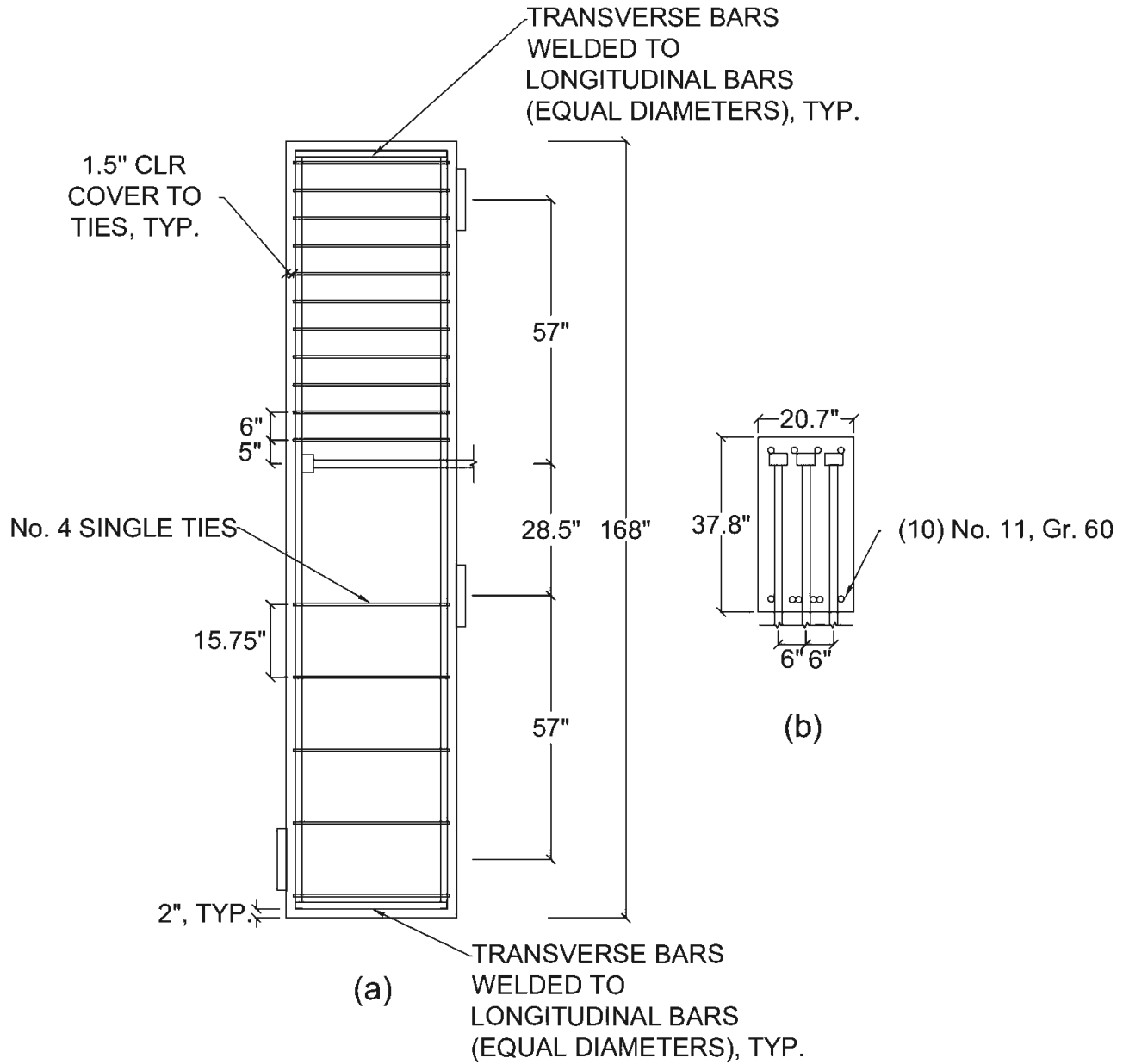


Figure C.17 Details of reinforcement layout for No. 14 headed bar specimen 14-7: (a) elevation, (b) cross-section

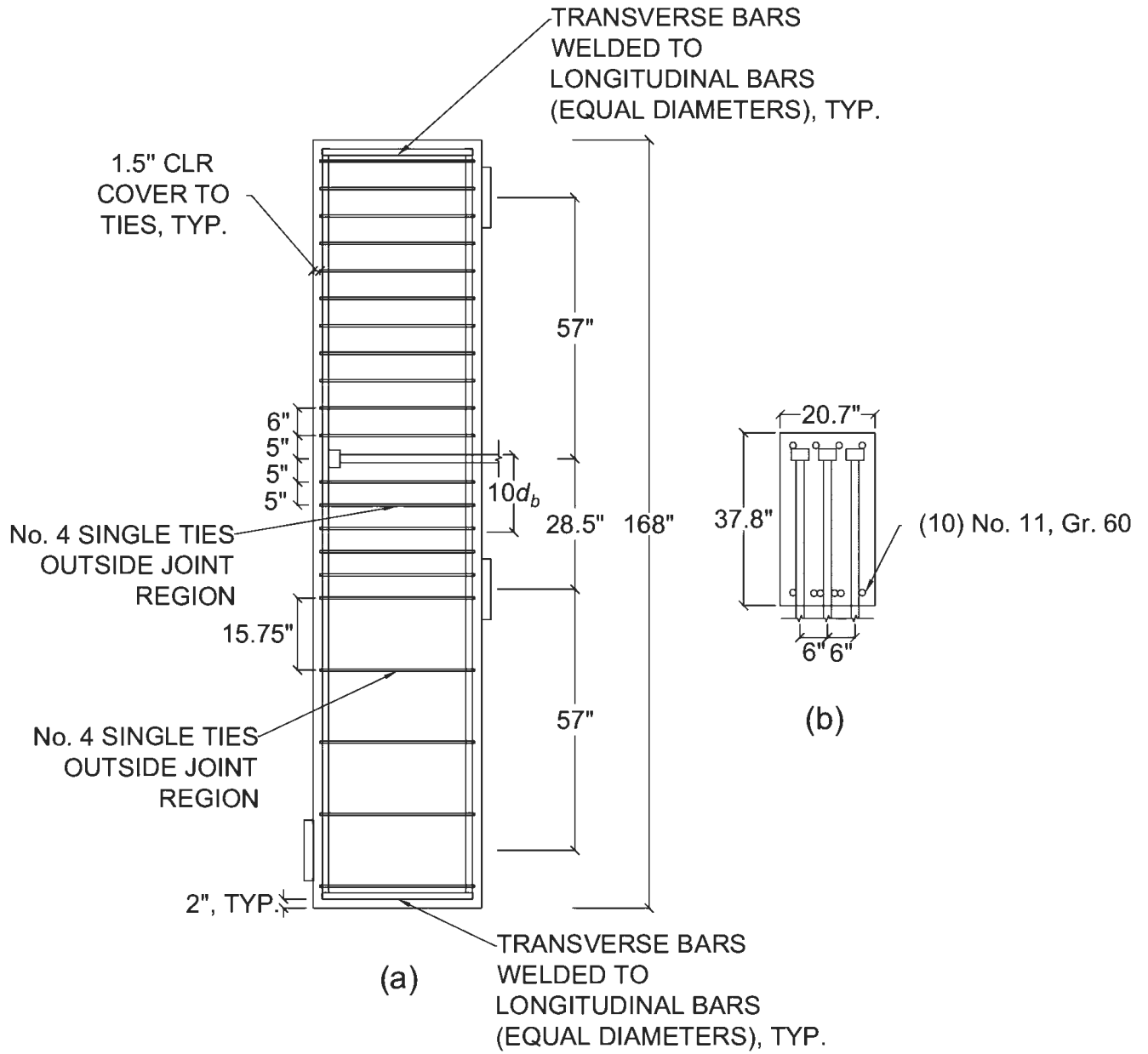


Figure C.18 Details of reinforcement layout for No. 14 headed bar specimen 14-8: (a) elevation, (b) cross-section

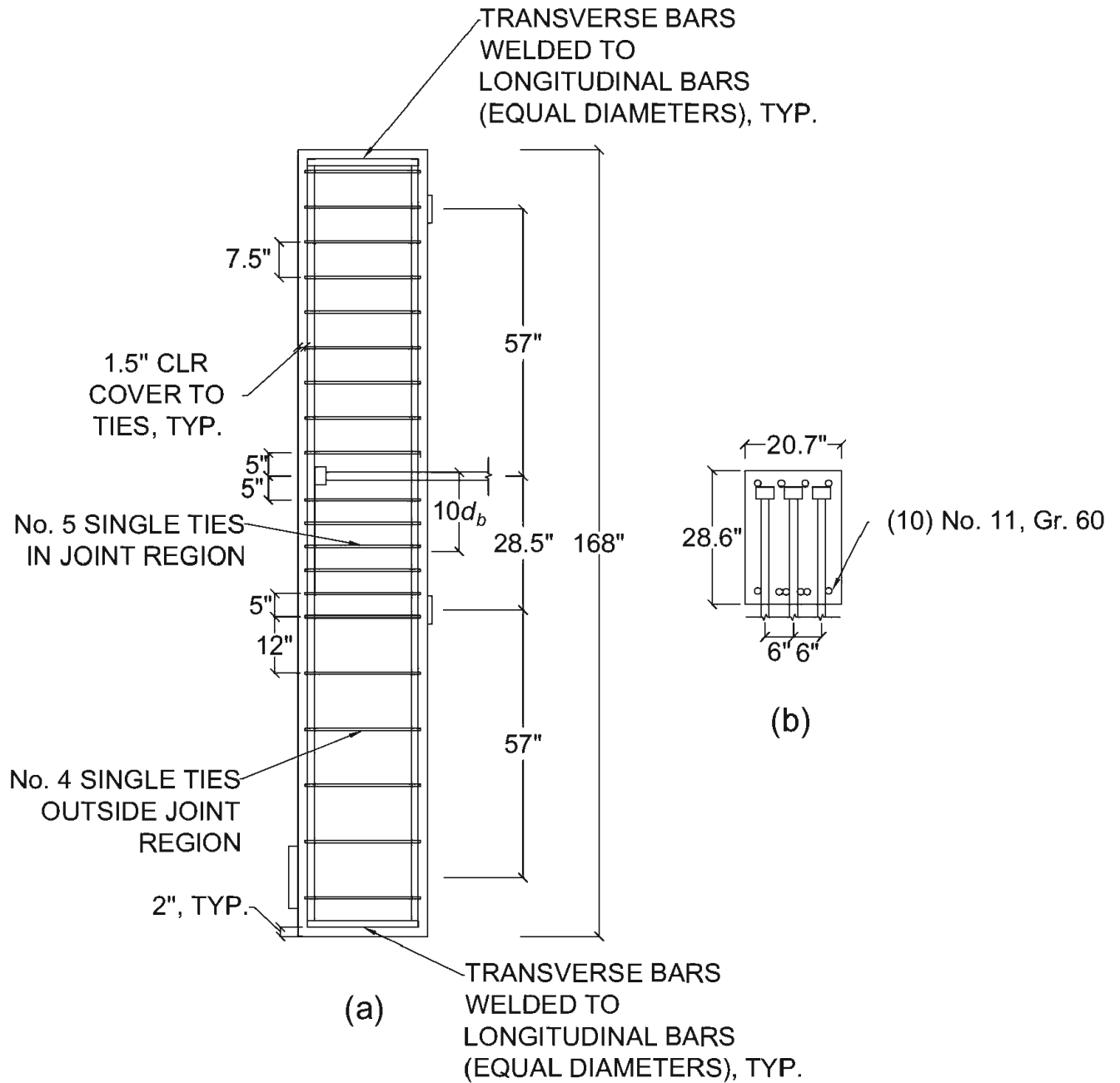


Figure C.19 Details of reinforcement layout for No. 14 headed bar specimen 14-9: (a) elevation, (b) cross-section

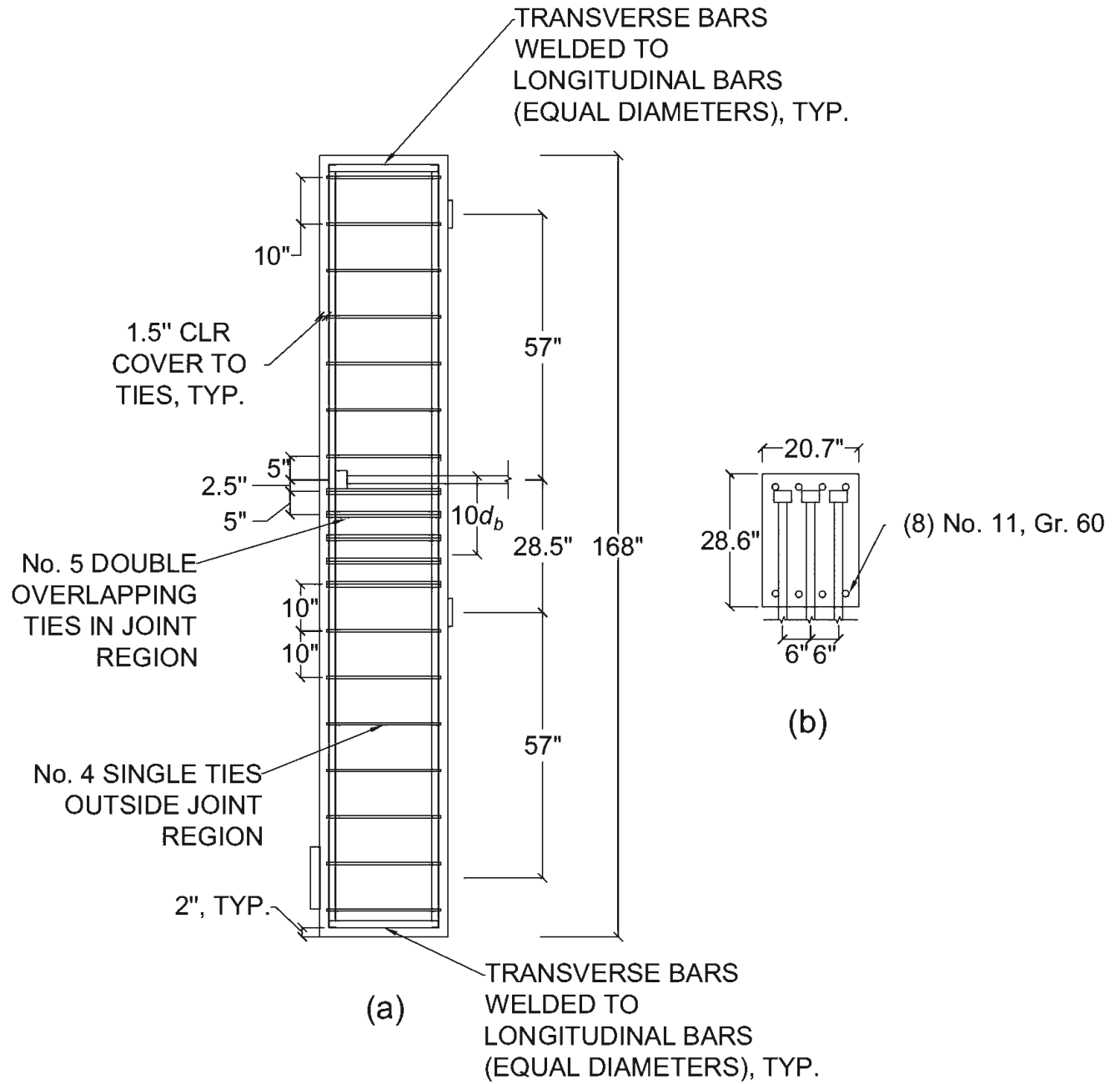


Figure C.20 Details of reinforcement layout for No. 14 headed bar specimen 14-10: (a) elevation, (b) cross-section

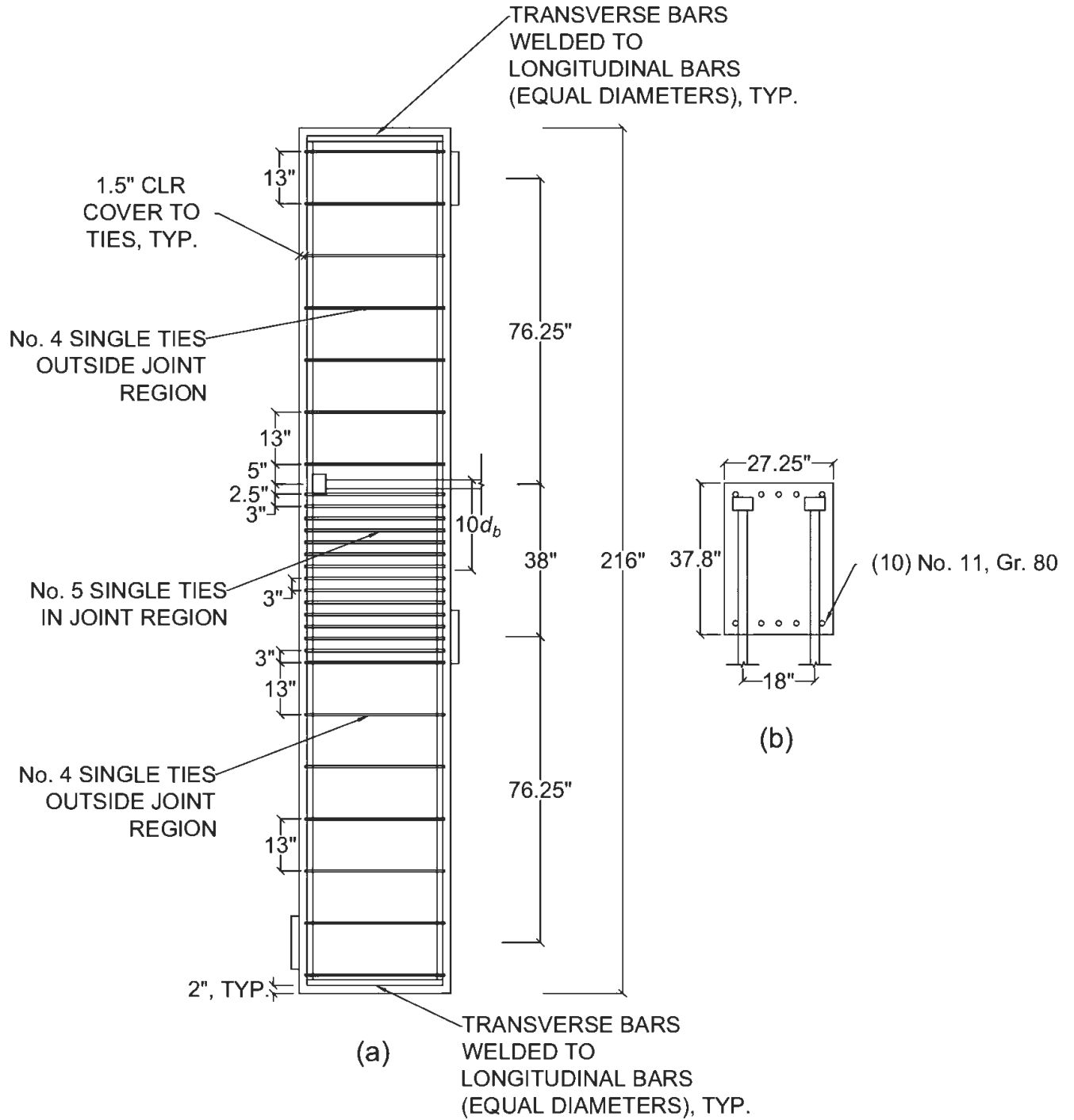


Figure C.21 Details of reinforcement layout for No. 18 headed bar specimen 18-1: (a) elevation, (b) cross-section

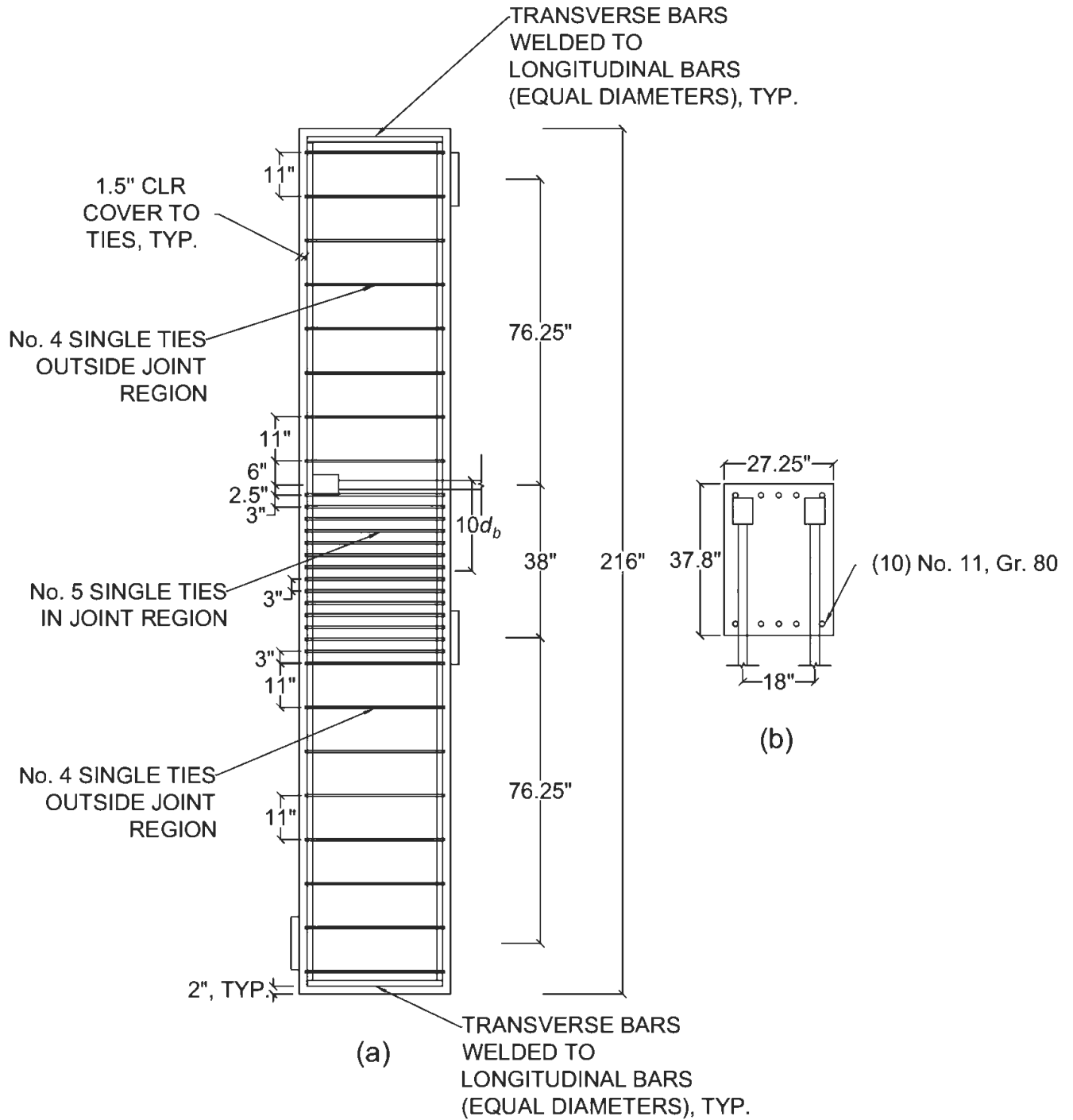


Figure C.22 Details of reinforcement layout for No. 18 headed bar specimen 18-2: (a) elevation, (b) cross-section

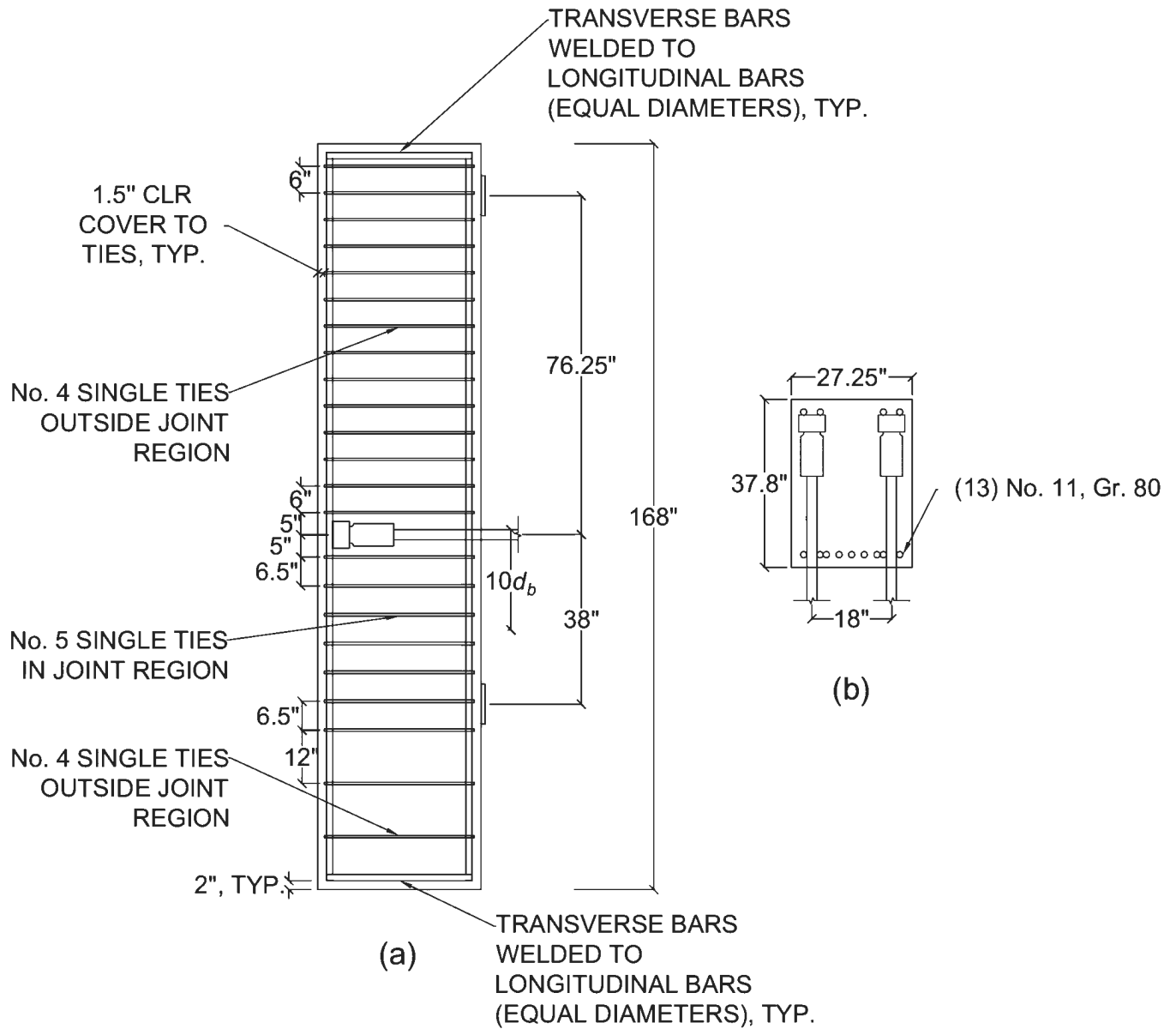


Figure C.23 Details of reinforcement layout for No. 18 headed bar specimen 18-3: (a) elevation, (b) cross-section

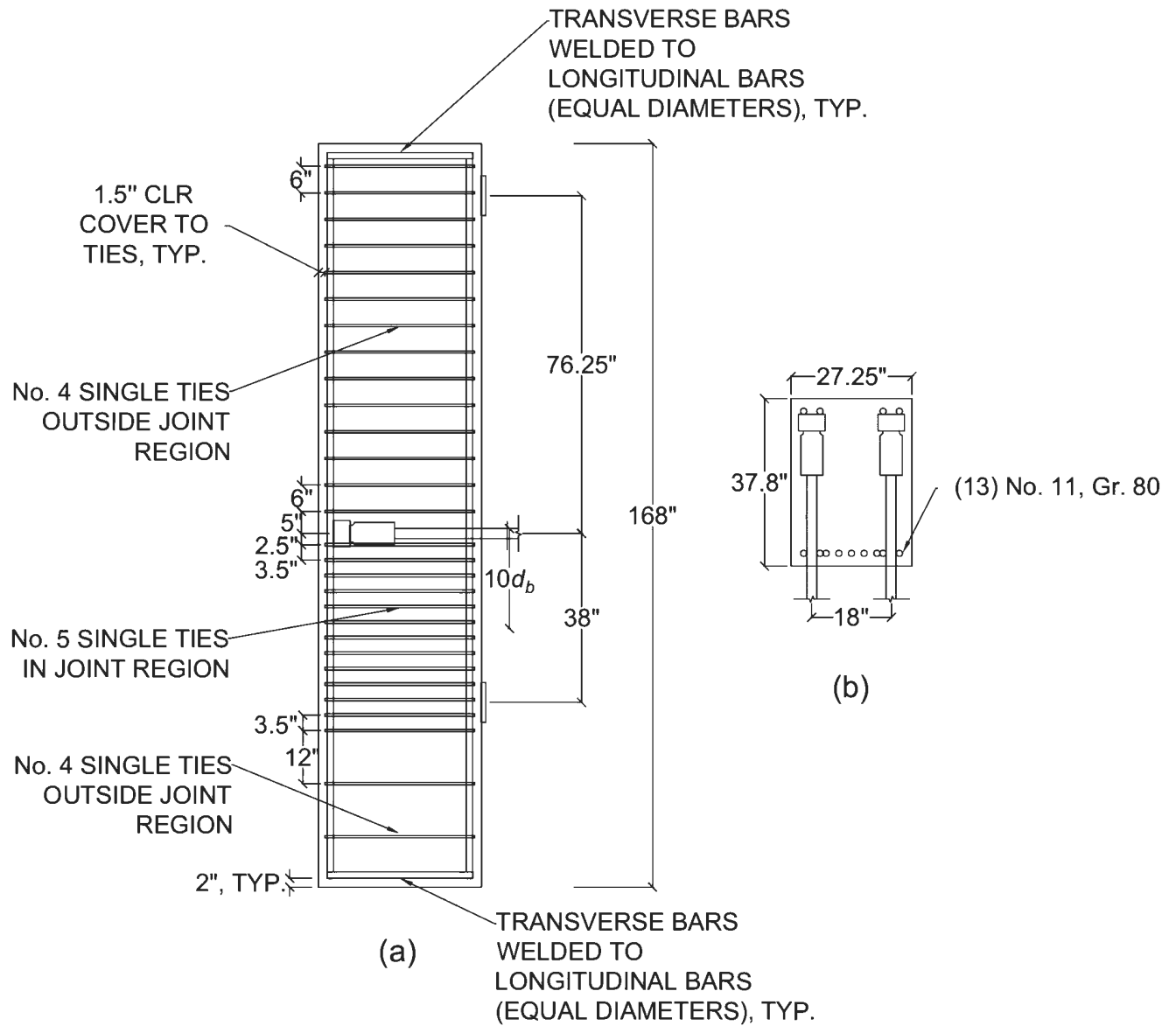


Figure C.24 Details of reinforcement layout for No. 18 headed bar specimen 18-4: (a) elevation, (b) cross-section

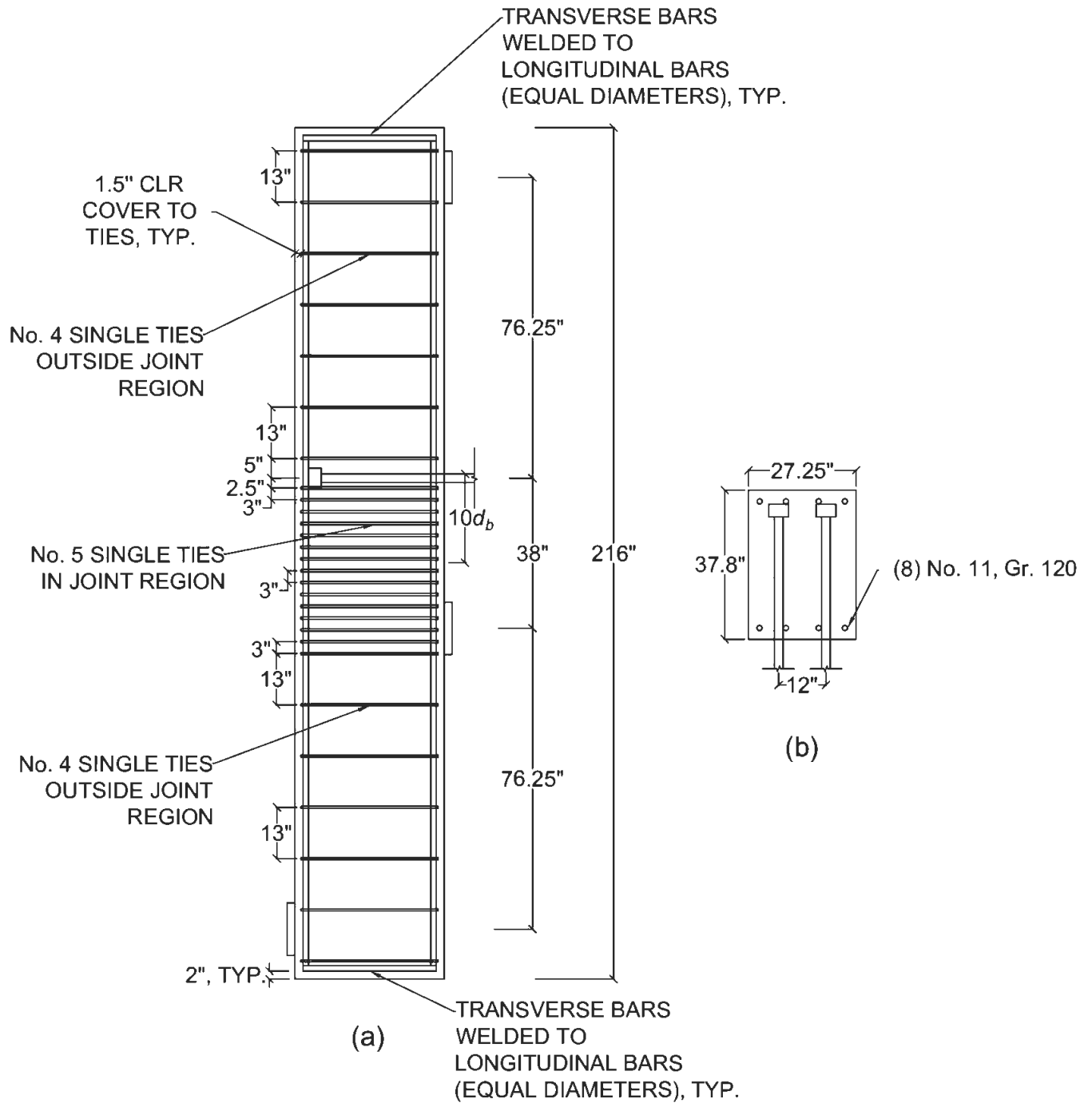


Figure C.25 Details of reinforcement layout for No. 18 headed bar specimen 18-5: (a) elevation, (b) cross-section

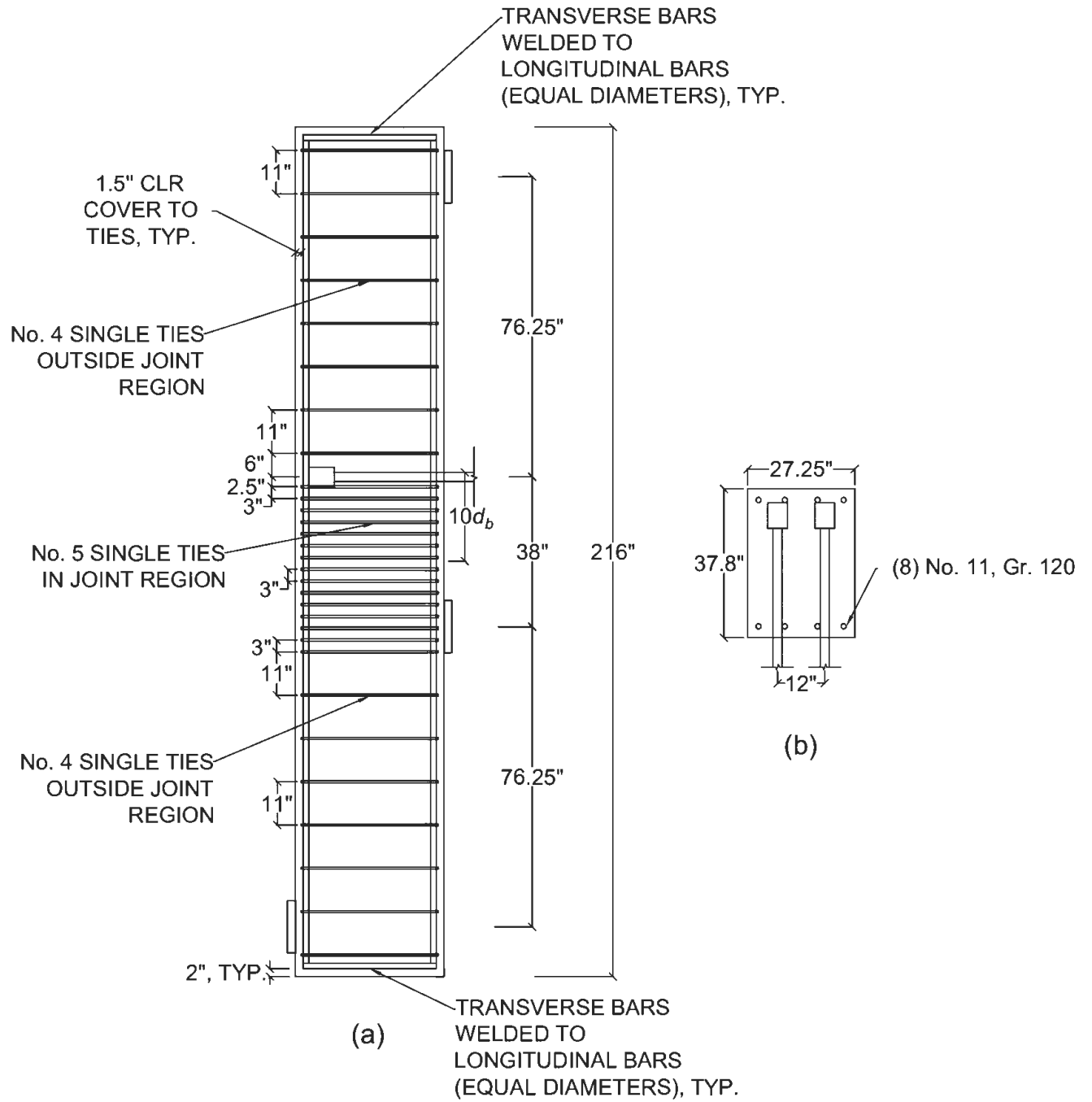


Figure C.26 Details of reinforcement layout for No. 18 headed bar specimen 18-6: (a) elevation, (b) cross-section

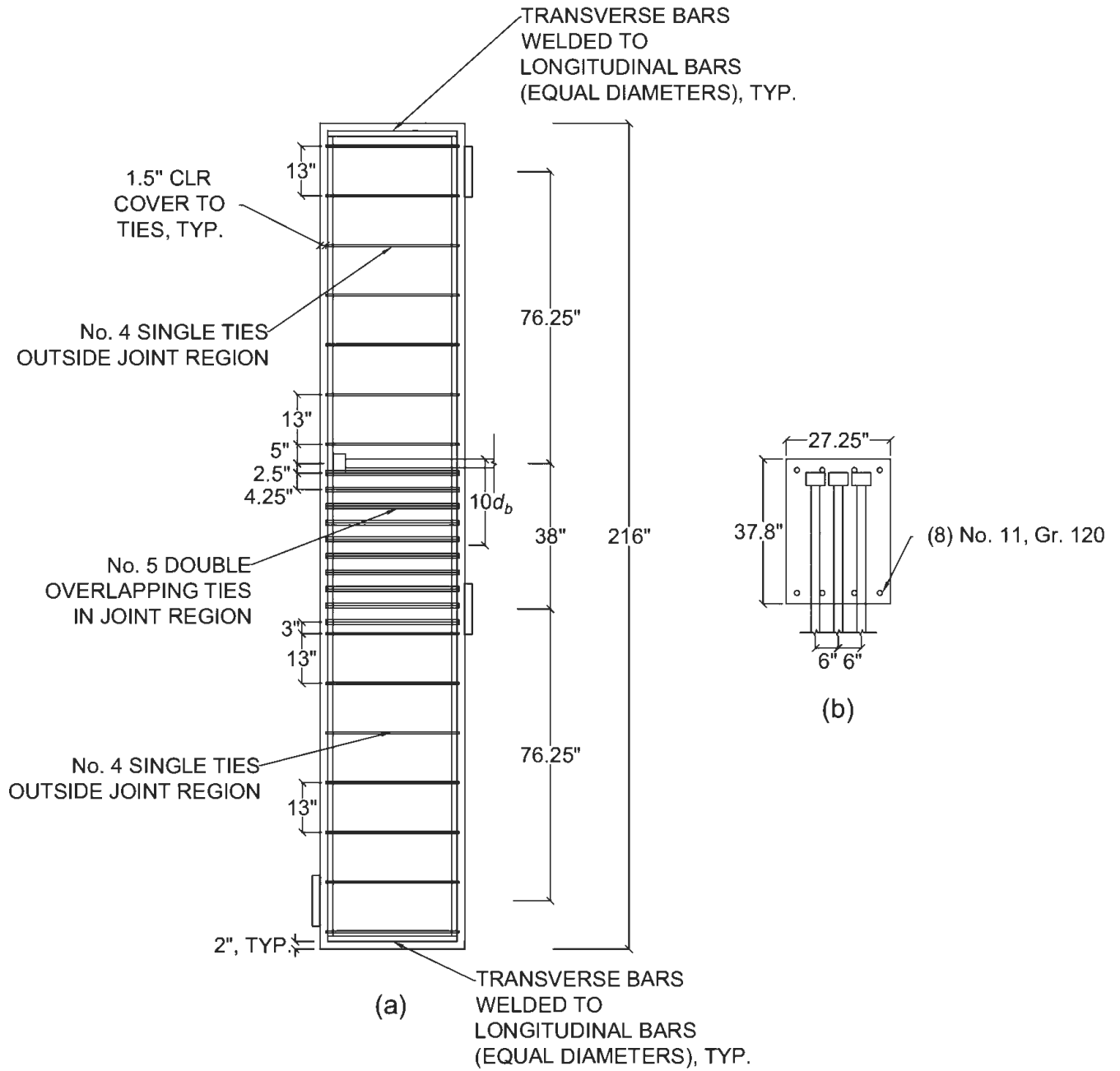


Figure C.27 Details of reinforcement layout for No. 18 headed bar specimen 18-7: (a) elevation, (b) cross-section

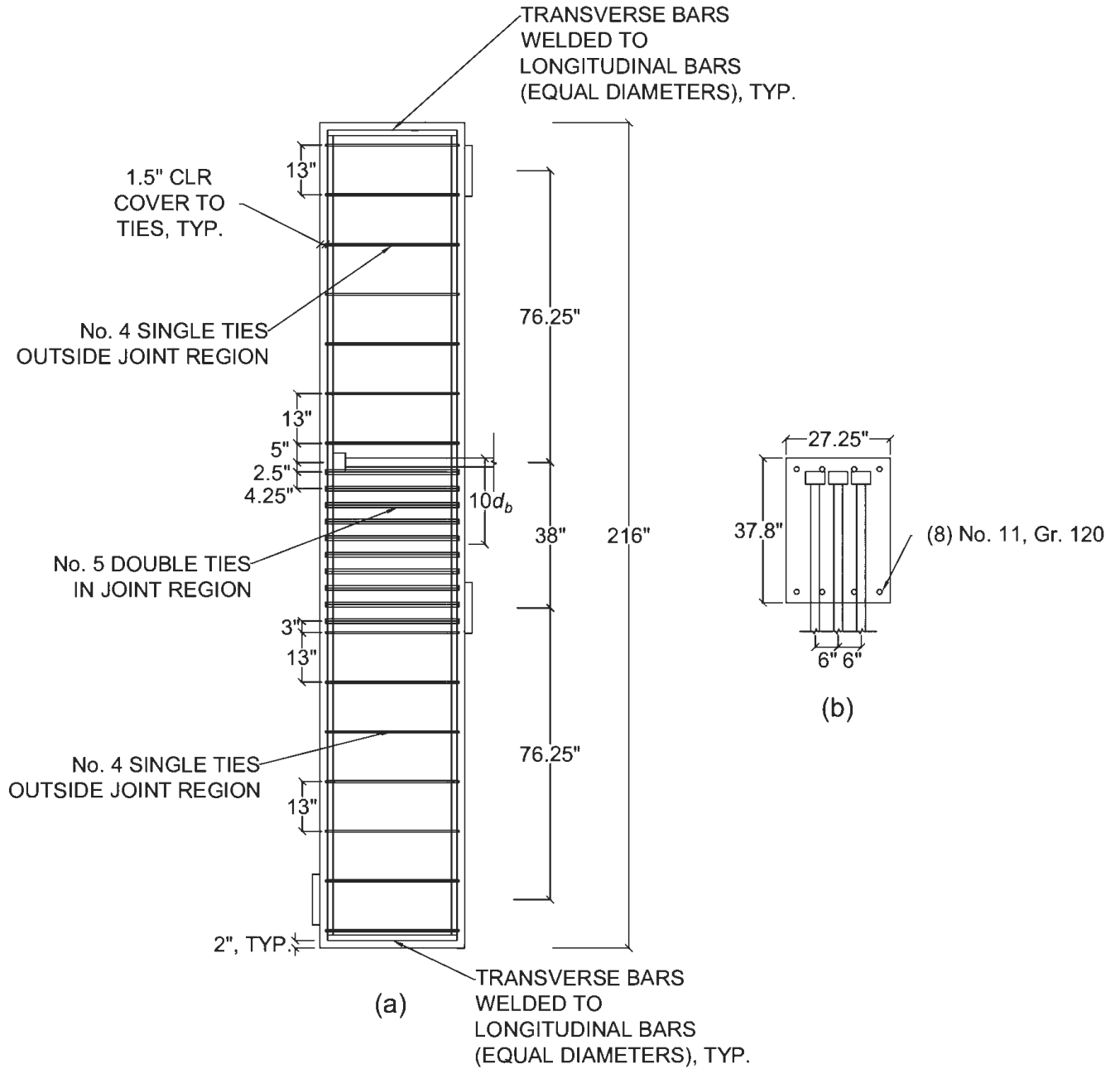


Figure C.28 Details of reinforcement layout for No. 18 headed bar specimen 18-8: (a) elevation, (b) cross-section

**C.2 DETAILED PROPERTIES AND TEST RESULTS FOR NO. 14 AND NO. 18 BAR
SPECIMENS TESTED IN CURRENT STUDY**

Table C.1 Detailed properties and test results for No. 14 and No. 18 bar specimens tested in current study

ID	Designation	n	Head	ℓ_{eh}	$\ell_{eh,avg}$	f_{cm}	Age	d_b	A_b	A_{brg}
				in.	in.	psi	Days	in.	in. ²	
11-1	(2@10)11-15-O4.5-i- 3.5-3.5-18.25	2	A	18.5	18.5	16,210	265	1.41	1.56	4.5
			B	18.5						
11-2	(2@10)11-15-O4.5-7#3-i- 3.5-3.5-18.25	2	A	18.5	18.5	15,850	275	1.41	1.56	4.5
			B	18.5						
14-2	(2@10.6)14-15-B4.2-5#4-i-3.5-3.5-20.5	2	A	20.5	20.5	12,830	69	1.693	2.25	4.2
			B	20.5						
14-3	(2@10.6)14-7-L4.2-i-3.5-3.5-31.9	2	A	32.1	31.8	8,510	170	1.693	2.25	4.2
			B	31.4						
14-4	(2@10.6)14-7-L4.2-5#4-i-3.5-3.5-31.9	2	A	32.0	32.0	7,700	16	1.693	2.25	4.2
			B	32.0						
14-15	(2@10.6)14-7-L4.2-i-3.5-3.5-22.7	2	A	22.6	22.8	6,190	21	1.693	2.25	4.2
			B	23.1						
14-16	(2@10.6)14-7-L4.2-3#4-i-3.5-3.5-22.7	2	A	23.1	22.6	5,390	8	1.693	2.25	4.2
			B	22.0						
14-16A	(2@10.6)14-7-L4.2-3#4-i-3.5-3.5-22.7	2	A	22.6	22.4	8,350	14	1.693	2.25	4.2
			B	22.3						
14-1A	(2@10.6)14-15-L4.2-i-3.5-3.5-22.7	2	A	22.3	22.4	12,030	122	1.693	2.25	4.2
			B	22.6						
14-2A	(2@10.6)14-15-L4.2-5#4-i-3.5-3.5-22.7	2	A	23.1	23.0	13,750	136	1.693	2.25	4.2
			B	22.9						
14-16B	(2@10.6)14-7-L4.2-3#4-i-3.5-3.5-22.7	2	A	22.5	22.1	7,500	28	1.693	2.25	4.2
			B	21.8						
14-16C	(2@10.6)14-7-L4.2-7#4-i-3.5-3.5-22.7	2	A	22.8	22.6	6,470	7	1.693	2.25	4.2
			B	22.4						
14-16D	(2@10.6)14-7-L4.2-10#5-i-3.5-3.5-22.7	2	A	22.8	22.9	6,900	32	1.693	2.25	4.2
			B	23.0						
14-16E	(2@10.6)14-7-L4.2-6#5-i-3.5-3.5-22.7	2	A	22.3	22.4	6,170	16	1.693	2.25	4.2
			B	22.5						
14-16F	(2@10.6)14-7-L4.2-6#5-i-3.5-3.5-22.7	2	A	22.1	22.1	5,640	8	1.693	2.25	4.2
			B	22.1						
14-17	(2@7.1)14-7-L4.2-6#5-i-6.5-3.5-22.7	2	A	22.5	22.4	6,540	16	1.693	2.25	4.2
			B	22.3						

Table C.1 Cont. Detailed properties and test results for No. 14 and No. 18 bar specimens tested in current study

ID	b	h	h_{cl}	b_{BP}	d_{eff}	d_{eff}/ℓ_{eh}	c_{so}	c_o	c_{bc}	s	s/d_b	Bar spacing
	in.	in.	in.	in.	in.		in.	in.	in.	in.		
11-1	22.5	24.5	20.5	6	22.12	1.20	3.5	2.3	3.5	14.1	10.0	Wide
11-2	22.5	24.5	20.5	6	22.74	1.23	3.5	2.3	3.5	14.1	10.0	Wide
14-2	26.7	28.6	25.5	6	27.55	1.34	3.5	2.4	3.5	18	10.6	Wide
14-3	26.7	37.8	25.5	6	30.37	0.95	3.5	2.4	3.5	18	10.6	Wide
14-4	26.7	37.8	25.5	6	31.28	0.98	3.5	2.4	3.5	18	10.6	Wide
14-15	26.7	28.6	25.5	6	29.48	1.29	3.5	2.4	3.5	18	10.6	Wide
14-16	26.7	28.6	25.5	6	28.13	1.24	3.5	2.4	3.5	18	10.6	Wide
14-16A	26.7	28.6	25.5	6	28.56	1.28	3.5	2.4	3.5	18	10.6	Wide
14-1A	26.7	28.6	25.5	6	27.34	1.22	3.5	2.4	3.5	18	10.6	Wide
14-2A	26.7	28.6	25.5	6	27.99	1.22	3.5	2.4	3.5	18	10.6	Wide
14-16B	26.7	28.6	25.5	6	28.88	1.31	3.5	2.4	3.5	18	10.6	Wide
14-16C	26.7	28.6	25.5	6	29.45	1.30	3.5	2.4	3.5	18	10.6	Wide
14-16D	26.7	28.6	25.5	6	30.79	1.34	3.5	2.4	3.5	18	10.6	Wide
14-16E	26.7	28.6	25.5	6	29.75	1.33	3.5	2.4	3.5	18	10.6	Wide
14-16F	26.7	28.6	25.5	6	29.56	1.34	3.5	2.4	3.5	18	10.6	Wide
14-17	26.7	28.6	25.5	6	29.39	1.31	6.5	5.4	3.5	12	7.1	Close

Table C.1 Cont. Detailed properties and test results for No. 14 and No. 18 bar specimens tested in current study

ID	d_{to}	N_{tp}	n_{tp}	n_{ut}	d_{tp}	A_{tp}	A_{tt}	A_{hs}	A_{tt}/A_{hs}	L. C.
	in.				in.	in. ²	in. ²	in. ²		
11-1	0.38	0	0	0	0	0	0	3.12	0	B
11-2	0.38	7	4	8	0.375	0.11	0.88	3.12	0.282	B
14-2	0.5	5	3	6	0.5	0.2	1.2	4.50	0.267	A
14-3	0.5	0	0	0	0	0	0	4.50	0	B
14-4	0.5	5	3	6	0.5	0.2	1.2	4.50	0.267	A
14-15	0.5	0	0	0	0	0	0	4.50	0	B
14-16	0.5	3	2	4	0.5	0.2	0.8	4.50	0.178	A
14-16A	0.5	3	2	4	0.5	0.2	0.8	4.50	0.178	A
14-1A	0.5	0	0	0	0	0	0	4.50	0	B
14-2A	0.5	5	3	6	0.5	0.2	1.2	4.50	0.267	B
14-16B	0.5	3	2	4	0.5	0.2	0.8	4.50	0.178	B
14-16C	0.5	7	4	8	0.5	0.2	1.6	4.50	0.356	B
14-16D	0.5	5	3	12	0.625	0.31	3.72	4.50	0.827	A
14-16E	0.5	5	2	8	0.625	0.31	2.48	4.50	0.551	A
14-16F	0.5	3	2	8	0.625	0.31	2.48	4.50	0.551	A
14-17	0.5	3	2	8	0.625	0.31	2.48	4.50	0.551	A

Table C.1 Cont. Detailed properties and test results for No. 14 and No. 18 bar specimens tested in current study

ID	Δ_{max}	Δ_{ind}	T_{max}	$f_{s,max}$	T_{ind}	T_{total}	T	f_s	Failure Type
	in.	in.	kips	ksi	kips	kips	kips	ksi	
11-1	2.22	0.84	165.2	105.91	165.1	326.0	163.0	104.5	CB+SS
	1.02	0.76	160.2	102.71	160.2				
11-2	0.61	0.26	229.7	147.23	229.7	442.0	221.0	141.7	SS
	2.35	0.30	212.8	136.4	212.8				
14-2	1.48	0.25	194	86.2	193.5	381.2	190.6	84.7	SF
	1.48	0.21	188.1	83.6	187.8				
14-3*	-	0.26	289.9	128.8	289.5	606.0	303.0	134.7	SS
	0.90	0.24	316.1	140.5	273.5				
14-4	0.17	0.08	331.1	147.2	328.5	667.2	333.6	148.3	SS
	0.33	0.14	339.1	150.7	339.1				
14-15	1.07	0.52	217.2	96.5	217.2	409.6	204.8	91.0	CB+SS
	1.39	0.26	192.4	85.5	192.4				
14-16	1.2	0.08	127.8	56.8	127.8	247.2	123.6	54.9	SF
	1.3	0.05	119.4	53.1	119.4				
14-16A	0.71	0.26	190.8	84.8	190.8	372.0	186.0	82.7	SF
	0.70	0.15	181.5	80.7	181.1				
14-1A	0.15	0.04	159.2	70.7	159.0	320.0	160.0	71.1	SF
	0.72	0.42	163.5	72.6	163.5				
14-2A	0.41	0.36	258.2	114.8	258.1	496.2	248.1	110.3	CB
	0.63	0.20	238.0	105.8	237.8				
14-16B	1.91	1.60	201.1	89.4	200.9	383.4	191.7	85.2	CB+SS
	0.96	0.67	182.4	81.1	182.4				
14-16C	0.26	0.11	192.1	85.4	191.1	416.9	208.4	92.6	SS
	0.51	0.41	225.8	100.4	225.7				
14-16D*	0.67	0.25	304.4	135.3	273.5	579.6	289.8	128.8	SS
	0.21	0.18	275.3	122.4	275.1				
14-16E	1.28	0.21	219	97.3	219.0	437.2	218.6	97.2	SS
	1.10	0.05	227.4	101.1	218.2				
14-16F	0.93	0.13	198.09	88.0	198.1	395.6	197.8	87.9	SS
	1.20	0.14	197.5	87.8	197.5				
14-17	0.81	0.19	203.5	90.5	203.5	413.4	206.7	91.9	CB
	0.90	0.25	210.1	93.4	209.9				

* Bars failed independently, so T is the average of the maximum force on individual bar

Table C.1 Cont. Detailed properties and test results for No. 14 and No. 18 bar specimens tested in current study

ID	Designation	n	Head	ℓ_{eh}	$\ell_{eh,avg}$	f_{cm}	Age	d_b	A_b	A_{brg}
				in.	in.	psi	Days	in.	in. ²	
14-5	(3@3.5)14-7-L4.2-5#4-i-3.5-3.5-22.7	3	A	22.3	22.3	6,830	31	1.693	2.25	4.2
			B	22.3						
			C	22.4						
14-6	(3@3.5)14-7-L4.2-5#5-i-3.5-3.5-22.7	3	A	22.3	22.4	6,890	51	1.693	2.25	4.2
			B	22.5						
			C	22.5						
14-7	(3@3.5)14-7-L4.2-i-3.5-3.5-31.9	3	A	32.0	32.1	7,080	102	1.693	2.25	4.2
			B	32.1						
			C	32.3						
14-8	(3@3.5)14-7-L4.2-5#5-i-3.5-3.5-31.9	3	A	31.6	31.7	7,100	109	1.693	2.25	4.2
			B	31.8						
			C	31.6						
14-9	(3@3.5)14-12-L4.2-5#5-i-3.5-3.5-22.7	3	A	22.3	22.1	11,480	38	1.693	2.25	4.2
			B	22.0						
			C	22.1						
14-10	(3@3.5)14-7-L4.2-10#5-i-3.5-3.5-22.7	3	A	22.3	22.3	6,820	42	1.693	2.25	4.2
			B	22.1						
			C	22.4						
18-1	(2@8.0)18-7-L4.4-14#5-i-3.5-3.5-31.1	2	A	32.5	32.6	5,750	20	2.257	4.00	4.4
			B	32.6						
18-2	(2@8.0)18-15-H4.4-14#5-i-3.5-3.5-27.8	2	A	28.3	28.4	11,770	45	2.257	4.00	4.4
			B	28.6						
18-3	(2@8.0)18-7-O4.3-6#5-i-3.5-3.5-30.6	2	A	31.1	30.9	6,540	8	2.257	4.00	4.3
			B	30.8						
18-4	(2@8.0)18-7-O4.3-12#5-i-3.5-3.5-30.6	2	A	30.8	30.9	7,200	15	2.257	4.00	4.3
			B	31.0						
18-5	(2@5.3)18-7-L4.4-14#5-i-6.5-3.5-31.1	2	A	32.0	32.5	5,310	23	2.257	4.00	4.4
			B	33.0						
18-6	(2@5.3)18-15-H4.4-14#5-i-6.5-3.5-27.8	2	A	28.6	28.6	10,230	53	2.257	4.00	4.4
			B	28.6						
18-7	(3@2.7)18-7-L4.4-20#5-i-6.5-3.5-31.1	3	A	32.0	32.1	5,890	20	2.257	4.00	4.4
			B	32.0						
			C	32.3						
18-8	(3@2.7)18-7-L4.4-20#5-i-6.5-3.5-31.1	3	A	32.3	32.3	6,380	27	2.257	4.00	4.4
			B	32.0						
			C	32.8						

Table C.1 Cont. Detailed properties and test results for No. 14 and No. 18 bar specimens tested in current study

ID	b	h	h_{cl}	b_{BP}	d_{eff}	d_{eff}/ℓ_{eh}	c_{so}	c_o	c_{bc}	s	s/d_b	Bar spacing
	in.	in.	in.	in.	in.		in.	in.	in.	in.		
14-5	20.7	28.6	24.0	9	30.45	1.37	3.5	2.4	3.5	6	3.5	Close
14-6	20.7	28.6	24.0	9	30.34	1.35	3.5	2.4	3.5	6	3.5	Close
14-7	20.7	37.8	24.0	9	32.76	1.02	3.5	2.4	3.5	6	3.5	Close
14-8	20.7	37.8	24.0	9	33.53	1.06	3.5	2.4	3.5	6	3.5	Close
14-9	20.7	28.6	25.5	6	29.51	1.34	3.5	2.4	3.5	6	3.5	Close
14-10	20.7	28.6	24.0	9	31.33	1.40	3.5	2.4	3.5	6	3.5	Close
18-1	27.3	37.8	33.7	9	39.99	1.23	3.5	2.1	3.5	18	8.0	Wide
18-2	27.3	37.8	35.2	6	39.74	1.40	3.5	2.1	3.5	18	8.0	Wide
18-3	27.3	37.8	33.7	9	40.34	1.31	3.5	1.7	3.5	18	8.0	Wide
18-4	27.3	37.8	33.7	9	40.25	1.30	3.5	1.7	3.5	18	8.0	Wide
18-5	27.3	37.8	33.7	9	39.88	1.23	6.5	5.1	3.5	12	5.3	Close
18-6	27.3	37.8	35.2	6	40.60	1.42	6.5	5.1	3.5	12	5.3	Close
18-7	27.3	37.8	32.2	12	39.49	1.23	6.5	5.1	3.5	6	2.7	Close
18-8	27.3	37.8	32.2	12	40.35	1.25	6.5	5.1	3.5	6	2.7	Close

Table C.1 Cont. Detailed properties and test results for No. 14 and No. 18 bar specimens tested in current study

ID	d_{to}	N_{tp}	n_{tp}	n_{tt}	d_{tp}	A_{tp}	A_{tt}	A_{hs}	A_{tt}/A_{hs}	L. C.
	in.				in.	in. ²	in. ²	in. ²		
14-5	0.5	5	3	6	0.5	0.2	1.2	6.75	0.178	B
14-6	0.5	5	3	6	0.625	0.31	1.86	6.75	0.276	B
14-7	0.5	0	0	0	0	0	0	6.75	0	B
14-8	0.5	5	3	6	0.625	0.31	1.86	6.75	0.276	B
14-9	0.5	5	3	6	0.625	0.31	1.86	6.75	0.276	B
14-10	0.5	5	3	12	0.625	0.31	3.72	6.75	0.551	A
18-1	0.5	14	7	14	0.625	0.31	4.34	8.00	0.543	A
18-2	0.5	14	7	14	0.625	0.31	4.34	8.00	0.543	A
18-3	0.5	6	3	6	0.625	0.31	1.86	8.00	0.233	B
18-4	0.5	12	6	12	0.625	0.31	3.72	8.00	0.465	B
18-5	0.5	14	7	14	0.625	0.31	4.34	8.00	0.543	A
18-6	0.5	14	7	14	0.625	0.31	4.34	8.00	0.543	A
18-7	0.5	10	5	20	0.625	0.31	6.2	12.00	0.517	A
18-8	0.5	10	5	20	0.625	0.31	6.2	12.00	0.517	A

Table C.1 Cont. Detailed properties and test results for No. 14 and No. 18 bar specimens tested in current study

ID	Δ_{max}	Δ_{ind}	T_{max}	$f_{s,max}$	T_{ind}	T_{total}	T	f_s	Failure Type
	in.	in.	kips	ksi	kips	kips	kips	ksi	
14-5	0.71	0.11	188.0	83.6	188.0	545.4	181.8	80.8	CB
	1.01	0.24	174.5	77.5	174.5				
	0.92	0.08	182.9	81.3	182.9				
14-6	0.66	0.06	179.7	79.9	179.5	538.5	179.5	79.8	CB
	0.78	0.25	176.3	78.4	176.3				
	0.73	0.20	182.7	81.2	182.6				
14-7	1.22	0.11	254.7	113.2	254.7	756.3	252.1	112.0	CB+SS
	2.03	0.27	248.8	110.6	248.6				
	1.73	0.28	253.2	112.5	253.2				
14-8	0.64	0.10	279.1	124.1	279.1	823.8	274.6	122.0	CB+SS
	0.57	0.13	266.0	118.2	266.0				
	0.34	0.02	278.7	123.9	278.7				
14-9	0.94	0.32	178.8	79.4	178.8	521.7	173.9	77.3	CB
	0.87	0.40	165.5	73.6	165.4				
	1.00	0.45	177.8	79.0	177.4				
14-10	0.60	0.26	208.1	92.5	207.9	619.8	206.6	91.8	CB
	0.81	0.30	205.3	91.3	205.3				
	0.73	0.28	206.4	91.7	206.4				
18-1	0.90	0.24	366.7	91.7	323.8	644.0	322.0	80.5	SS
	0.74	0.31	320.1	80.0	320.1				
18-2	2.74	1.35	406.3	101.6	404.7	813.2	406.6	101.7	CB+SS
	1.86	1.38	408.5	102.1	408.5				
18-3	1.07	0.34	366.0	91.5	364.8	733.0	366.5	91.6	CB
	1.07	0.34	368.3	92.1	368.3				
18-4	0.99	0.13	382.1	95.5	382.1	760.0	380.0	95.0	SS
	1.08	0.04	378.4	94.6	378.0				
18-5	1.20	0.98	300.5	75.1	300.5	601.6	300.8	75.2	CB
	1.16	0.02	301.1	75.3	301.1				
18-6	1.64	1.33	418.4	104.6	418.4	839.6	419.8	105.0	SS
	1.73	1.41	421.3	105.3	421.3				
18-7	0.49	0.13	256.4	64.1	256.2	756.3	252.1	63.0	CB+SS
	0.54	0.30	241.6	60.4	241.6				
	0.46	0.20	258.5	64.6	258.5				
18-8	2.32	0.48	291.7	72.9	291.7	885.9	295.3	73.8	CB+SS
	1.98	0.28	303.6	75.9	303.6				
	2.07	0.23	290.8	72.7	290.5				

C.3 SPECIMENS TESTED AT THE UNIVERSITY OF KANSAS

This section presents the specimens tested at the University of Kansas, including No. 5, No. 8, and No. 11 bar specimens tested by Shao et al. (2016), and No. 14 and No. 18 bar specimens tested in this study. Specimens are tabulated in four categories: widely-spaced bars without parallel ties (Table C2), closely-spaced bars without parallel ties (Table C3), widely-spaced bars with parallel ties (Table C4), and closely-spaced bars with parallel ties (Table C5). In each category, specimens not used to develop descriptive equations, Eq. (5.5) and (5.7), are identified, if any.

Table C.2 Detailed properties and test results for headed bar specimens having widely-spaced bars without parallel ties tested at the University of Kansas

SN	ID	<i>b</i>	<i>h</i>	$\ell_{eh,avg}$	f_{cm}	d_b	A_b	<i>s</i>	s/d_b
		in.	in.	in.	psi	in.	in. ²	in.	
1	5-5-F4.0-0-i-2.5-5-4	12.9	9.6	4.1	4810	0.625	0.31	7.3	11.7
2	5-5-F4.0-0-i-2.5-3-6	14.9	9.5	6.0	4690	0.625	0.31	7.3	11.7
3	5-12-F4.0-0-i-2.5-5-4	12.9	9.6	4.1	11030	0.625	0.31	7.3	11.7
4	5-12-F4.0-0-i-2.5-3-6	15.0	9.5	6.0	11030	0.625	0.31	7.4	11.8
5	8-5g-T4.0-0-i-2.5-3-12.5	16.8	17.1	12.6	5910	1	0.79	10.8	10.8
6	8-5g-T4.0-0-i-3.5-3-12.5	17.1	17.0	12.5	6320	1	0.79	11.1	11.1
7	8-5-T4.0-0-i-2.5-3-12.5	16.8	17.1	12.6	6210	1	0.79	10.8	10.8
8	8-5-T4.0-0-i-3.5-3-12.5	16.4	17.2	12.7	6440	1	0.79	10.4	10.4
9	8-8-F4.1-0-i-2.5-3-10.5	16.9	14.5	10.5	8450	1	0.79	10.9	10.9
10	8-12-F4.1-0-i-2.5-3-10	16.9	13.7	9.7	11760	1	0.79	10.9	10.9
11	8-5-S6.5-0-i-2.5-3-11.25	16.8	15.8	11.1	5500	1	0.79	10.8	10.8
12	8-5-S6.5-0-i-2.5-3-14.25	16.6	19.0	14.3	5500	1	0.79	10.6	10.6
13	8-5-O4.5-0-i-2.5-3-11.25	16.9	19.5	11.3	5500	1	0.79	10.9	10.9
14	8-5-O4.5-0-i-2.5-3-14.25	17.0	22.4	14.1	5500	1	0.79	11.0	11.0
15	8-5-T9.5-0-i-2.5-3-14.5	16.9	18.9	14.4	4970	1	0.79	10.9	10.9
16	8-5-O9.1-0-i-2.5-3-14.5	17.0	22.6	14.4	4970	1	0.79	11.0	11.0
17	8-15-T4.0-0-i-2.5-4.5-9.5	17.0	15.5	9.5	16030	1	0.79	11.0	11.0

Table C.2 Cont. Detailed properties and test results for headed bar specimens having widely-spaced bars without parallel ties tested at the University of Kansas

SN	n	A_{tt}	A_{hs}	A_{tt}/A_{hs}	h_{cl}	x_{mid}	d_{eff}	d_{eff}/ℓ_{eh}	θ
		in. ²	in. ²		in.	in.	in.		°
1	2	0	0.62	0	5.25	9.44	6.40	1.58	66.7
2	2	0	0.62	0	5.25	9.44	6.60	1.10	57.6
3	2	0	0.62	0	5.25	9.44	5.97	1.47	66.7
4	2	0	0.62	0	5.25	9.44	6.16	1.03	57.6
5	2	0	1.58	0	10.0	14.19	13.07	1.04	48.5
6	2	0	1.58	0	10.0	14.19	12.77	1.02	48.6
7	2	0	1.58	0	10.0	14.19	12.54	1.00	48.4
8	2	0	1.58	0	10.0	14.19	12.81	1.01	48.3
9	2	0	1.58	0	10.0	14.19	11.95	1.14	53.5
10	2	0	1.58	0	10.0	14.19	11.31	1.17	55.7
11	2	0	1.58	0	10.0	14.19	12.48	1.13	52.1
12	2	0	1.58	0	10.0	14.19	12.92	0.91	44.9
13	2	0	1.58	0	10.0	14.19	12.20	1.08	51.6
14	2	0	1.58	0	10.0	14.19	12.76	0.90	45.1
15	2	0	1.58	0	10.0	14.19	13.20	0.92	44.6
16	2	0	1.58	0	10.0	14.19	13.29	0.92	44.6
17	2	0	1.58	0	10.0	14.19	11.11	1.17	56.2

Table C.2 Cont. Detailed properties and test results for headed bar specimens having widely-spaced bars without parallel ties tested at the University of Kansas

SN	T	$T_h^{[1]}$	T/T_h	f_{su}	$f_{su}/f_{s,calc}^{[2]}$	$f_{su}/f_{s,calc}^{[3]}$
	lb	lb		ksi		
1	24500	22194	1.10	79.0	1.48	1.48
2	32700	31887	1.03	105.5	1.35	1.35
3	28300	26355	1.07	91.3	1.39	1.39
4	41700	38065	1.10	134.5	1.39	1.39
5	97700	84758	1.15	123.7	1.44	1.44
6	93400	85541	1.09	118.2	1.36	1.36
7	83300	85808	0.97	105.4	1.21	1.21
8	91900	86910	1.06	116.3	1.32	1.32
9	77100	77095	1.00	97.6	1.24	1.24
10	71800	76548	0.94	90.9	1.15	1.15
11	75555	74071	1.02	95.6	1.29	1.29
12	87720	94024	0.93	111.0	1.16	1.16
13	67390	75268	0.90	85.3	1.13	1.13
14	85000	93279	0.91	107.6	1.13	1.13
15	91650	92862	0.99	116.0	1.23	1.23
16	94800	92862	1.02	120.0	1.27	1.27
17	83300	80113	1.04	105.4	1.26	1.26

^[1] Based on descriptive equations, Eq. (5.5) and (5.7)

^[2] Based on proposed design equation, Eq. (6.32), using full expression for ψ_p , Eq. (6.29)

^[3] Based on proposed design equation, Eq. (6.32), using simplified expression for ψ_p , Eq. (6.30)

Table C.2 Cont. Detailed properties and test results for headed bar specimens having widely-spaced bars without parallel ties tested at the University of Kansas

SN	ID	<i>b</i>	<i>h</i>	$\ell_{eh,avg}$	f_{cm}	d_b	A_b	<i>s</i>	s/d_b
		in.	in.	in.	psi	in.	in. ²	in.	
18	8-15-S9.5-0-i-2.5-3-9.5	17.0	15.3	9.5	16030	1	0.79	11.0	11.0
19	8-8-T9.5-0-i-2.5-3-9.5	17.0	13.9	9.4	9040	1	0.79	11.0	11.0
20	(2@9)8-12-F4.1-0-i-2.5-3-12	15.0	16.1	12.1	12080	1	0.79	9.0	9.0
21	(2@9)8-12-F9.1-0-i-2.5-3-12	14.9	15.9	11.9	12080	1	0.79	8.9	8.9
22	8-8-O4.5-0-i-2.5-3-9.5	17.1	17.4	9.2	6710	1	0.79	11.1	11.1
23	(2@9)8-8-O4.5-0-i-2.5-3-9.5	15.1	17.3	9.0	6710	1	0.79	9.1	9.1
24	(2@9)8-8-T4.0-0-i-2.5-3-9.5	15.1	13.9	9.4	6790	1	0.79	9.1	9.1
25	11-5a-F3.8-0-i-2.5-3-17	21.9	20.9	16.6	4050	1.41	1.56	15.5	11.0
26	11-5-F3.8-0-i-2.5-3-17	21.4	21.6	17.3	5760	1.41	1.56	15.0	10.6
27	11-12-O4.5-0-i-2.5-3-16.75	21.4	26.9	17.1	10860	1.41	1.56	15.0	10.6
28	11-12-S5.5-0-i-2.5-3-16.75	21.7	22.7	16.9	10120	1.41	1.56	15.3	10.9
29	11-5-O4.5-0-i-2.5-3-19.25	21.5	29.2	19.4	5430	1.41	1.56	15.1	10.7
30	11-5-S5.5-0-i-2.5-3-19.25	21.5	25.1	19.4	6320	1.41	1.56	15.1	10.7
31	11-1	22.5	24.5	18.5	16210	1.41	1.56	14.1	10.0
32	14-3	26.7	37.8	31.8	8510	1.693	2.25	18.0	10.6
33	14-15	26.7	28.6	22.8	6190	1.693	2.25	18.0	10.6
34	14-1A*	26.7	28.6	22.4	12030	1.693	2.25	18.0	10.6

* Specimen failed in shear, not used to develop descriptive equations, Eq. (5.5) and (5.7)

Table C.2 Cont. Detailed properties and test results for headed bar specimens having widely-spaced bars without parallel ties tested at the University of Kansas

SN	n	A_{tt}	A_{hs}	A_{tt}/A_{hs}	h_{cl}	x_{mid}	d_{eff}	d_{eff}/ℓ_{eh}	θ
		in. ²	in. ²		in.	in.	in.		°
18	2	0	1.58	0	10.0	14.19	11.08	1.17	56.2
19	2	0	1.58	0	10.0	14.19	11.54	1.23	56.5
20	2	0	1.58	0	10.0	14.19	11.58	0.96	49.6
21	2	0	1.58	0	10.0	14.19	11.54	0.97	50.1
22	2	0	1.58	0	10.0	14.19	11.67	1.27	57.1
23	2	0	1.58	0	10.0	14.19	11.91	1.32	57.6
24	2	0	1.58	0	10.0	14.19	12.00	1.28	56.5
25	2	0	3.12	0	19.5	23.69	22.55	1.36	55.0
26	2	0	3.12	0	19.5	23.69	22.82	1.32	53.9
27	2	0	3.12	0	19.5	23.69	22.14	1.29	54.1
28	2	0	3.12	0	19.5	23.69	22.40	1.32	54.4
29	2	0	3.12	0	19.5	23.69	23.59	1.21	50.6
30	2	0	3.12	0	19.5	23.69	23.67	1.22	50.7
31	2	0	3.12	0	20.5	23.50	22.12	1.20	51.8
32	2	0	4.5	0	25.5	28.54	30.33	0.95	41.9
33	2	0	4.5	0	25.5	28.54	29.44	1.29	51.4
34	2	0	4.5	0	25.5	28.54	27.30	1.22	51.9

Table C.2 Cont. Detailed properties and test results for headed bar specimens having widely-spaced bars without parallel ties tested at the University of Kansas

SN	T	T_h ^[1]	T/T_h	f_{su}	$f_{su}/f_{s,calc}$ ^[2]	$f_{su}/f_{s,calc}$ ^[3]
	lb	lb		ksi		
18	81650	80113	1.02	103.4	1.24	1.24
19	65200	70305	0.93	82.5	1.16	1.16
20	79050	94579	0.84	100.1	1.01	1.01
21	76500	93249	0.82	96.8	1.00	1.00
22	58350	64836	0.90	73.9	1.14	1.14
23	58800	63573	0.92	74.4	1.17	1.17
24	61800	66259	0.93	78.2	1.18	1.18
25	97500	120635	0.81	62.5	1.02	1.02
26	132700	134846	0.98	85.1	1.22	1.22
27	169600	152764	1.11	108.7	1.33	1.33
28	175900	148975	1.18	112.8	1.42	1.42
29	157900	149070	1.06	101.2	1.30	1.30
30	176800	153383	1.15	113.3	1.41	1.41
31	163000	178441	0.91	104.5	1.07	1.07
32	303000	284810	1.06	134.7	1.25	1.25
33	204800	194950	1.05	91.0	1.27	1.27
34	160000	220013	0.73	71.1	0.86	0.86

^[1] Based on descriptive equations, Eq. (5.5) and (5.7)

^[2] Based on proposed design equation, Eq. (6.32), using full expression for ψ_p , Eq. (6.29)

^[3] Based on proposed design equation, Eq. (6.32), using simplified expression for ψ_p , Eq. (6.30)

Table C.3 Detailed properties and test results for headed bar specimens having closely-spaced bars without parallel ties tested at the University of Kansas

SN	ID	<i>b</i>	<i>h</i>	$\ell_{eh,avg}$	f_{cm}	d_b	A_b	s	s/d_b
		in.	in.	in.	psi	in.	in. ²	in.	
35	(3@5.9)5-12-F4.0-0-i-2.5-4-5	13.2	9.5	5.0	11030	0.625	0.31	3.8	6.1
36	(4@3.9)5-12-F4.0-0-i-2.5-4-5	12.8	9.7	5.2	11030	0.625	0.31	2.4	3.8
37	(3@3)8-8-F4.1-0-i-2.5-3-10.5	12.0	14.6	10.6	8450	1	0.79	3.0	3.0
38	(3@3)8-8-F4.1-0-i-2.5-3-10.5-HP	11.8	14.3	10.3	8450	1	0.79	2.9	2.9
39	(3@4)8-8-F4.1-0-i-2.5-3-10.5	14.0	14.8	10.8	8450	1	0.79	4.0	4.0
40	(3@5)8-8-F4.1-0-i-2.5-3-10.5	16.0	14.4	10.4	8050	1	0.79	5.0	5.0
41	(3@5)8-8-F4.1-0-i-2.5-3-10.5-HP	16.1	14.3	10.3	8260	1	0.79	5.1	5.1
42	(3@3)8-12-F4.1-0-i-2.5-3-10	12.0	13.9	9.9	11040	1	0.79	3.0	3.0
43	(3@4)8-12-F4.1-0-i-2.5-3-10	14.0	13.9	9.9	11440	1	0.79	4.0	4.0
44	(3@5)8-12-F4.1-0-i-2.5-3-10	16.0	13.9	9.9	11460	1	0.79	5.0	5.0
45	(3@5.5)8-5-T9.5-0-i-2.5-3-14.5	16.5	18.8	14.3	4960	1	0.79	5.3	5.3
46	(3@5.5)8-5-O9.1-0-i-2.5-3-14.5	16.5	22.6	14.4	4960	1	0.79	5.3	5.3
47	(4@3.7)8-5-T9.5-0-i-2.5-3-14.5	17.4	18.8	14.3	5570	1	0.79	3.8	3.8
48	(4@3.7)8-5-O9.1-0-i-2.5-3-14.5	16.8	22.3	14.1	5570	1	0.79	3.6	3.6
49	(3@4)8-8-T9.5-0-i-2.5-3-9.5	14.0	13.8	9.3	9040	1	0.79	4.0	4.0
50	(3@5)8-8-T9.5-0-i-2.5-3-9.5	16.0	14.0	9.5	9940	1	0.79	5.0	5.0

Table C.3 Cont. Detailed properties and test results for headed bar specimens having closely-spaced bars without parallel ties tested at the University of Kansas

SN	n	A_{tt}	A_{hs}	A_{tt}/A_{hs}	h_{cl}	x_{mid}	d_{eff}	d_{eff}/ℓ_{eh}	θ
		in. ²	in. ²		in.	in.	in.		°
35	3	0	0.93	0	5.25	9.44	6.29	1.25	61.9
36	4	0	1.24	0	5.25	9.44	6.56	1.26	61.2
37	3	0	2.37	0	10.0	14.19	12.93	1.22	53.3
38	3	0	2.37	0	10.0	14.19	12.75	1.23	53.9
39	3	0	2.37	0	10.0	14.19	12.69	1.17	52.6
40	3	0	2.37	0	10.0	14.19	12.70	1.23	53.9
41	3	0	2.37	0	10.0	14.19	12.45	1.21	54.2
42	3	0	2.37	0	10.0	14.19	11.73	1.18	55.1
43	3	0	2.37	0	10.0	14.19	11.66	1.18	55.0
44	3	0	2.37	0	10.0	14.19	11.63	1.17	55.0
45	3	0	2.37	0	10.0	14.19	13.95	0.98	44.9
46	3	0	2.37	0	10.0	14.19	14.07	0.98	44.7
47	4	0	3.16	0	10.0	14.19	13.83	0.97	44.8
48	4	0	3.16	0	10.0	14.19	13.99	1.00	45.3
49	3	0	2.37	0	10.0	14.19	11.73	1.27	56.9
50	3	0	2.37	0	10.0	14.19	11.52	1.21	56.2

Table C.3 Cont. Detailed properties and test results for headed bar specimens having closely-spaced bars without parallel ties tested at the University of Kansas

SN	T	T_h ^[1]	T/T_h	f_{su}	$f_{su}/f_{s,calc}$ ^[2]	$f_{su}/f_{s,calc}$ ^[3]
	lb	lb		ksi		
35	28033	27686	1.01	90.4	1.38	1.38
36	25633	22569	1.14	82.7	1.50	1.50
37	54800	47606	1.15	69.4	1.42	1.40
38	50500	45945	1.10	63.9	1.35	1.32
39	58700	54950	1.07	74.3	1.38	1.38
40	64000	58092	1.10	81.0	1.46	1.46
41	59900	58169	1.03	75.8	1.36	1.36
42	42200	47266	0.89	53.4	1.10	1.08
43	48900	53869	0.91	61.9	1.16	1.16
44	55100	60053	0.92	69.7	1.20	1.20
45	73400	72826	1.01	92.9	1.34	1.34
46	75700	73307	1.03	95.8	1.37	1.37
47	60800	63981	0.95	77.0	1.22	1.22
48	61225	61495	1.00	77.5	1.27	1.27
49	40300	48037	0.84	51.0	1.09	1.09
50	44500	55983	0.79	56.3	1.05	1.05

^[1] Based on descriptive equations, Eq. (5.5) and (5.7)

^[2] Based on proposed design equation, Eq. (6.32), using full expression for ψ_p , Eq. (6.29)

^[3] Based on proposed design equation, Eq. (6.32), using simplified expression for ψ_p , Eq. (6.30)

Table C.3 Cont. Detailed properties and test results for headed bar specimens having closely-spaced bars without parallel ties tested at the University of Kansas

SN	ID	<i>b</i>	<i>h</i>	$\ell_{eh,avg}$	f_{cm}	d_b	A_b	<i>s</i>	<i>s/d_b</i>
		in.	in.	in.	psi	in.	in. ²	in.	
51	(3@7)8-8-T9.5-0-i-2.5-3-9.5	19.9	14.0	9.5	10180	1	0.79	7.0	7.0
52	(3@4)8-8-T9.5-0-i-2.5-3-14.5	14.0	19.1	14.6	9040	1	0.79	4.0	4.0
53	(3@5)8-8-T9.5-0-i-2.5-3-14.5	15.8	19.1	14.6	9940	1	0.79	4.9	4.9
54	(3@7)8-8-T9.5-0-i-2.5-3-14.5	20.0	19.0	14.5	10180	1	0.79	7.0	7.0
55	(3@4.5)8-12-F4.1-0-i-2.5-3-12	14.8	16.2	12.2	12040	1	0.79	4.4	4.4
56	(3@4.5)8-12-F9.1-0-i-2.5-3-12	15.0	16.0	12.0	12040	1	0.79	4.5	4.5
57	(4@3)8-12-F4.1-0-i-2.5-3-12	15.0	16.0	12.0	12040	1	0.79	3.0	3.0
58	(4@3)8-12-F9.1-0-i-2.5-3-12	15.0	16.2	12.2	12360	1	0.79	3.0	3.0
59	(2@7)8-8-O4.5-0-i-2.5-3-9.5	13.0	17.5	9.3	6710	1	0.79	7.0	7.0
60	(2@5)8-8-O4.5-0-i-2.5-3-9.5	11.3	17.3	9.0	6710	1	0.79	5.3	5.3
61	(2@3)8-8-O4.5-0-i-2.5-3-9.5	9.1	17.3	9.0	6710	1	0.79	3.1	3.1
62	(3@4.5)8-8-T4.0-0-i-2.5-3-9.5	15.0	13.8	9.3	6790	1	0.79	4.5	4.5
63	(4@3)8-8-T4.0-0-i-2.5-3-9.5	15.0	14.0	9.5	6650	1	0.79	3.0	3.0
64	(3@3)8-8-T4.0-0-i-2.5-3-9.5	12.2	14.0	9.5	6790	1	0.79	3.1	3.1
65	(3@5.35)11-12-O4.5-0-i-2.5-3-16.75	21.3	26.7	16.9	10860	1.41	1.56	7.5	5.3
66	(3@5.35)11-12-S5.5-0-i-2.5-3-16.75	21.4	22.7	16.9	10120	1.41	1.56	7.5	5.3
67	(3@5.35)11-5-O4.5-0-i-2.5-3-19.25	21.5	29.3	19.5	5430	1.41	1.56	7.6	5.4
68	(3@5.35)11-5-S5.5-0-i-2.5-3-19.25	21.4	25.0	19.3	6320	1.41	1.56	7.5	5.3
69	14-7	20.7	37.8	32.1	7080	1.693	2.25	6.0	3.5

Table C.3 Cont. Detailed properties and test results for headed bar specimens having closely-spaced bars without parallel ties tested at the University of Kansas

SN	<i>n</i>	<i>A_{tt}</i>	<i>A_{hs}</i>	<i>A_{tt}/A_{hs}</i>	<i>h_{cl}</i>	<i>x_{mid}</i>	<i>d_{eff}</i>	<i>d_{eff}/ℓ_{eh}</i>	<i>θ</i>
		in. ²	in. ²		in.	in.	in.		°
51	3	0	2.37	0	10.0	14.19	11.84	1.25	56.2
52	3	0	2.37	0	10.0	14.19	13.29	0.91	44.2
53	3	0	2.37	0	10.0	14.19	13.22	0.91	44.2
54	3	0	2.37	0	10.0	14.19	12.77	0.88	44.3
55	3	0	2.37	0	10.0	14.19	12.29	1.01	49.3
56	3	0	2.37	0	10.0	14.19	12.27	1.02	49.7
57	4	0	3.16	0	10.0	14.19	11.98	1.00	49.8
58	4	0	3.16	0	10.0	14.19	11.97	0.98	49.4
59	2	0	1.58	0	10.0	14.19	12.06	1.30	56.9
60	2	0	1.58	0	10.0	14.19	12.22	1.36	57.6
61	2	0	1.58	0	10.0	14.19	12.57	1.40	57.6
62	3	0	2.37	0	10.0	14.19	11.99	1.28	56.7
63	4	0	3.16	0	10.0	14.19	11.72	1.24	56.3
64	3	0	2.37	0	10.0	14.19	12.36	1.31	56.3
65	3	0	4.68	0	19.5	23.69	22.01	1.30	54.5
66	3	0	4.68	0	19.5	23.69	22.23	1.31	54.5
67	3	0	4.68	0	19.5	23.69	24.50	1.26	50.5
68	3	0	4.68	0	19.5	23.69	24.38	1.26	50.8
69	3	0	6.75	0	24.0	28.54	32.73	1.02	41.6

Table C.3 Cont. Detailed properties and test results for headed bar specimens having closely-spaced bars without parallel ties tested at the University of Kansas

SN	T	$T_h^{[1]}$	T/T_h	f_{su}	$f_{su}/f_{s,calc}^{[2]}$	$f_{su}/f_{s,calc}^{[3]}$
	lb	lb		ksi		
51	68700	67522	1.02	87.0	1.32	1.32
52	76600	73720	1.04	97.0	1.31	1.31
53	93200	82924	1.12	118.0	1.44	1.44
54	104000	101224	1.03	131.6	1.30	1.30
55	75233	69227	1.09	95.2	1.38	1.38
56	75400	69067	1.09	95.4	1.39	1.39
57	49300	57675	0.85	62.4	1.03	1.02
58	50325	58762	0.86	63.7	1.03	1.02
59	54500	60661	0.90	69.0	1.19	1.19
60	51200	50557	1.01	64.8	1.36	1.36
61	47700	39480	1.21	60.4	1.53	1.52
62	40700	48252	0.84	51.5	1.12	1.12
63	26150	40814	0.64	33.1	0.81	0.79
64	39367	41479	0.95	49.8	1.20	1.19
65	106800	119889	0.89	68.5	1.14	1.14
66	109000	118568	0.92	69.9	1.18	1.18
67	128700	119541	1.08	82.5	1.41	1.41
68	137400	121678	1.13	88.1	1.47	1.47
69	252100	181632	1.39	112.0	1.67	1.67

^[1] Based on descriptive equations, Eq. (5.5) and (5.7)

^[2] Based on proposed design equation, Eq. (6.32), using full expression for ψ_p , Eq. (6.29)

^[3] Based on proposed design equation, Eq. (6.32), using simplified expression for ψ_p , Eq. (6.30)

Table C.4 Detailed properties and test results for headed bar specimens having widely-spaced bars with parallel ties tested at the University of Kansas

SN	ID	<i>b</i>	<i>h</i>	$\ell_{eh,avg}$	f_{cm}	d_b	A_b	<i>s</i>	s/d_b
		in.	in.	in.	psi	in.	in. ²	in.	
70	5-5-F4.0-2#3-i-2.5-5-4	13.0	9.3	3.8	4810	0.625	0.31	7.4	11.8
71	5-5-F4.0-5#3-i-2.5-5-4	13.0	9.7	4.2	4810	0.625	0.31	7.4	11.8
72	5-5-F4.0-2#3-i-2.5-3-6	13.0	9.5	6.0	4690	0.625	0.31	7.4	11.8
73	5-5-F4.0-5#3-i-2.5-3-6	13.0	9.6	6.1	4690	0.625	0.31	7.4	11.8
74	5-12-F4.0-2#3-i-2.5-5-4	12.9	9.6	4.1	11030	0.625	0.31	7.3	11.7
75	5-12-F4.0-5#3-i-2.5-5-4	13.0	9.7	4.2	11030	0.625	0.31	7.4	11.8
76	8-5-T4.0-4#3-i-3-3-12.5	17.9	16.9	12.4	5070	1	0.79	10.9	10.9
77	8-5-T4.0-4#3-i-4-3-12.5	20.0	16.6	12.1	5380	1	0.79	11.0	11.0
78	8-5-T4.0-4#4-i-3-3-12.5	17.6	16.9	12.4	5070	1	0.79	10.6	10.6
79	8-5-T4.0-4#4-i-4-3-12.5	20.1	16.7	12.2	4850	1	0.79	11.1	11.1
80	8-5g-T4.0-5#3-i-2.5-3-9.5	16.8	14.1	9.6	5090	1	0.79	10.8	10.8
81	8-5g-T4.0-5#3-i-3.5-3-9.5	19.3	14.1	9.6	5910	1	0.79	11.3	11.3
82	8-5g-T4.0-4#4-i-2.5-3-9.5	16.5	13.7	9.2	5180	1	0.79	10.5	10.5
83	8-5g-T4.0-4#4-i-3.5-3-9.5	16.3	14.0	9.5	5910	1	0.79	10.3	10.3
84	8-5-T4.0-5#3-i-2.5-3-9.5	16.5	13.8	9.3	5960	1	0.79	10.5	10.5
85	8-5-T4.0-5#3-i-3.5-3-9.5	18.8	13.6	9.1	6440	1	0.79	10.8	10.8
86	8-5-T4.0-4#4-i-2.5-3-9.5	16.5	13.8	9.3	6440	1	0.79	10.5	10.5
87	8-5-T4.0-4#4-i-3.5-3-9.5	18.8	13.8	9.3	6210	1	0.79	10.8	10.8
88	8-8-F4.1-2#3-i-2.5-3-10	17.1	13.9	9.9	8450	1	0.79	11.1	11.1
89	8-12-F4.1-5#3-i-2.5-3-10	17.0	14.0	10.0	11760	1	0.79	11.0	11.0
90	8-5-S6.5-2#3-i-2.5-3-9.25	17.3	13.9	9.1	5750	1	0.79	11.3	11.3
91	8-5-S6.5-2#3-i-2.5-3-12.25	17.0	17.1	12.3	5750	1	0.79	11.0	11.0
92	8-5-O4.5-2#3-i-2.5-3-9.25	17.0	17.6	9.4	5750	1	0.79	11.0	11.0
93	8-5-O4.5-2#3-i-2.5-3-12.25	16.8	20.3	12.0	5750	1	0.79	10.8	10.8
94	8-5-S6.5-5#3-i-2.5-3-8.25	17.0	13.1	8.3	5900	1	0.79	11.0	11.0
95	8-5-S6.5-5#3-i-2.5-3-11.25	17.8	15.7	10.9	5900	1	0.79	11.8	11.8
96	8-5-O4.5-5#3-i-2.5-3-8.25	17.0	16.3	8.0	5900	1	0.79	11.0	11.0
97	8-5-O4.5-5#3-i-2.5-3-11.25	16.8	19.4	11.1	5900	1	0.79	10.8	10.8
98	8-5-T9.5-5#3-i-2.5-3-14.5	17.0	18.9	14.4	5420	1	0.79	11.0	11.0

Table C.4 Cont. Detailed properties and test results for headed bar specimens having widely-spaced bars with parallel ties tested at the University of Kansas

SN	<i>n</i>	<i>A_{tt}</i>	<i>A_{hs}</i>	<i>A_{tt}/A_{hs}</i>	<i>h_{cl}</i>	<i>x_{mid}</i>	<i>d_{eff}</i>	<i>d_{eff}/ℓ_{eh}</i>	<i>θ</i>
		in. ²	in. ²		in.	in.	in.		°
70	2	0.22	0.62	0.355	5.25	9.44	6.16	1.62	68.0
71	2	0.66	0.62	1.065	5.25	9.44	6.48	1.56	66.2
72	2	0.22	0.62	0.355	5.25	9.44	7.04	1.17	57.6
73	2	0.66	0.62	1.065	5.25	9.44	7.30	1.21	57.3
74	2	0.22	0.62	0.355	5.25	9.44	6.08	1.47	66.4
75	2	0.66	0.62	1.065	5.25	9.44	6.23	1.48	65.9
76	2	0.66	1.58	0.418	10.0	14.19	12.85	1.04	48.9
77	2	0.66	1.58	0.418	10.0	14.19	12.69	1.05	49.6
78	2	0.8	1.58	0.506	10.0	14.19	13.61	1.09	48.8
79	2	0.8	1.58	0.506	10.0	14.19	13.03	1.07	49.3
80	2	0.66	1.58	0.418	10.0	14.19	12.72	1.33	56.0
81	2	0.66	1.58	0.418	10.0	14.19	12.17	1.27	56.0
82	2	0.8	1.58	0.506	10.0	14.19	13.16	1.43	57.1
83	2	0.8	1.58	0.506	10.0	14.19	13.13	1.38	56.2
84	2	0.66	1.58	0.418	10.0	14.19	12.36	1.33	56.7
85	2	0.66	1.58	0.418	10.0	14.19	12.15	1.34	57.4
86	2	0.8	1.58	0.506	10.0	14.19	12.75	1.38	56.9
87	2	0.8	1.58	0.506	10.0	14.19	12.33	1.33	56.9
88	2	0.22	1.58	0.139	10.0	14.19	11.84	1.20	55.1
89	2	0.66	1.58	0.418	10.0	14.19	11.58	1.16	54.8
90	2	0.22	1.58	0.139	10.0	14.19	11.97	1.31	57.2
91	2	0.22	1.58	0.139	10.0	14.19	12.71	1.03	49.1
92	2	0.22	1.58	0.139	10.0	14.19	12.14	1.29	56.5
93	2	0.22	1.58	0.139	10.0	14.19	12.51	1.04	49.8
94	2	0.66	1.58	0.418	10.0	14.19	11.93	1.44	59.6
95	2	0.66	1.58	0.418	10.0	14.19	12.51	1.14	52.4
96	2	0.66	1.58	0.418	10.0	14.19	12.12	1.52	60.6
97	2	0.66	1.58	0.418	10.0	14.19	12.59	1.13	51.9
98	2	0.66	1.58	0.418	10.0	14.19	13.97	0.97	44.6

Table C.4 Cont. Detailed properties and test results for headed bar specimens having widely-spaced bars with parallel ties tested at the University of Kansas

SN	T	$T_h^{[1]}$	T/T_h	f_{su}	$f_{su}/f_{s,calc}^{[2]}$	$f_{su}/f_{s,calc}^{[3]}$
	lb	lb		ksi		
70	19700	26065	0.76	63.5	1.08	1.13
71	26500	28524	0.93	85.5	1.33	1.33
72	37900	37047	1.02	122.3	1.33	1.39
73	43500	38004	1.14	140.3	1.51	1.51
74	32700	31943	1.02	105.5	1.34	1.41
75	38900	33148	1.17	125.5	1.56	1.56
76	87509	96598	0.91	110.8	1.16	1.16
77	96172	95603	1.01	121.7	1.28	1.28
78	109032	96967	1.12	138.0	1.43	1.43
79	101480	94697	1.07	128.5	1.38	1.38
80	78700	79159	0.99	99.6	1.34	1.34
81	79500	81155	0.98	100.6	1.31	1.31
82	90700	77064	1.18	114.8	1.60	1.60
83	96700	80768	1.20	122.4	1.60	1.60
84	74200	79652	0.93	93.9	1.25	1.25
85	80600	79041	1.02	102.0	1.37	1.37
86	90500	80293	1.13	114.6	1.51	1.51
87	85600	79807	1.07	108.4	1.44	1.44
88	73400	78237	0.94	92.9	1.07	1.26
89	87200	94462	0.92	110.4	1.16	1.16
90	63350	67844	0.93	80.2	1.10	1.29
91	85960	88117	0.98	108.8	1.11	1.30
92	67910	69451	0.98	86.0	1.15	1.35
93	78510	86156	0.91	99.4	1.04	1.22
94	62040	73036	0.85	78.5	1.18	1.18
95	84480	89999	0.94	106.9	1.22	1.22
96	68390	71017	0.96	86.6	1.35	1.35
97	82230	91214	0.90	104.1	1.16	1.16
98	121000	110155	1.10	153.2	1.35	1.35

^[1] Based on descriptive equations, Eq. (5.5) and (5.7)

^[2] Based on proposed design equation, Eq. (6.32), using full expression for ψ_p , Eq. (6.29)

^[3] Based on proposed design equation, Eq. (6.32), using simplified expression for ψ_p , Eq. (6.30)

Table C.4 Cont. Detailed properties and test results for headed bar specimens having widely-spaced bars with parallel ties tested at the University of Kansas

SN	ID	<i>b</i>	<i>h</i>	$\ell_{eh,avg}$	f_{cm}	d_b	A_b	<i>s</i>	s/d_b
		in.	in.	in.	psi	in.	in. ²	in.	
99	8-15-T4.0-2#3-i-2.5-4.5-7	17.0	13.1	7.1	16030	1	0.79	11.0	11.0
100	8-15-S9.5-2#3-i-2.5-3-7	16.9	12.8	7.1	16030	1	0.79	10.9	10.9
101	8-15-T4.0-5#3-i-2.5-4.5-5.5	17.0	11.5	5.5	16030	1	0.79	11.0	11.0
102	8-15-S9.5-5#3-i-2.5-3-5.5	17.0	11.4	5.6	16030	1	0.79	11.0	11.0
103	8-8-T9.5-2#3-i-2.5-3-9.5	16.8	13.7	9.2	9040	1	0.79	10.8	10.8
104	(2@9)8-12-F4.1-5#3-i-2.5-3-12	15.0	16.0	12.0	12080	1	0.79	9.0	9.0
105	(2@9)8-8-T4.0-5#3-i-2.5-3-9.5	15.1	14.0	9.5	6790	1	0.79	9.1	9.1
106	11-5a-F3.8-2#3-i-2.5-3-17	21.5	21.8	17.4	4050	1.41	1.56	15.1	10.7
107	11-5a-F3.8-6#3-i-2.5-3-17	21.4	21.1	16.7	4050	1.41	1.56	15.0	10.6
108	11-5-F3.8-6#3-i-2.5-3-17	21.4	21.3	16.9	5970	1.41	1.56	15.0	10.6
109	11-12-O4.5-6#3-i-2.5-3-16.75	21.4	26.6	16.8	10860	1.41	1.56	15.0	10.6
110	11-12-S5.5-6#3-i-2.5-3-16.75	21.8	22.6	16.8	10120	1.41	1.56	15.4	10.9
111	11-5-O4.5-6#3-i-2.5-3-19.25	21.4	29.4	19.6	5430	1.41	1.56	15.0	10.6
112	11-5-S5.5-6#3-i-2.5-3-19.25	21.7	24.9	19.1	6320	1.41	1.56	15.3	10.9
113	11-2	22.5	24.5	18.5	15850	1.41	1.56	14.1	10.0
114	14-4	26.7	37.8	32.0	7700	1.693	2.25	18.0	10.6
115	14-2A	26.7	28.6	23.0	13750	1.693	2.25	18.0	10.6
116	14-16B	26.7	28.6	22.1	7500	1.693	2.25	18.0	10.6
117	14-16C	26.7	28.6	22.6	6470	1.693	2.25	18.0	10.6
118	14-16D	26.7	28.6	22.9	6900	1.693	2.25	18.0	10.6
119	14-16E	26.7	28.6	22.4	6170	1.693	2.25	18.0	10.6
120	14-16F	26.7	28.6	22.4	5640	1.693	2.25	18.0	10.6
121	14-2*	26.7	28.6	20.5	12830	1.693	2.25	18.0	10.6
122	14-16*	26.7	28.6	22.6	5390	1.693	2.25	18.0	10.6
123	14-16A*	26.7	28.6	22.4	8350	1.693	2.25	18.0	10.6
124	18-1	27.3	37.8	32.6	5750	2.257	4	18.0	8.0
125	18-2	27.3	37.8	28.4	11770	2.257	4	18.0	8.0
126	18-3	27.3	37.8	30.9	6540	2.257	4	18.0	8.0
127	18-4	27.3	37.8	30.9	7200	2.257	4	18.0	8.0

* Specimen failed in shear, not used to develop descriptive equations, Eq. (5.5) and (5.7)

Table C.4 Cont. Detailed properties and test results for headed bar specimens having widely-spaced bars with parallel ties tested at the University of Kansas

SN	<i>n</i>	<i>A_{tt}</i>	<i>A_{hs}</i>	<i>A_{tt}/A_{hs}</i>	<i>h_{cl}</i>	<i>x_{mid}</i>	<i>d_{eff}</i>	<i>d_{eff}/ℓ_{eh}</i>	<i>θ</i>
		in. ²	in. ²		in.	in.	in.		°
99	2	0.22	1.58	0.139	10.0	14.19	10.78	1.53	63.5
100	2	0.22	1.58	0.139	10.0	14.19	10.90	1.54	63.5
101	2	0.66	1.58	0.418	10.0	14.19	10.84	1.97	68.8
102	2	0.66	1.58	0.418	10.0	14.19	11.01	1.96	68.4
103	2	0.22	1.58	0.139	10.0	14.19	11.64	1.27	57.1
104	2	0.66	1.58	0.418	10.0	14.19	12.24	1.02	49.8
105	2	0.66	1.58	0.418	10.0	14.19	12.48	1.31	56.2
106	2	0.22	3.12	0.071	19.5	23.69	23.27	1.33	53.6
107	2	0.66	3.12	0.212	19.5	23.69	23.22	1.39	54.8
108	2	0.66	3.12	0.212	19.5	23.69	23.22	1.37	54.4
109	2	0.66	3.12	0.212	19.5	23.69	22.64	1.35	54.6
110	2	0.66	3.12	0.212	19.5	23.69	22.74	1.35	54.6
111	2	0.66	3.12	0.212	19.5	23.69	24.22	1.23	50.4
112	2	0.66	3.12	0.212	19.5	23.69	23.93	1.25	51.1
113	2	0.88	3.12	0.282	20.5	23.50	22.74	1.23	51.8
114	2	1.2	4.5	0.267	25.5	28.54	31.24	0.98	41.7
115	2	1.2	4.5	0.267	25.5	28.54	27.95	1.22	51.1
116	2	0.8	4.5	0.178	25.5	28.54	28.84	1.30	52.2
117	2	1.6	4.5	0.356	25.5	28.54	29.41	1.30	51.7
118	2	3.72	4.5	0.827	25.5	28.54	30.75	1.34	51.3
119	2	2.48	4.5	0.551	25.5	28.54	29.71	1.33	51.9
120	2	2.48	4.5	0.551	25.5	28.54	29.52	1.32	51.9
121	2	1.24	4.5	0.276	25.5	28.54	27.51	1.34	54.3
122	2	0.8	4.5	0.178	25.5	28.54	28.09	1.24	51.6
123	2	0.8	4.5	0.178	25.5	28.54	28.52	1.27	51.9
124	2	4.34	8	0.543	33.7	38.15	40.04	1.23	49.5
125	2	4.34	8	0.543	35.2	38.15	39.79	1.40	53.3
126	2	1.86	8	0.233	33.7	38.15	40.39	1.31	51.0
127	2	3.72	8	0.465	33.7	38.15	40.30	1.31	51.0

Table C.4 Cont. Detailed properties and test results for headed bar specimens having widely-spaced bars with parallel ties tested at the University of Kansas

SN	T	T_h ^[1]	T/T_h	f_{su}	$f_{su}/f_{s,calc}$ ^[2]	$f_{su}/f_{s,calc}$ ^[3]
	lb	lb		ksi		
99	59000	66018	0.89	74.7	1.02	1.21
100	67100	66018	1.02	84.9	1.17	1.37
101	63300	63505	1.00	80.1	1.41	1.41
102	75800	64570	1.17	95.9	1.65	1.65
103	68700	74398	0.92	87.0	1.06	1.24
104	111900	109525	1.02	141.6	1.23	1.23
105	76700	82668	0.93	97.1	1.23	1.23
106	118200	132304	0.89	75.8	1.07	1.17
107	116200	138665	0.84	74.5	1.02	1.20
108	151900	150483	1.01	97.4	1.19	1.40
109	201500	167009	1.21	129.2	1.37	1.62
110	197400	164831	1.20	126.5	1.37	1.61
111	181400	167374	1.08	116.3	1.26	1.48
112	189600	168453	1.13	121.5	1.30	1.53
113	221100	200186	1.10	141.7	1.25	1.47
114	333600	312075	1.07	148.3	1.33	1.40
115	248100	263338	0.94	110.3	1.19	1.25
116	191700	218167	0.88	85.2	1.11	1.17
117	208400	236732	0.88	92.6	1.23	1.23
118	289800	247121	1.17	128.8	1.66	1.66
119	218600	238520	0.92	97.2	1.31	1.31
120	197800	234993	0.84	87.9	1.22	1.22
121	190600	237632	0.80	84.7	1.04	1.10
122	123600	208846	0.59	54.9	0.76	0.80
123	186000	224958	0.83	82.7	1.04	1.09
124	322000	396331	0.81	80.5	1.17	1.17
125	406600	402909	1.01	101.7	1.42	1.42
126	366500	353676	1.04	91.6	1.36	1.44
127	380000	395312	0.96	95.0	1.38	1.38

^[1] Based on descriptive equations, Eq. (5.5) and (5.7)

^[2] Based on proposed design equation, Eq. (6.32), using full expression for ψ_p , Eq. (6.29)

^[3] Based on proposed design equation, Eq. (6.32), using simplified expression for ψ_p , Eq. (6.30)

Table C.5 Detailed properties and test results for headed bar specimens having closely-spaced bars with parallel ties tested at the University of Kansas

SN	ID	<i>b</i>	<i>h</i>	$\ell_{eh,avg}$	f_{cm}	d_b	A_b	<i>s</i>	<i>s/d_b</i>
		in.	in.	in.	psi	in.	in. ²	in.	
128	(3@5.9)5-12-F4.0-2#3-i-2.5-4-5	13.2	9.7	5.2	11030	0.625	0.31	3.8	6.1
129	(3@5.9)5-12-F4.0-5#3-i-2.5-4-5	13.0	9.5	5.0	11030	0.625	0.31	3.7	5.9
130	(4@3.9)5-12-F4.0-2#3-i-2.5-4-5	13.1	9.5	5.0	11030	0.625	0.31	2.5	4.0
131	(3@3)8-8-F4.1-2#3-i-2.5-3-10	11.9	14.1	10.1	8260	1	0.79	3.0	3.0
132	(3@3)8-8-F4.1-2#3-i-2.5-3-10-HP	12.0	14.3	10.3	8260	1	0.79	3.0	3.0
133	(3@4)8-8-F4.1-2#3-i-2.5-3-10	14.0	13.9	9.9	8050	1	0.79	4.0	4.0
134	(3@4)8-8-F4.1-2#3-i-2.5-3-10-HP	14.3	14.3	10.3	8050	1	0.79	4.2	4.2
135	(3@5)8-8-F4.1-2#3-i-2.5-3-10.5	15.6	13.8	9.8	8260	1	0.79	4.8	4.8
136	(3@5)8-8-F4.1-2#3-i-2.5-3-10.5-HP	16.1	14.0	10.0	8260	1	0.79	5.1	5.1
137	(3@3)8-12-F4.1-5#3-i-2.5-3-10	12.1	14.0	10.0	11040	1	0.79	3.1	3.1
138	(3@4)8-12-F4.1-5#3-i-2.5-3-10	13.9	13.8	9.8	11440	1	0.79	4.0	4.0
139	(3@5)8-12-F4.1-5#3-i-2.5-3-10	16.3	13.6	9.6	11460	1	0.79	5.2	5.2
140	(3@5.5)8-5-T9.5-5#3-i-2.5-3-14.5	17.1	18.9	14.4	5370	1	0.79	5.6	5.6
141	(4@3.7)8-5-T9.5-5#3-i-2.5-3-14.5	17.4	19.0	14.5	5570	1	0.79	3.8	3.8
142	(3@4)8-8-T9.5-2#3-i-2.5-3-9.5	14.0	14.1	9.6	9040	1	0.79	4.0	4.0
143	(3@5)8-8-T9.5-2#3-i-2.5-3-9.5	16.0	13.9	9.4	9940	1	0.79	5.0	5.0
144	(3@7)8-8-T9.5-2#3-i-2.5-3-9.5	20.1	14.1	9.6	10180	1	0.79	7.1	7.1
145	(3@4)8-8-T9.5-2#3-i-2.5-3-14.5	14.0	18.9	14.4	9040	1	0.79	4.0	4.0
146	(3@5)8-8-T9.5-2#3-i-2.5-3-14.5	16.0	18.6	14.1	9940	1	0.79	5.0	5.0
147	(3@7)8-8-T9.5-2#3-i-2.5-3-14.5	20.0	19.0	14.5	10180	1	0.79	7.0	7.0

Table C.5 Cont. Detailed properties and test results for headed bar specimens having closely-spaced bars with parallel ties tested at the University of Kansas

SN	<i>n</i>	<i>A_{tt}</i>	<i>A_{hs}</i>	<i>A_{tt}/A_{hs}</i>	<i>h_{cl}</i>	<i>x_{mid}</i>	<i>d_{eff}</i>	<i>d_{eff}/ℓ_{eh}</i>	<i>θ</i>
		in. ²	in. ²		in.	in.	in.		°
128	3	0.22	0.93	0.237	5.25	9.44	6.56	1.27	61.4
129	3	0.66	0.93	0.710	5.25	9.44	6.71	1.34	62.0
130	4	0.22	1.24	0.177	5.25	9.44	6.80	1.35	61.9
131	3	0.22	2.37	0.093	10.0	14.19	13.42	1.33	54.6
132	3	0.22	2.37	0.093	10.0	14.19	13.11	1.27	54.0
133	3	0.22	2.37	0.093	10.0	14.19	12.67	1.28	55.1
134	3	0.22	2.37	0.093	10.0	14.19	13.29	1.29	53.9
135	3	0.22	2.37	0.093	10.0	14.19	12.36	1.26	55.4
136	3	0.22	2.37	0.093	10.0	14.19	12.67	1.27	54.8
137	3	0.66	2.37	0.278	10.0	14.19	12.50	1.25	54.8
138	3	0.66	2.37	0.278	10.0	14.19	12.24	1.25	55.4
139	3	0.66	2.37	0.278	10.0	14.19	12.03	1.25	55.9
140	3	0.66	2.37	0.278	10.0	14.19	14.65	1.02	44.5
141	4	0.66	3.16	0.209	10.0	14.19	14.84	1.02	44.4
142	3	0.22	2.37	0.093	10.0	14.19	12.22	1.28	56.0
143	3	0.22	2.37	0.093	10.0	14.19	11.91	1.26	56.4
144	3	0.22	2.37	0.093	10.0	14.19	11.79	1.23	56.0
145	3	0.22	2.37	0.093	10.0	14.19	13.66	0.95	44.5
146	3	0.22	2.37	0.093	10.0	14.19	13.59	0.97	45.2
147	3	0.22	2.37	0.093	10.0	14.19	13.02	0.90	44.3

Table C.5 Cont. Detailed properties and test results for headed bar specimens having closely-spaced bars with parallel ties tested at the University of Kansas

SN	T	$T_h^{[1]}$	T/T_h	f_{su}	$f_{su}/f_{s,calc}^{[2]}$	$f_{su}/f_{s,calc}^{[3]}$
	lb	lb		ksi		
128	35133	33584	1.05	113.3	1.21	1.53
129	38633	34700	1.11	124.6	1.30	1.30
130	30900	27915	1.11	99.7	1.44	1.53
131	61900	57369	1.08	78.4	1.51	1.48
132	56700	58670	0.97	71.8	1.35	1.33
133	55500	60679	0.91	70.3	1.28	1.36
134	69800	63840	1.09	88.4	1.52	1.64
135	56100	63998	0.88	71.0	1.21	1.37
136	65500	66344	0.99	82.9	1.35	1.53
137	61600	66202	0.93	78.0	1.04	1.02
138	65700	69943	0.94	83.2	1.05	1.10
139	69700	74981	0.93	88.2	1.02	1.19
140	94600	94050	1.01	119.7	1.08	1.30
141	76867	82141	0.94	97.3	1.13	1.18
142	51800	60391	0.86	65.6	1.20	1.27
143	55900	65003	0.86	70.8	1.18	1.33
144	67600	75489	0.90	85.6	1.14	1.28
145	85400	87381	0.98	108.1	1.31	1.39
146	105200	93460	1.13	133.2	1.48	1.67
147	113400	109767	1.03	143.5	1.26	1.42

^[1] Based on descriptive equations, Eq. (5.5) and (5.7)

^[2] Based on proposed design equation, Eq. (6.32), using full expression for ψ_p , Eq. (6.29)

^[3] Based on proposed design equation, Eq. (6.32), using simplified expression for ψ_p , Eq. (6.30)

Table C.5 Cont. Detailed properties and test results for headed bar specimens having closely-spaced bars with parallel ties tested at the University of Kansas

SN	ID	<i>b</i>	<i>h</i>	$\ell_{eh,avg}$	f_{cm}	d_b	A_b	<i>s</i>	<i>s/d_b</i>
		in.	in.	in.	psi	in.	in. ²	in.	
148	(3@4.5)8-12-F4.1-5#3-i-2.5-3-12	14.9	16.2	12.2	12040	1	0.79	4.5	4.5
149	(3@4.5)8-12-F9.1-5#3-i-2.5-3-12	15.0	15.9	11.9	12040	1	0.79	4.5	4.5
150	(4@3)8-12-F4.1-5#3-i-2.5-3-12	15.0	16.0	12.0	12360	1	0.79	3.0	3.0
151	(4@3)8-12-F9.1-5#3-i-2.5-3-12	15.0	16.0	12.0	12360	1	0.79	3.0	3.0
152	(3@4.5)8-8-T4.0-5#3-i-2.5-3-9.5	15.4	13.7	9.2	6650	1	0.79	4.7	4.7
153	(4@3)8-8-T4.0-5#3-i-2.5-3-9.5	15.0	14.2	9.7	6650	1	0.79	3.0	3.0
154	(3@3)8-8-T4.0-5#3-i-2.5-3-9.5	12.1	13.8	9.3	6650	1	0.79	3.1	3.1
155	(3@5.35)11-12-O4.5-6#3-i-2.5-3-16.75	21.4	26.8	17.0	10860	1.41	1.56	7.5	5.3
156	(3@5.35)11-12-S5.5-6#3-i-2.5-3-16.75	21.3	22.5	16.8	10120	1.41	1.56	7.5	5.3
157	(3@5.35)11-5-O4.5-6#3-i-2.5-3-19.25	21.6	29.1	19.4	5430	1.41	1.56	7.6	5.4
158	(3@5.35)11-5-S5.5-6#3-i-2.5-3-19.25	21.5	25.0	19.3	6320	1.41	1.56	7.6	5.4
159	14-17	26.7	28.6	22.4	6540	1.693	2.25	12.0	7.1
160	14-5	20.7	28.6	22.3	6830	1.693	2.25	6.0	3.5
161	14-6	20.7	28.6	22.4	6890	1.693	2.25	6.0	3.5
162	14-8	20.7	37.8	31.7	7100	1.693	2.25	6.0	3.5
163	14-9	20.7	28.6	22.1	11480	1.693	2.25	6.0	3.5
164	14-10	20.7	28.6	22.3	6820	1.693	2.25	6.0	3.5
165	18-5	27.3	37.8	32.5	5310	2.257	4	12.0	5.3
166	18-6	27.3	37.8	28.6	10230	2.257	4	12.0	5.3
167	18-7	27.3	37.8	32.1	5890	2.257	4	6.0	2.7
168	18-8	27.3	37.8	32.3	6380	2.257	4	6.0	2.7

Table C.5 Cont. Detailed properties and test results for headed bar specimens having closely-spaced bars with parallel ties tested at the University of Kansas

SN	<i>n</i>	<i>A_{tt}</i>	<i>A_{hs}</i>	<i>A_{tt}/A_{hs}</i>	<i>h_{cl}</i>	<i>x_{mid}</i>	<i>d_{eff}</i>	<i>d_{eff}/ℓ_{eh}</i>	<i>θ</i>
		in. ²	in. ²		in.	in.	in.		°
148	3	0.66	2.37	0.278	10.0	14.19	12.65	1.04	49.4
149	3	0.66	2.37	0.278	10.0	14.19	13.26	1.11	50.0
150	4	0.66	3.16	0.209	10.0	14.19	12.51	1.04	49.7
151	4	0.66	3.16	0.209	10.0	14.19	13.43	1.12	49.9
152	3	0.66	2.37	0.278	10.0	14.19	13.00	1.42	57.1
153	4	0.66	3.16	0.209	10.0	14.19	13.20	1.37	55.7
154	3	0.66	2.37	0.278	10.0	14.19	13.46	1.44	56.7
155	3	0.66	4.68	0.141	19.5	23.69	22.67	1.33	54.3
156	3	0.66	4.68	0.141	19.5	23.69	23.37	1.40	54.7
157	3	0.66	4.68	0.141	19.5	23.69	24.97	1.29	50.7
158	3	0.66	4.68	0.141	19.5	23.69	24.91	1.29	50.9
159	2	2.48	4.5	0.551	25.5	28.54	29.35	1.31	51.9
160	3	1.20	6.75	0.178	24.0	28.54	30.41	1.36	52.0
161	3	1.86	6.75	0.276	24.0	28.54	30.30	1.35	51.8
162	3	1.86	6.75	0.276	24.0	28.54	33.49	1.06	42.0
163	3	1.86	6.75	0.276	25.5	28.54	29.47	1.33	52.2
164	3	3.72	6.75	0.551	24.0	28.54	31.29	1.41	52.1
165	2	4.344	8	0.543	33.7	38.15	39.88	1.23	49.6
166	2	4.344	8	0.543	35.2	38.15	40.60	1.42	53.1
167	3	6.516	12	0.543	32.2	38.15	7.34	0.23	49.9
168	3	6.516	12	0.543	32.2	38.15	8.20	0.25	49.7

Table C.5 Cont. Detailed properties and test results for headed bar specimens having closely-spaced bars with parallel ties tested at the University of Kansas

SN	T	$T_h^{[1]}$	T/T_h	f_{su}	$f_{su}/f_{s,calc}^{[2]}$	$f_{su}/f_{s,calc}^{[3]}$
	lb	lb		ksi		
148	87700	87901	1.00	111.0	1.07	1.16
149	108567	86555	1.25	137.4	1.34	1.47
150	64175	76549	0.84	81.2	0.99	0.97
151	87800	76107	1.15	111.1	1.37	1.34
152	62467	63550	0.98	79.1	1.14	1.28
153	48600	56489	0.86	61.5	1.09	1.07
154	56533	57108	0.99	71.6	1.16	1.14
155	135800	143119	0.95	87.1	1.19	1.42
156	153800	139041	1.11	98.6	1.40	1.66
157	141700	141112	1.00	90.8	1.29	1.54
158	152900	144108	1.06	98.0	1.35	1.62
159	206700	236469	0.87	91.9	1.22	1.22
160	181800	167221	1.09	80.8	1.37	1.40
161	179500	177273	1.01	79.8	1.14	1.16
162	274600	237013	1.16	122.0	1.22	1.24
163	173900	192173	0.90	77.3	0.98	1.00
164	206600	187191	1.10	91.8	1.22	1.22
165	300800	343107	0.88	75.2	1.12	1.12
166	419800	347541	1.21	105.0	1.51	1.51
167	252100	284797	0.89	63.0	0.93	0.93
168	295300	290162	1.02	73.8	1.06	1.06

^[1] Based on descriptive equations, Eq. (5.5) and (5.7)

^[2] Based on proposed design equation, Eq. (6.32), using full expression for ψ_p , Eq. (6.29)

^[3] Based on proposed design equation, Eq. (6.32), using simplified expression for ψ_p , Eq. (6.30)

C.4 SPECIMENS TESTED IN OTHER STUDIES

This section presents the specimens tested outside the University of Kansas, including those by Bashandy (1996), Chun et al. (2017a), and Sim and Chun (2022a, 2022b), as tabulated in Table C.6. None of these specimens were used in developing descriptive equations, Eq. (5.5) and (5.7).

Table C.6 Detailed properties and test results for hooked bar specimens tested outside the University of Kansas

Study	SN	ID	<i>b</i>	<i>h</i>	$\ell_{eh,avg}$	f_{cm}	d_b	A_b	<i>s</i>	<i>s/d_b</i>
			in.	in.	in.	psi	in.	in. ²	in.	
Bashandy (1996)	169	T9	15.0	12.0	11.0	5000	1.41	1.56	4.7	3.3
	170	T10**	15.0	12.0	12.5	5000	1.41	1.56	7.6	5.4
	171	T12**	12.0	12.0	9.8	5110	1	0.79	8.0	8.0
	172	T13**	15.0	12.0	12.8	5560	1	0.79	8.0	8.0
	173	T14	15.0	12.0	11.0	5400	1.41	1.56	4.7	3.3
	174	T16	18.0	12.0	14.0	5740	1.41	1.56	4.7	3.3
	175	T20	12.0	12.0	8.2	5110	1.41	1.56	4.7	3.3
	176	T21	12.0	12.0	8.3	5110	1	0.79	5.0	5.0
	177	T22	12.0	12.0	8.3	5110	1	0.79	5.0	5.0
	178	T23	15.0	12.0	11.2	4820	1.41	1.56	4.7	3.3
	179	T24	15.0	12.0	11.2	4690	1.41	1.56	4.7	3.3
	180	T25	15.0	12.0	11.0	4690	1.41	1.56	4.7	3.3
	181	T26	21.0	12.0	17.0	4550	1.41	1.56	4.7	3.3
	182	T27	12.0	12.0	8.0	4550	1.41	1.56	4.7	3.3
	183	T28	15.0	12.0	11.2	4830	1.41	1.56	4.7	3.3
	184	T29	15.0	12.0	11.0	4830	1.41	1.56	4.7	3.3
185	T30	15.0	12.0	11.3	3210	1	0.79	5.0	5.0	
186	T32	12.0	12.0	8.0	4830	1	0.79	5.0	5.0	

** Specimens with bars outside column core and parallel ties, therefore Att/Ahs = 0 when calculating ψ_p

Table C.6 Cont. Detailed properties and test results for hooked bar specimens tested outside the University of Kansas

SN	n	A_u	A_{hs}	A_u/A_{hs}	h_{cl}	x_{mid}	d_{eff}	d_{eff}/ℓ_{eh}	θ
		in. ²	in. ²		in.	in.	in.		°
169	2	2.00	3.12	0.641	11.0	14.0	14.02	1.27	51.9
170	2	1.86	3.12	0.596	11.0	14.0	13.41	1.07	48.3
171	2	0.88	1.58	0.557	11.0	14.0	12.95	1.32	55.0
172	2	1.24	1.58	0.785	11.0	14.0	13.27	1.04	47.6
173	2	0.66	3.12	0.212	11.0	14.0	14.51	1.32	51.9
174	2	3.20	3.12	1.026	11.0	14.0	13.88	0.99	45.0
175	2	3.20	3.12	1.026	11.0	14.0	14.81	1.81	59.7
176	2	3.20	1.58	2.025	11.0	14.0	13.39	1.61	59.4
177	2	3.20	1.58	2.025	11.0	14.0	13.01	1.57	59.4
178	2	3.20	3.12	1.026	11.0	14.0	13.79	1.23	51.4
179	2	3.20	3.12	1.026	11.0	14.0	14.32	1.28	51.4
180	2	6.12	3.12	1.962	11.0	14.0	14.95	1.36	51.9
181	2	3.20	3.12	1.026	11.0	14.0	14.36	0.84	39.5
182	2	3.20	3.12	1.026	11.0	14.0	13.35	1.67	60.3
183	2	3.20	3.12	1.026	11.0	14.0	14.92	1.33	51.4
184	2	3.20	3.12	1.026	11.0	14.0	14.50	1.32	51.9
185	2	3.20	1.58	2.025	11.0	14.0	14.47	1.28	51.1
186	2	3.20	1.58	2.025	11.0	14.0	13.46	1.68	60.3

Table C.6 Cont. Detailed properties and test results for hooked bar specimens tested outside the University of Kansas

SN	T	$T_h^{[1]}$	T/T_h	f_{su}	$f_{su}/f_{s,calc}^{[2]}$	$f_{su}/f_{s,calc}^{[3]}$
	lb	lb		ksi		
169	76400	89600	0.85	49.0	0.97	0.97
170	60900	77800	0.92	39.0	1.21	1.21
171	40000	65100	0.72	50.6	0.90	0.90
172	61400	85100	0.84	77.7	1.04	1.04
173	93500	79100	1.18	59.9	1.60	1.60
174	95800	108500	0.88	61.4	0.92	0.92
175	78500	74100	1.06	50.3	1.32	1.32
176	49000	61400	0.8	62.0	0.96	0.96
177	41100	61400	0.67	52.0	0.81	0.81
178	68800	90100	0.76	44.1	0.86	0.86
179	80300	89800	0.89	51.5	1.01	1.01
180	95800	88700	1.08	61.4	1.23	1.23
181	111300	120600	0.92	71.3	0.93	0.93
182	44500	71800	0.62	28.5	0.79	0.79
183	97100	90200	1.08	62.2	1.22	1.22
184	86600	89100	0.97	55.5	1.10	1.10
185	62700	71600	0.88	79.4	1.02	1.02
186	48600	59400	0.82	61.5	1.01	1.01

^[1] Based on descriptive equations, Eq. (5.5) and (5.7)

^[2] Based on proposed design equation, Eq. (6.32), using full expression for ψ_p , Eq. (6.29)

^[3] Based on proposed design equation, Eq. (6.32), using simplified expression for ψ_p , Eq. (6.30)

Table C.6 Cont. Detailed properties and test results for hooked bar specimens tested outside the University of Kansas

Study	SN	ID ^{[1][2][3]}	<i>b</i>	<i>h</i>	$\ell_{eh,avg}$	f_{cm}	d_b	A_b	<i>s</i>	<i>s/d_b</i>
			in.	in.	in.	psi	in.	in. ²	in.	
Chun et al. (2017a)	187	D43-L7-C1-S42	21.3	14.8	11.9	6950	1.693	2.25	16.3	9.6
	188	D43-L7-C1-S42-HP0.5	21.3	14.8	11.9	6950	1.693	2.25	16.3	9.6
	189	D43-L7-C1-S70	21.3	14.8	11.9	9890	1.693	2.25	16.3	9.6
	190	D43-L10-C1-S42	21.3	19.8	16.9	7570	1.693	2.25	16.3	9.6
	191	D43-L10-C1-S42- HP0.5	21.3	19.8	16.9	7570	1.693	2.25	16.3	9.6
	192	D43-L10-C1-S70	21.3	19.8	16.9	11,770	1.693	2.25	16.3	9.6
	193	D43-L13-C1-S42	13.5	24.9	22	6640	1.693	2.25	8.5	5
	194	D43-L13-C2-S42	16.9	24.9	22	6420	1.693	2.25	8.5	5
	195	D43-L13-C1-S42-T1.5	13.5	24.9	22	5870	1.693	2.25	8.5	5
	196	D43-L13-C2-S42-T1.5*	16.9	24.9	22	6060	1.693	2.25	8.5	5
	197	D43-L16-C1-S42	13.5	30.0	27.1	6640	1.693	2.25	8.5	5
	198	D43-L16-C2-S42*	16.9	30.0	27.1	6640	1.693	2.25	8.5	5
	199	D43-L16-C1-S42-T1.5	13.5	30.0	27.1	6060	1.693	2.25	8.5	5
	200	D43-L16-C2-S42-T1.5*	16.9	30.0	27.1	6420	1.693	2.25	8.5	5
	201	D57-L7-C1-S42	23.0	18.9	15.8	7450	2.257	4	16.3	7.2
	202	D57-L7-C1-S42-HP0.5	23.0	18.9	15.8	7450	2.257	4	16.3	7.2
	203	D57-L7-C1-S70	23.0	18.9	15.8	11,150	2.257	4	16.3	7.2
	204	D57-L10-C1-S42	23.0	25.7	22.6	7450	2.257	4	16.3	7.2
	205	D57-L10-C1-S42-HP0.5	23.0	25.7	22.6	7450	2.257	4	16.3	7.2
	206	D57-L10-C1-S70	23.0	25.7	22.6	11,150	2.257	4	16.3	7.2
	207	D57-L13-C1-S42	23.0	32.4	29.3	5870	2.257	4	16.3	7.2
	208	D57-L13-C1-S42-HP0.5*	23.0	32.4	29.3	5870	2.257	4	16.3	7.2
	209	D57-L13-C1-S42-HP1.0a*	23.0	32.4	29.3	5870	2.257	4	16.3	7.2
210	D57-L13-C1-S42-HP1.0b*	23.0	32.4	29.3	5870	2.257	4	16.3	7.2	
211	D57-L13-C2-S42	27.5	32.4	29.3	5870	2.257	4	16.3	7.2	
212	D57-L16-C1-S42	23.0	39.2	36.1	6060	2.257	4	16.3	7.2	
213	D57-L16-C2-S42*	27.5	39.2	36.1	6060	2.257	4	16.3	7.2	

^[1] No specimen used in developing descriptive equations, Eq. (5.5) and 95.7)

^[2] Bars outside column core in all specimens

^[3] HP and T at the end of the designations denote a "confined" specimen. In all other cases, bars are outside parallel ties, therefore $A_{tr}/A_{hs} = 0$ when calculating ψ_p .

* Bars yielded

Table C.6 Cont. Detailed properties and test results for hooked bar specimens tested outside the University of Kansas

SN	<i>n</i>	<i>A_{tt}</i>	<i>A_{hs}</i>	<i>A_{tt}/A_{hs}</i> *	<i>h_{cl}</i>	<i>x_{mid}</i>	<i>d_{eff}</i>	<i>d_{eff}/ℓ_{eh}</i>	<i>θ</i>
		in. ²	in. ²		in.	in.	in.		°
187	2	1.8	4.5	0.4	5.5	7.9	7.79	0.65	33.7
188	2	1.8	4.5	0.4	5.5	7.9	8.56	0.72	33.7
189	2	1.8	4.5	0.4	5.5	7.9	8.29	0.70	33.7
190	2	1.8	4.5	0.4	8.8	11.3	11.91	0.70	33.7
191	2	1.8	4.5	0.4	8.8	11.3	12.31	0.73	33.7
192	2	1.8	4.5	0.4	8.8	11.3	11.61	0.69	33.7
193	2	1.8	4.5	0.4	10.7	14.7	16.36	0.74	33.7
194	2	1.8	4.5	0.4	10.7	14.7	15.95	0.72	33.7
195	2	1.8	4.5	0.4	10.7	14.7	16.69	0.76	33.7
196	2	1.8	4.5	0.4	10.7	14.7	17.17	0.78	33.7
197	2	1.8	4.5	0.4	14.1	18.1	20.92	0.77	33.7
198	2	1.8	4.5	0.4	14.1	18.1	19.89	0.73	33.7
199	2	1.8	4.5	0.4	14.1	18.1	19.43	0.72	33.7
200	2	1.8	4.5	0.4	14.1	18.1	20.20	0.75	33.7
201	2	3.2	8	0.4	6.9	10.5	10.81	0.68	33.7
202	2	3.2	8	0.4	6.9	10.5	11.86	0.75	33.7
203	2	3.2	8	0.4	6.9	10.5	10.13	0.64	33.7
204	2	3.2	8	0.4	11.4	15.1	15.73	0.70	33.7
205	2	3.2	8	0.4	11.4	15.1	16.97	0.75	33.7
206	2	3.2	8	0.4	11.4	15.1	15.06	0.67	33.7
207	2	3.2	8	0.4	14.8	19.5	20.70	0.71	33.7
208	2	3.2	8	0.4	14.8	19.5	22.66	0.77	33.7
209	2	3.2	8	0.4	14.8	19.5	22.66	0.77	33.7
210	2	3.2	8	0.4	14.8	19.5	22.69	0.77	33.7
211	2	3.2	8	0.4	14.8	19.5	20.98	0.72	33.7
212	2	3.2	8	0.4	19.4	24.1	26.05	0.72	33.7
213	2	3.2	8	0.4	19.4	24.1	25.81	0.71	33.7

* Cap of 0.4 applied to all specimens

Table C.6 Cont. Detailed properties and test results for hooked bar specimens tested outside the University of Kansas

SN	T	$T_h^{[1]}$	T/T_h	f_{su}	$f_{su}/f_{s,calc}^{[2]}$	$f_{su}/f_{s,calc}^{[3]}$
	lb	lb		ksi		
187	102000	91892	1.11	45.3	1.36	1.36
188	136000	132039	1.03	60.4	1.72	1.72
189	163600	99152	1.65	72.7	1.99	1.99
190	142700	130917	1.09	63.4	1.31	1.31
191	161000	171277	0.94	71.6	1.40	1.40
192	193400	144328	1.34	86.0	1.59	1.59
193	155000	126016	1.23	68.9	1.55	1.55
194	176200	124965	1.41	78.3	1.78	1.78
195	152800	171685	0.89	67.9	1.09	1.09
196	210200	172295	1.22	93.4	1.48	1.48
197	186800	153115	1.22	83.0	1.52	1.52
198	198000	153488	1.29	88.0	1.61	1.61
199	138400	203529	0.68	61.5	0.79	0.79
200	205000	205000	1.00	91.1	1.16	1.16
201	193800	133655	1.45	48.5	1.82	1.82
202	246000	212069	1.16	61.5	1.99	1.99
203	230000	145570	1.58	57.5	1.95	1.95
204	212800	186667	1.14	53.2	1.39	1.39
205	274200	268824	1.02	68.6	1.55	1.55
206	258000	203150	1.27	64.5	1.53	1.53
207	254800	227500	1.12	63.7	1.37	1.37
208	340000	311927	1.09	85.0	1.57	1.57
209	340000	311927	1.09	85.0	1.57	1.57
210	341200	310182	1.10	85.3	1.58	1.58
211	319200	228000	1.40	79.8	1.71	1.71
212	296000	279245	1.06	74.0	1.28	1.28
213	341200	279672	1.22	85.3	1.47	1.47

^[1] Based on descriptive equations, Eq. (5.5) and (5.7)

^[2] Based on proposed design equation, Eq. (6.32), using full expression for ψ_p , Eq. (6.29)

^[3] Based on proposed design equation, Eq. (6.32), using simplified expression for ψ_p , Eq. (6.30)

Table C.6 Cont. Detailed properties and test results for hooked bar specimens tested outside the University of Kansas

Study	SN	ID ^{[1][2][3]}	<i>b</i>	<i>h</i>	$\ell_{eh,avg}$	f_{cm}	d_b	A_b	s	s/d_b^{**}
			in.	in.	in.	psi	in.	in. ²	in.	
Sim and Chun (2022a)	214	D43-L13-C1-42	21.4	25.2	22.0	6260	1.693	2.25	1.7	1
	215	D43-L13-C2-42	24.8	25.2	22.0	6260	1.693	2.25	3.4	2
	216	D43-L13-C2-70	24.8	25.2	22.0	12590	1.693	2.25	3.4	2
	217	D43-L13-C2-42-C	24.8	25.2	22.0	6260	1.693	2.25	3.4	2
	218	D43-L16-C1-42	21.4	30.2	27.1	6850	1.693	2.25	1.7	1
	219	D43-L16-C2-42	24.8	30.2	27.1	6850	1.693	2.25	3.4	2
	220	D43-L16-C2-70	24.8	30.2	27.1	11450	1.693	2.25	3.4	2
	221	D43-L16-C2-42-C*	24.8	30.2	27.1	6850	1.693	2.25	3.4	2
	222	D43-L20-C1-42	21.4	37.0	33.9	6260	1.693	2.25	1.7	1
	223	D43-L20-C2-42	24.8	37.0	33.9	6260	1.693	2.25	3.4	2
Sim and Chun (2022b)	224	D22-L6-C1	14.4	6.9	5.3	12020	0.875	0.6	11.8	13.5
	225	D22-L6-C1.5	15.3	6.9	5.3	12020	0.875	0.6	11.8	13.5
	226	D22-L6-C1-TR	14.4	6.9	5.3	12020	0.875	0.6	11.8	13.5
	227	D22-L9-C1	14.4	9.5	7.9	12020	0.875	0.6	11.8	13.5
	228	D32-L6-C1	15.6	10.1	7.6	12020	1.27	1.27	11.8	9.3
	229	D32-L6-C1.5	16.9	10.1	7.6	12020	1.27	1.27	11.8	9.3
	230	D32-L6-C1-TR	15.6	10.1	7.6	12020	1.27	1.27	11.8	9.3
	231	D32-L9-C1	15.6	13.9	11.4	12020	1.27	1.27	11.8	9.3
	232	D22-L6-C1	14.4	6.9	5.3	16680	0.875	0.6	11.8	13.5
	233	D22-L6-C1.5	15.3	6.9	5.3	16680	0.875	0.6	11.8	13.5
	234	D22-L6-C1-TR	14.4	6.9	5.3	16680	0.875	0.6	11.8	13.5
	235	D22-L9-C1	14.4	9.5	7.9	16680	0.875	0.6	11.8	13.5
	236	D32-L6-C1	15.6	10.1	7.6	16680	1.27	1.27	11.8	9.3
	237	D32-L6-C1.5	16.9	10.1	7.6	16680	1.27	1.27	11.8	9.3
	238	D32-L6-C1-TR	15.6	10.1	7.6	16680	1.27	1.27	11.8	9.3
	239	D32-L9-C1	15.6	13.9	11.4	16680	1.27	1.27	11.8	9.3

^[1] No specimen used in developing descriptive equations, Eq. (5.5) and 95.7)

^[2] Bars outside column core in all specimens

^[3] C and TR at the end of the designations denote a "confined" specimen. In all other cases, bars are outside parallel ties, therefore $A_{tr}/A_{hs} = 0$ when calculating ψ_p .

* Bars yielded

** Center-to-center spacing between the two layers of headed bars was taken as s for Sim and Chun (2022a)

Table C.6 Cont. Detailed properties and test results for hooked bar specimens tested outside the University of Kansas

SN	n	A_u	A_{hs}	A_u/A_{hs}^*	h_{cl}	x_{mid}	d_{eff}	d_{eff}/ℓ_{eh}	θ
		in. ²	in. ²		in.	in.	in.		°
214	4	3.6	9	0.4	**	22.0	**	**	45.0
215	4	3.6	9	0.4	**	22.0	**	**	45.0
216	4	3.6	9	0.4	**	22.0	**	**	45.0
217	4	3.6	9	0.4	**	22.0	**	**	45.0
218	4	3.6	9	0.4	**	27.1	**	**	45.0
219	4	3.6	9	0.4	**	27.1	**	**	45.0
220	4	3.6	9	0.4	**	27.1	**	**	45.0
221	4	3.6	9	0.4	**	27.1	**	**	45.0
222	4	3.6	9	0.4	**	33.9	**	**	45.0
223	4	3.6	9	0.4	**	33.9	**	**	45.0
224	2	0.48	1.2	0.4	**	3.5	**	**	33.7
225	2	0.48	1.2	0.4	**	3.5	**	**	33.7
226	2	0.48	1.2	0.4	**	3.5	**	**	33.7
227	2	0.48	1.2	0.4	**	5.3	**	**	33.7
228	2	1.016	2.54	0.4	**	5.1	**	**	33.7
229	2	1.016	2.54	0.4	**	5.1	**	**	33.7
230	2	1.016	2.54	0.4	**	5.1	**	**	33.7
231	2	1.016	2.54	0.4	**	7.6	**	**	33.7
232	2	0.48	1.2	0.4	**	3.5	**	**	33.7
233	2	0.48	1.2	0.4	**	3.5	**	**	33.7
234	2	0.48	1.2	0.4	**	3.5	**	**	33.7
235	2	0.48	1.2	0.4	**	5.3	**	**	33.7
236	2	1.016	2.54	0.4	**	5.1	**	**	33.7
237	2	1.016	2.54	0.4	**	5.1	**	**	33.7
238	2	1.016	2.54	0.4	**	5.1	**	**	33.7
239	2	1.016	2.54	0.4	**	7.6	**	**	33.7

* Cap of 0.4 applied to all specimens

** Information not provided

Table C.6 Cont. Detailed properties and test results for hooked bar specimens tested outside the University of Kansas

SN	T	$T_h^{[1]}$	T/T_h	f_{su}	$f_{su}/f_{s,calc}^{[2]}$	$f_{su}/f_{s,calc}^{[3]}$
	lb	lb		ksi		
214*	88900	73471	1.21	39.5	N/A	N/A
215*	103400	86167	1.20	46.0	N/A	N/A
216*	143200	99444	1.44	63.6	N/A	N/A
217*	145600	138667	1.05	64.7	N/A	N/A
218*	114600	90952	1.26	50.9	N/A	N/A
219*	134100	106429	1.26	59.6	N/A	N/A
220*	156200	119237	1.31	69.4	N/A	N/A
221*	164300	164300	1.00	73.0	N/A	N/A
222*	123100	109911	1.12	54.7	N/A	N/A
223*	135600	129143	1.05	60.3	N/A	N/A
224	41400	34500	1.20	69.0	1.50	1.50
225	33700	34388	0.98	56.2	1.22	1.22
226	47900	44766	1.07	79.8	1.48	1.48
227	44000	50575	0.87	73.3	1.07	1.07
228	104700	59153	1.77	82.4	2.19	2.19
229	102900	59138	1.74	81.0	2.15	2.15
230	91300	80796	1.13	71.9	1.62	1.62
231	92600	86542	1.07	72.9	1.29	1.29
232	38700	36857	1.05	64.5	1.29	1.29
233	31500	37059	0.85	52.5	1.05	1.05
234	39000	46988	0.83	65.0	1.11	1.11
235	35900	54394	0.66	59.8	0.80	0.80
236	108100	63216	1.71	85.1	2.08	2.08
237	108500	63081	1.72	85.4	2.09	2.09
238	101500	85294	1.19	79.9	1.66	1.66
239	103200	92143	1.12	81.3	1.32	1.32

^[1] Based on descriptive equations, Eq. (5.5) and (5.7)

^[2] Based on proposed design equation, Eq. (6.32), using full expression for ψ_p , Eq. (6.29)

^[3] Based on proposed design equation, Eq. (6.32), using simplified expression for ψ_p , Eq. (6.30)

* Proposed design provisions do not apply since $s < 3d_b$

